UNIVERSITAT DE BARCELONA

Engineered nanomaterials release from nano-enabled products

Vicenç Pomar-Portillo

UNIVERSITAT DE BARCELONA

Faculty of Chemistry

Doctoral program in Nanoscience

Engineered nanomaterials release from nano-enabled products

Vicenç Pomar-Portillo

PhD Thesis

Barcelona, September 2021

Supervisor

Dr. Socorro Vázquez-Campos

(LEITAT Technolofical Center)

Tutor

Dr. Daniel Sainz Garcia

(UB, Faculty of Chemistry)

LEITAT Technological Center
managing your technologies
member of TECNIO

To my family and friends for
supporting me through all the process

Summary

The increased presence of nano-enabled products in multiple applications has raised concerns about its potential risks to human health and the environment. Therefore, there is a need for a responsible and coordinated approach to ensure that potential safety issues are being addressed at the same time as the technology is developing. The research presented in this PhD Thesis has the objective to contribute to the understanding of the potential human and environmental risks associated with engineered nanomaterials and nano-enabled products by generating relevant data on engineered nanomaterials released from nano-enabled products along their life cycle.

The objective has been tackled from three different perspectives: Firstly, by upgrading and refining material flow models that allow the prediction of engineered nanomaterials concentration in the environment; secondly, by generating release data from experimental simulations with multiple nano-enabled products; and thirdly, by evaluating the current research performed in Nanosafety Projects funded by the European Commission and suggesting where future research on release studies should focus.

The material flow model refinement is presented in the form of one peer-reviewed publication. In this study, a country-specific assessment of the flows to the environment from production to end-of-life of nano-Ag, -TiO_2 and -ZnO within Europe is described. The MF model provided insights on potential exposure to the environment. The outcomes from the model were ENM concentrations (tonnes/km^2) in different environmental compartments due to release. From these data, via realistic fate and exposure assessment, the data could be used to determine the potential risk that nano-TiO_2, -ZnO and -Ag releases could pose to the environment.

The release data generation from experiments is presented by two peer-reviewed publications and five unpublished results. In the first publication, the release from a fluorescent ink containing CdTe quantum dots during inkjet printing is evaluated. In the second publication, the release mechanisms of Polyamide 6 nanocomposites under weathering conditions are assessed. Nanocomposites containing nano-SiO_2, -TiO_2, -ZnO, multiwalled carbon nanotubes and two nano-organoclays were included in the study. Regarding the five unpublished studies, three of them are related to the use phase: household washing of curtains containing nano-TiO_2, weathering and abrasion of an asphalt coating containing nano-TiO_2 and household washing of a textile incorporating nano-Ag in different forms (nanoparticles and two nanowires of different lengths). The other two unpublished studies are related to the end-of-life, both of them considering the potential leaching that occurs in landfills. One study evaluates a camping tent

containing nano-Ag and the other a printed circuit for electronics with conductive ink containing nano-Ag. . An exhaustive characterisation was done in all the cases on both starting materials (engineered nanomaterials before being incorporated in the product), in the nano-enabled products before and after the respective experiments, and also on the released materials. The main outcomes were release rates and release forms, which were included in publically accessible databases to be used by the entire nanosafety community.

The evaluation of the current research performed in Nanosafety Projects funded by the European Commission and the suggestions where future research on release studies should focus is presented in the form of one peer-reviewed publication. The purpose of analysing the nanosafety research was to provide an overview of the products studied compared to what can realistically be found in the market (i.e. the exposure relevant materials that workers, consumers and the environment may be exposed to). In addition, the inventory also provided a rich source of information from which readers with different data needs can extract their own conclusions, providing relevant insights for the nanosafety community

The combination of key information and analyses deriving from the different studies allowed the extraction of conclusions and recommendations to contribute to the understanding of the potential human and environmental risks associated with engineered nanomaterials and nano-enabled products, which is described in the discussions and conclusions section.

Resum

La major presència de productes amb nanomaterials en múltiples aplicacions ha suscitat preocupacions sobre els seus possibles riscos per a la salut humana i el medi ambient. Per tant, cal un enfocament responsable i coordinat per garantir que s'aborden els possibles problemes de seguretat a el mateix temps que es desenvolupa la tecnologia. La investigació presentada en aquesta tesi doctoral té com a objectiu contribuir a la comprensió dels possibles riscos humans i ambientals associats amb els nanomaterials i els productes que en continguin, mitjançant la generació de dades rellevants sobre el seu alliberament al llarg del seu cicle de vida.

L'objectiu s'ha abordat des de tres perspectives diferents: en primer lloc, mitjançant l'actualització i perfeccionament dels models de flux de materials,; en segon lloc, generant dades d'alliberament a partir d'experiments amb múltiples productes que contenen nanomaterials; i en tercer lloc, avaluant la investigació realitzada en Projectes de Nanoseguretat finançats per la Comissió Europea.

El perfeccionament del model de flux de materials es presenta mitjançant una publicació científica. En aquest estudi, es descriu una avaluació específica per a cada país Europeu dels fluxos a l'entorn, des de la producció fins al final de la vida útil de nano-Ag, -TiO_2 i -ZnO.

La generació de dades d'alliberament a partir d'experiments es presenta mitjançant dues publicacions científiques i cinc resultats no publicats. Per a tots els experiments es van determinar les velocitats d'alliberament i les formes d'alliberament.

Mitjançant l'avaluació de la recerca realitzada en Projectes de Nanoseguretat finançats per la Comissió Europea s'han generat suggeriments sobre en qué hauria de centrar-se la investigació futura sobre estudis d'alliberament, el qual es presenta també mitjançant una publicació científica.

La combinació de la informació generada i l'anàlisi derivat dels diferents estudis permet l'extracció de conclusions i recomanacions que contribueixen a la comprensió dels possibles riscos humans i ambientals associats als nanomaterials i els productes que en continguin, el que es descriu a la secció de discussions i conclusions.

RESUMEN

La mayor presencia de productos con nanomateriales en múltiples aplicaciones ha suscitado preocupaciones sobre sus posibles riesgos para la salud humana y el medio ambiente. Por lo tanto, es necesario un enfoque responsable y coordinado para garantizar que se aborden los posibles problemas de seguridad al mismo tiempo que se desarrolla la tecnología. La investigación presentada en esta Tesis Doctoral tiene como objetivo contribuir a la comprensión de los posibles riesgos humanos y ambientales asociados con los nanomateriales y los productos que los contengan, mediante la generación de datos relevantes sobre su liberación a lo largo de su ciclo de vida.

El objetivo se ha abordado desde tres perspectivas diferentes: en primer lugar, mediante la actualización y perfeccionamiento de los modelos de flujo de materiales, los cuales permiten predecir la concentración de nanomateriales en el medio ambiente; en segundo lugar, generando datos de liberación a partir de experimentos con múltiples productos que contienen nanomateriales; y en tercer lugar, evaluando la investigación realizada en Proyectos de Nanoseguridad financiados por la Comisión Europea.

El perfeccionamiento del modelo de flujo de materiales se presenta mediante una publicación científica. En este estudio, se describe una evaluación específica para cada país Europeo de los flujos al medio ambiente, desde la producción hasta el final de la vida útil de nano-Ag, -TiO_2 y -ZnO.

La generación de datos de liberación a partir de experimentos se presenta mediante dos publicaciones científicas y cinco resultados no publicados. Para todos los experimentos se determinaron las velocidades de liberación y las formas de liberación.

Mediante la evaluación de la investigación realizada en Proyectos de Nanoseguridad financiados por la Comisión Europea se generaron sugerencias sobre en lo que debería centrarse la investigación futura sobre estudios de liberación, lo cual se presenta también mediante una publicación científica.

La combinación de la información generada y el análisis derivado de los diferentes estudios permite la extracción de conclusiones y recomendaciones que contribuyen a la comprensión de los posibles riesgos humanos y ambientales asociados a los nanomateriales y los productos que los contengan, lo que se describe en la sección de discusiones y conclusiones.

Table of contents

1. INTRODUCTION

1.1. Nanotechnology – Origin, definitions and basic principles

On December 29, 1959, physicist Richard Feynman presented in the American Physical Society meeting a talk entitled "There's Plenty of Room at the Bottom: An Invitation to Enter a New Field of Physics". In his talk, professor Feynman described a process in which scientists would be able to manipulate and control individual atoms and molecules, providing the first ideas and concepts behind nanoscience and nanotechnology (United States National Nanotechnology Initiative (NNI), 2021). However, it was not until 1974, that the Japanese scientist Norio Taniguchi used the term "nano-technology" for the first time, in a conference in Tokyo(Norio, 1974). The term was not used again until 1981, when Eric Drexler, who was unaware of Taniguchi's prior use of the term, published his first paper on nanotechnology in 1981 (Drexler, 1981) and developed and popularized the concept. In parallel, also in 1981, with the development of the scanning tunneling microscope (STM), which could image and manipulate individual atoms (Binnig and Rohrer, 1983), modern nanotechnology began (United States National Nanotechnology Initiative (NNI), 2021).

Nowadays, according to the International Standards Organization, Nanotechnology is defined as “the application of scientific knowledge to manipulate and control matter predominantly in the nanoscale to make use of size- and structure- dependent properties and phenomena from those associated with individual atoms or molecules, or extrapolation from larger sizes of the same material” (International Standards Organization, 2015). Understanding nanoscale as the “length range approximately from 1 nm to 100 nm” (International Standards Organization, 2015). Following those definitions, a nanomaterial is a “material with any external dimension in the nanoscale or having an internal structure or surface in the nanoscale” (International Standards Organization, 2015). Therefore, according to that definition, nanomaterials are not something new. Indeed, nanomaterials have been abundant during Earth’s formation and throughout its evolution over the past 4.54 billion years (Hochella et al., 2019). Nanomaterials can be divided into three categories based on their origin:

- ***Natural nanomaterials***: Occur from a natural process like a geological source (e.g. an erupting volcano) or a biological source (e.g. silica formed in rice husks).

- ***Incidental nanomaterials***: Arise as a by-product from human activity like welding fume particles, the smoke created when using a wood-burning stove or particles generated in car diesel exhaust.

- ***Engineered or manufactured nanomaterials***: Intentionally produced to have selected properties or composition.

By designing its size and shape, certain nanomaterials can present interesting properties that are not observed in the bulk form. For this reason, in this last third category – i.e. engineered nanomaterials (ENM), is where most of the focus has been put in the last decades. The difference in the properties of materials at the nanoscale arise for two main reasons. Firstly, nanomaterials have a relatively **larger surface area** when compared to the same mass of material produced in a larger form, which can make materials more chemically reactive and affect their functional properties. Secondly, **quantum effects** can begin to dominate the behaviour of matter at the nanoscale - particularly at the lower end - affecting the optical, electrical and magnetic behaviour of materials (The Royal Society & The Royal Academy of Engineering, 2004). When ENM are incorporated into products those properties can be transferred, , improving its performance and/or providing them with new functionalities (Stark et al., 2015). Different techniques can be employed for transferring the ENM' properties into the NEP. Generally, the ENM are incorporated in the NEP' surface as a coating or within the matrix. However, specific properties can also be obtained by the generation of nanometric patterns on the surface for example, without the incorporation of any ENM (Muñoz-García et al., 2014). The specific technique will depend on multiple parameters like the NEP and the ENM composition, the desired funcitionality, the production scale (industrial or lab-scale) or the specific application, among others.

The products incorporating nanomaterials are called nano-enabled or nano-enhanced products. Strictly speaking, nano-enabled products are defined as "*those products exhibiting a specific function or performance only possible with nanotechnology*"; while nano-enhanced products are "*those improving or enhancing their function or performance by applying nanotechnology or by the inclusion of nanosized materials*" (International Standards Organization, 2015). However, the scientists and other stakeholders involved in the field, generally do not discriminate between both terms. Therefore, in this thesis, all references to products incorporating engineered nanomaterials will be referred to as nano-enabled products (NEP).

1.2. Nanosafety – an overview

When nanotechnology research started increasing due to its promising benefits in multiple applications, concerns started arising about the idea that the properties that make ENM extremely interesting for multiple purposes, may be also responsible for undesired effects on humans and the environment (Zielińska et al., 2020). Therefore, there was a need for a responsible and coordinated approach to ensure that potential safety issues were being addressed at the same time as the technology was developing. Consequently, nanosafety, which is the field that studies all the safety issues associated with nanotechnology, started to grow to be able to cover all the areas of concern.

In the last 20 years, multiple agencies, including the European Commission (EC) and the National Nanotechnology Initiative (NNI) in the United States, have funded high number of nanosafety research projects to identify and understand any potential risks that ENM may pose to humans and the environment. However, before summarizing the state of the art achieved by those initiatives, the basic principles of risks must be defined.

1.2.1. Risk definition and assessment

The potential risk of a chemical (or in this case ENM) is defined by two general parameters, hazard and exposure.

Risk = Hazard x Exposure

According to the International Standards Organization (ISO), a **hazard** is any situation, substance, activity, or event, that could potentially cause human injury or ill health (International Standards Organization, 2018)Click or tap here to enter text., while **exposure** describes the measurement of both the amount of, and the frequency with which a substance comes into contact with a person or the environment (American Chemistry Council, 2021). Consequently, the **risk** is a measure of the probability that harm will occur under defined conditions of exposure to a substance (International Union of Pure and Applied Chemistry (IUPAC), 2001), in this case, ENM. If there is no exposure to an ENM, no matter how dangerous (hazardous) it may be, there is no risk of harm. Likewise, ENM which pose only a small hazard but to which there is frequent or continuous exposure may pose as much risk as ENM which have a high degree of hazard but with low exposure potential (International Union of Pure and Applied Chemistry (IUPAC), 2001). Another relevant term generally employed when talking about risk is “toxicity”. According to the Organisation for Economic Co-operation and Development (OECD), toxicity is the ability of a substance to cause poisonous effects resulting in severe biological harm or death (“OECD Glossary of Statistical Terms - Toxicity Definition,” 2021). Therefore, a toxic substance is

considered hazardous. However, a substance can be hazardous without being toxic (e.g an explosive).

In order to characterise the risk of a specific substance, the risk characterisation shall consider the human populations (exposed as workers, consumers or indirectly via the environment and if relevant a combination thereof) and the environmental spheres for which exposure to the substance is known or reasonably foreseeable (EcoMole, 2021). For that purpose, the **risk assessment** is performed, which aims at assessing the likelihood of occurrence of a given hazard in a certain exposure situation.

Within the European Union (EU), the *Registration, Evaluation, Authorisation and Restriction of Chemicals* (REACH) legislation is the current regulatory framework for chemical risk assessment and management, which also applies to ENM (Alenius et al., 2010). REACH considers dose (concentration)–response (effect) assessment with the objective to predict the concentration of the substance below which adverse effects of concern are not expected to occur (Syberg and Foss Hansen, 2016). REACH defines the Derived no-effect level (DNEL) as the exposure to a substance above which humans should not be exposed. Similarly, the Predicted no-effect concentration (PNEC) determines those concentrations that do not produce adverse effects on various environmental spheres (water, air, soil, accumulation through the food chain) as well as the potential effect on the microbiological activity of sewage treatment systems (European Commission, 2006).

The final step in the risk assessment is the risk characterisation. Therefore, for humans, the exposure of each human population known to be or likely to be exposed, should be compared with the appropriate DNEL. For the environment, the Predicted exposure concentration (PEC) should be compared with the PNEC for any given compartment, so that a PEC/PNEC ratio may be derived. If the PEC/PNEC ratio is ≤1, it implies that there is no immediate concern according to the available information. If the ratio is ≥1, the competent authority shall judge the case and act accordingly (European Chemicals Agency (ECHA), 2016; Syberg and Foss Hansen, 2016).

In order to perform the risk assessment both exposure and hazard assessment are needed, which require data. For the hazard assessment *in vitro* and *in vivo* experiments are performed in order to derive the DNEL and PNEC (Morimoto et al., 2010). In the exposure assessment a quantitative or qualitative estimate of the dose/concentration of the substance to which humans and the environment are or may be exposed should be made, considering all stages of the life cycle (Abbott and Maynard, 2010). Since the research presented in this thesis is mainly focused on exposure assessment, the concepts around that topic will be further described.

1.2.2. Life cycle stages and release pathway analysis

In the first nanosafety studies, there was a need for increasing the understanding of the interaction of engineered nanomaterials with the environment and the living world. Accordingly, the focus was on understanding the more fundamental aspects of toxicology and eco-toxicology (European Commission, 2004), which led to studies being focused on pristine ENM (without capping, linker or incorporation into any product). However, ENM are synthesized with multiple coatings, linkers and are incorporated in a large number of matrices for many different applications (Giese et al., 2018; Stark et al., 2015). In addition, further transformations may occur during the multiple activities that they might experienced and due to interactions with different substances and media before they are potentially released. As a result of all these possible transformations, which in some cases are not evident or easy to predict, a very wide diversity of materials may be generated inadvertently (Schug et al., 2013), which may potentially cause potential human or environmental health impacts. Therefore, the assessment implies studies not only focused on pristine ENM, but also on these ENM and nano-enabled products, along their life cycle (Mitrano et al., 2016).

The life cycle of a product is generally considering different stages: (i) synthesis, (ii) manufacturing (or in the case of ENM, their incorporation into the product), (iii) use and (iv) end-of-life (including recycling). Each of the stages, depending on the ENM and its application, may present multiple **release pathways**, i.e. - the scenarios through which the ENM goes through before being released to the environment or reaching the humans. Given the multiple pathways through which ENM may be released, it is important to prioritize the evaluation of those more likely to present a higher concern, which are known as critical release pathways. In order to identify them, certain indicators (e.g. NEP characteristics or specific activities) can be distinguished. In addition, certain pathways are not only associated with a determined risk probability but also with release to a specific compartment (human or environmental), which also provides relevant information on the potential impact.

The most relevant release pathways through which ENM may reach humans or environment, as well as the main factors contributing to release during the different life cycle stages are described here below and summarized in Figure 1.

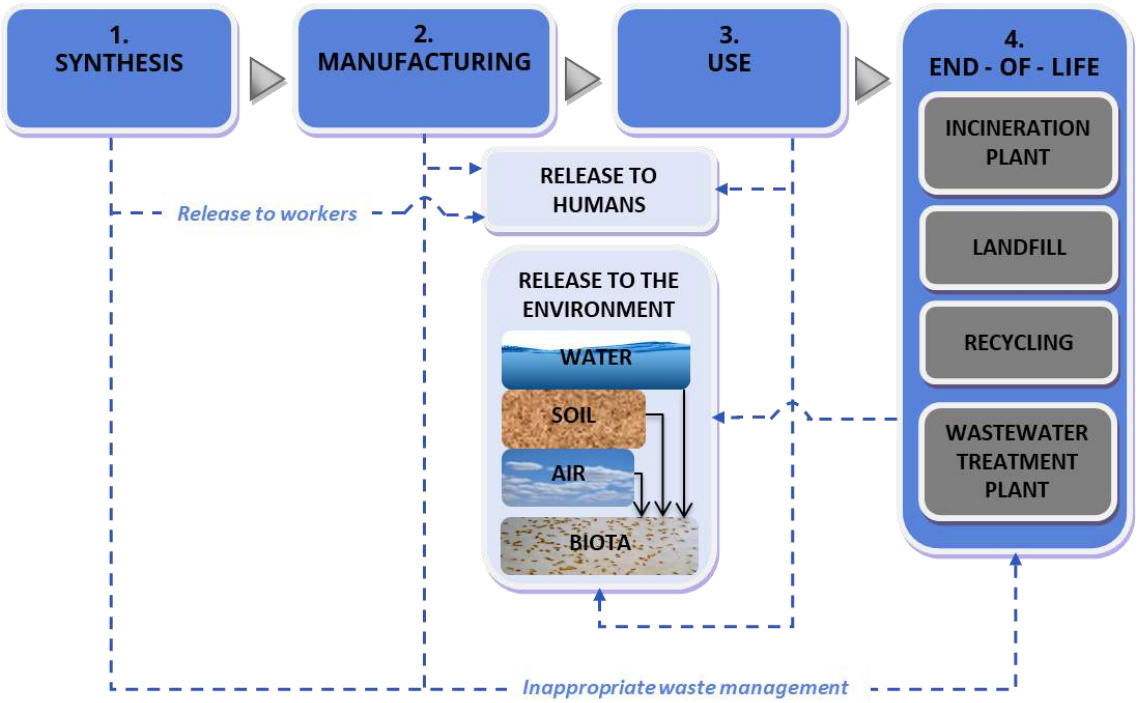

Figure 1 – Potential release pathways of ENM to humans and the environment from the different life cycle stages.

1.2.2.1. Production and manufacturing

Releases to both humans and the environment can occur during production and manufacturing processes of ENM. During those stages, there is an especially high concern with exposure to workers. For exposure and risk assessment in occupational settings involving engineered nanomaterials, it is important to understand the mechanisms of release and how they are influenced by the physico-chemical characteristics of ENM and those of the matrix material, and the process characteristics (Ding et al., 2017a). While workers may be exposed to ENM via inhalation, ingestion or dermal absorption, the inhalation route is the most likely to result in larger systemic doses (Oberdörster et al., 2005). Due to the high dustiness of ENM in powder form, especial attention should be taken with those processes involving powders (Schulte et al., 2014).

Regarding releases to the environment, concerns are mainly focused on inappropriate waste management. First, leftovers discharged in the sewage system, from where released ENM arrive at Wastewater Treatment Plants (WWTP) and may be released to the environment. Addittionally, containers or instruments used during the production or manufacturing processes, which may contain ENM and if are not disposed appropriately may also reach the environment.

1.2.2.2. Use

Emissions from the use phase are more complex to monitor due to the wide range of products in which ENM are present in a high variety of applications. Moreover, for a single product application multiple release pathways may occur, each of them with a different release rate, release form and ending-up in different compartments (i.e. humans and environment).

Typically, the releases of ENM occur due to an stress being applied to the NEP. During use, NEP are submitted to multiple stresses, which can be classified in: (i) chemical, (ii) mechanical or (iii) thermal. Chemical stresses during the consumption stage can be very broad, ranging from strong acid attacks to slight surface oxidation of the products. Depending on the chemical stress applied and the product resistance to such stress, it could lead to higher or lower release rates and different release forms. Generally, chemical stresses alter the release form by modifying the matrix and/or ENM composition and/or properties. Regarding mechanical stresses, during the use phase many products experience processes such as abrasion, cutting, drilling, sanding or shredding. Release of ENM and the form in which these materials will be released during these activities, will depend on the frequency, duration and energy involved. Regarding thermal stresses, except for specific applications, very high thermal stresses are not common during the use phase, but a moderate temperature during a prolonged time or a rapid change of temperature might also affect the material degradation and consequently leading to releases. It should be highlighted, that most of the processes that the products experienced during the use phase are a combination of the stresses described above, not just one of them.

1.2.2.3. End-of-life

Once the products arrive at the end-of-life stage they can pass through different processes depending on the product category, their intrinsic characteristics and the regulations of each country (Adam and Nowack, 2017). Most of the products will be treated via one of the three main end-of-life processes: landfilling, recycling or incineration (Caballero-Guzman et al., 2015). The potential release pathways of the three processes, which are more likely to pose a risk for the environment than for humans, are described below.

It is estimated that around 50% of ENM produced worldwide end up in landfills (Keller et al., 2013), which is a consequence of the high share of this practice in waste treatment around the world. During the time period that the products remain in the landfill, liquids present in the waste or from rainwaters may percolate through the nano-enabled products causing potential ENM releases. In addition, contact with leachates may also have an impact on the form in which these ENM will be released (Dulger et al., 2016). After reaching the soil, leachates containing

ENM might continue percolating until reaching groundwater. Despite modern engineered landfills being designed and constructed to prevent leachate emissions, leakage still occurs because of the failure of the liner system (Ya et al., 2019). Therefore, potential ENM emissions to the environment from the landfill, in this case to soil and water, should be taken into consideration.

Recycling is defined as any recovery operation in which waste materials are reprocessed into other products, materials or substances whether for the original or other purposes (European Commission, 2008). On the one hand, recycling is an ENM re-entrance pathway to the life cycle, by which new releases may occur. Adittionally, usual recycling processes applied to used products may cause releases. However, not all products are recycled, and in case they are, different conditions are applied depending on the nature of the product. Nevertheless, since most of the cases the processes applied are similar to those ones for manufacturing, release predictions can be made.

Incineration is applied to remove highly toxic organic substances from the waste, reduce its volume and potentially recover some of the energy stored in it. Incineration facilities burn wastes at high temperatures (850 – 1200 °C) in oxidative environments to ensure complete combustion of the waste (Holder et al., 2013). During incineration releases to air may occur, but most of the remaining ashes from incineration, which may contain ENM (Vejerano et al., 2014), are disposed into landfills leading to potential releases into soil or water.

End-of-life is the last stage of the life cycle, but the final release rate and form is the result of all the stresses previously experienced. For this reason, in order to properly understand the release process, all the cumulative contribution of the different stresses experienced should be taken into account (Mitrano et al., 2016). Moreover, in case the NEP has suffered release in previous stages, the ENM amount available to be released during the end-of-life will be lower compared with an unaged NEP, which also is an important consideration when evaluating the risk of ENM during the end-of-life stage.

1.2.2.4. Accidents

Although accidents usually are not considered as a life cycle stage, their contribution to release may be very relevant. Not considering accidental releases may not only lead to underestimating mass flows but also prevent integrating qualitative aspects of the fate of the accidentally released nanomaterials. The amount released during accidents varies from a few kg to several tons transferred to the surrounding environment. Although their probability is low, at a local scale, major releases cannot be overlooked because when they occur they can contribute

significantly to the total released amount, more than other types of releases over a given period of time.

1.3. Material flow analysis

An elementary step towards a quantitative assessment of the risks of new compounds or pollutants (e.g. engineered nanomaterials) is to estimate their concentrations in the compartments of interest (Gottschalk et al., 2010) (e.g humans and environment). In the case of nanosafety, since the number of different situations to which ENM and NEP are submitted is very broad, material flow (MF) models are a useful tool to determine the releases that may occur in each stage of the life cycle to different compartments (Dale et al., 2015), supporting risk asssessment. The Organisation for Economic Co-operation and Development (OECD), define **material flow analysis** as "*the study of physical flows of natural resources and materials into, through and out of a given system*" (Organisation for Economic Co-operation and Development (OECD), 2008). Material flow (MF) models are not exclusively applied to nanosafety. Indeed, its applications are very broad, ranging from business optimization, energy management or carbon dioxide emissions control, to name a few (Organisation for Economic Co-operation and Development (OECD), 2008). In Figure 2, an exemplification of a MF analysis for ENM is included.

Multiple MF analysis have been generated in the nanosafety field to predict the release of ENM. Up to now, the focus has mainly been on the environment, although releases to humans could also be assessed. The complexity of the models are very variable, each of them requiring different inputs, depending on the scope. Some models have focused on global estimations (Keller et al., 2013), while others have provided results for United States or Europe as a whole (Gottschalk et al., 2009; Rajkovic et al., 2020), or on smaller regions like Denmark (Gottschalk et al., 2015), Switzerland (Caballero-Guzman et al., 2015; Gottschalk et al., 2010, 2009) or Japan (Suzuki et al., 2018). Different models also consider different ENM (Gottschalk et al., 2010; Wang et al., 2016), concentrate their efforts in specific life cycle stages (Adam and Nowack, 2017; Caballero-Guzman et al., 2015; Rajkovic et al., 2020; Suzuki et al., 2018) or put more emphasis on information on release forms (Adam et al., 2018). For all those models, the inputs required are:

- ***ENM production volume***: Determines the flows into the model. It is a critical parameter since it will determine the total amount of material in the model. An example of ENM production volume is:
    - 38900 tonnes of nano-TiO_2 per year are produced in Europe.

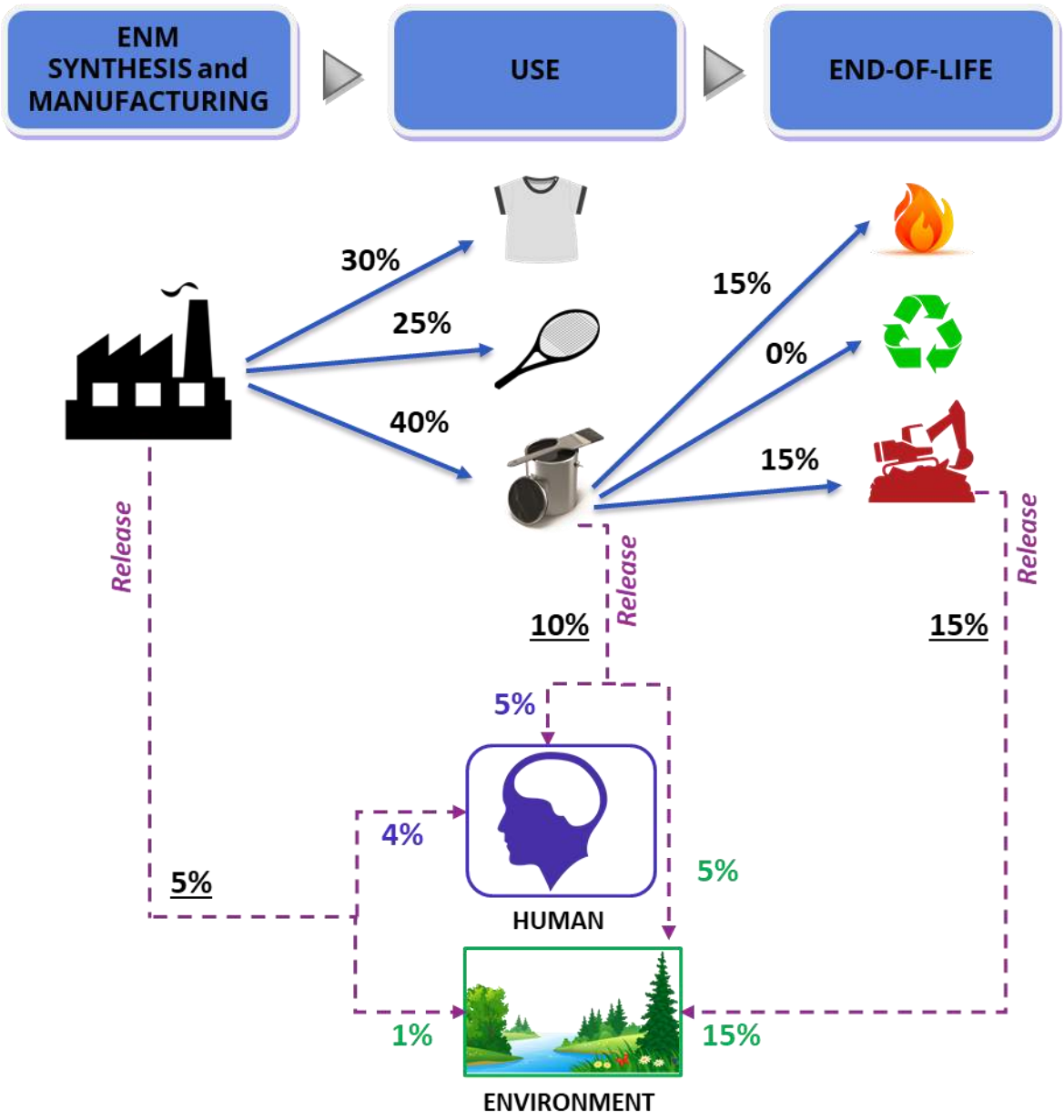

Figure 2 – Mass Flow analysis exemplification. The values represented are randomly attributed for the purpose of example. Blue arrows represent ENM distribution into products and further allocation to end-of-life processes, while purple arrows represent releases to humans and the environment

- ***ENM allocation to product categories***: Distribution of the ENM production volumes into specific products. Different products will be submitted to different stresses and different disposal practices, what will determine the release pathways that the ENM/ NEP will experienced. An example of ENM allocation to product category is:
  - 57% of the nano-TiO_2 produced in Europe is incorporated in sunscreens.

- ***Transfer coefficients***: Values describing the fractions of ENM flowing from one compartment represented in the model to another. Multiple types of transfer coefficients, determining the material flow among compartments, are included in a single model. The specific flow that the transfer coefficient defines, will depend on the scope of the model. An example of transfer coefficient is:
  - 90% of the nano-TiO_2 incorporated in sunscreens is released to water.

The main limitation of MF models typically are uncertainties associated with the data used as input to determine the ENM production volumes, their allocation to product categories and the transfer coefficients. To consider the uncertainties, some models have provided values using "high estimates" and "low estimates" (Keller et al., 2013), while others have used more sophisticated approaches incorporating probabilistic data treatments, what considers the uncertainties originated from each step of the model, providing probability distributions representing the range and likelihood of possible ENM concentrations in the environment (Gottschalk et al., 2010; Sun et al., 2014; Wang et al., 2016).

Some models have combined dynamic material flow modelling with probabilistic modelling, generating Dynamic Probabilistic Material Flow Analysis methods (Bornhöft et al., 2016). Unlike the static models, the dynamic MF analysis takes a reasonable time frame as the temporal system boundary and tracks the flows over many years (Sun et al., 2016). As a consequence, dynamic models can include a time variable, what can be useful for multiple considerations like the accumulation of ENM over years or even seasonal variations (e.g. higher use of sunscreens in the summer). In Figure 3, examples of the outputs of different MF analysis are included.

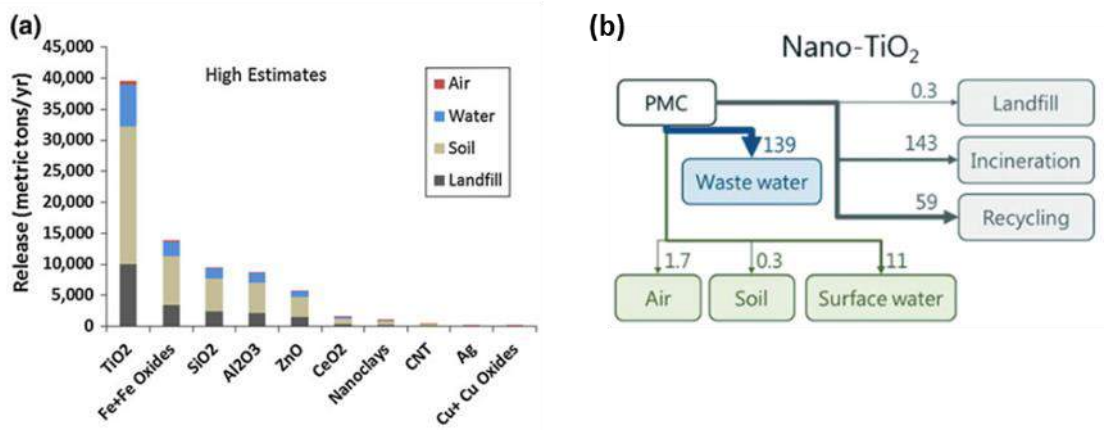

Figure 3 – (a) Final disposal in landfills and emissions to soil, water and air for ENM used in coatings, paints and pigments, considering a maximum global production and high release estimates. Figure obtained from (Keller et al., 2013). (b) Flow chart of nano-TiO2 in Belgium. The modes of the probability distributions are expressed in tonnes per year. PMC: production, manufacturing and consumption. Figure obtained from (Adam and Nowack, 2017).

1.4. Extracting release rates and release forms from experiments

In order to obtain realistic values from the MF models and use them for risk assessment purposes, release data must be generated to be used as input in the models. For that purpose, experimental release studies provide the most concrete basis (Keller et al., 2013). From the release experiments two main factors can be extracted: the **release rate**, which refers to the amount of substance/material released, and the **release form**, which refers to the physicochemical properties of these released materials/substances.

For production and manufacturing, field measurements provide data to directly derive the release rates and forms (Fonseca et al., 2021; Salmatonidis et al., 2020). However, laboratory tests are also used to determine relevant specific materials properties like dustiness, determining the tendency of materials to produce airborne dust during some production or typical manufacturing processes such as handling (Bach and Schmidt, 2008; Hamelmann and Schmidt, 2003; Shandilya et al., 2019), which has a direct impact on ENM exposure. The methodology commonly used to obtain release and exposure data during consumption and end-of-life stages, is based on laboratory-controlled experiments simulating real scenarios. Experimental designs shall be based on standardized protocols whenever possible, to waranty the reliability and reproducibility of the data generated. Specific protocols to simulate real scenarios for ENM and nano-enabled products are not always available. In these cases, non-nanomaterial specific protocols can be used performing the adaptations required. Generally, standardized protocols are not designed to determine the release, but to test the product performance against a specific stress. Thus, adaptations must be implemented to collect and analyse the released materials in order to obtain the data required to be used as input for the models.

Consumption phase experimental simulations have been performed for different products containing ENM (Koivisto et al., 2017), but more data is still required in order to refine the models. Some of the real scenarios that have been simulated with lab-based experimental setups and from which experimental data was generated are described below.

- ***Exposure to outdoor conditions***: When nano-enabled products are exposed outdoors, weathering effects may damage the material leading to release. In order to simulate weathering processes in laboratory-controlled conditions, climatic chambers are usually employed, which submit the samples to an accelerated weathering. When nano-enabled products are exposed to outdoor conditions, if they are located in cities,

released ENMs may be released to the sewage systems and from there to WWTPs. In case they are not located in very populated areas, ENMs might be released in soil instead. Multiple standardized protocols are available with indications on how to perform lab-based experiments using relevant conditions (e.g. UV dose, temperature, humidity) for specific products and climates (International Standards Organization, 2013).

- ***Mechanical stresses***: In order to evaluate the impact on release due to mechanical stresses, depending on the type of stress that needs to be experimentally simulated, different protocols can be used. Most of the protocols currently employed by researchers were originally developed to test products resistance to mechanical stresses, but the same principle can be used to evaluate the release. Abrasion is one of the most tested mechanical stresses for evaluating the release. Two of the most used instruments to simulate it are the Martindale and the Taber. In both techniques, by changing the abrasion material and the number of cycles, the intensity of the abrader can be adjusted. Apart from abrasion, the release due to other common stresses like cutting (Ogura et al., 2019), drilling (Ding et al., 2017b; Starost et al., 2017) or linear abrasion (International Standards Organization, 2019) can also be evaluated. Multiple standardized protocols provide indications on how to perform these assays depending on the product of interest that is being tested (meaning to which type of mechanical stress is the product submitted to during the use/manufacturing phase) and the instrument that should be used in each case (International Standards Organization, 2016, 2003). Mechanical stress experiments can also be combined with air measurements to determine the potential occupational releases that could be generated during these processes (Golanski et al., 2011; Kuijpers et al., 2019; Nored et al., 2018).

- ***Washings (textiles)***: ENM are commonly applied on textiles to provide different properties such as antibacterial or photocatalytic activity (Ferraris et al., 2014; Memon et al., 2015; Scott et al., 2017). In those cases, textiles washings represent a relevant activity concerning ENM release to the environment. In order to simulate the real conditions applied to a product in a washing scenario, a protocol commonly used to test the textiles colour fastness is employed (International Standards Organization, 2010). The standard protocol focuses on monitoring the properties of the textile after being washed (several washing cycles can be applied), but to be able to monitor the materials

released during the washing of a nano-enabled textile then the collection of washing waters and its analyses can provide information regarding release rates and release forms.

As previously mentioned in section 1.2.2.3, at the end-of-life stage, most of the products will be treated via one of the three main end-of-life processes: landfilling, recycling or incineration (Caballero-Guzman et al., 2015). To these three processes, releases from wastewater treatment plants should be added. Although WWTP are not involved in the end-of-life of many products, it is a compartment where many potential released materials could end up. Therefore, it is considered as a technical compartment with direct impact in the quantification of the releases to the environment.

- ***Leaching (landfill simulation)***: Since in landfills, the main concern is the ENM leaching, standardized protocols considering different types of leachates and waste products are typically used (European Standards, 2003; United States Environmental Protection Agency (EPA), 1992). In addition, release studies with samples from field-scale landfills have also been performed, which basically consist of leachates characterization (Kaegi et al., 2017). However, the challenge that researches are currently trying to overcome is the nano-waste detection and tracking of ENM in complex waste matrices and the differentiation of ENMs from naturally-occurring nanomaterials, which hampers the characterization (Part et al., 2018, 2015).

- ***Incineration***: To determine the release rates and the fate of ENM after an incineration process, researchers have performed measurements in real municipal solid waste incineration plants (Baran and Quicker, 2017; Oischinger et al., 2019; Walser et al., 2012). However, due to the complexity of those assays and availability to real municipal incineration plants, studies were also performed in laboratory-based incineration systems and pilot-scale incineration plants (Bouillard et al., 2013; Vejerano et al., 2014). During incineration, a special attention is paid on the fate of the ENM, since due to the high temperatures that are reached during the process, it is likely that ENM suffer modifications (Part et al., 2018).

- ***Recycling***: In general, ENM-containing wastes can be chemically, biologically, thermally, or physically treated for recycling purposes, and consequently influencing the fate of ENM. To date, there is no clear evidence of ENM release in existing waste recycling plants (Part et al., 2018). However, the main concerns are associated with occupational

exposure to workers (personnel working in the recycling plant) during mechanical waste recycling processes, such as sieving, shredding, milling, grinding, or sorting (Part et al., 2018). Therefore, in order to assess the potential release, occupational field measurements should be carried out in the reclycling plants as well as mechanical stress experimental simulations (to simulate waste stresses in the recycling processes).

- ***Wastewater treatment plants***: To determine the releases in WWTP, laboratory-scale experiments can be performed by evaluating the interaction of the ENM of interest with wastewater bacteria biomass stock solution (Kiser et al., 2009) or using wastewater sludge from municipal wastewater treatment plants (Lombi et al., 2012). However, if the facilities are available, studies with pilot WWTP fed with real municipal wastewater are performed (Kaegi et al., 2011), or even monitorization in real wastewater facilities (Kiser et al., 2009). In this type of experiments, it is important to determine which amount of ENM will remain in the sludge and which amount will be released in the water effluent, as well as the ENM form (composition and potential materials attached to it), to realistically determine the potential risks.

In Table 1, a compilation of some of the standardized protocols used to experimentally simulate potential release in real scenarios using laboratory-controlled experiments are compiled.

Table 1 - Compilation of some relevant standardized protocols used to simulate real life cycle scenarios to evaluate ENM release from nano-enabled products in laboratory-controlled experiments.

EXPERIMENTAL SIMULATION	DESCRIPTION	REFERENCE
WEATHERING	Plastics – Methods of exposure to laboratory light sources – Part 2: Xenon-arc lamps	ISO 4892-2:2013
	Paints and varnishes – Methods of exposure to laboratory light sources	ISO 16474:2013
	Textiles – Tests for colour fastness – Part B10: Artificial weathering – Exposure to filtered xenon-arc radiation	ISO 105-B10:2011
MECHANICAL STRESS	Rubber- or plastics-coated fabrics – Determination of abrasion resistance – Part 1: Taber abrader	ISO 5470-1:2016
	Rubber or plastics coated fabrics – Determination of abrasion resistance – Part 2: Martindale abrader	ISO 5470-2:2003

	Paints and varnishes – Determination of the resistance to rubbing using a linear abrasion tester (crockmeter)	ISO 21546:2019
WASHING	Textiles – Tests for colour fastness – Part C06: Colour fastness to domestic and commercial laundering	ISO 105-C06:2010
LEACHING	Test for leaching of granular waste materials and sludges – Part 4: One stage batch test at a liquid to solid ratio of 10 l/kg for materials with particle size below 10 mm (without or with size reduction)	EN – 12457-4
	Toxicity characterization leaching procedure (TCLP)	EPA Test Method 1311

2. OBJECTIVES

The objective of the thesis is to contribute to the understanding of the potential human and environmental risks associated to ENM and nano-enabled products. The specific contribution will be focused on generating relevant data on engineered nanomaterials release from nano-enabled products along their life cycle. The objective has been tackled from three different perspectives: Firstly, by upgrading and refining material flow models that allow the prediction of ENM concentration in the environment; secondly, by generating release data from experimental simulations with multiple nano-enabled products; and thirdly, by evaluating the current research performed in Nanosafety Projects funded by the European Commission and suggesting where future research on release studies should focus. The three approaches to achieve the thesis' objective are interralated and complement each other, which is exemplified in the infographic here below.

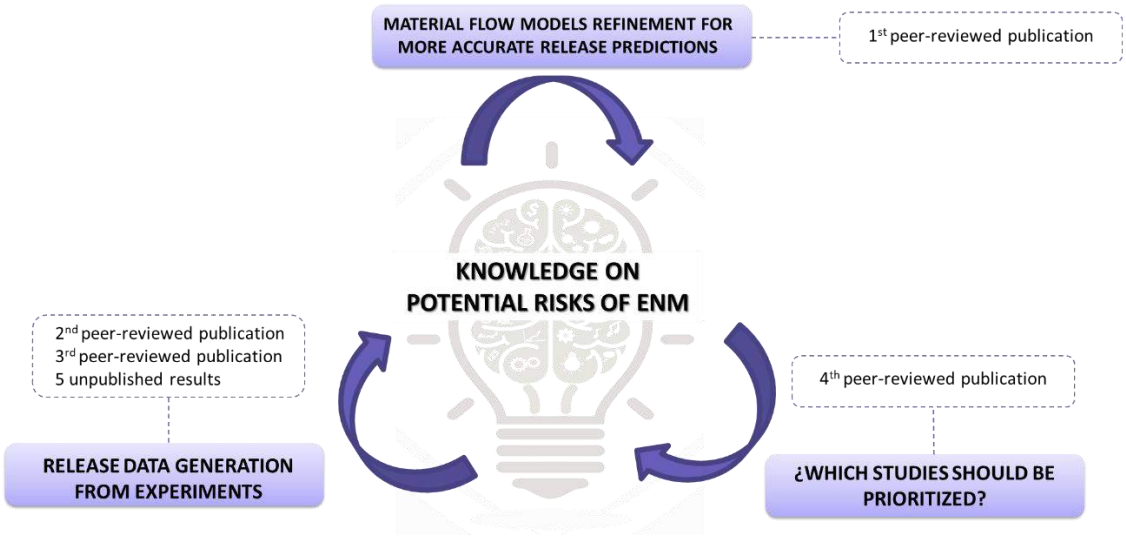

Figure 4 – Infographic exemplifying the thesis' objective and the three approaches to accomplish it.

In order to differentiate the three approaches, the results are divided in three sections, one for each of the approaches.

3. RESULTS

The results are divided in three sections, representing the three main focus of the thesis:

(i) Material flow model refinement

(ii) Release data generation from experimental simulations

(iii) Nanosafety research in Europe and future studies prioritization

The first section is comprised by one peer-reviewed publication with the title "I*nventory of country-specific emissions of engineered nanomaterials throughout the life cycle*". The second section is comprised by two peer-reviewed publications with the title "*Release mechanisms for PA6 nanocomposites under weathering conditions simulating their outdoor uses*" and "*Release and cytotoxicity screening of the printer emissions of a CdTe quantum dots-based fluorescent ink*"; one paper under preparation with the title "Silver nanoparticles and nanowires release from cotton textiles during household washings" and 4 experimental case studies not published in peer-reviewed journals, but reported in the European Project NANOFASE (Grant Agreement 646002). The third section is comprised by the last peer-reviewed publication published, "*Nanosafety research in Europe – Towards a focus on nano-enabled products*".

In each of the peer-reviewed publications, since they were performed with multiple co-authors, the specific work done within the context of this thesis by the author (Vicenç Pomar-Portillo) is indicated.

3.1. Material flow model refinement

3.1.1. First peer-reviewed publication

Inventory of country-specific emissions of engineered nanomaterials throughout the life cycle

Jeroen Kuenen, *[a] Vicenç Pomar-Portillo,[b] Alejandro Vilchez,[b] Antoon Visschedijk,[a] Hugo Denier van der Gon,[a] Socorro Vázquez-Campos,[b] Bernd Nowack[c] and Véronique Adam[c]

[a] *Department of Climate, Air and Sustainability, TNO, Princetonlaan 6, 3584 CBUtrecht, The Netherlands.*

[b] *Materials Safety Unit, Human & Environmental Health & Safety Division, LEITAT Technological Center, Carrer de la Innovació 2, 08225 Terrassa, Barcelona, Spain*

[c] *EMPA, Swiss Federal Laboratories for Materials Science and Technology, Lerchenfeldstrasse 5, 9014 St. Gallen, Switzerland*

*Corresponding author e-mail address: jeroen.kuenen@tno.nl

Contribution to the peer-reviewed publication within the context of this thesis: In this paper substantial contributions to the acquisition and analysis of data for the work were provided. More specifically, to the data needed to allocate the engineered nanomaterials production to specific countries, what is described in section 2.1.1 of the publication. In order to allocate the production to specific countries, the applications of the ENM (i.e the products where are incorporated) had to be refined, a work that was performed within the context of the thesis together with colleagues from the same group (Dr. Alejandro Vilchez). The results obtained from this work are described in section 3.1. of the paper. Moreover, contribution to the Discussion and Conclusion sections, critically revising the work for important intellectual content addition, were also provided.

The following manuscript is a version of record reproduced from Environ. Sci.: Nano, 2020,7, 3824 with permission from the Royal Society of Chemistry.

The online version can be accessed from:

https://doi.org/10.1039/D0EN00422G

Environmental Science Nano

ROYAL SOCIETY OF CHEMISTRY

PAPER

Cite this: *Environ. Sci.: Nano*, 2020, 7, 3824

Inventory of country-specific emissions of engineered nanomaterials throughout the life cycle†

Jeroen Kuenen, *[a] Vicenç Pomar-Portillo,[b] Alejandro Vilchez,[b] Antoon Visschedijk,[a] Hugo Denier van der Gon,[a] Socorro Vázquez-Campos,[b] Bernd Nowack[c] and Véronique Adam[c]

Engineered nanomaterials (ENMs) are being increasingly produced for various applications. In order to evaluate potential environmental impacts, knowledge on their environmental releases is needed. In this study, we present a country-specific assessment of the flows to the environment from production to end-of-life of nano-Ag, -TiO_2 and -ZnO within Europe. This paper includes a revision of the different applications in which the ENMs are used and their shares in Europe, as well as the distributions of ENM production, manufacturing and consumption over European countries using a surrogate-variable approach. Material flow analysis was used to quantify the probability distributions of ENM releases from each lifecycle stage to air, water and soil. Results show that the main applications of nano-TiO_2 and nano-ZnO are in cosmetics and personal care products, while nano-Ag is mainly used for electronic printing. While the production of these ENMs takes place in a limited number of countries, manufacturing and consumption are more homogeneously spread over Europe. In general, sludge-treated soil is the environmental compartment receiving the highest releases, while recycling is a technical compartment in the waste management system receiving significant ENM shares, especially for nano-Ag. Due to different waste management systems and sizes of countries, releases to surface water and soils normalised by the areas of these compartments vary by several orders of magnitude between countries, showing the relevance of a country-specific model. The results of this study can be used for the country-specific assessment of environmental fate and risks of ENMs and ENM-containing products.

Received 24th April 2020,
Accepted 1st November 2020

DOI: 10.1039/d0en00422g

rsc.li/es-nano

Environmental significance

To quantify environmental impacts and risks of engineered nanomaterials (ENMs), knowledge on their toxicities and environmental concentrations is required. Given the very limited availability of concentration measurements, modelling environmental releases of engineered nanomaterials is necessary. This paper presents an improved country-specific European release dataset that will aid environmental fate and risk assessments. In particular it includes updates of production amounts, an improved representation of applications containing ENMs and a material-specific distribution of ENM production, manufacturing and consumption among countries. Releases to surface water and soils vary across several orders of magnitude among countries, showing very different potentials for high concentrations (and consequent risks) within Europe. Environmental releases of nano-Ag are about one order of magnitude lower than previously assessed.

1. Introduction

Releases of engineered nanomaterials (ENMs) into the environment may have harmful impacts on the environment and human health.[1] Since concerns for possible harmful effects of ENMs on the environment are growing with the increased use of nano-enabled products and consequent release of nanomaterials, several studies have addressed the issue of quantifying these effects.[2–6] To assess this impact, knowledge about the actual concentrations of ENMs in the different environmental compartments is needed. Given the

[a] *Department of Climate, Air and Sustainability, TNO, Princetonlaan 6, 3584 CBUtrecht, The Netherlands. E-mail: jeroen.kuenen@tno.nl*
[b] *Materials Safety Unit, Human & Environmental Health & Safety Division, LEITAT Technological Center, Carrer de la Innovació 2, 08225 Terrassa, Barcelona, Spain*
[c] *EMPA, Swiss Federal Laboratories for Materials Science and Technology, Lerchenfeldstrasse 5, 9014 St. Gallen, Switzerland*

† Electronic supplementary information (ESI) available: Contains information on allocation of production, manufacturing and consumption amounts among countries as well as product allocations and raw results. See DOI: 10.1039/d0en00422g

limited information on the releases and dispersion of ENMs through the environment and the difficulty in measuring actual ENM concentrations in the environment, most studies use modelling approaches to address this issue.[7,8] Material flow models have been used to evaluate the ways ENMs move through the environment and to estimate their concentrations in different environmental compartments.[9,10] An input to such models and a prerequisite for an environmental assessment of the exposure and fate of ENMs is knowledge on the releases of ENMs to the different environmental compartments.

Most of the material flow models attempt to quantify the values and major uncertainties about the annual fluxes and related environmental emissions of ENMs into the environment. However, since data are scarce, releases in both space and time is highly variable. This implies that the releases of ENM from nano-enabled products along their life cycle is expressed as an annual release, and geographic variation of ENM releases or ENM concentrations in the environment has been considered in several studies, mainly focusing on a single country or watershed.[5,11–14]

Several studies have aimed at quantifying the production amounts of different ENMs at European and global levels.[5,15–18] These estimates show large variations between different studies, which are illustrative of the uncertainties in these estimates.

In this study, the aim is to go beyond these assessments and select the best estimates available for building up an application- and country-specific release model for selected ENMs. This work is partially built on part of a recent study that made a country-specific assessment of the flows in and out of the different waste sectors.[19] Instead of using Gross Domestic Product (GDP) to distribute production, manufacturing and consumption amounts to each European country, a country-specific assessment of these life-cycle stages was performed herein. We also present an updated representation of the different products containing ENMs. The improved and country specific ENM releases presented in this paper are a first step towards a high resolution spatially explicit release model to be integrated in environmental fate models.

In this work, we focus on three ENMs: nano-TiO_2, nano-ZnO and nano-Ag. These are selected since they are incorporated in many different products and used in a wide range of applications.[20,21] Additionally, they are among the most studied ENMs, both in terms of release monitoring in different exposure scenarios along their life cycle and of material flow analysis (MFA), therefore we can build on available information from previous studies. In addition, these three are of specific interest from an environmental fate modelling perspective.

2. Methodology and data collection

The flows of nano-Ag, -TiO_2 and -ZnO have been investigated within each European country (EU28, Norway and Switzerland) through their life cycles towards the environment, for the year 2015. The life cycle of ENMs starts with their production, then these ENMs are incorporated into products (*via* different manufacturing processes), which then are subsequently used by consumers. Finally, once the products are being used, the ENMs are distributed among the waste streams (end-of-life) to waste incineration, landfill and recycling. Flows to recycling should be understood as flows in waste that is intended to be recycled, so collected separately from mixed waste and entering sorting processes. Herein, recycling means recycling of the materials in which the ENMs are contained (*e.g.* plastic, textile, *etc.*), not of the ENMs themselves. During each of the life cycle stages, releases to air, water and soil may occur, as illustrated by Fig. 1. Imports and exports have also been assessed at the national level, as described in section 2.1.

In this work, we focused on the assessment of the amount of selected ENMs produced, manufactured and used in each individual country in Europe, as well as the different products in which they are incorporated and their shares. Subsequent release factors, describing the releases from each of the stages to the different environmental compartments (air, surface water and soil), were taken from previous studies.[19,22]

2.1. Production, manufacturing and consumption

The approach to estimate the amounts of ENMs being produced, manufactured and used is schematically shown in Fig. 2. Where A represents the amount (mass) of ENMs, which depends on the stage s, application a and country x. The different steps are briefly introduced here and described in detail in the other sections.

The total production A(s) in Europe is determined for each ENM and then allocated to the country by gathering available information on the production of various producers and production sites in Europe. While the methodology has been applied only to nano-Ag, -TiO_2 and -ZnO, it could be applied for any specific type of ENM, as long as this is defined such that individual applications can be identified for each of them.

For the manufacturing and consumption stages, A(s) is first stratified into the different products or applications in which the ENMs are incorporated, which results in amounts for Europe by stage s and by application a: A(s,a). Thereafter, A(s,a) is distributed over each of the European countries (x) by applying surrogate variables. This means that a relevant available parameter is chosen, for example population, that is expected to resemble the distribution of manufacturing and/or consumption, and which is subsequently applied to disaggregate the European total to the individual country level. This way, for each ENM and application the manufacturing and use of the product is distributed over the countries by using the best available data to represent the physical reality of the product use.

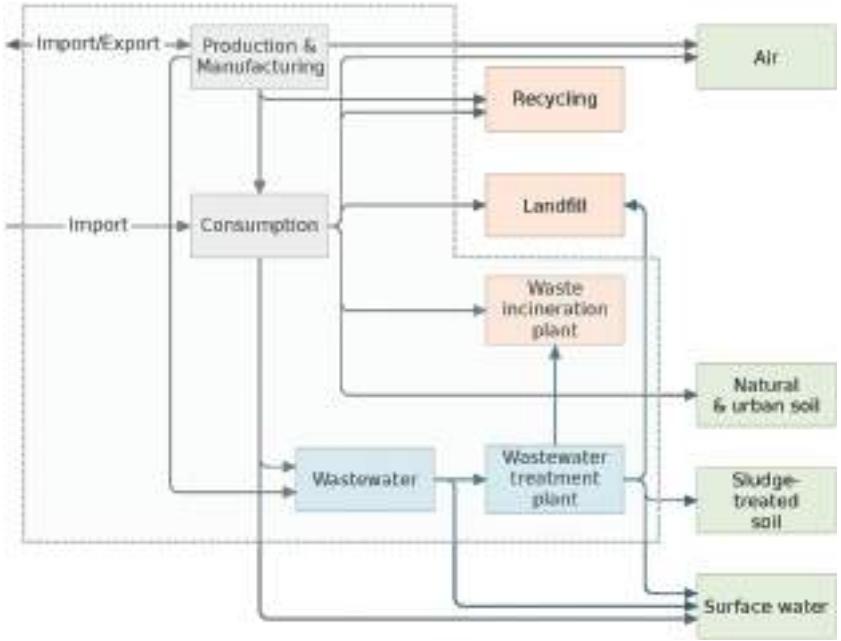

Fig. 1 System under study. The grey box includes the life cycle stages from which outflows were assessed. The fate of ENMs in the other life cycle stages and in environmental compartments was out of the scope of this study.

2.1.1. Production stage. Total European production volumes of nano-TiO_2 (38 900 tonnes on average) and nano-ZnO (7260 tonnes on average) are taken from literature.[22] For Ag, however, new information suggests that the 50 tonnes reported in the same study may be overestimating the European production. This is partly based on a report from the French government,[23] where it is stated that in 2017 the total amount of nano-Ag produced in or imported to France was between 1 and 10 kg, which is much lower than what would be expected if the whole European production would be 50 tonnes per year. Secondly, there is a fast increase of nano-Ag production in China and other parts of Asia producing for the European market,[18] implying that there is a large share of nano-Ag used in Europe which is actually produced elsewhere. Therefore, the nano-Ag production was decreased by one order of magnitude from the amount reported in Sun *et al.* (2016),[22] to 5 tonnes produced in Europe as a whole. This is in line with values reported in other literature sources, describing a production of 22 tonnes globally[24] or 5.5 tonnes in Europe.[17]

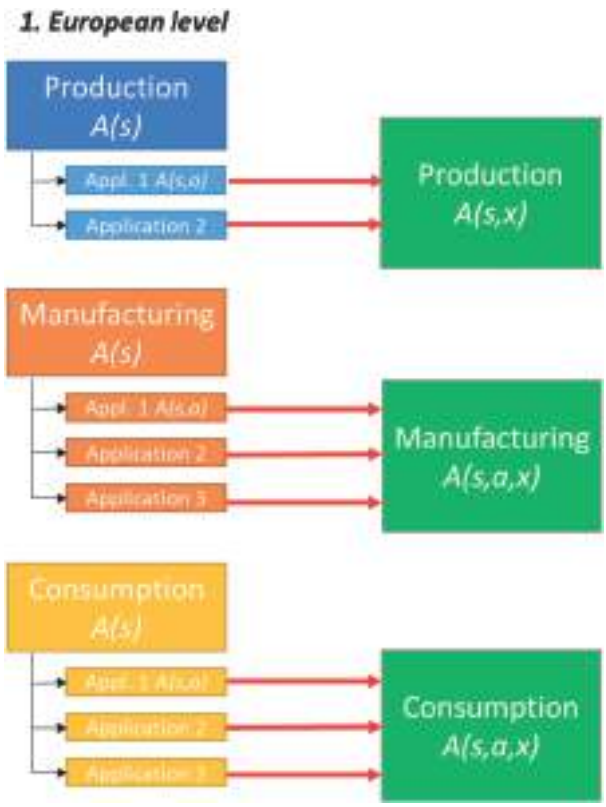

Fig. 2 Schematic illustration of the methodology used to calculate the amounts *A*(s,a,x) of ENM for each stage s, application a and country x.

Since most of the producers focused their production of ENMs for a specific application, it is important to distinguish between the main applications for each of the ENMs before distributing the production to individual countries (or producers). To do this, the product distributions were obtained from a comprehensive market report[20] supplemented with nano-registration databases.[25–28]

Allocation to countries. Next, European production of ENMs is distributed to individual countries following a new methodology based on information of the main ENM producers in Europe and the countries where their production facilities are located. Such information is obtained from market reports, industry associations and

companies' websites. Since the producers are different for each ENM, a specific study is performed for each ENM. First, the information provided by the market reports (*i.e.* main ENM producers) is verified by checking if the companies mentioned matched with the members (companies) of the respective producers' associations (*e.g.* TDMA – Titanium Dioxide Manufacturers Association or ZOPA – Zinc Oxide Producers Association), to make sure that all main producers are included. In all cases, the companies mentioned in the market reports as main producers are also part of the producers' association. Then, to calculate the contribution of each production plant to the production volume in each country, the following equation is used:

$$\begin{pmatrix}\text{Plant contribution to production (\%) in a specific country}\end{pmatrix} = \begin{pmatrix}\text{Overall share of ENMs produced for a given application (\%)}\end{pmatrix} \cdot \begin{pmatrix}\text{Company contribution to total European production for the application (\%)}\end{pmatrix} \cdot \begin{pmatrix}\text{Contribution of plant(s) in the country to company's European production (\%)}\end{pmatrix} \quad (1)$$

As observed in eqn (1), the contribution of each production plant depends on three parameters: (1) the overall share of the ENMs produced for a given application; (2) the company contribution to the total European production for the specific application and (3) the contribution of the plant(s) to the company's European production in the specific country under consideration. The three parameters range from 0 to 100%. The methodology to determine the share of the application for which the ENM is produced (and sold to a manufacturer) is described below (section 2.1.2). Then, in order to determine the company production capacity, for each application, the producing companies are identified using information available from the companies' websites, market reports and respective producers' associations. The producer companies have been grouped in high (H), medium (M) or low (L), depending on their production volume capacities, where for each group a total contribution to the overall production is defined (see below sections specific to each ENM and Tables S1–S3†). The third parameter represents the geographical distribution of these companies, taking into consideration that companies may have production plants in more than one European country. For companies with production plants in only one country the value used in the equation is 100%, otherwise the corresponding contribution (ranging from 0 to 100%) of the production plants in the country under consideration is used. It should be highlighted that the location of the production plants of each company is known, which allows allocating the respective production volumes not only to a specific country, but to a specific geographical location, obtaining the exact location from where release may occur.

Nano-TiO_2 country allocation. Unfortunately, data on the exact production amount of each plant is typically not available due to confidentiality issues given the commercially sensitive nature of production information in a competitive market. Therefore, qualitative information on the production capacities (high, medium or low) is collected based on information provided by the companies themselves where available, but mostly from knowledge of the market and the major players therein by the authors and experts that were consulted. A default production estimation is assumed for each group, where high production companies represent 80% of the total production, medium production companies account for 15% and small production companies for 5%. Suppliers mentioned in the market report are divided into companies dominating the market and secondary suppliers. Large producers are included in the high production group. Plants from nano-TiO_2 producer companies not mentioned in the market reports but being part of the TiO_2 manufacturers association are included in the medium and the companies mentioned in the market reports as secondary suppliers are included in the low production group. Regarding the product allocation, a distinction has been made between companies that produce for sunscreens and cosmetics and those producing for other applications. Four main companies have been identified to sell the nano-TiO_2 they produce for sunscreens and cosmetics applications (two of them with high production capacity, one with medium and one with low). For other applications, seven companies have been identified (two of them with high production capacity, three with medium and two with low (Table S1†)). Three of the companies produce nano-TiO_2 for multiple applications (including sunscreens and cosmetics), so they are considered in both categories ("*sunscreens and cosmetics*" and "*others*"). Company 2 (C2) and company three (C3), had production plants in different countries. Since information

on the production volumes of each of them is not available, production sites in each country are assumed to have the same share in the production. In the case of C2, two production plants are identified in Germany, therefore the production in Germany is assumed to be twice as high as the production in other countries.

To illustrate how the contribution of each production plant to a specific country is determined using eqn (1), here we explain an example for company C1, which produces nano-TiO_2 for sunscreens and cosmetic applications. From the product allocation, it is estimated that 76% of the nano-TiO_2 production is used in sunscreens and cosmetic applications (Table S1†), which means that a value of 76% is used as input for the first parameter in eqn (1). As explained above, high production companies are estimated to account for 80% of the total nano-TiO_2 production. Since the high production group is formed by 2 companies (C1 and C2), a production volume of 40% is assumed for each of them, which is the second parameter of eqn (1). The nano-TiO_2 production plants of C1 for sunscreens and cosmetics are based in one single production plant in Spain, which means that the value of the third parameter is 100%. Thus, its production plant contribution (in this case to Spain) is 76%·40%·100% = 30.4%. With a total of 38 900 tonnes estimated for the total European production volume of nano-TiO_2, the production allocated to this plant is 11 826 tonnes nano-TiO_2.

Nano-ZnO country allocation. Similar to nano-TiO_2, information on nano-ZnO production amount of each plant is not available. However, the market report differentiates between companies dominating the market (high production group) and other main suppliers (medium production group). The remainder of nano-ZnO producer companies mentioned in the market report, but not in the high or medium production groups, are included in the small production group. Since the difference between the medium and the small production groups is large, 1% contribution is estimated for the low production group and 19% for the medium, while the high production companies are assumed to represent 80% of the total production (like TiO_2). As in the case of nano-TiO_2, a distinction has been made between companies producing nano-ZnO for sunscreens and cosmetics, and companies producing for other applications. Five companies are the main producers of nano-ZnO used in sunscreens and cosmetics, three of them with high production capacity, one with medium and one with low (Table S2†). Since information on the amount produced in the different plants of C1 and C3 is not available, the same share has been given to each of the production plants.

Nano-Ag country allocation. Information on the amount of commercialized Ag ENMs is generally scarce, so there is no information on the amounts produced by individual companies. Therefore, each company producing for a specific application has been given the same share of the total ENMs for that application (Table S3†). Here, a distinction is made between companies producing for printed electronics and companies producing for other applications. For applications in printed electronics, seven companies are identified as main nano-Ag producers, while four companies have been identified to produce nano-Ag for other applications.

2.1.2. Manufacturing and consumption stage. During the manufacturing stage, the ENMs that are being produced in Europe (or beyond) are used in a variety of applications. To best attribute the different ENM releases to individual countries, information on the applications in which they are used is critical. As a principle, we have assumed that all ENMs produced in Europe are also being manufactured into products or applications and used within Europe, in the absence of any data to assume otherwise. Therefore, potential imports or exports of ENMs towards or out of Europe as a whole are out of the scope of this study. An exception is made for nano-Ag, where it was found that most of the production and manufacturing for nano-Ag containing products takes place outside Europe, whereas they may be used within Europe, as described in section 2.1.1.

Especially in China or elsewhere in Asia, a significant share of the global production and manufacturing of ENMs may take place.[18] Here we adopted a value of 20 tonnes of nano-Ag in the consumption phase, in contrast to 5 tonnes for production and manufacturing, based on the estimated nano silver market volume in the EU Scientific Committee on Emerging and Newly Identified Health Risks opinion on nanosilver.[29] This implies that we assume 75% is imported to Europe, which is in line with our assessment that a large part of the nano-silver containing products is imported from outside the EU.

Allocation to countries. As a next step, the amounts of ENMs being manufactured and used are distributed to the European countries. The approach is dependent on the stage and/or application. Relatively large point sources, such as larger industrial companies where ENMs are being manufactured into products, for which the location of the production facility (country, or even exact coordinates) is known, can be placed in their respective country along with the relevant share of the production.

However, for more diffuse sources, especially during the use phase of ENM-containing products, there is typically no specific information on the geographical distribution. One approach to derive a spatially distributed release dataset for these sources is by using surrogate datasets which have the necessary spatial distribution and are suitable to mimic the spatial distribution for the target variable itself.[30–32]

For the country distribution in the manufacturing and consumption stages, a suitable surrogate variable for each individual combination of ENM, stage and application is identified. A tiered approach is followed, which implies that the most important sources are examined in higher detail while relatively minor sources of emissions are dealt with in a more simple manner.[30] The complete overview of the surrogate variables used is given in the ESI† (Table S4). Gross domestic product[33] and population[34] for the year 2015 are used in case no other data are readily available, and for those

applications that have a relatively low share in the overall manufacturing/consumption. Other sources that have been used include the following:

- For manufacturing, the Eurostat statistics on manufactured goods (PRODCOM database)[35] is used as a proxy for multiple applications. PRODCOM is a database which holds information on the annual production (in physical and monetary terms) of detailed product categories per European country. For the year 2015, all monetary data (production in Euros) are selected for those applications for which the data are available. Monetary data are selected since these are more complete because they are less sensible to confidentiality issues than physical/mass-based production figures. The explanation of which PRODCOM codes are used for which application is given in the ESI† (Table S5).
- For cement production, data from the USGS Minerals Yearbook[36] are used (production data for 2012 per country).
- For paint consumption, data based on European sales of paints containing volatile organic compounds (VOCs) are used, based on 2013 production figures of paints in Europe.[37]
- For cosmetics (including sunscreens), a specific method is developed, given their importance in the overall ENM share of TiO_2 and ZnO, based on a study on the European Cosmetics industry for the EU DG Enterprise & Industry.[38] This study lists for each Member State the expenditure on cosmetics per person, and breaks this down into different products, including sun care. By multiplying the amounts spent per person on sunscreens and other cosmetics with the total population,[34] the total amount spent on sunscreens and other cosmetics is calculated for each country and used as the downscaling factor for distributing these applications over the European countries. For manufacture of both cosmetics and sunscreens, information on the market volume and net export (both in Euros) is obtained at country level from the annual report of the European sector organisation.[39] The sum of total market volume and net export by country is used as a proxy for distributing the manufacturing of cosmetics over Europe.

2.2. Waste management

After use, ENMs in solid waste are assumed to enter three different waste treatment processes: landfilling, waste incineration and recycling. In the model, ENM flows to recycling are equivalent to those collected separately from mixed waste and entering sorting processes, while flows towards landfilling and incineration are ENMs contained in mixed (or residual) waste. The proportions in which the different waste categories arising from ENM-containing products enter the different waste treatment processes have already been assessed in earlier work.[19] The uncertainties associated with each transfer coefficient within and out of waste treatment are assessed based on three data quality indicators: geographical relevance, temporal relevance and source reliability (or type).[19] These transfer coefficients and associated probability distributions are used as such in the present study.

ENMs can also be released to wastewater during use, and are consequently transferred to wastewater treatment plants, sludge, soil and surface water. Transfer coefficients related to wastewater management are taken from Sun *et al.*[6] the differentiation of these transfer coefficients at the national level is out of the scope of this study, except for those coefficients relating to sludge management. Flows of sludge to landfills, incineration plants or agricultural soils are based on data from the Eurostat database (see Table S6†).

2.3. Probabilistic material flow analysis

Data and associated uncertainties regarding production, manufacturing and consumption amounts, product allocations, waste treatment and other transfer coefficients describing the flows of ENMs within their life cycles are combined in a code written in R, enabling probabilistic material flow analysis.[40] This code uses matrix algebra to solve eqn (2):

$$A \cdot X = I \quad (2)$$

In this equation, I is the input vector containing all initial inputs to each compartment, which are production and potential imports to manufacturing and consumption. A is a matrix containing all transfer coefficients between the n compartments and X is the output vector of the model, which contains the flows to all compartments. 100 000 simulations have been run, so the final result given by the model is a matrix containing the probability distributions associated with the ENM masses flowing between the compartments of the model.

2.4. Comparison of releases among countries

To allow for a meaningful comparison of released masses among countries of different sizes, the masses of ENMs released in the environment are normalised by the areas of soil or surface water in each country. By normalising the releases by square kilometres, the differences in potential for high concentrations of ENMs can be highlighted. Therefore, releases to surface water are normalised by the area of freshwater (see Table S7† for references) to which a coastal line of seawater is added to account for releases during bathing. The width of this seawater band is 10 meters. The coastal line has been taken from the World Resource Institute.[41] The releases to soils (sludge-treated, natural and urban) are divided by the surface area of land in the countries of interest, which is calculated by subtracting the freshwater surface area from the total country surface area (see Table S7† for references).

3. Results

3.1. Product allocation

The different product allocations from the literature are listed in Tables S8–S10.† For nano-TiO_2, the product distribution is determined from the mean values of a market report[20] and two nano-registration databases.[26,27] Personal

care products are the most important application of TiO_2 nanoparticles.

For nano-ZnO, the market report[20] allocates the products in cosmetics (incl. sunscreens), paints and coatings and anti-bacterial applications, which was in relatively good agreement with other sources.[6,17] Product allocation also was determined through nano-registration databases.[26,27] However, since a low number of products were found, product allocation was exclusively based on the market report.[20] Since the allocation was determined with just one value, minimum and maximum values (as for nano-TiO_2) cannot be determined. Coefficients of variations are established to be ±50%.

The different sources give very different pictures of the tonnage values for nano-Ag as well as the main applications of nano-Ag. Electronics and appliances (more specifically: printing electronics), textiles, cosmetics, cleaning agents and medical technology appear to be the most important applications, although large differences between different data sources have been identified. Electronic printing is an emerging application that is growing rapidly.[42] This has been confirmed by discussion with experts in the NanoFASE project and its advisory board. Therefore, electronic printing was identified as the most important use of nano-Ag in Europe, estimated to be responsible of 80% of the total use. The remaining 20% were split in different applications based on the market report.[20] This market report also includes a category "*others*", without specifying which applications are included. Product categories found in nano-registration databases[25,27] that do not belong to the applications included individually are therefore placed in the category "*others*" (food, cleaning agents, appliances, small personal care items and filters). For anti-bacterial coatings, since information on the share allocated to indoor and outdoor applications was not available, 50% was attributed to each application. The same applied to medical applications (*i.e.* wound dressing and coatings on medical devices). Coefficients of variations are established to be ±50%.

Table 1 presents the resulting product distributions for each of the three selected ENMs. For nano-TiO_2 and nano-ZnO, personal care products (in particular sunscreens) are found to be the most important application, with smaller contributions from other applications such as coatings. For nano-Ag, the majority of manufactured products are printed electronics, with relatively small contributions from various other sources.

3.2. ENM distribution over countries

Fig. 3 shows the distribution of production, manufacturing and consumption over the EU member states, Norway and Switzerland. The share of each country in each of the 3 stages is given in Tables S11 and S12.† Results show that the

Table 1 Product distributions for nano-TiO2, nano-ZnO and nano-Ag. Largest contributing applications are shown in bold

Application	Description	Nano-TiO_2	Nano-ZnO	Nano-Ag
Personal care products				
Sunscreens		**57%**	**64%**	
Cosmetics	Liquid and gel products	19%	21%	2%
Coatings				
Paints and building surface treatments (*e.g.* photocatalytic, antimicrobial)		5%	13%	
Cement		3%		
Glass		3%		
Ceramic		3%		
Anti-bacterial coatings	Indoor and outdoor use, long-lasting products, applied on surfaces. 50% indoor use, 50% outdoor use.			5%
Other applications				
Food		5%		0.2%
Rubber, ceramic and plastic additives		2%		
Electronics and appliances	Examples include hairdryers and such types of electronic appliances. ENMs could be anywhere in the product.	2%		0.2%
Solar	Solar cells	0.3%		
Textiles		0.2%		2%
Antimicrobials (in plastics, textiles, *etc.*)			2%	
Printing electronics	**In circuit board**			**80%**
Medical	50% wound dressing, 50% coatings on medical devices			9%
Cleaning agents	Short-lasting products (*e.g.* cleansing bar and floor cleaner)	0.8%		0.2%
Small personal care items	Non-liquid, *e.g.* brushes or nail lacquers			0.2%
Filters	Nano-Ag incorporated in filters for purification of liquids (*e.g.* water filters) and air (*e.g.* vacuum cleaner filters)			0.2%

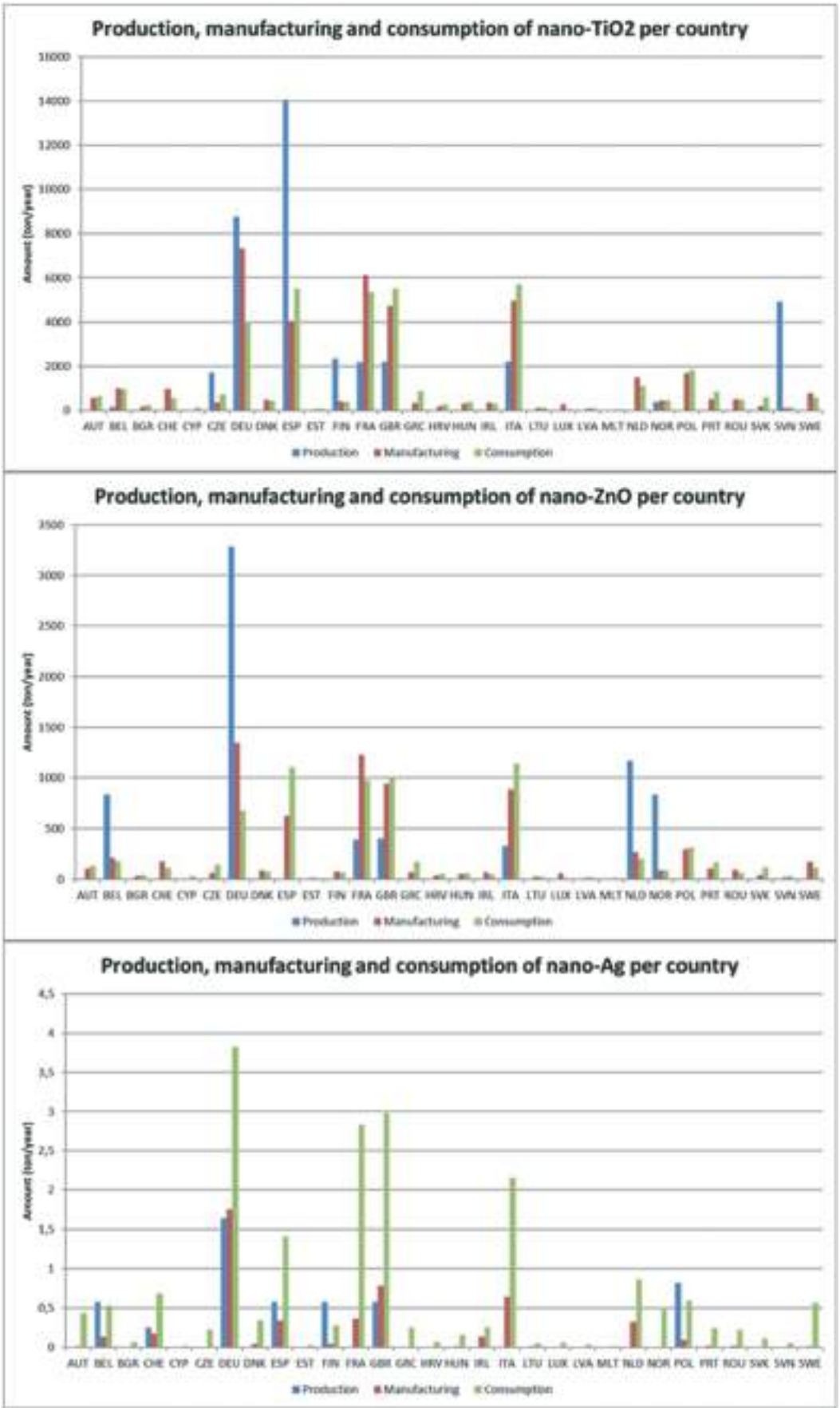

Fig. 3 Bar charts showing the distribution among countries of production, manufacturing and consumption of nano-TiO_2 (upper panel), nano-ZnO (middle) and nano-Ag (lower panel).

production of these specific ENMs only takes place in a limited number of European countries (*e.g.* TiO_2 production in Spain, ZnO production in Germany; see also Tables S1–S3†). In contrast, manufacturing and consumption are more homogeneously spread over Europe.

For nano-Ag, since the main application (printing electronics) is distributed using GDP, the country distribution obtained is similar to a distribution using GDP for all applications.

3.3. Modelling results for production and product allocation

In the rest of the paper, flows of ENMs within their life cycle and subsequent releases to the environment are described using the means of the probability distributions generated by the model. The United Kingdom is used as an example as it is representative for the European waste and sludge management, considering all compartments and processes included in the model.

Selected probability distributions are shown in Fig. 4 where flows to total consumption, consumption of personal liquid care products, wastewater and sludge-treated soil are described for nano-TiO_2 in the UK in year 2015. The latter three flows represent fractions of the first. Therefore, the shapes of their probability distributions are very similar (Fig. 4), and the flows decrease as the nano-TiO_2 initial amount is divided into the technical and environmental compartments of the model. While the modal value of total consumption is around 1890 tonnes, that of consumption of personal care liquid products is 1380 tonnes, of flows to wastewater is 1130 tonnes and finally to sludge-treated soil is 540 tonnes.

3.4. Releases

The means of the flows of nano-TiO_2, nano-ZnO and nano-Ag in the UK are shown in Fig. 5. A high share of nano-TiO_2 is present in personal care products, so most of the releases during use go to wastewater (4265 tonnes, Table S13†). This product allocation also explains why surface water receives a high amount of nano-TiO_2 (2539 tonnes). Recycling is the solid waste treatment process receiving the highest amount of nano-TiO_2 (875 tonnes). This is explained by the fact that packaging and construction waste make up a high share of waste categories in which nano-TiO_2 is embedded and recycled in relatively high rates. Most of the nano-ZnO released during use flows is to wastewater (773 tonnes, Table S14†), since a very high proportion of these ENMs is allocated to personal care products. A small proportion of these products remains in the packaging and follows the flows of solid waste. Sludge-treated soil is the largest environmental sink for nano-ZnO (447 tonnes).

The results also show that after use, the main part of nano-Ag goes to solid waste (0.76 tonnes, Table S15†), mainly entering recycling systems. This is because (1) printed electronics represent a high share of the product allocation (Table 1) and, (2) a high share of the waste arising from these products enters the recycling compartment (Fig. 2) in the end-of-life phase. When nano-Ag does not end up in solid

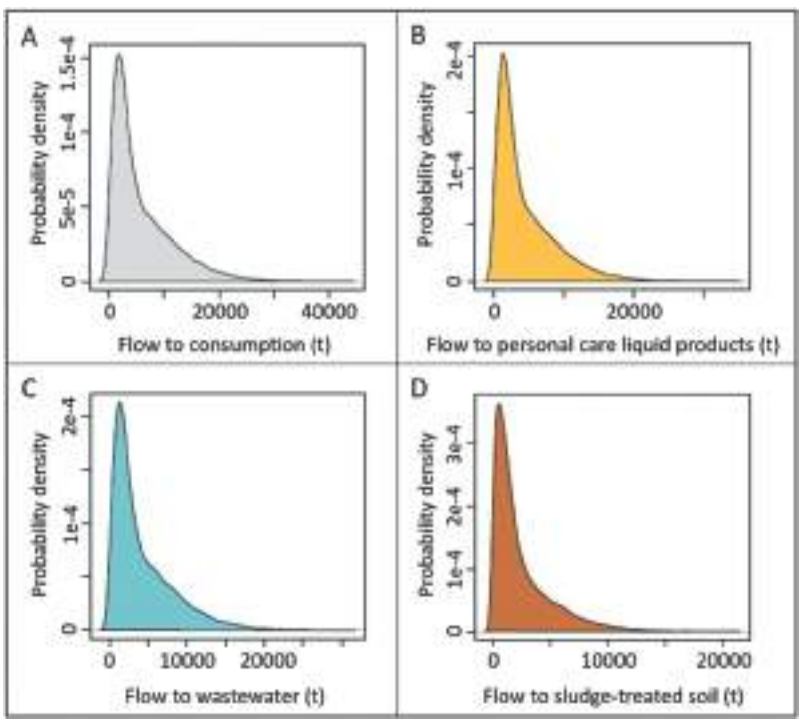

Fig. 4 Flows of nano-TiO_2 to total consumption (A), consumption of personal care liquid products (B), wastewater (C) and sludge-treated soil (D) in the UK, in tonnes for year 2015.

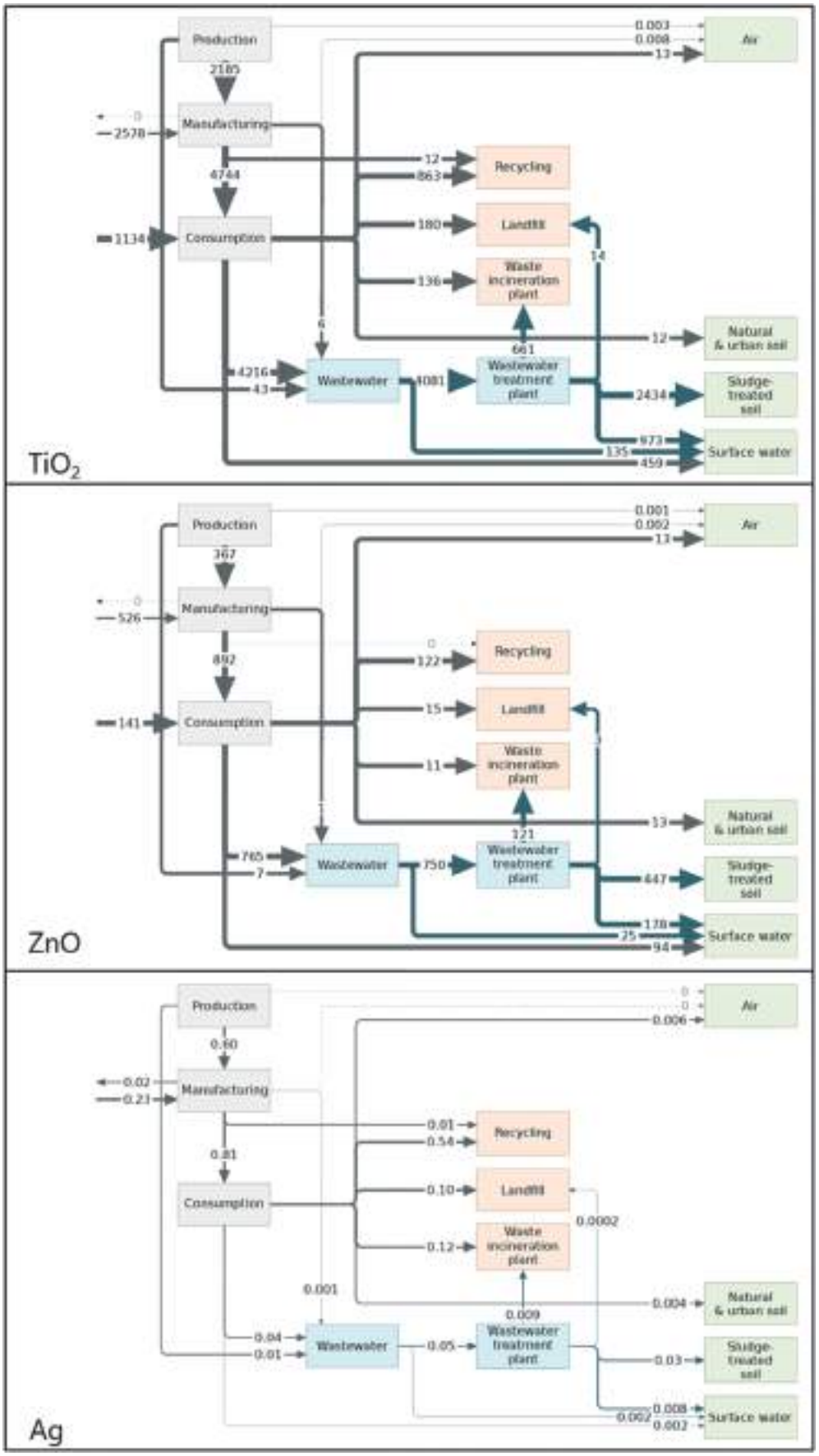

Fig. 5 Flows of nano-TiO_2, nano-ZnO and nano-Ag, in the United Kingdom in 2015. Values are in tonnes; they represent the means of the probability distributions.

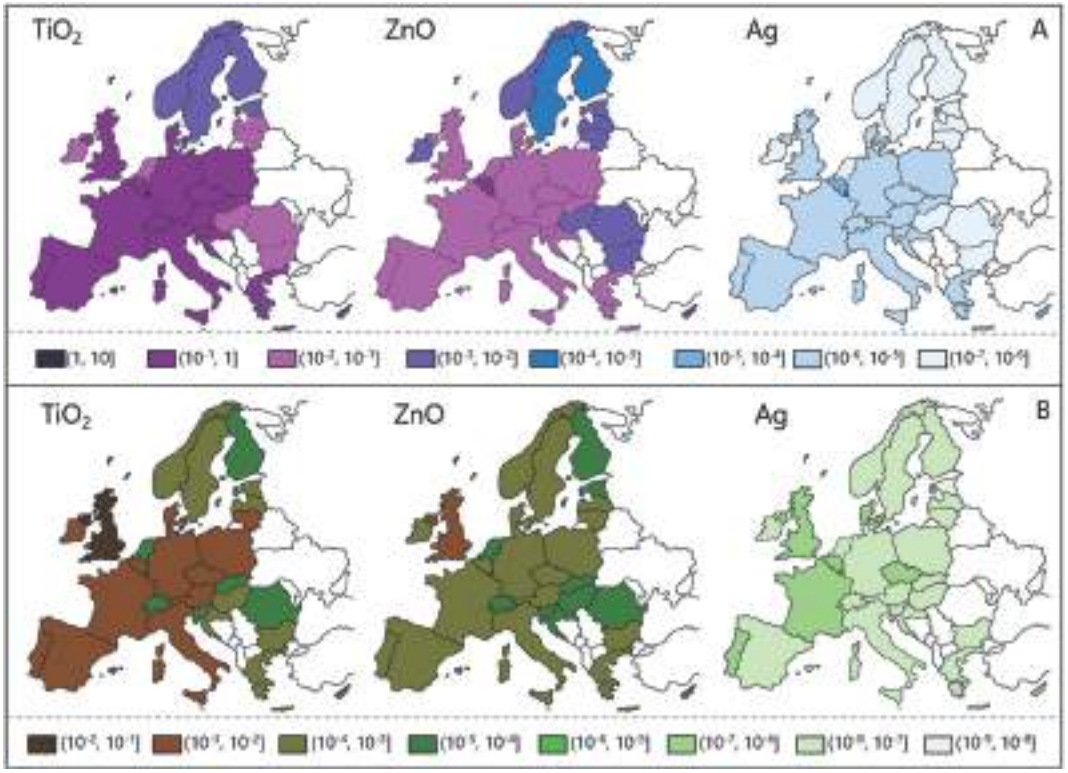

Fig. 6 Maps of releases of nano-TiO_2, nano-ZnO and nano-Ag to surface water (A) and soils (B) in European countries. The soil releases represent the sum of releases to natural & urban soil and sludge-treated soils. Values are in tonnes released per km^2.

waste, it flows to wastewater treatment plants, where most of it is removed with sludge. Therefore, sludge-treated soil is the environmental compartment receiving the highest emission of nano-Ag (0.03 tonnes).

The results expressed per unit of area of the respective environmental compartment are shown in Fig. 6 and in the ESI† (Tables S16 and S17). Concentrations of nano-Ag to surface water are lower compared to nano-TiO_2 and nano-ZnO due to lower production and release coefficients (Fig. 6A , Table S16†). The Scandinavian countries show lower releases of ENMs to surface water, reflecting the fact that less sunscreen is used, although this is also caused by these countries having a relatively large area of surface water compared to ENM released amounts. On the other hand, a small country like Cyprus has among the highest releases per surface water area (0.70 and 0.15 tonnes released per km^2 of surface water for nano-TiO_2 and nano-ZnO, respectively), since there is relatively little surface water except for the coastline as well as the relatively high use of sunscreens. Also in Hungary, Romania and Bulgaria the concentrations are lower, which is the result of a lower allocation of European sunscreen use to these countries.

Release estimates to soils do not necessarily correlate with used amounts of ENMs (Fig. 6B, Table S17†) since sludge management also plays a role, especially sludge application to agricultural soils. Therefore Cyprus, which is one of the countries with the lowest forecasted consumption of ENMs, but which applies all its sludge to agricultural land (Table S6†), presents high release estimates to soils (4.3×10^{-4}, 7.5 and 1.5 kg of nano-Ag, -TiO_2 and -ZnO per km^2, respectively). On the other hand, Switzerland and the Netherlands, for example, have fairly low estimated levels of consumption and incinerate all their sludge, leading to low releases to soils, in the orders of magnitude of 10^{-5} kg per km^2 for nano-Ag and 10^{-2} kg per km^2 for nano-TiO_2 and nano-ZnO.

4. Discussion

With this paper, we present an updated and country-specific European dataset of selected ENM releases to different environmental compartments in 2015.

Compared to the earlier studies[19,22] on which this work largely builds upon, one key change includes the revision of nano-Ag production and consumption volumes within Europe. Consequently, the environmental releases of nano-Ag have also been adjusted. In the paper we show that estimates for the total nano-Ag production in Europe as well as globally vary strongly between different sources, which makes it very difficult to select a realistic mean value. Since recent information such as the French product register[16] suggests that the actual production of nano-Ag in France is in the order of kilograms, the production value for nano-Ag was adopted from different sources stating production amounts on the lower side of the spectrum.[17,24] Because of import and export, production and consumption in Europe may differ substantially. Since we expect that a large part of the nano-Ag

containing products are imported into and used in Europe, we adjusted the consumption in this specific case to be 20 tonnes,[29] 4 times higher compared to the production in Europe.

Another major update is the revision of the different products or applications where the ENMs are used. While the main applications of nano-TiO_2 and nano-ZnO are similar to those previously reported, this revision had a high impact on nano-Ag. To further investigate the product distribution for nano-Ag, we compare the product distributions for nano-Ag with alternative product distributions reported in literature.[22,43] A direct comparison between the product allocations is provided in the supplementary information (Table S18†). Printed electronics were found to be a rapidly growing application[42] and while in earlier studies the importance of this application is considered to be smaller,[6] in a more recent study that reviewed the product distributions, consumer electronics (including mainly electronic printing) is found to be the most important application for nano-Ag, representing 65% of the total use,[43] which is in the same range as our estimation of 80%. At the same time, the application of nano-Ag in textiles appears to be decreasing. Where in earlier studies looking into the different applications, textiles were considered to be the most important application,[6] the latest market report that was used for this study indicates that this application is of lower importance.[20] Therefore, in this study it was decided to use the market report for the other sources than electronic printing, resulting in a relatively low share of textiles in nano-Ag.

Nevertheless, given the uncertainties associated with the product distribution for nano-Ag, it is important to assess the impact this could have on the estimated releases to the environmental compartments. To illustrate the impact this may have on the modelling results, alternative results for nano-Ag have been modelled using the product allocation presented in Giese *et al.* (2018),[43] where the total consumption of 20 tonnes per year has been preserved since it is roughly in line with global estimates presented in this paper. The comparison between the results resulting from both approaches is shown in Fig. S1 in the ESI.† The main difference compared to this study is that in Giese *et al.* (2018)[43] the share of electronic printing is lower and share of textiles is higher. While for electronic printing a large fraction of the ENMs ends up in recycling, for ENMs applied in textiles a significant portion of the ENMs is released to the environment (either through direct releases to air or through the wastewater system).This explains the higher releases to air, surface water and to sludge-treated soil and the lower share of recycling when applying the distribution from Giese *et al.* (2018).[43] Overall environmental releases with the high share of nano-Ag in textiles could be nearly a factor 3 higher.

It should be emphasized that the uncertainties in the country-specific release estimates are significant since different steps have been combined, each with its own uncertainty. In general, uncertainties arise from the (un) availability and quality of the data used. First, different estimates for the production (and consumption) of a specific ENM at European scale may differ by orders of magnitude, as shown in earlier studies[17,22] and explained in this paper. Uncertainties in these initial production estimates may arise from missing data in some of the assessment, or overestimates of production by others, the main reason being the commercially sensitive nature of this information, hence it is not publicly available. These uncertainties exist in the European assessment and remain after downscaling to the national level.

A second source of uncertainty is the quantification of the share of the different applications for each ENM. The comparison between different values reported in literature as presented in this paper shows that generally there exists a large variability between them. Like for the production estimates, this is largely related to the fact that the production figures are typically confidential information. Another reason is the rapidly changing market for products containing ENM which makes the use of ENMs in specific applications will come and go. While for nano-TiO_2 and nano-ZnO, most literature studies agree that cosmetics and sunscreens are the applications representing the highest share of ENM consumption, the share of these applications varies between different sources. And especially in the case of nano-Ag where even the main applications (*e.g.* electronics, medical technology, textiles) vary between different studies as explained in this study.

Third, the export of waste outside Europe could not be quantified due to lack of reliable data. For electronic waste for example, although there may be illegal and unreported export of such waste to developing countries outside Europe, information to that regard is lacking and could not be considered in this model. The officially reported flows of WEEE exported outside Europe are however very small (less than 0.001% of collected WEEE at the European scale[44]) and would not have changed the results presented here.

Uncertainty also arises from the distribution of ENM production, manufacturing and use to individual countries. In this study, we present an approach based on surrogate variables, which is often used for distributing environmental releases in space.[30–32] Also, for ENMs the distribution of production, manufacturing and consumption across countries has been attempted before. Keller and Lazareva (2013)[5] derived regional values from global by using population combined with human development index in major world regions. Adam and Nowack (2017)[19] downscaled European production, manufacturing and consumption to individual country scale using GDP as proxy. However, the method presented here allows to choose different means of distributing across countries depending on the stage and application. This allows both, the differentiation in country distribution between production, manufacturing and consumption and the differentiation between different applications. For the production (and manufacturing) stage,

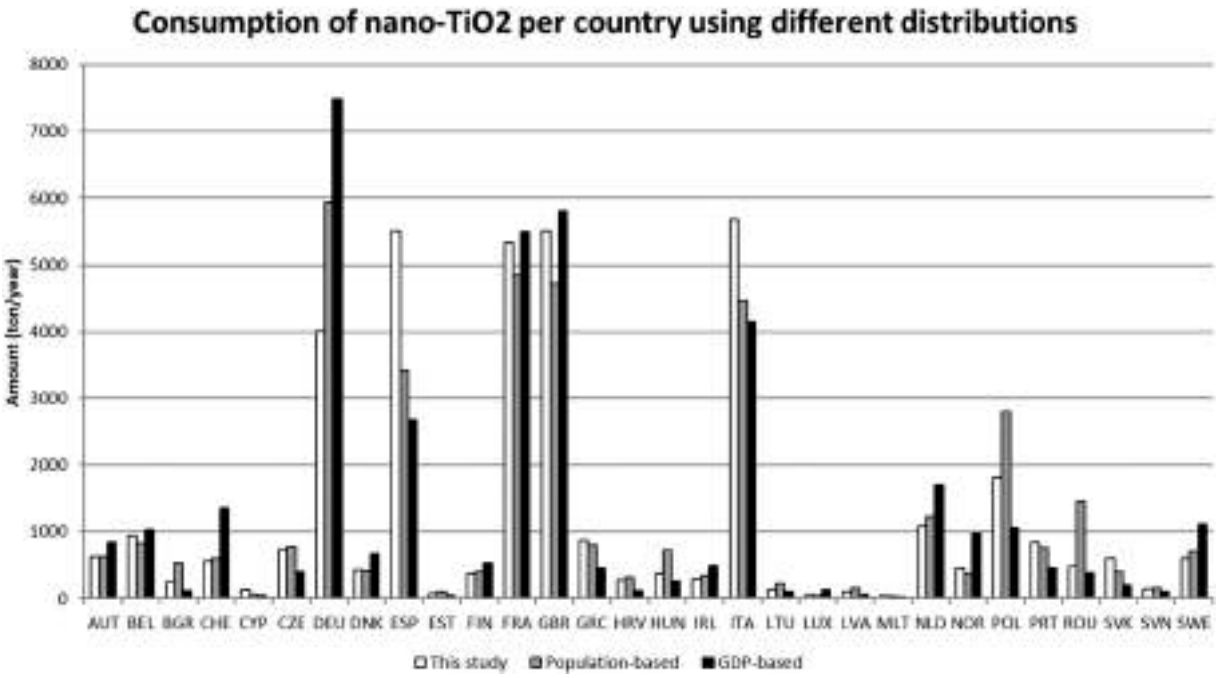

Fig. 7 Comparison of nano-TiO_2 consumption using different methods for distributing emissions over countries.

specific countries in which the production of specific ENMs or ENM-containing products takes place have been identified. While population density or GDP may be used for the allocation of production for different applications to countries; for products with higher share in the total ENM mass, specific country distributions have been developed where relevant information was available. For instance, for sunscreens the expenditure on sunscreens is used as a proxy. It should be emphasized that this is a first approximation which does not take into account the fact that prices of sunscreens vary within Europe and products bought in one country may be used in another country (*e.g.* part of the sunscreen use now attributed to the UK may be taken by holiday makers and used in southern Europe). However, in the absence of actual data this is not accounted for.

In order to assess the impact of this new methodology, Fig. 7 shows a comparison between the method presented in this paper and a distribution solely based on population or GDP as used in previous studies. The figure shows that in specific cases applying this more advanced method still may lead to differences up to a factor 2 or more in the allocation of releases from the consumption stage (*e.g.* TiO_2 consumption in Germany, ZnO consumption in Spain), which shows the importance of the application of a country-specific modelling as presented herein. Additionally, this will lead to varying environmental concentrations and potential risks among European countries.

The results from this study can be used as direct input to fate modelling. For assessing the fate of ENMs, the information at country level is a first step which supports country-specific modelling. However, for spatially and temporally explicit modelling of environmental fate a higher resolution of the release data would be required.[45] Therefore, the next step would be to quantify these releases in a grid, including point sources at exact locations for example at wastewater treatment plants.

Another remaining challenge is to quantify and model the flows coming out of recycling. For many applications such as electronics recycling presents a very important compartment where to a lot of the ENM mass flows in the end-of-life stage. A significant part of the selected ENM-containing products ending up in recycling could re-enter the manufacturing and/or consumption phases. Assessing these flows is particularly important for nano-Ag, since recycling is the compartment receiving most of this ENM after use. Given the importance of wastewater for ENM releases, an improved and country specific assessment of wastewater management, with country-specific connection rates of households to sewer and WWTPs and levels of treatment, should also be considered. In addition, the issue of wastewater overflows is something to be studied in more detail, as during these events large volumes of ENMs may end up in surface water. Finally, including time dynamics (how long ENMs stay in the use phase, and how waste management practices change over time) in this country-specific model would enable a quantification of stocks within the life cycle, and a more accurate estimation and timing of releases. Including these aspects will make the resulting dataset more useful for modelling the fate of the respective nanomaterials.

5. Conclusions

An updated and country-specific inventory for ENM releases has been prepared for nano-TiO_2, nano-ZnO and nano-Ag.

Specific attention has been paid to updating the share of ENMs over the various applications, and subsequently the country allocation for each of these applications.

The results show that cosmetics and sunscreens are the dominant applications of nano-TiO_2 and nano-ZnO. Therefore, the highest releases are found during the consumption stage and eventually end up in surface water and/or wastewater. The bulk of wastewater passes through wastewater treatment plants and consequently the ENMs end up in the sewage sludge which is then partially spread on agricultural soils. For nano-Ag, printing electronics is the main application and leads to potential ENM releases during solid waste treatment. However, printing electronics mostly enter the recycling compartment of solid waste treatment. A comparison with an alternative product distribution shows that potential ENM releases can be strongly influenced by this assumption, as other applications may have different pathways (*e.g.* nano-Ag in textiles ending up in the wastewater system).

The country-specific element of the ENM releases is brought in by means of using surrogate variables. These are selected at the level of individual applications of ENMs, in order to reflect the distribution more accurately compared to using a single distribution parameter such as GDP. For example, in the case of sunscreens, which is the most important application of nano-TiO_2 and nano-ZnO, a specific variable is developed based on sunscreen expenditure per country.

The results can be used to assess the fate of nanomaterials in Europe and specific countries. A next step is to further disaggregate the releases both spatially and temporally, in order to assess the fate of ENMs in a spatially and temporally explicit way. Further research is needed to analyse the flows of ENMs after entering the recycling compartment, since there is a significant portion of nanomaterials (especially nano-Ag) being collected, and with the efforts to increase European recycling rates, it is likely that the ENMs ending up in this compartment increase in the future. Finally, to provide the results with more confidence, more research should be undertaken to reduce the uncertainties in all the datasets that are used to derive the ENM releases to the environment.

Conflicts of interest

There are no conflicts to declare.

Acknowledgements

The work presented in this paper is based on the NanoFASE project, which receives funding from the European Union's Horizon 2020 research and innovation programme under grant agreement number 646002. We acknowledge the contributions from partners from the NanoFASE projects and its advisory board, in particular F. Gottschalk, B. Park. F. Klaessig and A. Crossley, for providing valuable inputs and comments to this work, especially regarding critical parts such as total production volumes and the share of different applications.

References

1 F. Gottschalk, E. Kost and B. Nowack, Engineered nanomaterials in water and soils: A risk quantification based on probabilistic exposure and effect modeling, *Environ. Toxicol. Chem.*, 2013, **32**, 1278–1287.

2 F. Gottschalk, T. Sun and B. Nowack, Environmental concentrations of engineered nanomaterials: Review of modeling and analytical studies, *Environ. Pollut.*, 2013, **181**, 287–300.

3 A. B. A. Boxall, Q. Chaudhry, C. Sinclair, A. Jones, R. Aitken, B. Jefferson and C. Watts, *Current and Future Predicted Environmental Exposure To Engineered Nanoparticles*, York, United Kingdom, 2007.

4 F. Gottschalk, T. Sonderer, R. W. Scholz and B. Nowack, Modeled Environmental Concentrations of Engineered Nanomaterials (TiO2, ZnO, Ag, CNT, Fullerenes) for Different Regions, *Environ. Sci. Technol.*, 2009, **43**, 9216–9222.

5 A. A. Keller and A. Lazareva, Predicted Releases of Engineered Nanomaterials: From Global to Regional to Local, *Environ. Sci. Technol. Lett.*, 2014, **1**, 65–70.

6 T. Y. Sun, F. Gottschalk, K. Hungerbühler and B. Nowack, Comprehensive probabilistic modelling of environmental emissions of engineered nanomaterials, *Environ. Pollut.*, 2014, **185**, 69–76.

7 B. Nowack, Evaluation of environmental exposure models for engineered nanomaterials in a regulatory context, *NanoImpact*, 2017, **8**, 38–47.

8 C. O. Hendren, M. Lowry, K. D. Grieger, E. S. Money, J. M. Johnston, M. R. Wiesner and S. M. Beaulieu, Modeling Approaches for Characterizing and Evaluating Environmental Exposure to Engineered Nanomaterials in Support of Risk-Based Decision Making, *Environ. Sci. Technol.*, 2013, **47**, 1190–1205.

9 F. von der Kammer, P. L. Ferguson, P. A. Holden, A. Masion, K. R. Rogers, S. J. Klaine, A. A. Koelmans, N. Horne and J. M. Unrine, Analysis of engineered nanomaterials in complex matrices (environment and biota): General considerations and conceptual case studies, *Environ. Toxicol. Chem.*, 2012, **31**, 32–49.

10 B. Nowack, M. Baalousha, N. Bornhöft, Q. Chaudhry, G. Cornelis, J. Cotterill, A. Gondikas, M. Hassellöv, J. Lead, D. M. Mitrano, F. von der Kammer and T. Wontner-Smith, Progress towards the validation of modeled environmental concentrations of engineered nanomaterials by analytical measurements, *Environ. Sci.: Nano*, 2015, **2**, 421–428.

11 A. L. Dale, G. V. Lowry and E. A. Casman, Stream Dynamics and Chemical Transformations Control the Environmental Fate of Silver and Zinc Oxide Nanoparticles in a Watershed-Scale Model, *Environ. Sci. Technol.*, 2015, **49**, 7285–7293.

12 E. Dumont, A. C. Johnson, V. D. J. Keller and R. J. Williams, Nano silver and nano zinc-oxide in surface waters – Exposure estimation for Europe at high spatial and temporal resolution, *Environ. Pollut.*, 2015, **196**, 341–349.

13 A. C. Johnson, M. J. Bowes, A. Crossley, H. P. Jarvie, K. Jurkschat, M. D. Jürgens, A. J. Lawlor, B. Park, P. Rowland, D. Spurgeon, C. Svendsen, I. P. Thompson, R. J. Barnes, R. J. Williams and N. Xu, An assessment of the fate, behaviour and environmental risk associated with sunscreen TiO2 nanoparticles in UK field scenarios, *Sci. Total Environ.*, 2011, **409**, 2503–2510.

14 T. Y. Sun, G. Conroy, E. Donner, K. Hungerbühler, E. Lombi and B. Nowack, Probabilistic modelling of engineered nanomaterial emissions to the environment: a spatio-temporal approach, *Environ. Sci.: Nano*, 2015, **2**, 340–351.

15 A. A. Keller, S. McFerran, A. Lazareva and S. Suh, Global life cycle releases of engineered nanomaterials, *J. Nanopart. Res.*, 2013, **15**, 1692.

16 H. Wigger, W. Wohlleben and B. Nowack, Redefining environmental nanomaterial flows: consequences of the regulatory nanomaterial definition on the results of environmental exposure models, *Environ. Sci.: Nano*, 2018, **5**, 1372–1385.

17 F. Piccinno, F. Gottschalk, S. Seeger and B. Nowack, Industrial production quantities and uses of ten engineered nanomaterials in Europe and the world, *J. Nanopart. Res.*, 2012, **14**, 1109.

18 P. A. Holden, F. Klaessig, R. F. Turco, J. H. Priester, C. M. Rico, H. Avila-Arias, M. Mortimer, K. Pacpaco and J. L. Gardea-Torresdey, Evaluation of Exposure Concentrations Used in Assessing Manufactured Nanomaterial Environmental Hazards: Are They Relevant?, *Environ. Sci. Technol.*, 2014, **48**, 10541–10551.

19 V. Adam and B. Nowack, European country-specific probabilistic assessment of ENM flows towards landfilling, incineration and recycling, *Environ. Sci.: Nano*, 2017, **4**, 1961–1973.

20 Future Markets Inc., *The Global Nanotechnology and Nanomaterials Market Opportunity Report*, 2016.

21 Allied Market Research, *Europe Nanomaterials Market: Trends, Share, Opportunities and Forecasts 2014–2022*, Allied Market Research, 2016.

22 T. Y. Sun, N. A. Bornhöft, K. Hungerbühler and B. Nowack, Dynamic Probabilistic Modeling of Environmental Emissions of Engineered Nanomaterials, *Environ. Sci. Technol.*, 2016, **50**, 4701–4711.

23 Ministère de la Transition écologique et Solidaire, *Éléments issus des déclarations des substances à l'état nanoparticulaire*, 2017.

24 European Commission, *Commission Staff Working Paper - Types and uses of nanomaterials, indcluding safety aspects. Accompanying the Communication from the Commission to the European Parliament, the Council and the European Economic and Social Committee on the Second Regulatory*, 2012.

25 Woodrow Wilson International Center for Scholars, *The project on emerging nanotechnologies - Consumer Products Inventory*, https://nanotechproject.org/.

26 Bund für Umwelt und Naturschutz Deutschland (BUND), *Datenbank für Nano-Produkte*, 2011.

27 D. C. C. DTU Environment, *Danish Ecological Council*, 2013.

28 StatNano, *Nanotechnology Products Database*, https://product.statnano.com/.

29 European Commission, *Scientific Committee on Emerging and Newly Identified Health Risks (SCENIHR) opinion on nanosilver: safety, health and environmental effects and role in antimicrobial resistance*, 2014.

30 EEA, *EMEP/EEA Air Pollutant Emission Inventory Guidebook, chapter on Spatial Emissions Mapping*, 2016.

31 J. J. P. Kuenen, A. J. H. Visschedijk, M. Jozwicka and H. A. C. Denier Van Der Gon, TNO-MACC-II emission inventory; A multi-year (2003-2009) consistent high-resolution European emission inventory for air quality modelling, *Atmos. Chem. Phys.*, 2014, **14**, 10963–10976.

32 M. Crippa, D. Guizzardi, M. Muntean, E. Schaaf, F. Dentener, J. A. Van Aardenne, S. Monni, U. Doering, J. G. J. Olivier, V. Pagliari and G. Janssens-Maenhout, Gridded emissions of air pollutants for the period 1970-2012 within EDGAR v4.3.2, *Earth Syst. Sci. Data*, 2018, **10**, 1987–2013.

33 Eurostat, *Gross Domestic Product at market prices (tec00001)*, year 2014, https://ec.europa.eu/eurostat/data/database?node_code=tec00001, (accessed 6 July 2016).

34 Eurostat, *Total population by age and sex on 1 January*, year 2014, https://ec.europa.eu/eurostat/web/population-demography-migration-projections/data/database, (accessed 11 July 2016).

35 Eurostat, *PRODCOM Statistics on Manufactured Goods*, year 2015, https://ec.europa.eu/eurostat/web/prodcom/data/excel-files-nace-rev.2, (accessed 25 January 2017).

36 USGS, *Minerals Yearbook 2012 for Cement*, https://prd-wret.s3-us-west-2.amazonaws.com/assets/palladium/production/atoms/files/myb1-2013-cemen.pdf, (accessed 11 July 2016).

37 J. K. Pearson, European solvent VOC emission inventories based on industry-wide information, *Atmos. Environ.*, 2019, **204**, 118–124.

38 Global Insight, *A study of the European Cosmetics Industry*, 2007.

39 Cosmetics Europe, *Activity Report 2014*, 2014.

40 F. Gottschalk, R. Scholz and B. Nowack, Probabilistic material flow modeling for assessing the environmental exposure to compounds: Methodology and an application to engineered nano-TiO2 particles, *Environ. Model. Softw.*, 2010, **25**, 320–332.

41 World Resource Institute, *Coastal and Marine Ecosystems-Marine Jurisdictions: Coastline length*, https://web.archive.org/web/20120419075053/http://earthtrends.wri.org/text/coastal-marine/variable-61.html#fn_2, (accessed 13 May 2019).

42 K. Rajan, I. Roppolo, A. Chiappone, S. Bocchini, D. Perrone and A. Chiolerio, Silver nanoparticle ink technology: state of the art, *Nanotechnol. Sci. Appl.*, 2016, **9**, 1–13.

43 B. Giese, F. Klaessig, B. Park, R. Kaegi, M. Steinfeldt, H. Wigger, A. Von Gleich and F. Gottschalk, Risks, Release and

Concentrations of Engineered Nanomaterial in the Environment, *Sci. Rep.*, 2018, **8**, 1–18.

44 Eurostat, *Waste electrical and electronic equipment (WEEE) by waste management operations*, https://ec.europa.eu/eurostat/web/waste/data/database, (accessed 15 October 2020).

45 R. J. Williams, S. Harrison, V. Keller, J. Kuenen, S. Lofts, A. Praetorius, C. Svendsen, L. C. Vermeulen and J. van Wijnen, Models for assessing engineered nanomaterial fate and behaviour in the aquatic environment, *Curr. Opin. Environ. Sustain.*, 2019, **36**, 105–115.

Electronic Supplementary Material (ESI) for Environmental Science: Nano.

Supplementary information

Inventory of country-specific emissions of engineered nanomaterials throughout the life cycle

Jeroen Kuenen[1], Vicenç Pomar-Portillo[2], Alejandro Vilchez[2], Antoon Visschedijk[1], Hugo Denier van der Gon[1], Socorro Vázquez-Campos[2], Bernd Nowack[3], Véronique Adam[3]

[1] TNO, Department of Climate, Air and Sustainability, Princetonlaan 6, 3584 CB Utrecht, The Netherlands

[2] LEITAT Technological Center, Materials Safety Unit, Human & Environmental Health & Safety Division, Carrer de la Innovació 2, 08225 Terrassa (Barcelona), Spain

[3]EMPA, Swiss Federal Laboratories for Materials Science and Technology, Lerchenfeldstrasse 5, 9014 St. Gallen, Switzerland

Country allocation of ENM production

Table S1: Nano-TiO_2 production percentages in European companies (C1 to C8). The countries that do not appear in the table do not produce nano-TiO_2.

Application and overall share of manufacturing *(A)*		Sunscreens & Cosmetics (76%)				Others (24%)						
Company		C1	C2	C3	C4	C2	C5	C3	C6	C7	C4	C8
Company production capacity at European level *(B)*		High	High	Medium	Low	High	High	Medium	Medium	Medium	Low	Low
Company contribution to European production *(C = B / number of companies at same level)*		40%	40%	15%	5%	40%	40%	5%	5%	5%	2.5%	2.5%
Contribution of plants in country to company European production *(D = number of plants in country / European number of plants)*	BEL								33%			
	CZE				100%						100%	
	DEU		27%			27%	100%		33%			
	ESP	100%	13%			13%						
	FIN		13%			13%						
	FRA		13%			13%				100%		
	GBR		13%			13%						
	ITA		13%			13%						
	NOR								33%			100%
	SVN			100%				100%				
Contribution of company to nano-ZnO production in country *(A x C x D)*	BEL								0.4%			
	CZE				4%						1%	
	DEU		8%			3%	10%		0.4%			
	ESP	30%	4%			1%						
	FIN		4%			1%						
	FRA		4%			1%				1%		
	GBR		4%			1%						
	ITA		4%			1%						
	NOR								0.4%			1%
	SVN			11%				1%				

Table S2: Nano-ZnO production percentages in European companies (C1 to C9). The countries that do not appear in the table do not produce nano-ZnO.

Application and overall share of manufacturing *(A)*		Sunscreens & Cosmetics (85%)					Others (15%)					
Company		C1	C2	C3	C4	C5	C3	C6	C7	C4	C8	C9
Company production capacity at European level *(B)*		High	High	High	Medium	Low	High	Medium	Medium	Medium	Low	Low
Company contribution to European production *(C = B / number of companies at same level)*		27%	27%	27%	19%	1%	80%	6%	6%	6%	0.5%	0.5%
Contribution of plants in country to company European production *(D = number of plants in country / European number of plants)*	BEL			33%			33%					
	CZE											100%
	DEU	20%	100%		100%			100%		100%		
	ESP										100%	
	FRA	20%				100%						
	GBR	20%							100%			
	ITA	20%										
	NLD	20%		33%			33%					
	NOR			33%			33%					
Contribution of company to nano-ZnO production in country *(A x C x D)*	BEL			8%			4%					
	CZE											0.1%
	DEU	4.5%	23%		16%			1%		1%		
	ESP										0.1%	
	FRA	4.5%				0.9%						
	GBR	4.5%							1%			
	ITA	4.5%										
	NLD	4.5%		8%			4%					
	NOR			8%			4%					

Table S3: Nano-Ag production percentages in European companies (C1 to C10). The countries that do not appear in the table do not produce nano-Ag.

Application and overall share of	Printed electronics (80%)	Other applications (20%)

manufacturing *(A)*											
Company		C1	C2	C3	C4	C5	C6	C7	C8	C9	C10	C5
Company production capacity at European level *(B)*		Medium	Medium	Medium	Medium	Medium	Medium	Medium	Medium	Medium	Medium	Medium
Company contribution to European production *(C = B / number of companies at same level)*		14%	14%	14%	14%	14%	14%	14%	25%	25%	25%	25%
Contribution of plants in country to company European production *(D = number of plants in country / European number of plants)*	BEL	100%										
	DEU				100%	100%					100%	100%
	ESP							100%				
	FIN						100%					
	GBR			100%						100%		
	POL		100%						100%			
Contribution of company to nano-ZnO production in country *(A x C x D)*	BEL	11%										
	DEU				11%	11%					5%	5%
	ESP							11%				
	FIN						11%					
	GBR			11%						5%		
	POL		11%						5%			

Country distribution

Table S4: Surrogate variables chosen for country distribution for the manufacturing and consumption stages. Numbered entries are further explained below.

Application	**Proxy for manufacturing stage**	**Proxy for consumption stage**
Anti-bacterial coatings	GDP	GDP
Anti-bacterials	GDP	GDP
Cement	Cement production	GDP
Ceramic	PRODCOM_Glass and ceramics	Population
Cleaning agents	PRODCOM_Cleaning agents	Population
Cosmetics	Proxy sunscreen and cosmetics production	Proxy cosmetics use
Printing electronics	PRODCOM_Electronic printing	GDP
Electronics and appliances	PRODCOM_Electronics and appliances	GDP
Filters	PRODCOM_Filters	GDP
Food	PRODCOM_Food	Population
Glass	PRODCOM_Glass	Population
Medical	PRODCOM_Medical technolog	GDP
Paints and building surface treatments	PRODCOM_Paints and Coatings	ESIG paint consumption
Rubber, ceramic and plastic additives	GDP	Population
Small personal care items	GDP	Population
Solar	PRODCOM_Solar	GDP
Sunscreens	Proxy sunscreen and cosmetics production	Proxy sunscreen use
Textiles	PRODCOM_Textiles	Population

Explanation of PRODCOM codes used for manufacturing of specific applications

Table S5: Explanation of PRODCOM codes used for each application

Application	**Selected PRODCOM codes**
Cleaning agents	20412020, 20412030, 20412050, 20412090, 20413150, 20413240, 20413250, 20413260, 20413270, 20414330, 20414350, 20414370, 20414383, 20414389, 20414400
Electronics and appliances	26112220, 26112240, 26114070, 27511133, 27511135, 27511150, 27511170, 27511200, 27511200, 27511300, 28295000, 28298510, 28942150, 28942230, 28945210
Filters	28945210, 17124330, 17291200, 17291951, 22292630, 28291350, 28298250, 32995910
Food	100000Z1, 100000Z2, 10851100, 10851200, 10851300, 10851410, 10851900
Glass	20302130
Glass and ceramics	20302130, 20302150, 20302170
Medical technology	13202020, 21201380, 21202420, 21202430, 21202440, 21202460, 32501200, 32501311, 32501313, 32501315, 32501317, 32501370, 32502255, 32502259, 32502290, 32505010, 32505020, 32505030
Paints and Coatings	20301150, 20301170, 20301225, 20301229, 20301230, 20301250, 20301270, 20301290, 20302130, 20302150, 20302170, 20302213, 20302215, 20302240, 20302253, 20302255, 20302260, 20302273, 20302279, 20302350, 20302370, 20302450, 20302470
Solar	26112240
Textiles	14121120, 14121240, 14121250, 14122120, 14122130, 14122240, 14122250, 14123013, 14123023, 14131110, 14131120, 14131230, 14131260, 14131270, 14131310, 14131320, 14131430, 14131460, 14131470, 14131480, 14131490, 14132115, 14132130, 14132200, 14132300, 14132442, 14132444, 14132445, 14132448, 14132449, 14132455, 14132460, 14133115, 14133130, 14133200, 14133330, 14133470, 14133480, 14133542, 14133548, 14133549, 14133551, 14133561, 14133563, 14133565, 14133569, 14141100, 14141220, 14141230, 14141240, 14141310, 14141420, 14141430, 14141440, 14141450, 14142100, 14142220, 14142230, 14142240, 14142300, 14142430, 14142450, 14142460, 14142480, 14142489, 14142530, 14142550, 14142570, 14143000, 14191210, 14191230, 14191240, 14191250, 14191290, 14191300, 14191960, 14192210, 14192220, 14192230, 14192240, 14192250, 14192370, 14192396, 14193175, 14193190, 14193200, 14311033, 14311035, 14311037, 14311050, 14311090, 14391031, 14391032, 14391033, 14391061, 14391062, 14391071, 14391072, 14391090

Sludge management

Table S6: Transfer coefficients relating to sludge management (adapted from Eurostat[1])

Country	Year	% Landfill	% Incineration	% Agricultural use
Belgium	2010	0%	87%	13%
Bulgaria	2014	34%	0%	66%
Czechia	2014	14%	6%	79%
Denmark	2010	1%	31%	68%
Germany	2014	0%	70%	30%
Estonia	2009	90%	0%	10%
Ireland	2014	1%	0%	99%
Greece	2014	39%	38%	23%
Spain	2012	16%	4%	80%
France	2014	5%	27%	68%
Croatia	2014	95%	0%	5%
Italy	2010	57%	5%	39%
Cyprus	2014	0%	0%	100%
Latvia	2013	3%	0%	97%
Lithuania	2014	0%	0%	100%
Luxembourg	2012	0%	16%	84%
Hungary	2014	14%	74%	12%
Malta	2014	100%	0%	0%
Netherlands	2014	0%	100%	0%
Austria	2014	2%	73%	25%
Poland	2014	14%	38%	48%
Portugal	2012	10%	0%	90%
Romania	2014	91%	1%	8%
Slovenia	2014	2%	97%	1%
Slovakia	2014	21%	79%	0%
Finland	2012	20%	65%	15%
Sweden	2014	6%	4%	90%
United Kingdom	2012	0%	21%	78%
Norway	2014	18%	0%	83%
Switzerland	2013	0%	100%	0%

Normalised releases to soil and surface water

Table S7: References used to calculate normalised releases to soil and surface water.

Country	**Total surface area**	**Freshwater surface**
Austria	Eurostat[2]	Eurostat
Belgium	Eurostat	Eurostat
Bulgaria	Eurostat	Eurostat
Switzerland	Steinmeier (2013)[3]	Steinmeier (2013)
Cyprus	Eurostat	Eurostat
Czech Republic	Eurostat	Eurostat
Germany	Eurostat	Eurostat
Denmark	Eurostat	Eurostat
Spain	Eurostat	Eurostat
Estonia	Eurostat	Klein (2000)[4]
Finland	Eurostat	Eurostat
France	Eurostat	Eurostat
United Kingdom	Eurostat	Eurostat
Greece	Eurostat	Eurostat
Croatia	Eurostat	Eurostat
Hungary	Eurostat	Eurostat
Ireland	Eurostat	Eurostat
Italy	Eurostat	Eurostat
Lithuania	Eurostat	Eurostat
Luxembourg	Eurostat	Eurostat
Latvia	Eurostat	Eurostat
Malta	Eurostat	Eurostat
Netherlands	Eurostat	Eurostat

Norway	Worldatlas[5]	Worldatlas
Poland	Eurostat	Eurostat
Portugal	Eurostat	Eurostat
Romania	Eurostat	Eurostat
Slovakia	Eurostat	Eurostat
Slovenia	Eurostat	Eurostat
Sweden	Eurostat	Eurostat

Production, manufacturing and consumption results

Table S8: Overview of different information sources for applications of nanosized TiO_2 and their relative importance

Application	Future markets (2016)	Bund (n=61)	Danish (n=111)	Mean	Min	Max
Total personal care*	72%	75%	81%	76%	72%	81%
Sunscreens**	72%	64%	21%	57%	21%	64%
Cosmetics**		11%	60%	19%	11%	60%
Coatings*	20%	21%		14%	0%	21%
Paints and building surface treatments (e.g. photocatalytic, antimicrobial)	10%	5%		5%	0%	10%
Cement	3%	5%		3%	0%	5%
Glass	3%	5%		3%	0%	5%
Ceramic	3%	5%		3%	0%	5%
Rubber, ceramic and plastic additives	5%	2%		2%	0%	5%
Solar	1%			0.3%	0%	1%
Electronics and appliances	0.5%	2%	3%	2%	0.5%	3%
Cleaning agents	0.5%		2%	0.8%	0%	2%
Food	0.5%		14%	5%	0%	14%
Textiles	0.5%			0.2%	0%	0.5%

(*) This category represents the contribution of multiple applications from this table.

(**) Sources provide opposite results, therefore the mean is not used here. Most references identify sunscreens as the most important application. Hence, it is assumed that sunscreens account for 57% of the total personal care products.

Table S9: Applications of nanosized ZnO and their relative importance.

Application	Future markets (2016)	Min	Max
Total personal care	85%	43%	100%
Paints and lacquers (coatings)	13%	7%	20%
Antibacterial	2%	1%	3%

Table S10: Applications of nanosized Ag and their relative importance.

Application	Final		Min	Max
Electronic printing	80%		40%	100%
Medical (including wound dressing and coatings in medical devices)	9%		4.5%	13.5%
Anti-bacterial coatings (indoor use, long-lasting products that are applied on surfaces, also paints)	5%		2.5%	7.5%
Cosmetics and personal care (liquids and gel)	2%		1%	3%
Textiles	2%		1%	3%
Food	0.2%		0.1%	0.3%
Cleaning agents (short-lasting products)	0.2%		0.1%	0.3%
Appliances	0.2%		0.1%	0.3%
Small personal care items (non-liquids)	0.2%		0.1%	0.3%
Filters	0.2%		0.1%	0.3%

Table S11: Total estimated production of ENMs in Europe (EU28 + Norway + Switzerland) and distributions over countries (in percentage). Countries not mentioned are assumed to have no production of each of the three ENMs.

Country	Nano-TiO2	Nano-ZnO	Nano-Ag
Average European total (tonnes)	38900	7260	5
BEL	0.4%	12%	11%
CHE			5%
CZE	4.4%	0.1%	
DEU	21%	45%	33%
ESP	36%	0.1%	11%
FIN	6.0%		11%
FRA	6.8%	5.4%	
GBR	5.7%	5.5%	11%
ITA	5.7%	4.6%	
NLD		16%	
NOR	1.0%	12%	
POL			16%
SVN	13%		

Values have been rounded to maximum 2 significant digit. All columns add up to 100%.

Table S12: Total estimated manufacturing and consumption of ENMs in Europe (EU28 + Norway + Switzerland) and distributions over countries (in percentage).

	Manufacturing			Consumption		
Country	**Nano-TiO2**	**Nano-ZnO**	**Nano-Ag**	**Nano-TiO2**	**Nano-ZnO**	**Nano-Ag**
AUT	1.5%	1.5%	0.3%	1.6%	1.8%	2.2%
BEL	2.6%	2.9%	2.6%	2.5%	2.4%	2.7%
BGR	0.4%	0.4%	0.1%	0.6%	0.5%	0.3%
CHE	2.5%	2.4%	3.5%	1.5%	1.5%	3.4%
CYP	0.0%	0.0%	0.0%	0.3%	0.4%	0.1%
CZE	0.9%	0.9%	0.2%	1.9%	2.0%	1.1%
DEU	19%	19%	35.6%	11%	9.5%	19%
DNK	1.2%	1.2%	0.8%	1.1%	1.0%	1.7%
ESP	11%	8.7%	6.8%	14%	15%	7.1%
EST	0.2%	0.2%	0.0%	0.2%	0.2%	0.1%
FIN	1.0%	1.1%	0.9%	1.0%	0.9%	1.4%
FRA	16%	17%	7.3%	14%	14%	14%
GBR	12%	13%	16%	14%	14%	15%
GRC	0.8%	0.9%	0.2%	2.3%	2.4%	1.2%
HRV	0.5%	0.5%	0.1%	0.7%	0.7%	0.3%
HUN	0.7%	0.7%	0.3%	1.0%	0.8%	0.8%
IRL	0.9%	1.0%	2.6%	0.7%	0.7%	1.2%
ITA	13%	12%	13%	15%	16%	11%
LTU	0.3%	0.3%	0.2%	0.3%	0.3%	0.3%
LUX	0.7%	0.8%	0.0%	0.1%	0.1%	0.3%
LVA	0.2%	0.2%	0.0%	0.3%	0.2%	0.2%
MLT	0.0%	0.0%	0.0%	0.1%	0.1%	0.1%
NLD	3.9%	3.7%	6.5%	2.9%	2.8%	4.4%
NOR	1.2%	1.2%	0.2%	1.2%	1.2%	2.4%
POL	4.4%	4.1%	1.8%	4.8%	4.5%	3.0%
PRT	1.3%	1.4%	0.5%	2.2%	2.3%	1.2%
ROU	1.3%	1.3%	0.4%	1.2%	0.9%	1.1%
SVK	0.5%	0.5%	0.1%	1.6%	1.7%	0.5%
SVN	0.2%	0.2%	0.0%	0.4%	0.4%	0.3%
SWE	2.0%	2.3%	0.2%	1.5%	1.6%	2.8%

Values have been rounded to maximum 2 significant digits. All columns add up to 100%.

Modelling results

Table S13: 25th quantiles, means and 75th quantiles of flows of nano-TiO_2 (tonnes)

		Austria			Belgium			Bulgaria		
From	**To**	**Q25**	**Mean**	**Q75**	**Q25**	**Mean**	**Q75**	**Q25**	**Mean**	**Q75**
Import	Manufacturing	31	558	556	47	835	845	8	149	149
Import	Consumption	4	114	113	0	0	0	5	98	100
Production	Manufacturing	0	0	0	128	155	271	0	0	0
Production	Wastewater	0	0	0	0	3	3	0	0	0
Production	Air	0	0	0	0	0	0	0	0	0
Production	Export	0	0	0	0	0	0	0	0	0
Manufacturing	Consumption	107	556	669	167	954	1078	65	246	347
Manufacturing	Wastewater	0	1	1	0	1	1	0	0	0
Manufacturing	Air	0	0	0	0	0	0	0	0	0
Manufacturing	Recycling systems	0	1	1	0	1	1	0	0	0
Manufacturing	Export	0	0	0	0	34	77	0	0	0
Consumption	Wastewater	78	481	559	118	685	772	45	177	245
Consumption	Air	0	1	2	0	2	2	0	1	1
Consumption	Surface water	8	52	61	13	74	84	5	19	26
Consumption	Natural & urban soil	0	1	2	0	2	2	0	0	1
Consumption	Landfill	1	4	5	0	1	1	3	13	17
Consumption	Waste incineration plant	5	32	36	6	40	45	0	0	0
Consumption	Recycling systems	14	98	112	23	150	168	8	36	47
Wastewater	WWTP	77	466	543	116	663	749	45	171	239
Wastewater	Surface water	3	15	18	4	22	25	1	6	8
WWTP	Sludge	50	355	398	76	508	570	27	130	164
WWTP	Surface water	12	111	121	19	155	171	5	41	43
Sludge	Sludge-treated soil	12	87	98	10	68	76	18	86	108
Sludge	Landfill	1	7	8	0	0	0	10	44	59
Sludge	Waste incineration plant	39	261	295	69	440	495	0	0	0
		Switzerland			**Cyprus**			**Czech Republic**		
From	**To**	**Q25**	**Mean**	**Q75**	**Q25**	**Mean**	**Q75**	**Q25**	**Mean**	**Q75**
Import	Manufacturing	58	983	1025	0	4	4	0	0	0
Import	Consumption	0	0	0	8	125	126	22	409	430
Production	Manufacturing	0	0	0	0	0	0	17	308	319
Production	Wastewater	0	0	0	0	0	0	2	34	35
Production	Air	0	0	0	0	0	0	0	0	0
Production	Export	0	0	0	0	0	0	77	1389	1442
Manufacturing	Consumption	33	575	595	5	4	5	165	307	596
Manufacturing	Wastewater	0	1	1	0	0	0	0	0	0
Manufacturing	Air	0	0	0	0	0	0	0	0	0
Manufacturing	Recycling systems	0	1	1	0	0	0	0	1	1
Manufacturing	Export	23	406	422	0	0	0	0	0	0
Consumption	Wastewater	24	412	427	9	93	94	130	514	727
Consumption	Air	0	1	1	0	0	0	0	2	2
Consumption	Surface water	2	45	47	1	10	10	14	56	77
Consumption	Natural & urban soil	0	1	1	0	0	0	0	1	2
Consumption	Landfill	0	0	0	1	7	7	9	38	51
Consumption	Waste incineration plant	1	22	23	0	0	0	2	11	14
Consumption	Recycling systems	5	93	96	2	19	19	20	94	125
Wastewater	WWTP	23	399	413	8	90	91	129	498	711
Wastewater	Surface water	1	13	13	0	3	3	4	16	24
WWTP	Sludge	16	304	311	6	69	69	82	378	497
WWTP	Surface water	3	95	99	1	21	23	15	120	122
Sludge	Sludge-treated soil	0	0	0	6	69	69	65	300	394
Sludge	Landfill	0	0	0	0	0	0	14	54	77
Sludge	Waste incineration plant	16	304	312	0	0	0	6	24	33

Table S13 (continued): 25th quantiles, means and 75th quantiles of flows of nano-TiO_2 (tonnes)

		Germany			Denmark			Spain		
From	**To**	**Q25**	**Mean**	**Q75**	**Q25**	**Mean**	**Q75**	**Q25**	**Mean**	**Q75**
Import	Manufacturing	0	0	0	27	477	475	0	0	0
Import	Consumption	0	0	0	0	0	0	71	1593	1619
Production	Manufacturing	402	7271	7303	0	0	0	226	3868	3988
Production	Wastewater	7	164	167	0	0	0	14	283	293
Production	Air	0	0	0	0	0	0	0	0	0
Production	Export	13	865	888	0	0	0	593	10109	10457
Manufacturing	Consumption	215	3971	3998	23	422	426	1224	3853	5503
Manufacturing	Wastewater	1	19	19	0	1	1	0	5	5
Manufacturing	Air	0	0	0	0	0	0	0	0	0
Manufacturing	Recycling systems	0	5	6	0	0	0	0	10	10
Manufacturing	Export	174	3275	3322	0	55	61	0	0	0
Consumption	Wastewater	152	2850	2876	16	303	306	902	3907	5036
Consumption	Air	0	9	9	0	1	1	2	12	14
Consumption	Surface water	16	309	316	2	33	34	95	424	544
Consumption	Natural & urban soil	0	8	8	0	1	1	2	11	14
Consumption	Landfill	0	1	1	0	7	7	65	319	402
Consumption	Waste incineration plant	8	164	166	1	15	15	11	55	69
Consumption	Recycling systems	31	631	641	3	63	64	136	718	887
Wastewater	WWTP	150	2759	2774	16	293	296	895	3782	4942
Wastewater	Surface water	5	91	89	1	10	10	30	125	166
WWTP	Sludge	106	2095	2088	11	224	228	523	2876	3516
WWTP	Surface water	21	664	718	2	68	71	110	906	956
Sludge	Sludge-treated soil	32	638	636	8	152	155	417	2295	2807
Sludge	Landfill	0	0	0	0	3	3	108	460	591
Sludge	Waste incineration plant	75	1457	1460	4	70	71	27	121	154
		Estonia			**Finland**			**France**		
From	**To**	**Q25**	**Mean**	**Q75**	**Q25**	**Mean**	**Q75**	**Q25**	**Mean**	**Q75**
Import	Manufacturing	4	62	65	0	0	0	346	6229	6341
Import	Consumption	1	18	18	0	0	0	0	0	0
Production	Manufacturing	0	0	0	20	341	353	190	158	191
Production	Wastewater	0	0	0	2	46	47	0	3	3
Production	Air	0	0	0	0	0	0	0	0	0
Production	Export	0	0	0	112	1913	1972	0	0	0
Manufacturing	Consumption	16	62	82	19	323	333	465	5605	5802
Manufacturing	Wastewater	0	0	0	0	1	1	1	8	9
Manufacturing	Air	0	0	0	0	0	0	0	0	0
Manufacturing	Recycling systems	0	0	0	0	0	0	0	5	5
Manufacturing	Export	0	0	0	0	17	25	9	770	849
Consumption	Wastewater	12	58	71	13	232	239	329	4020	4173
Consumption	Air	0	0	0	0	1	1	1	12	12
Consumption	Surface water	1	6	8	1	25	26	35	438	458
Consumption	Natural & urban soil	0	0	0	0	1	1	1	11	12
Consumption	Landfill	0	1	1	0	4	4	9	122	127
Consumption	Waste incineration plant	1	4	5	0	8	8	13	164	170
Consumption	Recycling systems	2	11	13	3	53	55	64	838	864
Wastewater	WWTP	11	56	69	13	224	231	323	3891	4034
Wastewater	Surface water	0	2	2	0	7	7	11	129	136
WWTP	Sludge	7	43	50	9	170	175	234	2967	3063
WWTP	Surface water	2	13	15	2	54	56	52	925	971
Sludge	Sludge-treated soil	1	4	5	1	25	26	158	2004	2070
Sludge	Landfill	6	38	46	2	34	35	13	149	155
Sludge	Waste incineration plant	0	0	0	6	111	115	66	813	848

Table S13 (continued): 25th quantiles, means and 75th quantiles of flows of nano-TiO_2 (tonnes)

		United Kingdom			Greece			Croatia		
From	**To**	**Q25**	**Mean**	**Q75**	**Q25**	**Mean**	**Q75**	**Q25**	**Mean**	**Q75**
Import	Manufacturing	153	2578	2662	19	331	341	11	194	202
Import	Consumption	41	1134	1137	31	549	563	4	88	89
Production	Manufacturing	1146	2185	4256	0	0	0	0	0	0
Production	Wastewater	2	43	44	0	0	0	0	0	0
Production	Air	0	0	0	0	0	0	0	0	0
Production	Export	0	0	0	0	0	0	0	0	0
Manufacturing	Consumption	1879	4744	7381	195	329	651	64	193	286
Manufacturing	Wastewater	2	6	9	0	0	0	0	0	0
Manufacturing	Air	0	0	0	0	0	0	0	0	0
Manufacturing	Recycling systems	3	12	15	0	1	1	0	0	0
Manufacturing	Export	0	0	0	0	0	0	0	0	0
Consumption	Wastewater	1350	4216	6039	158	630	858	47	202	267
Consumption	Air	3	13	17	0	2	2	0	1	1
Consumption	Surface water	142	459	646	17	68	92	5	22	29
Consumption	Natural & urban soil	4	12	16	0	2	2	0	1	1
Consumption	Landfill	51	180	247	11	48	63	4	19	24
Consumption	Waste incineration plant	39	136	187	0	0	0	0	0	0
Consumption	Recycling systems	245	863	1184	28	128	166	7	38	48
Wastewater	WWTP	1334	4081	5895	157	610	839	47	195	261
Wastewater	Surface water	45	135	196	5	20	27	2	6	9
WWTP	Sludge	863	3108	4268	101	465	599	28	149	183
WWTP	Surface water	165	973	1027	19	145	152	6	47	50
Sludge	Sludge-treated soil	677	2434	3338	23	106	136	1	7	9
Sludge	Landfill	10	14	28	43	181	240	28	141	177
Sludge	Waste incineration plant	195	661	915	39	179	229	0	0	0
		Hungary			**Ireland**			**Italy**		
From	**To**	**Q25**	**Mean**	**Q75**	**Q25**	**Mean**	**Q75**	**Q25**	**Mean**	**Q75**
Import	Manufacturing	17	289	300	21	368	378	158	2849	2940
Import	Consumption	4	94	97	0	0	0	40	1097	1090
Production	Manufacturing	0	0	0	0	0	0	1187	2187	4404
Production	Wastewater	0	0	0	0	0	0	2	43	44
Production	Air	0	0	0	0	0	0	0	0	0
Production	Export	0	0	0	0	0	0	0	0	0
Manufacturing	Consumption	79	288	386	16	295	304	1917	5017	7718
Manufacturing	Wastewater	0	0	0	0	0	0	2	6	9
Manufacturing	Air	0	0	0	0	0	0	0	0	0
Manufacturing	Recycling systems	0	1	1	0	0	0	3	13	16
Manufacturing	Export	0	0	0	2	73	75	0	0	0
Consumption	Wastewater	58	274	344	11	212	218	1374	4387	6260
Consumption	Air	0	1	1	0	1	1	3	13	18
Consumption	Surface water	6	30	37	1	23	24	144	477	671
Consumption	Natural & urban soil	0	1	1	0	1	1	4	12	17
Consumption	Landfill	4	22	27	0	8	8	39	144	197
Consumption	Waste incineration plant	1	4	5	0	4	4	38	140	191
Consumption	Recycling systems	9	50	61	2	47	49	265	941	1292
Wastewater	WWTP	58	266	336	11	205	211	1359	4247	6117
Wastewater	Surface water	2	9	11	0	7	7	45	140	202
WWTP	Sludge	34	203	241	8	156	159	883	3229	4458
WWTP	Surface water	8	63	68	2	49	52	166	1017	1060
Sludge	Sludge-treated soil	5	28	33	8	155	157	340	1252	1726
Sludge	Landfill	7	31	39	0	2	2	516	1832	2532
Sludge	Waste incineration plant	25	144	171	0	0	0	49	146	215

Table S13 (continued): 25th quantiles, means and 75th quantiles of flows of nano-TiO_2 (tonnes)

		Lithuania			Luxemburg			Latvia		
From	**To**	**Q25**	**Mean**	**Q75**	**Q25**	**Mean**	**Q75**	**Q25**	**Mean**	**Q75**
Import	Manufacturing	6	113	115	16	278	288	4	74	75
Import	Consumption	1	23	23	0	0	0	1	25	26
Production	Manufacturing	0	0	0	0	0	0	0	0	0
Production	Wastewater	0	0	0	0	0	0	0	0	0
Production	Air	0	0	0	0	0	0	0	0	0
Production	Export	0	0	0	0	0	0	0	0	0
Manufacturing	Consumption	23	113	137	3	55	57	21	74	100
Manufacturing	Wastewater	0	0	0	0	0	0	0	0	0
Manufacturing	Air	0	0	0	0	0	0	0	0	0
Manufacturing	Recycling systems	0	0	0	0	0	0	0	0	0
Manufacturing	Export	0	0	0	13	223	230	0	0	0
Consumption	Wastewater	17	98	115	2	39	41	15	71	89
Consumption	Air	0	0	0	0	0	0	0	0	0
Consumption	Surface water	2	11	12	0	4	4	2	8	10
Consumption	Natural & urban soil	0	0	0	0	0	0	0	0	0
Consumption	Landfill	1	8	9	0	0	0	1	6	7
Consumption	Waste incineration plant	0	0	0	0	2	2	0	0	0
Wastewater	WWTP	17	95	111	2	38	39	15	69	87
Wastewater	Surface water	1	3	4	0	1	1	1	2	3
WWTP	Sludge	10	72	81	1	29	30	9	52	62
WWTP	Surface water	3	23	25	0	9	9	2	16	18
Sludge	Sludge-treated soil	10	72	81	1	24	25	9	51	60
Sludge	Landfill	0	0	0	0	0	0	0	1	2
Sludge	Waste incineration plant	0	0	0	0	5	5	0	0	0
Consumption	Recycling systems	3	20	23	0	9	9	3	14	17
		Malta			**Netherlands**			**Norway**		
From	**To**	**Q25**	**Mean**	**Q75**	**Q25**	**Mean**	**Q75**	**Q25**	**Mean**	**Q75**
Import	Manufacturing	0	4	4	60	1097	1132	3	76	76
Import	Consumption	2	43	44	0	0	0	2	65	65
Production	Manufacturing	0	0	0	261	383	752	79	375	444
Production	Wastewater	0	0	0	0	8	7	0	7	8
Production	Air	0	0	0	0	0	0	0	0	0
Production	Export	0	0	0	0	0	0	0	0	0
Manufacturing	Consumption	4	4	5	229	1098	1384	139	449	556
Manufacturing	Wastewater	0	0	0	0	2	2	0	1	1
Manufacturing	Air	0	0	0	0	0	0	0	0	0
Manufacturing	Recycling systems	0	0	0	0	1	1	0	1	1
Manufacturing	Export	0	0	0	54	379	452	0	0	0
Consumption	Wastewater	4	34	36	160	788	988	99	369	446
Consumption	Air	0	0	0	0	2	3	0	1	1
Consumption	Surface water	0	4	4	17	86	106	10	40	48
Consumption	Natural & urban soil	0	0	0	0	2	3	0	1	1
Consumption	Landfill	0	3	3	0	1	1	0	1	1
Consumption	Waste incineration plant	0	0	0	9	52	63	6	25	30
Consumption	Recycling systems	1	6	7	29	167	203	17	77	92
Wastewater	WWTP	4	33	34	159	762	964	98	357	432
Wastewater	Surface water	0	1	1	5	25	31	3	12	14
WWTP	Sludge	3	25	26	96	584	696	57	273	325
WWTP	Surface water	1	8	8	21	178	192	13	85	94
Sludge	Sludge-treated soil	0	0	0	0	0	0	47	225	268
Sludge	Landfill	3	25	26	0	0	0	10	48	57
Sludge	Waste incineration plant	0	0	0	101	584	703	0	0	0

Table S13 (continued): 25th quantiles, means and 75th quantiles of flows of nano-TiO_2 (tonnes)

		Poland			Portugal			Romania		
From	**To**	**Q25**	**Mean**	**Q75**	**Q25**	**Mean**	**Q75**	**Q25**	**Mean**	**Q75**
Import	Manufacturing	77	1334	1381	32	530	531	29	499	517
Import	Consumption	10	305	309	17	338	342	0	0	0
Production	Manufacturing	276	387	769	0	0	0	0	0	0
Production	Wastewater	0	8	7	0	0	0	0	0	0
Production	Export	0	0	0	0	0	0	0	0	0
Production	Air	0	0	0	0	0	0	0	0	0
Manufacturing	Consumption	560	1714	2335	213	528	861	28	487	507
Manufacturing	Wastewater	0	2	3	0	1	1	0	1	1
Manufacturing	Air	0	0	0	0	0	0	0	0	0
Manufacturing	Recycling systems	1	4	5	0	1	1	0	0	0
Manufacturing	Export	0	0	0	0	0	0	0	11	29
Consumption	Wastewater	398	1449	1882	160	621	846	20	349	365
Consumption	Air	1	4	5	0	2	2	0	1	1
Consumption	Surface water	41	157	203	17	68	91	2	38	40
Consumption	Natural & urban soil	1	4	5	0	2	2	0	1	1
Consumption	Landfill	22	92	115	10	42	55	2	35	36
Consumption	Waste incineration plant	4	17	21	4	17	23	0	0	0
Consumption	Recycling systems	69	296	372	25	114	147	3	63	65
Wastewater	WWTP	395	1403	1835	160	601	832	19	338	353
Wastewater	Surface water	13	46	59	5	20	27	1	11	12
WWTP	Sludge	243	1066	1333	97	460	581	14	258	266
WWTP	Surface water	51	337	363	18	142	150	3	80	83
Sludge	Sludge-treated soil	117	512	639	87	413	522	1	21	22
Sludge	Landfill	42	151	196	13	46	65	13	235	244
Sludge	Waste incineration plant	94	403	505	1	0	2	0	2	2
		Slovakia			**Slovenia**			**Sweden**		
From	**To**	**Q25**	**Mean**	**Q75**	**Q25**	**Mean**	**Q75**	**Q25**	**Mean**	**Q75**
Import	Manufacturing	11	195	197	0	0	0	46	802	831
Import	Consumption	23	421	435	2	48	49	0	0	0
Production	Manufacturing	0	0	0	1	35	36	0	0	0
Production	Wastewater	0	0	0	5	97	99	0	0	0
Production	Air	0	0	0	0	0	0	0	0	0
Production	Export	0	0	0	275	4808	4931	0	0	0
Manufacturing	Consumption	124	195	391	16	35	57	34	612	633
Manufacturing	Wastewater	0	0	0	0	0	0	0	1	1
Manufacturing	Air	0	0	0	0	0	0	0	0	0
Manufacturing	Recycling systems	0	0	0	0	0	0	0	1	1
Manufacturing	Export	0	0	0	0	0	0	6	188	194
Consumption	Wastewater	103	441	586	12	60	76	24	439	454
Consumption	Air	0	1	2	0	0	0	0	1	1
Consumption	Surface water	11	48	63	1	6	8	3	48	50
Consumption	Natural & urban soil	0	1	2	0	0	0	0	1	1
Consumption	Landfill	6	31	40	1	4	5	0	0	0
Consumption	Waste incineration plant	1	5	7	0	0	0	1	23	24
Consumption	Recycling systems	18	87	110	2	13	16	5	99	103
Wastewater	WWTP	102	427	573	12	58	74	24	425	441
Wastewater	Surface water	3	14	18	0	2	2	1	14	14
WWTP	Sludge	64	325	411	7	44	53	16	324	330
WWTP	Surface water	13	102	107	2	14	14	3	101	105
Sludge	Sludge-treated soil	0	0	0	0	1	1	15	291	297
Sludge	Landfill	16	69	90	0	1	1	1	21	21
Sludge	Waste incineration plant	51	256	325	7	43	51	1	13	13

Table S14: 25th quantiles, means and 75th quantiles of flows of nano-ZnO (tonnes)

		Austria			Belgium			Bulgaria		
From	**To**	**Q25**	**Mean**	**Q75**	**Q25**	**Mean**	**Q75**	**Q25**	**Mean**	**Q75**
Import	Manufacturing	16	101	113	0	0	0	6	27	31
Import	Consumption	1	25	28	0	0	0	1	9	10
Production	Manufacturing	0	0	0	35	184	205	0	0	0
Production	Wastewater	0	0	0	1	15	17	0	0	0
Production	Air	0	0	0	0	0	0	0	0	0
Production	Export	0	0	0	111	585	653	0	0	0
Manufacturing	Consumption	38	101	119	29	152	170	11	27	33
Manufacturing	Wastewater	0	0	0	0	0	0	0	0	0
Manufacturing	Air	0	0	0	0	0	0	0	0	0
Manufacturing	Export	0	0	0	0	31	36	0	0	0
Consumption	Wastewater	28	93	109	21	112	125	9	27	32
Consumption	Air	0	2	2	0	2	2	0	0	1
Consumption	Surface water	3	11	13	2	14	15	1	3	4
Consumption	Natural & urban soil	0	2	2	0	2	2	0	0	1
Consumption	Landfill	0	0	0	0	0	0	0	1	1
Consumption	Waste incineration plant	1	2	3	0	3	3	0	0	0
Consumption	Recycling	5	16	18	3	19	21	1	4	5
Wastewater	WWTP	28	90	106	24	127	142	8	26	31
Wastewater	Surface water	1	3	4	1	4	5	0	1	1
WWTP	Sludge	16	69	82	9	97	110	5	20	24
WWTP	Surface water	3	22	24	2	30	31	1	6	7
Sludge	Sludge-treated soil	4	17	20	1	13	15	3	13	16
Sludge	Landfill	0	1	2	0	0	0	2	7	8
Sludge	Waste incineration plant	12	50	61	8	84	96	0	0	0
		Switzerland			**Cyprus**			**Czech Republic**		
From	**To**	**Q25**	**Mean**	**Q75**	**Q25**	**Mean**	**Q75**	**Q25**	**Mean**	**Q75**
Import	Manufacturing	31	167	188	0	0	0	11	55	61
Import	Consumption	0	0	0	5	25	28	12	72	81
Production	Manufacturing	0	0	0	0	0	0	6	5	6
Production	Wastewater	0	0	0	0	0	0	0	0	0
Production	Air	0	0	0	0	0	0	0	0	0
Production	Export	0	0	0	0	0	0	0	0	0
Manufacturing	Consumption	19	107	120	0	0	0	38	60	81
Manufacturing	Wastewater	0	0	0	0	0	0	0	0	0
Manufacturing	Air	0	0	0	0	0	0	0	0	0
Manufacturing	Export	9	60	68	0	0	0	0	0	0
Consumption	Wastewater	14	79	89	3	18	20	37	98	120
Consumption	Air	0	1	2	0	0	0	1	2	2
Consumption	Surface water	2	10	11	0	2	3	4	12	15
Consumption	Natural & urban soil	0	1	2	0	0	0	1	2	2
Consumption	Landfill	0	0	0	0	1	1	2	4	5
Consumption	Waste incineration plant	0	1	1	0	0	0	0	1	1
Consumption	Recycling	2	14	16	1	3	3	5	14	17
Wastewater	WWTP	14	77	86	3	18	20	36	95	117
Wastewater	Surface water	0	3	3	0	1	1	1	3	4
WWTP	Sludge	5	59	67	1	14	15	22	73	89
WWTP	Surface water	1	18	18	0	4	4	4	22	27
Sludge	Sludge-treated soil	0	0	0	1	14	15	17	58	70
Sludge	Landfill	0	0	0	0	0	0	3	10	13
Sludge	Waste incineration plant	6	59	67	0	0	0	1	5	6

Table S14 (continued): 25th quantiles, means and 75th quantiles of flows of nano-ZnO (tonnes)

		Germany			Denmark			Spain		
From	**To**	**Q25**	**Mean**	**Q75**	**Q25**	**Mean**	**Q75**	**Q25**	**Mean**	**Q75**
Import	Manufacturing	0	0	0	16	84	93	108	588	661
Import	Consumption	0	0	0	0	0	0	66	458	516
Production	Manufacturing	218	1219	1359	0	0	0	4	5	5
Production	Wastewater	5	61	68	0	0	0	0	0	0
Production	Air	0	0	0	0	0	0	0	0	0
Production	Export	310	1810	2027	0	0	0	0	0	0
Manufacturing	Consumption	108	614	684	13	72	80	302	593	772
Manufacturing	Wastewater	0	2	2	0	0	0	0	1	1
Manufacturing	Air	0	0	0	0	0	0	0	0	0
Manufacturing	Export	98	603	676	0	12	14	0	0	0
Consumption	Wastewater	78	454	506	9	53	59	270	777	953
Consumption	Air	1	8	9	0	1	1	4	13	16
Consumption	Surface water	8	56	62	1	7	7	31	96	119
Consumption	Natural & urban soil	1	8	9	0	1	1	4	13	17
Consumption	Landfill	0	0	0	0	1	1	12	37	46
Consumption	Waste incineration plant	1	9	10	0	1	1	2	6	8
Consumption	Recycling	13	79	88	1	9	10	36	108	133
Wastewater	WWTP	90	512	570	9	51	57	263	753	923
Wastewater	Surface water	3	17	19	0	2	2	9	25	30
WWTP	Sludge	36	390	449	4	39	45	162	573	700
WWTP	Surface water	9	122	124	1	12	12	33	181	212
Sludge	Sludge-treated soil	11	119	136	3	27	30	130	457	559
Sludge	Landfill	0	0	0	0	1	1	29	92	113
Sludge	Waste incineration plant	26	272	312	1	12	14	7	24	30
		Estonia			**Finland**			**France**		
From	**To**	**Q25**	**Mean**	**Q75**	**Q25**	**Mean**	**Q75**	**Q25**	**Mean**	**Q75**
Import	Manufacturing	3	13	14	14	75	83	138	795	888
Import	Consumption	0	0	0	0	0	0	0	0	0
Production	Manufacturing	0	0	0	0	0	0	252	359	523
Production	Wastewater	0	0	0	0	0	0	1	7	8
Production	Air	0	0	0	0	0	0	0	0	0
Production	Export	0	0	0	0	0	0	0	0	0
Manufacturing	Consumption	3	13	14	12	65	72	307	930	1137
Manufacturing	Wastewater	0	0	0	0	0	0	1	2	2
Manufacturing	Air	0	0	0	0	0	0	0	0	0
Manufacturing	Export	0	0	0	0	10	12	45	222	277
Consumption	Wastewater	2	10	11	9	48	53	225	688	842
Consumption	Air	0	0	0	0	1	1	4	12	14
Consumption	Surface water	0	1	1	1	6	7	26	85	103
Consumption	Natural & urban soil	0	0	0	0	1	1	3	12	14
Consumption	Landfill	0	0	0	0	0	0	3	10	12
Consumption	Waste incineration plant	0	0	0	0	0	0	4	13	16
Consumption	Recycling	0	1	2	2	9	10	35	110	135
Wastewater	WWTP	2	9	10	9	46	52	224	675	829
Wastewater	Surface water	0	0	0	0	2	2	7	22	28
WWTP	Sludge	1	7	8	3	35	40	137	514	629
WWTP	Surface water	0	2	2	1	11	11	28	162	182
Sludge	Sludge-treated soil	0	1	1	0	5	6	93	347	425
Sludge	Landfill	1	6	7	1	7	8	8	26	32
Sludge	Waste incineration plant	0	0	0	2	23	26	39	141	173

Table S14 (continued): 25th quantiles, means and 75th quantiles of flows of nano-ZnO (tonnes)

		United Kingdom			Greece			Croatia		
From	**To**	**Q25**	**Mean**	**Q75**	**Q25**	**Mean**	**Q75**	**Q25**	**Mean**	**Q75**
Import	Manufacturing	94	526	586	13	65	72	7	33	37
Import	Consumption	6	141	155	17	97	109	1	14	16
Production	Manufacturing	221	367	515	0	0	0	0	0	0
Production	Wastewater	1	7	8	0	0	0	0	0	0
Production	Air	0	0	0	0	0	0	0	0	0
Production	Export	0	0	0	0	0	0	0	0	0
Manufacturing	Consumption	410	892	1165	39	65	92	15	33	41
Manufacturing	Wastewater	0	1	2	0	0	0	0	0	0
Manufacturing	Air	0	0	0	0	0	0	0	0	0
Manufacturing	Export	0	0	0	0	0	0	0	0	0
Consumption	Wastewater	304	765	976	42	120	148	12	35	41
Consumption	Air	5	13	17	1	2	3	0	1	1
Consumption	Surface water	35	94	120	5	15	18	1	4	5
Consumption	Natural & urban soil	5	13	17	1	2	3	0	1	1
Consumption	Landfill	6	15	20	1	4	5	0	1	2
Consumption	Waste incineration plant	4	11	15	0	0	0	0	0	0
Consumption	Recycling	47	122	155	6	19	24	2	5	6
Wastewater	WWTP	301	750	957	41	116	144	11	34	40
Wastewater	Surface water	10	25	32	1	4	5	0	1	1
WWTP	Sludge	186	571	717	25	88	108	7	26	31
WWTP	Surface water	37	178	205	5	27	32	1	8	9
Sludge	Sludge-treated soil	146	447	562	6	20	25	0	1	2
Sludge	Landfill	1	3	3	10	34	42	7	25	30
Sludge	Waste incineration plant	41	121	152	9	34	41	0	0	0
		Hungary			**Ireland**			**Italy**		
From	**To**	**Q25**	**Mean**	**Q75**	**Q25**	**Mean**	**Q75**	**Q25**	**Mean**	**Q75**
Import	Manufacturing	10	50	56	14	70	77	102	537	599
Import	Consumption	0	7	8	0	0	0	16	262	293
Production	Manufacturing	0	0	0	0	0	0	192	304	431
Production	Wastewater	0	0	0	0	0	0	1	6	7
Production	Air	0	0	0	0	0	0	0	0	0
Production	Export	0	0	0	0	0	0	0	0	0
Manufacturing	Consumption	16	50	57	9	46	51	439	840	1139
Manufacturing	Wastewater	0	0	0	0	0	0	0	1	1
Manufacturing	Air	0	0	0	0	0	0	0	0	0
Manufacturing	Export	0	0	0	3	24	27	0	0	0
Consumption	Wastewater	12	42	48	6	34	38	334	814	1056
Consumption	Air	0	1	1	0	1	1	5	14	18
Consumption	Surface water	1	5	6	1	4	5	39	101	129
Consumption	Natural & urban soil	0	1	1	0	1	1	5	14	18
Consumption	Landfill	1	2	2	0	0	0	4	10	12
Consumption	Waste incineration plant	0	0	0	0	0	0	4	9	12
Consumption	Recycling	2	6	7	1	6	7	56	139	180
Wastewater	WWTP	12	41	47	6	33	37	329	796	1035
Wastewater	Surface water	0	1	2	0	1	1	11	26	34
WWTP	Sludge	6	31	37	2	25	29	206	609	780
WWTP	Surface water	1	10	10	1	8	8	40	188	219
Sludge	Sludge-treated soil	1	4	5	2	25	28	79	236	302
Sludge	Landfill	1	4	5	0	0	0	118	345	441
Sludge	Waste incineration plant	5	23	27	0	0	0	10	27	35

Table S14 (continued): 25th quantiles, means and 75th quantiles of flows of nano-ZnO (tonnes)

		Lithuania			Luxemburg			Latvia		
From	**To**	**Q25**	**Mean**	**Q75**	**Q25**	**Mean**	**Q75**	**Q25**	**Mean**	**Q75**
Import	Manufacturing	4	19	21	11	54	60	2	12	14
Import	Consumption	0	3	3	0	0	0	0	4	4
Production	Manufacturing	0	0	0	0	0	0	0	0	0
Production	Wastewater	0	0	0	0	0	0	0	0	0
Production	Air	0	0	0	0	0	0	0	0	0
Production	Export	0	0	0	0	0	0	0	0	0
Manufacturing	Consumption	6	19	22	2	10	11	5	12	15
Manufacturing	Wastewater	0	0	0	0	0	0	0	0	0
Manufacturing	Air	0	0	0	0	0	0	0	0	0
Manufacturing	Export	0	0	0	9	44	49	0	0	0
Consumption	Wastewater	5	16	18	1	7	8	4	12	14
Consumption	Air	0	0	0	0	0	0	0	0	0
Consumption	Surface water	1	2	2	0	1	1	0	1	2
Consumption	Natural & urban soil	0	0	0	0	0	0	0	0	0
Consumption	Landfill	0	1	1	0	0	0	0	0	1
Consumption	Waste incineration plant	0	0	0	0	0	0	0	0	0
Consumption	Recycling	1	3	3	0	1	1	1	2	2
Wastewater	WWTP	4	16	18	1	7	8	4	11	13
Wastewater	Surface water	0	1	1	0	0	0	0	0	0
WWTP	Sludge	2	12	14	1	5	6	2	9	10
WWTP	Surface water	1	4	4	0	2	2	0	3	3
Sludge	Sludge-treated soil	2	12	14	0	4	5	2	8	10
Sludge	Landfill	0	0	0	0	0	0	0	0	0
Sludge	Waste incineration plant	0	0	0	0	1	1	0	0	0
		Malta			**Netherlands**			**Norway**		
From	**To**	**Q25**	**Mean**	**Q75**	**Q25**	**Mean**	**Q75**	**Q25**	**Mean**	**Q75**
Import	Manufacturing	0	1	1	0	0	0	0	0	0
Import	Consumption	1	7	8	0	0	0	0	0	0
Production	Manufacturing	0	0	0	45	230	255	13	69	77
Production	Wastewater	0	0	0	2	22	24	1	16	17
Production	Air	0	0	0	0	0	0	0	0	0
Production	Export	0	0	0	164	848	939	134	706	785
Manufacturing	Consumption	1	1	1	33	172	192	12	67	75
Manufacturing	Wastewater	0	0	0	0	0	0	0	0	0
Manufacturing	Air	0	0	0	0	0	0	0	0	0
Manufacturing	Export	0	0	0	3	58	65	0	2	4
Consumption	Wastewater	2	6	7	24	128	142	9	50	56
Consumption	Air	0	0	0	0	2	2	0	1	1
Consumption	Surface water	0	1	1	3	16	17	1	6	7
Consumption	Natural & urban soil	0	0	0	0	2	2	0	1	1
Consumption	Landfill	0	0	0	0	0	0	0	0	0
Consumption	Waste incineration plant	0	0	0	1	3	3	0	2	2
Consumption	Recycling	0	1	1	4	22	24	1	8	9
Wastewater	WWTP	2	6	7	29	149	165	13	66	74
Wastewater	Surface water	0	0	0	1	5	5	0	2	2
WWTP	Sludge	1	4	5	11	113	129	5	51	58
WWTP	Surface water	0	1	1	3	36	36	1	16	16
Sludge	Sludge-treated soil	0	0	0	0	0	0	4	42	48
Sludge	Landfill	1	4	5	0	0	0	1	9	10
Sludge	Waste incineration plant	0	0	0	12	113	130	0	0	0

Table S14 (continued): 25th quantiles, means and 75th quantiles of flows of nano-ZnO (tonnes)

		Poland			Portugal			Romania		
From	**To**	**Q25**	**Mean**	**Q75**	**Q25**	**Mean**	**Q75**	**Q25**	**Mean**	**Q75**
Import	Manufacturing	52	273	305	19	98	109	18	91	102
Import	Consumption	2	46	51	8	58	65	0	0	0
Production	Manufacturing	0	0	0	0	0	0	0	0	0
Production	Wastewater	0	0	0	0	0	0	0	0	0
Production	Air	0	0	0	0	0	0	0	0	0
Production	Export	0	0	0	0	0	0	0	0	0
Manufacturing	Consumption	93	273	317	46	98	123	12	65	72
Manufacturing	Wastewater	0	0	0	0	0	0	0	0	0
Manufacturing	Air	0	0	0	0	0	0	0	0	0
Manufacturing	Export	0	0	0	0	0	0	2	26	30
Consumption	Wastewater	69	236	273	39	115	140	9	48	53
Consumption	Air	1	4	5	1	2	2	0	1	1
Consumption	Surface water	8	29	34	5	14	17	1	6	7
Consumption	Natural & urban soil	1	4	5	1	2	2	0	1	1
Consumption	Landfill	2	7	9	1	5	6	0	2	3
Consumption	Waste incineration plant	0	1	1	1	2	2	0	0	0
Consumption	Recycling	11	38	44	5	16	20	1	7	8
Wastewater	WWTP	68	229	264	38	112	135	9	46	52
Wastewater	Surface water	2	8	9	1	4	4	0	2	2
WWTP	Sludge	36	175	207	23	85	103	3	35	40
WWTP	Surface water	8	54	59	5	27	31	1	11	11
Sludge	Sludge-treated soil	18	84	99	21	76	93	0	3	3
Sludge	Landfill	6	25	29	3	9	10	3	32	37
Sludge	Waste incineration plant	14	66	78	0	0	0	0	0	0
		Slovakia			**Slovenia**			**Sweden**		
From	**To**	**Q25**	**Mean**	**Q75**	**Q25**	**Mean**	**Q75**	**Q25**	**Mean**	**Q75**
Import	Manufacturing	7	36	41	3	16	18	33	160	176
Import	Consumption	13	77	86	1	9	10	0	0	0
Production	Manufacturing	0	0	0	0	0	0	0	0	0
Production	Wastewater	0	0	0	0	0	0	0	0	0
Production	Air	0	0	0	0	0	0	0	0	0
Production	Export	0	0	0	0	0	0	0	0	0
Manufacturing	Consumption	25	36	52	8	16	21	21	107	119
Manufacturing	Wastewater	0	0	0	0	0	0	0	0	0
Manufacturing	Air	0	0	0	0	0	0	0	0	0
Manufacturing	Export	0	0	0	0	0	0	7	52	58
Consumption	Wastewater	28	84	103	6	19	23	15	80	88
Consumption	Air	0	1	2	0	0	0	0	1	2
Consumption	Surface water	3	10	13	1	2	3	2	10	11
Consumption	Natural & urban soil	0	1	2	0	0	0	0	1	2
Consumption	Landfill	1	3	3	0	0	1	0	0	0
Consumption	Waste incineration plant	0	0	1	0	0	0	0	1	1
Consumption	Recycling	4	13	16	1	3	4	3	14	16
Wastewater	WWTP	28	81	100	6	18	22	15	77	85
Wastewater	Surface water	1	3	3	0	1	1	0	3	3
WWTP	Sludge	17	62	76	4	14	17	6	59	67
WWTP	Surface water	3	19	22	1	4	5	1	18	19
Sludge	Sludge-treated soil	0	0	0	0	0	0	6	53	60
Sludge	Landfill	4	13	16	0	0	0	0	4	4
Sludge	Waste incineration plant	13	49	60	4	13	16	0	2	3

Table S15: 25th quantiles, means and 75th quantiles of flows of nano-Ag (tonnes)

		Austria			Belgium			Bulgaria		
From	**To**	**Q25**	**Mean**	**Q75**	**Q25**	**Mean**	**Q75**	**Q25**	**Mean**	**Q75**
Import	Manufacturing	0.004	0.017	0.024	0.000	0.000	0.000	0.002	0.006	0.008
Import	Consumption	0.082	0.333	0.459	0.064	0.292	0.388	0.011	0.047	0.064
Production	Manufacturing	0.009	0.053	0.064	0.032	0.124	0.176	0.007	0.052	0.064
Production	Wastewater	0.000	0.001	0.001	0.002	0.012	0.015	0.000	0.001	0.001
Production	Export	0.000	0.000	0.000	0.114	0.476	0.648	0.000	0.000	0.000
Manufacturing	Consumption	0.019	0.068	0.099	0.038	0.122	0.186	0.012	0.057	0.075
Manufacturing	Wastewater	0.000	0.000	0.000	0.000	0.000	0.000	0.000	0.000	0.000
Manufacturing	Recycling system	0.000	0.001	0.001	0.000	0.002	0.002	0.000	0.001	0.001
Manufacturing	Export	0.000	0.000	0.000	0.000	0.000	0.000	0.000	0.000	0.000
Consumption	Wastewater	0.004	0.019	0.026	0.004	0.020	0.026	0.001	0.005	0.006
Consumption	Air	0.001	0.003	0.004	0.001	0.003	0.004	0.000	0.001	0.001
Consumption	Surface water	0.000	0.001	0.001	0.000	0.001	0.001	0.000	0.000	0.000
Consumption	Natural & urban soil	0.000	0.002	0.002	0.000	0.002	0.002	0.000	0.000	0.001
Consumption	Landfill	0.001	0.005	0.007	0.000	0.001	0.002	0.007	0.031	0.041
Consumption	Waste incineration plant	0.015	0.061	0.083	0.019	0.081	0.110	0.001	0.005	0.007
Consumption	Recycling system	0.077	0.310	0.429	0.075	0.306	0.422	0.014	0.061	0.082
Wastewater	WWTP	0.005	0.020	0.027	0.008	0.031	0.042	0.001	0.006	0.008
Wastewater	Surface water	0.000	0.001	0.001	0.000	0.001	0.001	0.000	0.000	0.000
WWTP	Sludge	0.004	0.017	0.022	0.006	0.026	0.035	0.001	0.005	0.006
WWTP	Surface water	0.000	0.003	0.003	0.000	0.005	0.005	0.000	0.001	0.001
Sludge	Sludge-treated soil	0.001	0.004	0.005	0.001	0.004	0.005	0.001	0.003	0.004
Sludge	Landfill	0.000	0.000	0.001	0.000	0.000	0.000	0.001	0.002	0.002
Sludge	Waste incineration plant	0.004	0.012	0.018	0.006	0.023	0.034	0.000	0.000	0.000
		Switzerland			**Cyprus**			**Czech Republic**		
From	**To**	**Q25**	**Mean**	**Q75**	**Q25**	**Mean**	**Q75**	**Q25**	**Mean**	**Q75**
Import	Manufacturing	0.000	0.000	0.000	0.000	0.001	0.001	0.002	0.009	0.013
Import	Consumption	0.000	0.000	0.000	0.005	0.019	0.026	0.042	0.168	0.231
Production	Manufacturing	0.048	0.182	0.258	0.007	0.052	0.064	0.013	0.052	0.062
Production	Wastewater	0.001	0.005	0.007	0.000	0.001	0.001	0.000	0.001	0.001
Production	Export	0.006	0.079	0.099	0.000	0.000	0.000	0.000	0.000	0.000
Manufacturing	Consumption	0.044	0.175	0.243	0.009	0.052	0.064	0.022	0.060	0.081
Manufacturing	Wastewater	0.000	0.000	0.000	0.000	0.000	0.000	0.000	0.000	0.000
Manufacturing	Recycling system	0.001	0.002	0.003	0.000	0.001	0.001	0.000	0.001	0.001
Manufacturing	Export	0.000	0.004	0.020	0.000	0.000	0.000	0.000	0.000	0.000
Consumption	Wastewater	0.002	0.008	0.011	0.001	0.003	0.004	0.003	0.011	0.014
Consumption	Air	0.000	0.001	0.002	0.000	0.001	0.001	0.000	0.002	0.002
Consumption	Surface water	0.000	0.000	0.001	0.000	0.000	0.000	0.000	0.001	0.001
Consumption	Natural & urban soil	0.000	0.001	0.001	0.000	0.000	0.000	0.000	0.001	0.001
Consumption	Landfill	0.000	0.000	0.000	0.008	0.038	0.049	0.014	0.053	0.070
Consumption	Waste incineration plant	0.008	0.035	0.048	0.001	0.003	0.004	0.007	0.026	0.035
Consumption	Recycling system	0.032	0.129	0.178	0.005	0.024	0.031	0.037	0.135	0.184
Wastewater	WWTP	0.003	0.013	0.018	0.001	0.004	0.005	0.003	0.012	0.016
Wastewater	Surface water	0.000	0.000	0.001	0.000	0.000	0.000	0.000	0.000	0.001
WWTP	Sludge	0.003	0.011	0.015	0.001	0.004	0.004	0.002	0.010	0.013
WWTP	Surface water	0.000	0.002	0.002	0.000	0.001	0.001	0.000	0.002	0.002
Sludge	Sludge-treated soil	0.000	0.000	0.000	0.001	0.004	0.004	0.002	0.008	0.010
Sludge	Landfill	0.000	0.000	0.000	0.000	0.000	0.000	0.001	0.001	0.003
Sludge	Waste incineration plant	0.003	0.011	0.017	0.000	0.000	0.000	0.000	0.001	0.002

Table S15 (continued): 25th quantiles, means and 75th quantiles of flows of nano-Ag (tonnes)

		Germany			Denmark			Spain		
From	**To**	**Q25**	**Mean**	**Q75**	**Q25**	**Mean**	**Q75**	**Q25**	**Mean**	**Q75**
Import	Manufacturing	0.034	0.281	0.337	0.012	0.045	0.063	0.000	0.000	0.000
Import	Consumption	0.000	0.000	0.000	0.055	0.229	0.312	0.175	0.778	1.033
Production	Manufacturing	0.624	1.714	2.410	0.022	0.052	0.070	0.094	0.354	0.501
Production	Wastewater	0.006	0.034	0.042	0.000	0.001	0.001	0.002	0.012	0.015
Production	Export	0.000	0.000	0.000	0.000	0.000	0.000	0.034	0.244	0.310
Manufacturing	Consumption	0.326	1.080	1.439	0.054	0.096	0.122	0.110	0.348	0.527
Manufacturing	Wastewater	0.001	0.002	0.003	0.000	0.000	0.000	0.000	0.000	0.000
Manufacturing	Recycling system	0.000	0.000	0.000	0.000	0.001	0.002	0.001	0.005	0.007
Manufacturing	Export	0.252	0.889	1.177	0.000	0.000	0.000	0.000	0.000	0.000
Consumption	Wastewater	0.014	0.052	0.068	0.005	0.016	0.020	0.012	0.054	0.072
Consumption	Air	0.002	0.008	0.011	0.001	0.002	0.003	0.002	0.009	0.011
Consumption	Surface water	0.001	0.003	0.004	0.000	0.001	0.001	0.001	0.003	0.004
Consumption	Natural & urban soil	0.001	0.005	0.006	0.000	0.001	0.002	0.001	0.005	0.006
Consumption	Landfill	0.000	0.001	0.001	0.001	0.002	0.002	0.069	0.282	0.386
Consumption	Waste incineration plant	0.068	0.233	0.307	0.030	0.094	0.124	0.025	0.103	0.140
Consumption	Recycling system	0.233	0.779	1.035	0.069	0.209	0.279	0.168	0.670	0.923
Wastewater	WWTP	0.024	0.085	0.113	0.005	0.016	0.021	0.016	0.064	0.088
Wastewater	Surface water	0.001	0.003	0.004	0.000	0.001	0.001	0.001	0.002	0.003
WWTP	Sludge	0.019	0.072	0.093	0.004	0.014	0.018	0.012	0.054	0.072
WWTP	Surface water	0.002	0.013	0.013	0.000	0.003	0.003	0.001	0.010	0.010
Sludge	Sludge-treated soil	0.006	0.022	0.028	0.003	0.009	0.012	0.010	0.043	0.058
Sludge	Landfill	0.000	0.000	0.000	0.000	0.000	0.000	0.004	0.009	0.017
Sludge	Waste incineration plant	0.017	0.050	0.070	0.002	0.004	0.007	0.001	0.002	0.005
		Estonia			**Finland**			**France**		
From	**To**	**Q25**	**Mean**	**Q75**	**Q25**	**Mean**	**Q75**	**Q25**	**Mean**	**Q75**
Import	Manufacturing	0.000	0.001	0.001	0.000	0.000	0.000	0.102	0.387	0.554
Import	Consumption	0.005	0.021	0.029	0.041	0.171	0.228	0.451	1.893	2.570
Production	Manufacturing	0.007	0.052	0.063	0.008	0.034	0.046	0.043	0.052	0.057
Production	Wastewater	0.000	0.001	0.001	0.002	0.012	0.015	0.000	0.001	0.001
Production	Export	0.000	0.000	0.000	0.141	0.559	0.770	0.000	0.000	0.000
Manufacturing	Consumption	0.010	0.052	0.064	0.010	0.034	0.050	0.349	0.433	0.518
Manufacturing	Wastewater	0.000	0.000	0.000	0.000	0.000	0.000	0.000	0.000	0.000
Manufacturing	Recycling system	0.000	0.001	0.001	0.000	0.000	0.001	0.002	0.006	0.008
Manufacturing	Export	0.000	0.000	0.000	0.000	0.000	0.000	0.000	0.000	0.000
Consumption	Wastewater	0.001	0.004	0.004	0.002	0.010	0.013	0.035	0.112	0.145
Consumption	Air	0.000	0.001	0.001	0.000	0.002	0.002	0.006	0.018	0.023
Consumption	Surface water	0.000	0.000	0.000	0.000	0.001	0.001	0.002	0.006	0.008
Consumption	Natural & urban soil	0.000	0.000	0.000	0.000	0.001	0.001	0.003	0.010	0.013
Consumption	Landfill	0.001	0.005	0.006	0.002	0.008	0.010	0.049	0.151	0.196
Consumption	Waste incineration plant	0.008	0.039	0.049	0.006	0.026	0.035	0.103	0.316	0.411
Consumption	Recycling system	0.005	0.025	0.032	0.039	0.157	0.214	0.585	1.714	2.269
Wastewater	WWTP	0.001	0.004	0.006	0.005	0.021	0.028	0.037	0.110	0.144
Wastewater	Surface water	0.000	0.000	0.000	0.000	0.001	0.001	0.001	0.004	0.005
WWTP	Sludge	0.001	0.004	0.005	0.004	0.018	0.023	0.029	0.093	0.120
WWTP	Surface water	0.000	0.001	0.001	0.000	0.003	0.003	0.003	0.017	0.018
Sludge	Sludge-treated soil	0.000	0.000	0.000	0.001	0.003	0.003	0.020	0.063	0.081
Sludge	Landfill	0.001	0.003	0.004	0.001	0.004	0.005	0.003	0.005	0.008
Sludge	Waste incineration plant	0.000	0.000	0.000	0.003	0.012	0.017	0.012	0.025	0.038

Table S15 (continued): 25th quantiles, means and 75th quantiles of flows of nano-Ag (tonnes)

		United Kingdom			Greece			Croatia		
From	**To**	**Q25**	**Mean**	**Q75**	**Q25**	**Mean**	**Q75**	**Q25**	**Mean**	**Q75**
Import	Manufacturing	0.041	0.239	0.305	0.002	0.009	0.013	0.002	0.006	0.008
Import	Consumption	0.000	0.000	0.000	0.047	0.189	0.261	0.011	0.045	0.062
Production	Manufacturing	0.267	0.599	0.849	0.013	0.053	0.062	0.012	0.052	0.062
Production	Wastewater	0.002	0.012	0.015	0.000	0.001	0.001	0.000	0.001	0.001
Production	Export	0.000	0.000	0.000	0.000	0.000	0.000	0.000	0.000	0.000
Manufacturing	Consumption	0.277	0.807	1.084	0.022	0.061	0.082	0.016	0.057	0.072
Manufacturing	Wastewater	0.000	0.001	0.001	0.000	0.000	0.000	0.000	0.000	0.000
Manufacturing	Recycling system	0.004	0.010	0.014	0.000	0.001	0.001	0.000	0.001	0.001
Manufacturing	Export	0.000	0.020	0.118	0.000	0.000	0.000	0.000	0.000	0.000
Consumption	Wastewater	0.012	0.039	0.051	0.003	0.012	0.016	0.001	0.005	0.006
Consumption	Air	0.002	0.006	0.008	0.000	0.002	0.003	0.000	0.001	0.001
Consumption	Surface water	0.001	0.002	0.003	0.000	0.001	0.001	0.000	0.000	0.000
Consumption	Natural & urban soil	0.001	0.004	0.005	0.000	0.001	0.001	0.000	0.000	0.001
Consumption	Landfill	0.034	0.101	0.134	0.015	0.059	0.079	0.015	0.056	0.073
Consumption	Waste incineration plant	0.039	0.117	0.155	0.003	0.012	0.016	0.001	0.005	0.006
Consumption	Recycling system	0.184	0.539	0.723	0.044	0.163	0.223	0.009	0.035	0.046
Wastewater	WWTP	0.017	0.050	0.067	0.003	0.013	0.017	0.001	0.006	0.007
Wastewater	Surface water	0.001	0.002	0.002	0.000	0.000	0.001	0.000	0.000	0.000
WWTP	Sludge	0.013	0.042	0.055	0.003	0.011	0.014	0.001	0.005	0.006
WWTP	Surface water	0.001	0.008	0.008	0.000	0.002	0.002	0.000	0.001	0.001
Sludge	Sludge-treated soil	0.010	0.033	0.043	0.001	0.002	0.003	0.000	0.000	0.000
Sludge	Landfill	0.001	0.000	0.001	0.002	0.004	0.007	0.001	0.005	0.006
Sludge	Waste incineration plant	0.004	0.009	0.013	0.001	0.004	0.006	0.000	0.000	0.000
		Hungary			**Ireland**			**Italy**		
From	**To**	**Q25**	**Mean**	**Q75**	**Q25**	**Mean**	**Q75**	**Q25**	**Mean**	**Q75**
Import	Manufacturing	0.004	0.013	0.019	0.035	0.134	0.193	0.169	0.644	0.912
Import	Consumption	0.026	0.108	0.147	0.000	0.000	0.000	0.000	0.000	0.000
Production	Manufacturing	0.015	0.052	0.063	0.032	0.052	0.068	0.048	0.052	0.054
Production	Wastewater	0.000	0.001	0.001	0.000	0.001	0.001	0.000	0.001	0.001
Production	Export	0.000	0.000	0.000	0.000	0.000	0.000	0.000	0.000	0.000
Manufacturing	Consumption	0.025	0.065	0.084	0.030	0.090	0.123	0.165	0.583	0.774
Manufacturing	Wastewater	0.000	0.000	0.000	0.000	0.000	0.000	0.000	0.001	0.001
Manufacturing	Recycling system	0.000	0.001	0.001	0.001	0.002	0.003	0.002	0.009	0.011
Manufacturing	Export	0.000	0.000	0.000	0.031	0.094	0.129	0.000	0.104	0.158
Consumption	Wastewater	0.002	0.008	0.011	0.001	0.004	0.006	0.007	0.028	0.036
Consumption	Air	0.000	0.001	0.002	0.000	0.001	0.001	0.001	0.004	0.006
Consumption	Surface water	0.000	0.000	0.001	0.000	0.000	0.000	0.000	0.002	0.002
Consumption	Natural & urban soil	0.000	0.001	0.001	0.000	0.000	0.001	0.001	0.003	0.003
Consumption	Landfill	0.012	0.041	0.054	0.004	0.013	0.017	0.022	0.079	0.105
Consumption	Waste incineration plant	0.004	0.016	0.021	0.003	0.010	0.014	0.029	0.106	0.139
Consumption	Recycling system	0.031	0.104	0.139	0.020	0.061	0.084	0.101	0.362	0.479
Wastewater	WWTP	0.003	0.009	0.012	0.002	0.005	0.007	0.008	0.029	0.038
Wastewater	Surface water	0.000	0.000	0.000	0.000	0.000	0.000	0.000	0.001	0.001
WWTP	Sludge	0.002	0.008	0.010	0.001	0.005	0.006	0.007	0.024	0.032
WWTP	Surface water	0.000	0.001	0.001	0.000	0.001	0.001	0.001	0.004	0.005
Sludge	Sludge-treated soil	0.000	0.001	0.001	0.001	0.004	0.006	0.003	0.009	0.012
Sludge	Landfill	0.001	0.001	0.002	0.000	0.000	0.000	0.005	0.014	0.019
Sludge	Waste incineration plant	0.002	0.006	0.008	0.000	0.000	0.000	0.001	0.001	0.002

Table S15 (continued): 25th quantiles, means and 75th quantiles of flows of nano-Ag (tonnes)

		Lithuania			Luxemburg			Latvia		
From	**To**	**Q25**	**Mean**	**Q75**	**Q25**	**Mean**	**Q75**	**Q25**	**Mean**	**Q75**
Import	Manufacturing	0.001	0.006	0.007	0.000	0.001	0.001	0.000	0.001	0.001
Import	Consumption	0.007	0.031	0.041	0.012	0.049	0.068	0.007	0.026	0.036
Production	Manufacturing	0.012	0.052	0.064	0.008	0.053	0.065	0.007	0.053	0.064
Production	Wastewater	0.000	0.001	0.001	0.000	0.001	0.001	0.000	0.001	0.001
Production	Export	0.000	0.000	0.000	0.000	0.000	0.000	0.000	0.000	0.000
Manufacturing	Consumption	0.016	0.057	0.072	0.012	0.053	0.069	0.010	0.052	0.065
Manufacturing	Wastewater	0.000	0.000	0.000	0.000	0.000	0.000	0.000	0.000	0.000
Manufacturing	Recycling system	0.000	0.001	0.001	0.000	0.001	0.001	0.000	0.001	0.001
Manufacturing	Export	0.000	0.000	0.000	0.000	0.000	0.000	0.000	0.000	0.000
Consumption	Wastewater	0.001	0.004	0.005	0.001	0.005	0.006	0.001	0.004	0.005
Consumption	Air	0.000	0.001	0.001	0.000	0.001	0.001	0.000	0.001	0.001
Consumption	Surface water	0.000	0.000	0.000	0.000	0.000	0.000	0.000	0.000	0.000
Consumption	Natural & urban soil	0.000	0.000	0.000	0.000	0.000	0.001	0.000	0.000	0.000
Consumption	Landfill	0.004	0.015	0.019	0.001	0.003	0.004	0.009	0.043	0.055
Consumption	Waste incineration plant	0.001	0.004	0.005	0.004	0.019	0.025	0.001	0.004	0.005
Consumption	Recycling system	0.016	0.063	0.081	0.017	0.073	0.097	0.006	0.027	0.035
Wastewater	WWTP	0.001	0.005	0.007	0.001	0.006	0.008	0.001	0.005	0.006
Wastewater	Surface water	0.000	0.000	0.000	0.000	0.000	0.000	0.000	0.000	0.000
WWTP	Sludge	0.001	0.004	0.005	0.001	0.005	0.006	0.001	0.004	0.005
WWTP	Surface water	0.000	0.001	0.001	0.000	0.001	0.001	0.000	0.001	0.001
Sludge	Sludge-treated soil	0.001	0.004	0.005	0.001	0.004	0.005	0.001	0.004	0.005
Sludge	Landfill	0.000	0.000	0.000	0.000	0.000	0.000	0.000	0.000	0.000
Sludge	Waste incineration plant	0.000	0.000	0.000	0.000	0.001	0.001	0.000	0.000	0.000
		Malta			**Netherlands**			**Norway**		
From	**To**	**Q25**	**Mean**	**Q75**	**Q25**	**Mean**	**Q75**	**Q25**	**Mean**	**Q75**
Import	Manufacturing	0.000	0.000	0.000	0.077	0.296	0.418	0.001	0.004	0.005
Import	Consumption	0.001	0.005	0.006	0.000	0.000	0.000	0.096	0.383	0.534
Production	Manufacturing	0.006	0.052	0.064	0.040	0.052	0.062	0.011	0.052	0.064
Production	Wastewater	0.000	0.001	0.001	0.000	0.001	0.001	0.000	0.001	0.001
Production	Export	0.000	0.000	0.000	0.000	0.000	0.000	0.000	0.000	0.000
Manufacturing	Consumption	0.011	0.051	0.063	0.072	0.233	0.311	0.018	0.056	0.079
Manufacturing	Wastewater	0.000	0.000	0.000	0.000	0.000	0.000	0.000	0.000	0.000
Manufacturing	Recycling system	0.000	0.001	0.001	0.001	0.004	0.006	0.000	0.001	0.001
Manufacturing	Export	0.000	0.000	0.000	0.040	0.130	0.173	0.000	0.000	0.000
Consumption	Wastewater	0.001	0.003	0.003	0.003	0.011	0.015	0.005	0.021	0.028
Consumption	Air	0.000	0.000	0.001	0.001	0.002	0.002	0.001	0.003	0.004
Consumption	Surface water	0.000	0.000	0.000	0.000	0.001	0.001	0.000	0.001	0.002
Consumption	Natural & urban soil	0.000	0.0002	0.000	0.000	0.001	0.001	0.000	0.002	0.003
Consumption	Landfill	0.005	0.026	0.032	0.000	0.001	0.002	0.000	0.002	0.003
Consumption	Waste incineration plant	0.001	0.003	0.003	0.026	0.088	0.116	0.022	0.088	0.120
Consumption	Recycling system	0.005	0.024	0.029	0.040	0.130	0.173	0.083	0.321	0.447
Wastewater	WWTP	0.001	0.004	0.004	0.004	0.012	0.016	0.005	0.022	0.029
Wastewater	Surface water	0.000	0.000	0.000	0.000	0.000	0.001	0.000	0.001	0.001
WWTP	Sludge	0.001	0.003	0.004	0.003	0.010	0.014	0.004	0.018	0.024
WWTP	Surface water	0.000	0.001	0.001	0.000	0.002	0.002	0.000	0.003	0.003
Sludge	Sludge-treated soil	0.000	0.000	0.000	0.000	0.000	0.000	0.003	0.015	0.020
Sludge	Landfill	0.001	0.003	0.004	0.000	0.000	0.000	0.001	0.003	0.004
Sludge	Waste incineration plant	0.001	0.002	0.003	0.004	0.010	0.014	0.000	0.000	0.000

Table S15 (continued): 25th quantiles, means and 75th quantiles of flows of nano-Ag (tonnes)

		Poland			Portugal			Romania		
From	**To**	**Q25**	**Mean**	**Q75**	**Q25**	**Mean**	**Q75**	**Q25**	**Mean**	**Q75**
Import	Manufacturing	0.000	0.000	0.000	0.002	0.013	0.016	0.001	0.011	0.013
Import	Consumption	0.091	0.384	0.520	0.041	0.167	0.229	0.038	0.155	0.213
Production	Manufacturing	0.019	0.077	0.107	0.016	0.052	0.067	0.015	0.052	0.066
Production	Wastewater	0.003	0.017	0.021	0.000	0.001	0.001	0.000	0.001	0.001
Production	Export	0.196	0.780	1.077	0.000	0.000	0.000	0.000	0.000	0.000
Manufacturing	Consumption	0.023	0.076	0.113	0.026	0.065	0.087	0.023	0.062	0.083
Manufacturing	Wastewater	0.000	0.000	0.000	0.000	0.000	0.000	0.000	0.000	0.000
Manufacturing	Recycling system	0.000	0.001	0.001	0.000	0.001	0.001	0.000	0.001	0.001
Manufacturing	Export	0.000	0.000	0.000	0.000	0.000	0.000	0.000	0.000	0.000
Consumption	Wastewater	0.005	0.022	0.029	0.003	0.011	0.015	0.003	0.010	0.014
Consumption	Air	0.001	0.004	0.005	0.000	0.002	0.002	0.000	0.002	0.002
Consumption	Surface water	0.000	0.001	0.002	0.000	0.001	0.001	0.000	0.001	0.001
Consumption	Natural & urban soil	0.000	0.002	0.003	0.000	0.001	0.001	0.000	0.001	0.001
Consumption	Landfill	0.025	0.108	0.144	0.013	0.049	0.065	0.048	0.173	0.234
Consumption	Waste incineration plant	0.012	0.053	0.071	0.009	0.032	0.042	0.003	0.012	0.016
Consumption	Recycling system	0.066	0.270	0.369	0.039	0.137	0.186	0.005	0.019	0.026
Wastewater	WWTP	0.009	0.038	0.052	0.003	0.012	0.016	0.003	0.011	0.015
Wastewater	Surface water	0.000	0.001	0.002	0.000	0.000	0.001	0.000	0.000	0.000
WWTP	Sludge	0.007	0.032	0.043	0.003	0.010	0.013	0.002	0.009	0.012
WWTP	Surface water	0.001	0.006	0.006	0.000	0.002	0.002	0.000	0.002	0.002
Sludge	Sludge-treated soil	0.003	0.016	0.021	0.002	0.009	0.012	0.000	0.001	0.001
Sludge	Landfill	0.002	0.005	0.008	0.001	0.001	0.002	0.003	0.009	0.013
Sludge	Waste incineration plant	0.004	0.012	0.019	0.000	0.000	0.001	0.000	0.000	0.000
		Slovakia			**Slovenia**			**Sweden**		
From	**To**	**Q25**	**Mean**	**Q75**	**Q25**	**Mean**	**Q75**	**Q25**	**Mean**	**Q75**
Import	Manufacturing	0.000	0.002	0.002	0.000	0.001	0.001	0.001	0.006	0.007
Import	Consumption	0.021	0.083	0.114	0.010	0.041	0.056	0.111	0.444	0.612
Production	Manufacturing	0.008	0.052	0.064	0.007	0.052	0.064	0.012	0.053	0.065
Production	Wastewater	0.000	0.001	0.001	0.000	0.001	0.001	0.000	0.001	0.001
Production	Export	0.000	0.000	0.000	0.000	0.000	0.000	0.000	0.000	0.000
Manufacturing	Consumption	0.014	0.053	0.071	0.011	0.052	0.066	0.019	0.057	0.081
Manufacturing	Wastewater	0.000	0.000	0.000	0.000	0.000	0.000	0.000	0.000	0.000
Manufacturing	Recycling system	0.000	0.001	0.001	0.000	0.001	0.001	0.000	0.001	0.001
Manufacturing	Export	0.000	0.000	0.000	0.000	0.000	0.000	0.000	0.000	0.000
Consumption	Wastewater	0.001	0.007	0.009	0.001	0.004	0.006	0.006	0.024	0.032
Consumption	Air	0.000	0.001	0.001	0.000	0.001	0.001	0.001	0.004	0.005
Consumption	Surface water	0.000	0.000	0.000	0.000	0.000	0.000	0.000	0.001	0.002
Consumption	Natural & urban soil	0.000	0.001	0.001	0.000	0.000	0.001	0.000	0.002	0.003
Consumption	Landfill	0.016	0.064	0.086	0.005	0.023	0.029	0.000	0.001	0.001
Consumption	Waste incineration plant	0.004	0.017	0.023	0.001	0.005	0.006	0.025	0.105	0.140
Consumption	Recycling system	0.011	0.047	0.063	0.013	0.060	0.079	0.094	0.364	0.501
Wastewater	WWTP	0.002	0.007	0.010	0.001	0.005	0.007	0.006	0.024	0.033
Wastewater	Surface water	0.000	0.000	0.000	0.000	0.000	0.000	0.000	0.001	0.001
WWTP	Sludge	0.001	0.006	0.008	0.001	0.005	0.006	0.005	0.021	0.027
WWTP	Surface water	0.000	0.001	0.001	0.000	0.001	0.001	0.000	0.004	0.004
Sludge	Sludge-treated soil	0.000	0.000	0.000	0.000	0.000	0.000	0.004	0.018	0.024
Sludge	Landfill	0.001	0.001	0.002	0.000	0.000	0.000	0.000	0.001	0.002
Sludge	Waste incineration plant	0.001	0.005	0.007	0.001	0.004	0.006	0.001	0.001	0.004

Table S16: Normalised releases to surface water. Values are in tonnes / km² of surface water (freshwater and a band of 10 m along the coastlines).

Country	**Nano-TiO_2**	**Nano-ZnO**	**Nano-Ag**
Austria	1.2E-01	2.5E-02	3.42E-06
Belgium	5.7E-01	1.1E-01	1.57E-05
Bulgaria	5.8E-02	9.2E-03	8.76E-07
Switzerland	1.0E-01	2.1E-02	2.03E-06
Cyprus	7.0E-01	1.5E-01	2.05E-05
Czech Republic	1.8E-01	3.5E-02	2.76E-06
Germany	1.6E-01	3.0E-02	2.91E-06
Denmark	1.6E-01	2.9E-02	7.21E-06
Spain	3.1E-01	6.5E-02	3.23E-06
Estonia	7.5E-03	1.3E-03	3.49E-07
Finland	2.5E-03	5.4E-04	1.46E-07
France	2.0E-01	3.6E-02	3.59E-06
United Kingdom	3.7E-01	7.0E-02	2.84E-06
Greece	1.4E-01	2.7E-02	1.73E-06
Croatia	1.1E-01	2.0E-02	1.46E-06
Hungary	5.2E-02	8.3E-03	5.13E-07
Ireland	4.6E-02	7.6E-03	5.85E-07
Italy	2.9E-01	5.6E-02	1.25E-06
Lithuania	2.8E-02	4.7E-03	7.57E-07
Luxembourg	1.8E+00	3.4E-01	1.25E-04
Latvia	1.8E-02	3.2E-03	6.95E-07
Malta	2.1E+00	3.9E-01	1.34E-04
Netherlands	7.4E-02	1.5E-02	7.70E-07
Norway	6.8E-03	1.2E-03	2.49E-07
Poland	1.0E-01	1.7E-02	1.51E-06
Portugal	1.9E-01	3.6E-02	2.42E-06
Romania	3.6E-02	5.1E-03	8.28E-07
Slovakia	3.0E-01	5.8E-02	1.80E-06
Slovenia	1.4E-01	4.6E-02	6.35E-06
Sweden	4.0E-03	7.6E-04	1.49E-07

Table S17: Normalised releases to soils. Values are in tonnes / km^2 of soil

Country	**Nano-TiO_2**	**Nano-ZnO**	**Nano-Ag**
Austria	1.1E-03	2.3E-04	7.27E-08
Belgium	2.3E-03	4.9E-04	1.99E-07
Bulgaria	7.8E-04	1.2E-04	2.73E-08
Switzerland	2.9E-05	3.4E-05	2.01E-08
Cyprus	7.5E-03	1.5E-03	4.34E-07
Czech Republic	3.9E-03	7.6E-04	1.16E-07
Germany	1.8E-03	3.6E-04	7.67E-08
Denmark	3.6E-03	6.5E-04	2.35E-07
Spain	4.7E-03	9.5E-04	9.72E-08
Estonia	1.0E-04	2.0E-05	1.65E-08
Finland	8.4E-05	2.0E-05	1.32E-08
France	3.7E-03	6.6E-04	1.35E-07
United Kingdom	1.0E-02	1.9E-03	1.52E-07
Greece	8.2E-04	1.7E-04	2.30E-08
Croatia	1.4E-04	3.3E-05	1.25E-08
Hungary	3.1E-04	5.1E-05	2.20E-08
Ireland	2.3E-03	3.7E-04	7.25E-08
Italy	4.3E-03	8.5E-04	4.06E-08
Lithuania	1.1E-03	1.9E-04	6.24E-08
Luxembourg	9.4E-03	1.8E-03	1.55E-06
Latvia	8.0E-04	1.4E-04	6.24E-08
Malta	3.0E-04	3.4E-04	9.65E-07
Netherlands	6.4E-05	6.5E-05	2.95E-08
Norway	7.4E-04	1.4E-04	5.59E-08
Poland	1.7E-03	2.9E-04	5.83E-08
Portugal	4.7E-03	8.9E-04	1.14E-07
Romania	9.4E-05	1.6E-05	8.49E-09
Slovakia	2.5E-05	3.0E-05	2.06E-08
Slovenia	3.7E-05	2.5E-05	2.49E-08
Sweden	7.1E-04	1.3E-04	4.88E-08

Product allocation for nano-Ag

Table S18: Comparison between product allocation in this study and two other studies

Country	Sun et al. 2016[6]	Giese et al. 2018[7]	This study
Textiles	**25%**	**31%**	2.4%
Cleaning agents	6%	1%	0.2%
Paints	3%		
Consumer electronics / Electronic printing	**38%**	**65%**	**80%**
Cosmetics	10%	0%	2.6%
Medical technology	4%	1%	9.3%
Plastics	3%	1%	
Food	7%	0%	0.2%
Glass and ceramics	1%		
Metals	2%	0.5%*	
Soil remediation	1%		
Filters		0.5%*	0.2%
Coatings		1%	4.9%

* in the original reference presented as Other (incl. metals, filters, …) accounting for 1%, for comparison in this table presented as metals and filters with each 0.5% contribution.

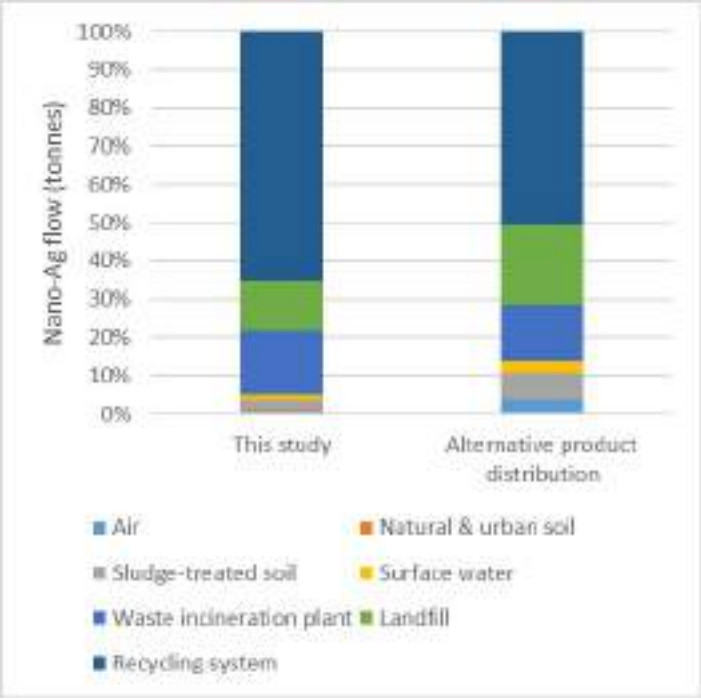

Figure S1 Modelled results of nano-Ag using the product distribution presented in this study and the product distribution presented by Giese et al. (2018)[7]

References

1 Eurostat, Sewage sludge production and disposal from urban wastewater.

2 Eurostat, Freshwater and total land cover.

3 C. Steinmeier, *CORINE land cover 2000 / 2006 - Switzerland - Final Report*, 2013.

4 L. Klein, *Habitat fragmentation due to transportation, Estonia*, 2016.

5 Worldatlas, Worldatlas, https://www.worldatlas.com/webimage/countrys/europe/no.htm, (accessed 13 May 2019).

6 T. Y. Sun, N. A. Bornhöft, K. Hungerbühler and B. Nowack, Dynamic Probabilistic Modeling of Environmental Emissions of Engineered Nanomaterials, *Environ. Sci. Technol.*, 2016, **50**, 4701–4711.

7 B. Giese, F. Klaessig, B. Park, R. Kaegi, M. Steinfeldt, H. Wigger, A. Von Gleich and F. Gottschalk, Risks, Release and Concentrations of Engineered Nanomaterial in the Environment, *Sci. Rep.*, 2018, **8**, 1–18.

3.2. Release data generation from experimental simulations

3.2.1. Second peer-reviewed publication

Release mechanisms for PA6 nanocomposites under weathering conditions simulating their outdoor uses

E. Fernández-Rosas,[a*] V. Pomar-Portillo,[a] D. González-Gálvez,[a] G. Vilar,[a] and S. Vázquez-Campos[a]

[a] *LEITAT Technological Center, C/de la Innovació 2, 08225 Terrassa (Barcelona), Spain*

*Corresponding author e-mail address: efernandez@leitat.org

Contribution to the peer-reviewed publication within the context of this thesis: In this paper substantial contribution to the analysis and interpretation of data as well as to reflect the work done and the outcomes obtained in the text of the manuscript were provided. Since all the work was performed from researchers from the same group (LEITAT – Materials safety), the work was divided equally and all the authors contributed to the whole paper.

The following manuscript is a version of record reproduced NanoImpact 20 (2020) 100260 with permission from Elsevier.

The online version can be accessed from:

https://doi.org/10.1016/j.impact.2020.100260

NanoImpact 20 (2020) 100260

Contents lists available at ScienceDirect

NanoImpact

journal homepage: www.elsevier.com/locate/nanoimpact

Release mechanisms for PA6 nanocomposites under weathering conditions simulating their outdoor uses

E. Fernández-Rosas*, V. Pomar-Portillo, D. González-Gálvez, G. Vilar, S. Vázquez-Campos

LEITAT Technological Center, C/de la Innovació 2, 08225 Terrassa (Barcelona), Spain

ARTICLE INFO

Keywords:
Release
Nanosafety
Weathering
Nanocomposite
Polyamide

ABSTRACT

The increased use of polymer nanocomposites in different applications could lead to potential nanofiller release into different human and environmental compartments and consequently, increase the exposure of human and environmental species to nanomaterials. This study aims at determining how the inclusion of nanofillers with diverse chemical nature (SiO_2, TiO_2, ZnO, multiwalled carbon nanotubes and two nano-organoclays) in polyamide 6 composites influences the nanomaterial release during the use of these products. The different nanocomposites were exposed to accelerated ageing processes, simulating outdoor conditions, through irradiation with UV light under a combination of dry-wet cycles. Release monitoring consisted of nanocomposites characterisation, run-off waters collection and released materials quantification and characterisation. The study confirmed that the chemical surface nature of the nanofiller strongly impacts on polymer degradation, in some cases enhancing its protection and in others promoting polyamide hydrolysis and/or photo-degradation processes. Polymer degradation and nanomaterial-polymer compatibility are the main determinants for the release and consequent exposure to nanofillers.

1. Introduction

Whenever a new technology is widely incorporated in our everyday consumer goods, a variety of concerns about its potential risks on human health and the environment are raised. Nanotechnology is not an exception, due to the expected exponential incorporation of nanomaterials (NMs) in consumer goods, together with the unawareness of the behaviour and hazards of NMs, lots of efforts have been dedicated to the nanosafety field during the last decade.(Krejsa and Middleton, 1997; Krug, 2014; Maynard et al., 2006; Nel et al., 2015; Read et al., 2014) One of the remaining challenges in the area of nanosafety is the detection, quantification and characterisation of NMs in complex matrices at very low concentrations.(Fadel et al., 2015; Gottschalk et al., 2013; Hischier and Walser, 2012; López-Serrano et al., 2014; Stamm et al., 2012; von der Kammer et al., 2012) NMs may be released in any step of a nano-enabled product life cycle, depending on multiple variables such as the type of manufacturing process, its storage conditions, or multiple stresses that the product could suffer during its use and end-of-life processes.(Nowack et al., 2013) Once a nanocomposite (NC) reaches the consumer, NMs can be released from the matrix to the surrounding environment during different use processes, leading to potential impacts of these materials on human health and ecosystems.(Bello et al., 2009; Chen et al., 2008; Du et al., 2013; Fujiwara et al., 2008; Njuguna et al., 2014; Wohlleben et al., 2014a) NMs release from nano-enabled products is not only caused by the product intended use (e.g., intended exposure in the case of a cosmetic vs. unintended exposure for some polymeric NC) or by external stresses (e.g., mechanical stress, abrasion or sunlight degradation), but also is dependent on the nature of the matrix, the NM properties on the compatibility of the NM and the matrix, and on homo−/heterogeneous dispersion of the NMs in the matrix.(Duncan, 2015; Froggett et al., 2014; Vílchez et al., 2015) The number of studies focussed on NMs release from NCs is growing, as it is reflected in reviews on the area.(Froggett et al., 2014; Harper et al., 2015; Koivisto et al., 2017; Mackevica and Hansen, 2016; Vílchez et al., 2015) There are still knowledge/data gaps that need to be covered to improve our understanding of the risks of NCs. In general the data generated so far have shown that under accelerated ageing conditions such as abrasion, sanding or UV/sunlight radiation, different released materials could be observed (i.e., isolated NM, NM embedded or attached to the polymer, polymeric microparticles).(Duncan, 2015; Froggett et al., 2014; Golanski et al., 2012; Jacobs et al., 2016; Kim et al., 2016; Mitrano et al., 2015; Rhiem et al., 2016; Wohlleben et al., 2014b, 2016).

The work presented herein is focused on nanoreinforced polyamide

Abbreviations: nanomaterial, NM; nanocomposite, NC; polyamide 6, PA6; nanoparticles, NPs; multi-walled carbon nanotubes, MWCNT; montmorillonites, MMT; Thermogravimetric Analysis, TGA; Differential Scanning Calorimetry, DSC

* Corresponding author.
E-mail address: efernandez@leitat.org (E. Fernández-Rosas).

https://doi.org/10.1016/j.impact.2020.100260
Received 12 May 2020; Received in revised form 23 September 2020; Accepted 25 September 2020
Available online 09 October 2020

6 (PA6, also known as nylon 6). PA6 is highly used in a wide variety of applications such as textile fibres, electrical & electronic components, pipes, industrial components and consumer goods among others. (Francisco et al., 2019; Kausar, 2020) Additivation of PA6 leads to composites with enhanced properties. Nanoclays are the most common nanoadditive for reinforcement purposes, replacing metal-based additives in many applications in which they can provide the required strength, wear and impact resistance with lower weight and corrosion concerns.(Battegazzore et al., 2019; García et al., 2004; Kashiwagi et al., 2004) Carbon nanotubes provide fire resistance and increase conductivity, valuable properties in applications as diverse as packaging, electronics, automotive or charge dissipation in personal protective materials.(Al Sheheri et al., 2019; De Volder et al., 2013) Moreover, metal oxide nanoparticles (NPs) enhance the mechanical properties of the polymers (SiO_2, ZnO), can be used as flame retardants (SiO_2), or used as UV barriers or antimicrobials (TiO_2, ZnO).(Kango et al., 2013)

Polyamides can undergo different degradation processes due to its nature. On one hand, it may be photo-oxidised by the combined effect of UV radiation and oxygen, and this oxidation may even cause chain scission, which is usually observed in the outer layers of the polymer. (Carroccio et al., 2003; Kroes, 1963; Rabek, 1995) Additionally, water uptake can cause hydrolysis of the amide (depolymerisation), reaction promoted at high temperatures.(Chaupart et al., 1998; Davis and Sims, 1983; Shamey and Sinha, 2003) Nanofillers can enhance or protect the polymer from these degradation processes.(Chen et al., 2013; da Silva Freitas and Claudio Mendes, 2020; Franze et al., 2012; Ray et al., 2002; Wohlleben and Neubauer, 2016) For instance, previous studies have shown that the photocatalytic activity of ZnO and TiO_2 NPs promotes the production of ROS (reactive oxygen species) that assist polymer chains scission resulting in the degradation of the matrix, whilst the opacity of carbon nanotubes can prevent UV radiation from reaching and degrading underlying polymer layers, by absorbing the UV radiation and thermally dissipating the radiation as heat. In addition, CNTs can scavenge radicals that would otherwise lead to chain scission and photo-oxidation, preventing the polymer degradation.(Fernández-Rosas et al., 2016; Nguyen et al., 2012; Pellegrin et al., 2009; Wohlleben et al., 2014b) One of the consequences of polymer/composite degradation is the potential release of materials that could then have an impact on human health or the environment. Thus, the monitoring of polymer degradation is essential to understand and control nanomaterials release from polymeric nanocomposites.

Good compatibility between the polymer matrix and the nanoadditives ensures good dispersion quality.(Bilotti et al., 2014; Kango et al., 2013; Mistretta et al., 2015) NMs in the present study were synthesized and surface functionalised to both, achieve a good NM-matrix compatibility and to keep other original properties of the polymer matrix unaffected. Metal oxides NPs were modified with hydroxyl functional groups that were expected to easily interact with PA6 amide groups by formation of hydrogen bonds and, moreover, protecting the matrix of direct contact with the metal oxides surface. Multiwalled carbon nanotubes (MWCNT) were functionalised with amine groups, as these functional groups interact with the amides in the matrix avoiding polymer hydrolysis, which is known to be enhanced by carbon nanotubes with carboxylic acids.(Chen et al., 2013; Zhao et al., 2009) Finally, nanoclays with high content of organomodifiers were synthesized to enhance their compatibility with PA6 polymeric chains.

The present work aims at determining the effect of nanofillers with different physicochemical properties (size, shape, composition, and chemical nature) on PA6 NCs degradation, and consequent monitoring of the potential NM release, from a safety perspective. The release monitoring was carried out considering that these NCs are to be used for outdoor applications and following accelerated ageing, simulating weathering conditions. Different PA6 NCs were prepared containing different metal oxide NPs, nanoclays or MWCNT. These NCs were exposed to an accelerated ageing process including rain cycles, temperature and UV radiation. Rain cycles allowed to evaluate the effect of water uptake potentially causing amide hydrolysis (depolymerisation). Moreover, the run-off waters were collected, and the released materials isolated. Physicochemical degradation of NC specimens and the properties of the released materials generated during ageing, were monitored using a combination of analytical techniques.

2. Experimental

2.1. Nanomaterials production and properties

Metal oxide NPs (SiO_2, TiO_2 and ZnO) synthesized by flame spray pyrolysis were obtained from Centro Tecnológico L'Urederra and surface functionalised by the company Polyrise SAS. Surface modification was reached by introducing organic coatings covalently attached onto the NPs surface, using as precursors 3-isocyanatopropyltriethoxysilane in presence of diethanolamine to obtain SiO_2-OH NPs, and 3-glycidoxypropyltrimethoxysilane to generate TiO_2-OH and ZnO-OH NPs (Fig. 1 Fig. S1 and Table S1).

MWCNT (97.8% pure, average diameter of 25–27 nm) were synthesized and functionalized by Glonatech in a fluidised bed chemical vapour deposition system. Amine groups were incorporated by MWCNT sonication in presence of *N*,*N*-dimethylformamide (DMF) and subsequent reaction with ethylenediamine to obtain MWCNT-NH_2 (4% of N content) (Fig. 1, Fig. S1 and Table S1).

Nanoclays, Dellite® montmorillonites (MMT) were obtained from Laviosa Chimica Mineraria S.p.A. Nanoclays (90% smectite, 0.5% cristoballite, cation exchange capacity of 100 meq / 100 g) had been functionalised with a dimethyl dihydrogenated tallow ammonium chloride salt (Stepan, USA) (43–48% content) to obtain MMT67G and small-sized $MMT67G_{small}$ (with an additional milling step) nanoclays. According to the supplier, these were 1 × 500 nm plates structured as 7–9 μm or 5–7 μm aggregates in dry form, respectively, determined by the company Sympatec GmbH (see Fig. 1, Fig. S1 and Table S1). The intersheet distance reported by the provider for MMT67G and MMT67Gsmall is 3–4 nm and 2–4 nm respectively.

The physicochemical properties of the NMs were characterized by multiple techniques. For extra information regarding the NMs physicochemical properties and methods used for their characterisation, see Supporting Information (Section 1 in SI).

2.2. Extrusion and injection of the nanocomposites

To produce the NCs (without any type of protecting agent or other additive), PA6 (PA6 Novamid® B24) was pre-dried in a dehumidifier (Portable Drying Conveyor, Wittmann PDC), to prevent hydrolytic degradation and alteration of its properties, as PA6 fibres can absorb up to 2.4 wt% of water. All the NCs were prepared using the same batch of PA6. NC pellets were prepared with a theoretical 3 wt% nanofiller content by melt mixing PA6 with the desired NM on a co-rotating twin-screw extruder incorporating a water cooling system and a pelletiser. The nanocomposites were prepared in three different twin-extruders: A 45 mm extruder (Wener & Pleiderer) for metal oxide NPs, a ZSE 27 HP extruder (Leistritz) to produce nanoclay NCs, and a TSE20 (Brabender) for MWCNT NCs. The operating variables (i.e., temperature, pressure and screw speed) were selected depending on the NM used, based on the industrial partners expertise. Dilution and mixing were done at i) 225–245 °C, 10 bar and 80 rpm for metal oxide NPs, ii) 230–240 °C, 2 bar and 180 rpm for MWCNT, and iii) 240 °C, 20 bar and 250 rpm for nanoclays. A specific twin interpenetrating helical screws system ensured a uniform flow from feeder to extruder.

Pellets were injected to generate standard test specimens type 1A, as described by the ISO 527-2 norm, with an exposed surface of 94.3 cm^2 and a total volume of 9 cm^3.(International Standards Organization, 2012) Previously, NCs had been dried in a dehumidifier. Injection moulding was done in three different injection moulding machines: a

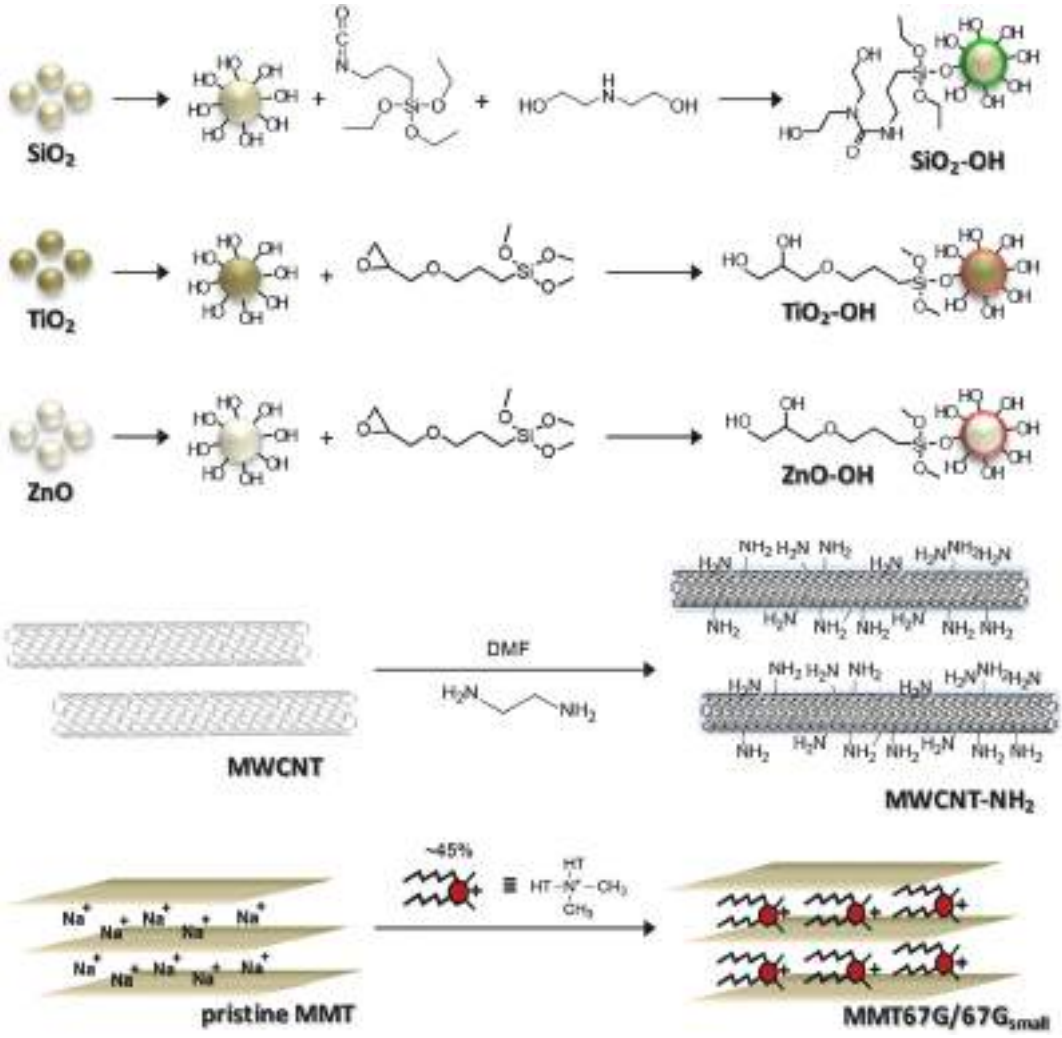

Fig. 1. Schematic representation of the tailored surface functionalisations applied in the nanofillers. Hydrogenated Tallow (HT) = CH_3–$(CH_2)_{12–16}$–CH_2–.

FM21 industrial injection machine (Sandreto) for NCs containing metal oxide NPs and non-additivated samples, a KM80-160E (KraussMaffei) for MWCNT NC, and a 200/45 injection moulding machine (Engel Victory) for NCs with nanoclays. Operation conditions differ depending on the nanofiller. With metal oxides, 230–240 °C, 135 bars and a speed of 14 mm/s in the injection unit, with 30 °C in the moulding unit. MWCNT NCs were injected at 240–280 °C, 450 bars and 20 mm/s, keeping a mould temperature of 40 °C. Finally, nanoclay NCs injection was done at 240–245 °C, 650 bars and 31 mm/s, using a mould temperature of 80 °C. As a reference for physicochemical and mechanical studies, plain PA6 was injection moulded under the same conditions as metal oxides NC.

Extrusion and injection conditions for the PA6 and PA6 NCs are summarised in Table S2, and representative SEM/TEM microtome cuts of the NC after injection are shown in Fig. S2.

2.3. Exposure to accelerated ageing and released material quantification

NC standard test specimens were submitted to accelerated ageing in a Suntest XXL+ climatic chamber (Atlas). Exposure conditions were based on the norm ISO 4892-2 Plastics – Methods of exposure to laboratory light sources – Part 2: Xenon-arc lamps. (ISO, 2013) Samples were subjected to continuous irradiation for 1000 h at 60 W/m^2 (interval 300–400 nm), a standard temperature of 65 °C (± 3 °C) and 50% (± 5%) relative humidity. During the process, dry/wet (i.e. sprayed water) rain cycles were adjusted (this specific norm conditions were changed with the objective of avoiding dilution of the release material collected during the ageing process) from 102/18 min to 29/1 min (± 0.5 min), maintaining the other parameters invariable (temperature and irradiation). In previous studies, the results obtained with these parameters were proven to be comparable to results obtained with the standard rain cycles. (Wohlleben et al., 2014b)These conditions are equivalent to 1 year of outdoor exposure in a low mountain Mediterranean climate with an average annual temperature of 15 °C: Temperate winters, rainy springs and autumns, hot and dry summers. The entire surface of the specimens (from 10 to 16, depending on the NC type) was homogeneously irradiated by turning upside down, rotating and changing their position in the climatic chamber, in each weathering cycle (4 cycles of 250 h), to achieve homogenous ageing throughout all the surface.

Run-off waters from the wet cycles were collected independently for each NC type at different time points along all the experiment to characterize the potential release materials generated during the ageing process. An empty position was used to collect the waters to be used as blank. Released materials were isolated by freeze-drying (CoolSafe 100–9 PRO Freeze Dryer, LaboGene APS, Denmark; water sublimation at −95 °C and ~ 0.3 mbar) the collected run-off waters. At least 2.5 L (≥4% *v*/v) of the total collected water was lyophilised as representative sample (at least three different volumes of water were independently lyophilized for each sample to calculate the total

released material), obtaining a dry residue ≥3 mg in all cases. The lyophilized fractions were extracted from a homogenized mixture of the total run-off waters collected for each sample.

2.4. Physicochemical characterisation of NCs and run-off waters

Different characterisation techniques were used to study chemical and physical degradation and changes in NCs structure and to quantify NM release during the outdoors ageing process. Changes in the physicochemical properties occurring during the ageing process were monitored (NC surfaces and inner regions of the composites).

2.4.1. Surface chemistry characterisation

Plain PA6 and PA6 NCs (original and artificially aged) surfaces, isolated materials from run-off waters were analysed by Fourier Transform Infrared Spectroscopy using an Attenuated Total Reflection measurement accessory (ATR-FTIR spectroscopy; IR Affinity-18,400, Shimadzu, Japan), in order to study the chemical changes during artificial ageing and to detect potential releases (isolated materials, including NM, present in run-off waters) and NM accumulation in NC surfaces (present in aged-NCs surfaces). All the infrared spectra were processed through an ATR correction (at 1800 cm^{-1}) and subsequent multiple points baseline correction. Moreover, ATR-FTIR spectra of NC surfaces were normalised using a representative peak for comparison purposes. The peak at 1261 cm^{-1} was chosen as it is far from the IR areas in which deeper changes are observed due to the different degradation mechanisms.

2.4.2. Microscopy

The composite morphology and NMs distribution were analysed by a JSM-6010 LV (JEOL Ltd.) scanning electron microscope (SEM) with an InTouchScope™ operation system (V1.06, JEOL Ltd., Japan), and by a high-resolution transmission electron microscope (HR-TEM; JEM 2010, JEOL Ltd., Japan) coupled to an EDX detector (SDD X-Max^N, Oxford Instruments, UK). For SEM analyses of the internal distribution of nanofillers and the physical degradation effects on the surface, NCs samples were sectioned with a 10 µm thickness in a 2040 Autocut microtome (Leica Reichert-Jung, Germany) and metallised using a 108 auto sputter coater (Cressington Scientific Instruments Ltd., UK). To observe the distribution of nanoclays in PA6 and its inter-sheet distances, 2 mm^2 sections of the NCs were included in Epon resin. After curing for 48 h at 60 °C, ultrafine sections generated in an EM UC7 ultramicrotome (Leica, Germany) were placed on TEM grids (formvar/carbon-coated 200 mesh Cu grids, EMS) for subsequent TEM analysis.

The morphological analysis of the released fragments and their atomic composition was determined by HR-TEM coupled to an EDX detector. For this measurement, samples were deposited on TEM grids (formvar/carbon-coated 200 mesh Cu grids, EMS) after their redispersion in ultrapure water at a concentration of 0.25 mg/mL.

2.4.3. Thermal characterisation

Both, Thermogravimetric Analysis (TGA) and Differential Scanning Calorimetry (DSC) were used for thermal characterisation of the NMs and NCs (before and after ageing). Representative samples were extracted from the centre of the NC specimens, cutting a proportional amount of surface and inner part. The Hi-Res TGA allowed quantifying NMs content and determining thermal stability of NCs; changes in the degradation profile can be directly related to polymer degradation and/or changes in the nanofiller (i.e., concentration, hydration, dissolution…). These analyses were performed (Q500, TA instruments, USA) applying a temperature increase of 10 °C/min from 30 to 1000 °C and gas flow rate of 10 mL/min. TGA were performed under N_2 atmosphere. The influence of NMs in the melting and crystallisation behaviour of PA6, and NCs crystalline structure, were studied using differential scanning calorimetry (mDSC, Q20, TA Instruments, USA) in a N_2 atmosphere. Samples were heated from 30 to 250 °C at 20 °C/min and held at 250 °C for 2 min before cooling back to 30 °C at 10 °C/min. Melting and crystallisation temperatures (T_m^a and T_c^a respectively), and their enthalpies (ΔH_m and ΔH_c) were obtained from the thermogram. The degree of crystallinity (X_c) of PA6 in the NC was calculated using the equation $X_c = (\Delta H_m/(\Delta H_{m0}\cdot(1\text{-}W_f)))\cdot 100$, where ΔH_{m0} is the melting enthalpy of 100% crystalline PA6, considered as 190.6 J/g. (Macknight et al., 1985), and W_f is the weight fraction of NM in a NC. For NCs, the % of nanofiller load was taken from the ashes quantification (see the following section).

2.4.4. Nanomaterial content quantification

Ash analysis was used to quantify the nanofiller content in the NCs before and after ageing. Ash analysis was performed following the norm ISO 3451-4, which is a test specifically used to quantify inorganic material content in polyamides. A specific amount of NC was used to run this test in order to obtain ≥5 mg of ashes, the sample was heated in a ceramic crucible under a Bunsen burner until release of gases stopped, before being exposed to 600 °C for a period ranging between 2 and 3 h in a 12PR/300 "PAD" furnace (Hobersal); masses were determined after reaching room temperature in a desiccator using an analytical balance with an accuracy of 0.1 mg. Released NM (m_{NM}) were calculated using total material isolated (m_{NC}) and its inorganic residue (IR_{NC}) at 840 °C (see Fig. S4), and later corrected with the residue of raw NM (IR_{NM}): $m_{NM} = m_{NC}\cdot(IR_{NC}/IR_{NM})$. One-way analysis of variance (ANOVA) was employed to evaluate differences among groups. Triplicates were generated for each assay. This methodology cannot be used for MWCNT content quantification as they were combusted.

Nanofiller content in the material isolated from run-off waters with the freeze-dryer (as previously explained in Section 3.3) was determined by TGA analysis, as the total amount of material was too low (from 27,5 to 1071 mg) to follow the analysis of the ashes described above. TGA was performed applying a temperature increase of 20 °C/min from 50 to 300 °C, 10 °C/min since reaching 600 °C (range in which most of the material was consumed) and 20 °C/min from 600 to 750 °C under N_2 (10 mL/min), at 750 °C the gas was changed to air and a temperature increase of 10 °C/min applied up to 900 °C. The material remaining at 840 °C was considered inorganic residue, as it is the maximum temperature before nano-TiO_2 starts degrading. Total NM content was calculated taking into account the inorganic residue of original NMs. It is important to mention that MWCNT content had to be determined at 600 °C and under N_2 to avoid MWCNT combustion.

3. Results and discussion

3.1. Nanomaterials dispersion in PA6 composites

The distribution of the nanofillers in the polymer was evaluated by SEM imaging (Fig. 2). At the microscale, NM were spread over the whole surface for the different NCs. However, at the nanoscale, scattered large aggregates (< 50 µm) could be observed in both PA6/nanoclay and PA6/SiO_2 NCs (Fig. S2). (Laoutid et al., 2013) For PA6/TiO_2 and PA6/ZnO composites, NPs were distributed in the polymeric matrix, with essentially isolated NPs below 30 nm and a few aggregates between 100 and 200 nm. The best distribution in the polymer was obtained with PA6/MWCNT NCs, where almost all the nanotubes observed by electron microscopy were isolated as single MWCNT and had length dimensions above 200 µm. For PA6/nanoclay NCs, TEM sections showed a good compatibilisation of the matrix with the nanofiller, and nanosized layered structures of nanoclays around 1 nm thickness with an interlayer distance of 3–4 nm were observed (Fig. S2). (Kalpokaitė-Dičkuvienė et al., 2013) This distribution indicates that the organomodifier intercalation effectively facilitated the 67G nanoclays dispersion in PA6. However, much larger aggregates with sizes up to few micrometres were also present in those samples, possibly caused by the high content of organomodifier. These aggregates could be a hindrance to

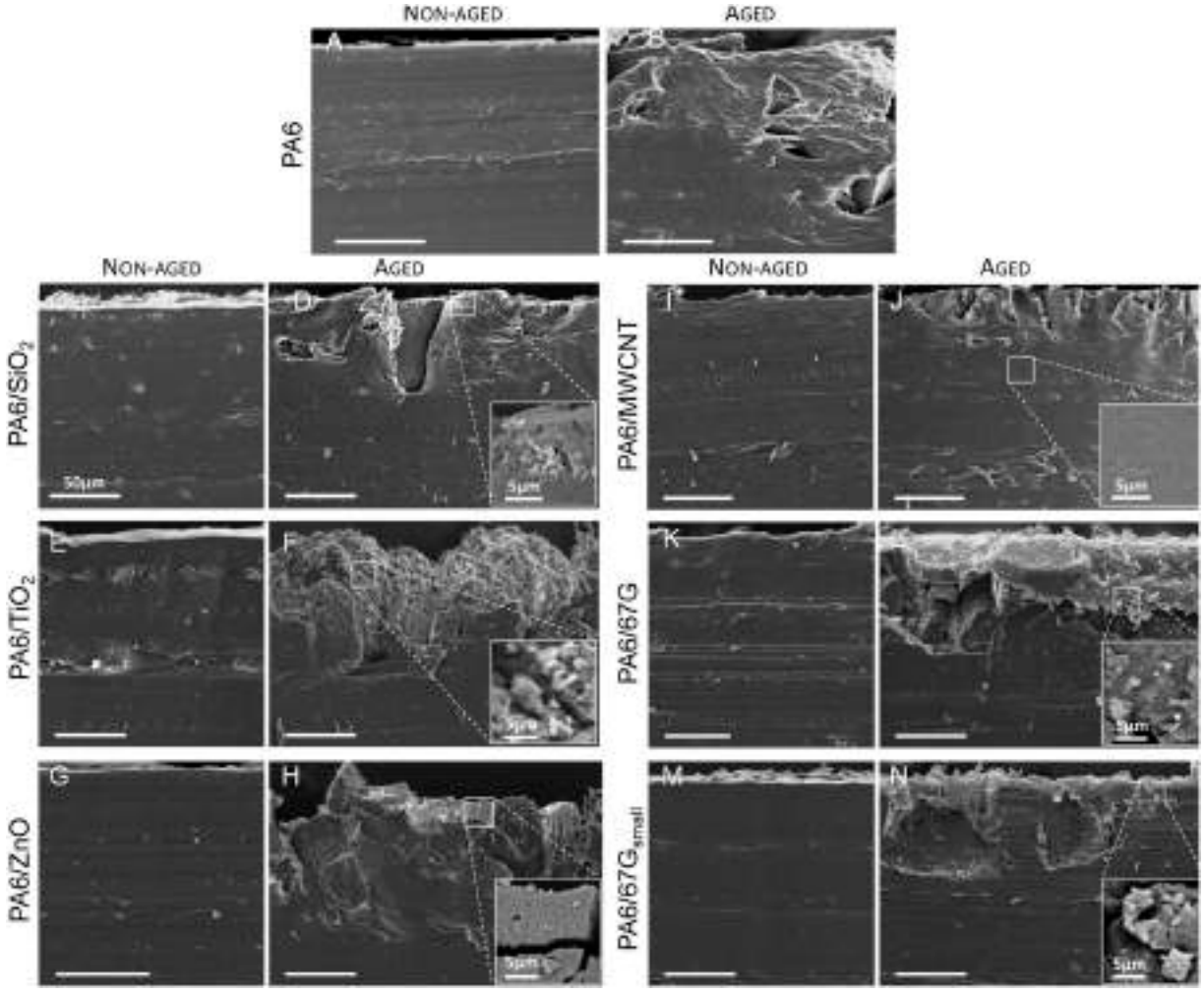

Fig. 2. Representative SEM images of transversal cuts of aged and non-aged PA6 and PA6 NCs; material surfaces always on the top of the image. Scale bars correspond to 50 µm, except when indicated.

Table 1
Estimation of the nanofiller content in PA6 NCs by ashes content analysis.

NC	Ashes Content (SD, n = 3)		TGA residue of NM[b]	NM content[c]	Corrected NM content[d]
PA6	0.05%	(0.04%)	–	–	–
$PA6/SiO_2$	2.63%	(0.24%)	83.2%	3.16%	3.10%
$PA6/TiO_2$	1.95%	(0.30%)	75.4%	2.59%	2.52%
PA6/ZnO	2.68%	(0.28%)	84.3%	3.18%	3.12%
PA6/MWCNT	1.1%[a]	(0.1%)	33.0%	3.3%	3.1%
PA6/67G	1.53%	(0.04%)	54.7%	2.80%	2.71%
$PA6/67G_{small}$	1.78%	(0.07%)	54.8%	3.24%	3.16%

[a] Calculated by TGA under N_2.
[b] Calculated from TGA of raw NM used in NC manufacturing.
[c] Considering all the inorganic residue as NM.
[d] Considering all the inorganic residue but 0.05% present in plain PA6 as NM.

confer the desired properties (e.g., barrier) to the composite,(Alix et al., 2012) however optimisation of the production process to obtain the desired performance of these NCs was out of the scope of the authors. Calcination of the NCs also indicated that the distribution of all the nanofillers was quite uniform within the samples (low standard deviation) (Table 1).

3.2. Physicochemical properties of nanocomposites and changes caused by ageing

An interlaboratory study of nanosilica release from a polyamide NC due to weathering, indicated that direct quantification and characterisation in run-off waters becomes necessary for materials release evaluation.(Wohlleben et al., 2014b) Another interlaboratory study conducted with PA6 NCs containing MWCNTs, showed that ISO4892-2 was a reproducible method to obtain quantitative release rates values since good agreement was obtained in the results of the 4 laboratories involved in the study.(Wohlleben et al., 2017) In the present work, outdoors weathering of NCs was simulated following the ISO4892-2(ISO, 2013) norm with a slight modification in the protocol and experimental set-up, allowing the collection of run-off waters. In the cited interlaboratory study, the analyses were performed on released materials obtained after the weathered samples were immersed in water, however in our study, analyses were directly performed on the materials released in the run-off waters collected during the ageing process.

3.2.1. Chemical and structural surface alterations

PA6 is a polymer highly resistant to abrasion and to chemicals such as alcohols, ketones and alkalis, but sensitive to acidic environments that catalyse amide hydrolysis. Additionally, polyamide degradation is favoured under outdoor conditions, where UV light combined with rain and high temperatures promotes both PA6 photo-oxidation and amide cleavage. Some NMs exert a protective effect on polyamide, delaying its

degradation (e.g., acting as UV-filter), while other nanofillers can promote degradation (e.g., acids that catalyse amide hydrolysis or photocatalysts that promote polymer oxidation) (Fernández-Rosas et al., 2016). Understanding the degradation mechanism occurring in each NC is crucial for understanding and monitoring potential nanoparticle releases. In our studies, all the NMs used were surface modified, aiming at improving NM dispersion in the polymer.

Polymer degradation was studied by SEM analysis of transversal section of the specimens and by FT-IR analysis of the surfaces. SEM images (Fig. 2) showed the type of defect (e.g., cracking, porosity, burn-like), whether the NM accumulates in the surface or not, and the depth of the area damaged. The FT-IR analysis was used to determine the chemical degradation mechanisms affecting each NC and their intensity (Fig. S5 to S12); furthermore, it also permitted to observe the accumulation of some NM in the surface (Fig. 2 and S2). Photooxidation was monitored mainly by the appearance of a complex signal around 1750 cm^{-1}, corresponding to different carbonyl groups (carboxylic acid or peracid, ketone, aldehyde, ester or peresters), multiple signals in the fingerprint area due to oxidation (C−O, C–O–H, C═C, C–O–O, etc.) and the appearance of a very wide peak between 2500 and 3500 cm^{-1} corresponding to O−H of carboxylic acids or peracids. However, amide cleavage was mainly followed by monitoring N−H stretching wide peak at 3200–3400 cm^{-1} (negative ΔAbs in Fig. 3), which partially changes to a narrower N−H stretching peak that superposes at 3300 cm^{-1} (positive ΔAbs in Fig. 3) and to a very wide O−H from carboxylic acid at 2500–3500 cm^{-1}.

SEM analysis showed a smooth surface for PA6 specimens. Ageing caused the appearance of sharp squared cracks of about 200 μm^2 and smaller longitudinal and aligned fractures with lengths ranging from < 100 nm to 2 μm; these effects reached 100 μm mean-depth, deeper than any of the other NCs (Fig. 2 and S3). This may be attributed to the increasing of the NC barrier properties favoured by the presence of nanofillers. FT-IR spectra showed a reduction in all PA6 signals and increases in the bands indicating photo-oxidation (Fig. 3).

In PA6/nanoclay composites, the surface showed protruding round-shaped plates (Fig. S3) of 25–30 μm (PA6/67G) or 10–20 μm (PA6/$67G_{small}$), which clearly flaked off after ageing (Fig. 2). Ageing effects were observed to a mean depth of 66 μm in both organoclay NCs. PA6/67G and PA6/$67G_{small}$ showed similar chemical degradation in the FTIR spectra, but more intense in the NC containing the smaller nanoclays. The clearest change is the enhancement of the signals corresponding to clays (Si–O–Si, ~1000 cm^{-1}), which corroborates the increase of organoclays concentration on the surface (compare to organoclay FTIR in Fig. S8). As it has been previously observed in other studies (Ray et al., 2002), FTIR spectra showed that clays catalyzed amide cleavage (changes in N–H_{st} band, 3300 cm^{-1}, an effect that was more significant for the nanoclays with smaller size). SEM images (Fig. 2 and S3) showed that clays protruded from the NC surface, probably due to more intense PA6 degradation around organoclays combined with their hydrophobicity, which minimised their release during the rain cycles in the weathering process. Images also showed that surface degradation seems stronger than for neat PA6 but, as indicated, the damages are more superficial than in neat PA6. The difference between the two nanoclays may be explained by the size difference, but also could be due to other factors as the effects of nanoclays over polyamide degradation have been reported amply in the literature, and there are several factors to consider: Size, organomodifier, nanoclay impurities such as iron, length of the amide monomer, pollutants in the air, etc. (Abdelwahab et al., 2020; Battegazzore et al., 2019; Davis et al., 2003; Fornes et al., 2003; Jang and Wilkie, 2005; Kiliaris et al., 2009; Mistretta et al., 2015; Monticelli et al., 2007; Shelley et al., 2001).

In PA6/SiO_2 NC, NPs could be observed through the entire surface and distributed inside the matrix. The SiO_2 NPs observed were mainly isolated but scattered big aggregates (with a diameter up to 50 μm) were also present (Fig. 2 and S3). After ageing, the degradation of the surface was less evident than in plain PA6, and the penetration of the structural damages was lower (about 50 μm mean depth). Moreover, low chemical degradation compared to neat PA6 was observed by FTIR on the surface of PA6/SiO_2 NC: Small changes in the carbonyl area, and some hydrolysis (Fig. 3). SEM images showed that SiO_2 NPs were accumulated on the surface area after ageing, but they remained in the subsurface and in the cracks, and were not observed in the outer surface (Fig. 2 and S3), indicating that PA6 degrades without preferential SiO_2 release. These observations strengthen the importance of NPs presence to reduce SiO_2-nanocomposite degradation (and consequently materials release) as reported in our previous work, where SiO_2 NPs accumulation on the surface was observed after PA6/SiO_2 ageing.(Fernández-Rosas et al., 2016) A study by Sung and co-workers showed high release from an epoxy/nano-SiO_2 coating when water was sprayed periodically during the ageing process.(Sung et al., 2014) These differences may be explained due to different matrix material, to the distribution of the NPs on the surface and also to their surface functionalisation.

Contrary to what was observed for organoclays and SiO_2 NCs, the surfaces of PA6/TiO_2 and PA6/ZnO NCs were intensively affected by the ageing process. Polymer surface presented some fractures, and essentially isolated NPs were observed uniformly distributed. Ageing conditions created highly porous and cracked surfaces, with more rounded corners in the case of PA6/TiO_2. The alterations described penetrated more than 80 μm (Fig. 2 and S3) and in many regions there was cracking propagation and material loss. These polymer degradation processes can be attributed to the catalytic activity associated with both nanofillers, which accelerated PA6 chains scission and could not be reduced by the addition of organosilanes in the NPs surface. However, TiO_2 and ZnO NPs affected the matrix differently during ageing as each type of nanofiller enhanced a different degradation pathway, even though both fillers are known by their photocatalytic activity. As it shows the FTIR spectra (Fig. 3), the main routes that lead to PA6 degradation in the PA6/TiO_2 NC was the photo-oxidation (Miyauchi et al., 2008), as shown by the characteristic bands of different oxidation functional groups such as carbonyl groups (1750 cm^{-1}), alcohols and carboxylic acids (3000–3500 cm^{-1}), and an increase of complexity in the fingerprint area; FTIR spectra also showed important TiO_2 NPs accumulation detected by a signal increase around 650 cm^{-1} (compare Fig. 3). In the case of PA6/ ZnO NCs, FTIR spectra showed that ZnO NPs catalyse amide cleavage (N−H st at 3300 cm^{-1}) causing the scission of the polymer chains (Klun and Krzan, 2002); water reaches the inner layers of PA6 in contrast to UV irradiation which only affects the upper layers of the polymer. Another important difference between TiO_2 and ZnO, which is observed by SEM, is that while TiO_2 NPs remain on the surface, which is not the case for ZnO NPs. The fact that TiO_2 NPs remain on the surface may explain the intensity of photodegradation in PA6/ TiO_2 NCs samples compared to PA6/ ZnO NCs; an additional factor to be considered would be that ZnO NPs catalyses much slower the photodegradation than the amide cleavage (the kinetics were not monitored during these studies).

PA6/MWCNT NC presented a uniform distribution with cross-linking and a striated surface (Fig. S2-D), with roughness observed after ageing of the NC: The surface appeared cracked with deep sharp-edged tear (> 10 μm depth) and the observed damage was around 50 μm mean depth (Fig. 2 and S3). The low degradation is attributed to two different phenomena: The ability of carbon nanotubes to shield UV-light slowing down PA6 degradation, and to an increase in the mechanical properties (hardening of the NC) due to the presence of MWCNTs, which at the same time makes the material more brittle (Dintcheva et al., 2015; Kashiwagi et al., 2005). A signal increase in FTIR was observed after ageing, suggesting amide cleavage due to scission of the polymer chains (N-H_{st} at 3300 cm^{-1}); this amide cleavage might be attributed to hydrolysis catalyzed by MWCNT-metal content (e.g. Fe) or MWCNT enhancing thermal degradation. Neither aggregates nor carbon nanotubes protruding from the surface could be observed, before or after the ageing process. These results differ from

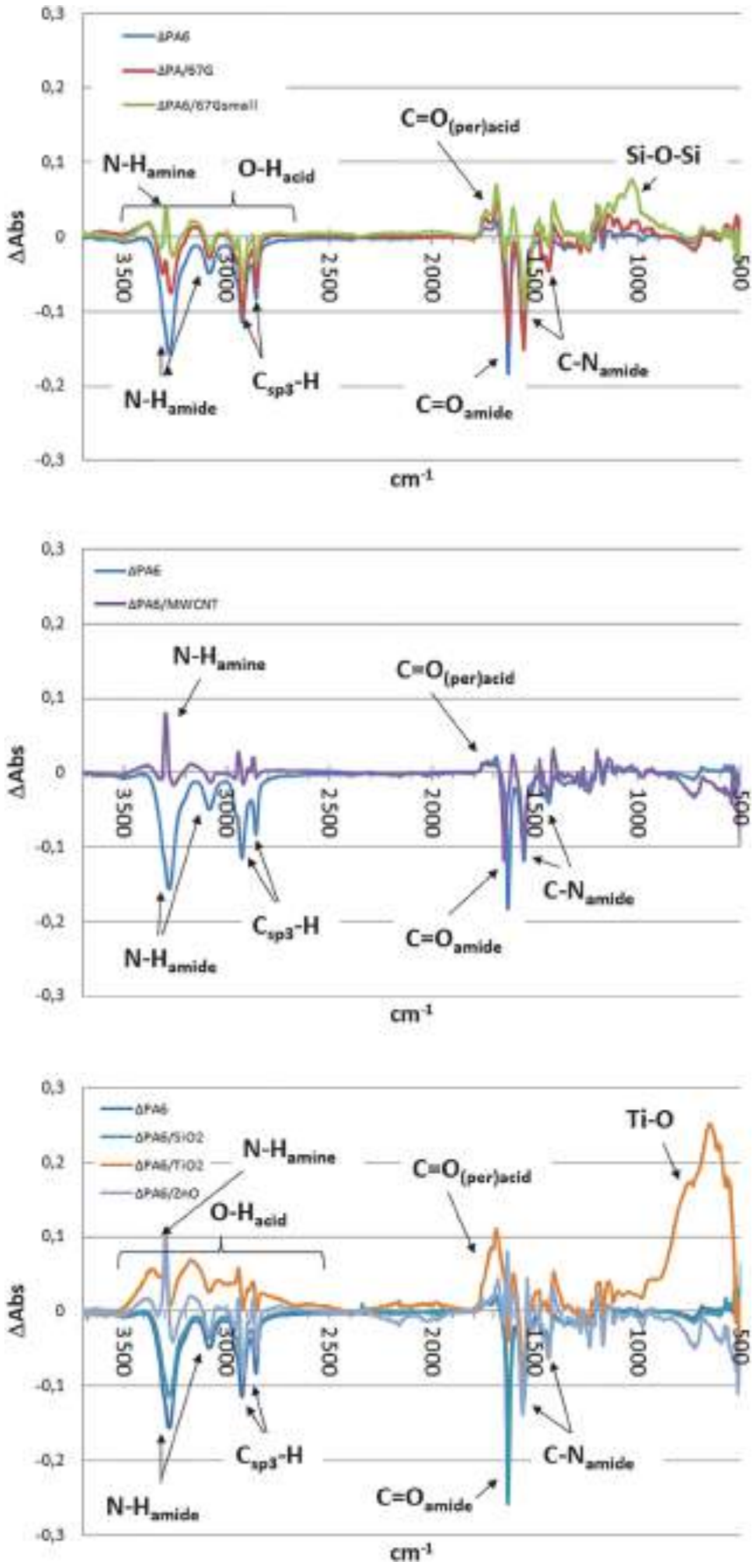

Fig. 3. Difference between FTIR spectra of aged and non-aged PA6 and PA6 NCs (normalised at 1261 cm^{-1}).

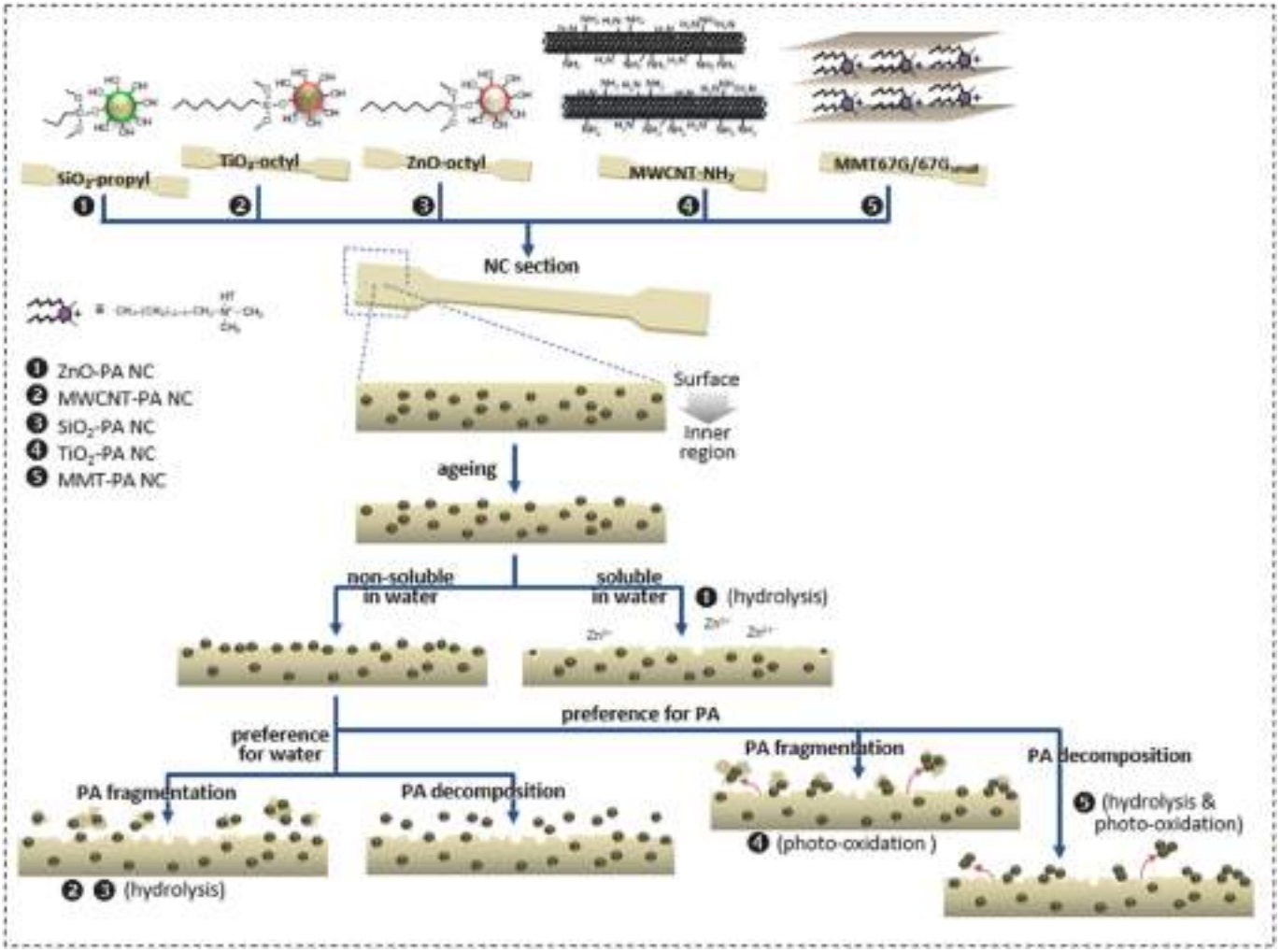

Scheme 1. Schematic representation of the degradation mechanism of the different NCs under ageing conditions.

other ageing studies done with MWCNT NC (Duncan, 2015), which report MWCNT protruding and accumulating on the surface; in most cases, the difference could be explained by the differences in the polymer or by the ageing energy applied in each case.

In summary, most of the studied NMs were satisfactorily dispersed into the PA6 matrix using industrial processes. However, the presence of some aggregates in nanoclays and SiO_2 NPs nanocomposites could not be avoided even in the presence of an organomodifier or surface functionalisation, respectively. Additionally, in most of the cases, surface functionalisation was not enough to protect the polymer from the nanofiller catalysing the photo-oxidation and/or amide hydrolysis of PA6 matrix. Scheme 1 illustrates the degradation mechanisms described in this section for each NC. As it has been monitored by FTIR and SEM analyses, most NM accumulated in the outer layers during the ageing process as PA6 degrades, but different behaviours were observed, ZnO was freely exposed in the surface or in the cracks, TiO_2 NPs and nanoclays accumulated on the surface, and SiO_2 NPs remained in cracks but could not be observed in the outer surface. These results complement existing studies that reported NM accumulation in NC surfaces during ageing,(Ging et al., 2014; Nguyen et al., 2011, 2012; Wohlleben et al., 2014b) and contribute to the understanding of potential release pathways that could be followed by some nanofillers. Therefore, some of the observations from these analyses indicate that matrix degradation may be enhanced or reduced depending on: i) the NM chemical nature, ii) the proper compatibilisation between the NM and the polymer (distribution of the NM in the matrix and the presence of agglomerates or aggregates), and iii) if the NM could strongly interact with the polymer network (Duncan, 2015).

3.2.2. *Changes in thermal properties after NCs weathering*

The chemical nature of the polymer, the nanofiller, their interaction and the crystalline structure of the composite material, are key parameters that influence the thermal degradation profile of a NC (TGA of NCs in Fig. 4 and Fig. S13). The same parameters, have an effect in the degradation mechanism of the NCs during weathering and, consequently could influence the potential release of the nanofillers from the polymeric matrix during NC use in outdoor conditions. Therefore, by studying the thermal degradation profiles of NCs, relevant information could be obtained to support the understanding of released materials.

Monitoring of thermal decomposition profile of polymeric specimens, under nitrogen atmosphere, showed that among the non-aged samples, the plain polymer was the composite experiencing degradation at a higher temperature, evidencing that the nanomaterials incorporation did not delay the thermal degradation.

When comparing the thermogravimetric analysis of the aged and non-aged composites, significant differences were not found for PA6/SiO2, PA6/TiO2, nor for the NCs containing nanoclays. The main differences were found in plain composite, PA6/ZnO and PA6/MWCNT. Changes in thermal degradation suggest that there are internal modifications in the composites, which may affect the release behaviour.

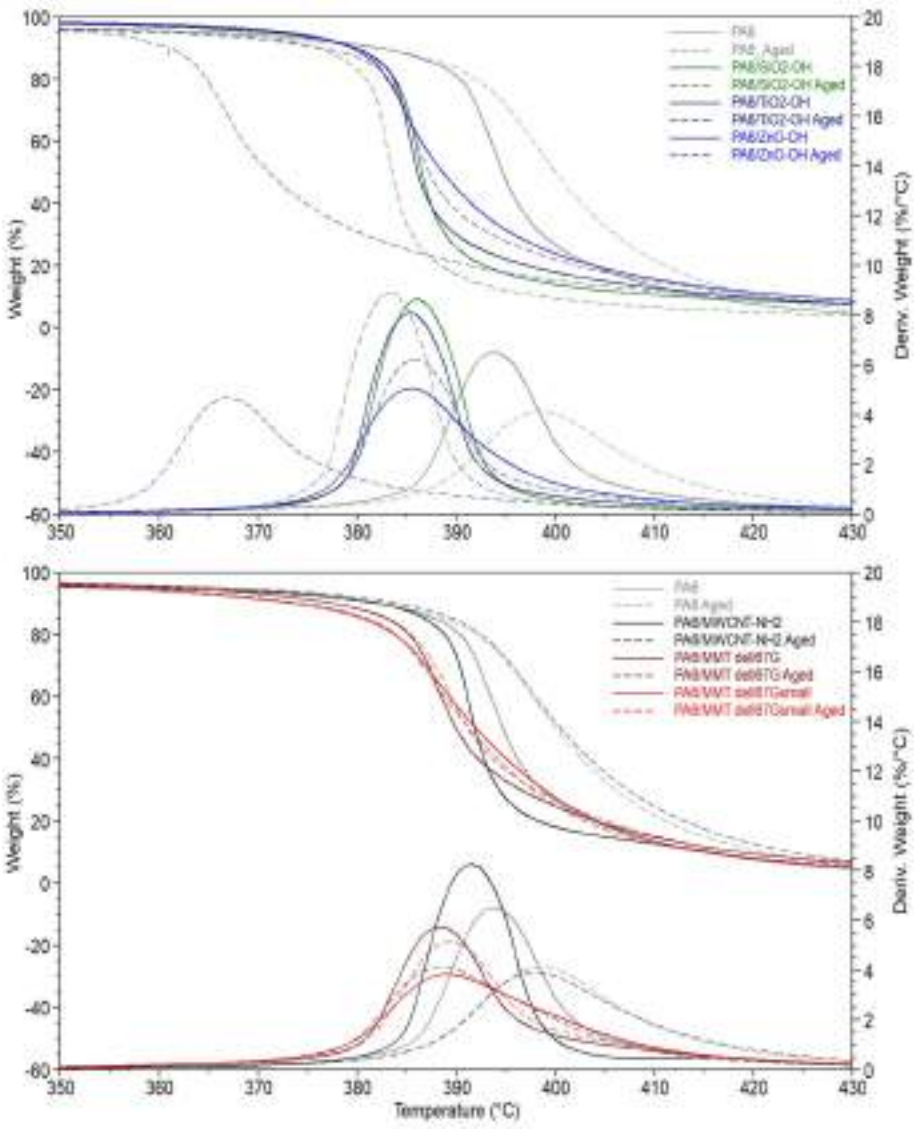

Fig. 4. TGA of PA6 polymer and PA6 NCs in nitrogen at a 10 °C/min heating rate. In the top part of the graphs the Weight (%) is presented while in the bottom part the respective weight derivates (%/°C) are plotted.

Table 2
Quantification of the released material collected by freeze-drying from the run-off waters.

NC	Residue (%)[a]	TOTAL released (%)[c] SD (n = 3)	TOTAL released (mg/m^2)[d] SD (n = 3)	NM released (mg/m^2)[e]	NM concentration in released material (%)
PA6	–	0.064 (0.019)	742 (220)	–	–
PA6/SiO_2	15.32	0.031 (0.005)	338 (50)	62	18
PA6/TiO_2	10.37	0.031 (0.006)	341 (66)	47	14
PA6/ZnO	5.28	0.686 (0.037)	7576 (414)	474	6
PA6/MWCNT	19.57[b]	0.129 (0.011)	1458 (127)	865	59
PA6/67G	14.69	0.025 (0.008)	265 (82)	71	27
PA6/67G$_{small}$	12.63	0.056 (0.014)	601 (151)	139	23

[a] Material remaining calculated from TGA under air at 840 °C.
[b] Calculated from TGA under N_2 at 600 °C.
[c] Ratio of recovered material from run-off waters vs. total amount of NC. SD calculated using 3 independent lyophilized volumes of water.
[d] Ratio of recovered material from run-off waters vs. NC specimens surface.
[e] Ratio of NM recovered from run-off waters vs. NC specimens surface. Released NM (m_{NM}) is calculated using total material isolated (m_{NC}) and its inorganic residue (IR_{NC}) at 840 °C (see Fig. S4), and later corrected with the residue of raw NM (IR_{NM}): $m_{NM} = m_{NC}$·(IRNC/IR_{NM}).

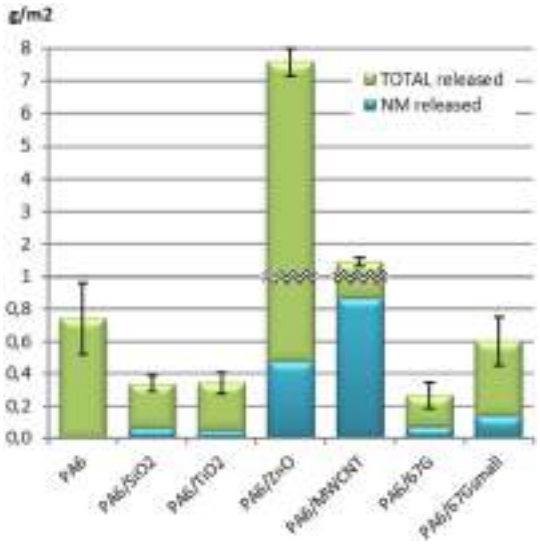

Fig. 5. Comparison of the total material released and NM content estimated based on the corresponding TGA isotherms. Error bars = SD.

These results are in agreement with the total material released measured (Table 2 and Fig. 5), since these three samples were the ones in which a higher release was found, especially for PA6/ZnO.

These results indicate that the macroscopic degradation of the samples during the weathering process is not always enough (in terms of mass) to show changes in the thermal profiles that could differ from those observed before ageing. Only in the case of plain polymer, PA6/ZnO and PA6/MWCNT NCs these changes were significant.

3.3. Characterisation of the released materials from nanocomposites during accelerated ageing

Considerable differences in PA6 degradation were detected through direct observation of the different NCs using a combination of analytical techniques. However, the collection of released materials during the exposure to accelerated ageing conditions (simulating outdoor scenarios) is the most direct and reliable source of information. Collection of run-off waters from the ageing process and further material isolation (Fig. S14) was the procedure followed to quantify NC releases. Besides, their characterisation included the determination of the total amount of nanofillers in the released material and if the NM were isolated, aggregated or embedded in PA6 (or any derived degradation compound). However, this quantification method presents two drawbacks: On one side, part of the polymer can be degraded to volatiles and, therefore not directly collected during the process (Achhammer et al., 1951; Smith et al., 2012); and, furthermore, some nanofillers can remain on the surface of the NC which will only be released by applying some mechanical forces, not included during the ageing process, but that can be done as a second step after the samples have been aged, as it was shown by Wohlleben et al. (Wohlleben et al., 2014b). Therefore, this quantification method presented here only measures spontaneous release during weathering. In any case, monitoring of polymer NC surfaces after weathering allows predicting potential exposure by direct contact (potential consumer exposure).

Quantification of the released material (Table 2 and Fig. 5) showed that two NCs produced higher released materials than plain PA6 (742 mg/m^2, only ~0.06% of material lose): PA6/ZnO NCs lost the highest amount of material by far (7576 mg/m^2, ten-fold plain PA), followed by PA6/MWCNT (1458 mg/m^2). Most of these results were in agreement with the characterisation of aged NCs described in previous sections (high release in PA6/ZnO or the low release in PA6/SiO_2 and in PA6/nanoclays) and the results suggest that the increased release mass is the result of PA6/ZnO and PA6/MWCNT mechanism of degradation is mainly via amide hydrolysis. Additionally, the results obtained for PA6/TiO_2 NCs point to a different mechanism (photooxidation), as high surface degradation was observed but small amounts of material (and the lowest amount of NM) were collected. The small amounts of TiO_2 observed can be explained by considering that TiO2 is known as a chemical opacifier, therefore the released material collected is due to the degradation occurring on the outer surface of the NC.

As in section 4.2.1, FTIR was used to determine the materials released and supports the understanding of the mechanism of degradation occurring to each composite (Fig. 7). Basically, FTIR spectra showed: i) presence of PA6 (Csp3-H as a double band between 2850 and 2950 cm^{-1}, carbonyl at 1640 cm-1, N—H bond at 1500 cm^{-1} and as double band at 3100 and 3200 cm^{-1}), which might come from PA6 oligomers derived from amide cleavage or from PA6 release due to thermal degradation or cracking; ii) presence of amine (narrow band at 3300 cm^{-1}) derived from amide hydrolysis; iii) presence of carboxylic acid (carbonyl band at 1750 cm^{-1} and very broad hydroxyl group at 2500–3500 cm^{-1}), which might come from amide hydrolysis and from polymer photooxidation; and iv) oxidation products in the form of alcohols, alkenes, ketones, etc. (complex bands in the fingerprint area, 1000–1500 cm^{-1}, and in the carbonyl area around 1750 cm^{-1}).

The NCs containing the smaller nanoclays released more than double amount of material than PA6/67G, confirming the higher surface degradation observed in PA6/67G$_{small}$ composites after ageing (see previous section). In both cases the amount of waxy material recovered after ageing was low (Table 2 and Fig. 5), but TGA characterisation indicated that nanoclays content in both cases were 10 (PA6/67G) and 7-fold (PA6/67G$_{small}$) higher in the released material than in the non-aged NCs (Table 1, Table 2 and Fig. 5), based on the weight losses. This might be due to a favourable release of the Nanoclays from the polymer surface during weathering or that the degradation of PA6 generates volatile residues that could be lost during the process. TEM images showed that the released material was composed of organic material and isolated nanoclay layers (Fig. 6). FTIR was not useful in this case to determine nanoclays presence in the sample as nanoclays signal (~1000 cm^{-1}) overlaps with PA6 degradation products. However, FTIR spectra indicate that, in both nanoclay composites, released materials were composed by a mixture of PA6 degradation products, mainly from those ones due to PA6 hydrolysis (Fig. 7).

PA6/SiO_2 NCs presented low total release material in the form of a semi-waxy powder (Table 2, Fig. 5 and S14) but with high concentration of nano-SiO_2 (based on the TGA weight losses of the NC and its run-off waters). These results match with the physicochemical characterisation of the aged NC, as PA6/SiO_2 presented low surface degradation. The high concentration of silica in the released material of PA6/SiO_2 is explained by PA6 degradation, this is corroborated in the FTIR spectrum, with very broad peaks, and in the TGA, with material loss all along the analysis (Figs. 7 and 8). TEM images clearly showed the presence of silica NPs embedded in organic matter (Fig. 6), but no isolated silica could be detected. Together with the fact that silica NPs did not accumulate in the NC surface, indicating a strong interaction nanofiller-PA6, and a protective effect of the PA6 surface degradation using functionalised silica NPs. Two previous works from our group with other PA6/nanosilica composites already shown the importance of surface functionalisation for improving NM-polymer interaction and nanofiller protective effect.(Fernández-Rosas et al., 2016; Wohlleben et al., 2014b) In the first study we observed that the use of organo-modified nanosilica reduced PA6 degradation by minimizing silica surface and PA6 interaction, though in that case, the organomodifier did not help in NM-matrix compatibilisation, increasing NM release. In the second study, different nanosilica and PA6 protecting agents were used, but the amount of released material was comparable. However, SiO_2 NPs-polymer interactions were minimised (i.e. less compatibilized), resulting in a much lower concentration of SiO_2 NPs in the

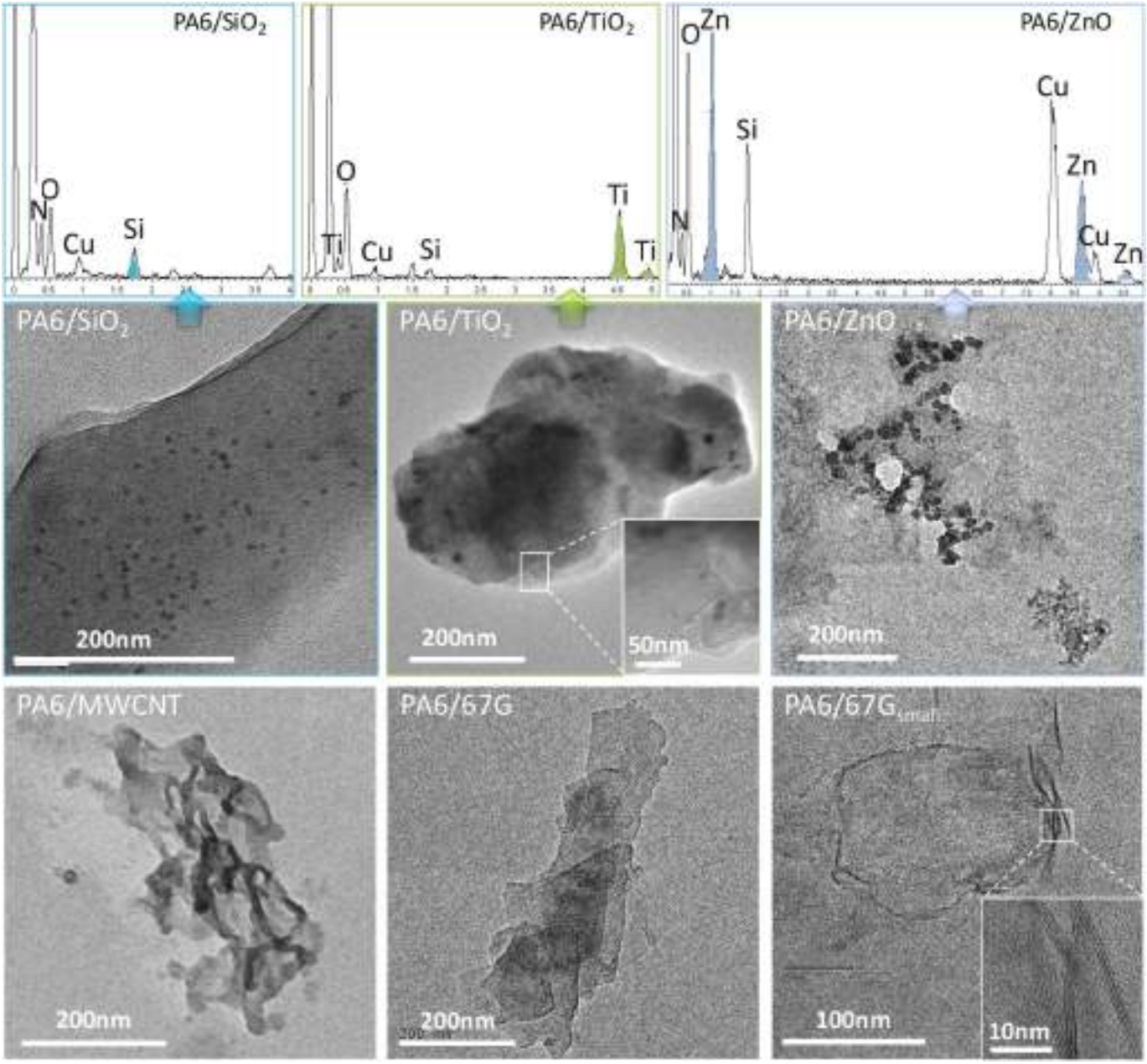

Fig. 6. TEM representative images of recovered material from the run-off waters generated during the NC ageing process, and the corresponding EDX graphs for materials collected form PA6/SiO_2, PA6/TiO_2 and PA6/ZnO NCs.

released material (~10%) containing isolated SiO_2 aggregates. (Wohlleben et al., 2014b)

The quantification and characterisation of released materials of PA6/TiO_2 NCs is almost identical to PA6/SiO_2. However, based on the characterisation of aged NCs, a higher amount of released materials was expected. The low amount of recovered material could be hypothetically explained by the photo-oxidation of the material due to TiO_2, which would release most of the material as volatiles. In addition, most TiO_2 remained attached to the NC surface. TEM images showed that TiO_2 released was embedded in organic matter, small fragments of NCs.

Oppositely, PA6/ZnO NCs released a large amount of material in a more granulated form (Fig. S14). This was expected based on the surface characterisation of aged NCs, as PA6/ZnO presented high degradation (see previous section). In this case, FTIR spectrum shows that most of the organic content is composed of products derived from PA6 hydrolysis (NH_{amine} ~ 3300 cm^{-1}) (Figs. 3 and 7). TEM images showed ZnO aggregates embedded in organic matter and also isolated ZnO aggregates; this corroborates that ZnO NPs are released once exposed at the NCs surface, as well as embedded particles in small NC fragments similarly to PA6/SiO_2 and PA6/TiO_2. Additionally, isolated aggregates of smaller ZnO NPs (smaller than the original NPs incorporated in the composites) were observed, which indicated that they were partially dissolved in run-off waters (Fig. 6).

Finally, a large amount of material was recovered from PA6/MWCNT run-off waters. Both TGA and TEM images showed that most of the material is composed of released MWCNT with some highly degraded material (Figs. 6, 8 and S14). Additionally, FTIR spectra (Fig. 7) showed the presence of a mixture of PA6 and its oxidation products. The presence of PA6 degradation products might be explained by a strong impact of the radiation on the NC surface, where the natural colouring of MWCNT under the UV irradiation during the weathering process causes an increase of temperature, compared to plain PA6 and

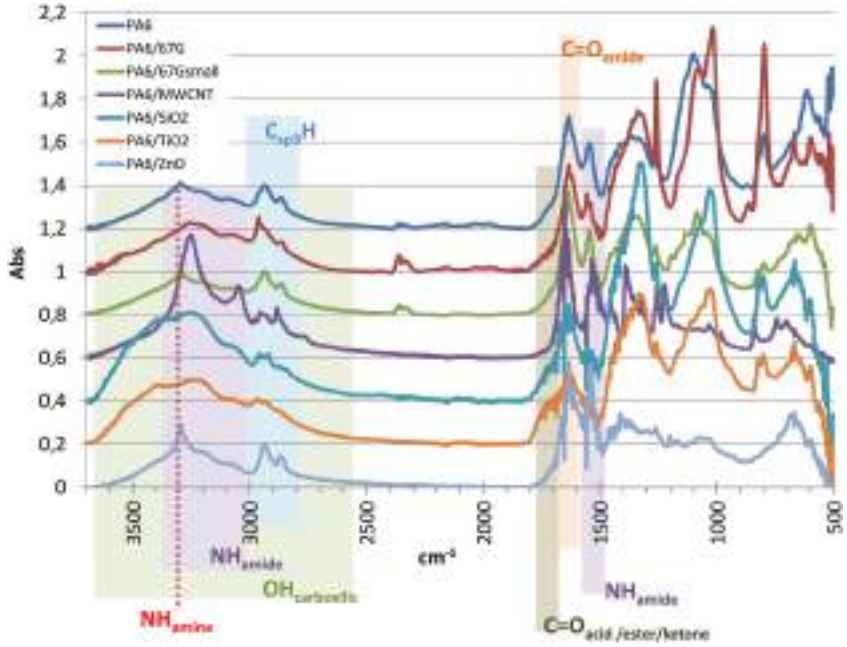

Fig. 7. FTIR spectra of released materials from PA6 and PA6 NCs ageing (normalised at 2935 cm^{-1}).

the other NCs, blocking a deeper penetration and consequent degradation. This effect cannot be offset by the presence of the amine-modifier. Thus, high release of MWCNT from the cracks were detected, as well as the presence of impurities or remaining reactants coming from MWCNT functionalisation process and some matrix degradation residues.

In conclusion, FTIR spectra and TGA showed that most of the released materials were PA6 and polymer degradation compounds derived from PA6 photo-oxidation and/or hydrolysis; depending on the nanofillers, one type of degradation compound dominates over the other. ZnO NPs, MWCNTs and nanoclays NCs showed predominance of released materials derived from hydrolysed PA6, while TiO_2 and SiO_2 NCs showed predominance of released materials derived from oxidised PA6. TEM images showed that most released materials were due to the release of small fragments of NCs, as it is clearly observed in PA6/SiO_2, PA6/TiO_2 and PA6/ZnO images (Fig. 6). However, isolated particles or aggregates were still observed in some cases (ZnO NPs, MWCNT and nanoclays). In general, the amount of total material released is low (< 1.5 g/m^2) other than in the case of PA6/ZnO (7.6 g/m^2); moreover, most NC showed less release than plain polymer. NM content in the released material is always (minimum two-fold) higher than in the NC, which indicates that most degraded polymer is released as volatiles.

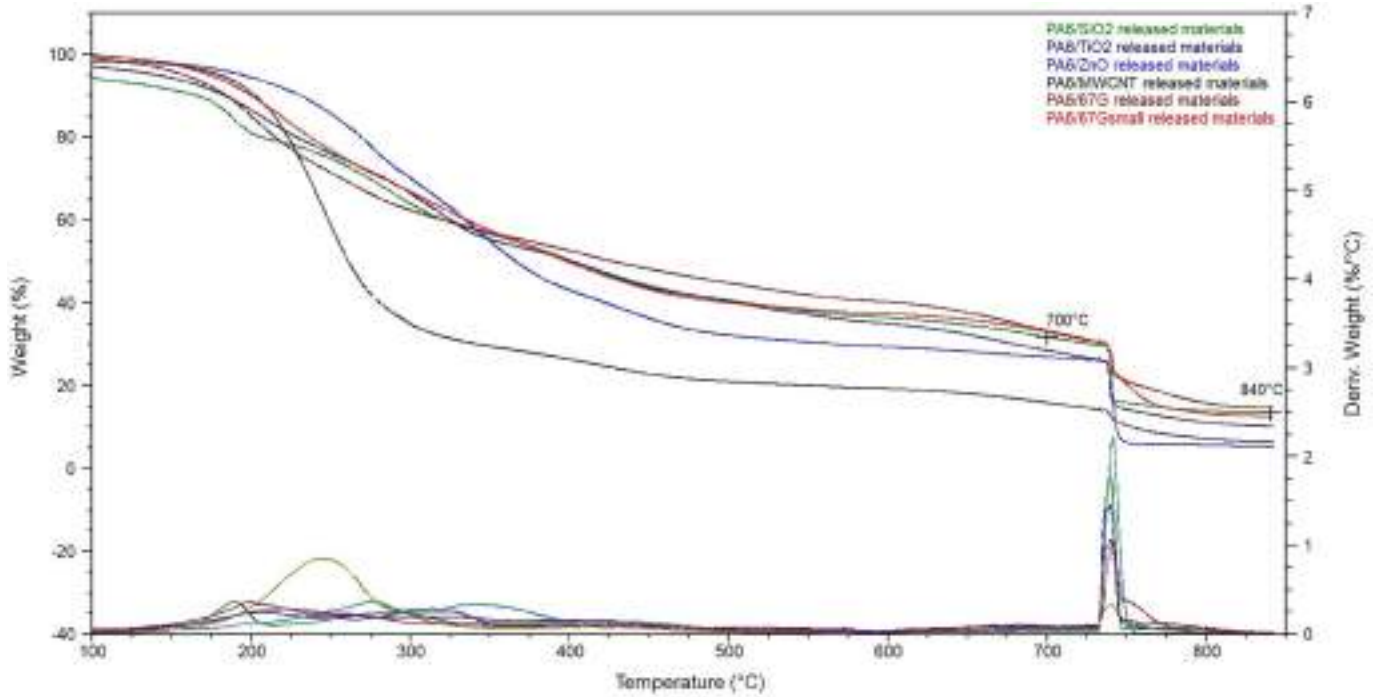

Fig. 8. TGA isotherm corresponding to the released materials collected from the run-off waters from PA6 and PA6 NCs after ageing.

Table 3
Summary of the most relevant observations and characterisation results.

	Released material		Surface characterisation		
NC	NM released observed (SEM/TEM)	Chemical characterisation (FTIR)	NM accumulation on polymer surface (SEM)	Surface morphology (SEM)	Surface chemistry (FTIR)
PA6	–	Oxidised and hydrolysed PA6	–	Degraded, irregular with little cracking	Mainly degraded by oxidation, also some hydrolysis
PA6/SiO_2	Yes, embedded in polymer	Mainly oxidised PA6	In the subsurface and cracks	Degraded with some plain surface, round-shaped cracks	More hydrolysis than plain PA6, no SiO_2 accumulation
PA6/TiO_2	Yes, embedded in polymer	Mainly oxidised PA6	Yes	Very degraded, highly porous in the outer surface and highly round-shaped cracked (with TiO_2 in the tips)	Much more oxidation than plain PA6, large TiO_2 accumulation
PA6/ZnO	Yes, embedded in polymer + free aggregates	Mainly strongly hydrolysed PA6	Some accumulation in the subsurface	Very degraded, highly porous (sponge-like), large broken fragments	Much more hydrolysis than plain PA6
PA6/MWCNT	Yes, free + embedded	PA6 (degraded)	Not observable	Plain surface, deep sharp-edged cracks	More hydrolysis and less oxidation than plain PA6
PA6/67G	Isolated (few)	Oxidised and hydrolysed PA6 (more oxidised than plain PA6)	Yes	Degraded, with plates all over a plain surface	More oxidation and hydrolysis than plain PA6, some clays accumulation
PA6/$67G_{small}$	Isolated (few)	Oxidised and hydrolysed PA6 (similar to plain PA6)	Yes	Degraded, with plates all over a plain surface	More oxidation and hydrolysis than plain PA6, strong clays accumulation

Total release has to be determined case by case and cannot be indirectly predicted based on the characterisation of the aged NCs until there are no standard procedures established for the full process.

4. Conclusions

The most used nanofillers in industrial processes for PA6 NCs (including SiO_2 NPs, ZnO NPs, TiO_2 NPs, MWCNT and nanoclays) were surface functionalised to improve their compatibility with PA6 and PA6 NCs were prepared. These NCs were exposed to accelerated weathering processes (UV irradiation, temperature, and simulated rain) to study NM release during their use phase.

Nanofillers used have different physicochemical properties, including different shapes, which affected polymer degradation and therefore polymer thermal, chemical, and mechanical properties (summary of observations in Table 3). Therefore, large differences were observed when comparing the results on the mechanism of polymer degradation and consequent potential release of nanofillers for the different NCs. Strong surface degradation was observed (SEM and FTIR) in the cases of PA6/TiO_2 and PA6/ZnO, although following different degradation pathways: Nano-TiO_2 acted as photocatalyst and degrades the polymer around the particles, leading to isolated aggregates on the surface, while nano-ZnO and/or dissolved Zn^{2+} catalyse amide hydrolysis leading to direct release of different species (smaller NPs and ions) not observed on the surface. In both cases, the release of significant amounts of polymer fragments was observed. PA6/MWCNT NCs suffered amide hydrolysis and physical cracking was detected. However, the other NCs (SiO_2 and nanoclays) did not experience significant chemical degradation of the matrix, although NM accumulation in the outer layers was observed for silica and nanoclays NCs. Surface damages never reached the 100 μm mean-depth observed in plain PA6, which may be attributed to the higher opacity and crystallinity of the NCs due to the presence of nanofillers. Schematic representation of the different mechanisms followed by the different NCs is depicted in Scheme 1.

The quantification and characterisation of released materials collected from the run-off waters sometimes pointed in different directions than NC surface characterisation, due to a combination of processes taken place during the ageing process. MWCNT and ZnO NCs presented a higher material release: Releases from PA6/ZnO NCs could be explained by the strong polymer hydrolysis and NM dissolution processes during ageing; and the case of PA6/MWCNT due to stronger physical polymer degradation that caused direct release of small fragments of NC. Additionally, low releases measured for PA6/TiO_2 are explained by polymer degradation into not detected volatiles and a subsequent TiO_2 accumulation in the NC surface.

In summary, this work shows the importance of the chemical nature of nanofillers on the degradation of nano-enabled products when exposed to weathering conditions, and their consequent effect on NMs releases. Moreover, it indicates the importance of combining the NC and released material characterisation to fully understand the mechanism causing release (concentration and form of release). The work presented in this paper combines different analytical techniques that contribute to the identification of the route of exposure as well as the identification of the exposure relevant material towards a meaningful exposure assessment: NMs in some cases tend to accumulate in the NC surface increasing potential dermal exposure to the consumer, while in other cases they are released with the rain waters leading to potential environmental exposures. These results are therefore an important input for the human and environmental risk assessment of nano-enabled products, since release quantification values obtained in this work can be used as direct inputs for exposure assessment in risk and impact assessment analysis. Furthermore, the insights on the mechanism of release followed by NM with different chemical nature, particle shape and size will contribute to the design strategies towards

safer nano-enabled products along their life cycle (implementation of the safe-by-design concept in the industrial innovation processes).

Declaration of Competing Interest

The authors declare that they have no known competing financial interests or personal relationships that could have appeared to influence the work reported in this paper.

Acknowledgements

The research leading to these results was funded by the project "Toxicological impact of nanomaterials derived from processing, weathering and recycling from polymer nanocomposites used in various industrial applications" (NANOPOLYTOX) from the European Community's Seventh Framework Programme (FP7/2007–2013) under Grant Agreement n. 247899.

Appendix A. Supplementary data

Supplementary data to this article can be found online at https://doi.org/10.1016/j.impact.2020.100260.

References

Abdelwahab, M., Codou, A., Anstey, A., Mohanty, A.K., Misra, M., 2020. Studies on the dimensional stability and mechanical properties of nanobiocomposites from polyamide 6-filled with biocarbon and nanoclay hybrid systems. Compos. Part A Appl. Sci. Manuf. 129. https://doi.org/10.1016/j.compositesa.2019.105695.

Achhammer, B.G., Reinhart, F.W., Kline, G.M., 1951. Mechanism of the degradation of polyamides. J. Res. Natl. Bur. Stand. (1934) 46, 391–421. https://doi.org/10.6028/jres.046.044.

Al Sheheri, S.Z., Al-Amshany, Z.M., Al Sulami, Q.A., Tashkandi, N.Y., Hussein, M.A., El-Shishtawy, R.M., 2019. The preparation of carbon nanofillers and their role on the performance of variable polymer nanocomposites. Des. Monomers Polym. 22, 8–53. https://doi.org/10.1080/15685551.2019.1565664.

Alix, S., Follain, N., Tenn, N., Alexandre, B., Bourbigot, S., Soulestin, J., Marais, S., 2012. Effect of highly exfoliated and oriented organoclays on the barrier properties of polyamide 6 based nanocomposites. J. Phys. Chem. C 116, 4937–4947. https://doi.org/10.1021/jp2052344.

Battegazzore, D., Sattin, A., Maspoch, M.L., Frache, A., 2019. Mechanical and barrier properties enhancement in film extruded bio-polyamides with modified nanoclay. Polym. Compos. 40, 2617–2628. https://doi.org/10.1002/pc.25056.

Bello, D., Wardle, B.L., Yamamoto, N., Guzman, deVilloria R., Garcia, E.J., Hart, A.J., Ahn, K., Ellenbecker, M.J., Hallock, M., 2009. Exposure to Nanoscale Particles and Fibers during Machining of Hybrid Advanced Composites Containing Carbon Nanotubes. https://doi.org/10.1007/s11051-008-9499-4.

Bilotti, E., Duquesne, E., Deng, H., Zhang, R., Quero, F., Georgiades, S.N., Fischer, H.R., Dubois, P., Peijs, T., 2014. In situ polymerised polyamide 6/sepiolite nanocomposites: effect of different interphases. Eur. Polym. J. 56, 131–139. https://doi.org/10.1016/j.eurpolymj.2014.04.004.

Carroccio, S., Puglisi, C., Montaudo, G., 2003. New vistas in the photo-oxidation of nylon 6. Macromolecules 36, 7499–7507. https://doi.org/10.1021/ma0344137.

Chaupart, N., Serpe, G., Verdu, J., 1998. Molecular weight distribution and mass changes during polyamide hydrolysis. Polymer (Guildf) 39, 1375–1380. https://doi.org/10.1016/S0032-3861(97)00414-X.

Chen, Z., Meng, H., Xing, G., Yuan, H., Zhao, F., Liu, R., Chang, X., Gao, X., Wang, T., Jia, G., Ye, C., Chai, Z., Zhao, Y., 2008. Age-related differences in pulmonary and cardiovascular responses to SiO2 nanoparticle inhalation: nanotoxicity has susceptible population. Environ. Sci. Technol. 42, 8985–8992.

Chen, H.M., Feng, C.X., Zhang, W. Bin, Yang, J.H., Huang, T., Zhang, N., Wang, Y., 2013. Hydrolytic degradation behavior of poly(l-lactide)/carbon nanotubes nanocomposites. Polym. Degrad. Stab. 98, 198–208. https://doi.org/10.1016/j.polymdegradstab.2012.10.009.

da Silva Freitas, D., Claudio Mendes, L., 2020. Water resistance, mechanical, and morphological characteristics in polyamide-6/zirconium phosphate nanocomposites. J. Compos. Mater. 54, 259–269. https://doi.org/10.1177/0021998319857120.

Davis, A., Sims, D., 1983. Weathering of Polymers, 1st ed. Springer Netherlands, Amsterdam (The Netherlands).

Davis, R.D., Gilman, J.W., VanderHart, D.L., 2003. Processing degradation of polyamide 6/montmorillonite clay nanocomposites and clay organic modifier. Polym. Degrad. Stab. 79, 111–121. https://doi.org/10.1016/S0141-3910(02)00263-X.

De Volder, M.F.L., Tawfick, S.H., Baughman, R.H., Hart, A.J., 2013. Carbon nanotubes: present and future commercial applications. Science 339, 535–539. https://doi.org/10.1126/science.1222453.

Dintcheva, N.T., Arrigo, R., Catalanotto, F., Morici, E., 2015. Improvement of the photostability of polystyrene-block-polybutadiene-block-polystyrene through carbon nanotubes. Polym. Degrad. Stab. 118, 24–32. https://doi.org/10.1016/j.polymdegradstab.2015.04.011.

Du, J., Wang, S., You, H., Zhao, X., 2013. Understanding the toxicity of carbon nanotubes in the environment is crucial to the control of nanomaterials in producing and processing and the assessment of health risk for human: a review. Environ. Toxicol. Pharmacol. 36, 451–462. https://doi.org/10.1016/j.etap.2013.05.007.

Duncan, T.V., 2015. Release of engineered nanomaterials from polymer nanocomposites: the effect of matrix degradation. ACS Appl. Mater. Interfaces 7, 20–39. https://doi.org/10.1021/am5062757.

Fadel, T.R., Steevens, J.A., Thomas, T.A., Linkov, I., 2015. The challenges of nanotechnology risk management. Nano Today 10, 6–10. https://doi.org/10.1016/j.nantod.2014.09.008.

Fernández-Rosas, E., Vilar, G., Janer, G., González-Gálvez, D., Puntes, V., Jamier, V., Aubouy, L., Vázquez-Campos, S., 2016. Influence of nanomaterial compatibilization strategies on polyamide nanocomposites properties and nanomaterial release during the use phase. Environ. Sci. Technol. 50, 2584–2594. https://doi.org/10.1021/acs.est.5b05727.

Fornes, T.D., Yoon, P.J., Paul, D.R., 2003. Polymer matrix degradation and color formation in melt processed nylon 6/clay nanocomposites. Polymer (Guildf) 44, 7545–7556. https://doi.org/10.1016/j.polymer.2003.09.034.

Francisco, D.L., Paiva, L.B., Aldeia, W., 2019. Advances in polyamide nanocomposites: A review. Polym. Compos. https://doi.org/10.1002/pc.24837.

Franze, B., Strenge, I., Engelhard, Carsten, Egger, S., Lehmann, R., Height, M., Loessner, M., Schuppler, M., Chaloupka, K., Malam, Y., Seifalian, A.M., Chen, X., Schluesener, H.J., Lee, H.Y., Park, H.K., Lee, Y.M., Kim, K., Park, S.B., Farkas, J., Peter, H., Christian, P., Hasselloev, M., Elechiguerra, J.L., Burt, J.L., Morones, J.R., Camacho-Bragado, A., Gao, X., Lara, H.H., Yacaman, M.J., Panyala, N., Mendez, E.P., Havel, J., Phalen, R.F., Morrow, P.E., Larese, F.F., D'Agostin, F., Crosera, M., Adami, G., Renzi, N., Bovenzi, M., Maina, G., Vogt, A., Combadiere, B., Hadam, S., Stieler, K., Lademann, J., Schaefer, H., Rosenman, K., Moss, A., Kon, S., Sue, Y., Lee, J., Wang, M., Lin, T., Sung, J., Huang, J., Marshall, J.P., Schneider, R.P., Gulbranson, S.H., Hud, J.A., Hansen, R.C., Luoma, S., Ho, Y., Bryan, G., Croteau, M.N., Misra, S.K., Luoma, S.N., Valsami-Jones, E., Albright, L., Wilson, E., Griffitt, R., Luo, J., Gao, J., Bonzongo, J., Barber, D., Howard, A., Engelhard, C., Krystek, P., Ulrich, A., Garcia, C.C., Manohar, S., Ritsema, R., Scheffer, A., Engelhard, C., Sperling, M., Buscher, W., Jimenez, M.S., Gomez, M.T., Bolea, E., Laborda, F., Castillo, J., Engelhard, C., Vielhaber, T., Scheffer, A., Brocksieper, M., Buscher, W., Karst, U., Garcia, C., Murtazin, A., Groh, S., Horvatic, V., Niemax, K., Murtazin, A., Groh, S., Niemax, K., Gschwind, S., Flamigni, L., Koch, J., Borovinskaya, O., Groh, S., Niemax, K., Günther, D., Degueldre, C., Favarger, P., Ho, K., Chan, W., Laborda, F., Jimenez-Lamana, J., Bolea, E., Castillo, J.R., Degueldre, C., Favarger, P., Wold, S., Zook, J.M., Long, S.E., Cleveland, D., Geronimo, C.L.A., MacCuspie, R.I., Kittler, S., Greulich, C., Diendorf, J., Koller, M., Epple, M., Almagro, B., Ganan-Calvo, A.M., Hidalgo, M., Canals, A., 2012. Single particle inductively coupled plasma mass spectrometry: evaluation of three different pneumatic and piezo-based sample introduction systems for the characterization of silver nanoparticles. J. Anal. At. Spectrom. 27, 1074. https://doi.org/10.1039/c2ja00003b.

Froggett, S.J., Clancy, S.F., Boverhof, D.R., Canady, R.A., 2014. A Review and Perspective of Existing Research on the Release of Nanomaterials from Solid Nanocomposites.

Fujiwara, K., Suematsu, H., Kiyomiya, E., Aoki, M., Sato, M., Moritoki, N., 2008. Size-dependent toxicity of silica nano-particles to Chlorella kessleri. J. Environ. Sci. Health A Tox. Hazard. Subst. Environ. Eng. 43, 1167–1173. https://doi.org/10.1080/10934520802171675.

García, M., García-Turiel, J., Norder, B., Chavez, F., Kooi, B.J., van Zyl, W.E., Verweij, H., Blank, D.H.A., 2004. Polyamide-6/silica nanocomposites. Adv. Eng. Mater. 6, 724–729. https://doi.org/10.1002/adem.200400059.

Ging, J., Tejerina-Anton, R., Ramakrishnan, G., Nielsen, M., Murphy, K., Gorham, J.M., Nguyen, T., Orlov, A., 2014. Development of a conceptual framework for evaluation of nanomaterials release from nanocomposites: environmental and toxicological implications. Sci. Total Environ. 473–474, 9–19. https://doi.org/10.1016/j.scitotenv.2013.11.135.

Golanski, L., Guiot, A., Pras, M., Malarde, M., Tardif, F., 2012. Release-ability of nano fillers from different nanomaterials (toward the acceptability of nanoproduct). J. Nanopart. Res. 14, 962. https://doi.org/10.1007/s11051-012-0962-x.

Gottschalk, F., Sun, T., Nowack, B., 2013. Environmental concentrations of engineered nanomaterials : review of modeling and analytical studies. Environ. Pollut. https://doi.org/10.1016/j.envpol.2013.06.003.

Harper, S., Wohlleben, W., Doa, M., Nowack, B., Clancy, S., Canady, R., Maynard, A., 2015. Measuring nanomaterial release from carbon nanotube composites: review of the state of the science. J. Phys. Conf. Ser. 617, 012026. https://doi.org/10.1088/1742-6596/617/1/012026.

Hischier, R., Walser, T., 2012. Life cycle assessment of engineered nanomaterials: state of the art and strategies to overcome existing gaps. Sci. Total Environ. 425, 271–282. https://doi.org/10.1016/j.scitotenv.2012.03.001.

International Standards Organization, 2012. ISO 527-2:2012 - Plastics - Determination of Tensile Properties - Part 2: Test Conditions for Moulding and Extrusion Plastics.

ISO, 2013. ISO 4892-2:2013 Plastics – Methods of Exposure to Laboratory Light Sources – Part 2: Xenon-arc Lamps. International Standards Organization.

Jacobs, D.S., Huang, S.R., Cheng, Y.L., Rabb, S.A., Gorham, J.M., Krommenhoek, P.J., Yu, L.L., Nguyen, T., Sung, L., 2016. Surface degradation and nanoparticle release of a commercial nanosilica/polyurethane coating under UV exposure. J. Coat. Technol. Res. 13, 735–751. https://doi.org/10.1007/s11998-016-9796-2.

Jang, B.N., Wilkie, C.A., 2005. The effect of clay on the thermal degradation of polyamide 6 in polyamide 6/clay nanocomposites. Polymer (Guildf) 46, 3264–3274. https://doi.org/10.1016/j.polymer.2005.02.078.

Kalpokait-Dičkuvien, R., Lukošiūt, I., Ččsnien, J., Baltušnikas, A., Brinkien, K., 2013. Influence of the Organically Modified Nanoclay on Properties of Cement Paste.

Kango, S., Kalia, S., Celli, A., Njuguna, J., Habibi, Y., Kumar, R., 2013. Surface modification of inorganic nanoparticles for development of organic–inorganic nanocomposites—A review. Prog. Polym. Sci. 38, 1232–1261. https://doi.org/10.1016/j.progpolymsci.2013.02.003.

Kashiwagi, T., Harris, R.H., Zhang, X., Briber, R.M., Cipriano, B.H., Raghavan, S.R., Awad, W.H., Shields, J.R., 2004. Flame retardant mechanism of polyamide 6–clay nanocomposites. Polymer (Guildf) 45, 881–891. https://doi.org/10.1016/j.polymer.2003.11.036.

Kashiwagi, T., Du, F., Winey, K.I., Groth, K.M., Shields, J.R., Bellayer, S.P., Kim, H., Douglas, J.F., 2005. Flammability properties of polymer nanocomposites with single-walled carbon nanotubes: effects of nanotube dispersion and concentration. Polymer (Guildf) 46, 471–481. https://doi.org/10.1016/j.polymer.2004.10.087.

Kausar, A., 2020. A review of high performance polymer nanocomposites for packaging applications in electronics and food industries. J. Plast. Film Sheet. https://doi.org/10.1177/8756087919849459.

Kiliaris, P., Papaspyrides, C.D., Pfaendner, R., 2009. Influence of accelerated aging on clay-reinforced polyamide 6. Polym. Degrad. Stab. 94, 389–396. https://doi.org/10.1016/j.polymdegradstab.2008.11.016.

Kim, Y.S., Davis, R., Uddin, N., Nyden, M., Rabb, S.A., 2016. Quantification of nanoparticle release from polymer nanocomposite coatings due to environmental stressing. J. Occup. Environ. Hyg. 13, 303–313. https://doi.org/10.1080/15459624.2015.1116696.

Klun, U., Krzan, A., 2002. Degradation of polyamide-6 by using metal salts as catalyst. Polym. Adv. Technol. 13, 817–822. https://doi.org/10.1002/pat.250.

Koivisto, A.J., Jensen, A.C.Ø., Kling, K.I., Nørgaard, A., Brinch, A., Christensen, F., Jensen, K.A., 2017. Quantitative material releases from products and articles containing manufactured nanomaterials: towards a release library. NanoImpact 5, 119–132. https://doi.org/10.1016/j.impact.2017.02.001.

Krejsa, M.R., Middleton, J.C., 1997. NMR Analysis of UV- and Heat-Aged Nylon-6. 6 9297. pp. 4695–4703.

Kroes, G.H., 1963. The photo-oxidation of nylon 6 and 66. Recl. des Trav. Chim. des Pays-Bas 82, 979–987. https://doi.org/10.1002/recl.19630821006.

Krug, H.F., 2014. Nanosafety research–are we on the right track? Angew. Chem. Int. Ed. Eng. 53, 12304–12319. https://doi.org/10.1002/anie.201403367.

Laoutid, F., François, D., Paint, Y., Bonnaud, L., Dubois, P., 2013. Using nanosilica to fine-tune morphology and properties of polyamide 6/poly(propylene) blends. Macromol. Mater. Eng. 298, 328–338. https://doi.org/10.1002/mame.201200047.

López-Serrano, A., Olivas, R.M., Landaluze, J.S., Cámara, C., 2014. Nanoparticles: a global vision. Characterization, separation, and quantification methods. Potential environmental and health impact. Anal. Methods 6, 38–56. https://doi.org/10.1039/C3AY40517F.

Mackevica, A., Hansen, S.F., 2016. Release of nanomaterials from solid nanocomposites and consumer exposure assessment - a forward-looking review. Nanotoxicology 10, 641–653. https://doi.org/10.3109/17435390.2015.1132346.

Macknight, W.J., Lenz, R.W., Musto, P.V., Somani, R.J., 1985. Binary alloys of nylon 6 and ethylene-methacrylic acid copolymers: morphological, thermal and mechanical analysis. Polym. Eng. Sci. 25, 1124–1134. https://doi.org/10.1002/pen.760251803.

Maynard, A.D., Aitken, R.J., Butz, T., Colvin, V., Donaldson, K., Oberdörster, G., Philbert, M.A., Ryan, J., Seaton, A., Stone, V., Tinkle, S.S., Tran, L., Walker, N.J., Warheit, D.B., 2006. Safe handling of nanotechnology. Nature 444, 267–269. https://doi.org/10.1038/444267a.

Mistretta, M.C., Fontana, P., Ceraulo, M., Morreale, M., La Mantia, F.P., 2015. Effect of compatibilization on the photo-oxidation behaviour of polyethylene/polyamide 6 blends and their nanocomposites. Polym. Degrad. Stab. 112, 192–197. https://doi.org/10.1016/j.polymdegradstab.2015.01.002.

Mitrano, D.M., Motellier, S., Clavaguera, S., Nowack, B., 2015. Review of nanomaterial aging and transformations through the life cycle of nano-enhanced products. Environ. Int. 77, 132–147. https://doi.org/10.1016/j.envint.2015.01.013.

Miyauchi, M., Li, Y., Shimizu, H., 2008. Enhanced degradation in nanocomposites of TiO 2 and biodegradable polymer. Environ. Sci. Technol. 42, 4551–4554. https://doi.org/10.1021/es800097n.

Monticelli, O., Musina, Z., Frache, A., Bellucci, F., Camino, G., Russo, S., 2007. Influence of compatibilizer degradation on formation and properties of PA6/organoclay nanocomposites. Polym. Degrad. Stab. 92, 370–378. https://doi.org/10.1016/j.polymdegradstab.2006.12.010.

Nel, A.E., Parak, W.J., Chan, W.C.W., Xia, T., Hersam, M.C., Brinker, C.J., Zink, J.I., Pinkerton, K.E., Baer, D.R., Weiss, P.S., 2015. Where are we heading in nanotechnology environmental health and safety and materials characterization? ACS Nano 9, 5627–5630. https://doi.org/10.1021/acsnano.5b03496.

Nguyen, T., Pellegrin, B., Bernard, C., Gu, X., Gorham, J.M., Stutzman, P., Stanley, D., Shapiro, A., Byrd, E., Hettenhouser, R., Chin, J., 2011. Fate of nanoparticles during life cycle of polymer nanocomposites. J. Phys. Conf. Ser. 304, 012060. https://doi.org/10.1088/1742-6596/304/1/012060.

Nguyen, T., Pellegrin, B., Bernard, C., Rabb, S., Stuztman, P., Gorham, J.M., Gu, X., Yu, L.L., Chin, J.W., 2012. Characterization of surface accumulation and release of nanosilica during irradiation of polymer nanocomposites by ultraviolet light. J. Nanosci. Nanotechnol. 12, 6202–6215. https://doi.org/10.1166/jnn.2012.6442.

Njuguna, J., Pielichowski, K., Zhu, H. (Eds.), 2014. Health and Environmental Safety of Nanomaterials: Polymer Nancomposites and Other Materials Containing Nanoparticles. Elsevier Science.

Nowack, B., Brouwer, C., Geertsma, R.E., Heugens, E.H.W., Ross, B.L., Toufektsian, M., Wijnhoven, S.W.P., Aitken, R.J., 2013. Analysis of the occupational, consumer and environmental exposure to engineered nanomaterials used in 10 technology sectors. Nanotoxicology 7, 1152–1156. https://doi.org/10.3109/17435390.2012.711863.

Pellegrin, B., Nguyen, T., Mermet, L., Shapiro, A., Gu, X., Chin, J., 2009. Degradation and nanoparticle release of polymer nanocomposites exposed to UV. Nanotech 1, 94–97.

Rabek, J.F., 1995. Polymer Photodegradation: Mechanisms and Experimental Methods. Springer Netherlands, Amsterdam (The Netherlands). https://doi.org/10.1007/978-94-011-1274-1.

Ray, S.S., Yamada, K., Okamoto, M., Ueda, K., 2002. Polylactide-layered silicate nanocomposite: a novel biodegradable material. Nano Lett. 2, 1093–1096. https://doi.org/10.1021/nl0202152.

Read, S.A.K., Jiménez, A.S., Ross, B.L., Aitken, R.J., van Tongeren, M., 2014. Nanotechnology and Exposure Scenarios, Handbook of Nanosafety: Measurement, Exposure and Toxicology. Elsevierhttps://doi.org/10.1016/B978-0-12-416604-2.00002-0.

Rhiem, S., Barthel, A.-K., Meyer-Plath, A., Hennig, M.P., Wachtendorf, V., Sturm, H., Schäffer, A., Maes, H.M., 2016. Release of 14C-labelled carbon nanotubes from polycarbonate composites. Environ. Pollut. 215, 356–365. https://doi.org/10.1016/j.envpol.2016.04.098.

Shamey, R., Sinha, K., 2003. A review of degradation of nylon 6. 6 as a result of exposure to environmental conditions. Rev. Prog. Color. Relat. Top. 33, 93–107. https://doi.org/10.1111/j.1478-4408.2003.tb00147.x.

Shelley, J.S., Mather, P.T., DeVries, K.L., 2001. Reinforcement and environmental degradation of nylon-6/clay nanocomposites. Polymer (Guildf) 42, 5849–5858. https://doi.org/10.1016/S0032-3861(00)00900-9.

Smith, J.N., White, G.V., White, M.I., Bernstein, R., Hochrein, J.M., 2012. Characterization of volatile nylon 6.6 thermal-oxidative degradation products by selective isotopic labeling and cryo-GC/MS. J. Am. Soc. Mass Spectrom. 23, 1579–1592. https://doi.org/10.1007/s13361-012-0415-x.

Stamm, H., Gibson, N., Anklam, E., 2012. Detection of nanomaterials in food and consumer products: bridging the gap from legislation to enforcement. Food Addit. Contam. Part A. Chem. Anal. Control. Expo. Risk Assess. 29, 1175–1182. https://doi.org/10.1080/19440049.2012.689778.

Sung, L., Stanley, D., Gorham, J.M., Rabb, S., Gu, X., Yu, L.L., Nguyen, T., 2014. A quantitative study of nanoparticle release from nanocoatings exposed to UV radiation. J. Coat. Technol. Res. 12, 121–135. https://doi.org/10.1007/s11998-014-9620-9.

Vílchez, A., Fernández-Rosas, E., González-Gálvez, D., Vázquez-Campos, S., 2015. Nanomaterials release from nano-enabled products. In: Viana, M. (Ed.), Indoor and Outdoor Nanoparticles: Determinants of Release and Exposure Scenarios (the Handbook of Environmental Chemistry Series). Springer, Berlin Heidelberg, Switzerland, pp. 1–32. https://doi.org/10.1007/698_2015_409.

von der Kammer, F., Ferguson, P.L., Holden, P.A., Masion, A., Rogers, K.R., Klaine, S.J., Koelmans, A.A., Horne, N., Unrine, J.M., 2012. Analysis of engineered nanomaterials in complex matrices (environment and biota): general considerations and conceptual case studies. Environ. Toxicol. Chem. 31, 32–49. https://doi.org/10.1002/etc.723.

Wohlleben, W., Neubauer, N., 2016. Quantitative rates of release from weathered nanocomposites are determined across 5 orders of magnitude by the matrix, modulated by the embedded nanomaterial. NanoImpact 1, 39–45. https://doi.org/10.1016/j.impact.2016.01.001.

Wohlleben, W., Kuhlbusch, T.A., Schnekenburger, J., Lehr, C.-M., 2014a. Safety of Nanomaterials along their Lifecycle: Release, Exposure, and Human Hazards. CRC Press, LLC Taylor & Francis, Boca Raton, CL, USA.

Wohlleben, W., Vilar, G., Fernández-Rosas, E., González-Gálvez, D., Gabriel, C., Hirth, S., Frechen, T., Stanley, D., Gorham, J., Sung, L.-P., Hsueh, H.-C., Hsiang-Chun H.-C., Chuang, Y.-F., Nguyen, T., Vazquez-Campos, S., 2014b. A pilot interlaboratory comparison of protocols that simulate aging of nanocomposites and detect released fragments. Environ. Chem. 11, 402–418. https://doi.org/10.1071/EN14072.

Wohlleben, W., Meyer, J., Muller, J., Müller, P., Vilsmeier, K., Stahlmecke, B., Kuhlbusch, T.A.J., 2016. Release from nanomaterials during their use phase: combined mechanical and chemical stresses applied to simple and multi-filler nanocomposites mimicking wear of nano-reinforced tires. Environ. Sci. Nano. https://doi.org/10.1039/C6EN00094K.

Wohlleben, W., Kingston, C., Carter, J., Sahle-Demessie, E., Vázquez-Campos, S., Acrey, B., Chen, C.-Y., Walton, E., Egenolf, H., Müller, P., Zepp, R., 2017. NanoRelease: pilot interlaboratory comparison of a weathering protocol applied to resilient and labile polymers with and without embedded carbon nanotubes. Carbon N. Y. 113, 346–360. https://doi.org/10.1016/J.CARBON.2016.11.011.

Zhao, Y., Qiu, Z., Yang, W., 2009. Effect of multi-walled carbon nanotubes on the crystallization and hydrolytic degradation of biodegradable poly (L -lactide). Compos. Sci. Technol. 69, 627–632. https://doi.org/10.1016/j.compscitech.2008.12.008.

Release mechanisms for PA6 nanocomposites under weathering conditions simulating their outdoor uses

E. Fernández-Rosas,[a] V. Pomar-Portillo,[a] D. González-Gálvez,[a] G. Vilar,[a] and S. Vázquez-Campos[a]

[a]LEITAT Technological Center, C/de la Innovació 2, 08225 Terrassa (Barcelona), Spain

Supporting Information

Index

Section SI_1 – NMs physicochemical properties and methods for its characterization

ICP-MS

Samples were directly weighed (0.5g sample) into the microwave vessels using an AG245 Balance (Mettler Toledo), readability 0.0001g. Samples were digested with an acid solution in an analytical microwave digestion system (MARS, CEM, 1600W):

- General (Zn, Al, Fe): 10 ml of 70% HNO_3.
- Si digestion: 10 ml of HNO_3:HCl:HF 5:4:1 mixture (special vessels and ICP-MS injection system).
- Ti digestion: 5 ml of 70% HNO_3 and 5 ml of 49% HF.

Specifically, the microwave digestion program consists on heating from room temperature to 200 °C in 10 min, then maintain this temperature 15 min and, finally, cold down to room temperature to manipulate the samples safely. After having carried out the described digestion program, all samples were filled with MilliQ water to 50 ml. Then, further dilutions were made with 2% HNO_3 aqueous solution to obtain the desired concentrations for ICP-MS characterization.

ICP-MS analyses (Agilent 7500, Agilent Technologies) were performed by the Scientific & Technical Services Unit at LEITAT (Dr. Beatriz Guerrero, Clara Bagán and Aleix Conesa). Samples are diluted properly with an aqueous solution of HNO_3 2% w/w. The quantification is done by interpolation in a standard curve obtained from commercial 1000 ppm standards of the elements under study (Sigma Aldrich).

TEM

Raw NMs were analyzed by high-resolution transmission electron microscope (HR-TEM; JEM 2010, JEOL Ltd.) coupled to an EDX detector (SDD X-Max^N, Oxford Instruments).

NM sizes and distributions were determined using ImageJ (http://imagej.nih.gov/ij/).[1,2]

TGA

Hi-Res TGA was performed (Q500, TA instruments, USA) applying a temperature increase of 10°C/min from 30-1000 °C and gas flow rate of 10 mL/min. TGA were performed both under nitrogen atmosphere (Figure S6).

Dynamic light scattering and ζ-Potential

Initially, 1 mg/ml NM dispersions in water were prepared by tip sonication (3 mm tip, 15 min, 20% amplitude) (Ultrasonic Processors – VCX Series, 750 Watts, Sonics & Materials Inc.)

Hydrodynamic size and stability of the sonicated NM in water was studied at different times after the sonication process (90 min and 24 h)

Hydrodynamic size was measured by dynamic light scattering (DLS) using a Zetasizer (nano series Nano ZS, Malvern Instruments Ltd.). The dispersion stability was studied observing hydrodynamic size and derived count rate evolutions and measuring the ζ-Potential of the samples (Zetasizer Nano ZS, Malvern Instruments Ltd.).

Both hydrodynamic size and ζ-potential were measured using disposable capillary cells (DTS1070), after two minutes of equilibration at 25 °C.

UV-Visible Spectrophotometry

Initially, 1 mg/ml NM dispersions in water were prepared by tip sonication (3 mm tip, 15 min, 20% amplitude) (Ultrasonic Processors – VCX Series, 750 Watts, Sonics & Materials Inc.). 0.1 mg/ml dispersions were prepared by dilution in Mili-Q water and vortex mixing.

UV-Vis analyses were performed in 190-900 nm wavelength range at 1 nm/s rate (UV-240, Shimadzu Corp.).

FTIR

NMs were analyzed by Fourier Transform Infrared Spectroscopy by Attenuated Total Reflection (ATR-FTIR spectroscopy; IR Affinity-1 8400, Shimadzu).

BET

Surface area and porosity of nanoclays were measured by a multipoint isotherm Brunauer–Emmett–Teller (BET) assay (equilibration time 60s), using N_2 as adsorbate, in a BET surface area analyser (Nova 2200e series, Quantachrome, Germany).

Prior to BET analyses, the clays were degassed overnight under vacuum at 105 °C. Surface area was calculated using 12 data points of relative pressure in the range of 0.05 to 0.3 ($r^2 > 0.995$, in all analyses), and porosity was obtained using the Barrett–Joyner–Halenda (BJH) method in the desorption branch of the isotherm.

XRD

X-ray crystallography was performed by X-Ray powder diffraction (X'Pert 1 Powder, Cu Kα radiation, Philips Analytical) to identify the crystalline composition of each nanomaterial.

Table S1 Physicochemical properties of the NM used as nanofillers in PA6.

		SiO_2-OH	TiO_2-OH	ZnO-OH	MWCNT-NH_2	MMTdell67G	MMTdell67G$_{small}$
ICP-MS		28.5% Si	37.2% Ti	79.9% Zn	0.04% Al 0.13% Fe	17.74% Si	17.39% Si
TEM (nm)		14 ± 9	18 ± 8	30 ± 17	25 - 27 (ø)	25 - 3230	25 - 820
TGA (% residue in N_2)		89.8	79.6	89.6	33.0	54.7	54.8
ζ-Ave Diam (nm)	90 s	332.8	623.3	1047.0	---	2816.0	1657.0
	24 h	94.5	341.5	881.2		341.9	318.8
ζ-Pot (mV)		-43.7	-27	44.2	-25.2	-26.0	-23.5
UV-Vis (nm)		209	190	373	337	238	239
FTIR (cm^{-1})		799, 1051, 1406, 1610/1547, 2901/2988, ~3321	~650, 1078, 1406, 2910/2970, 3350	~550, 788, 883, 1015/1099, 1420, 2884/2934, 3275	1649, 2116, 3157, ~3350	721, 799, 885, 914, 1005, 1111, 1468, 1647, 2924/2860, 3628	717, 797, 887, 916, 1009, 1108 , 1461, 1647, 2910/2840, 3628
surface area (m^2/g)		122.45	4.843	21.700	23.896	3.521	3.525
porosity (BJH) (cm^3/g)		0.444	0.054	0.108	0.099	0.032	0.027
porous diam. (nm)		10.7	10.4	22.4	3.3	3.9	3.9
XRD (%)		amorphous material	78.8 anatase 21.1 rutile	100 zincite	---	90 smectite 0.5 cristobalite	90 smectite 0.5 cristobalite

Section SI_2 – Conditions of extrusion and injection

Table S2 Conditions of extrusion and injection for PA6 and PA6 NCs.

	EXTRUSION				INJECTION								
NC	**Profile T (°C)**	**Speed (rpm)**	**Pressure (bar)**	**Torque (Nm)**	**Profile T (°C)**	**Dosing (mm)**	**Inject time (s)**	**Inject speed (mm/s)**	**Hold press. (bar)**	**Hold time (s)**	**Cool time (s)**	**Speed screw (rpm)**	**Mould T (°C)**
PA	-	-	-	-	240-240-230-230	50	28	14	135	10	30	120	30
PA/SiO_2	245-240-235-230-225	80	10	0.28	240-240-230	50	28	14	135	10	30	120	30
PA/TiO_2	"	"	"	"	"	"	"	"	"	"	"	"	"
PA/ZnO	"	"	"	"	"	"	"	"	"	"	"	"	"
PA/MWCNT	240-235-235-230-230	180	2-2.5	41-43	280-240	25	1	20	450	10	12	60	40
PA6/67G	240-240-240	250	20	30	245-240-240-240	41	1	31	650	12	8	120	80
PA6/67G_{small}	"	"	"	"	"	"	"	"	"	"	"	"	"

Section SI_3 – DSC results and discussion

Semicrystalline polymer PA6 can exhibit two stable crystalline forms, α and β, and the thermodynamically unstable mesomorphic form γ. They coexist and are present in a different degree depending on the processing conditions. In DSC isotherms the first melting peak (<200 °C) is attributed to form γ, with parallel chains but ordered in a twisted/pleated conformation. Forms α and β, with longer parallel chain axes and intra-/inter-sheet hydrogen bonds respectively, melt at higher temperatures (around 214 °C for α and 220 °C for β).[3] Yet, β and γ forms may reorganise into α during a DSC scan. Furthermore, crystalline organization changes with the addition of nanofillers. The relatively high heating rate applied of 20 °C/min should be enough to minimise this reorganization.

In the present study in the first melting isotherm, γ form was observed in all the samples analysed, though the melting peak shifted from 105-155 °C. In plain PA6 also the presence of the stable crystalline form α was evident in the first melting isotherm, with the characteristic peak at 221 and 219 °C before and after being submitted to ageing conditions respectively (Table S1); nevertheless, only moved from 219 °C to 222 °C in the case of NCs. Referring to form β, in the NCs after injection only was observed in the nanoclay-filled PA6 samples (at approximately 212 °C). After undergoing ageing, melting of form β was apparent in those same NCs and temperatures, but also in PA6/SiO_2 (217 °C), PA6/TiO_2 (212 °C) and PA6/MWCNT (219 °C) in a much reduced degree. Mohamadi and co-workers had demonstrated previously that the addition of nanometric organoclays (i.e., cloisite 20A) increased the presence of the crystalline form β.[4]

Table S3: Values of DSC and percentage of crystallinity

	NC	midpoint T^a_c (°C)	ΔH_c (J/g)	midpoint T^a_m * (°C)	ΔH_m * (J/g)	crystallinity † of the NC (%)	Δ crystallintiy *vs* PA (%)	Δ crystallintiy *vs* AGING (%)
NON-AGED	PA	189,9	79,9 ± 4,1	221,2 126,1	76,5 ± 0,1	40,1%	-	-
	PA/SiO_2-OH	190,9	77,6 ± 1,1	221,5 123,3	68,8 ± 3,3	37,2%	-2,9%	-
	PA/TiO_2-OH	190,6	82,7 ± 0,4	220,9 129,9	77,8 ± 1,8	41,8%	1,7%	-
	PA/ZnO-OH	191,3	81,8 ± 2,0	222,1 129,0	79,0 ± 0,4	42,8%	2,6%	-
	PA/MWCNT-NH_2	196,3	82,1 ± 0,8	221,4 133,4	80,5 ± 1,6	43,6%	3,4%	-
	PA/67G	188,9	73,5 ± 1,8	221,0 153,1	70,2 ± 0,8	37,9%	-2,3%	-
	PA/67G_{small}	189,3	77,4 ± 0,5	221,2 137,4	67,0 ± 2,0	36,3%	-3,9%	-
AGED	PA	190,2	80,5 ± 1,2	218,8 110,6	76,6 ± 2,7	40,2%	-	0,0%
	PA/SiO_2-OH	191,0	77,7 ± 1,8	220,5 120,4	71,4 ± 3,4	38,6%	-1,5%	1,4%
	PA/TiO_2-OH	191,0	76,6 ± 3,7	220,7 132,4	70,4 ± 0,1	37,9%	-2,3%	-4,0%
	PA/ZnO-OH	191,2	78,3 ± 3,7	220,2 104,6	74,1 ± 3,4	40,1%	-0,1%	-2,7%
	PA/MWCNT-NH_2	196,4	80,4 ± 1,0	221,8 109,4	81,4 ± 0,1	44,1%	3,9%	0,5%
	PA/67G	188,9	76,0 ± 1,1	220,7 136,7	72,2 ± 0,0	38,9%	-1,2%	1,1%
	PA/67G_{small}	189,0	76,1 ± 1,4	220,5 139,1	72,6 ± 0,0	39,3%	-0,8%	3,1%

* *obtained from 1st melting*

† *NM content % taken from calcination results (table 3)*

Crystallization temperature (T_c) and the degree of crystallinity (X_c) were determined from DSC crystallization exotherms. Interestingly, crystallinity of plain PA6 and NCs was always above 40% apart from those cases where a melting peak of form β was observable (Table S1). The exception was PA6/SiO_2, with a 37.2% of crystallinity. PA6/MWCNT NC exhibited the highest crystallinity both before and after ageing (43.5% and 44.0% respectively). The presence of TiO_2, ZnO and MWCNT increased crystallinity during injection moulding, but it was only maintained in the PA6/MWCNT NC after ageing. The lowest crystallinity by DSC was determined for PA6 composed with nanoclays and TiO_2 NPs, which showed almost the same crystalline degree as aged PA6/SiO_2 and aged PA6/TiO_2. The general increase of crystallinity with ageing can be explained by a rearrangement of the polymer chains during this process. Ageing reduced crystallinity only in PA6/TiO_2 and especially in PA6/ZnO which can be attributed to the stronger degradation of PA6 observed by FT-IR as well (i.e., amide hydrolysis, chain scission) and, consequently, by a reduced regularity in chain structure and the increasing spaces between chains [5].

Compared to plain polyamide, PA6/SiO_2 and (in a lesser extent) PA6/MWCNT showed narrower melting peaks. It could be caused by still a more reduced presence of the crystalline form β, which could not even be detected in the melting isotherm of PA6[6,7] or could be a direct consequence of a narrower crystallite

size distribution.[8] After ageing, melting occurred in a narrower range of temperatures in all the cases excepting in PA6/ZnO, most probably caused by polymer chains reordering. The broadest melting peak of the latter NC could be caused by a stronger degradation of polyamide (smaller molecular sizes with different thermal stabilities) and/or ZnO NPs aggregation.

DSC thermograms indicated as well that PA6/MWCNT crystallisation midpoint temperature was the highest one, at least 6 °C higher than for plain PA6 both before and after being subjected to ageing. It points clearly to a nucleating effect triggered by the presence of nanotubes in PA6 crystallisation. Other authors had observed before that nanofillers act as heterogeneous sites for spherulite growth in molten polyamide, increasing the crystalline portion [7,9]. It reduces the need for meeting the barrier activation energy of thermal homogeneous nucleation, allowing the NCs crystallization process to begin at higher temperatures.

Essentially, DSC analysis showed that crystalline structures of PA6 consisted predominantly on α form, with a much lower proportion of γ form and traces of β form. The highest crystallinity was shown by nanotube-based NCs independently of the ageing process, and crystallization shifted to higher temperatures (>5 °C). The lowest degree of crystallinity was shown by the silica-based NCs (i.e., PA6/SiO_2, PA6/67G and PA6/67G_{small}). In a specific NC, the proportion of crystalline forms and the degree of crystallinity might influence its performance, as the presence of the more thermodynamically unstable γ phase leads to a lower density and stiffness in the NCs. Reorganisation and degradation of PA6 chains caused by the ageing process modified NCs crystalline structure, which could translate in changes in the performance of the composites.

Section SI_4 – Figures

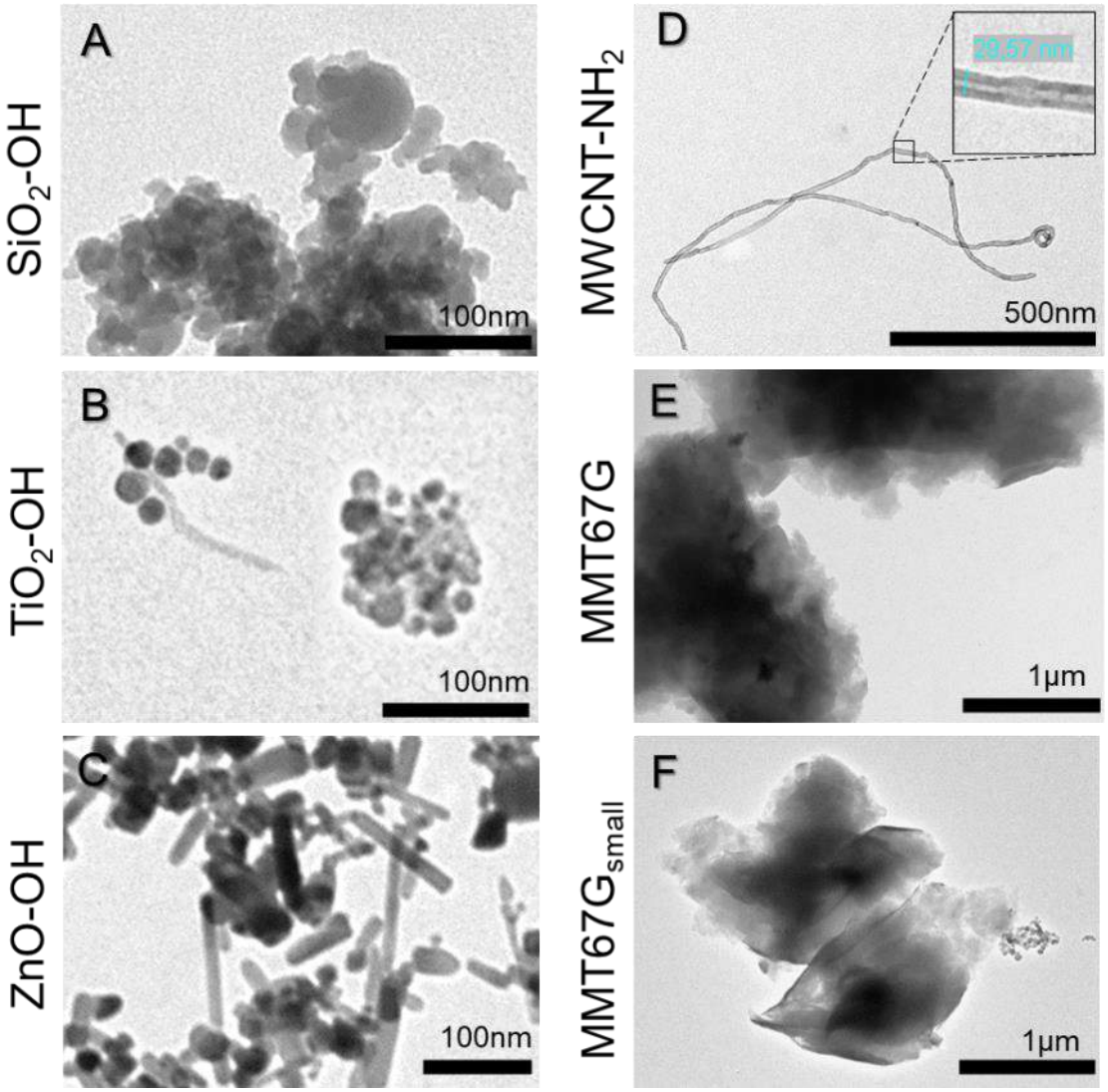

Figure S1: TEM images of the NM used as nanofillers for PA6 NC.

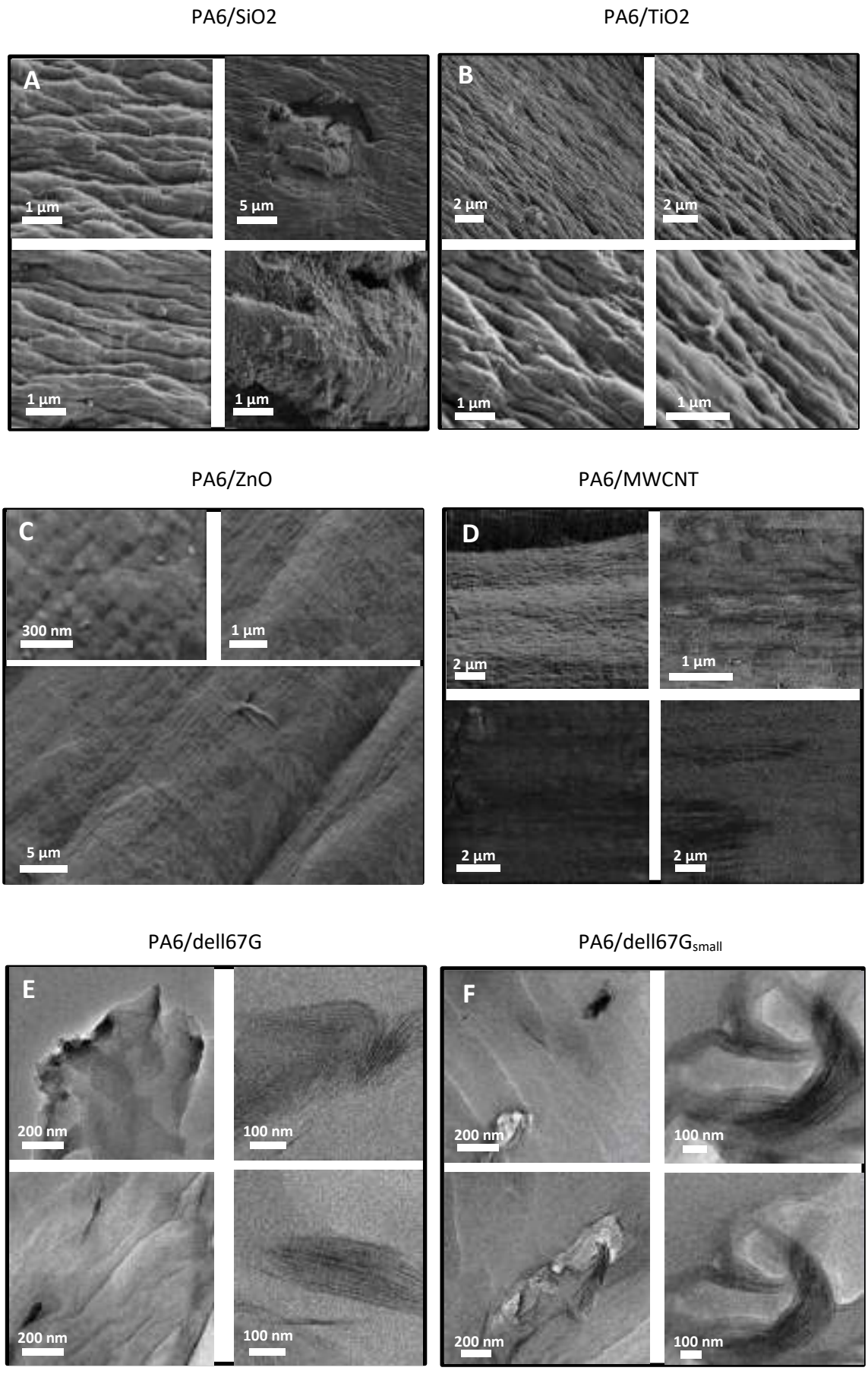

Figure S2: SEM (A-D) and TEM (E-F) microtome cuts of the NCs studied after its injection.

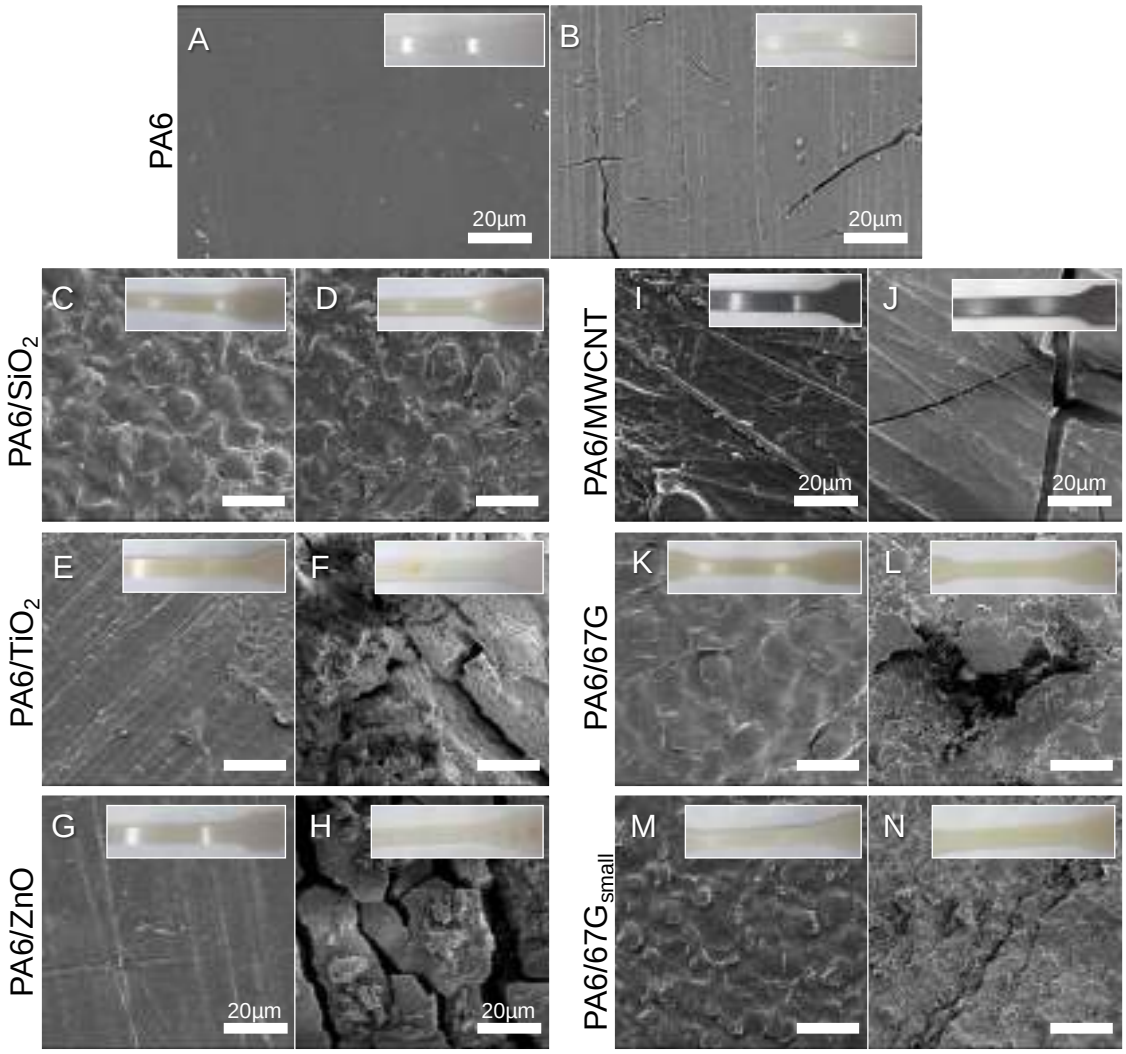

Figure S3: SEM Images of the PA6 NCs surface: non-aged (left) and aged NCs (right); inserts correspond to the specimen appearance at sight. Bar = 50µm except when indicated.

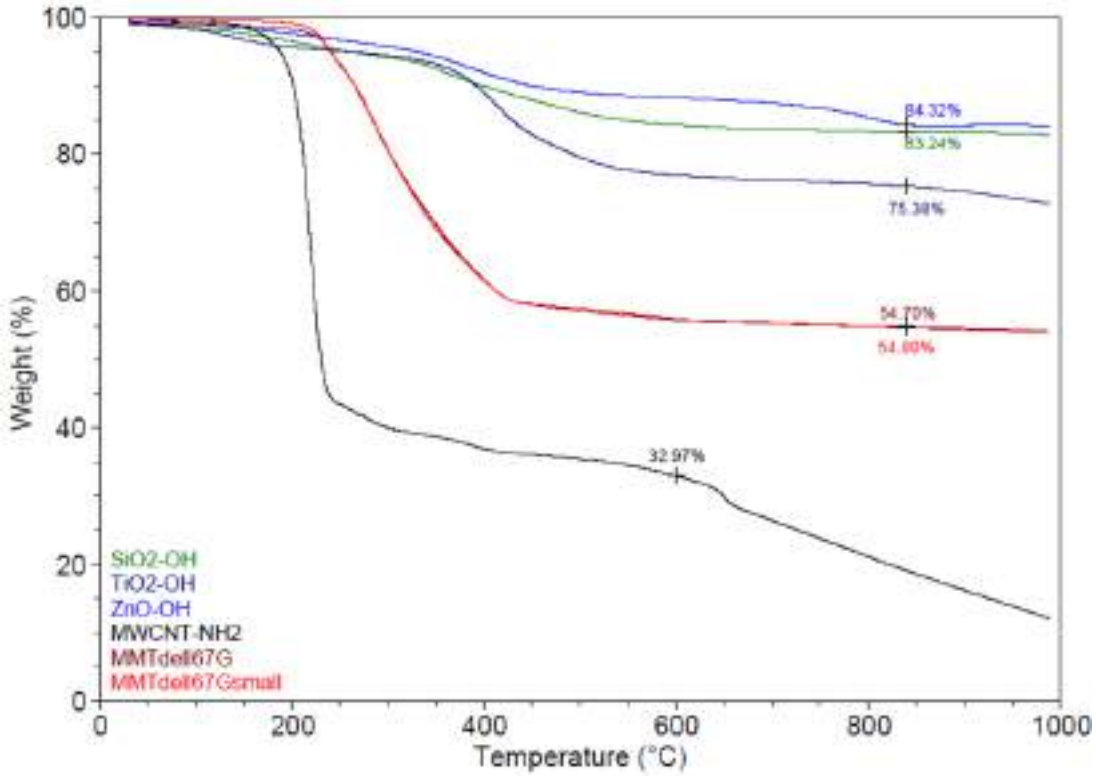

Figure S4: TGAs of functionalised nanomaterials in Nitrogen atmosphere.

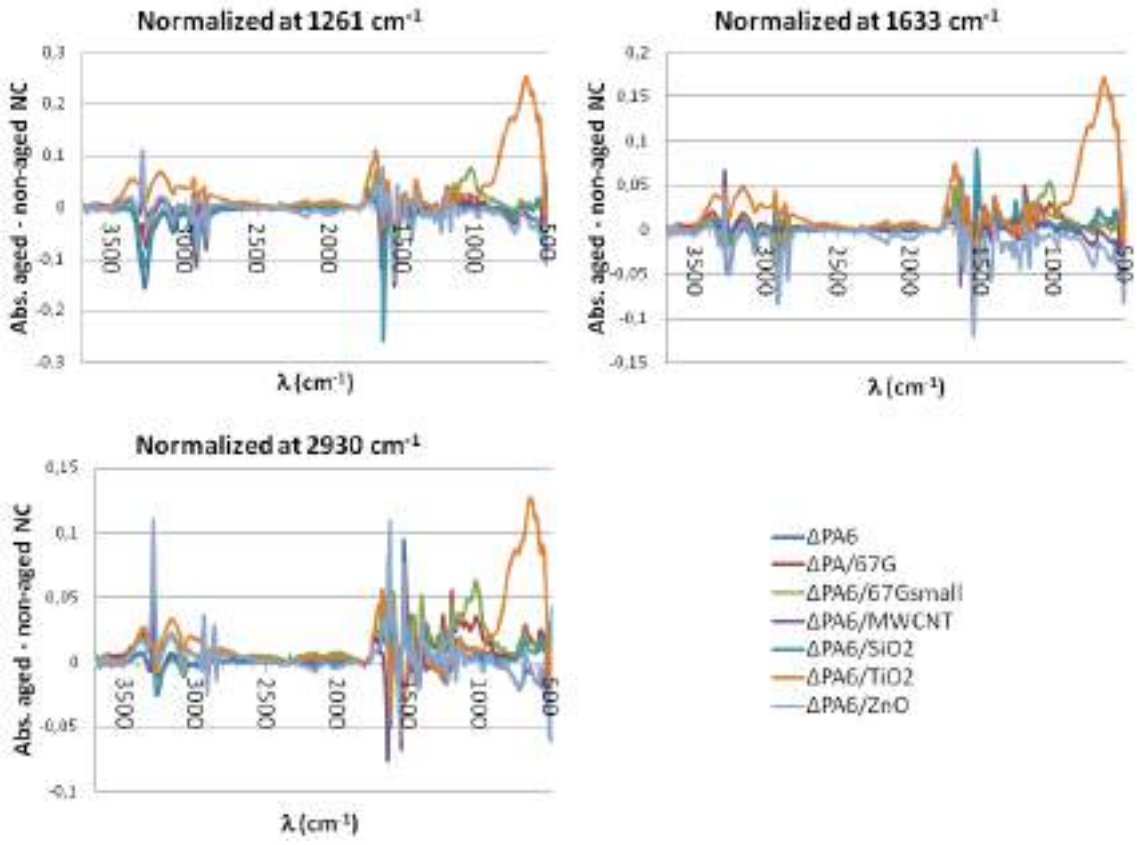

Figure S5: FT-IR spectrograms.

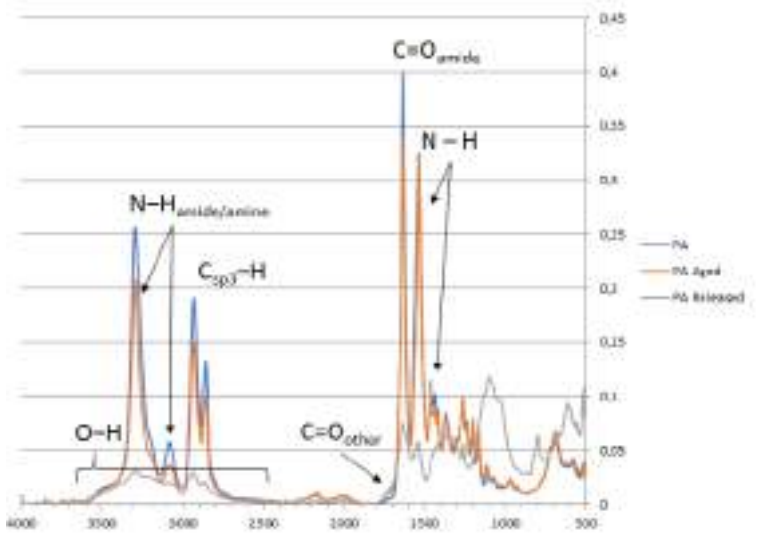

Figure S6: FT-IR spectrograms of PA specimens and released material.

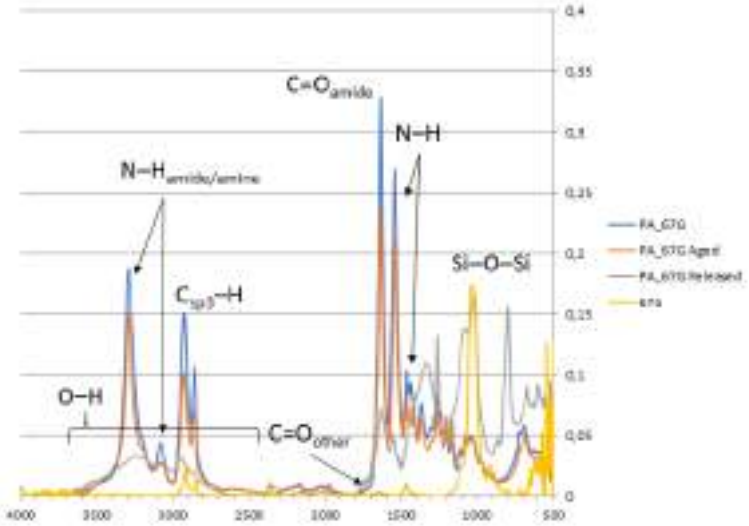

Figure S7: FT-IR spectrograms of 67G, PA/67G specimens and released material.

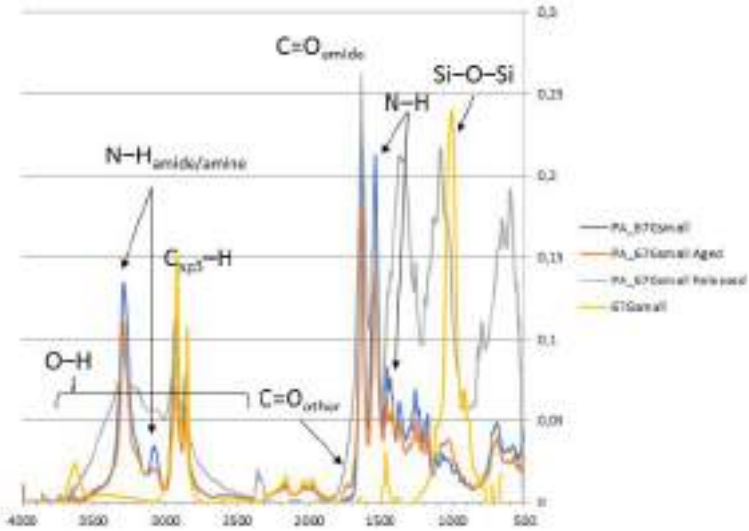

Figure S8: FT-IR spectrograms of 67 G_{SMALL}, PA/67G_{SMALL} specimens and released material.

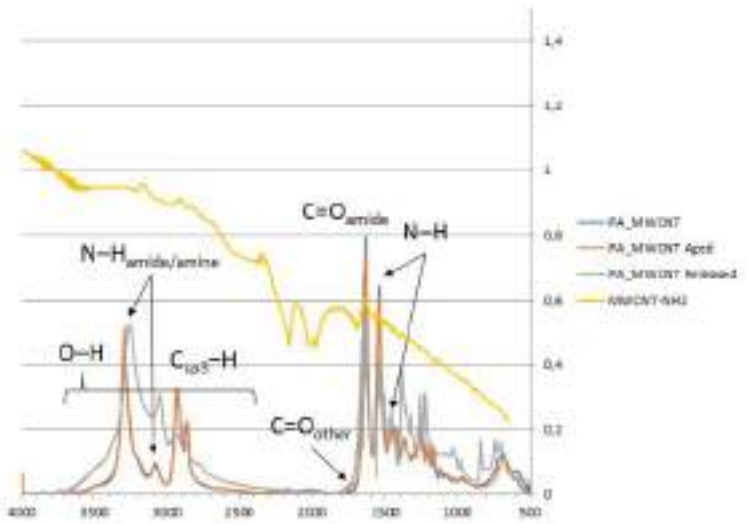

Figure S9: FT-IR spectrograms of MWCNT, PA/MWCNT specimens and released material.

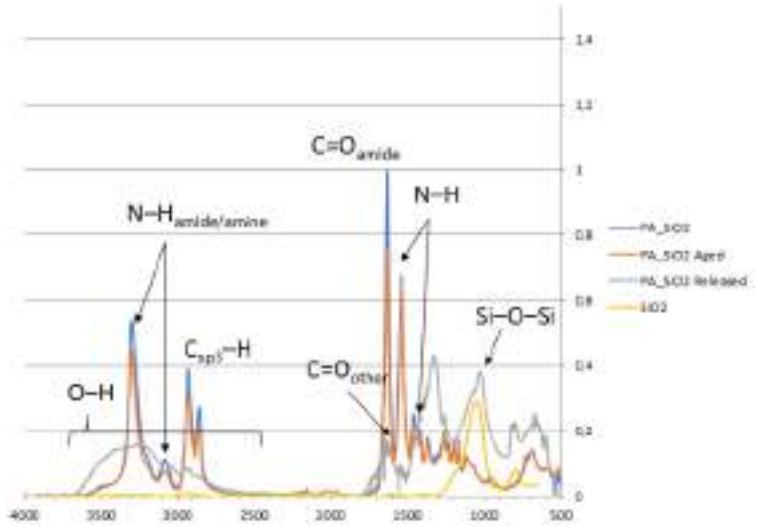

Figure S10: FT-IR spectrograms of SiO_2, PA/SiO_2 specimens and released material.

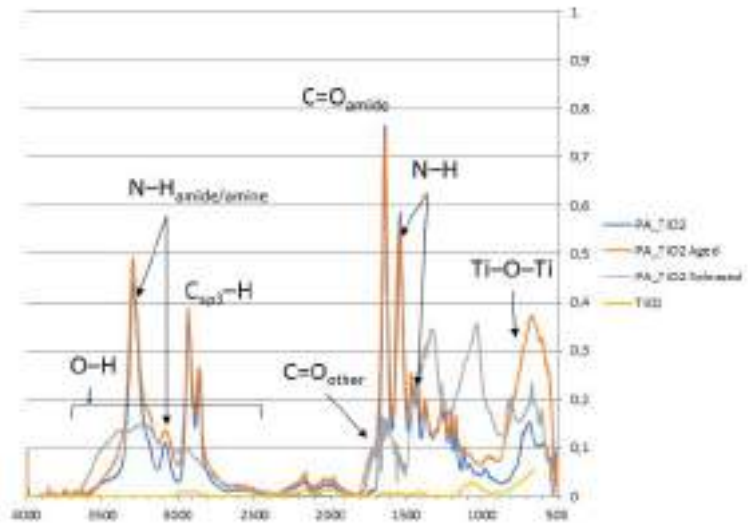

Figure S11: FT-IR spectrograms of TiO_2, PA/TiO_2 specimens and released material.

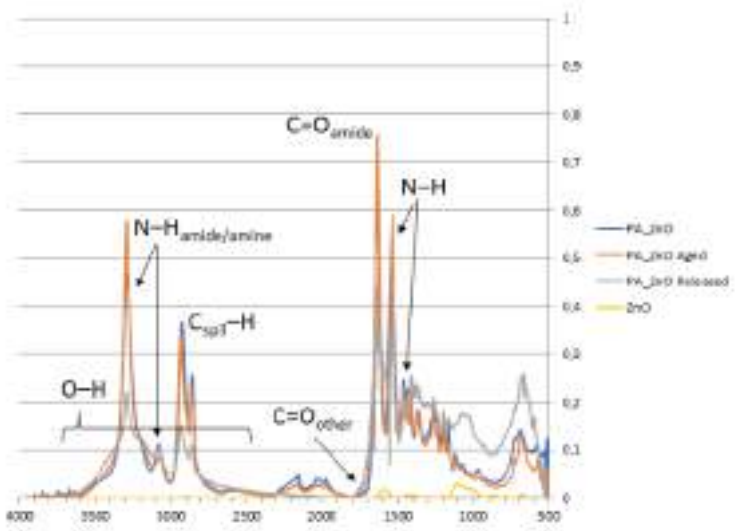

Figure S12: FT-IR spectrograms of ZnO, PA/ZnO specimens and released material.

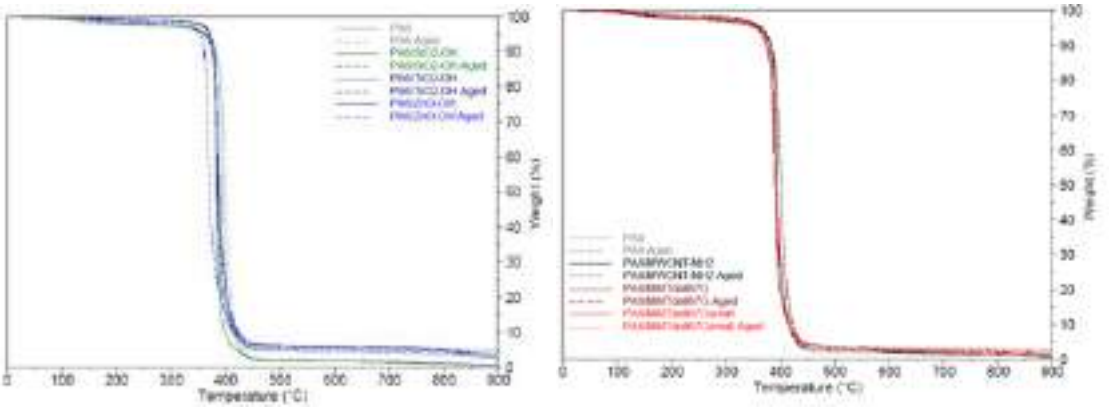

Figure S13: Complete TGA isotherms in nitrogen of non-aged and aged PA6 and PA6 NCs.

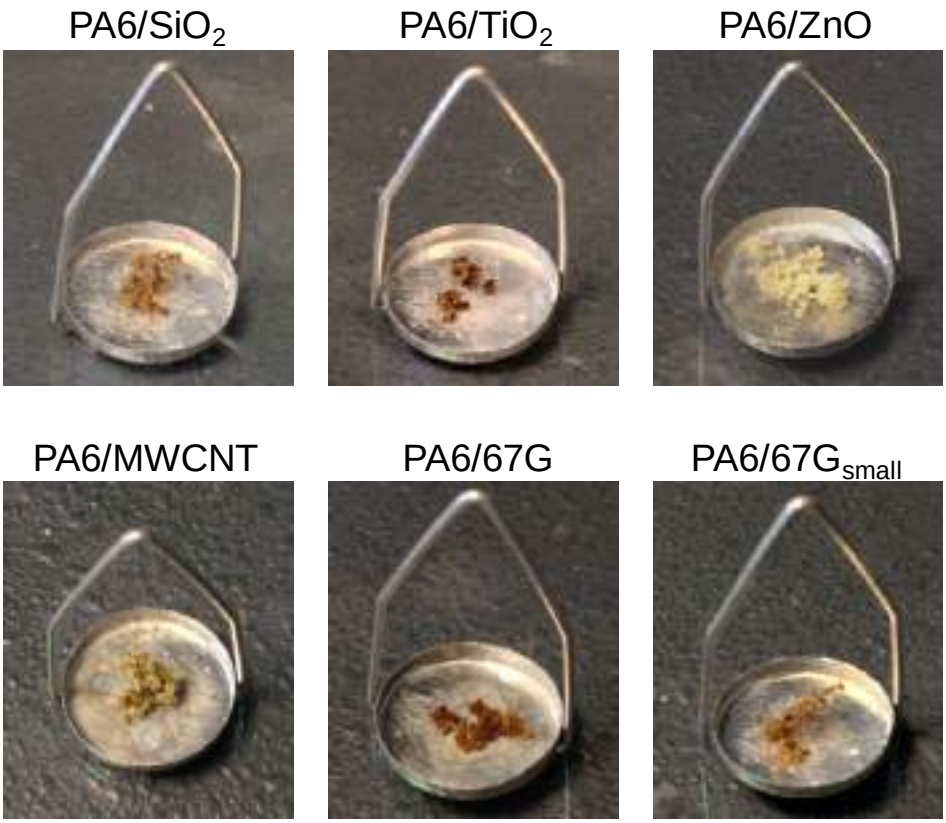

Figure S14: Images of the material collected from runoff waters after freeze-drying.

Section SI_5 – References

1 C. A. Schneider, W. S. Rasband and K. W. Eliceiri, *Nat. Methods*, 2012, **9**, 671–675.

2 M. D. Abramoff, P. J. Magalhães and S. J. Ram, *Biophotonics Int.*, 2004, 11, 36–42.

3 Y. Liu, L. Cui, F. Guan, Y. Gao, N. E. Hedin, L. Zhu and H. Fong, *Macromolecules*, 2007, **40**, 6283–6290.

4 S. Mohamadi, N. S. Sanjani, N. T. Qazvini and M. Barari, *J. Nanosci. Nanotechnol.*, 2009, **9**, 3959–65.

5 N. Nakayama and T. Hayashi, *Polym. Degrad. Stab.*, 2007, **92**, 1255–1264.

6 J. Zheng, R. W. Siegel and C. G. Toney, *J. Polym. Sci. Part B Polym. Phys.*, 2003, **41**, 1033–1050.

7 Q. Xu, F. Chen, X. Li and Z. Zhang, 20–24.

8 X. Liao, A. V Nawaby and H. E. Naguib, .

9 Y. Katoh and M. Okamoto, *Polymer*, 2009, **50**, 4718–4726.

Release and cytotoxicity screening of the printer emissions of a CdTe quantum dots-based fluorescent ink

María Blázquez Sánchez[a,b], Inge Nelissen[c], Vicenç Pomar-Portillo[d], Alejandro Vílchez[d], Jo Van Laer[c], An Jacobs[c], Evelien Frijns[c], Socorro Vázquez-Campos[d], Elisabet Fernandez-Rosas[d,*]

[a] *INKOA SISTEMAS SL, Ribera de Axpe 11, Edificio D1, Dpto 208, 48950, Erandio, Bizkaia, Spain*

[b] *CBET Research Group, Department of Zoology and Animal Cell Biology, Faculty of Science and Technology and Research Centre for Experimental Marine Biology and Biotechnology PiE, University of the Basque Country UPV/EHU, Barrio Sarriena s/n, 48940, Leioa, Bizkaia, Spain*

[c] *VITO NV, Health Unit, Boeretang 200, 2400, Mol, Belgium*

[d] *LEITAT Technological Center, Carrer de la Innovació 2, 08225, Terrassa, Barcelona, Spain*

*Corresponding author e-mail address: efernandez@leitat.org

Contribution to the peer-reviewed publication within the context of this thesis: This paper can be divided in two differentiated areas. On the one hand, the one related to exposure and, on the other hand, the one related to toxicity. The section that belongs to this thesis is the one related to the exposure evaluation, methodology described in section 2.2 and results in section 3.2. Any contribution was provided to the toxicity assays. Contribution was also provided to the characterisation of the ink (section 2.1 and 3.1), and to the Discussion and Conclusion sections, critically revising the work for important intellectual content addition.

The following manuscript is a version of record reproduced from Toxicology Letters 347 (2021) 1–11 with permission from the Royal Society of Chemistry.

The online version can be accessed from:

http://dx.doi.org/10.1016/j.toxlet.2021.04.009

Toxicology Letters 347 (2021) 1–11

Contents lists available at ScienceDirect

Toxicology Letters

journal homepage: www.elsevier.com/locate/toxlet

Release and cytotoxicity screening of the printer emissions of a CdTe quantum dots-based fluorescent ink

María Blázquez Sánchez[a,b], Inge Nelissen[c], Vicenç Pomar-Portillo[d], Alejandro Vílchez[d], Jo Van Laer[c], An Jacobs[c], Evelien Frijns[c], Socorro Vázquez-Campos[d], Elisabet Fernandez-Rosas[d,*]

[a] INKOA SISTEMAS SL, Ribera de Axpe 11, Edificio D1, Dpto 208, 48950, Erandio, Bizkaia, Spain
[b] CBET Research Group, Department of Zoology and Animal Cell Biology, Faculty of Science and Technology and Research Centre for Experimental Marine Biology and Biotechnology PiE, University of the Basque Country UPV/EHU, Barrio Sarriena s/n, 48940, Leioa, Bizkaia, Spain
[c] VITO NV, Health Unit, Boeretang 200, 2400, Mol, Belgium
[d] LEITAT Technological Center, Carrer de la Innovació 2, 08225, Terrassa, Barcelona, Spain

HIGHLIGHTS

- Water-based ink containing PEG coated CdTe QDs has been used for inkjet printing.
- PEG-CdTe QDs released, maintaining their individual identity (3–5 nm diameter) at the use phase.
- Cytoxicological assessment by ink atomization was done using BEAS-2B cells in an ALI culture.
- PEG-CdTe QDs decreased cell viability by 25.6 % when compared with clean air.
- The ALI integrated approach is appropriate to explore in-depth *in vitro* inhalation toxicity.

GRAPHICAL ABSTRACT

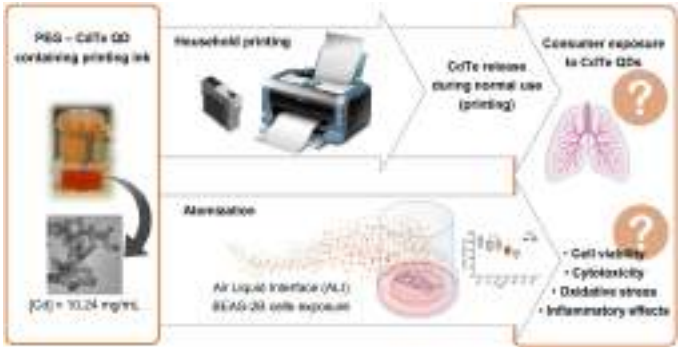

ARTICLE INFO

Article history:
Received 20 October 2020
Received in revised form 26 February 2021
Accepted 13 April 2021
Available online 18 April 2021

Keywords:
CdTe quantum dots
printing ink
release
airborne exposure
cytotoxicity

ABSTRACT

The fluorescent properties of cadmium telluride (CdTe) containing quantum dots (QDs) have led to novel products and applications in the ink and pigment industry. The toxic effects of the emissions associated to the use of printing ink containing CdTe QDs might differ from those of conventional formulations which do not integrate nanoparticles, as CdTe QDs might be emitted. Within this work, the airborne emissions of a water-soluble fluorescent ink containing polyethylene glycol (PEG)-coated CdTe QDs of 3–5 nm diameter have been characterized and studied under controlled conditions during household inkjet printing in a scenario simulating the use phase. Subsequently, the cytotoxicological potential of atomized CdTe QDs ink in an acute exposure regimen simulating an accidental, worse-case scenario has been evaluated *in vitro* at the air-liquid interface (ALI) using the pulmonary cell line BEAS-2B. Endpoints screened included cell viability, oxidative stress and inflammatory effects. We have observed that CdTe QDs ink at 54.7 ng/mL decreased cell viability by 25.6 % when compared with clean air after 1h of exposure; a concentration about 65 times higher was needed to observe a similar effect in submerged

* Corresponding author.
E-mail address: maria@inkoa.com (E. Fernandez-Rosas).

http://dx.doi.org/10.1016/j.toxlet.2021.04.009
0378-4274/

conditions. However, we did not observe oxidative stress or inflammatory effects. The present study integrates the development of scenarios simulating the use phase of nano-additivated inks and the direct cell exposure for *in vitro* effects assessment, thus implementing a life-cycle oriented approach in the assessment of the toxicity of CdTe QDs.

1. Introduction

The use of nanoparticles (NPs) in ink formulations is leading to products with new or enhanced properties and applications. This has opened new market opportunities and several companies are taking advantage of these nano-based technologies. Quantum dots (QDs) confer a wide range of optical properties to pigments/inks, covering the most requested needs in applications for the near future. They have a broad absorption and narrow band emission that can be tuned based on their composition and size, change electrical conductivity or improve thermal and photochemical stability (Kshirsagar et al., 2013; Lange and Wedel, 2017). One of the most widely used are cadmium telluride (CdTe) QDs, due to their ease of tunability, high photoluminescence, quantum efficiency and stability in water (Wuister et al., 2003).

Inkjet printing is an attractive technology for microscale patterning since it can eject tiny droplets (with diameters in the range 50–100 μm), which are composed of either solutions or dispersions of functional materials, onto addressable sites on a substrate (Tekin et al., 2007). To date, whereas most of the research studies have focused on emissions from laser printers and their corresponding effects towards human health (Karrasch et al., 2017; Nakadate et al., 2018; Pirela et al., 2015; Terunuma et al., 2019), no solid scientific evidence has been reported in the literature confirming the emission of airborne particles from inkjet printers (Shi et al., 2015; The Danish Environmental Protection Agency, 2015). However, Konga and coworkers concluded that inkjet printer emissions exert a synergistic effect in the presence of environmental tobacco smoke and induce intense damage to the lung mitochondria in an asthmatic murine model by disrupting the structural and functional integrity of the mitochondrial membrane (Konga et al., 2009).

In general, focus of the research so far has been placed on the type of printers and printing parameters, but the emissions and health effects that can be attributed to the nature of the ink have not been investigated. Furthermore, the toxicological effects of the emissions of inkjet printing ink containing NPs, used as additives, might differ from those of conventional formulations. In this regard, the CEPE European Council of the Paint, Printing Ink and Artists 'Colours Industry, in a communication from 2012, argued that (i) *NPs used in paints, printing inks and Artists 'Colours are bound either in a liquid matrix (mixture before application) or in a solid matrix (final film after application and drying) and that by definition, the term "bound" includes all types of physical/chemical bonds (e.g. covalent, ionic, Van der Waals) which prevent any release of NPs from such matrices* and; (ii) *NPs used in paints, printing inks and Artists 'Colours are not likely to be extracted or released (from the mixture or the final film) under normal or reasonably foreseeable conditions of use* (CEPE, 2012).

Cadmium and cadmium-containing compounds have been classified as carcinogenic to humans at the lungs by the International Agency for Research on Cancer (IARC, 2012), based on the evidence that ionic cadmium causes genotoxic effects in different types of eukaryotic cells, including human cells. Nevertheless, a number of cadmium-based chemicals along with CdTe have been developed in Europe (International Cadmium Association (ICdA, 2020) and are registered in REACH (ECHA, 2020a, b).

Specifically concerning CdTe QDs, Nguyen et al. investigated their effects on mitochondria in human hepatocellular carcinoma HepG2 cells, concluding that CdTe QDs caused disruption of the mitochondrial membrane potential, increased intracellular calcium levels, impaired cellular respiration, and decreased adenosine triphosphate synthesis (Nguyen et al., 2015). In another study, Su et al. compared the cytotoxicity values of QDs and free cadmium ions, and found that CdTe QDs were more cytotoxic than $CdCl_2$ solutions, even when the intracellular Cd^{2+} concentrations were identical in HEK293 cells (Su et al., 2010). Of main relevance concerning the respiratory exposure route, Zheng et al. (2018) studied the cytotoxicity and carcinogenicity of uncapped CdTe QDs concluding that acute exposure to CdTe QDs with diameter < 5 nm for 24 and 48 h elicited dose-dependent cytotoxicity in BEAS-2B cells, suggesting that CdTe QDs are potent human lung carcinogens. In 2019, Xu et al. characterized the proteome response of BEAS-2B observing that uncapped CdTe QDs with diameter < 5 nm significantly altered the BEAS-2B proteome, inducing oxidative stress (Xu et al., 2019).

The present study is based on the hypothesis that the use of nano-additivated ink in normal or accidental conditions may lead to human exposure and associated health risks. It characterizes the emissions of a product under development consisting in a water-based ink containing PEG-CdTe QDs during household inkjet printing under controlled conditions, representing potential release pathways for the PEG-CdTe QDs during the ink's usage. Subsequently, an acute exposure regimen to high-dose PEG-CdTe QDs aerosol as an accidental, worse-case scenario is simulated. To attain such purpose, an approach is developed using atomization and *in vitro* exposure at the air liquid interface (ALI) of the human bronchial epithelial cell line BEAS-2B, representing the initial part of the airways in contact with inhaled aerosols, in order to assess the potential health effect of airborne emissions of the nano-additivated ink. Additionally, cell viability is assessed in submerged conditions using the same cell line for comparison. Finally, a selection of genes relevant to screen oxidative stress and inflammatory response are investigated at the ALI.

The approach undertaken, in addition to assuring reproducibility in exposure, is relevant for first toxicity screening purposes in a safer-by-design approach. Furthermore, the present study is useful in other situations potentially conveying an associated release of NPs under normal conditions of use since water-based inks can also be used in alternative printing methods including, amongst others: flexographic, lithographic, gravure or screen-printing, and serves as a model for inkjet printing inks containing other NPs (e.g. Ag NPs). To the best of the authors' knowledge, no previous studies have been published analyzing the toxicological effect of airborne emissions of CdTe QDs containing inks.

2. Materials and methods

2.1. Ink formulation and characterization

Ink containing CdTe QDs of 3−5 nm diameter capped with PEG (750)-O-C(=O)CH_2CH_2-SH and a λ emission maximum of 750 ± 5 nm was synthesized, manufactured and provided by PLASMACHEM GmbH (Germany) as a prototype. Its composition cannot be

detailed for confidentiality issues. The solvent ink formulation without QDs was also provided to be used as control material.

The PEG-CdTe QDs ink was analyzed by inductively coupled plasma mass spectrometry (ICP-MS, Agilent 7500, Agilent Technologies) to determine the Cd and Te concentration after digesting the ink with acid in an analytical microwave digestion system (MARS, CEM, 1600 W) (for a detailed protocol see supporting information section 1 (SI-S1)). Transmission electron microscopy (TEM, JEOL 1010) and high-resolution TEM (JEM-2011) coupled with energy-dispersive X-ray spectroscopy (EDX) were used to determine the shape and size of the QDs. The TEM images were analysed using FIJI software (Schindelin et al., 2012). Thermogravimetric analysis (TGA) was performed on the ink with and without QDs to determine the differences produced by the QDs' incorporation, using a TGA Q500 (TA Instruments) under a N_2 flow of 90 mL min^{-1} and heating from 25 °C to 995 °C at a heating rate of 10 °C min^{-1}. Fourier-transform infrared spectroscopy coupled to an Attenuated Total Reflectance (FTIR-ATR, Affinity-1 Shimadzu 8400) was performed to determine the presence of characteristic functional groups of the coating or impurities present in the sample; spectra were recorded in the region of 600−4000 cm^{-1}. Before TGA and FTIR-ATR were performed, the ink was freeze-dried (100−9 PRO Freeze Dryer, CoolSafe) at −95 °C and ∼0.3 mbar, to increase the PEG-CdTe QDs signal in the analysis by getting rid of the water.

2.2. QDs release during paper printing process at household scale

For the printing experiment, a household inkjet printer (Pixma P7250, Canon) with refillable ink cartridges PGI-525 and CLI-526, with auto-reset chips (Octopus) was used. The PEG-CdTe QDs ink was manually loaded into the cartridges after gentle shaking. Printing was done at maximum quality on greyscale to assure that the ink was exclusively printed from the refillable black cartridge for PGI-550 black, whereas the rest of the cartridges were inserted in the printer but intentionally left empty. Printing was performed on 100 % recycled paper 80 g/m^2 (Staples) and the printed pattern was maintained during the whole process to minimize variability.

The printer was enclosed in a hermetically closed methacrylate box of 1.00 × 0.60 × 0.40 m (0.24 m^3), which had a clean air polycarbonate filter (225–9542, SKC). Silicon tubes of 6 mm diameter were introduced inside the box and connected to the air measurement instruments to sample the air. Sampling points were located around 5 cm above the output tray of the printer. A schematic representation of the setup has been included in Fig. SI1. For particle number concentration (PNC) measurement two different instruments were used: an Scanning Mobility Particle Sizer (SMPS) spectrometer (NanoScan 3910, TSI) with size range of 10–420 nm, 60 s scan time and 0.75 L/min flow rate, and an Optical Particle Sizer (OPS 3330, TSI) with size range of 300–10000 nm, 60 s scan time and 1.00 L/min. Measurements of PNC were undertaken before, during and after the household printing process. Once a low background of particles inside the chamber (<150 particles/cm^3) was reached, a 10-minute printing cycle was performed followed by uninterrupted air monitoring for 75 min, to observe the evolution of PNC.

A transmission electron microscopy (TEM) sampler device (MPS, Ecomeasure) was connected to the SMPS outlet allowing to collect the released material directly onto copper TEM grids coated with carbon, which were later analyzed. In a different configuration of the setup and with the purpose of collecting particles emitted in each of the stages (i.e., before, during and after printing) a glass fibre filter (Type A/E filter, Pall Corporation) was placed into the OPS to capture the particles passing through it, and runs were conducted changing the filters at the end of each stage. The collected material was further observed using an optical microscope (Axioplan, Zeiss) equipped with epifluorescence and a multi-band fluorescence bandpass filter.

2.3. Ink aerosol generation for in vitro cell exposure at the ALI

A new setup based on atomization of the PEG-CdTe QDs ink was designed for ALI exposure of a pulmonary cell line in a Vitrocell® module (Fig. SI2) with four compartments. For the atomization experiments, 2 mL of each sample (solvent ink and PEG-CdTe QDs ink) were dispersed in 80 mL ultrapure water, to obtain a 1:40 dilution for an optimal atomization (among the several dilutions tested, this had the smallest particle mode without interference of smaller particles < 10 nm as measured in-line using the 3936 SMPS from TSI at particle size range 15−661 nm; see Fig. SI3). These dispersions were atomized in a fume cupboard, using a collision-type atomizer (ATM 220, Topas) and a pressure of 2 bar. The QD-containing air flow leaving the atomizer at 4 lpm was dried using a diffusion dryer (DDU 570, Topas). Using a T-split junction, 0.3 lpm of the aerosol flow entered the dispersion unit of the Vitrocell® exposure module, and the remaining flow of 3.7 lpm was led into the exhaust of the fume hood using a pump connected to a mass flow controller. Each of the four positions of the exposure module extracted 0.003 lpm from the dispersion unit using a pump with a four way flow splitter with, for each flow, adjustable high precision valves.

During the exposure, temperature was controlled through a circulating 37 °C water bath and the exposure period was 1 h. Four replicate cultures were treated in parallel in the Vitrocell® system.

2.4. Cell culture settings

The BEAS-2B cell line (CLR-9609, ATCC), originally derived from normal bronchial epithelial cells, was cultured as described by Verstraelen et al. (2014). Briefly, cells were seeded at a ratio of 0.2 mL/cm^2 surface area, in growth medium (BEGM), consisting of bronchial epithelial cell basal medium (BEBM, Lonza) supplemented with 0.5 mL retinoic acid, 0.5 mL epinephrine, 0.5 mL triiodothyronine, 0.5 mL human recombinant epidermal growth factor, 0.5 mL insulin, 0.5 mL gentamicin sulfate amphotericin-B, 0.5 mL transferrin, 0.5 mL hydrocortisone, and 2 mL bovine pituitary extract (BulletKit, Lonza). Cells were kept in a humidified atmosphere at 37 °C and 5% CO_2, and subcultured before reaching 80 % confluence. Medium was refreshed every 2–3 days and cells were subcultured every 4–5 days (1500–3000 cells/cm^2).

For the exposure at the ALI, cells were seeded at a density of 15000 cells/cm^2 on precoated Corning® Transwell® polyester membrane inserts, pore size 0.4 μm as described elesewere (Geys et al., 2006), membrane diameter 24 mm (Sigma-Aldrich Chemie Gmbh). Inserts were placed in a sterile 6-well plate, and BEGM was added to both sides: 2 mL basolateral and 1 mL apical. Plates were incubated for 48 h at 37 °C, 5% CO_2 in a humidified incubator before replacing the growth medium by BEBM without growth factors, 16 h prior to ALI exposures to synchronize cell growth. Immediately before exposure, culture medium was completely removed from the apical side of the inserts and cells were washed with sterile phosphate buffered saline (PBS). Next, cells were transferred into the chambers of the *in vitro* exposure module (6PT-CF, Vitrocell® Systems) with 4 compartments to hold 24 mm inserts. The basolateral chambers were filled with 15−16 mL pre-warmed BEBM.

2.5. Deposition efficiency and dose quantification

To calculate the deposition efficiency, aerosolized PEG-CdTe QDs ink generated by the atomizer during 1 h was collected in 0.5 mL ultrapure water (quadruplicates, corresponding to the 4

positions in the Vitrocell® module) using the same setup as for the cell exposures at the ALI. Cd and Te concentrations were determined using a quadrupole ICP-MS instrument (Nexion 300 s Perkin Elmer) after microwave oven digestion with nitric acid, as described in SI-S2.

To quantify only the ions concentration to which cells had been exposed in the Vitrocell® module, Cd and Te ions were collected in BEGM medium without cells and separated from non-ionic particulate compounds by transferring the medium to centrifuge tubes (Pall Microsep™ Advance with 10 kDa Omega™ membrane) and centrifugation at 4000xg for 10 min (Hettich, Rotanta 460R). Ions were quantified using non-destructive ICP-MS analysis. Recovery tests of an internal standard Rhodium (^{103}Rh) showed 20 % signal suppression due to matrix interference during sample analysis, and this correction was applied to the results.

2.6. In vitro cell exposure at the ALI

BEAS-2B cells were exposed in the Vitrocell® module to PEG-CdTe QDs ink (QDs Ink) and solvent ink (S. Ink). An optimal flow rate of 3 mL/min during 1 h of exposure was selected, based on prior experiments with synthetic clean air, in order to minimise mechanical stress and dehydration of the cells, as well as to maintain cell viability after exposure. As vehicle and positive controls for cell viability and oxidative stress assessment and cytokine production, cells were exposed to synthetic clean air (C. Air, vehicle control) and to 10 ppm NO_2, respectively. Additionally, untreated cells on inserts without apical medium were kept for 1 h in a humidified 37 °C incubator with 5% CO_2 were used to control basal cell growth and viability on the inserts (IC-). Finally, as additional negative and positive control conditions for cytokine induction, cells submerged in apical medium for 24 h without treatment (IC+) or containing 20 μg/mL lipopolysaccharide (LPS) from *Escherichia coli* (Sigma-Aldrich Chemie Gmbh) were used, respectively. Two biologically independent runs (2 replicate inserts/run) were performed for each exposure condition (Fig. 1).

After exposure, cells were post-incubated by placing the inserts in a new sterile six-well plate with 2 and 1 mL BEGM basolateral and apically, respectively, and allowing cell recovery in a humidified 37 °C incubator with 5% CO_2, in agreement with previous works (Persoz et al., 2012). Specifically, cells in two replicate inserts were post-incubated for 23 h along with the incubator controls (without or with apical medium, and LPS-treated cells) for evaluation of cell viability and cytokine secretion, whereas the other two replicate inserts were post-incubated for 1 h and analysed for oxidative stress and inflammatory response by gene expression using RT-qPCR (Fig. 1).

Complementarily, and taking into consideration previous studies reporting direct association between Cd ions from CdTe-QDs in the cell culture medium and cytotoxicity in other epithelial cell lines (Du et al., 2019; Su et al., 2010), BEAS-2B was exposed to six serial 1/5 dilutions of PEG-CdTe QDs from 8.6–27000 ng/mL in submerged conditions, and Cd and Te ions were quantified by ICP-MS (see the details in SI-S3). Previous data from our laboratories exposing the same cell line in submerged conditions to $CdCl_2$ were also used with comparison purposes.

2.7. Viability assessment

Cell viability was assessed using the Prestoblue™ Cell Viability Reagent (Life Technologies), according to the manufacturer's instructions. The apical medium was replaced with 1 mL of a 10 % Prestoblue™ solution in growth medium to allow living cells to metabolize resazurin. After 2 h of incubation at 37 °C, fluorescence of the collected apical solution was measured in a 96-well plate at an excitation wavelength of 530 nm, and an emission wavelength of 620 nm using a Fluoroskan Ascent® reader (ThermoFisher Scientific, Waltham, MA, USA). Cell viability was expressed as the percentage of fluorescence relative to the vehicle control (i.e. C. Air) cells.

In submerged conditions cell viability was assessed by neutral red assay and by trypan blue (vital) staining and counting using a Countess Automated Cell Counter (Invitrogen), for $CdCl_2$ and the solvent and CdTe QDs inks respectively (SI-S4).

2.8. Oxidative stress and inflammatory response

For gene expression analysis, the medium was aspirated from the apical surface of the cells after 1 h post-incubation and cells were lysed with RLT lysis buffer (Qiagen) containing 1% 2-mercaptoethanol (Sigma-Aldrich Chemie Gmbh). Total RNA was isolated using the mini RNeasy RNA isolation kit (Qiagen), according to the manufacturer's specifications. The RNA concentration was determined using a NanoDrop Spectrophotometer (NanoDrop Technologies). RNA was stored in RNase-free water (Qiagen) at −80 °C.

For cDNA synthesis, the Transcriptor First Strand cDNA Synthesis Kit (Roche Applied Science) was used, based on the use of random hexamer and oligo-dT primers. The procedure is described in the manufacturer's specifications. The amount of

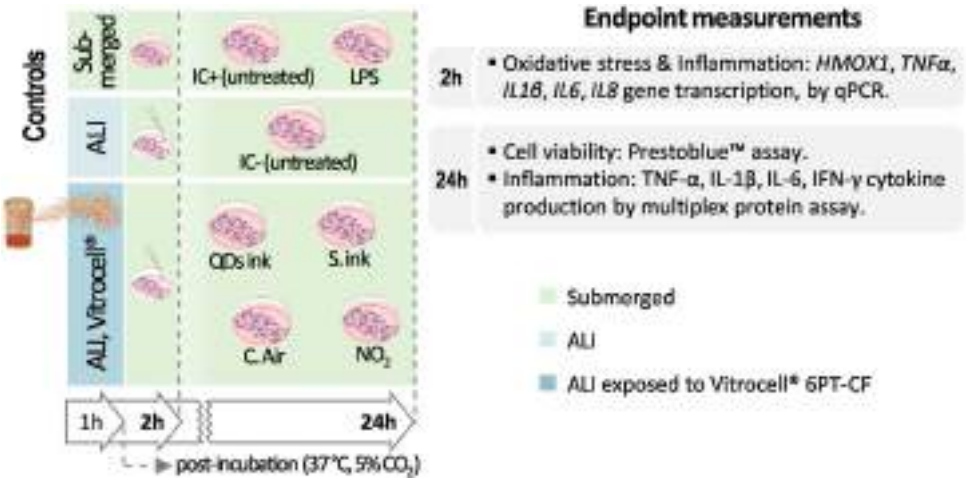

Fig. 1. Schematic representation of the different *in vitro* cell conditions, with indication of exposure and post-incubation times, control conditions and the respective endpoint measurements. Abbreviations: IFN: interferon; IL: interleukin; LPS: lipopolysaccharide; TNF: tumour necrosis factor.

starting RNA in the reverse transcription reaction was 0.5 μg. cDNA samples were further diluted in nuclease-free water and stored at −20 °C.

After cDNA synthesis, qPCR was performed in 96-well plates in duplicate for each sample using a LightCycler 480 Probes Master Mix on a LightCycler 480 instrument (Roche Applied Science). Amplification reactions for genes encoding interleukin (IL)-8, IL-6, heme oxygenase (HMOX)1, tumor necrosis factor (TNF)-α and IL-1β proteins, and reference genes Ribosomal Protein Lateral Stalk Subunit P0 (*RPLP0*), Guanine Nucleotide-binding protein subunit Beta-2-like 1 (*GNB2L1*), and Peptidyl-Prolyl cis-trans Isomerase A (*PPIA*) were monitored using double-quenched probes™ designed using PrimerQuest Tool and supplied as PrimeTime qPCR probe assays (Integrated DNA technologies). All samples were measured in the same run for a given target (i.e. sample maximization strategy according to Hellemans et al. (2007)). Gene expression changes were analysed using the qBase software. The expression levels obtained were normalized against the reference genes and fold changes in expression levels of conditions at the ALI (QDs and S. ink and NO_2) were given relative to the vehicle control (i.e. C. Air).

At the protein level, the pro-inflammatory cytokines interferon (IFN)-γ, IL-1 β, IL-6 and TNF-α were also measured using a multiplex protein assay. After 23 h post-incubation apical culture supernatants were collected and centrifuged at 300 x g for 5 min to remove cell debris. Protease inhibitor cocktail (0.2 % v/v; Sigma–Aldrich Chemie Gmbh) was added to the samples before freezing at -80 °C, and samples were stored until analysis. The cytokines were quantified using the human pro-inflammatory I (4-plex) kit (Meso Scale Discovery) on a MESO QuickPlex SQ120 instrument, according to the manufacturer's instructions. Calibration curves were used to calculate the cytokine concentrations, expressed in ng/mL. Fold changes in of cytokine concentrations measured in the different conditions at the ALI (QDs and S. ink and NO_2) were given relative to the vehicle control (i.e. C. Air).

2.9. Statistical analysis

The biological response data for ALI experiments are shown as mean values ± standard deviation of duplicate inserts from two independent experiments. For the statistical tests and graphical representations, the GraphPad Prism 7.04 software was used. For the evaluation of the biological data normality was assessed both for cytotoxicity (D'Agostino & Pearson test, K2), inflammation and oxidative stress (Shapiro-Wilk test) datasets before applying a 2-way ANOVA (Tukey's multiple comparison tests).

3. Results

3.1. PEG CdTe-QDs ink characterization

Results from the ICP-MS elemental analysis indicated Cd and Te concentrations in the PEG CdTe-QDs ink of 10.24 (±0.86) mg/mL and 3.53 (±0.18) mg/mL, respectively. Thus, the total concentration

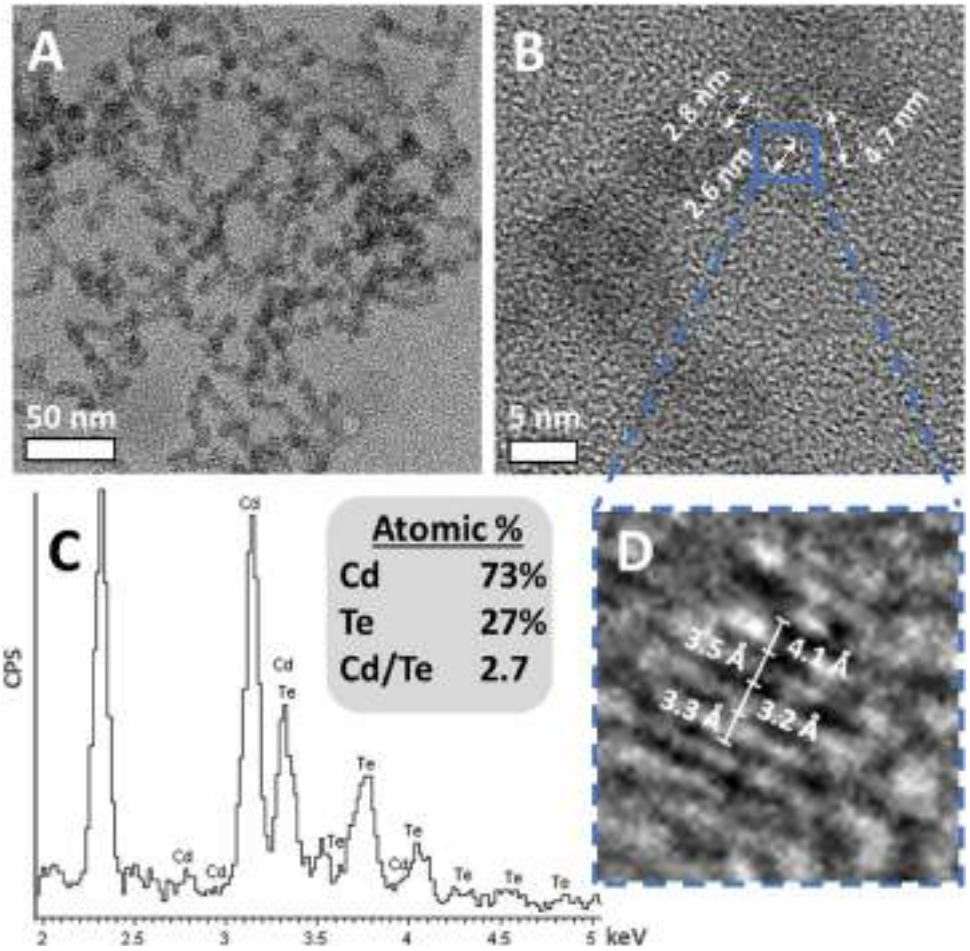

Fig. 2. A) TEM image of the ink showing aggregated PEG-CdTe QDs networks. B) Section of the PEG-CdTe QDs network where individual QDs are indicated by a white dashed line and their diameter measured. C) EDX spectrum of the PEG-CdTe QDs ink showing the atomic percentage of Cadmium and Tellurium: Counts per Second (CPS) are displayed against voltage (keV). D) Higher magnification image of a QD where the interplanar distances were measured.

of CdTe-QDs in the ink was 13.77 mg/mL. Considering that the atomic mass of Cd is 112.4 u and 127.6 u for Te (Meija et al., 2016) the Cd and Te ratio was around 3:1. The higher Cd content can be explained by the fact that Cd atoms are located around the QDs' surface, as a result of the synthesis method employed. Cadmium is needed in the surface to attach the QDs to the ligand (PEG) through a Cd-S bond. For control samples of ultrapure water and solvent ink, values under the limit of detection (<0.1 ng/mL) were obtained for both Cd and Te.

From the TEM characterization it can be observed that the particles were slightly aggregated, forming networks (Fig. 2A). Particles size measurements (Fig. 2B) confirmed that the QDs contained in the ink presented the size claimed by the manufacturer, from 3 to 5 nm. The EDX measurements showed a Cd:Te molar ratio of 2.7 (Fig. 2C), a result concordant to the one determined by ICP-MS. At higher magnifications (Fig. 2D) the interplanar distances could be observed and measured, resulting in an average distance of 3.53 Å, which was close to the expected interplanar distance between (111) planes in CdTe structures (3.75 Å) (Guillén-Cervantes et al., 2015).

TGA allowed to determine the inorganic mass percentage in the PEG-CdTe QDs ink (Fig. SI4), since Cd and Te remained after the temperature raised over 400 °C while the organic components were volatilized. For the solvent ink almost no residue remained, whilst for the PEG-CdTe QDs ink the residue represented a 6.7 % of the weight. Considering that after the freeze-drying process only the 20.9 % of the ink mass remained (which was a viscous liquid), the 6.7 % measured in the TGA corresponds to the 1.4 % of the ink. Since the ink's density is close to 1 g/cm^3, the concentration is equivalent to 14.0 mg/mL, which was close to the results obtained in the ICP-MS measurements (Cd plus Te). This suggests that, as expected, the only inorganic material in the ink (the TGA residue) corresponds to the PEG-CdTe QDs. Moreover, for both the solvent ink and the PEG-CdTe QDs ink, the two main weight losses were observed at the same temperatures, at 200°C and 350°C, suggesting that there were no alterations on the solvent ink after the CdTe QDs addition.

The FTIR-ATR spectrum of the freeze-dried PEG-CdTe QDs ink (Fig. SI5) showed the characteristic absorption bands of PEG, at 2800 cm^{-1} (stretching CH—) and at around 1100 cm^{-1} (stretching CO—). Interestingly, another peak was observed at around 1630 cm^{-1} which could be related with thioglycolic acid which is a common reagent employed in CdTe QDs synthesis (Abd El-sadek and Babu, 2011; Arivarasan et al., 2014). The presence of a broad band observed around 3400 cm^{-1} might be related with the presence of residual water.

3.2. QDs release during paper printing process at household scale

Variations of PNC in air before, during and after the household PEG-CdTe QDs ink printing process measured with the SMPS and OPS (size range from 10 to 10000 nm) are shown in Fig. 2. Before printing, the pumps incorporated in the air measurement instrument circulated the air outside the chamber allowing new air to enter through the polycarbonate filter and renewing the air inside the chamber. As a result, the PNC decreased along time, going from 350 to 140 particles/cm^3 after 90 min. When the printing process started (grey shadowed region), a quick increase in PNC could be clearly observed, reaching a maximum value of 593 particles/cm^3. After the printing stopped, due to the recirculation of air with the instruments' pump, PNC progressively decreased. One hour was needed to reach a PNC around 220 particles/cm^3. As can be seen in the top part of Fig. 3, no fluorescence (related to PEG-CdTe QDs) was observed in the filter corresponding to the background stage. However, intense fluorescence was observed on the filter placed during the printing process, meaning that QDs were released into the air. After printing, fluorescence was also detected (with a lower intensity than in the filter belonging to the printing process), suggesting that some QDs remained in the air after printing.

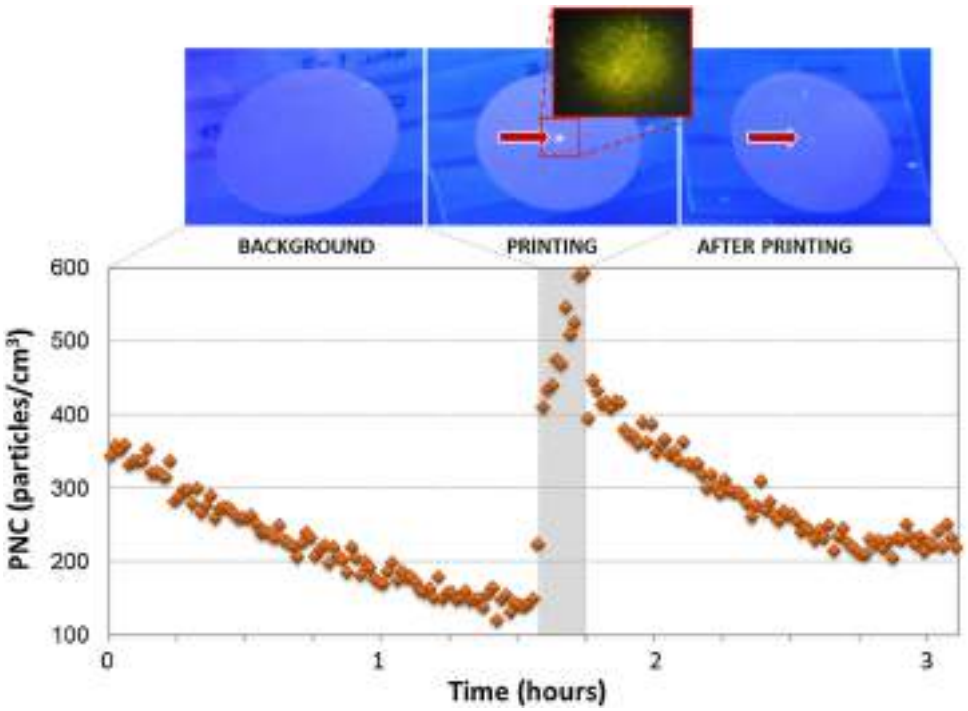

Fig. 3. Particles number concentration (PNC) in air during the PEG-CdTe QDs ink household printing process measured using an SMPS and OPS in the defined setup, and filters (images at the top) containing material collected for 10 min before (background), during and after printing. The insert shown in the image during printing corresponds to an epifluorescence image of the filter.

Electron microscopy images of the particles released during the household printing process and retained on the TEM grid are shown in Fig. 3. Evidences of the PEG-CdTe QDs collected during the printing process were found. Similar aggregates to the ones observed in the ink (Fig. 2) were observed, suggesting that released materials did not contain isolated PEG-CdTe QDs, but droplets containing PEG-CdTe QDs aggregates instead (Fig. 4A-B). At higher magnifications, the crystallographic planes of the PEG-CdTe QDs were observed, presenting an approximate interplanar distance around 3.23 Å, which is very close to the size measured in the original PEG-CdTe QDs ink sample (Fig. 4C-D). Measurements of released individual PEG-CdTe QDs provided diameter sizes similar to the ones observed in the ink, 3–5 nm, while aggregates presented diameter sizes around 20 nm. EDX measurements (Fig. SI6) confirmed that the observed structures contained Cd and Te.

3.3. Deposition efficiency and dose quantification after in vitro ink exposure

The maximum possible dose of 1246.9 ng per well was calculated with the average PNC of $6.741^{*}0^{6}$ particles per cm^3 and the average diameter of 69.5 nm, both determined by SMPS. Dose quantification by ICP-MS of the aerosolized particles in the Vitrocell® module for each compartment determined that BEAS-2B cells were exposed to a total dose of 37.1 (±6.2) ng/mL of Cd, and 17.6 (±2.6) ng/mL of Te (Table 1). It corresponds to a Cd:Te ratio of 2.4:1 and a total CdTe concentration of 54.7 ng/mL (± 8.6), implying an exposure of 12.1 ng/cm^2. A deposition efficiency of 4.39 % was determined by SMPS based on the average particle size. Solvent ink gave values under

Concerning the exposure in submerged conditions, the percentage of dissolved Cd and Te ions determined was inversely proportional to dose (Table SI1), as could be expected at low concentrations, where the dissolution rate increases to reach an equilibrium. Though, when compared to the dose determined for cells in the Vitrocell® module, the estimated ionic dose was much higher for Cd, with a 63.1 % (46.9 ng/mL) present in its ionic form, whilst Te was ionized by 45.0 % (15.9 ng/mL).

3.4. Cell viability assessment

Atomized solvent and PEG-CdTe QDs inks decreased cell viability by 9.0 % (±11.9 %) and 25.6 % (±15.7 %) respectively, whereas NO_2 –positive control– decreased cell viability by 32.8 % (±11.7 %) in contrast to clean air condition.

Differences in the cytotoxicological response between all the conditions tested at the ALI were statistically significant, with p-values <0.001 (see Fig. 5). Regarding complementary controls, IC- (incubator control at the ALI) showed statistically significant differences ($p < 0.0001$) when compared with IC+ (incubator control in submerged conditions); whereas the cytokine induction

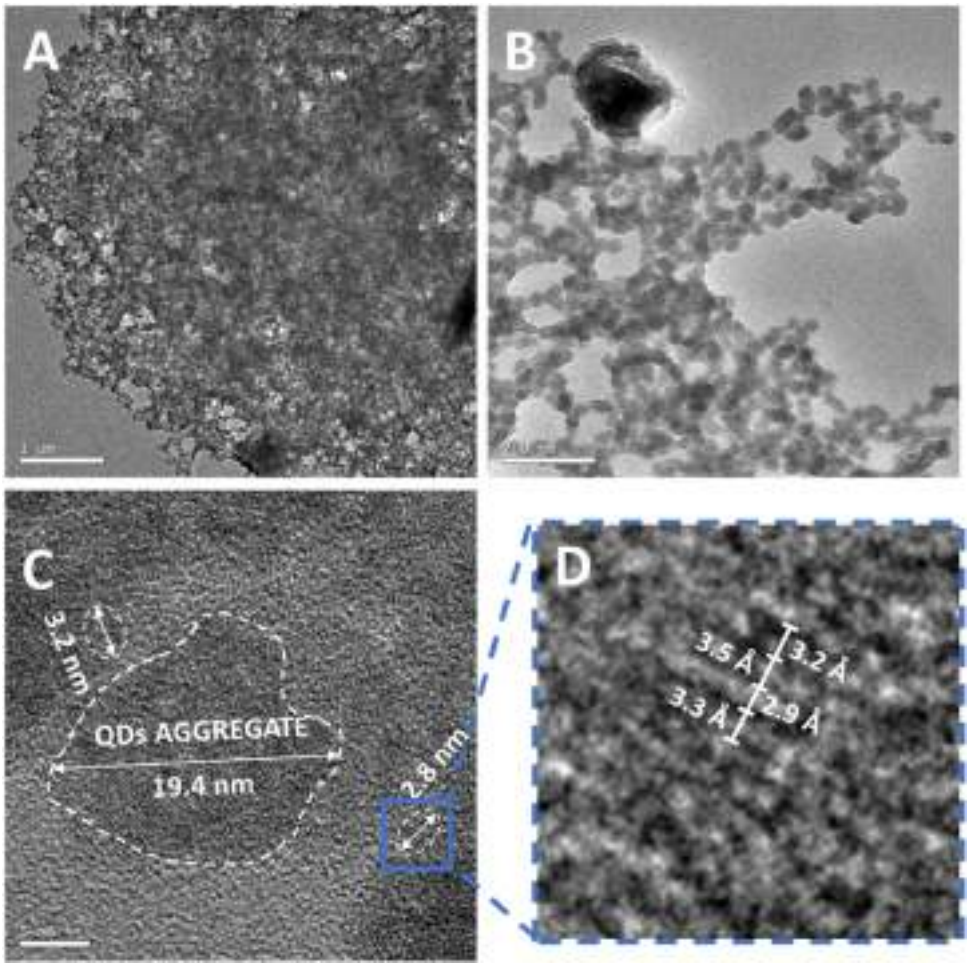

Fig. 4. TEM images of the airborne CdTe-QDs emitted during PEG-CdTe QDs ink household printing collected with sampler device. **A**) TEM image of aggregated ink on the TEM grid. **B**) PEG-CdTe QDs networks **C**) Section of the PEG-CdTe QDs network where individual QDs and QDs aggregates are indicated by a white dashed line and their diameter measured. **D**) Higher magnification image of a QD where the interplanar distances were measured.

Table 1
Dose quantification after 1 h exposure to the aerosolized PEG-CdTe QDs ink in the Vitrocell® module using ICP-MS. Total and ionic doses of CdTe, Cd and Te are indicated.

Total CdTe (ng/mL)	Total Cd (ng/mL)	Ionic Cd		Total Te (ng/mL)	Ionic Te	
		(ng/mL)	(%)		(ng/mL)	(%)
54.7 ± 8.6	37.1 ± 6.2	10.9 ± 3.6	29.4	17.6 ± 2.6	16.0 ± 4.5	90.9

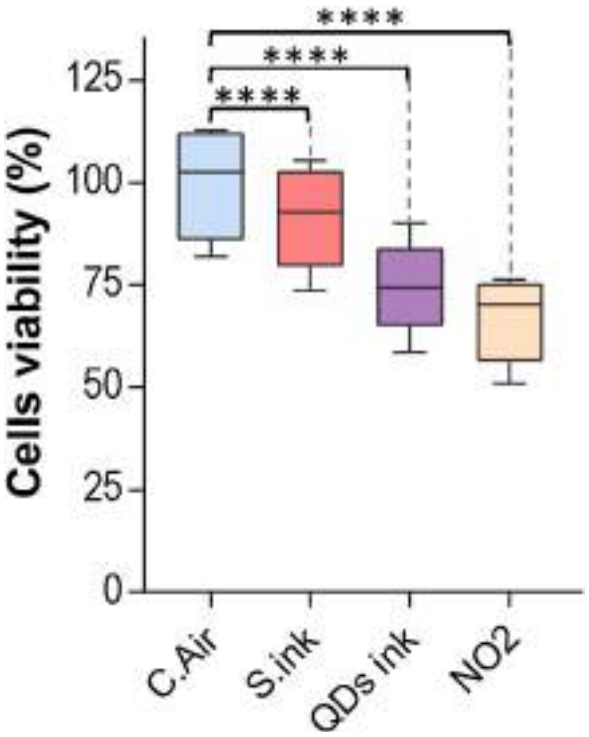

Fig. 5. Box-and-whisker plot showing the mean viability of BEAS-B2 cells exposed for 1 h at the ALI to different conditions, compared to a clean air (C. Air) atmosphere: solvent ink (S. Ink), PEG-CdTe QDs ink (QDs Ink) and nitrogen dioxide (NO_2) as cytotoxicity control for cytokine induction control. Error bars indicate standard deviation. **** = $p < 0.001$.

control with LPS (performed also in submerged conditions) compared to IC + did not show significant differences.

Results in submerged conditions showed that cytotoxicity had a good correlation ($r^2 = 0.872$) with Cd ionic concentration, whether it had been added as QDs or as a salt. However, no cytotoxicity could be observed below 500 ng/mL of Cd in ionic form ($p > 0.05$). A similar cell survival attributed to PEG-CdTe QDs at the ALI (i.e. 74.4 % cell viability compared to vehicle control, 83.4 % compared to solvent ink control), with 10.9 ng/mL Cd ions, corresponded to 890 ng/mL of Cd ions in submerged conditions (Fig. SI7). This remarkable change in the dose-effect may be due to a differential impact caused by the exposure route, highlighting the importance of the model used for cytotoxicity assessments relevant to airways.

3.5. Oxidative stress and inflammatory response assessment

It has previously been described that QD-induced cytotoxicity can at least partially be explained by oxidative stress (Lovrić et al., 2005), which is accompanied by the induction of antioxidant mechanisms in the cell. In addition, oxidant air pollutants, such as particulate matter and NO_2, have been shown to induce lung inflammation through stimulation of the oxidative stress process, which is a major pathway leading to pathological conditions in the lungs. Therefore, we investigated possible changes in gene expression of pro-inflammatory (IL-1β, IL-6, IL-8 and TNF-α) and oxidative stress (HMOX1) markers by real-time qPCR after *in vitro* exposure of BEAS-2B cells to both solvent and PEG-CdTe QDs inks at the ALI, and in submerged conditions for comparison.

IL-1β, IL-6, IL-8 and TNFα did not show altered transcription levels after atomized solvent and PEG-CdTe QDs inks exposure at the tested concentration when compared to clean air(Fig. 6A); for IL-1β, differences were observed only when comparing C. Air and NO_2 conditions ($p = 0.0333$). Similarly, HMOX1 which is a primary

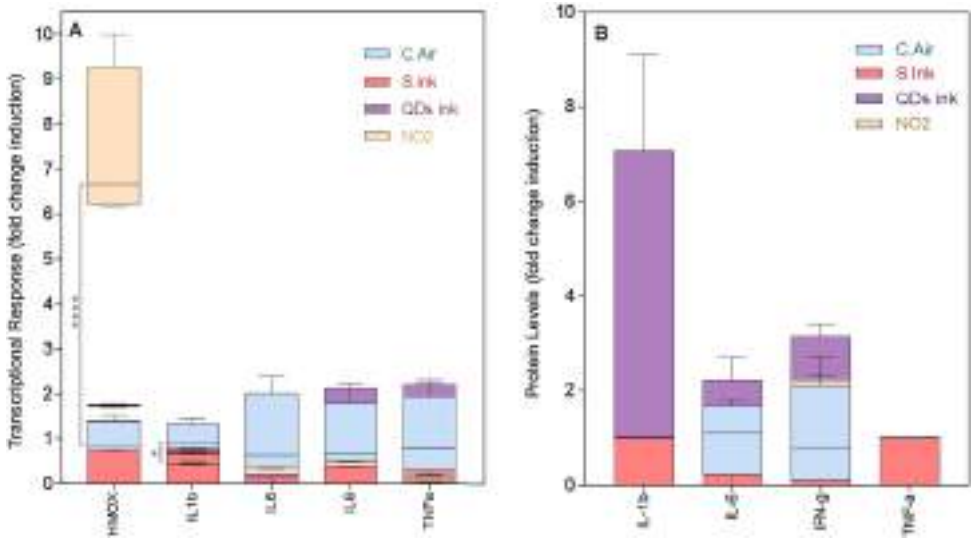

Fig. 6. Box-and-whisker plot showing the impact of solvent and PEG-CdTe QDs inks, and nitrogen dioxide (NO_2) in contrast to clean air (C. Air) on BEAS-2B cells after *in vitro* exposure for 1 h at the ALI, at two regulation levels: **A**) the transcription of oxidative stress (*HMOX1*) and pro-inflammatory cytokines (*IL1b*, *IL6*, *IL8* and *TNFa*) markers; **B**) the protein synthesis for the proinflammatory cytokines IL1-β, IL-6, INF-γ, and TNF-α. In both cases, fold-change was calculated compared to the vehicle control (C. Air). Error bars indicate standard deviation. * = $p < 0.05$; **** = $p < 0.0001$. the limit of detection (<0.1 ng/mL) for both elements in the conditions tested.

enzymatic anti-oxidant in the lungs induced by environmental components (heat stress, hypoxia, metals, endotoxins, hormones), was upregulated only by the positive control (NO_2).

In submerged conditions, transcription levels of HMOX1 were upregulated compared to the solvent ink control after exposure to ≥216 ng/mL of PEG-CdTe QDs ink, while IL-8 and IL-6 were upregulated after exposure to at least 5400 or 27000 ng/mL QDs ink, respectively. IL-1β and TNF-α mRNA levels remained unchanged after QDs ink treatment (Fig. SI8A).

The production of the pro-inflammatory cytokines IL-1β, IL-6, TNF-α and IFN-γ was also measured at the protein level using a multiplex protein assay. No significant changes in the cytokine levels could be detected in the apical cell medium conditioned with the cells during post-incubation following the solvent and PEG-CdTe QDs inks exposure at the ALI compared to clean air condition (Fig. 6B). Concerning complementary controls, no significant differences were observed due to removal of the culture medium at the ALI (IC + vs IC-) for all selected proteins. LPS showed statistically significant differences ($p < 0.0001$) for IL-6 and IFN-g, and for TNFa ($p = 0.002$) when compared to IC+.

In submerged BEAS-2B cell cultures exposed to the PEG-CdTe QDs ink, IL-6 was also the only cytokine that was detected, showing increasing levels compared to solvent ink from 216 ng/mL onward (Fig. SI8B). The levels of the other 3 cytokines were not induced by the PEG-CdTe QDs ink, as they did not pass the respective detection limits of the assay (IL-6 0.448 pg/mL; IFN-γ 0.924 pg/mL; IL-1β 0.355 pg/mL; TNF-α 0.204 pg/mL).

4. Discussion

In this study we report the release of QDs into the air during inkjet printing of a prototype of PEG-CdTe QDs containing ink and the *in vitro* screening of its health effects. We simulated a household printing process and confirmed that airborne PEG-CdTe QDs were released during inkjet printing. Released particle formats were determined by TEM, and revealed aggregated PEG-CdTe QDs forming networks, although their individual identity (with 3–5 nm diameter) was not lost. This is in contrast to Shi and colleagues who did not observe NP emission from 5 inkjet printers in a normal office environment (Shi et al., 2015). The discrepancy may be explained by the a priori presence of NPs (PEG-CdTe QDs) in the ink in our study.

The simulated release scenario of nano-ink aerosols may cause relevant human exposure and associated health risks. To assess potential health effects from respiratory exposure to aerosolized PEG-CdTe QDs ink, we performed an *in vitro* investigation using human bronchial epithelial cells that were exposed to PEG-CdTe QDs ink aerosol at the ALI in contrast to the not nano-additivated solvent ink. Such ALI exposure has been proven to provide a controlled, yet more practically and physiologically relevant approach for biological response assessment (Ihalainen et al., 2019; Lacroix et al., 2018), as the cells undergo an acute exposure scenario (1 h) followed by a physiological response time ranging from 1 to 23 h for mRNA expression and protein expression and metabolic response, respectively. To our knowledge this approach has not been applied to QDs toxicity assessment before and studies investigating the inhalation route of exposure are scarce (Zheng et al., 2018).

PEG-CdTe QDs contained in ink was delivered to the cells at a concentration of 37.1 ng/mL Cd and 17.6 ng/mL Te (54.7 ng/mL PEG-CdTe QDs), decreasing cell metabolic activity by 25.6 % (±15.7 %) in the ALI inhalation simulating conditions. A 9.0 % (±11.9 %) decrease of cell viability was also observed for atomized solvent ink. Notwithstanding the relevance of the results obtained, 1 h cell exposure at relatively high concentrations of aerosolized ink does not reflect long-term exposure to low concentrations of particles resulting from household inkjet printing. We have used the Multiple Particle Path Dosimetry Model (MPPD) (v3.04) (Anjilvel and Asgharian, 1995) to calculate the lung deposition and deposition mass flux for particles emitted during inkjet printing on the human respiratory system. Values used as input for the model were 500.14 particle/cm^3; 62 nm and 5.85 g/cm^3 for average particle concentration, mean particle diameter and particle density, respectively. The pulmonary deposited mass rate per unit area estimated by the MPPD model corresponded to a concentration of $9.30^{*}10^{-16}$ μg/min/cm^2, equivalent to $9.30^{*}10^{-12}$ ng/cm^2 for a 10 min printing period whereas the dose calculated during 1 h atomization (12.1 ng/cm^2) corresponds to 2.02 ng/cm^2 if a 10 min period is taken as a reference. Despite the considerable difference with the estimated pulmonary deposited mass, the exact dose delivered to the cells in ALI is difficult to measure or estimate. For instance, Oldham and coworkers (2020) have recently reported experimentally measured deposition efficiencies ranging from 0.013 to 0.86 % in a Vitrocell® 24/48 ALI *in vitro* exposure system whereas we have reported a 4.39 % deposition efficiency. Delivering nanoparticles in the form of suspensions is susceptible to inaccuracies related to dispersion techniques, dispersant media, re-agglomeration and setting behavior. An additional difficulty is related to the deposition rates of nanoparticle aerosols which are generally quite low (Paur et al., 2011), liming the accuracy of the calculated dose. The instrumentation used for dose measurement represents another obstacle: we have derived the dose on the basis of PNC and average particle diameter measured by an SMPS in conjunction with an OPS or by an SMPS only during the inkjet printing scenario and the atomization process, respectively (see M&M sections 2.2. and 2.3.), this implying that the full spectrum of particles generated during the inkjet printing and/or atomization process might not be covered within the particle size range measured by these instruments.

Long-term exposure is not possible with current *in vitro* ALI systems, such as Vitrocell®, since the survival of the cells is low (<4−8 hours) as the models lack culture medium and thus nutrients at the apical side. Alternatively, we have represented an acute worse-case- exposure scenario. In this set-up, aerosol generation by atomization was needed to obtain high nanoparticle levels and reproducibility in exposure. Even if the dose that we have selected is unrealistic, the composition of the aerosolized inks corresponds to that of particles released during inject printing: we have not exclusively focused on the toxicological effects associated to PEG-CdTe QDs used as an additive in inkjet printing ink. In this sense, Pirela et al. (2017) highlighted the use of toner particles instead of “real world” exposures as a major research gap in a review describing the toxicological effects derived from nanoparticle exposures from toner-based printing.

An additional limitation is related to the short culture times (16 h) of the cells before onset of experiments at the ALI restricting their mucociliary differentiation. In fact, our BEAS-2B cell model is only suitable for basal cell toxicity screening purposes. Epithelial cells contribute to lung immunity by secretion of chemokines, cytokines and antimicrobial compounds (e.g. ROS) (Parker and Prince, 2011). For further studies, to observe integrated cell responses such as interactions with mucus-secreting goblet cells and ciliar clearance of foreign particles, more complex models would be needed. In any case, only *in vivo* exposure models would allow to assess effects over the full human airway physiology: bronchus or conductive part and alveoli or terminal branches where gas exchange occurs; vascular endothelium and immune cells (alveolar macrophages being the front line cell type); or systemic effects such as translocation/accumulation of nanoparticles in secondary organs, and the subsequent responses.

Despite the aforementioned, ALI *in vitro* inhalation models mimic more closely the pulmonary region than classic (i.e.,

submerged) *in vitro* methods. In this sense, in previous studies also based on the assessment of metabolic cell activity, a similar toxicity level was reached around 37.5 nM (9 ng/mL) CdTe QDs in HEK293 cells (Su et al., 2010), 1 μg/mL in MCF-7 cells (Lovrić et al., 2005), and 15 μg/mL in HeLa cells (Du et al., 2019) after 24 h exposure in submerged culture conditions. Differences of 4 orders of magnitude are observed, which may have several causes related to the key intrinsic QDs properties (including size, surface ligand) and purity of the suspension (Su et al., 2009). Furthermore, exposure time, exposure concentration, assay type, cell anatomical type and cell origin seem to also be major attributes to QD-induced toxicity response (Oh et al., 2016), as is the *in vitro* exposure format (ALI *versus* submerged cultures). The latter highlights the importance of the model used for cytotoxicity assessments related to airways. Of main relevance for nanoadditivated products, the exposure conditions at the ALI prevent from possible changes undergone in NP's physicochemical properties (e.g. dissolution, agglomeration) resulting from interactions with the cell culture medium.

Moreover, the use of ALI models has the potential to reduce the number of animals used in research as they may provide better previous information on *in vivo* processes in humans, since some specific mechanisms might differ or do not exist in animal models due to physiological differences (Lacroix et al., 2018).

The CdTe QDs' cytotoxicity observed in this study could be due to the eventual entering of these toxic species into the cells, thereby causing a synergistic effect between CdTe-QDs' nanotoxicity and Cd ions-induced cytotoxicity (Zheng et al., 2018). Su et al. also reported a direct association between the total CdTe-QDs ingested by HEK293 cells and cytotoxicity (Su et al., 2010). However, they did not find a direct relationship between intracellular Cd^{2+} ions and CdTe QDs concentration supplied to the cells, and concluded that the nanoscale properties of the QDs played an important role in their cytotoxicity. Since Cd and its compounds are classified as group 1 carcinogens, its dissolution even capped must however be considered of high relevance for human and environmental health. Yet, in a recent study on *in vivo* biodistribution and systemic effects, Nguyen et al. observed that Cd alone cannot fully explain the toxicity of CdTe-QDs (Nguyen et al., 2019). Intrinsic QDs properties can also be major contributors of toxicity including size, surface ligands and residual reagents from the QDs synthesis process (Oh et al., 2016). The size (between 3 and 5 nm) of the PEG-CdTe QDs used in our study, as well as the observed presence of QDs' stabilizing reagent thioglycolic acid in the inks have been related to increased toxicity by others (Liu et al., 2013; Zheng et al., 2018; Xu et al., 2015; Du et al., 2019). In addition, but generally less well considered, tellurium is mildly toxic and thus can be partially responsible for the observed effects. *In vitro* studies by Vij and Hardej (2012) indicated that diphenyl ditelluride and tellurium tetrachloride significantly decreased cell viability in transformed (HT-29, Caco-2) and non-transformed colon cells (CCD-18Co), starting from 31.25 (4.0 μg/mL) and 500 μM (63.8 μg/mL) respectively. In our study, the total aerosol delivered Te dose to BEAS-2B cells was ~113 times lower, and therefore unlikely to contribute to the observed toxicity. Finally, PEG capping was applied to the QDs' surfaces in our study, which is known to reduce their non-specific binding to cells and subsequent uptake, as well as the release of Cd^{2+}, thus resulting in higher biocompatibility. Also, PEG conjugation to CdTe QDs having a similar surface ligand (i.e. thioglycolyl acid/ mercapto-acetohydrazide) and primary size (3.8 nm) as in our study has been shown to significantly reduce their *in vitro* and *in vivo* toxicity *(Du et al.*, 2019). Nevertheless, we have demonstrated that cells exposed at the ALI with aerosolized PEG-CdTe QDs ink at 135 times lower effective dose show residual cellular toxicity. This shift can be attributed to a different reactivity of the PEG-CdTe QDs at a given concentration, as cell exposure in the ALI scenario represents a different, yet more relevant mechanism of cell-particle interaction.

HMOX1 was selected to screen the oxidative potential of PEG-CdTe QDs ink, one of the most important mechanisms of cell toxicity (Lovrić et al., 2005). QDs have been observed to elicit reactive oxygen species (ROS) production and to impact on antioxidant glutathione levels. We investigated whether the PEG-CdTe QDs ink altered antioxidant HMOX1 expression in the cells, but did not measure differential gene regulation. We did not observe either an inflammatory response at the ALI compared to the clean air condition.

5. Conclusions

The emissions of a water-based printing ink containing coated PEG-CdTe QDs during a household inkjet printing scenario simulated under controlled conditions have been characterized, showing the release of PEG-CdTe QDs in the use phase of the ink. Release forms consisted of aggregated PEG-CdTe QDs forming networks, though maintaining their individual identity (with 3–5 nm diameter).

An integrated approach using atomization of nano-additivated ink and exposure of BEAS-2B cells at the ALI for the *in vitro* screening of the cytotoxicological effect of airborne emissions has been developed. Using this approach, aerosol of PEG-CdTe QDs ink was delivered to the cells under the ALI inhalation simulating conditions at a concentration of 54.7 ng/mL (37.1 ng/mL Cd and 17.6 ng/mL Te), resulting in decreased cell viability by 25.6 % (±15.7 %) when compared with the clean air condition. A 9.0 % (±11.9 %) decrease of cell viability was also observed for atomized solvent ink.

Our *in vitro* basal acute toxicity screening study indicates potential health impact of CdTe-QDs particles derived from inkjet printing emissions. These findings warrant further exploration using more complex *in vitro/ex vivo* models and *in vivo* studies, to enable proper data collection for risk assessment.

Declaration of Competing Interest

The authors report no declarations of interest.

Acknowledgements

This work was supported by the European Union's Seventh Framework Programme (EU FP7) under grant agreement No. 309329 (NanoSolutions) and from the QualityNano Project which is financed by the European Community Research Infrastructures under the FP7 Capacities Programme (Grant No. INFRA-2010-262163), and its partner VITO nv. Authors thank PlasmaChem GmbH, specially Alexei Antipov, for providing both the PEG CdTe-QDs ink and the solvent ink.

Appendix A. Supplementary data

Supplementary material related to this article can be found, in the online version, at doi:https://doi.org/10.1016/j.toxlet.2021.04.009.

References

Abd El-sadek, M.S., Babu, S.M., 2011. A controlled approach for synthesizing CdTe@CrOOH (core-shell) composite nanoparticles. Curr. Appl. Phys. 11, 926–932. doi:http://dx.doi.org/10.1016/j.cap.2010.12.022.

Anjilvel, S., Asgharian, B., 1995. A Multiple-Path Model of Particle Deposition in the Rat Lung. Fundam. Appl. Toxicol. 28, 41–50. doi:http://dx.doi.org/10.1006/faat.1995.1144.

Arivarasan, A., Sasikala, G., Jayavel, R., 2014. In situ synthesis of CdTe:CdS quantum dot nanocomposites for photovoltaic applications. Mater. Sci. Semicond. Process. 25, 238–243. doi:http://dx.doi.org/10.1016/j.mssp.2013.12.018.

CEPE, 2012. Position Paper on the French Decree and Order on Nanomaterials. Available on line at: https://www.cepe.org/wp-content/uploads/2018/01/CEPE-Position-on-the-French-Decree-and-Order-on-Nanomaterials.pdf. Last accessed on 01 September 2020. .

Du, Y., Zhong, Y., Dong, J., Qian, C., Sun, S., Gao, L., Yang, D., 2019. The effect of PEG functionalization on the *in vivo* behavior and toxicity of CdTe quantum dots. RSC Adv. 9, 12218–12225. doi:http://dx.doi.org/10.1039/C9RA00022D.

ECHA 2020a. https://echaa.europa.eu/es/substance-information/-/substanceinfo/100.239.172. Last accessed on 01 September 2020.

ECHA 2020b. https://echab.europa.eu/es/substance-information/-/substanceinfo/100.013.773. Last accessed on 01 September 2020.

Geys, J., Coenegrachts, L., Vercammen, J., Engelborghs, Y., Nemmar, A., Nemery, B., Hoet, P.H.M., 2006. In vitro study of the pulmonary translocation of nanoparticles: a preliminary study. Toxicol. Lett. 160, 218–226. doi:http://dx.doi.org/10.1016/j.toxlet.2005.07.005.

Guillén-Cervantes, A., Silva-López, H., Becerril-Silva, M., Arias-Cerón, J.S., Campos-González, E., Medina-Torres, A.C., Zelaya-Ángel, O., 2015. Photoluminescence of CdTe nanocrystals grown by pulsed laser ablation on a template of Si nanoparticles. Appl. Phys. A 118, 1039–1042. doi:http://dx.doi.org/10.1007/s00339-014-8866-5.

Hellemans, J., Mortier, G., De Paepe, A., Speleman, F., Vandesompele, J., 2007. qBase relative quantification framework and software for management and automated analysis of real-time quantitative PCR data. Genome Biol. 8, R19. doi:http://dx.doi.org/10.1186/gb-2007-8-2-r19.

IARC Working Group on the Evaluation of Carcinogenic Risks to Humans, International Agency for Research on Cancer, 2012. A Review of Human Carcinogens. Arsenic, Metals, Fibres, and Dusts. International Agency for Research on Cancer.

Ihalainen, M., Jalava, P., Ihantola, T., Kasurinen, S., Uski, O., Sippula, O., Hartikainen, A., Tissari, J., Kuuspalo, K., Lähde, A., Hirvonen, M.-R., Jokiniemi, J., 2019. Design and validation of an air-liquid interface (ALI) exposure device based on thermophoresis. Aerosol Sci. Technol. 53, 133–145. doi:http://dx.doi.org/10.1080/02786826.2018.1556775.

International Cadmium Association (ICdA), 2020. International Cadmium Association (ICdA) Website. . Last accessed on 1 September 2020 https://www.cadmium.org/cadmium-applications/cadmium-pigments.

Karrasch, S., Simon, M., Herbig, B., Langner, J., Seeger, S., Kronseder, A., Peters, S., Dietrich-Gümperlein, G., Schierl, R., Nowak, D., Jörres, R.A., 2017. Health effects of laser printer emissions: a controlled exposure study. Indoor Air 27, 753–765. doi:http://dx.doi.org/10.1111/ina.12366.

Konga, D.B., Kim, Y., Hong, S.C., Roh, Y.M., Lee, C.M., Kim, K.Y., Lee, S.M., 2009. Oxidative stress and antioxidant defenses in asthmatic murine model exposed to printer emissions and environmental tobacco smoke. J. Environ. Pathol. Toxicol. Oncol. 28, 325–340. doi:http://dx.doi.org/10.1615/jenvironpatholtoxicoloncol.v28.i4.70.

Kshirsagar, A., Jiang, Z., Pickering, S., Xu, J., Ruzyllo, J., 2013. Formation of photoluminescent patterns on paper using nanocrystalline quantum dot ink and mist deposition. ECS J. Solid State Sci. Technol. 2, R87–R90.

Lacroix, G., Koch, W., Ritter, D., Gutleb, A.C., Larsen, S.T., Loret, T., Zanetti, F., Constant, S., Chortarea, S., Rothen-Rutishauser, B., Hiemstra, P.S., Frejafon, E., Hubert, P., Gribaldo, L., Kearns, P., Aublant, J.-M., Diabaté, S., Weiss, C., de Groot, A., Kooter, I., 2018. Air–liquid interface *in vitro* models for respiratory toxicology research: consensus workshop and recommendations. Appl. Vitr. Toxicol. 4, 91–106. doi:http://dx.doi.org/10.1089/aivt.2017.0034.

Lange, A., Wedel, A., 2017. Organic light-emitting diode (OLED) and quantum dot (QD) inks and application. Handbook of Industrial Inkjet Printing. Wiley-VCH Verlag GmbH & Co. KGaA, Weinheim, Germany, pp. 225–238. doi:http://dx.doi.org/10.1002/9783527687169.ch12.

Liu, X., Tang, M., Zhang, T., Hu, Y., Zhang, S., Kong, L., Xue, Y., 2013. Determination of a threshold dose to reduce or eliminate CdTe-Induced toxicity in L929 cells by controlling the exposure dose. PLoS One 8, e59359 doi:http://dx.doi.org/10.1371/journal.pone.0059359.

Lovrić, J., Cho, S.J., Winnik, F.M., Maysinger, D., 2005. Unmodified cadmium telluride quantum dots induce reactive oxygen species formation leading to multiple organelle damage and cell death. Chem. Biol. 12, 1227–1234. doi:http://dx.doi.org/10.1016/J.CHEMBIOL.2005.09.008.

Meija, J., Coplen, T.B., Berglund, M., Brand, W.A., De Bièvre, P., Gröning, M., Holden, N. E., Irrgeher, J., Loss, R.D., Walczyk, T., Prohaska, T., 2016. Atomic weights of the elements 2013 (IUPAC Technical Report). Pure Appl. Chem. 88, 265–291. doi:http://dx.doi.org/10.1515/pac-2015-0305.

Nakadate, T., Yamano, Y., Yamauchi, T., Okubo, S., Nagashima, D., 2018. Assessing the chronic respiratory health risk associated with inhalation exposure to powdered toner for printing in actual working conditions: a cohort study on occupationally exposed workers over 10 years. BMJ Open 8, 22049. doi:http://dx.doi.org/10.1136/bmjopen-2018-022049.

Nguyen, K.C., Rippstein, P., Tayabali, A.F., Willmore, W.G., 2015. Mitochondrial toxicity of cadmium telluride quantum dot nanoparticles in mammalian hepatocytes. Toxicol. Sci. 146, 31–42. doi:http://dx.doi.org/10.1093/toxsci/kfv068.

Nguyen, K.C., Zhang, Y., Todd, J., Kittle, K., Patry, D., Caldwell, D., Lalande, M., Smith, S., Parks, D., Navarro, M., Massarsky, A., Moon, T.W., Willmore, W.G., Tayabali, A. F., 2019. Biodistribution and systemic effects in mice following intravenous administration of cadmium telluride quantum dot nanoparticles. Chem. Res. Toxicol. 32, 1491–1503. doi:http://dx.doi.org/10.1021/acs.chemrestox.8b00397.

Oh, E., Liu, R., Nel, A., Gemill, K.B., Bilal, M., Cohen, Y., Medintz, I.L., 2016. Meta-analysis of cellular toxicity for cadmium-containing quantum dots. Nat. Nanotechnol. 11, 479–486. doi:http://dx.doi.org/10.1038/nnano.2015.338.

Oldham, M.J., Castro, N., Zhang, J., Rostami, A., Lucci, F., Pithawalla, Y., Kuczaj, A.K., Gilman, I.G., Kosachevsky, P., Hoeng, J., Lee, K.M., 2020. Deposition efficiency and uniformity of monodisperse solid particle deposition in the Vitrocell® 24/48 Air–Liquid-Interface in vitro exposure system. Aerosol Sci. Technol. 54, 52–65. doi:http://dx.doi.org/10.1080/02786826.2019.1676877.

Parker, D., Prince, A., 2011. Innate immunity in the respiratory epithelium. Am. J. Respir. Cell Mol. Biol. doi:http://dx.doi.org/10.1165/rcmb.2011-0011RT.

Paur, H.R., Cassee, F.R., Teeguarden, J., Fissan, H., Diabate, S., Aufderheide, M., Kreyling, W.G., Hänninen, O., Kasper, G., Riediker, M., Rothen-Rutishauser, B., Schmid, O., 2011. In-vitro cell exposure studies for the assessment of nanoparticle toxicity in the lung-A dialog between aerosol science and biology. J. Aerosol Sci. 42, 668–692. doi:http://dx.doi.org/10.1016/j.jaerosci.2011.06.005.

Persoz, C., Achard, S., Momas, I., Seta, N., 2012. Inflammatory response modulation of airway epithelial cells exposed to formaldehyde. Toxicol. Lett. 211, 159–163. doi:http://dx.doi.org/10.1016/j.toxlet.2012.03.799.

Pirela, S.V., Sotiriou, G.A., Bello, D., Shafer, M., Bunker, K.L., Castranova, V., Thomas, T., Demokritou, P., 2015. Consumer exposures to laser printer-emitted engineered nanoparticles: a case study of life-cycle implications from nano-enabled products. Nanotoxicology 9, 760–768. doi:http://dx.doi.org/10.3109/17435390.2014.976602.

Pirela, S.V., Martin, J., Bello, D., Demokritou, P., 2017. Nanoparticle exposures from nano-enabled toner-based printing equipment and human health: state of science and future research needs. Crit. Rev. Toxicol. doi:http://dx.doi.org/10.1080/10408444.2017.1318354.

Schindelin, J., Arganda-Carreras, I., Frise, E., Kaynig, V., Longair, M., Pietzsch, T., Preibisch, S., Rueden, C., Saalfeld, S., Schmid, B., Tinevez, J.-Y., White, D.J., Hartenstein, V., Eliceiri, K., Tomancak, P., Cardona, A., 2012. Fiji: an open-source platform for biological-image analysis. Nat. Methods 9, 676–682. doi:http://dx.doi.org/10.1038/nmeth.2019.

Shi, X., Chen, R., Huo, L., Zhao, L., Bai, R., Long, D., Pui, D.Y.H., Rang, W., Chen, C., 2015. Evaluation of nanoparticles emitted from printers in a lean chamber, a copy center and office rooms: ealth risks of indoor air quality. J. Nanosci. Nanotechnol. 15, 9554–9564. doi:http://dx.doi.org/10.1166/jnn.2015.10314.

Su, Y., He, Y., Lu, H., Sai, L., Li, Q., Li, W., Wang, L., Shen, P., Huang, Q., Fan, C., 2009. The cytotoxicity of cadmium based, aqueous phase – synthesized, quantum dots and its modulation by surface coating. Biomaterials 30, 19–25. doi:http://dx.doi.org/10.1016/J.BIOMATERIALS.2008.09.029.

Su, Y., Hu, M., Fan, C., He, Y., Li, Q., Li, W., Wang, L.-H., Shen, P., Huang, Q., 2010. The cytotoxicity of CdTe quantum dots and the relative contributions from released cadmium ions and nanoparticle properties. Biomaterials 31, 4829–4834. doi:http://dx.doi.org/10.1016/J.BIOMATERIALS.2010.02.074.

Tekin, E., Smith, P.J., Hoeppener, S., Van Den Berg, A.M.J., Susha, A.S., Rogach, A.L., Feldmann, J., Schubert, U.S., 2007. InkJet printing of luminescent CdTe nanocrystal-polymer composites. Adv. Funct. Mater. 17, 23–28. doi:http://dx.doi.org/10.1002/adfm.200600587.

Terunuma, N., Ikegami, K., Kitamura, H., Ando, H., Kurosaki, S., Masuda, M., Kochi, T., Yanagi, N., Ogami, A., Higashi, T., 2019. A Cohort study on respiratory symptoms and diseases caused by toner-handling work: longitudinal analyses from 2003 to 2013. Atmosphere (Basel) 10, 647. doi:http://dx.doi.org/10.3390/atmos10110647.

The Danish Environmental Protection Agency, 2015. Release of Nanomaterials From Ink and Toner Cartridges for Printers. Copenhagen, Denmark. .

Verstraelen, S., Remy, S., Casals, E., De Boever, P., Witters, H., Gatti, A., Puntes, V., Nelissen, I., 2014. Gene expression profiles reveal distinct immunological responses of cobalt and cerium dioxide nanoparticles in two in vitro lung epithelial cell models. Toxicol. Lett. 228, 157–169. doi:http://dx.doi.org/10.1016/j.toxlet.2014.05.006.

Vij, P., Hardej, D., 2012. Evaluation of tellurium toxicity in transformed and non-transformed human colon cells. Environ. Toxicol. Pharmacol. 34, 768–782. doi:http://dx.doi.org/10.1016/J.ETAP.2012.09.009.

Wuister, S.F., Swart, I., van Driel, F., Hickey, S.G., de Mello Donegá, C., 2003. Highly luminescent water-soluble CdTe quantum dots. Nano Lett. 3, 503–507. doi:http://dx.doi.org/10.1021/nl034054t.

Xu, W., Du, T., Xu, C., Han, H., Liang, J., Xiao, S., 2015. Evaluation of biological toxicity of CdTe quantum dots with different coating reagents according to protein expression of engineering *Escherichia coli*. J. Nanomater 2015, 1–7. doi:http://dx.doi.org/10.1155/2015/583963.

Xu, Y.-M., Tan, H.W., Zheng, W., Liang, Z.-L., Yu, F.-Y., Wu, D.-D., Yao, Y., Zhong, Q.-H., Yan, R., Lau, A.T.Y., 2019. Cadmium telluride quantum dot-exposed human bronchial epithelial cells: a further study of the cellular response by proteomics. Toxicol. Res. (Camb). 8, 994–1001. doi:http://dx.doi.org/10.1039/c9tx00126c.

Zheng, W., Xu, Y.-M., Wu, D.-D., Yao, Y., Liang, Z.-L., Tan, H.W., Lau, A.T.Y., 2018. Acute and chronic cadmium telluride quantum dots-exposed human bronchial epithelial cells: The effects of particle sizes on their cytotoxicity and carcinogenicity. Biochem. Biophys. Res. Commun. 495, 899–903. doi:http://dx.doi.org/10.1016/J.BBRC.2017.11.074.

Supporting information

Release and Cytotoxicity screening of the printer emissions of a CdTe Quantum Dots-based fluorescent ink

María Blázquez Sánchez,[a,b] Nelissen Inge,[d] Vicenç Pomar-Portillo,[c] Alejandro Vílchez,[c] Jo Van Laer,[d] Jacobs An,[d] Evelien Frijns,[d] and Socorro Vázquez-Campos,[c] Elisabet Fernandez-Rosas [c*]

[a] INKOA SISTEMAS SL, Ribera de Axpe 11, Edificio D1, Dpto 208. 48950 Erandio, Bizkaia, Spain.; [b] CBET Research Group, Department of Zoology and Animal Cell Biology, Faculty of Science and Technology and Research Centre for Experimental Marine Biology and Biotechnology PiE, University of the Basque Country UPV/EHU, Barrio Sarriena s/n. 48940, Leioa, Bizkaia, Spain; [c] VITO NV, Health Unit, Boeretang 200, 2400 Mol, Belgium; [d] LEITAT Technological Center, Carrer de la Innovació 2, 08225 Terrassa (Barcelona), Spain.

Materials and methods

SI-S1. Ink formulation and characterization. Inductively coupled plasma mass spectrometry (ICP-MS) protocol

Samples were digested with an acid solution (10 ml of nitric acid 70%, HNO_3 for trace analysis, Sigma Aldrich) in an analytical microwave digestion system (MARS, CEM). Before the digestion, samples were directly weighed (0.01 g sample) into 55 mL perfluoroalkoxy alkanes (PFA) microwave vessels (MARSXPress, CEM). Then, 10 mL of nitric acid were placed into the vessel to perform the microwave acid digestion program. Specifically, the conditions and procedure of microwave digestions were as follows: heat from room temperature to 200ºC in 10 min, then maintain this temperature for 15 min and, finally, cool down to room temperature to manipulate the samples safely. After having carried out the described digestion program, all samples were filled with ultrapure water to 50 ml. Then, further dilutions were made with 2% HNO_3 aqueous solution to obtain the desired concentrations for ICP-MS characterization. Cadmium (Cd) and Tellurium (Te) analysis were performed by ICP-MS (Agilent 7500, Agilent Technologies). The quantification was done by interpolation in a standard curve obtained from 1000 ppm commercial standard (Sigma Aldrich).

SI-S2. Deposition efficiency and dose quantification after ink exposure at the ALI. ICP-MS protocol

For destructive ICP-MS analysis, an aliquot of 400 µl of the sample was transferred into a polypropylene (PP) 15 ml disposable test tube, and 400 µl of nitric acid (67-69% Fisher scientific Optima grade) was added. The test tubes were closed and transferred to a microwave oven (Milestone mls1200 mega) and heated three times for 2 minutes at 150 Watt. After cooling down 3.2 ml of ultrapure water was added resulting in a 10% (v/v) nitric acid digestion solution.

For non-destructive analysis samples were prepared by diluting them at least 10 times in 2% nitric acid and measured without further digestion.

The (non-)digested samples were measured using a quadrupole ICP-MS instrument (Nexion 300s, Perkin Elmer) equipped with an ESI SC2-DX autosampler with SC-FAST automated sample introduction system. In total 6 calibration standards, all matrix matched, together with a calibration blank were used to calibrate the ICP-MS in standard mode. Three calibration standards (1.0 µg/l, 10 µg/l and 50 µg/l) were used to calibrate for Cd and Te, and three calibration standards (same concentrations) were used for the calibration of tin (Sn) and molybdenum (Mo). The latter was necessary to determine the presence of these elements in the samples, since they are a source of interference on the different masses of Cd. After analysis there appeared no presence of Mo and Sn in the samples. The calibration was verified by independent control samples in the concentration range of 0.1 µg/l, 1.0 µg/l and 10 µg/l, also matrix matched. After the measurement of the samples the calibration blank was re-analysed together with the highest calibration standards. An Internal standard Rhodium (103Rh) was pumped online and mixed with all samples to control for non-spectral interference due to the sample matrix. All results obtained were corrected for this internal standard.

Results

SI-S3. Dose efficiency and quantification after in vitro ink exposure. Submerged conditions

To compare total and ionic exposure of cells to Cd and Te ions in the ALI vs. in submerged conditions, six serial 1/5 dilutions of PEG-CdTe QDs ink in BEGM medium were measured after 24 hours of exposure (Table S1). The range covered equitably concentrations above and below the CdTe dose value determined using the Vitrocell® module. ICP-MS readout series indicated a linear pattern of dissolved Te ions (r^2 = 0.846) and Cd ions (r^2 = 0.958) at all the dilutions tested, except for Te at the highest QDs concentration (27 µg/ml) (see next section SI-S4 and Figure SI8). In that case, ionic Te concentration decreased to values detected in the medium at ~1.1 µg/ml QDs, whereas Cd ion concentration increased further. These ionic Cd:Te ratio changes with concentration can be explained by the fact that at that the highest dose only the QDs' surfaces dissolve in the culture media, where Cd atoms dominate.

Table SI1. Cd and Te ionic concentrations detected by ICP-MS in filtered BEGM medium (submerged conditions) after 24 hours incubation with PEG-CdTe QDs ink. Solvent ink was used as negative control.

QDs exposure values*	Te ions detected*	Cd ions detected*	QDs ionic % detected*	Cd:Te ions ratio
0.0	<0.1	<0.1	N/A	N/A
8.6	2.3	3.8	71%	1.65
43	7.7	12	46%	1.56
216	29	37	31%	1.23
1080	99	122	20%	1.23
5400	160	427	11%	2.67
27000	102	1050	4,3%	10.29

** All the values indicated in ng/ml.*

SI-S4. Cell viability assessment. Submerged conditions

Potential *in vitro* cytotoxic effects of the PEG-CdTe QDs containing ink in submerged conditions was also assessed using the same human bronchial epithelial BEAS-2B cell line. Cells were exposed for 24 hours to the same 1/5 serial dilutions of PEG-CdTe QDs used for the deposition efficiency assay, from 8.6-27000 ng/ml. After submerged exposure of the BEAS-2B cells to the PEG-CdTe QDs ink, they were detached from the well plate by trypsinization, and 10 µl cell suspension was added to 10 µl of 0.4% trypan blue staining solution (Invitrogen) in an Eppendorf tube. The mixture was gently pipetted up and down, and 10 µL was added to a Countess™ Cell Counting Chamber slide (Invitrogen) which was read out on a Countess™ Automated Cell Counter after parameter adjustment. The changes in cell count for live, dead and total cells, and calculated percentage viability, as displayed on the screen, were used as a measure of toxicity in exposed compared to untreated BEAS-2B cells.

Results were compared to previous data from our laboratories, exposing the same cell line in submerged conditions to serial concentrations of $CdCl_2$ salt (190-50000 ng/ml). Briefly, the assay was done following the provider's specifications, and using a Multiskan Ascent spectrophotometer (Thermo Fisher) at 540 nm for the readouts. In submerged conditions, an exponential decline on cell viability related to Cd ions ($CdCl_2$) concentration within three orders of magnitude was observed (Figure SI8, golden dots), where EC_{50} calculated using neutral red assay was 2000 ng/ml.

Although a different protocol was followed (cell density and cytotoxicity test), highly similar EC_{50} values were obtained, and results relative to Cd ionic doses showed a good exponential correlation ($r^2 = 0.8721$) between both experiments. Consequently, Cd ions seemed to be the main cause of the observed cytotoxicity. Figure SI-S8 shows a comparison with cytotoxicity observed in ALI exposure.

Cells were not affected by concentrations of Cd ions lower than 500 ng/ml ($p \leq 0.05$), corresponding to a concentration of PEG-CdTe QDs in ink between 5400-27000 ng/ml). The observed IC_{20} was at 1050 ng/mL of Cd^{2+} (27 µg/mL of QDs) compared to the positive control. No cytotoxicity could be attributed to solvent ink in submerged conditions, tested at 0.25% v/v, the same final concentration as for the PEG-CdTe QDs ink.

At the ALI, viability observed for cells exposed to the PEG-CdTe QDs ink (Figure SI8, green square) was two orders of magnitude lower than in submerged conditions, 74.4%, though 2/3 of the cytotoxicity observed (16.6%) could be attributed to PEG-CdTe QDs, and 1/3 (9%) to the presence of solvent ink.

Figures

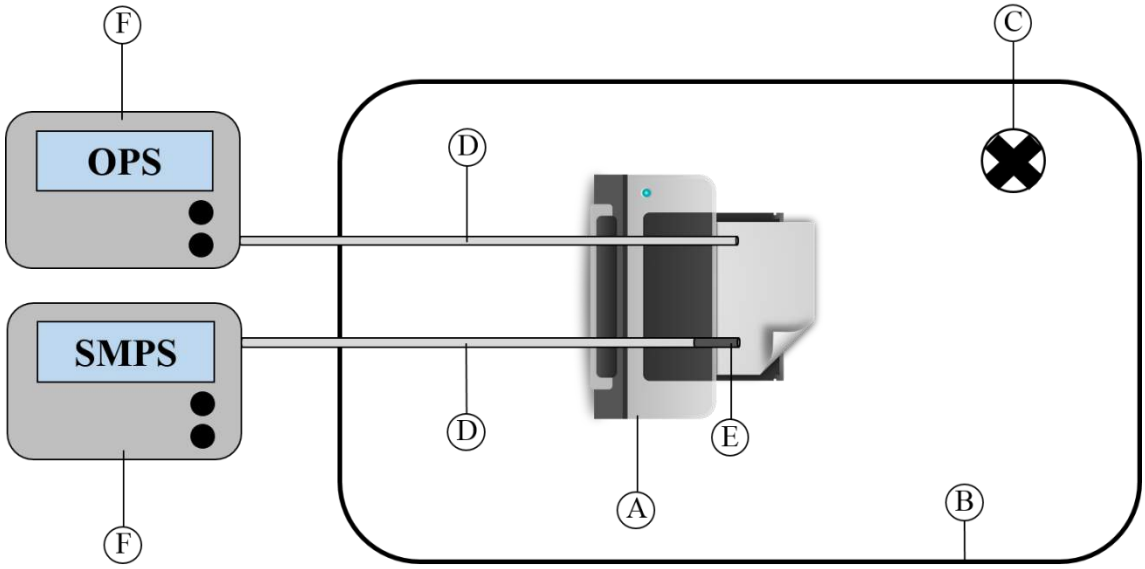

Figure SI1 - Schematic representation of the setup used to determine the Particle Number Concentration (PNC) in air during the household printing process using the Optical Particle Sizer (OPS) and Scanning Mobility Particle Sizer (SMPS). A) Printer; B) Methacrylate box; C) Polycarbonate filter; D) Silicon tubes; E) TEM sampler device; F) Air measurement instruments.

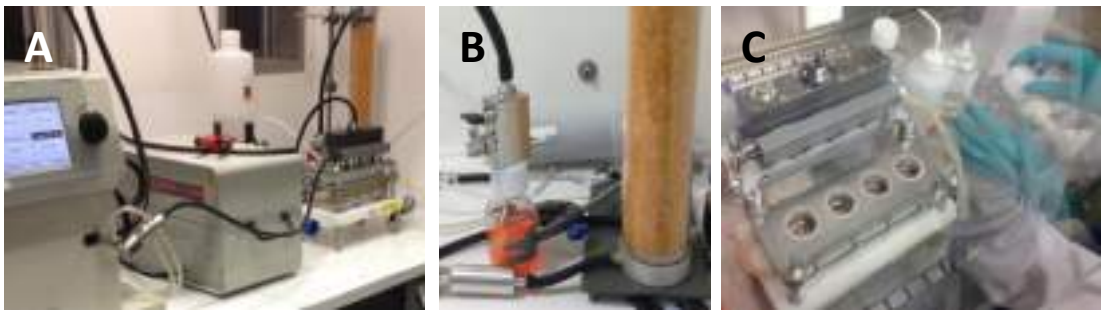

Figure SI2 - Experimental set up for the aerosol generation and air-liquid interface (ALI) exposure. A) PEG-CdTe QDs ink sample and diffusion dryer; B) Vitrocell® Module; C) Collison type atomizer; Instrumentation for particle measurement (3936 SMPS).

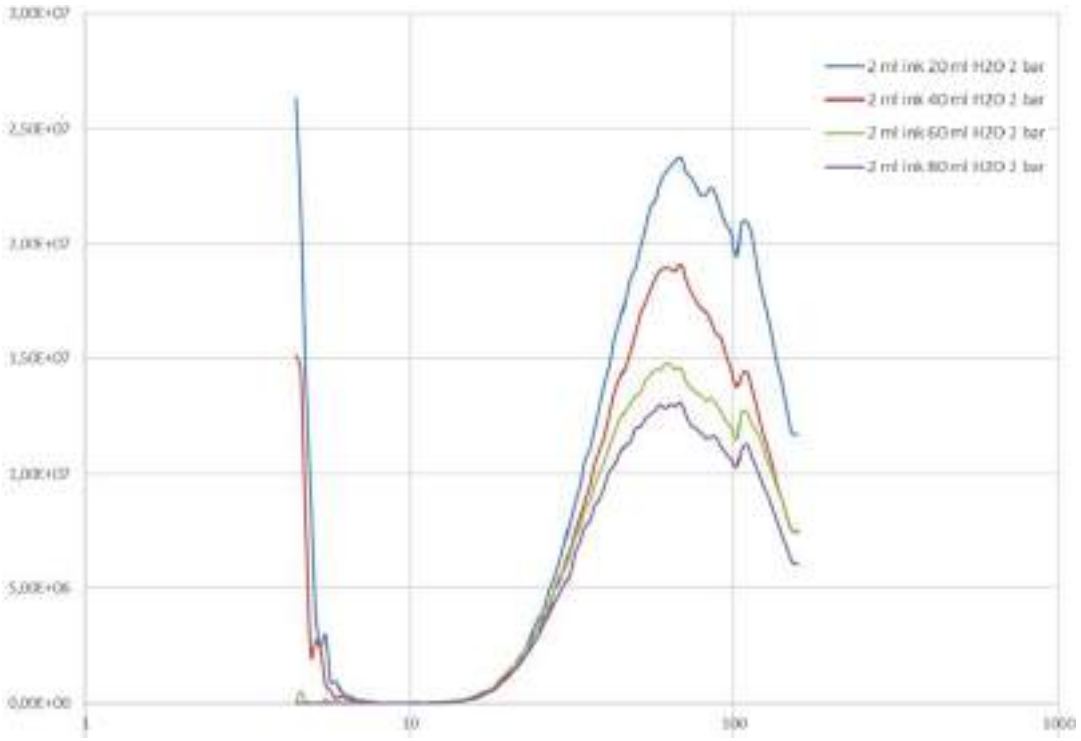

Figure SI3 – SMPS graph showing the size distribution measurements of different dilutions of the PEG-CdTe QDs ink tested to determine the most optimal atomization settings, evidencing that the 1:40 dilution (purple curve) has the smallest particle mode and no interference of smaller particles < 10 nm.

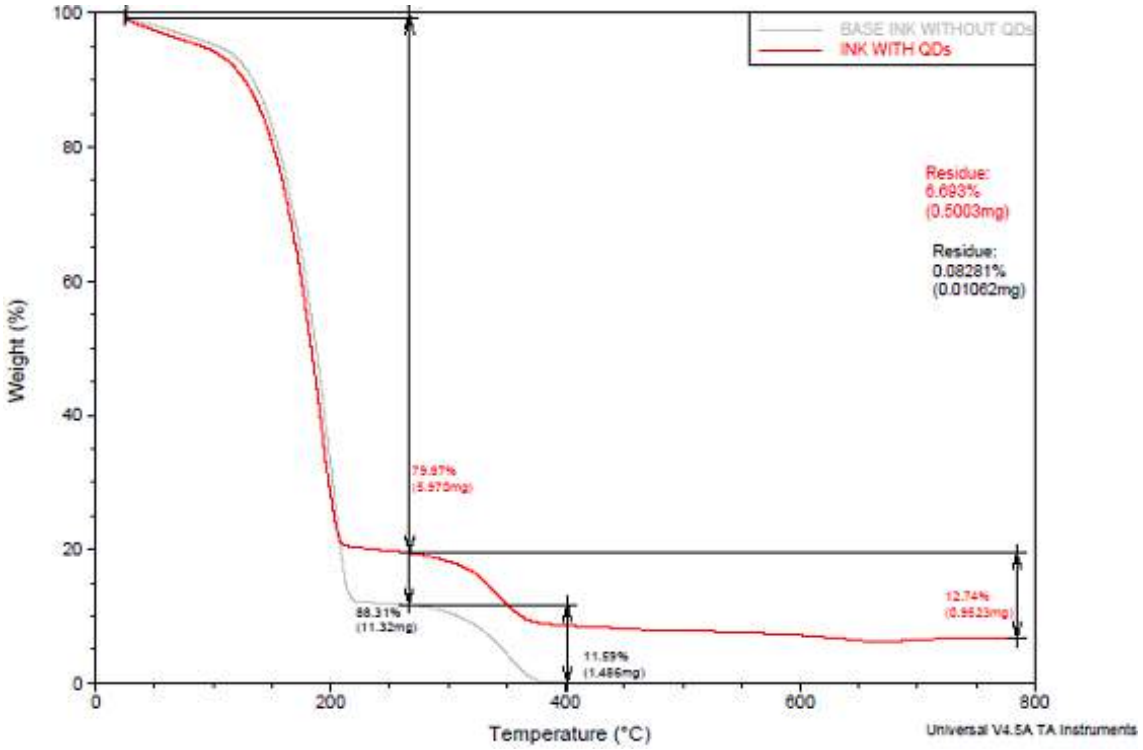

Figure SI4 - TGA curves for the base solvent ink (grey) and the PEG-CdTe QDs ink (red).

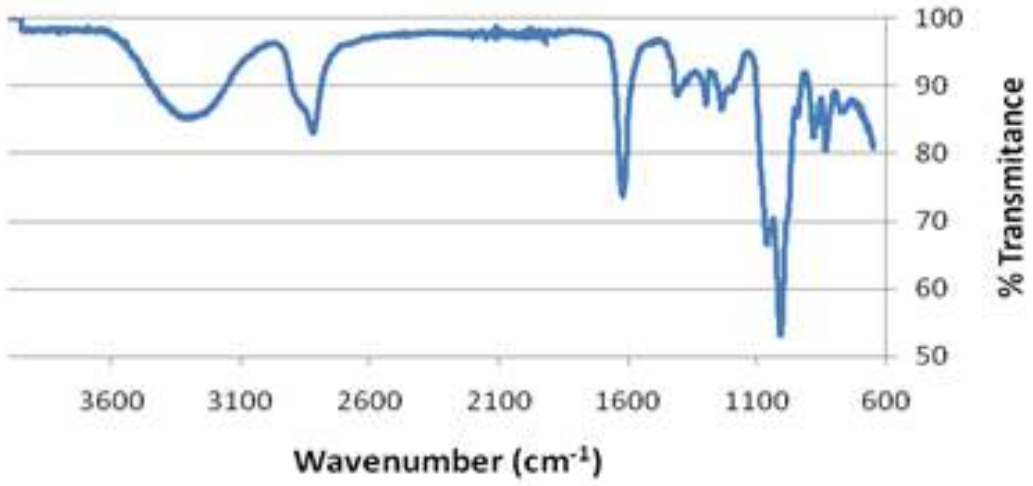

Figure SI5 - FTIR-ATR spectrum of PEG-CdTe QDs ink after freeze-drying.

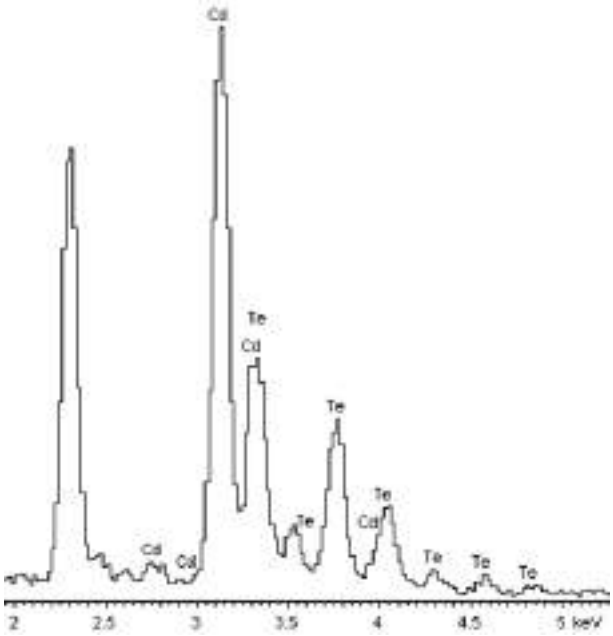

Figure SI6 - EDX spectrum of the PEG-CdTe QDs released during the printing process and collected on the TEM grid using the sampler device.

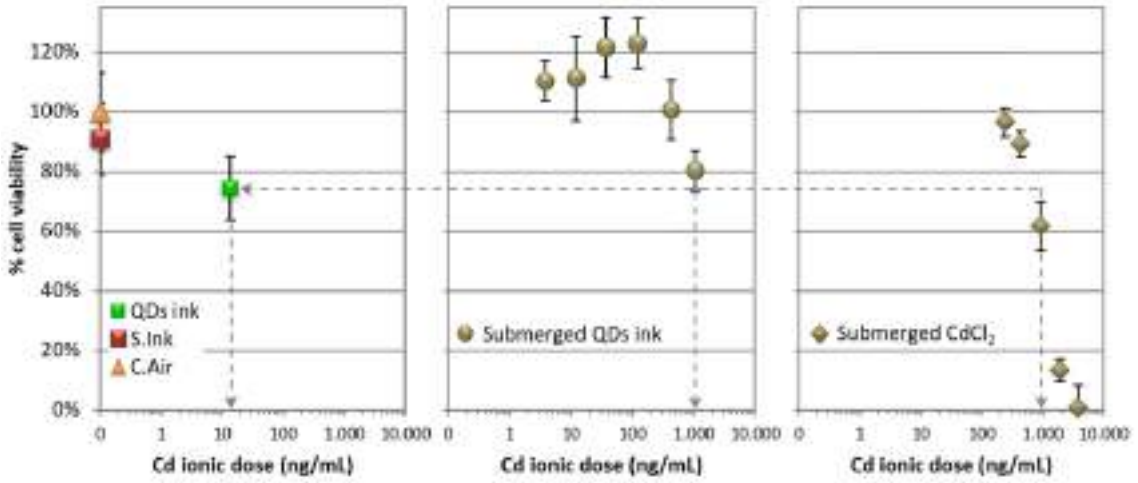

Figure SI7 - BEAS-B2 cells viability after 24 hours of exposure to Cd ions from different sources, compared to ALI control exposed to clean air (C.Air). Conditions tested: PEG-CdTe QDs ink at the ALI (QDs ink), solvent ink at the ALI (S.Ink), and Cd ions in submerged conditions (from PEG-CdTe QDs ink and $CdCl_2$). Error bars = SD (standard deviation).

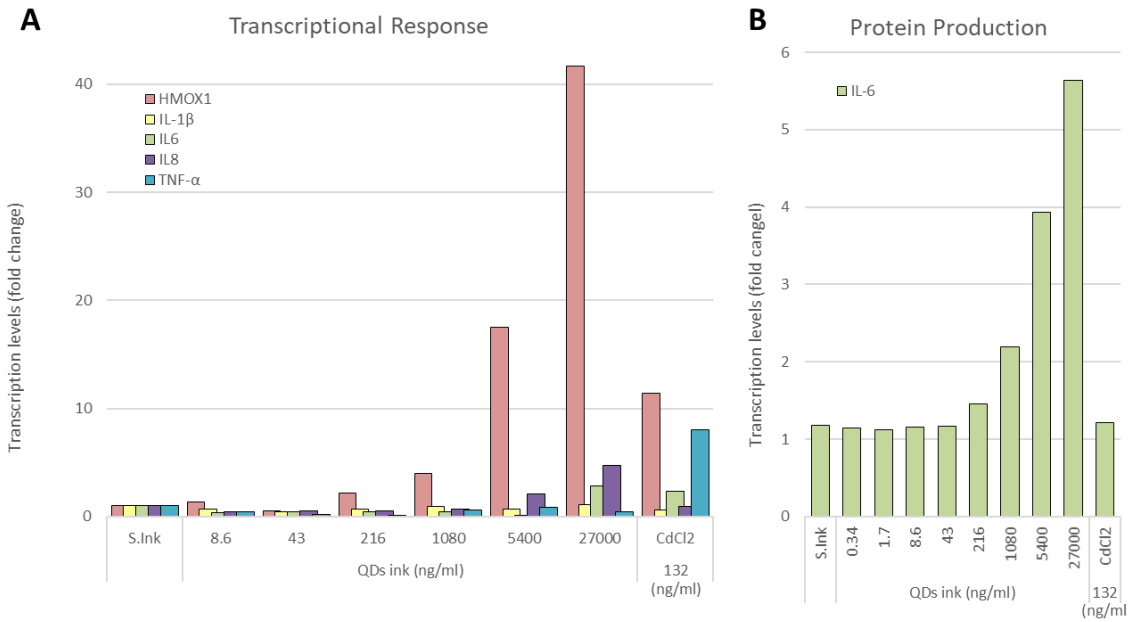

Figure SI8 - Evaluation of oxidative stress and pro-inflammatory cell response in BEAS-2B cells exposed for 24 hours to PEG-CdTe QDs ink (QDs ink) in submerged conditions, compared to the solvent ink control (S.Ink) and to cadmium in ionic form ($CdCl_2$). **A**) Potential alterations in the transcriptional response of HMOX1, IL-1β, IL-6, IL-8 and TNF-α measured by real-time qPCR; **B**) changes in protein production of IL-1β, IL-6, TNF-α and IFN-γ detected using a multiplex cytokine assay, where only IL-6 protein levels were over the detection limit of the assay.

3.2.3. Peer-reviewed publication under preparation

Silver nanoparticles and nanowires release from cotton textiles during household washings

Vicenç Pomar-Portillo,[a] Olga Chybová[b], Lenka Martinkova[b], Keana Scott [c] and Socorro Vázquez-Campos*[a]

[a] *LEITAT Technological Center, Carrer de la Innovació 2, 08225, Terrassa, Barcelona, Spain*

[b] *Inotex Ltd, 544 01 Dvur Kralove nad Labem, Czech Republic*

[c] *Material Measurement Laboratory, National Institute of Standards and Technology, 100 Bureau Drive, Gaithersburg, MD 20899, USA*

*Corresponding author e-mail address: svazquez@leitat.org

Contribution to the peer-reviewed publication under preparation within the context of this thesis: All the work needed to generate the information included in the manuscript was performed within the context of this thesis, but completed in two different institutions, LEITAT and the National Institute of Standards and Technology (NIST), where the internship of the PhD took place during 6 months. The co-authors affiliated to INOTEX provided the samples and Dr. Socorro Vázquez Campos and Dr. Keana Scott provided supervision in their respective facilities (LEITAT and NIST).

The following manuscript is a version generated to be submitted to the journal. The co-authors need to review the work, for this reason the paper could no be submitted yet. In any case, it provides a clear example of the work performed and the outcomes that can be obtained.

ARTICLE

Silver nanoparticles and nanowires release from cotton textiles during household washings

Received 00th January 20xx,
Accepted 00th January 20xx

DOI: 10.1039/x0xx00000x

Vicenç Pomar-Portillo,[a] Olga Chybová[b], Lenka Martinkova[b], Keana Scott[c] and Socorro Vázquez-Campos*[a]

Multiple studies evaluating silver nanoparticles (NP) release from textiles due to household washings can be found in literature. However, studies with silver nanowires (NW) are still lacking. Silver nanowires, like silver nanoparticles, have been proven to present antibacterial activity, and some studies claim that they may have the potential to further enhance the properties of nanosilver-containing products, including textiles. In this publication, the release behaviour of textiles containing Ag nanoparticles (around 50 nm diameter), Ag nanowires with a length around 5 µm and Ag nanowires with a length around 25 – 35 µm was evaluated. The amount of silver released along washings was quantified and the released materials were characterized in order to determine the release rates and release forms. In all the samples, release was higher in the first washings and decreased as more washings were performed. After ten washings, 30 ± 2%, 41 ± 9% and 27 ± 2% of the silver present in the unwashed textile remained for the samples containing Ag NPs, the shorter Ag NWs and the longer AgNWs, respectively. Based on the results, clear evidences on the size and shape effect on release rates could not be derived from this study. However, remarkable differences were found in release forms. Electron microscopy images on released waters suggest that ENMs preserve their size and shape characteristics when are released and then, they partially dissolve and sulphurize. Consequently, the size and shape properties of the nanomaterials incorporated will greatly define their release form. Release quantification values obtained in this work can be used as direct inputs for exposure assessment and the insights on release forms provide a basis to determine the potential hazard of the released materials. Thus, providing relevant information for risk assessment purposes.

1. Introduction

The textile industry is one of the most important industries in the manufactured goods sector. According to the World Trade Organization's International Trade Statistics, the top ten exporters of the textile and clothing industry accounted for 5.1% of the worldwide exports of manufactured goods ($673 billion) in 2019 (World Trade Organization, 2020). Textiles are present in multiple aspects of our lives and its applications are very diverse, ranging from the clothing we wear to fabrics in our home furnishing to materials for construction to medical products or the automotive sector among many others.

To improve the performance and to provide with new functionalities, manufacturers have started to incorporate engineered nanomaterials (ENMs) in textiles (Yetisen et al., 2016). Applications like self-cleaning (Lee et al., 2014), electrical conductivity (Chatterjee and Maity, 2018; Trovato et al., 2020), antibacterial activity (Qiu et al., 2020) or flame retardancy (Alongi et al., 2019; Kundu et al., 2020) are some of the purposes of ENMs' incorporation. Silver is typically incorporated to provide antibacterial activity, which can be used in different textile products, ranging from wound dressing to reduce bacteria proliferation avoiding potential infections (Mogrovejo-Valdivia et al., 2019) to sportswear to prevent the odor produced by bacteria (Chen et al., 2010).

When the intended use of the textile is clothing, household washings represent a critical exposure scenario of silver ENMs into the environment. The ENMs released from the textile during the washing cycle go through the seewage system and enter in a waste water treatment plant (WWTP). Conventional WWTP are relatively efficient in removing ENMs from the liquid phase of the WWTP and thus limiting the ENMs found in the final effluent (Loureiro et al., 2018). Mass-based removal efficiencies of different ENMs in different types of WWTP quantified in the literature vary widely between 0% and 100% (Alito and Gunsch, 2014; Kaegi et al., 2011; Kiser et al., 2009; Lombi et al., 2012). For silver, Kaegi et al. recently reported a removal efficiency of around 90%, meaning that most ENMs are attached to sludge particles (Kaegi et al., 2011). Then, the ENMs will be released together with the WWTP's sludge to terrestrial environments, where it is used as farm-land fertilizer (biosolids). Consequently, the soil could be contaminated with the released ENMs, which could further penetrate to groundwater and spread, potentially disrupting numerous biological ecosystems (Loureiro et al., 2018). ENMs remaining in the treated effluent stream may enter surface water, also posing a potential risk to the environment (Troy M. and Westerhoff, 2008).

[a] *LEITAT Technological Center, C/de la Innovació 2, 08225 Terrassa (Barcelona), Spain.*
[b] *Inotex Ltd, 544 01 Dvur Kralove nad Labem, Czech Republic*
[c] *Material Measurement Laboratory, National Institute of Standards and Technology, 100 Bureau Drive, Gaithersburg, MD 20899, USA*
† Footnotes relating to the title and/or authors should appear here.
Electronic Supplementary Information (ESI) available: [details of any supplementary information available should be included here]. See DOI: 10.1039/x0xx00000x

To properly assess the risk, ENMs release quantification and characterization is crucial. For that purpose, experimental simulations in laboratory-controlled conditions provide a concrete basis for estimating the release. Consequently, in the last years, multiple studies evaluating the silver nanoparticles (NPs) release from textiles have been published (Geranio et al., 2009; Lombi et al., 2014; Lorenz et al., 2012; Mitrano et al., 2016b). However, those studies mainly considered a single shape, spherical particles.

Silver nanowires, like silver nanoparticles, have been proven to present antibacterial activity (De Mori et al., 2020; Visnapuu et al., 2013), a feature that is transferred to textiles when they are incorporated (Nateghi and Shateri-Khalilabad, 2015). By tuning the size and shape of silver, researchers have been trying to refine its antibacterial effect (Helmlinger et al., 2016). Some papers claim that silver nanowires may have the potential to further enhance the properties of nanosilver-containing products, since they may present higher antimicrobial efficacy and lower cytotoxicity than silver nanoparticles (Jones et al., 2018; Rezvani et al., 2019). Conversely, other studies claim that different silver sizes and shapes may have different antibacterial effects but the same cytotoxicity (Helmlinger et al., 2016), while other experiments suggest that nanowires antibacterial activity may be lower than for nanoparticles (Hong et al., 2016).

Although the clear implications of size and shape on silver's antibacterial activity and cytotoxicity are not completely understood (Pal et al., 2007), different silver ENMs apart from spherical particles are likely to be incorporated in more and more products, including textiles (Giesz et al., 2017; Yao et al., 2019). Therefore, their potential impact on the environment should be investigated.

The aim of the present study is to determine how the size and shape of silver can affect to their release during washing, by comparing three different ENMs incorporated in textiles with the same conditions. The outcomes, release rates and release forms, may be useful to perform risk assessments of nano-enabled products.

2. Materials and methods

Three different silver engineered nanomaterials were incorporated on cotton textiles (one ENM in each fabric). Ag nanoparticles (NPs) with 50 nm diameter, coated with Polyvinylpyrrolidone (PVP) were obtained from Applied Nanoparticles SL. Ag nanowires with two different sizes, the shorter with 5 µm length and 40 nm diameter and the longer with 25 – 35 µm length and 70 nm diameter, both of them coated with PVP, were obtained from Nanogap. The three nanomaterials were purchased dispersed in water. To ease interpretation, we will refer to the shorter nanowires as AgNW_s and to the longer ones as AgNW_L. Before being incorporated on the textiles by impregnation, Ag nanomaterials dispersions were mixed with wetting agents (Erkantol NR, Tanatex Chemicals) and binders (Texafix SW, Inotex) with concentrations in the impregnation solutions of 1g/L and 20 g/L respectively. After impregnation, the textiles were dryed at 120ºC and cured at 140 ºC.

In commercial textiles evaluated in previous studies where the silver content was determined, concentrations ranging from 1.5 to 21600 ppm (mg Ag/ kg fabric) were measured, most of them containing around few tens to hundred ppm (Geranio et al., 2009; Lorenz et al., 2012; Mitrano et al., 2014). Besides, more recent studies determined that fabrics with as low as ~10 ppm of Ag can maintain high antibacterial efficacy under normal use phase conditions, but below this concentration efficacy significantly decreases (Spielman-Sun et al., 2018). Therefore, based on this information, the amount of silver was adjusted to obtain a final Ag concentration in textiles around 25 ppm, which seemed a realistic concentation. In addition to the three samples containing the different Ag ENMs, one control sample without silver but with wetting agents and binders was also generated. Images of the 4 samples, three with silver ENMs and one control without Ag, are included in supporting information (Figure S1).

2.1. Characterization of ENMs and unwashed textiles

The Ag dispersions were characterized with electron microscopy to check its morphology. Ag NPs were characterized by Transmisison electron microscopy (TEM, JEM-2100) while Ag NWs were characterized by Scanning electron microscopy (SEM, FEI Helios Nanolab 660) using the STEM (Scanning Transmission Electron Microscopy) detector. TEM images of the nanoparticles were processed using an automatic counting method for measuring the diameter of spherical objects, included in FIJI image processing Software (Schindelin et al., 2012). The same automatic counting could not be used for the nanowires due to their linear shape. Diameter and length of the nanowires were measured manually one by one. The longer nanowires usually presented bends, which hindered the measurement because the size measuring tool only measured straight-line distances. A specific FIJI plugin able to determine the length of curvilinear structures was used (Steger, 1998; Wagner et al., 2017), an example can be seen in supporting information (Figure S3).

After Ag incorporation by impregnation, the textile samples were digested with nitric acid (70%) in an analytical microwave digestion system (MARS, CEM, 1600W) and Ag content was quantified by Inductively Coupled Plasma Mass Spectrometry (ICPMS, Agilent 7500, Agilent Technologies). The nanomaterials distribution on the textiles were obtained with SEM (FEI Helios Nanolab 660).

2.2. Washing cycle protocol

The household washings simulations were performed according to an adaptation of the standardized protocol ISO 105-C06:2010 Textiles -- Tests for colour fastness -- Part C06: Colour fastness to domestic and commercial laundering (International Organization for Standardization, 2010). Each sample consisted of 2.95 ± 0.05 g of fabrics, which were cut in squares with approximately 14 cm side. All the samples were sewn with a cotton thread to avoid the textile fraying and yarns release in the washing waters, which would have hampered later characterization. The washings were performed in 550 ± 50 ml stainless steel vessels with 75 ± 5 mm diameter and 125 ± 10 mm height. Each vessel contained one sample, 10 stainless steel (SS) balls of 6 mm diameter (to simulate mechanical impact) and 150 ml of detergent solution (as shown in Figure S2). The detergent used (Adios al separar, Micolor) was a light-duty detergent with anionic and non-ionic surfactants, fabric care additives and enzymes. The dose used was 4 ml of detergent per distilled water liter, resulting in a washing pH of 7.4. The tests were carried out in a Gyrowash (James Heal) equipment at 40 ± 2 rpm and 40 ± 2 ºC.

Prior to the textile washing, the vessel with the detergent and the stainless steel balls were placed inside Gyrowash for 5 minutes in order to reach the desired temperature (i.e. 40 ± 2 ºC). Then, the textile was also introduced and washed for 30 minutes. The textile was retrieved and the washing waters were collected. Then, following the ISO protocol, two rinsing cycles of 1

minute at 40 ± 2 rpm, 40 ± 2ºC and with 100 ml of distilled water were performed (International Organization for Standardization, 2010). The rinsing solutions were also introduced in Gyrowash without textile for 5 minutes for temperature conditioning and waters were collected for further characterization. After the washing cycle, the samples were dried at ambient temperature.

2.3. Characterization of washed textiles and released waters

Ag concentration in textiles was analyzed at 1; 3; 5 and 10 washing cycles including three replicates per sample. When a sample reached the expected number of washings it was digested and analyzed by ICPMS, so a new textile was used for the following washings. Washing waters corresponding to 1, 2, 3, 5, 7 and 10 washing cycles were also analyzed by ICPMS. All the washing waters analyzed belonged to the textile washed 10 times. For both washed textiles and released waters, the same acidic digestion and ICPMS measurement protocols used for the unwashed textiles (previously described) was employed.

Since the concentration in released waters was expected to be quite low, a centrifugation step (clinical centrifuge, International Equipment Co.) at 1700g (3450 rpm) was applied on the released water samples for 2h before the collection for the deposition on TEM grids. Released waters sediments from the centrifugation process were observed through SEM (FEI Helios Nanolab 660) with STEM detector and EDX (Oxford Instruments X-Max 80 mm^2 SDD-EDS detector) for the elemental analysis.

3. Results

3.1. ENMs characterization

3.1.1. Electron microscopy characterization

Electron microscopy images of each ENM can be observed in Figure 1. The Ag NPs presented a circular shape, a homogeneous size and big NPs aggregates were not found. In Figure 1B it is clearly seen how the PVP covered all the nanoparticles. The amount of PVP was so high that it looked like a film covering most of the grid. Both nanowires dispersion presented a clear wire shape with a high aspect ratio (height-to-diameter ratio >>1). A clear difference in length between the longer and shorter nanowires was also observed (note change in scale of Figure 1 C and D). Longer nanowires were more difficult to measure because their size was close to that of the mesh holes in the TEM grid. As a consequence, some of the nanowires were partially laying in the copper grid framework, which prevented its measurement.

The size characteristics of the different nanomaterials are represented by means of frequency distributions (histograms) in Figure S4. The Ag nanoparticles presented a normal distribution with an average diameter of 64 ± 6 nm. The minimum and maximum diameters measured were 49 nm and 82 nm, respectively. For the nanowires, a clear difference was observed among samples. In the case of the nanowires expected to be shorter (AgNW_s) the average diameter was 44 nm, while for the longer ones (AgNW_L) it was 151 nm. This last value, according to the ISO definition (International Standards Organization, 2015), would invalidate the consideration of the longer wires as “nano” since none of their external dimensions was ≤100 nm.

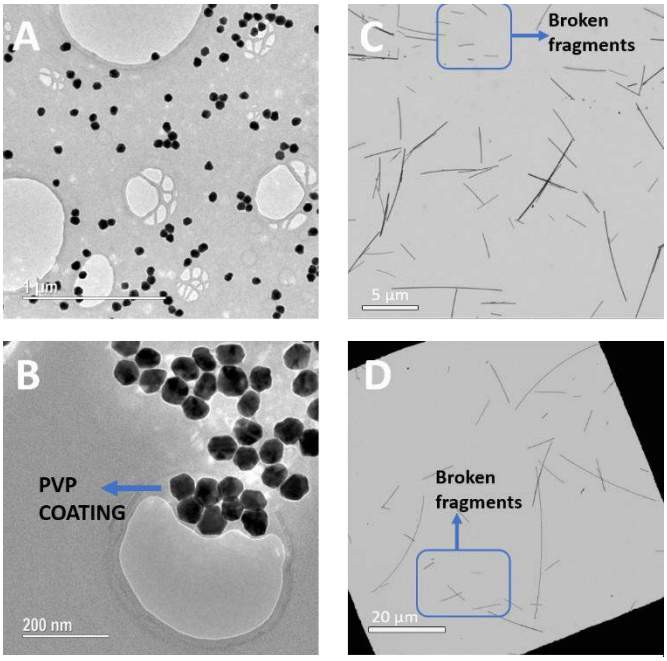

Figure 1 – Ag NMs electron microscopy images: A), B) Ag NPs; C) shorter Ag NWs (AgNW_s); D) longer Ag NWs (AgNW_L).

Regarding the length measurements, 3.5 ± 2.4 µm average length was measured for AgNW_s, while 15.1 ± 13.9 µm for AgNW_L. In the two cases, the histograms high frequency bins were mainly in the lower length range (left size of the graph, Figure S2), which means that in both dispersions there were more nanowires of short length than with long length. This fact can be easily appreciated in Figure 1C and Figure 1D. In both dispersions, the smaller fragments diameter was similar to that of longer NWs, what suggests that the size difference is not due to the synthesis process. Most probably, what is observed are just broken fragments. In the case of the longer nanowires, the histogram is even more shifted to the left (more smaller fragments). The reason could be that the longer the NWs the more likely it is that they break in smaller fragments, which can break again in even smaller fragments, ending up with a very disperse distribution and with most of the measurements reflecting nanowires of smaller length. The breakage could occur during the dispersion handling, the redispersion or during the sample preparation for microscopy. In any case, it gives information of how sensitive they are to breaking, something to consider when these kinds of samples must be manipulated in order to incorporate them in other products. As in the present case study, where they were impregnated on textiles.

3.2. Textiles characterization

3.2.1. Electron microscopy characterization

Nanomaterials distribution on the textiles after impregnation was observed by SEM. For the cotton textile containing Ag NPs, an uniform distribution was observed using backscattered electron imaging (BSE) mode. Silver, due to its higher atomic number, was observed brighter than textile yarns, organic components or other common salts (e.g. KCl or $CaCO_3$), making its detection easier. In Figure 2A, the Ag NPs presence along the textile yarns is observed. The nanoparticles were uniformly distributed and generally isolated, although some small aggregates were also found (Figure S2A). The area with the aggregate was used to perform an EDX analysis, which confirmed that the brighter dots observed were Ag (Figure S2B). Secondary electron imaging (SE) mode was used in higher magnification images. What allowed to measure the

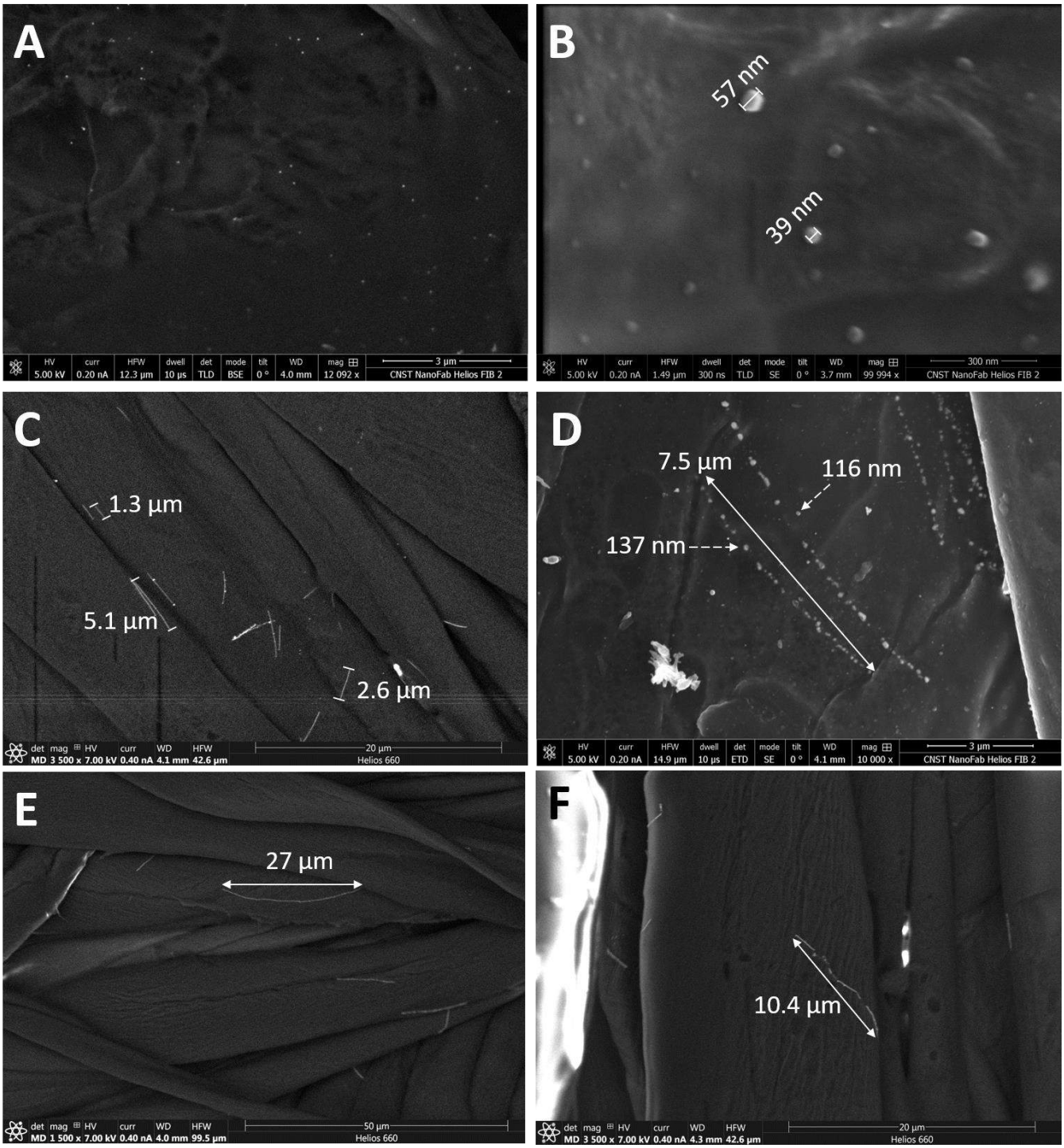

Figure 2 – SEM images of unwashed textiles containing the different ENMs: Ag NPs (A, B); Ag_NW_s (C, D); Ag_NW_L (E, F).

diameter size of the nanoaprticles impregnated on the textile. As shown in Figure 2B, the NPs size was measured. The specific diameter values measured (57 nm and 39 nm) were slightly smaller, but very close to the ones measured in the raw NPs dispersion (64 ± 6 nm; Figure 1 and Figure S4).

For the samples containing Ag nanowires, since they were easily recognized due to its wire shape, secondary electron (SE) mode was used in all the images. In Figure 2 (C, D) the AgNW_s on the cotton yarns are observed. The NWs were uniformly distributed along the textile and isolated, like the NPs. Although some overlapping nanowires were also found. The nanowires length measured were in the same size range than in the raw dispersion (3.5 ± 2.4 nm; Figure 1C and Figure S2). In certain areas, some nanowires presented an unexpected fragmentation (Figure 2D). The wire shape was still visible but not as a continuous line. The wire was formed by individual spherical particles around 100 nm one next to the other with a space between them. A length increase, compared with the compact nanowires, was also observed. These results were very significant since for some nanowires, the characteristics on the textile were completely different from the ones expected. It was not clear why the fragmentation phenomenon occured, but water contact together with exposure to high temperatures (drying at 120ºC

and curing at 140 ºC) during the impregnation process could have caused this effect. What was clear is that fragmentation occurred once the nanowires were on the textile surface, otherwise the wire shape would not have been maintained. EDX analysis confirmed that the fragmented wires were made of Ag (Figure S6). Although some of the nanowires observed were fragmented, most of them mantained the wire shape, meaning that the impregnation process succeeded and did not have a relevant impact for the purpose of the study. However, the influence of the impregnation and the following drying process on the nanowires integrity should be further evaluated by manufacturers, to ensure that the properties of the ENMs impregnated are mantained.

The results obtained for the longer nanowires were similar to the shorter ones. Multiple nanowires were observed on the textile surface. Some of them were isolated while others were overlapping one onto the other. Their length was in agreement with the lengths measured for the raw dispersion. Again, some of the NWs observed were fragmented (Figure 2F).

The control sample, although it did not contain any ENMs, was also observed with SEM (Figure S6). On the textile surface multiple particulate matter was identified. However, from the EDX analysis it was confirmed that they mainly were common salts like calcium carbonate ($CaCO_3$) probably coming from the water used in the impregnation process. No Ag ENMs were observed in the control sample. Particulate matter in some occasions can have a similar size to engineered nanomaterials causing confusion. For this reason EDX analysis is an indispensable technique to prove the nanomaterials presence in the sample.

3.2.2. Inductively coupled plasma mass spectrometry

The percentage of Ag remaining along washing cycles in the different textile samples is represented in Figure 3. The percentages were calculated considering the unwashed textiles concentration as a 100%. The height of the bars represents the mean value coming from the three replicates, while the error bars correspond to their standard deviation. In supporting information (Figure S9), a chart indicating the total Ag concentration in textiles measured by ICPMS is plotted. Both charts (Figure 3 and Figure S9) are built with the same data, but the different representations ease the observation of different conclusions. Control samples without silver were also washed and analysed through ICPMS but Ag was not detected. Thus, for simplicity, it was not included in the charts.

Looking at Figure 3, it can be concluded that for all the samples the concentration decreased with washings. Moreover, in all the cases, release was higher in the first washings and decreased as more washings were performed. According to the results, the sample with lowest release contained the shorter Ag NWs (AgNW_s) with 41% of Ag remaining after ten washing cycles. The sample containing Ag NPs presented around 10% more release, only 30% of Ag remained. Finally, the sample presenting a higher release was the one containing the longer nanowires (AgNW_L), in which only 27% of the silver remained after 10 washings. These results are in line with previous published studies, where with only 1 washing/rinsing cycle, releases from 10 to 35% were measured (Lorenz et al., 2012; Mitrano et al., 2016a, 2014).

Although the sample containing AgNW_s presented a slightly lower release, differences in release rates were not very remarkable and a similar release proportion was maintained along washings for the different samples.

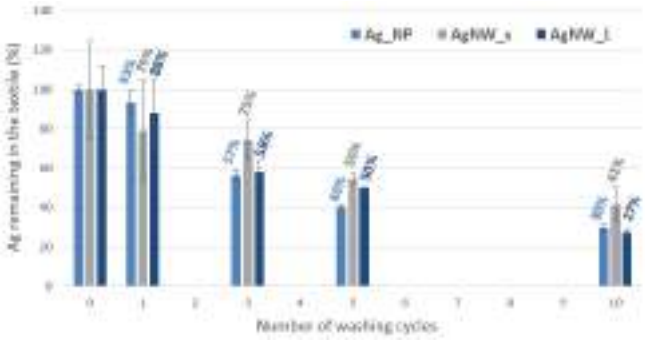

Figure 3 – Amount of silver (%) remaining in the textiles along washings.

Furthermore, the textiles containing Ag NPs and the longer Ag NWs presented very similar release values. Therefore, clear evidences on the size and shape effect on release rates could not be derived from this study.

Looking at the total silver concentration in the textiles (Figure S9), the values for the unwashed textiles show starting concentration values of 22 ppm, 19ppm and 18 ppm for the textiles with Ag NPs, AgNW_s and AgNW_L, respectively. As previously mentioned in methodology section, the textiles expected concentration was around 25 ppm. In none of the cases was the exact concentration achieved but very close values were obtained. Relative standard deviation values (RSD%) from 2% in AgNP to 25% and 12% in AgNW_s and AgNW_L were obtained, what gives an idea of the heterogeneity that the textiles can present. In previous studies, RSD% up to 60% were quantified in commercial textiles containing silver ENMs (Lorenz et al., 2012). Impregnation is a common and cost effective method used in the textile industry to impart additional functionality (Scott et al., 2017). Some heterogeneity is expected and does not impact on the quality of the product. Indeed, it is representative of many of the products present in the market.

For all the samples, almost the half of the silver had been released after only five washings, what corresponds to a total silver concentrations around 10 ppm for all the samples (Figure S9), meaning that the attachment was not very effective. According to Spielman-Sun et al., fabrics with as low as ~10 ppm of Ag can maintain high antibacterial efficacy under normal use phase conditions, but below this concentration efficacy significantly decreases (Spielman-Sun et al., 2018). Therefore, for the samples under study, with only 5 washings, the antibacterial efficacy would be in the limit of being greatly reduced, loosing the property for which the ENMs were incorporated. Based on the results, the starting silver concentration should be higher, or ideally, the attachment should be improved, what would maintain the textile functionality while limiting the release to the environment.

3.3. Released materials characterization

3.3.1. Electron microscopy characterization

In the released waters of the textile with Ag NPs, silver was not detected. As shown in supporting information (Figure S10), round shaped particles were found, but the EDX determined these were salts probably coming from the water or detergent, not silver. In the released waters there was a high amount of detergent, which hindered the identification of the NPs.

Nanowires, due to their high aspect ratio, were easier to identify than NPs. In the released waters of the textile with AgNW_s, a nanowire fragment was

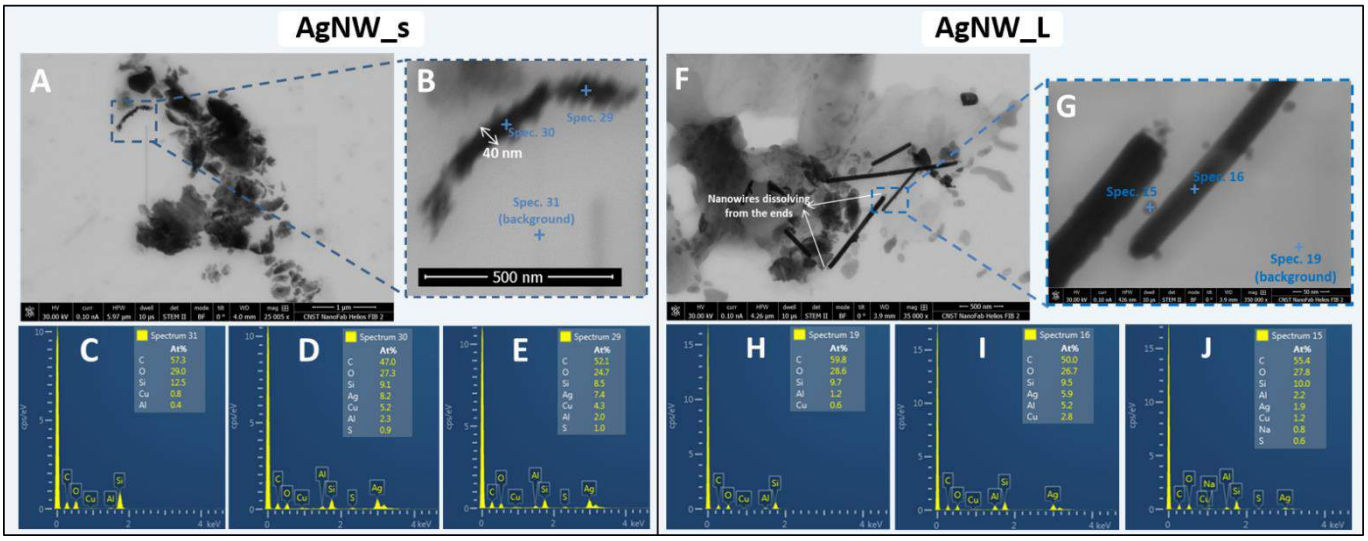

Figure 4 – Released waters' STEM images of the textiles containing AgNW_s (left), AgNW_L (right) and corresponding EDX analysis.

found together with detergent residues. As shown in Figure 4C, the background contained C, O, Si, Cu and Al. The Cu and some C probably came from the TEM grid, Si and Al from the detergent and O is highly abundant in the environment. In the EDX analysis of the nanowire, apart from the background elements, a high amount of Ag was detected confirming that it was a Ag nanowire. Sulphur was also measured, suggesting that part of the silver could be sulphurized, most likely in the surface. However, the intensity of the sulphur peak was so small that it could not be confirmed. Even more interesting is the fragment to which the spectrum 29 refers to (Figure 4E). In this occasion, the EDX analysis confirms that it is Ag but from the magnified image (Figure 4B) is seen that the wire shape is not maintained. Most probably what is being observed is the nanowire being dissolved. In this spectrum the S/Ag ratio (1.0/7.4=0.14) is higher than in the previous spectra (0.9/8.2=0.11), suggesting that the sulphurized silver amount is higher. The sulphur is probably originated from the detergent, which has ingredients containing sulfates and benzenesulfonic acid (CAS number 68891-38-3 and 68411-30-3). PVP is a protective coating, but as shown in previous work from Levard et al., it does not protect silver from sulfidation (Levard et al., 2011). In addition, in the lower part of the nanowire, an agglomerated structure similar to the one observed in the top is also present, suggesting that the nanowires start dissolving mainly from the ends, as would be expected. Small fragments protruding from the middle section of the wires are also seen, but they are not as abundant as the ones in the tips. Moreover, the diameter size of the nanowires was 40 nm, very close to the diameter size measured in the raw nanomaterials 44 ± 12 nm (Figure S2), meaning that silver was not released in a high amount in the inner sections of the nanowire.

In the released waters of the textiles containing AgNW_L, a high amount of nanowires were found. In this case, not only fragments were found as in the case of AgNW_s, but also nanowires of the same length of the original dispersions. In Figure 4F and Figure S9 some of the fragments are shown. In Figure 4, a higher magnification image of the nanowires with the corresponding EDX spectrum is presented. On this occasion, small particulate matter surrounds the nanowire not only in the tips but also in the central area. The information provided by the EDX is very similar to the one obtained from the shorter nanowire. The background spectra, as in the previous case, shows C, O, Si, Cu, Al. While the spectrum from the middle of the nanowire, apart from the background elements also measured Ag. When the EDX analysis was performed in the small particulate matter surrounding the nanowire, Ag was also detected together with S. Again it could be Ag dissolving from the nanowires, which was partially sulphurized.

3.3.2. Inductively coupled plasma mass spectrometry

In Figure 5, the Ag concentration in washing waters measured by ICPMS is plotted. The trend observed was to measure higher concentrations in the first washing waters and a decrease along washings, which agrees with the trend observed in textiles (Figure 3), where release also decreased with washings. During the first washings, especially in the first, there are relatively big concentration differences among the samples. However, as more washings are performed the closer the values are. Indeed, for ten washings, the Ag concentration for all the samples was almost the same, all the samples being in a range of 3.5 to 7.0 ppb.

Rinsing waters were also measured but the concentration of Ag was not high enough to be detected. The reason why the washings compared to the rinsing waters present a higher concentration is because the washing time was 30 minutes while the rinsing was only 1 minute. In any case, most probably, the rinsing also produced some release, although it was very small compared to the washings.

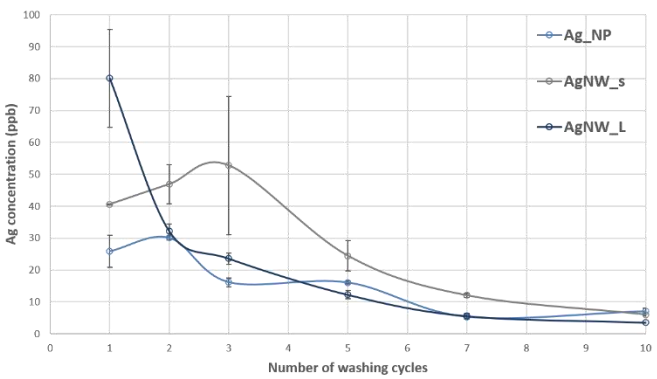

Figure 5 – Ag concentration in washing waters along washing cycles for the three different samples.

The concentrations measured in released waters can be related to the textiles concentration decrease along washings. For instance, the concentration difference between the unwashed textile containing Ag NPs and the sample washed one time is 1.4 ppm. Considering that the textile weight was 2.95 g and that the Ag was released to 150 ml of water with detergent, the expected silver concentration in released waters is 28 ppb (more details on the calculation in supporting information). In this particular case it exactly matches with the concentration experimentally measured in released waters. However, there is not the same level of accuracy for all the other cases, since as explained in the methodology section, once a textile reached the planned amount of washings it was digested and analyzed by ICPMS to determine the Ag concentration, so a new piece of textile was washed again to reach the next number of washings. The silver concentration variability in the textiles does not allow making precise calculations, but it allows knowing if the range of concentrations measured in release waters is in agreement with the Ag released from the textiles determined by ICPMS. In this case, for all the samples, the values found in released waters were in the same range as the expected concentrations coming from the textiles analyses, what means that both results were in agreement.

4. Conclusions

The release during washing from textiles containing three different silver ENMs was evaluated. After ten washings, 30 ± 2%, 41 ± 9% and 27 ± 2% of the silver present in the unwashed textile remained for the samples containing Ag NPs, AgNW_s and AgNW_L, respectively. Based on the values, clear evidences on the size and shape effect of the ENMs on the release rates could not be determined.

However, remarkable differences were found in release forms. Microscopy images on released waters suggest that ENMs preserve their size and shape characteristics when are released and then, they partially dissolve and sulphurizes. Previously published studies have shown that the rate and degree of the dissolution of PVP coated Ag-NPs depend on their surface functionalization, their concentration and the temperature, with faster dissolution rates at the beginning and finally leading to incompletely dissolved particles (Ahlberg et al., 2014; Kittler et al., 2010). Dissolution studies by Levard et al. have shown that PVP coated Ag-NPs of around 40 nm diameter (similar to the ones used in this study) reach equilibrium after one month, with around 2% dissolved Ag^+ species. Sulfidation in S/Ag ratio as low as 0.019 leaded to strong dissolution rates decrease with Ag^+ species in solution drop by a factor of 7 (Levard et al., 2011). Consequently, the size and shape properties of the ENMs incorporated will greatly define the form of the released ENMs.

To the author's knowledge, this paper represents the first published study of nanowires release from textiles, providing new insights on its release rates and forms. Release quantification values obtained in this work can be used as direct inputs for exposure assessment and the insights on release forms provide a basis to determine the potential hazard of the released materials. Therefore, the results presented are an important input for the risk assessment of nano-enabled products.

5. Conflicts of interest

There are no conflicts to declare.

6. Acknowledgements

The work presented in this paper is based on the NanoFASE project, which receives funding from the European Union's Horizon 2020 research and innovation programme under grant agreement number 646002.

7. Notes and references

Ahlberg, S., Antonopulos, A., Diendorf, J., Dringen, R., Epple, M., Flöck, R., Goedecke, W., Graf, C., Haberl, N., Helmlinger, J., Herzog, F., Heuer, F., Hirn, S., Johannes, C., Kittler, S., Köller, M., Korn, K., Kreyling, W.G., Krombach, F., Lademann, J., Loza, K., Luther, E.M., Malissek, M., Meinke, M.C., Nordmeyer, D., Pailliart, A., Raabe, J., Rancan, F., Rothen-Rutishauser, B.R., Rühl, E., Schleh, C., Seibel, A., Sengstock, C., Treuel, L., Vogt, A., Weber, K., Zellner, R., 2014. PVP-coated, negatively charged silver nanoparticles: A multi-center study of their physicochemical characteristics, cell culture and in vivo experiments. Beilstein J. Nanotechnol. https://doi.org/10.3762/bjnano.5.205

Alito, C.L., Gunsch, C.K., 2014. Assessing the effects of silver nanoparticles on biological nutrient removal in bench-scale activated sludge sequencing batch reactors. Environ. Sci. Technol. 48, 970–976. https://doi.org/10.1021/es403640j

Alongi, J., Ferruti, P., Manfredi, A., Carosio, F., Feng, Z., Hakkarainen, M., Ranucci, E., 2019. Superior flame retardancy of cotton by synergetic effect of cellulose-derived nano-graphene oxide carbon dots and disulphide-containing polyamidoamines. Polym. Degrad. Stab. 169. https://doi.org/10.1016/j.polymdegradstab.2019.108993

Chatterjee, A., Maity, S., 2018. Electroconductive Textiles, in: Advanced Textile Engineering Materials. John Wiley & Sons, Inc., Hoboken, NJ, USA, pp. 177–255. https://doi.org/10.1002/9781119488101.ch6

Chen, C.-C., Wang, C.-C., Yeh, J.-T., 2010. Improvement of Odor Elimination and Anti-bacterial Activity of Polyester Fabrics Finished with Composite Emulsions of Nanometer Titanium Dioxide-silver Particles-water-borne Polyurethane. Text. Res. J. Artic. Text. Res. J. 80, 291–300. https://doi.org/10.1177/0040517508100626

De Mori, A., Jones, R.S., Cretella, M., Cerri, G., Draheim, R.R., Barbu, E., Tozzi, G., Roldo, M., 2020. Evaluation of Antibacterial and Cytotoxicity Properties of Silver Nanowires and Their Composites with Carbon Nanotubes for Biomedical Applications. Int. J. Mol. Sci. 21, 2303. https://doi.org/10.3390/ijms21072303

Geranio, L., Heuberger, M., Nowack, B., 2009. The behavior of silver nanotextiles during washing. Environ. Sci. Technol. 43, 8113–8118. https://doi.org/10.1021/es9018332

Giesz, P., Mackiewicz, E., Grobelny, J., Celichowski, G., Cieślak, M., 2017. Multifunctional hybrid functionalization of cellulose fabrics with AgNWs and TiO2. Carbohydr. Polym. 177, 397–405. https://doi.org/10.1016/j.carbpol.2017.08.087

Helmlinger, J., Sengstock, C., Groß-Heitfeld, C., Mayer, C., Schildhauer, T.A., Köller, M., Epple, M., 2016. Silver nanoparticles with different size and shape: equal

cytotoxicity, but different antibacterial effects. RSC Adv. 6, 18490–18501. https://doi.org/10.1039/C5RA27836H

Hong, X., Wen, J., Xiong, X., Hu, Y., 2016. Shape effect on the antibacterial activity of silver nanoparticles synthesized via a microwave-assisted method. Environ. Sci. Pollut. Res. 23, 4489–4497. https://doi.org/10.1007/s11356-015-5668-z

International Organization for Standardization, 2010. ISO 105-C06:2010 Textiles -- Tests for colour fastness -- Part C06: Colour fastness to domestic and commercial laundering.

International Standards Organization, 2015. ISO/TS 80004-1:2015 Nanotechnologies — Vocabulary — Part 1: Core terms.

Jones, R., Draheim, R., Roldo, M., 2018. Silver Nanowires: Synthesis, Antibacterial Activity and Biomedical Applications. Appl. Sci. 8, 673. https://doi.org/10.3390/app8050673

Kaegi, R., Voegelin, A., Sinnet, B., Zuleeg, S., Hagendorfer, H., Burkhardt, M., Siegrist, H., 2011. Behavior of metallic silver nanoparticles in a pilot wastewater treatment plant. Environ. Sci. Technol. 45, 3902–3908. https://doi.org/10.1021/es1041892

Kiser, M.A., Westerhoff, P., Benn, T., Wang, Y., Pérez-Rivera, J., Hristovski, K., 2009. Titanium nanomaterial removal and release from wastewater treatment plants. Environ. Sci. Technol. 43, 6757–6763. https://doi.org/10.1021/es901102n

Kittler, S., Greulich, C., Diendorf, J., Köller, M., Epple, M., 2010. Toxicity of silver nanoparticles increases during storage because of slow dissolution under release of silver ions. Chem. Mater. 22, 4548–4554. https://doi.org/10.1021/cm100023p

Kundu, C.K., Li, Z., Song, L., Hu, Y., 2020. An overview of fire retardant treatments for synthetic textiles: From traditional approaches to recent applications. Eur. Polym. J. https://doi.org/10.1016/j.eurpolymj.2020.109911

Lee, H.J., Kim, J., Park, C.H., 2014. Fabrication of self-cleaning textiles by TiO2-carbon nanotube treatment. Text. Res. J. 84, 267–278. https://doi.org/10.1177/0040517513494258

Levard, C., Reinsch, B.C., Marc Michel, F., Oumahi, C., Lowry, G. V, Brown, G.E., 2011. Sulfidation Processes of PVP-Coated Silver Nanoparticles in Aqueous Solution: Impact on Dissolution Rate. Environ. Sci. Technol 45, 5260–5266. https://doi.org/10.1021/es2007758

Lombi, E., Donner, E., Scheckel, K.G., Sekine, R., Lorenz, C., Goetz, N. Von, Nowack, B., 2014. Silver speciation and release in commercial antimicrobial textiles as influenced by washing. Chemosphere 111, 352–358. https://doi.org/10.1016/j.chemosphere.2014.03.116

Lombi, E., Donner, E., Tavakkoli, E., Turney, T.W., Naidu, R., Miller, B.W., Scheckel, K.G., 2012. Fate of zinc oxide nanoparticles during anaerobic digestion of wastewater and post-treatment processing of sewage sludge. Environ. Sci. Technol. 46, 9089–9096. https://doi.org/10.1021/es301487s

Lorenz, C., Windler, L., Von Goetz, N., Lehmann, R.P., Schuppler, M., Hungerbühler, K., Heuberger, M., Nowack, B., 2012. Characterization of silver release from commercially available functional (nano)textiles. Chemosphere. https://doi.org/10.1016/j.chemosphere.2012.04.063

Loureiro, S., Tourinho, P.S., Cornelis, G., Van Den Brink, N.W., Díez-Ortiz, M., Vázquez-Campos, S., Pomar-Portillo, V., Svendsen, C., Van Gestel, C.A.M., 2018. Nanomaterials as Soil Pollutants, in: Soil Pollution. Elsevier, pp. 161–190. https://doi.org/10.1016/B978-0-12-849873-6.00007-8

Mitrano, D.M., Limpiteeprakan, P., Babel, S., Nowack, B., Cheever, B., Frost, P.C., Xenopoulos, M.A., Hintelmann, H., Metcalfe, C.D., Thiel, S., 2016a. Durability of nano-enhanced textiles through the life cycle: releases from landfilling after washing. Environ. Sci. Nano 3, 375–387. https://doi.org/10.1039/C6EN00023A

Mitrano, D.M., Lombi, E., Dasilva, Y.A.R., Nowack, B., 2016b. Unraveling the Complexity in the Aging of Nanoenhanced Textiles: A Comprehensive Sequential Study on the Effects of Sunlight and Washing on Silver Nanoparticles. Environ. Sci. Technol. 5790–5799. https://doi.org/10.1021/acs.est.6b01478

Mitrano, D.M., Rimmele, E., Wichser, A., Erni, R., Height, M., Nowack, B., 2014. Presence of nanoparticles in wash water from conventional silver and nano-silver textiles. ACS Nano 8, 7208–7219. https://doi.org/10.1021/nn502228w

Mogrovejo-Valdivia, A., Rahmouni, O., Tabary, N., Maton, M., Neut, C., Martel, B., Blanchemain, N., 2019. In vitro evaluation of drug release and antibacterial activity of a silver-loaded wound dressing coated with a multilayer system. Int. J. Pharm. 556, 301–310. https://doi.org/10.1016/j.ijpharm.2018.12.018

Nateghi, M.R., Shateri-Khalilabad, M., 2015. Silver nanowire-functionalized cotton fabric. Carbohydr. Polym. 117, 160–168. https://doi.org/10.1016/j.carbpol.2014.09.057

Pal, S., Tak, Y.K., Song, J.M., 2007. Does the Antibacterial Activity of Silver Nanoparticles Depend on the Shape of the Nanoparticle? A Study of the Gram-Negative Bacterium Escherichia coli. Appl. Environ. Microbiol. 73, 1712–1720. https://doi.org/10.1128/AEM.02218-06

Qiu, Q., Chen, S., Li, Y., Yang, Y., Zhang, H., Quan, Z., Qin, X., Wang, R., Yu, J., 2020. Functional nanofibers embedded into textiles for durable antibacterial properties. Chem. Eng. J. 384, 123241. https://doi.org/10.1016/j.cej.2019.123241

Rezvani, E., Rafferty, A., McGuinness, C., Kennedy, J., 2019. Adverse effects of nanosilver on human health and the environment. Acta Biomater. https://doi.org/10.1016/j.actbio.2019.05.042

Schindelin, J., Arganda-Carreras, I., Frise, E., Kaynig, V., Longair, M., Pietzsch, T., Preibisch, S., Rueden, C., Saalfeld, S., Schmid, B., Tinevez, J.-Y., White, D.J., Hartenstein, V., Eliceiri, K., Tomancak, P., Cardona, A., 2012. Fiji: an open-source platform for biological-image analysis. Nat. Methods 9, 676–682. https://doi.org/10.1038/nmeth.2019

Scott, K., Pomar-Portillo, V., Vázquez-Campos, S., 2017. Nanomaterials in Textiles, in: Metrology and Standardization of Nanotechnology. Wiley-VCH Verlag GmbH & Co. KGaA, Weinheim, Germany, pp. 559–572. https://doi.org/10.1002/9783527800308.ch31

Spielman-Sun, E., Zaikova, T., Dankovich, T., Yun, J., Ryan, M., Hutchison, J.E., Lowry, G. V., 2018. Effect of silver concentration and chemical transformations on release and antibacterial efficacy in silver-containing textiles. NanoImpact 11, 51–57. https://doi.org/10.1016/j.impact.2018.02.002

Steger, C., 1998. An unbiased detector of curvilinear structures. IEEE

Trans. Pattern Anal. Mach. Intell. 20, 113–125. https://doi.org/10.1109/34.659930

Trovato, V., Teblum, E., Kostikov, Y., Pedrana, A., Re, V., Nessim, G.D., Rosace, G., 2020. Sol-gel approach to incorporate millimeter-long carbon nanotubes into fabrics for the development of electrical-conductive textiles. Mater. Chem. Phys. 240, 122218. https://doi.org/10.1016/j.matchemphys.2019.122218

Troy M., B., Westerhoff, P., 2008. Nanoparticle Silver Released into Water from Commercially Available Sock Fabrics. Environ. Sci. Technol. 42, 4133–4139. https://doi.org/10.1021/es7032718

Visnapuu, M., Joost, U., Juganson, K., Künnis-Beres, K., Kahru, A., Kisand, V., Ivask, A., 2013. Dissolution of silver nanowires and nanospheres dictates their toxicity to escherichia coli. Biomed Res. Int. 2013. https://doi.org/10.1155/2013/819252

Wagner, T., Hiner, M., xraynaud, 2017. thorstenwagner/ij-ridgedetection: Ridge Detection 1.4.0. https://doi.org/10.5281/ZENODO.845874

World Trade Organization, 2020. World Trade Statistical Review 2020.

Yao, S., Yang, J., Poblete, F.R., Hu, X., Zhu, Y., 2019. Multifunctional Electronic Textiles Using Silver Nanowire Composites. https://doi.org/10.1021/acsami.9b07520

Yetisen, A.K., Qu, H., Manbachi, A., Butt, H., Dokmeci, M.R., Hinestroza, J.P., Skorobogatiy, M., Khademhosseini, A., Yun, S.H., 2016. Nanotechnology in Textiles. ACS Nano 10, 3042–3068. https://doi.org/10.1021/acsnano.5b08176

Supplemental Information

Silver nanoparticles and nanowires release from cotton textiles during household washings

Vicenç Pomar-Portillo,*[a] Olga Chybová[b], Lenka Martinkova[b], Keana Scott [c] and Socorro Vázquez-Campos[a]

[a] *LEITAT Technological Center, Carrer de la Innovació 2, 08225, Terrassa, Barcelona, Spain*

[b] *Inotex Ltd, 544 01 Dvur Kralove nad Labem, Czech Republic*

[c] *Material Measurement Laboratory, National Institute of Standards and Technology, 100 Bureau Drive, Gaithersburg, MD 20899, USA*

*Corresponding author e-mail address: svazquez@leitat.org

Impregnated textile samples

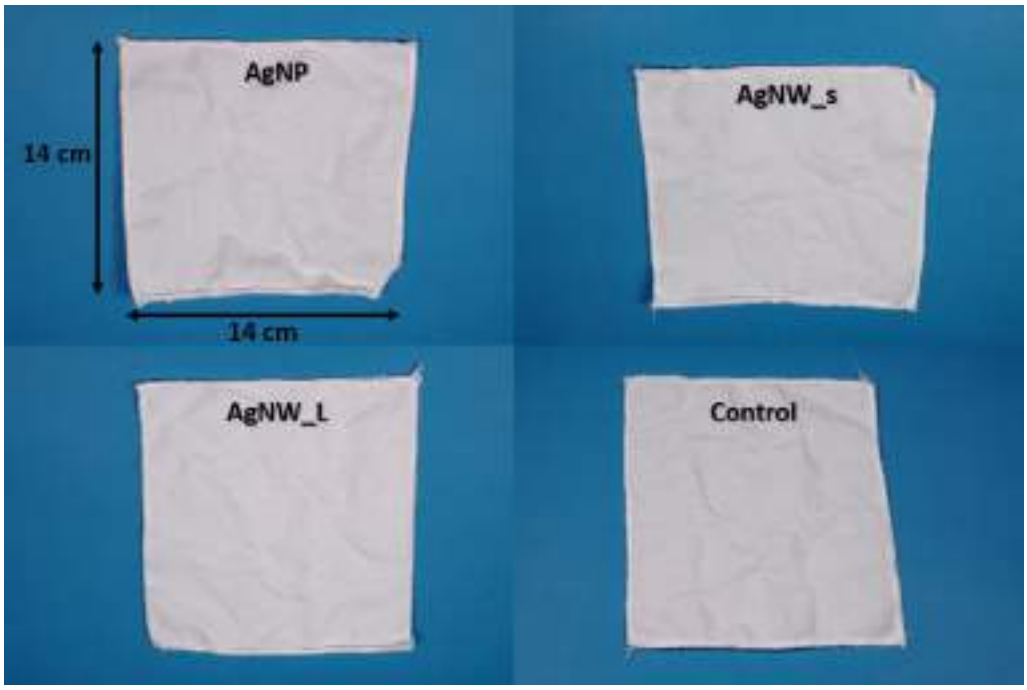

Figure S1 – Textile samples used in the experiments containing silver ENMs and control.

Washing vessels used for the experiments

Figure S 2 – Washing vessels containing the textiles, detergent solution and stainless steel balls (not observed because are covered by the foam).

Electron microscopy characterization of ENMs disperisons

Measuring the length and diameter of curvilinear nanowires

The longer nanowires usually presented bends, which hindered the measurement because the default size measuring FIJI tool only measured straight-line distances. A specific FIJI plugin able to determine the length of curvilinear structures was used (Steger, 1998; Wagner et al., 2017), an example showing the sensitivity of the plugin and the difference from using the default size measuring tool is included in Figure S1.

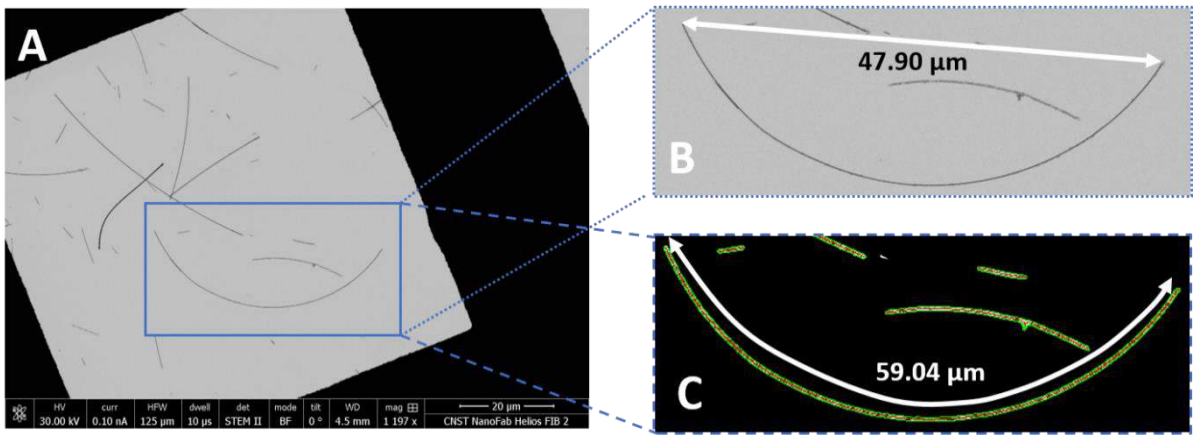

Figure S3 –A) AgNW_L STEM image; B) Nanowire's length using predetermined FIJI software for measuring distances; C) Nanowire recognition and length measurement using FIJI plugin.

ENMs morphology

The size characteristics of the different nanomaterials are shown in Figure S2 by means of frequency distributions (histograms). 223 nanoparticles and 120 nanowires of each size (AgNW_s and AgNW_L) were counted to generate the size distributions. For each set of measurements the corresponding average size with standard deviation and Relative Standard Deviation (RSD) are also shown. RSD, which is usually expressed as a percentage (RSD%), is a standardized measure of dispersion of the frequency distributions that is commonly used for comparing the uncertainty between different measurements. For Ag nanoparticles, due to their spherical shape, the diameter is the only size parameter considered, while for nanowires the length, diameter and length-to-diameter ratios are plotted.

The Ag nanoparticles presented a normal distribution with an average diameter of 64 ± 6 nm. The minimum and maximum diameters measured were 49 nm and 82 nm, respectively. This small difference between maximum and minimum values together with a low RSD% of 10% (the lowest for all the sets of

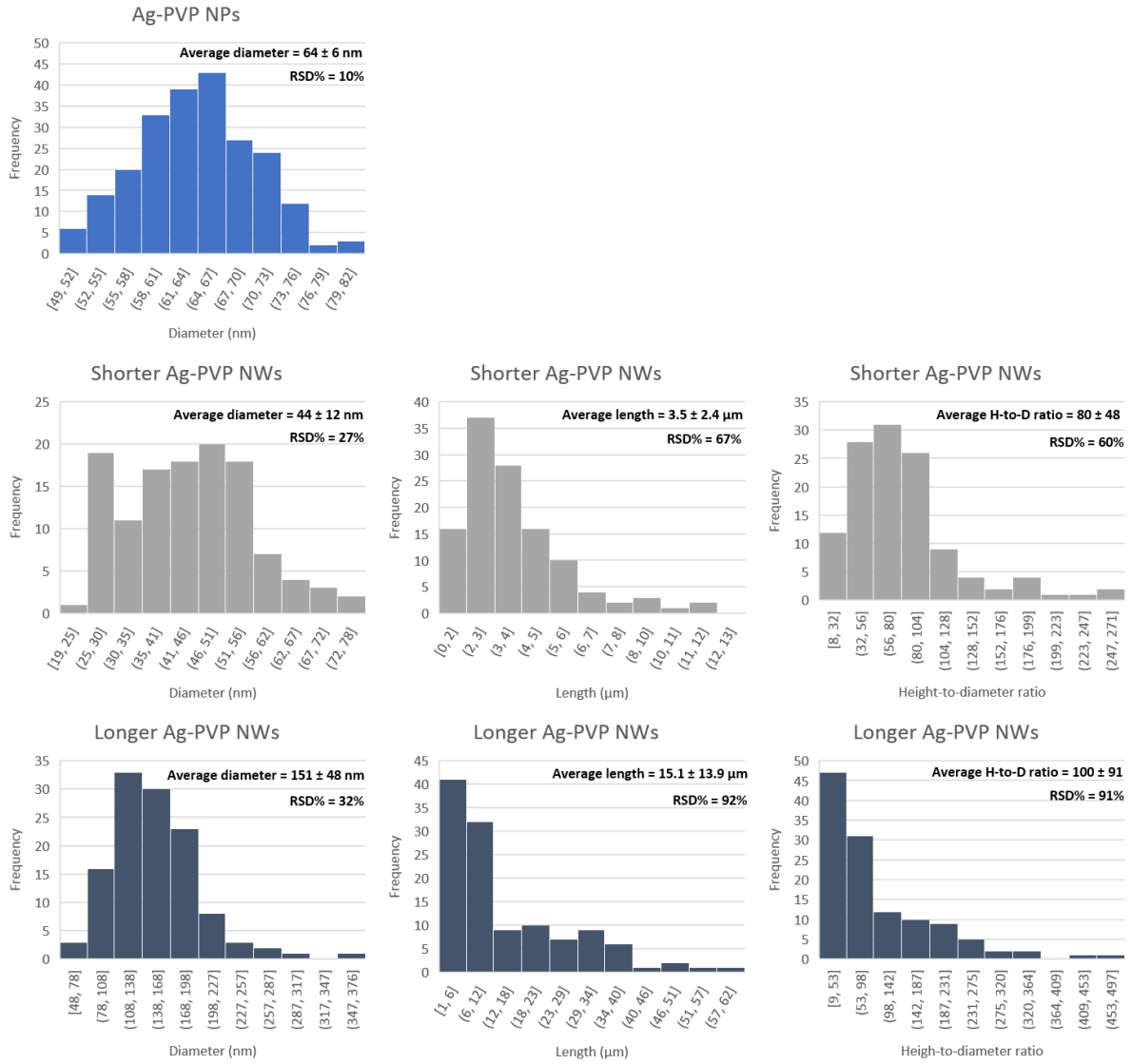

measurements) suggests that Ag-PVP NPs dispersion was very monodisperse. The length measurements of both nanowires samples confirmed what was inferred just by looking at the images, there was a significant difference between the length of the two nanowire samples. AgNW_s had a 3.5 ± 2.4 µm average length, while AgNW_L 15.1 ± 13.9 µm. For both nanowire samples the RSD% of the diameter measurements was around 3 times higher than for the Ag NPs, suggesting that the diameters size was more heterogeneous.

Figure S4 – Diameter, length and height-to-diameter ratio (H-to-D) size distribution of the Ag ENMs incorporated on the textiles. 223 nanoparticles and 120 nanowires of each size (AgNW_s and AgNW_L) were counted to generate the size distributions.

Unwashed impregnated textiles electron microscopy characterization

In Figure S5A, the Ag NPs distribution along a textile yarns is observed. The nanoparticles were uniformly distributed and generally isolated, although some small aggregates were also found. The area with the aggregate was used to perform an EDX analysis, which confirmed that the brighter dots observed corresponded to Ag (Figure S5B).

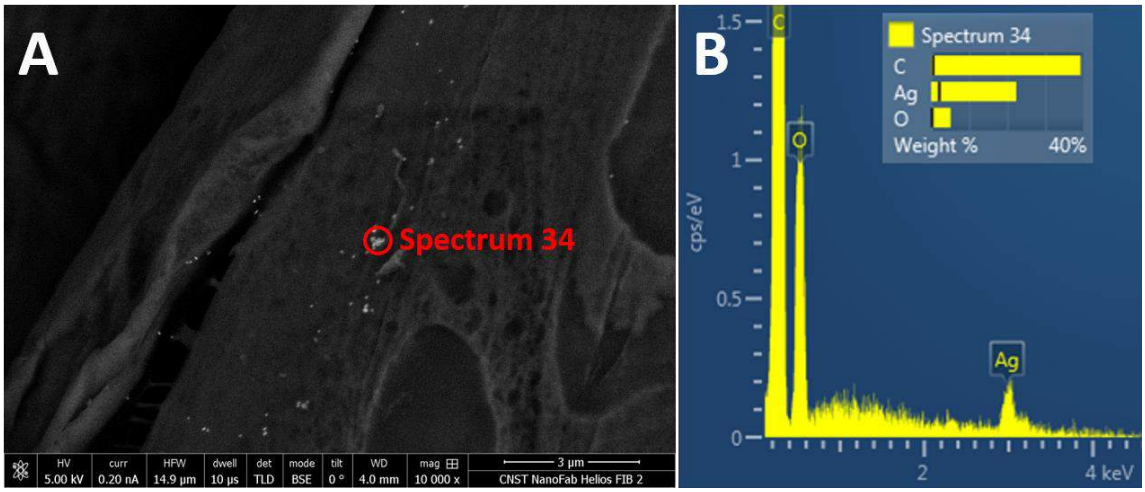

Figure S5 – A) SEM image in backscattered electron mode and B) corresponding EDX analysis of unwashed textile containing Ag NPs.

In Figure S6 and Figure S7, the AgNW_s and AgNW_L distribution along the textile is observed. The NWs were uniformly distributed along the textile and isolated, like the NPs. Although some overlapping nanowires were also found. EDX analysis confirmed that the fragments observed corresponded to Ag (Figure S6C).

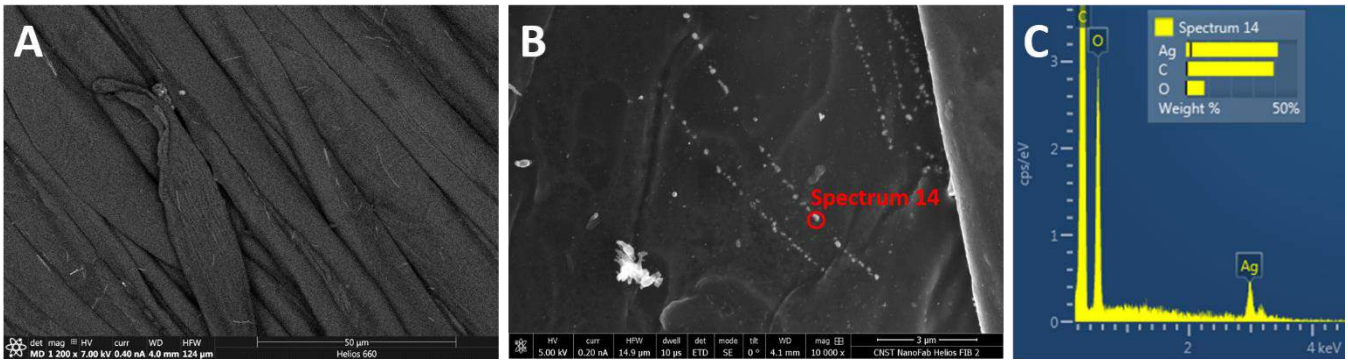

Figure S6 – A), B) SEM images in secondary electron mode and C) corresponding EDX analysis of textile containing AgNW_s.

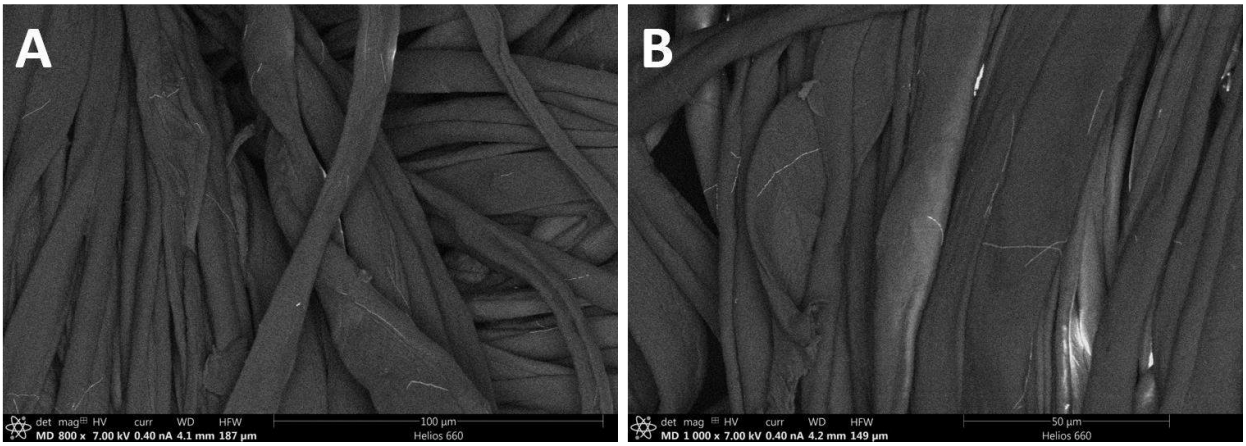

Figure S7 – SEM images in secondary electron mode of textile containing AgNW_L.

On the control sample surface multiple particulate matter was identified. However, from the EDX analysis it was confirmed that they mainly were common salts like calcium carbonate (CaCO3) probably coming from the water used in the impregnation process. No Ag NMs were observed in the control sample.

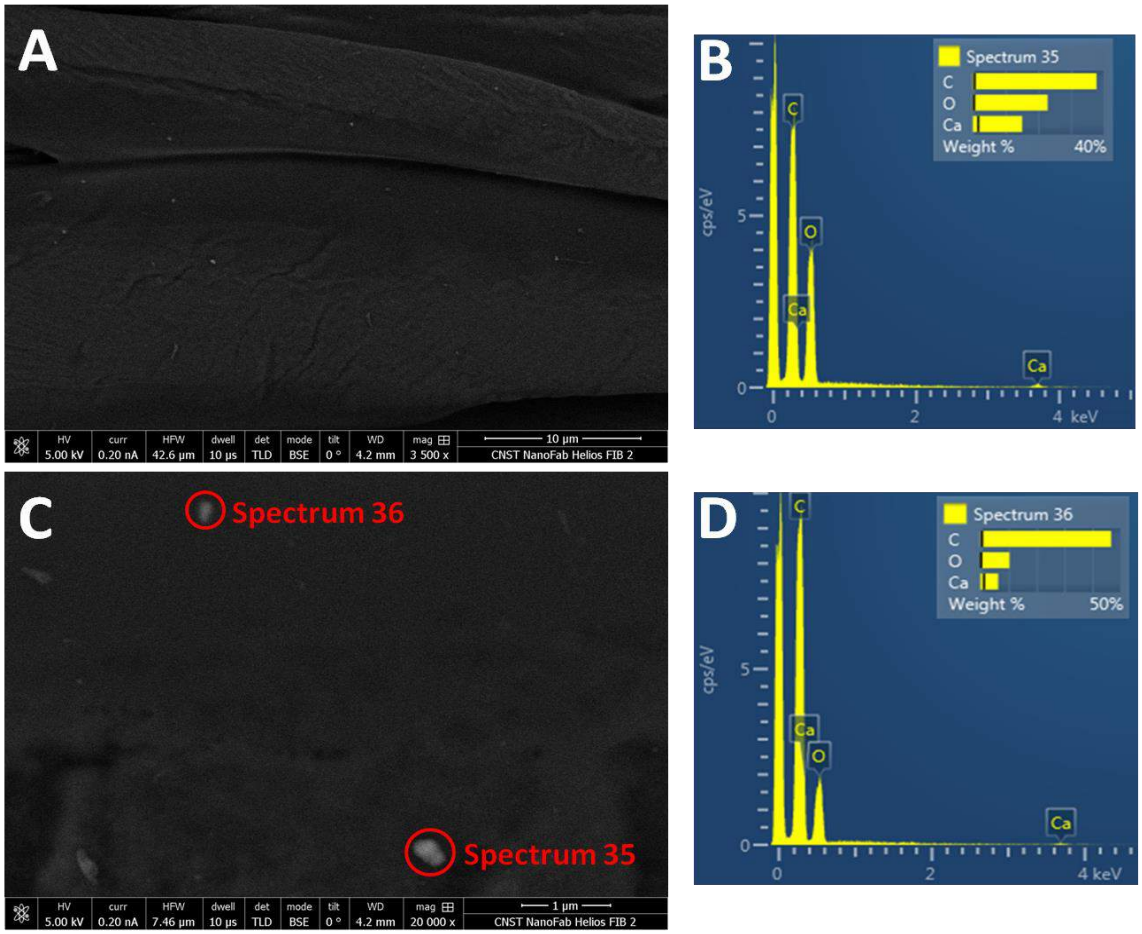

Figure S8 –A), C) SEM images in backscattered electron mode and B), D) corresponding EDX analysis of unwashed control (without silver) textile.

Analysis of silver content in textiles

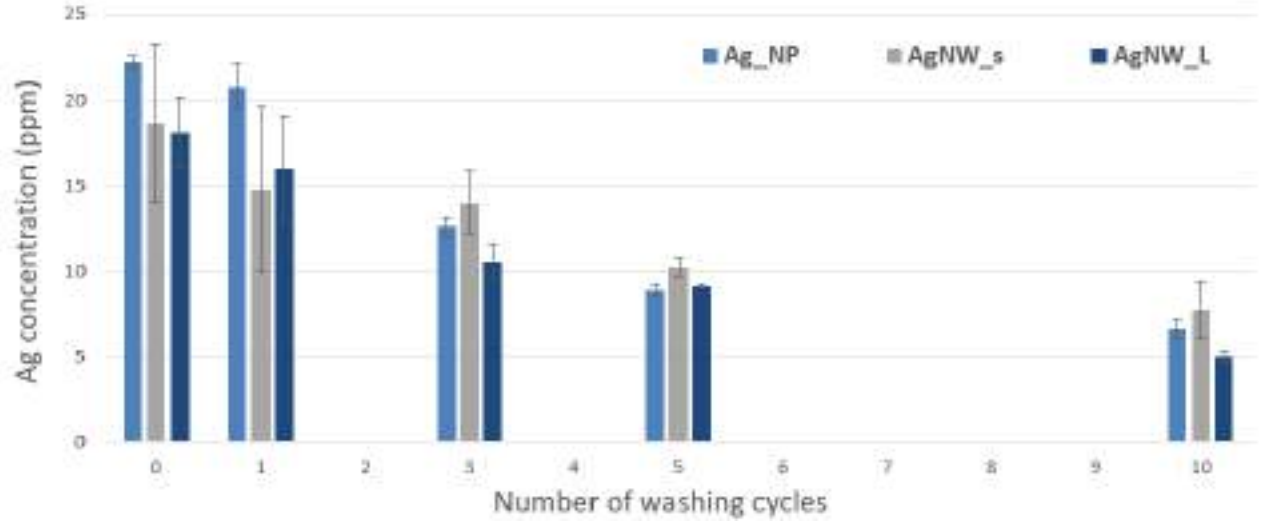

Figure S9 – Silver concentration in the textiles along washings.

Electron microscopy characterization of released waters

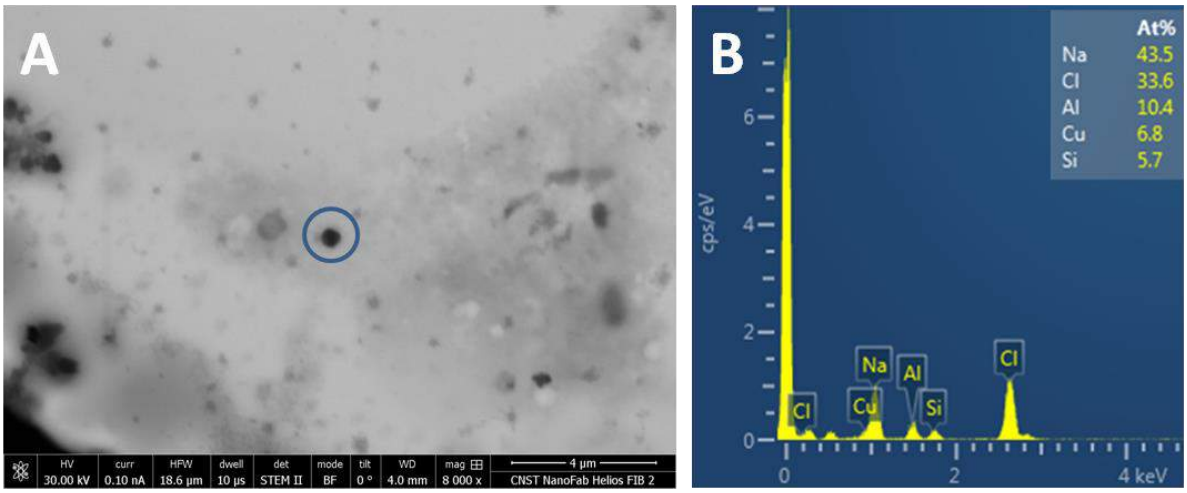

Figure S10 – STEM image and corresponding EDX analysis of release waters of the textile containing Ag NPs.

In all the images the nanowires appear next to detergent residues, to which they probably were adhered. In Figure S11C part of the nanowire can be seen without detergent. However, in Figure S11D, it can be seen how small residues of detergent are attached all along the nanowire.

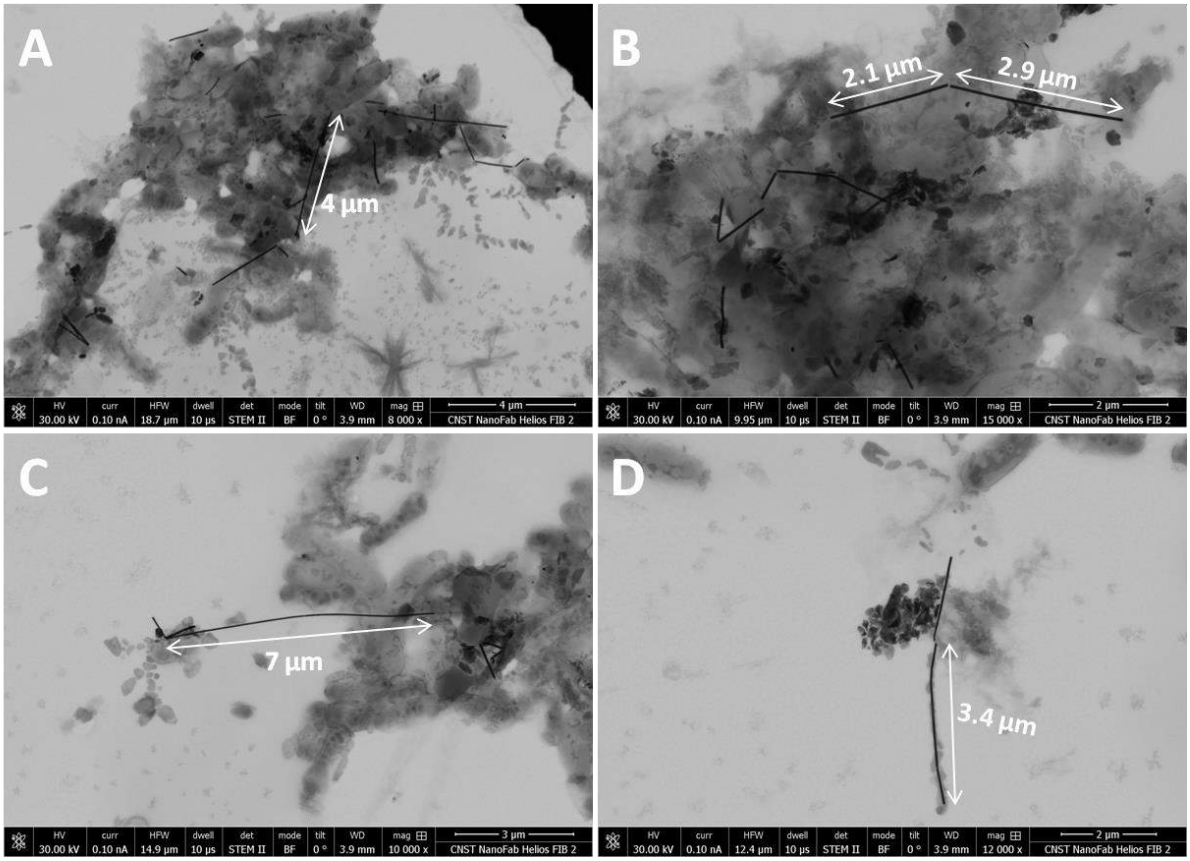

Figure S11 – STEM images of AgNW_L found in release waters.

Theoretical estimation of silver content in released waters

Based on the concentration difference in the textiles along washings, the silver concentration in released waters can be estimated with the following formula:

$$\textit{Ag concentration in released water} = \frac{\left(\textit{Ag concentration in the textile before washing} - \textit{Ag concentration in the textile after washing}\right) \cdot \textit{Textile weight}}{\textit{Amount of liquid inside the washing vessel}}$$

An example for the silver released during the first washing of the textile containing Ag NPs is shown below:

$$Ag\ concentration\ in\ released\ water = \frac{1.4\ \left[\frac{mg\ Ag}{kg\ Textile}\right] \cdot 2.95 \cdot 10^{-3}\ [kg\ Textile]}{0.15\ [L]} = 28 \cdot 10^{-3}\ ppm = \mathbf{28\ ppb}$$

References

Steger, C., 1998. An unbiased detector of curvilinear structures. IEEE Trans. Pattern Anal. Mach. Intell. 20, 113–125. https://doi.org/10.1109/34.659930

Wagner, T., Hiner, M., xraynaud, 2017. thorstenwagner/ij-ridgedetection: Ridge Detection 1.4.0. https://doi.org/10.5281/ZENODO.845874

3.2.4. Curtains with photocatalytic activity

Introduction

The present case study consists of polyester (PES) fabrics containing photocatalytic nano-TiO2 to be used as curtain material. From the application point of view, the interest of the case study remains in that the incorporation of nano-TiO2 provides photocatalytic activity to the textile. This property provides the curtain with the ability to degrade volatile organic compounds (VOCs) or other air contaminants that surround the fabric improving the air quality around the curtain. The nano-enabled product was manufactured by INOTEX. INOTEX Ltd (from Czech Republic) is a small private technological research, innovation and technology transfer company specialised in wet processing of textiles and (multi)functional textile developments using new methods. It supports implementation of tailor-made research and technological development by the use of own pilot production capacities.

From the environmental point of view potential TiO_2 ENM release from textiles should be investigated. In this case, the activity of most concern is washing the curtains, which could lead to ENM exposure to the environment via wastewater treatment works. To assess this potential risk, household-washing simulations of the nano-enabled curtains in controlled laboratory conditions were performed following an adaptation of a standardized protocol (ISO 105-C06:2010 (International Standards Organization, 2010)) with the aim to determine nano-TiO_2 release rates and forms.

Materials and methods

The nano-TiO_2 was incorporated in the textile together with a wetting agent (Tanawet RC-N) and a siloxane-acryl urethane binder (Sipurino) by impregnation in INOTEX's facilities. The treated textile samples and the chemicals used were provided for characterization and release experiments:

Table 2 – Overview of samples provided

NOMENCLATURE	DESCRIPTION
Curb_TiO_2	PES fabric treated with nano-TiO_2, wetting agent and binder
Curb (control sample)	PES fabric without nano-TiO_2
Tiodisper NA-AS (commercial name)	Nano-TiO_2 dispersion
Tanawet RC-N (commercial name)	Wetting agent

Multiple characterizations were performed on both starting and washed materials. The nano-TiO_2 dispersion (Tiodisper NA-AS) and washing waters were observed through high resolution transmission electron microscope (HR-TEM; JEOL JEM-2100) coupled with EDX (OI Aztec 80mm X-max) to determine the size and morphology of starting and released nanomaterials. XRD analysis (D5000, Bruker) was performed to determine the crystallographic structure of the nano-TiO_2. The washed and unwashed textiles were characterized by SEM (JEOL JSM6500F FEG-SEM) coupled with an EDAX EDX system with Genesis software. Titanium concentration was determined in Tiodisper NA-AS solution and in washed and unwashed textiles with and without nano-TiO_2 by Inductively Coupled Plasma Mass Spectrometry (ICPMS, Agilent 7500, Agilent Technologies). Before the measurements the textile samples were digested with an acid solution in an analytical microwave digestion system (MARS, CEM, 1600W). Titanium concentration in washing waters was also measured by ICPMS, but before the analysis optimization of the analytical procedure was performed in order to determine if liquid samples required digestion or not.

Washing cycle protocol

The household washings simulations were performed according to an adaptation of the standardized protocol ISO 105-C06:2010 Textiles -- Tests for colour fastness -- Part C06: Colour fastness to domestic and commercial laundering (International Standards Organization, 2010). Each sample consisted in 1.00 ± 0.05 g of fabrics, which were cut in squares with approximately 15 cm side. A temperature sealing was applied on the textiles edges in order to avoid the textile fraying and yarns release in the washing waters, what would have hampered its later characterization. The washings were performed in 550 ± 50 ml stainless steel vessels with 75 ± 5 mm diameter and 125 ± 10 mm height. Each vessel contained one sample, 10 stainless steel (SS) balls of 6 mm diameter (to simulate mechanical impact) and 150 ml of detergent solution. The detergent used was a light duty detergent with anionic and non-ionic surfactants, fabric care additives and enzymes. The dose used was 4 ml of detergent per distilled water liter, what provided a washing pH of 7.4. The tests were carried out in a Linitest+ equipment (Lab Dyeing System, Atlas) at 40 ± 2 rpm and 40 ± 2 ^{o}C.

Prior to the textile washing the vessel with the detergent and the stainless steel balls were placed inside Linitest+ during 5 minutes in order to reach the desired temperature. Then the textile was also introduced and washed during 30 minutes. The textile was removed and the washing waters were collected. Then, following the ISO protocol, two rinsing cycles of 1 minute at 40 ± 2 rpm, 40 ± 2 ^{o}C and using 100 ml of distilled water were performed (International Standards Organization, 2010). The rinsing solutions (distilled water) without the textile was also

introduced in Linitest+ during 5 minutes for temperature conditioning and after rinsing the waters were collected for further characterization. After the washing cycle the samples were dried at ambient temperature.

Two different textile samples were tested: 1) PES fabric treated with TiO_2 NPs, wetting agent and binder (Curb_TiO_2[1]); 2) PES fabric without TiO_2 NPs (control sample, Curb[1]). TiO_2 concentration in textiles was analyzed at 1; 3; 5 and 10 washing cycles including three replicates per sample. When a sample reached the expected number of washings it was digested and analyzed through ICPMS, so a new textile was used for the following washings, meaning that it was needed to start washing the new textile from the beginning (0 washings). Thus, multiple washing waters were obtained since every time that a washing started, new washing waters were produced. To avoid release differences due to different concentrations in textiles, all the washing waters analyzed belonged to the textile washed 10 times. From the textile washed 10 times, washing waters from the 1st, 2nd, 3rd, 5th, 7th and 10th washing cycles were analyzed by ICPMS.

Liquid samples ICPMS analysis optimization

ICPMS is an analytical technique which ionises chemical species in a plasma and then detects the ions by their mass to charge ratio. Some materials such as TiO_2, depending on the concentration, can be difficult to ionise. In these situations acidic digestion can be used, which dissolves the sample which is then introduced into the ICPMS equipment. However, this means the liquid sample is diluted and therefore the limit of detection is increased. Since we suspected that some of our liquid samples contained a relatively low concentration of Ti, acid digestion was avoided where possible in order to keep the limit of detection as low as possible.

To determine the capacity of the ICPMS equipment to ionize the sample without previous digestion, known concentrations of 1, 10 and 20 ppb of the original TiO_2 dispersion (Tiodisper NA-AS) were measured. For each of the concentrations three replicates were tested.

Results

ENMs

Electron microscopy

From the TEM images (Figure 5) it was confirmed that the Tiodisper NA-AS dispersion contained nanomaterials. Although some nanoparticles were isolated, most of them were forming aggregates that ranged from around 100 nm to few micrometers. Although spherical NPs were

[1] Sample's name

also observed, most of the NPs presented irregular shape. From the diffraction pattern shown in Figure 5A it was concluded that the sample was polycrystalline which provided diffraction in multiple directions thus generating the observed pattern. Due to the elevated amount of aggregates in the dispersion it was difficult to determine where a particle started and ended. For this reason, a particle size distribution could not be measured. High magnifications images (as the one shown in Figure 5D) showed it was not possible to distinguish discreet nanoparticles and therefore measure the size of the NPs present in the aggregates. However, the interplanar distances of the TiO_2 crystal could be distinguished and measured at around 3.5 Å which matches the (101) plane of anatase TiO_2.

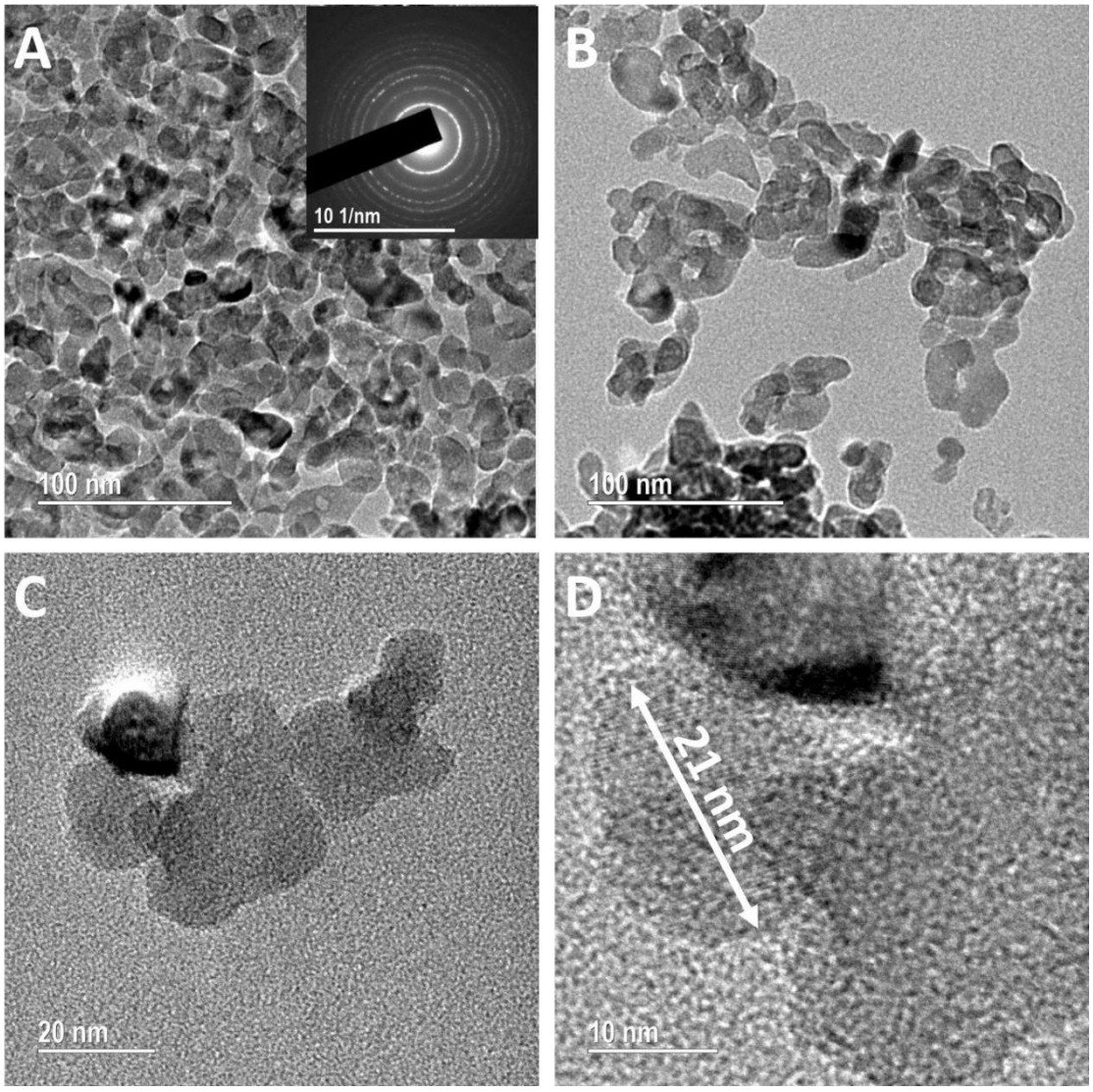

Figure 5 – TEM images of TiO2 nanoparticles before being impregnated in the textile.

X-Ray Diffraction

The XRD measurement performed on the nano-TiO_2 dispersion (Tiodisper NA-AS) are shown in Figure 6. The results match the ICDD (International Centre for Diffraction Data) database entry for anatase TiO_2, as expected, since that crystal form is the more photocatalitically active form of TiO_2 (Schneider et al., 2014).

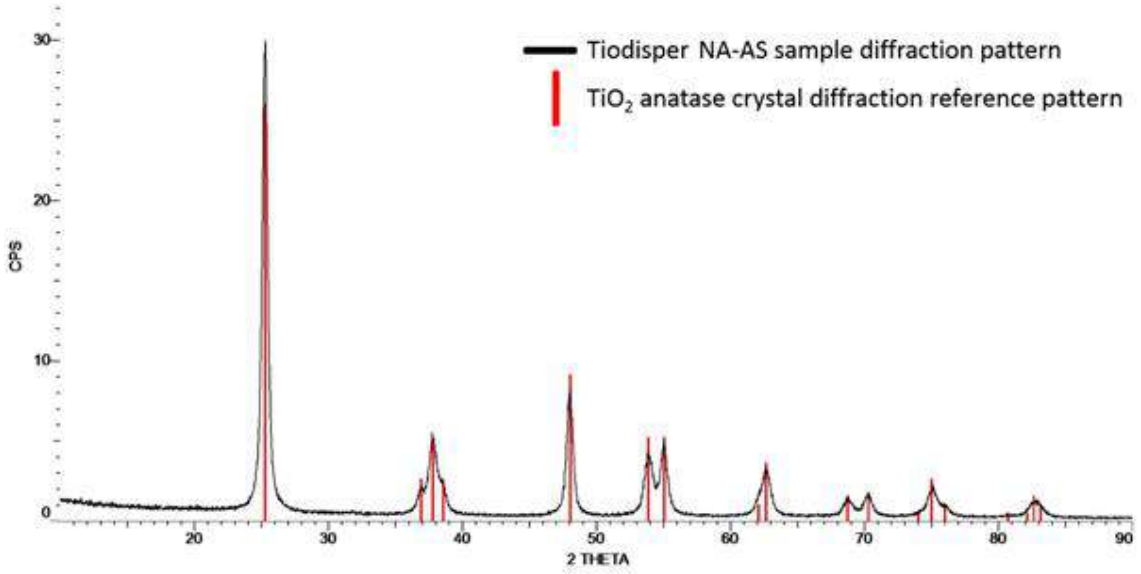

Figure 6 – Tiodisper NA-AS sample diffraction pattern

Inductively Coupled Plasma Mass Spectrometry

The ICPMS results obtained from the starting materials are shown in Table 3. It was concluded that the PES textile already contained Ti even before the incorporation of the nano-TiO_2. The reason could be the extensive use of TiO_2 as a delustering agent in synthetic fibres. A delustering agent is a substance added in synthetic fibres to reduce the lustre (sheen) and transparency of the fibre. Commonly, powdered anatase TiO_2 is used for that purpose. In any case, after the Tiodisper NA-AS addition, the amount of Ti increased significantly; by 1000 ppm, 50% of the original concentration. This means that in the textiles containing nano-TiO_2 two kinds of TiO_2 will be present, 1/3 of the TiO_2 will come from the Tiodisper NA-AS and 2/3 from the TiO_2 previously present in the textile. This fact shows the difficulty of working with real materials, since as in this case, the matrix can produce interferences with the materials of interest.

Table 3 - Ti concentration determined by ICP-MS in the samples provided by INOTEX.

SAMPLE	Ti CONCENTRATION (ppm)	RSD (%)
Control sample (Curb)	2111 ± 44	2.1

Textile with ENM (Curb_TiO_2)	3095 ± 123	4.0
ENM dispersion (Tiodisper NA-AS)	193847 ± 2691	1.4

Unwashed textiles characterization

Electron microscopy and EDX

In Figure 7A a SEM image of the Curb textile sample yarns is shown. On the yarns multiple particles can be seen, which are distributed along the entire surface. From the magnified image shown in Figure 7B is concluded that while some of the particles are a few micrometers in size, others have submicron size. The platinum in the EDX spectra of both background and particles is from a thin Pt coating applied to the sample to minimize sample charging problems. The large low energy peak (0.277 keV) is the C Kα characteristic X-ray and most of this signal comes from the textile (polyester). The oxygen Kα electron transmission has an energy of 0.525 keV and the titanium Lα emission has an energy of 0.452 keV but this is a much less intense X-ray line than the Kα line at 4.088 keV, which does not overlap with any of the elements of interest. For these reasons this peak is used for TiO_2 identification. Much of the oxygen peak will be signal from the PES. However, it is reasonable to assume when Ti is detected the particles are made of TiO_2.

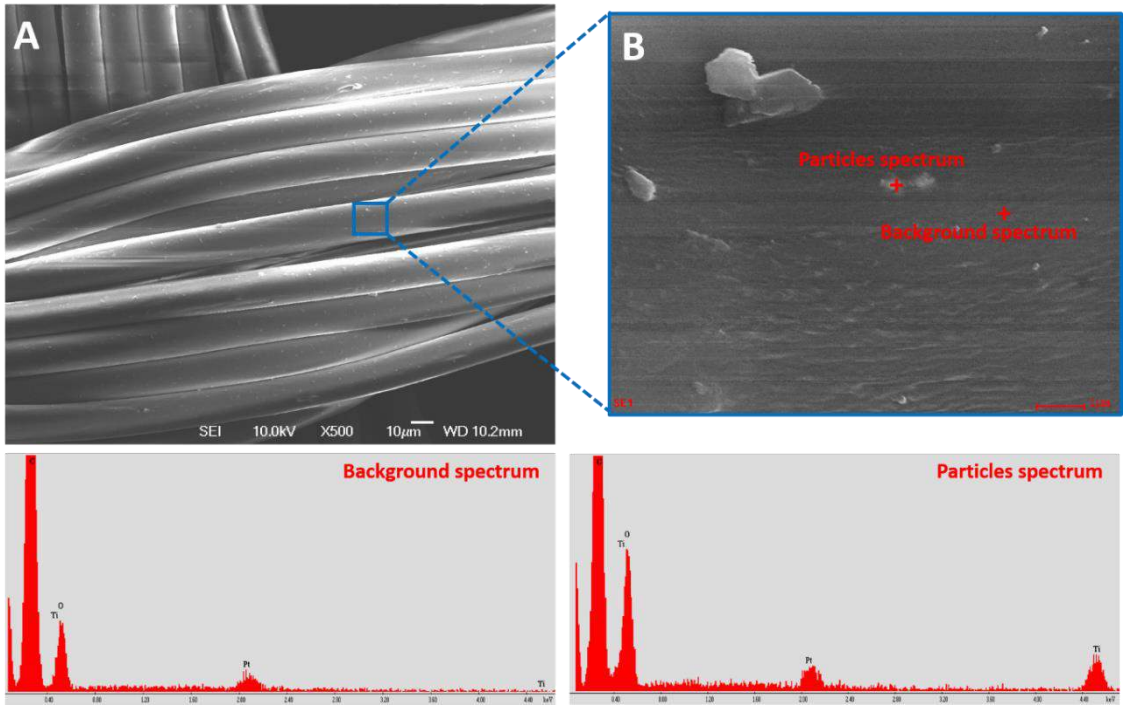

Figure 7 – SEM images and corresponding EDX spectrums of Curb sample.

For the Curb_TiO_2 sample a similar conclusion is obtained. In Figure 8A multiple particles can be seen in the yarn's surface. In the EDX analysis performed from Figure 8B, again in the background there is no Ti presence while in both particles (big and smaller) TiO_2 was detected.

Although the elemental analysis (EDX) of both samples lead to similar results, when the surface images of Curb and Curb_TiO_2 samples are compared some differences are apparent. When Figure 7B and Figure 8B are compared it is clearly seen that in Curb_TiO_2 sample there is a higher number of particles. Comparing Figure 7A and Figure 8A, although it is more difficult to detect, it is useful to realize that this is a general trend, it happens in all the yarns. Moreover, in Curb_TiO_2 sample there is a higher number of smaller particles forming aggregates, which is not seen in Curb sample. Most probably these small particles are the ones from the Tiodisper NA-AS that have attached to the textile during the impregnation process. Thus, it is possible to differentiate among the two TiO_2 particles distribution present in the samples. The bigger one originally coming from the textile and the second one lately added by impregnation.

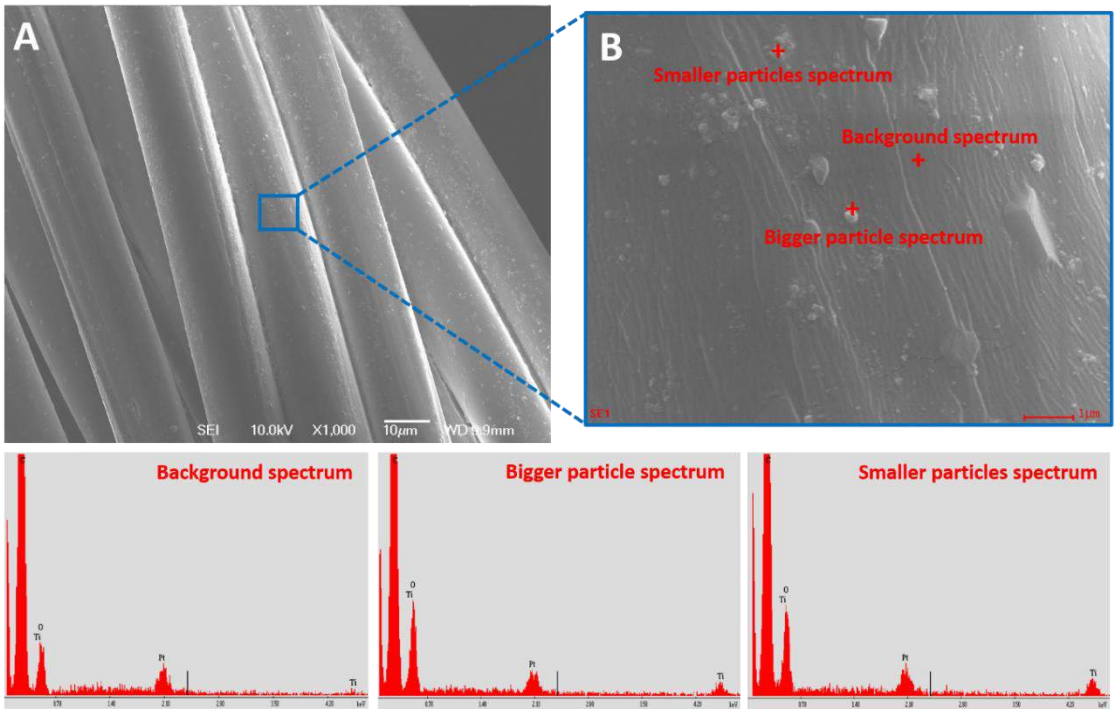

Figure 8 – SEM images and corresponding EDX spectrums of Curb_TiO_2 sample.

Washed textiles characterization

Electron microscopy and EDX

The main difference between washed and unwashed textiles observed by SEM was that in the former, a large amount of detergent partially covering the yarns was observed. As mentioned in the methods section the textiles are submitted to two rinsing processes after every washing. However, as demonstrated in the images it was not enough to rinse off all the detergent. In any

case, the detergent present on the textile should not have a direct impact on the release, so its presence is not highly relevant for our study. The aim of observing the textiles through SEM was to determine how the particles on the surface are affected by the washings. In this particular case study, as seen in Figure 9 and Figure 10, the particles distribution on the textiles was very similar to the one observed for unwashed textiles, suggesting that they are well attached (which has been confirmed with ICPMS). For washed textiles, like for unwashed textiles, the number of particles on the yarns' surface of Curb_TiO_2 sample was greater than for Curb, meaning that the TiO_2 concentration was higher, which was also later confirmed with the ICPMS analysis.

In Figure 9, SEM images of Curb_W5 (washed 5 times) are shown. In Figure 9A it is clearly seen how part of the yarns are covered by detergent and others are not. In Figure 9B EDX analysis was performed on different areas where particulate-like matter was found. However, in none of the spectra was Ti signal detected. There could be two reasons. First, that the particles on which the analyses were performed were organic, probably from the detergent. If they were made of other elements apart from Ti, the EDX would have also detected it, which was not the case. The second possibility is that the detergent layer on the particles is hampering the detection of Ti. As can be seen in the upper right side of Figure 9B, the area where the EDX was performed was covered by detergent, providing more arguments to think that the second possibility is what is actually happening.

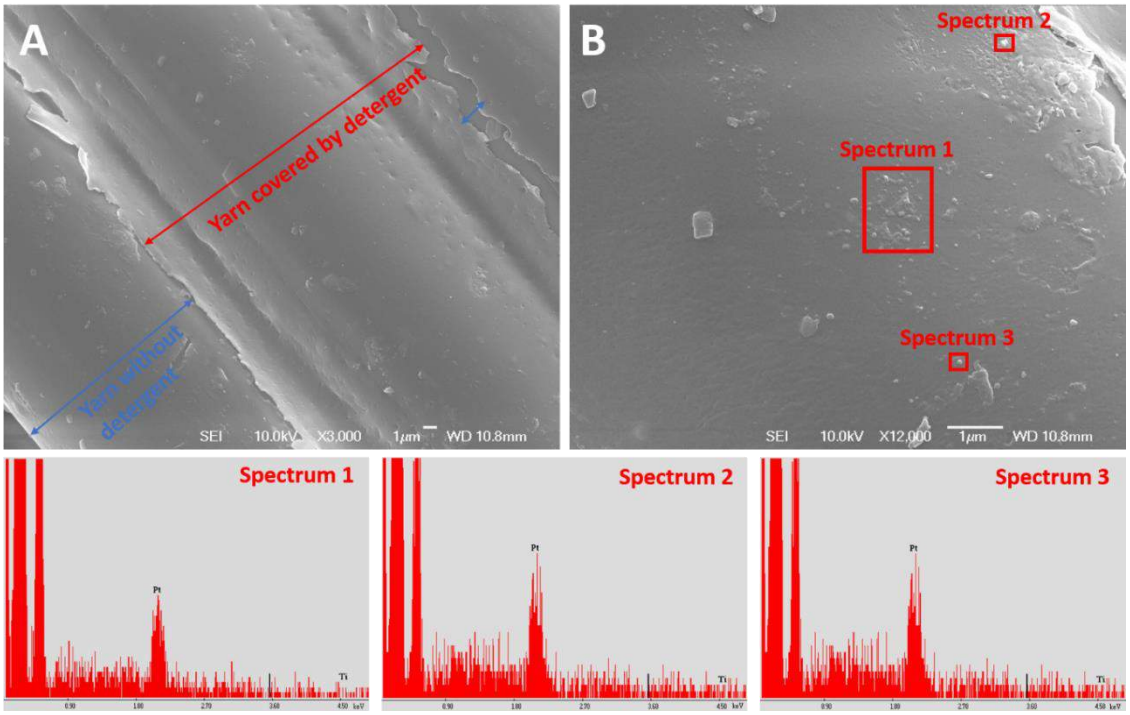

Figure 9 – SEM images and corresponding EDX spectrums of Curb_W5 (washed 5 times) sample.

Looking at Figure 10, the Curb_TiO_2 sample has a higher number of particles than in Curb. In the image with higher magnifications (Figure 10B) the nanoparticles aggregates can easily be seen. There are also some individual nanoparticles as the one pointed with the arrow, others are forming aggregates smaller than 100 nm, but most of them are forming bigger aggregates containing a high number of NPs. In the EDX analysis of Curb_TiO_2_W5 samples, Ti was detected, most probably because the area wasn't covered by detergent, making its detection easier.

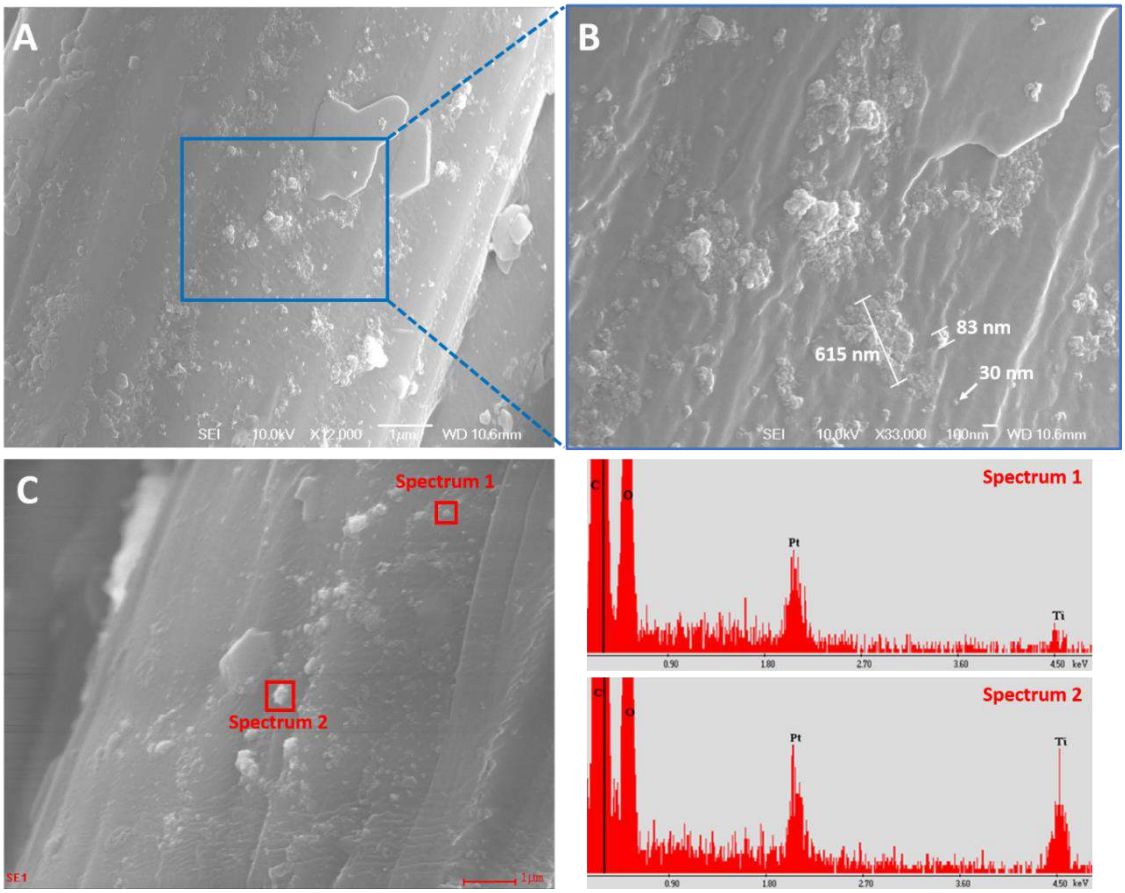

Figure 10 – SEM images and corresponding EDX spectrums of Curb_TiO_2_W5 (washed 5 times) sample.

Inductively Coupled Plasma Mass Spectrometry

The Ti concentration in Curb and Curb_TiO_2 textiles with washings was measured by ICPMS, the results are shown in Figure 11. The height of the bars represents the mean value from the three replicates, while the error bars correspond to their standard deviation. In the left-side chart, the Ti concentration in textiles is shown while in the right-side chart the TiO_2 (or Ti) remaining percentage is plotted considering the unwashed textile concentration as a 100%. Both charts are built with the same data, but different representations ease the observation of different conclusions.

From the left-side chart is clearly seen that the Ti concentration of the textiles where the nano-TiO_2 dispersion was applied (Curb_TiO_2) is higher than in the control (Curb). Since the lower concentration found in Curb_TiO_2 washed textiles is higher than the maximum (unwashed) Curb sample, the results suggest that nano-TiO_2 is still present in the textile after 10 washings. It is also remarkable that for both samples the concentration decrease is approximately the same. From around 3100 ppm to 2800 ppm for Curb_TiO_2 (300 ppm decrease) and from 2100 ppm to 1800 ppm for Curb (300 ppm decrease). However, since Curb sample has less TiO_2 than Curb_TiO_2, this 300 ppm decrease means a higher released percentage. This fact is easily appreciated in the right-side chart, where the released percentage in each sample is shown. After 10 washings around 90% of TiO_2 remains in Curb_TiO_2 sample and 80% in the case of Curb sample, meaning that Curb TiO_2 release is approximately 10% lower.

The Ti concentration decrease statistical relevance has been evaluated through an Analysis of Variance (ANOVA) data treatment with an α value equal to 0.05. For both Curb and Curb_TiO_2 samples the conclusion was the same. There is a significant Ti concentration decrease from the unwashed textile (0 washings) in comparison with the washed textiles (1, 3, 5, 10 washings). However, there is not a statistically relevant difference among washed textiles. Meaning that Ti concentration after 1 washing is not statistically different after 3, 5 or 10 washings. These results could be explained by the small decrease in concentration along washings compared with the Ti concentration variance among replicates. In other words, the concentration decrease after the first washing is so small that the standard deviation among replicates has a higher impact hiding it.

Considering that the Ti concentration in all the washed textiles is the same, the release percentage for Curb and Curb_TiO_2 can be determined as an average from the 1^{st}, 3^{rd}, 5^{th} and 10^{th} washings. For the Curb sample **17 ± 2%** of Ti is released, while for Curb_TiO_2 only the **9 ± 2%**. It is surprising that in Curb_TiO_2 sample, even though it has a higher concentration of TiO_2, the amount released is smaller. This effect is probably produced by the substances included in the nano-TiO_2 formulation to improve the attachment, as binders and wetting agents. However, it must be emphasized that the TiO_2 released in Curb sample, since it is the control, does not come from the nano-TiO_2 dispersion, it is the background TiO_2 used in the fibre as delustering agent. The same can be applied for Curb_TiO_2 sample. It doesn't mean that all the TiO_2 released was in the nanometer range. Most probably, part of it, belonged to the TiO_2 present in the textiles before the nano-TiO_2 incorporation.

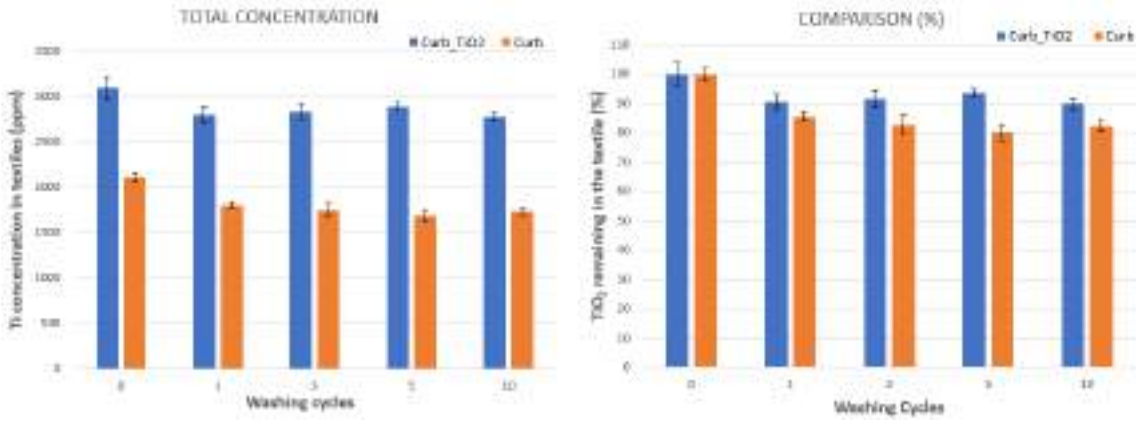

Figure 11 – Curb_TiO_2 and Curb samples Ti concentration in textiles along washings.

Washing waters characterization

Liquid samples ICPMS analysis optimization

From the results obtained in the ICPMS measurements without acid digestion of the known concentrations, shown in Figure 12, it is clearly observed that the ICPMS plasma ionization it is not enough to ionize all the titanium in the sample. For the three concentrations tested the measured concentration differs from the known concentration, a trend that is more noticeable as the Ti concentration increases. Therefore, even though it leads to an increase in the detection limit, acid digestion is needed before ICPMS measurements of the textiles washing waters.

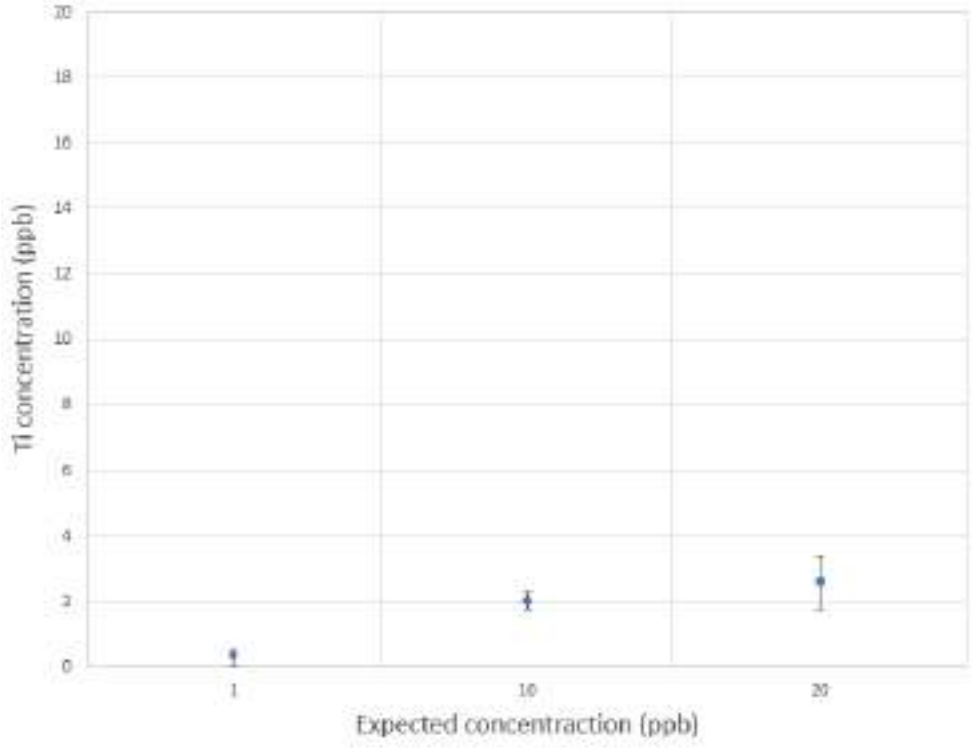

Figure 12 – ICPMS plasma ionization test.

Inductively Coupled Plasma Mass Spectrometry

The washing waters collected during the washing experiment were analyzed through ICPMS. Ti concentration in water was higher for Curb_TiO_2 sample than for Curb. Differences around one order of magnitude were measured.

For Curb sample, due to the low amount of Ti, concentrations above the limit of detection were only found for the first and second washing waters. Concentrations around 20 ppb were measured. Ti concentration in the second washing waters were lower than in the first, suggesting that release decreases along with washings.

For Curb_TiO_2 a decrease of Ti concentration along washings was also observed in washing waters. As can be seen in Figure 13, the release trend is exponentially negative, what means that during the first washings there is a big difference in concentration along with washings, whether for the last ones the difference is smaller. Indeed, from 7^{th} to 10^{th} washings a concentration difference was not observed. As shown in Figure 13, for Curb_TiO_2 sample, an exponential equation trendline was calculated to describe the release behaviour (red dashed line):

$$y = \frac{291.03}{x^{0.466}}$$

Where:

y = Ti concentration in washing waters (ppb)

x = The number of washings performed, should be a natural ($\mathbb{N}$) number.

The previous equation could be useful to predict the amount of Ti that could be found in washing waters if more washings were performed (e.g. 20, 30, 50 washings).

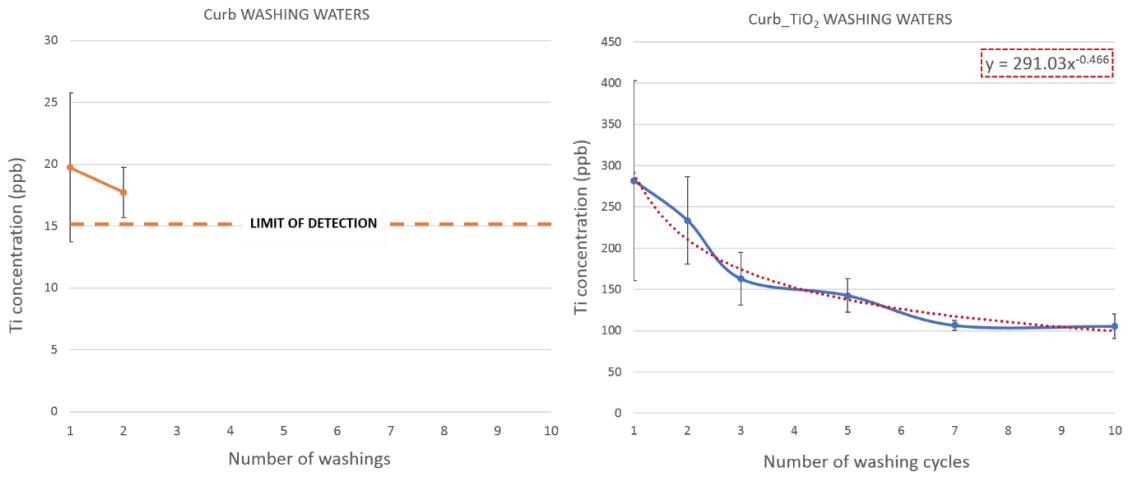

Figure 13 – Ti concentration in washing waters of Curb and Curb_TiO_2 samples. The orange and blue solid line representing washing waters Ti concentration experimentally determined by ICPMS for Curb and Curb_TiO_2, respectively. Red dashed line showing the exponential equation trendline (theoretical approach).

Electron microscopy

In order to not only determine the amount but also the form of TiO_2 released from the curtains, TEM images of the washing waters were obtained. In Figure 14, TEM images from a small amount of white sediment found in the vessel which had been used to store one of the water from the first washing of Curb_TiO_2 are shown. As seen in Figure 14 the nanoparticles released formed big aggregates surrounded by organic matter, most probably coming from the detergent. From the EDX results (Figure 14D) it was confirmed that the components observed were TiO_2. From the diffraction pattern obtained from the sample, which is shown in Figure 14C it was confirmed that the released TiO_2 was in anatase form since the pattern exactly matched with the one previously measured in Tiodisper NA-AS (Figure 5A). Curb washing waters were also observed by electron microscopy but no released TiO_2 was found.

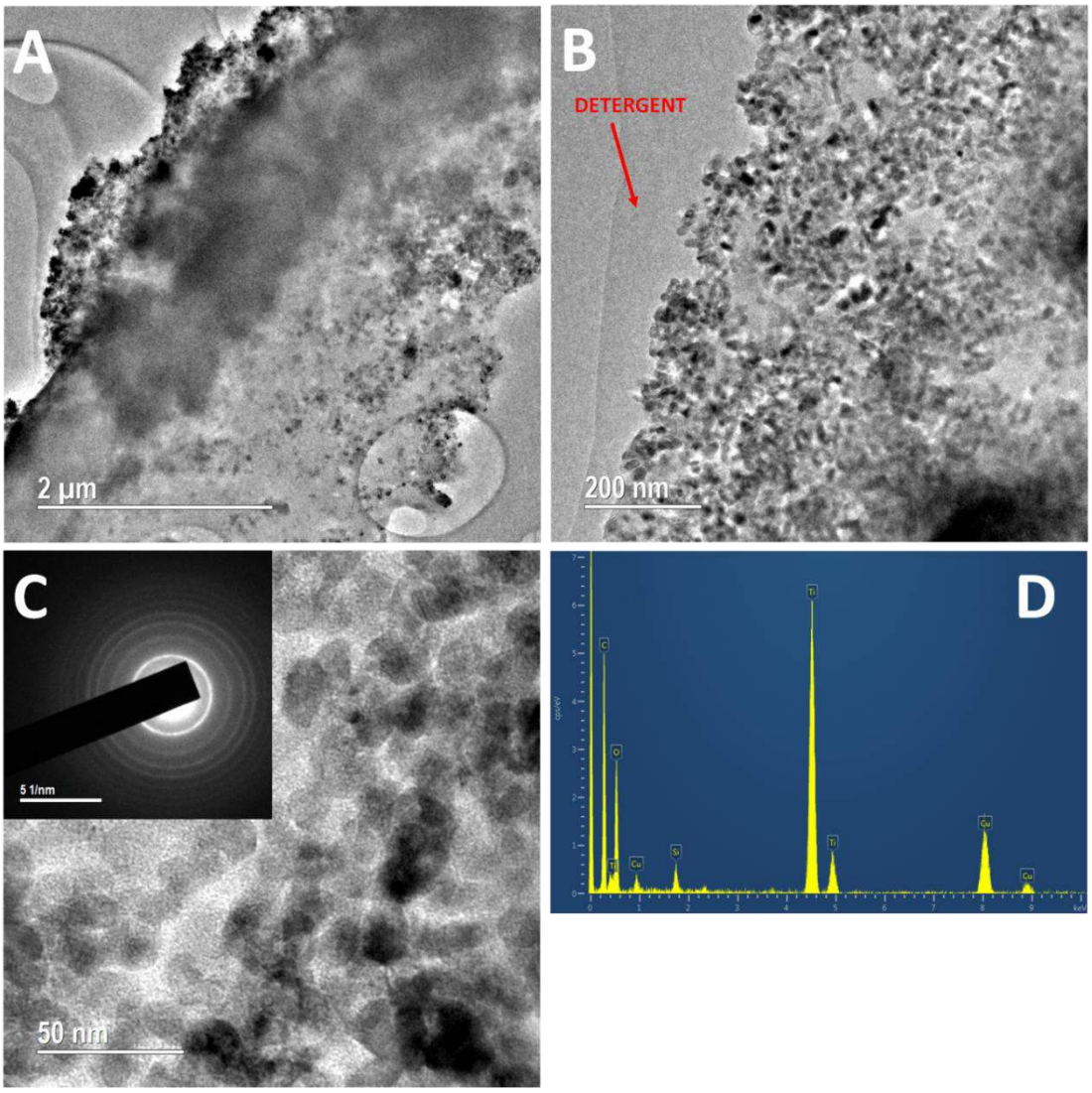

Figure 14 – TiO_2 NPs released from Curb_TiO_2 sample.

Conclusions

For both control (Curb) and nano-enabled curtains (Curb_TiO_2) a high release was observed for the first washing while statistically relevant difference in concentration for the following 9 washings was not measured.

In previous published studies, release of TiO_2 from textiles during household washings ranged from 0.01% to 3.4% of the initial elemental Ti concentration in the first washing and rinsing process (Koivisto et al., 2017), meaning that releases of 17 ± 2% and 9 ± 2% are relatively high. However, although in other published studies the release in the first washing is lower, in the present case study the release is very low during the following 9 washings. In order to do a relevant comparison, the current textiles should be compared with other textiles also washed 10 times.

Release forms were determined by electron microscopy, where large TiO_2 aggregates were observed.

3.2.5. Photocatalytic coating for roads

Introduction

Air pollution is a local, regional and international problem caused by the emission of pollutants, like NOx, which can lead to negative impacts on human health and ecosystems (European Environment Agency, 2018). In order to mitigate the problem, multiple initiatives are being developed, some of them considering the use of nanotechnology. One of them is the present case study, a photocatalytic coating for roads containing nano-TiO_2 to remove NO_x pollutants from air, using nano-TiO_2 photocatalytic properties (Schneider et al., 2014). The initiative consists of directly coating the roads in the most contaminated areas (mainly in the cities) in order to degrade some of these pollutants.

The photocatalytic coating has been developed by FCC Construcción (FCCCO), a leading company in the construction sector with civil engineering projects in more than 40 countries. As part of the FCC Group of Citizen Services it promotes transversal research and development in the areas of environment, buildings, infrastructures, waste recycling, water and energy.

Since the coating is exposed to outdoor conditions, concerns due to the potential release of nano-TiO_2 from the coating have been raised. Due to multiple stresses such as weathering and wheel abrasions, the coating/asphalt could be damaged leading to nanoparticles being released. In cities, released nano-TiO_2 may arrive into surface water drainage systems and from there to the environment, either discharged directly to rivers or via waste water treatment plants. In case that it was applied to more rural areas, released nano-TiO_2 may directly reach the soil or surface water. Since large areas of roads are present in all Europe, the application of this product could serve broad market needs, especially in those areas strongly affected by air pollution. Therefore, it is important to study and analyse if release could occur and in what forms and amounts.

Materials and methods

Hot Bituminous Mix (HBM) is the most used material in most city streets and highways. HBMs are manufactured in agglomerate plants at temperatures between 160 °C and 180 °C and are made of a combination of hydrocarbonated binders and aggregates. Combinations of different aggregates granulometrics and different percentages of bitumen, provides different kinds of mixes with different intrinsic properties, and consequently, their fields of application are also different. One of the most used mixes in cities is AC16 Surf S.

The AC16 surf S corresponds to a semi-dense mix that is commonly used in the surface layer of roads. The aggregates used are of porphyry nature for the coarse fraction and a combination of porphyry and limestone for the fine fraction together with calcium carbonate as a filler. A close view of AC16 Surf S asphalt is shown in Figure 15.

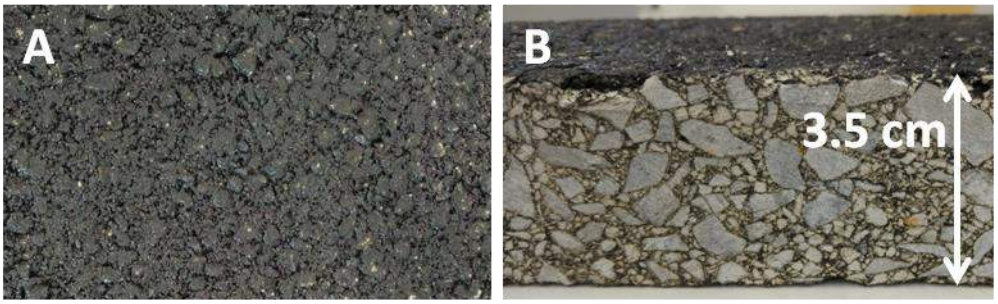

Figure 15 – Close view of the uncoated AC16 Surf S asphalt sample. A) top view, B) lateral view.

The asphalt materials with and without the photocatalytic coating were provided by FCCCO for release experiments as well as the nano-TiO_2 dispersion for characterization. 100% anatase nano-TiO_2 (PC 500, Crystal Global) were bought and modified by FCCCO with an organic resin made of a copolymer dispersion based on vinyl acetate and ethylene, in order to obtain the final product. The nano-TiO_2 dispersion was analysed by X-ray Diffraction (XRD) (D5000, Bruker) to confirm the crystalline phase and High Resolution-Transmission Electron Microscopy (JEOL JEM-2100) to show particle size and shape.

Coating application

The coating was applied in FCCCO's facilities using a paint spray gun, as shown in Figure 16B. Next to the coated samples, different sheets of paper were placed, which were digested in an analytical microwave digestion system (MARS, CEM, 1600W) and further analysed by ICPMS (Agilent 7500, Agilent Technologies) to determine the TiO_2 amount sprayed per area.

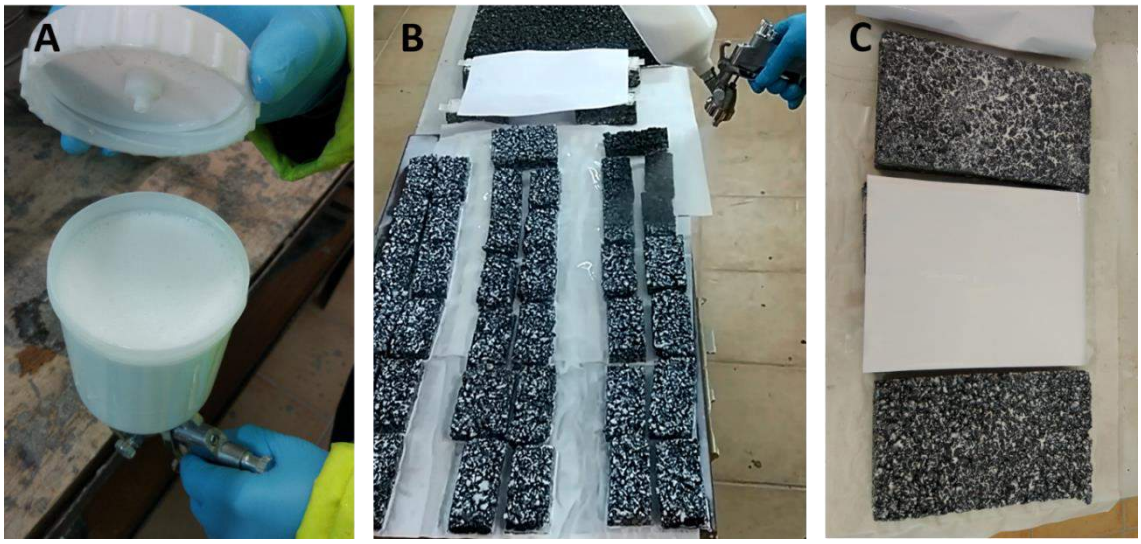

Figure 16 – TiO_2 coating application on asphalt samples. Nano-TiO_2 dispersion A) in the air spray gun container; B) being sprayed on the asphalt samples; C) drying on the asphalt samples and blank papers (which have been used to determine the amount of TiO_2 deposited).

After the coating was applied the samples were dried at ambient temperature.

TiO_2 release monitoring due to weathering and wheel abrasion

In the release experiments two samples were studied:

- AC16_TiO_2: AC16 surf S asphalt with the coating on it.
- AC16_blank: AC16 surf S asphalt without any coating.

The release rates and release forms of nano-TiO_2 coming from the photocatalytic coating on the different asphalts were evaluated. The four samples were introduced into a climatic chamber (Suntest XXL, Atlas) where dry and rain cycles were alternated (29 minutes dry and 1 minute rain). The weathering parameters are shown in Table 4. LEITAT's climatic chamber has been adapted to include individual sample holders and being able to collect the water from the rain cycles after being in contact with the samples, an image of the climatic chamber modification is shown in Figure 17.

Table 4 – Climatic chamber weathering parameters.

Irradiance at 320 nm ($W/(m^2 \cdot nm)$)	Black Standard Temperature (ºC)	Chamber Temperature (ºC)	Relative Humidity (%)	Dry cycle duration (min)	Wet cycle duration (min)
0.51 ± 0.02	65 ± 3	38 ± 3	50 ± 10	29	1

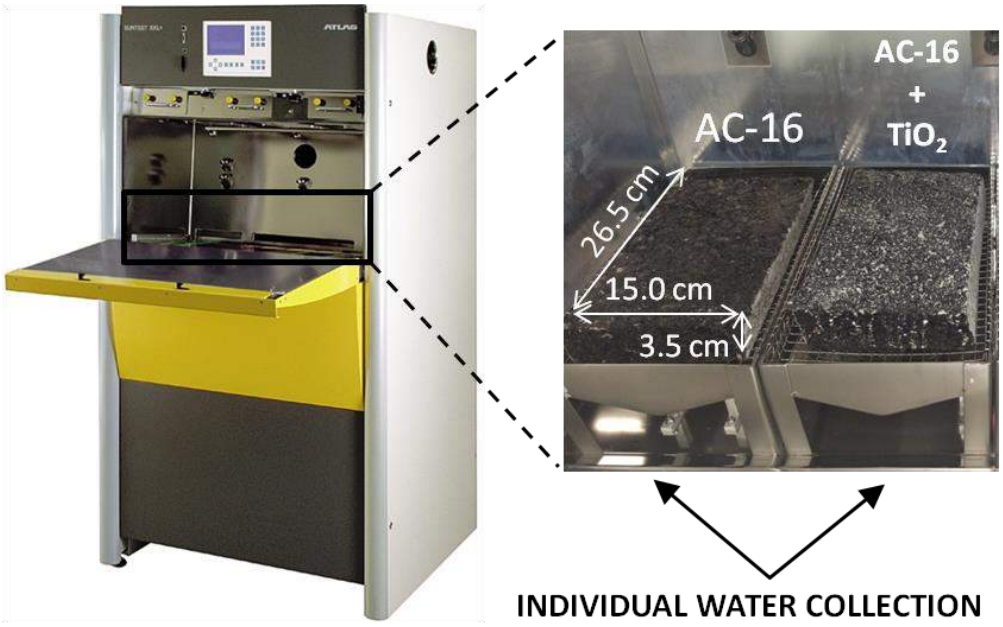

Figure 17 – Asphalt samples distribution inside the climatic chamber

After 14 and 28 days of weathering simulation the samples were taken out from the climatic chamber and were submitted to wheel tracking assays following an adaptation of EN 12697-22:2003 +A1:2007 (International Standards Organization, 2007)]. In Figure 18 an image of the standardized equipment to perform the assay is shown. The assays were performed at 25ºC with a load of 5000 ± 50 N. The wheel width was 80 ± 5 mm and a total of 2000 cycles were applied in each assay, considering one cycle as the wheel going back and forward at a frequency of 1.0 ± 0.1 Hz. After the wheel abrasion simulation, the samples were introduced in the climatic chamber to continue with the weathering simulation.

Figure 18 – Standardized equipment used to perform the wheel abrasion simulation.

During some of the rain cycles the water from each sample was individually collected, freeze-dried (CoolSafe 100-9 PRO Freeze Dryer, water sublimation at -95 °C and ~0.3 mbar), digested with acid and further analysed through ICP-OES (Inductively coupled plasma optical emission

spectroscopy, Optima 8000, Perkin Elmer) to determine the Ti concentration and the resulting release rate in each case. Characterization with HR-TEM (JEOL JEM-2100) and FE-SEM (field emission scanning electron microscopy, Merlin, Zeiss) with Energy Dispersive X-ray analysis (Oxford Instruments INCA X-Max) was also performed to obtain information regarding the release forms. To provide a more realistic scenario, weathering cycles were alternated with wheel abrasion. The samples collection and wheel abrasion times are shown in Figure 19. It shall be emphasized that waters were collected just before and after abrasion to determine its impact on release. The total simulation time was 42 days (1008h), which is equivalent to approximately 1 year exposure in outdoor conditions in a low altitude, Mediterranean climate with an average annual temperature of 15 °C: temperate winters, rainy springs and autumns, hot and dry summers.

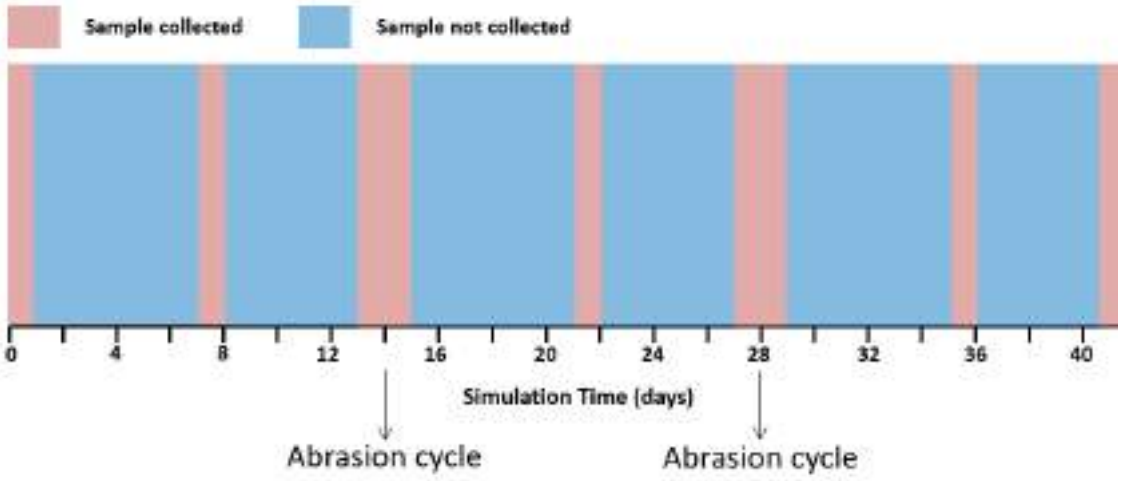

Figure 19 – Water collection and abrasion cycles planned for the climatic chamber simulation.

Results

ENM characterization

Electron microscopy

The initial concentration of the nano-TiO_2 dispersion was 30g of TiO_2 per litre. This was diluted to 100 ppm for HR-TEM. The images are shown in Figure 20. The nanoparticles were highly agglomerated but some individual nanoparticles were also observed. Due to the high agglomeration state, a size distribution analysis could not be performed, but as seen in Figure 20B some of the individual particles were around 10 – 20nm. Agglomerates sizes ranged from few nanometers to some micrometers.

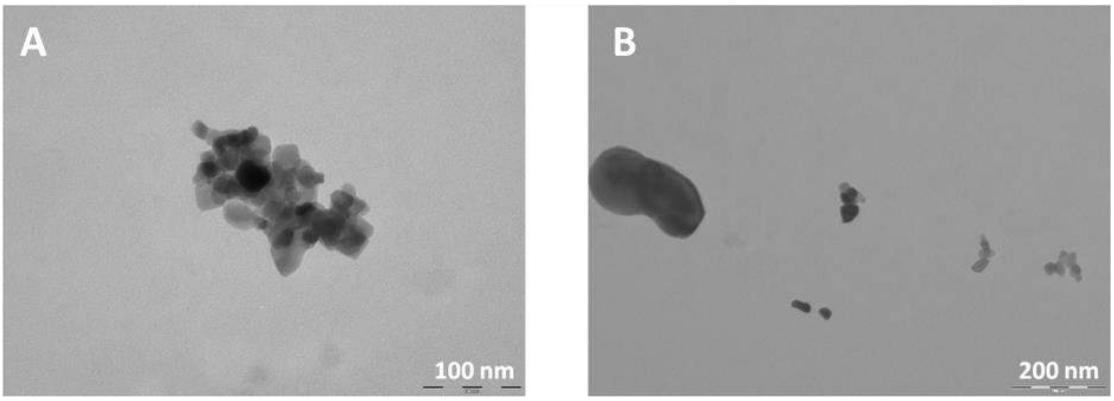

Figure 20 – HR-TEM images of TiO_2 dispersion used in FCCCO's case study.

X-Ray diffraction

XRD measurements of dried TiO_2 matched with the anatase TiO_2 entry in the International Centre for Diffraction Data (ICDD) powder diffraction database (www.ICDD.com) confirming this as the crystalline phase in the coating material, as expected since anatase is the crystallographic phase providing a higher photocatalytic activity.

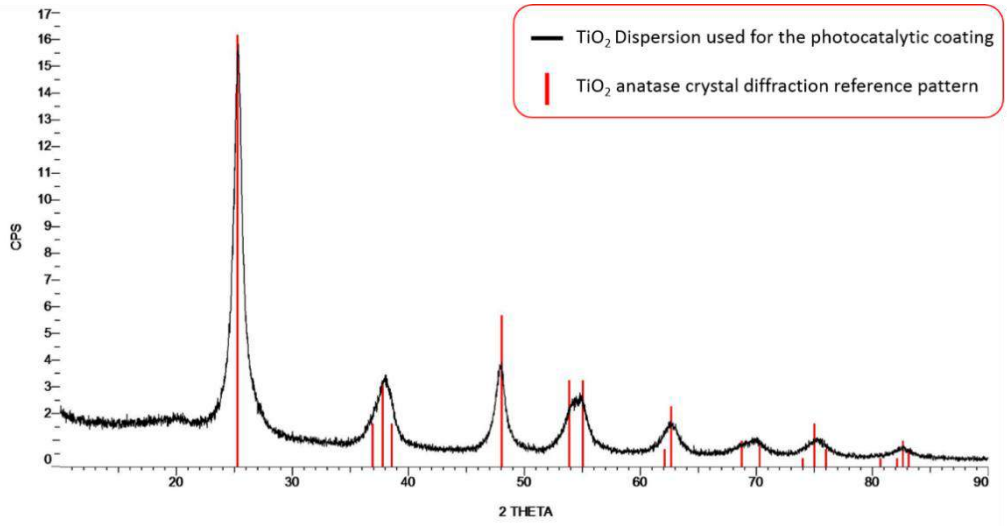

Figure 21 – XRD measurement of FCCCO TiO2 dispersion

Coating application

From all the sheet papers coated together with the samples, 6 representative areas of 65 cm^2 were cut, digested and analysed through ICPMS, the results are shown in Table 5. Apart from the coated paper, the uncoated paper was also analysed as a control. A small amount of Ti was detected in the uncoated paper as expected since paper whitening is a major use of TiO_2. However, this background Ti amount can be neglected since it is 4 orders of magnitude below

the concentrations detected in the coated paper. As the ICPMS results show, the TiO_2 concentration sprayed on the surface was around 2.5 TiO_2 g/m^2, a concentration very close to the one used in real applications.

Table 5 – ICPMS results of Ti and calculated TiO_2 concentration in coated papers.

Samples	Ti concentration (g/m^2)	TiO_2 concentration (g/m^2)
Coated Paper_A	1.6	2.6
Coated Paper_B	1.3	2.2
Coated Paper_C	1.8	3.1
Coated Paper_D	1.4	2.3
Coated Paper_E	1.6	2.6
Coated Paper_F	1.2	1.9
Average ± St. dev.	1.47 ± 0.23	2.45 ± 0.39

TiO_2 release due to weathering and wheel abrasion

Inductively Coupled Plasma Optical Emission Spectrometry

The concentrations of TiO_2 detected in the collected waters with time and normalized per m^2 are represented in Figure 22. The blank sample (without TiO_2 coating used as control) presented much smaller concentrations than the one with the TiO_2 coating, confirming that contamination during the experiment did not occur.

The release behaviour can be divided into three main different types, in the figure represented by A, B and C. High release occurs at the beginning (A). This may be due to weakly attached coating or weakly attached asphalt containing coating that is easily released with the first raining cycles in the climatic chamber. Then release diminishes and starts to increase again (B). This increase is probably related to matrix/coating degradation, which produces TiO_2 release. The longer time the sample is in the climatic chamber, the higher the degradation and as a consequence the higher the TiO_2 release is. A maximum is achieved, and the release diminishes again reaching a constant level (C). Probably, most of the TiO_2 available due to the sample surface damage has already been released, ending up in a release rate decrease.

When looking at the abrasion effect (around 350h and 700h), two different tendencies are observed. In the first abrasion, an effect on the TiO_2 release is not so significant. However, in the second abrasion, a clear release increase was measured. The reason could be that in the

beginning the asphalt/coating was not very damaged, so the sample could resist the abrasion and TiO_2 release did not increase (B tendency). When the second abrasion was performed, the asphalt/coating was more damaged, as can be seen by the previous TiO_2 release increase. In this occasion, the stress produced by the abrasion was more critical resulting in a release increase. These results suggest that it is very important to consider the state of the asphalt/coating when the abrasion is performed. Since the capacity of the sample to resist the mechanical stress will depend on its state.

Since the TiO_2 concentration with time is known and the total amount of water produced during the experiment is also known. The total amount of TiO_2 released in the experiment simulating one year was calculated as 0.93 g TiO_2/m^2. Since the initial amount of TiO_2 in the sample is also known (see coating application section (2.45 g TiO_2/m^2)) the release amount can be calculated with the following equation:

$$\frac{0.93 \frac{\text{g TiO}_2 \text{ released}}{m^2}}{2.45 \frac{\text{g TiO}_2 \text{ before aging}}{m^2}} \cdot 100 = \mathbf{38\%}$$

This means that 38% of the TiO_2 initially present in the sample was released in the experiment which simulated one-year weathering and wheel abrasion post-application.

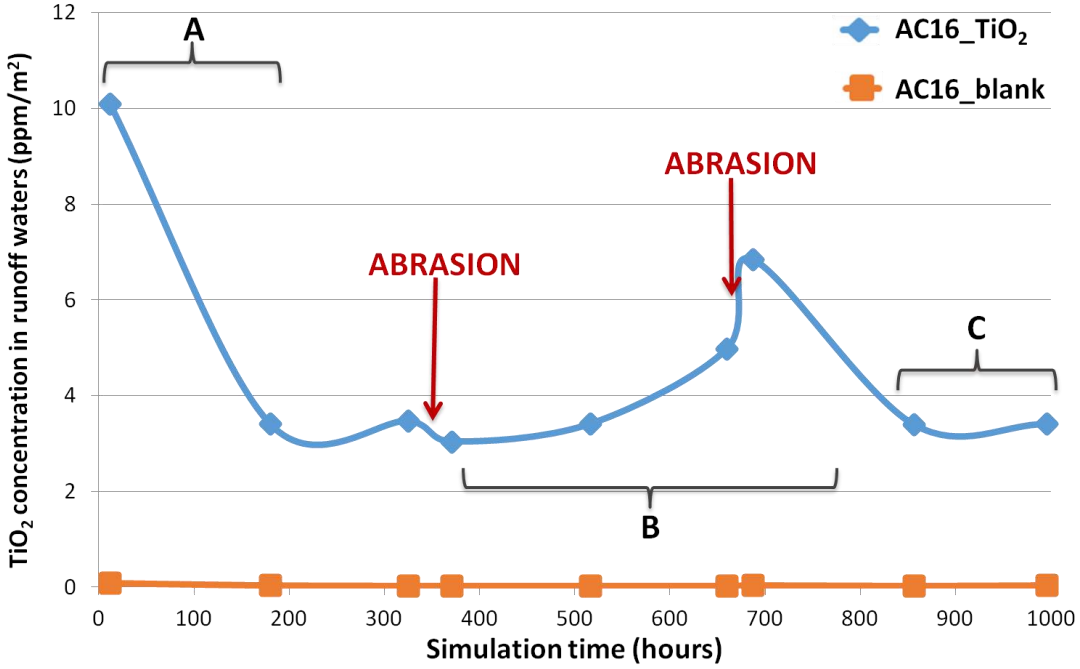

Figure 22 – TiO_2 release along time due to weathering and wheel abrasion.

It could seem that 38% is a lot, but indeed, if the samples before and after ageing are observed (Figure 23A) it can be clearly appreciated that most of the coating (whitish substance) have disappeared. Indeed, both blank and sample containing the coating look almost the same after the ageing (as shown in Figure 23B). Thus, the visual inspection agrees with the measurements, a high coating release is experienced.

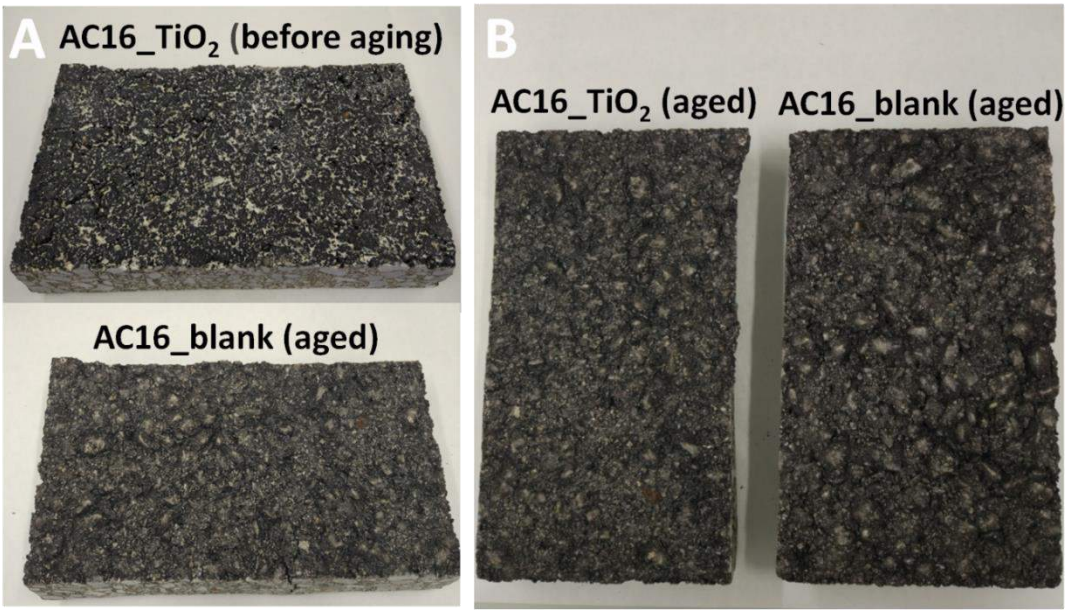

Figure 23 – Asphalt samples with and without coating, before and after aging.

Electron microscopy

The release waters presented a high amount of inorganic and organic content, which made it difficult to distinguish one component from the other. EDX provided an essential tool to determine what was being observed. Ti signal was detected in multiple aggregates always together with inorganic and organic content, presumably from the substrate. The aggregates found presented sizes of few micrometres.

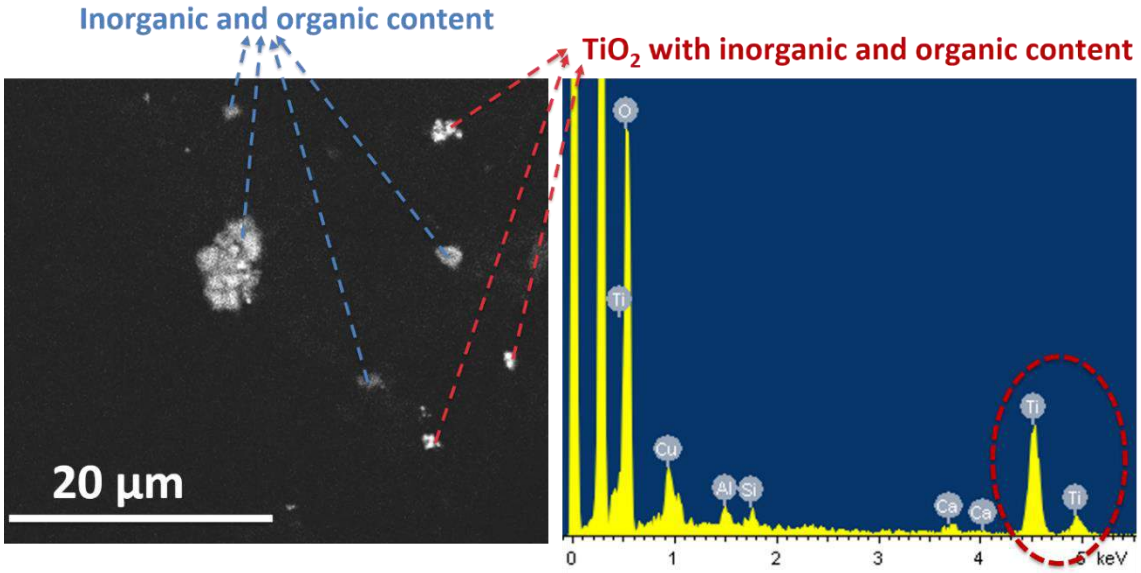

Figure 24 – Field emission SEM image with EDX analysis of the release waters from AC16_TiO_2.

Conclusion

It was confirmed that the crystallographic form of the TiO_2 present in the coating is anatase, which is the most photocatalytically active phase. The amount of TiO_2 sprayed on the lab-produced sample was also determined, which was in the range of the concentrations used in the real road coating applications.

A realistic and controlled use phase simulating weathering and wheel abrasion was performed and the corresponding released materials collected and characterized. From the experiments, it was determined that the amount of TiO_2 released varies with time and initially a higher release occurs. Wheel abrasion effect on release depended on the asphalt/coating condition. The release increased due to wheel abrasion when the sample was aged, while a release increase was not observed in the first abrasion when the weathering had not affected the sample for long. Through the whole duration of the experiment, which approximately relates to 1 year of weathering in outdoors conditions, 38% of the TiO_2 was released in the form of few micrometres sized aggregates together with other inorganic compounds and organic material presumably from the substrate.

3.2.6. Camping tents with antibacterial activity

Introduction

Nowadays, in the textile industry, there is interest in introducing silver ENM into products due to their well-known antibacterial properties (Besinis et al., 2014; Dallas et al., 2011; Ferraris et al., 2014; Hajipour et al., 2012; Kvitek et al., 2011; Wang et al., 2017). However, one of the inconveniences they are facing is the weak ENM attachment in the textiles. The textile manufacturers are aware of the problem and are looking for alternatives to ensure the maximum attachment of the nanoparticles, not only to achieve a long-term effect of the treatment but also to minimize nanoparticles release to the environment. The present case study is one of many examples of efforts to improve ENM attachment. The nano-enabled product was provided by INOTEX, who participated in a project where the product was developed by a third party.

Materials and methods

The case study consists of a cotton fabric modified with a fluorocarbon-based thin water repellent layer on both sides. In addition, a watertight impermeable layer of polyacrylic coating paste containing Ag nanoparticles, stabilized with polyethylenimine (PEI) polymer through a coordinate-covalent bond, was applied to one of the sides. The resulting textile-based composite is intended to be used as a material to fabricate camping tents. According to INOTEX, the Ag presence diminishes the potentially harmful effect of bacteria on the fabric, avoiding undesirable effects such as bad odours or mould appearance.

Four different samples were tested, all of them exemplified in Figure 25 and shown in Figure 26. All the samples of the cotton tent cloth were treated with a fluorocarbon finish preventing the coating paste penetration, and coated by one-side single or double polyacrylic coating with or without Ag-PEI NPs content. The four samples together with the Ag-PEI dispersion and the polyacrylic paste containing the Ag-PEI dispersion were evaluated.

From the environmental point of view, there is an interest in testing the potential release of Ag NPs to the environment. During the use phase, the textile will be exposed to weathering effects. However, for Ag to be released, the cotton textile would need to be destroyed first, which is not likely to happen in normal use. For this reason, the main release scenario and therefore the one studied is during the end-of-life stage, more specifically during landfilling. The leaching of silver nanoparticles from the textiles was studied simulating an accelerated end-of-life process according to the standardized protocol EN – 12457-4: Test for leaching of granular waste materials and sludges (European Standards, 2003).

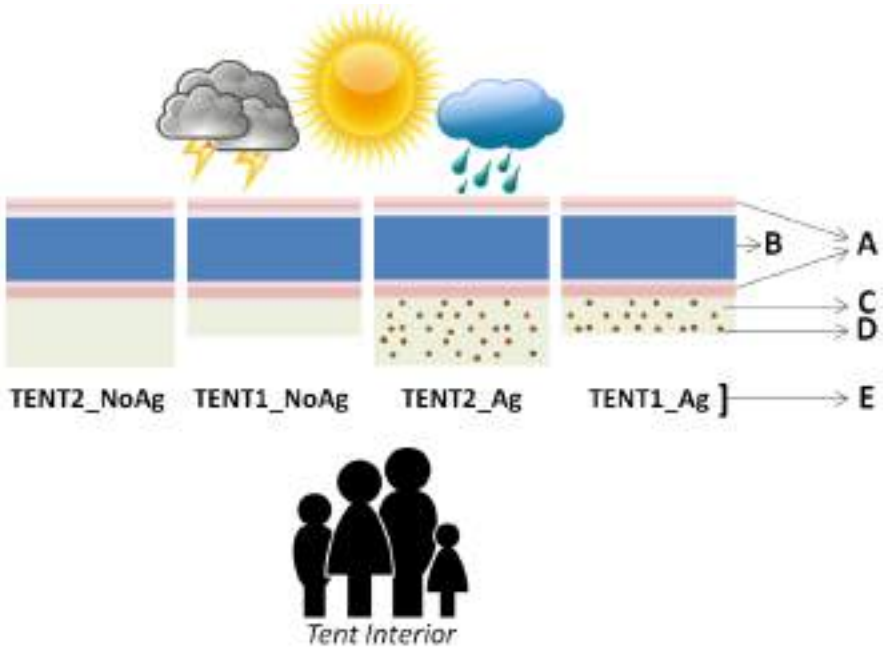

Figure 25 – Case study composition, textile for camping tent applications. A: Fluorocarbon based thin water repellent layer; B: Cotton fabric; C: Mixed dispersion of synthetic copolymers (acrylics and polyurethanes) impermeable layer; D: Ag nanoparticles coated with Polyethylenimine (PEI); E: Samples code.

The samples containing Ag NPs (both with 1 or 2 polyacrylic coating layers) are the ones intended for commercial applications, while the non-containing Ag were specifically designed for the test as control.

Figure 26 – Visual aspect of the 4 samples. A: Tent exterior side; B: Tent interior side (showing the polyacrylic coatings, see Figure 31 for the meaning of the codes).

In Figure 26A it is observed that the exterior side of all the textiles look the same, while the tent interior side showing the polyacrylic coating (Figure 26B) presents some differences from one sample to others. When the polyacrylic coating does not contain Ag-PEI NPs the samples are

whitish. However, since Ag-PEI NPs dispersion presented a brownish colour, the more silver the sample contains, the more brown-coloured the tent interior side looks.

The density of each sample, which was used in a later stage to calculate the release rate per area, was measured by weighing three replicates of the Ag containing samples in a 0.1 mg precision balance (Ohaus Adventurer SL, AS214). In order to precisely measure the area of each textile, a photo of the weighted textiles was taken and the images were processed with FIJI software (Schindelin et al., 2012) as can be seen in Figure 27.

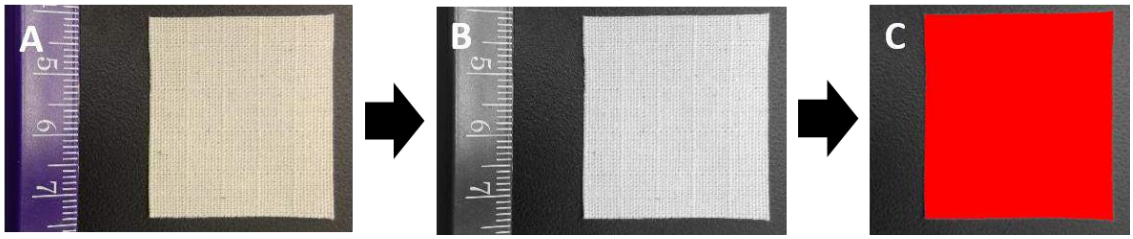

Figure 27 – A) Original picture; B) Image conversion to greyscale; C) Textile recognition and area measurement by the software.

The Ag-PEI dispersion was diluted to 100 ppm with ultrapure water and observed through high resolution transmission electron microscope (HR-TEM; JEM 2010, JEOL Ltd.) to determine the size and morphology of the nanomaterials (Figure 29). The TEM images were analysed using FIJI software (Schindelin et al., 2012) to obtain its size distribution. The four textile samples plus the original Ag-PEI NPs dispersion were digested in an analytical microwave (CEM, Mars) and analyzed through Inductively Coupled Plasma Mass Spectrometry (Agilent, 7500) to determine the Ag content. In addition, the textile's surface was observed with field emission scanning electron microscopy (JEOL 6500F FE-SEM).

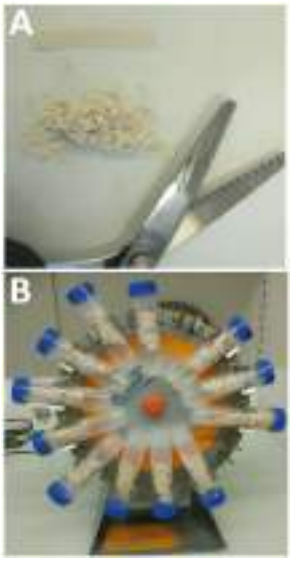

Figure 28 – A) Textile fragments. B) Fragments in contact with water being shacked.

Once the raw materials were characterized, they were submitted to the leaching test following the protocol specifications (European Standards, 2003). The textiles were cut into fragments ≤ 10 mm as seen in Figure 28A. They were cut with Pinking shears (zig-zag scissors) because unfinished textile edges can easily fray and the threads pull out easily, the saw-tooth pattern does not prevent the fraying but limits the length of the frayed thread minimizing the damage and helping to obtain fewer threads in the leaching waters, easing their further analysis and treatments. Once the textiles were cut, 3 g were introduced in 50 ml

polypropylene vial with 30 mL of ultrapure water (maintaining the 10 L/kg liquid to solid ratio proposed by the protocol). Then, the samples were shaken with an end-over-end shaker (OVAN, NR50 E) at 10 ± 3 rpm for 24h at ambient temperature (25ºC). Three replicates were tested for each textile ending up with a total of 12 samples. After the landfill simulation, the respective leaching waters were collected. In each vial, 30 mL were introduced, but after the experiment, due to the textile water absorption, only around 25 mL could be collected. 5 mL were directly collected for Ag determination through ICPMS; 5 mL were filtered through a filter paper of approximately 20 - 25 µm pore size (Filter-Lab quantitative filter paper, ANOIA); 5 mL were centrifugated with 3kDa centricons (Amicon Ultra-15 Centrifugal Filter Units, Millipore) and the remainder was collected, freeze-dried and observed through HR-TEM (JEOL JEM-2100).

Results

Starting materials

Transmission Electron Microscopy

The TEM images of the Ag-PEI dispersion show two differentiated size population of silver particles, which present a spherical shape. One of them is in the micro range and the other in the nano range. Figure 29A shows the bigger particles, Figure 29D shows the smaller ones and in Figure 29B, C the two different sizes populations can be appreciated. Moreover, especially in Figure 29A, the polyethylenimine coating can be observed as a darker substance surrounding the particles.

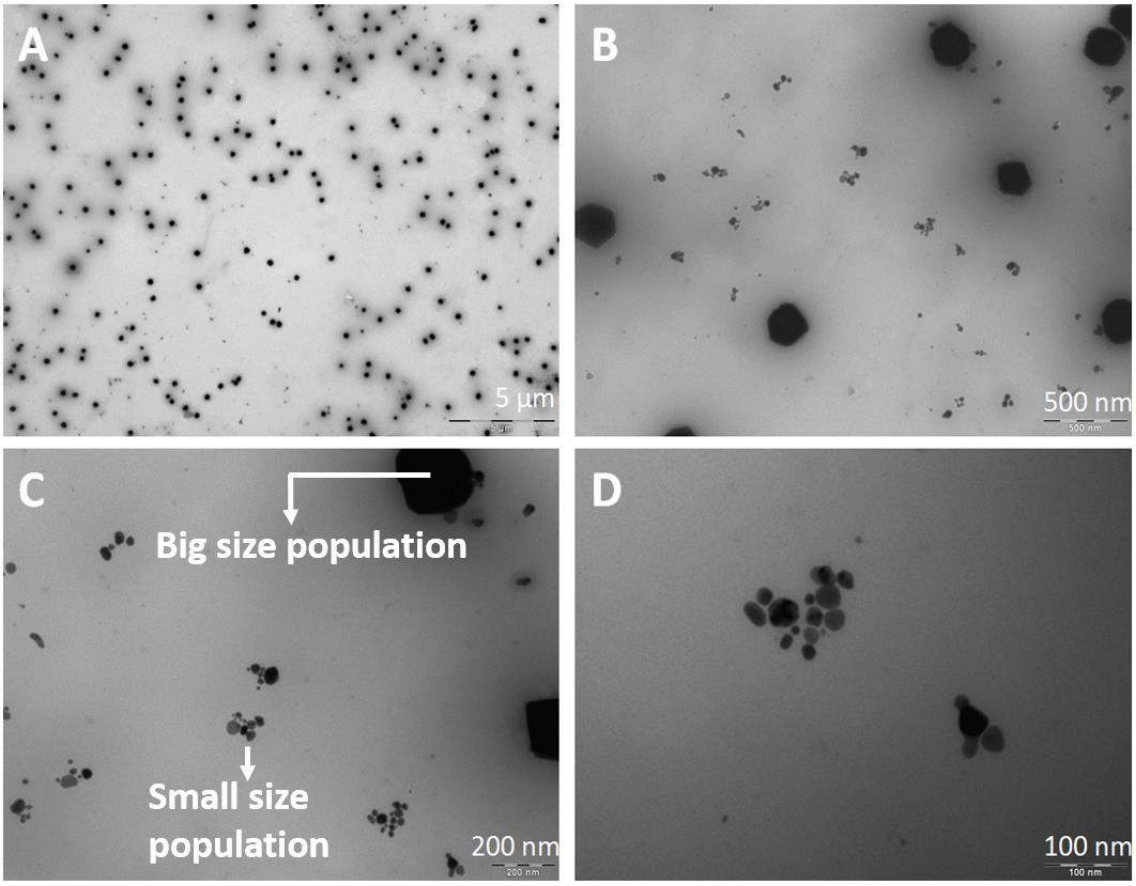

Figure 29 – HR-TEM images of Ag-PEI dispersion where the two size populations can be observed.

The size distributions of the two populations are presented in two different graphs for an easier interpretation. As can be seen in Figure 30 there is around one order of magnitude of difference between the two populations. The bigger particles presented a more uniform distribution (lower RSD%) while the smaller ones were more disperse. A total of 270 particles were counted, 50 for the smaller size population and 220 for the bigger size population.

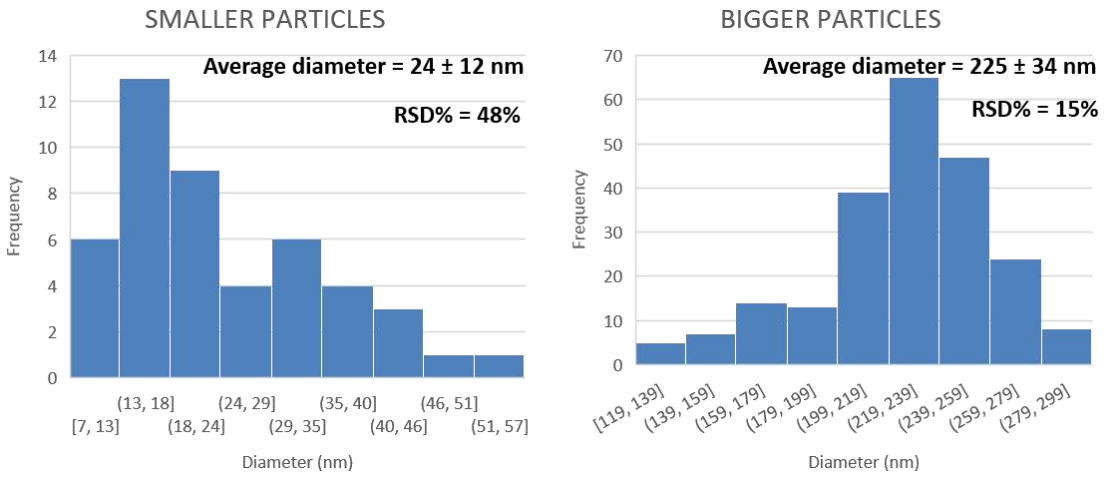

Figure 30 – Ag-PEI dispersion size distribution.

Scanning Electron Microscopy

From the SEM images of the camping tent samples before performing the leaching experiment a clear difference between the interior and exterior side of the textile sample was observed (Figure 31). While in the exterior side a regular textile pattern is seen, in the interior side containing the polyacrylate coating, a layer recovering the whole surface is clearly seen.

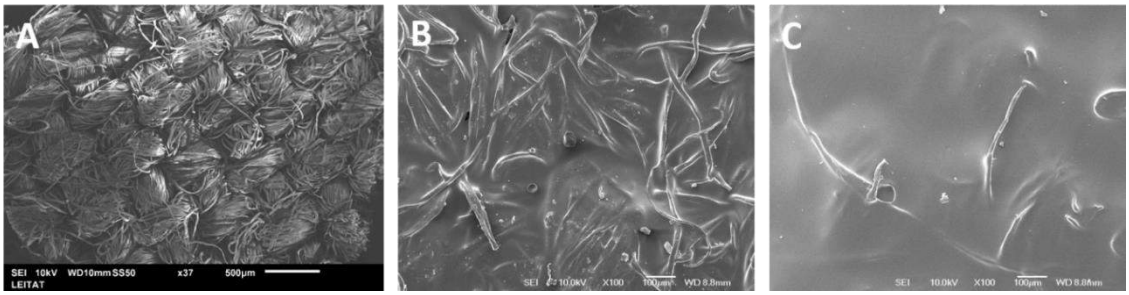

Figure 31 – SEM images of the camping tent samples before the leaching experiment. A) Tent exterior side, magnification: x37; B) tent interior side with one coating, magnification: x100; C) tent interior side with two coatings, magnification: x100.

A significant difference was found between samples with one and two coatings. While with one layer the textile fibres can be seen underneath the coating, with two layers, although some fibres can also be seen, most of the area is only covered by the coating providing a much more homogenous appearance.

Inductively Coupled Plasma Mass Spectrometry

The ICPMS results are shown in Table 6. As expected, in TENT2_NoAg and TENT1_NoAg silver was not detected, while in TENT2_Ag and TENT1_Ag it was. Moreover, the uncertainties (coming from three replicates) are very low, which suggests that the sample is quite homogeneous. As expected, the silver concentration in TENT2_Ag was higher than in TENT1_Ag. Since TENT2_Ag present one layer more than TENT1_Ag, the density measured also was higher, 24.9 ± 1.3 mg/cm^2 for TENT1_Ag and 27.0 ± 0.6 3 mg/cm^2 for TENT2_Ag.

Table 6 - Ag concentration in the original textiles and Ag-PEI dispersion determined by ICPMS.

SAMPLE	Ag CONCENTRATION (ppm)	RSD (%)
TENT2_NoAg	< 0.7 (not detected)	-
TENT1_NoAg	< 0.7 (not detected)	-
TENT2_Ag	111.9 ± 2.0	1.79
TENT1_Ag	68.9 ± 0.2	0.29
Ag-PEI dispersion	5000 (info provided by INOTEX)	-

Aged materials and leaching waters

Electron Microscopy

In Figure 32 the samples' surface after the leaching experiment are shown. No significant differences before and after the leaching experiment were found. The exterior side (made of cotton) looked a bit worn away. More yarns were protruding from the surface as a consequence of the mechanical wearing, but since this side does not contain any nanomaterials it doesn't have any effect on the release. Regarding the interior side, for both samples containing one and two coatings, the visual aspect was the same as for unwashed samples. In the images (both in Figure 32B and C) small holes or area without coating were observed. However, these areas were also detected before the experiments and are probably due to the application method of the coating, they were not caused by the leaching experiment. Most probably, the leaching produced some damage in the outer layers of the coating, but the damage was not enough to be observed through electron microscopy.

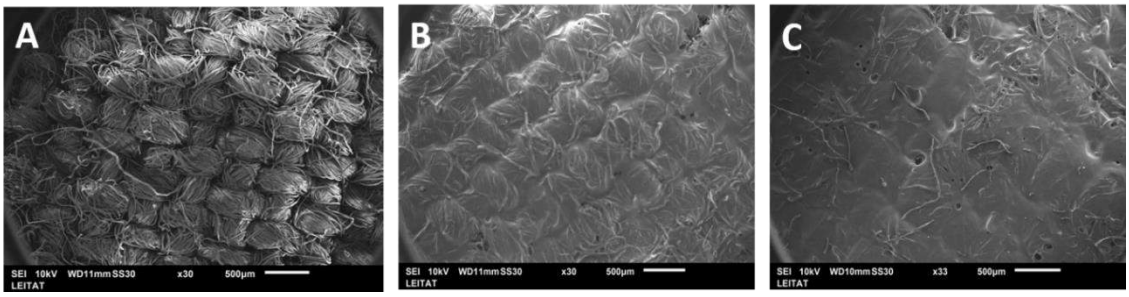

Figure 32 – SEM images of the camping tent samples after the leaching experiment. A) Tent exterior side, magnification: x30; B) tent interior side with one coating, magnification: x30; C) tent interior side with two coatings, magnification: x33.

As previously mentioned in the methodology section, part of the leaching waters were freeze-dried in order to obtain a solid residue to observe through SEM. The images corresponding to the freeze-dried residues are shown in Figure 33. In the residues, small fragments of the samples were found, which looked similar to the previously analysed fragments. Again, the same pattern was observed, for samples containing only 1 coating the yarns were more easily visualized than for those samples containing 2 coatings. Multiple EDX measurements were performed in different areas of all samples but Ag was not detected in any of them.

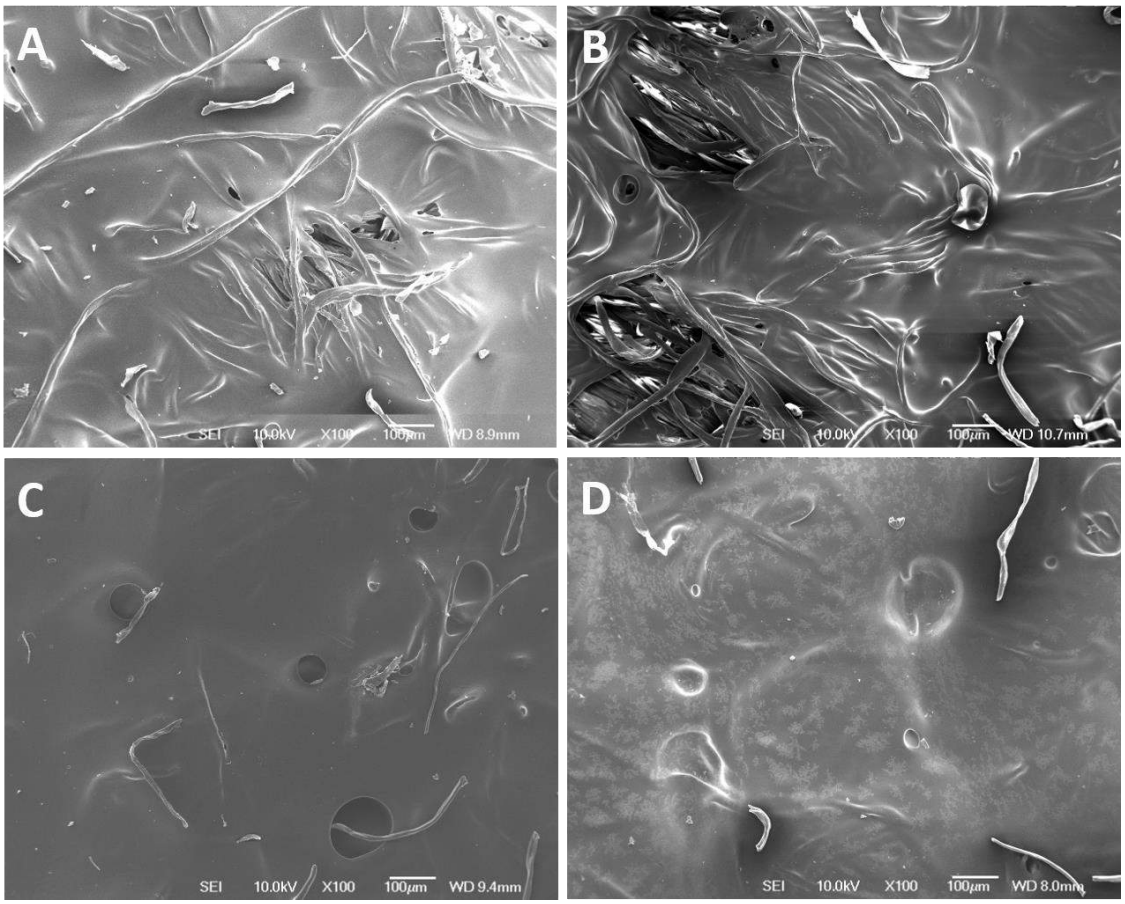

Figure 33 – SEM images of the residues from freeze-dried leaching waters of samples A) TENT1_NoAg; B) TENT1_Ag; C)TENT2_NoAg; D)TENT2_Ag.

Inductively Coupled Plasma Mass Spectrometry

Ag concentration in washing waters determined by ICPMS is shown in Figure 34. In the chart the total silver concentration is divided in three categories: (i) unfiltered water, (ii) filtered water with paper filter of 20 µm pore size and (iii) water filtered with 3 kDa centricons corresponding to the ionic content. For each of them, the corresponding standard deviations coming from three replicates were also included. Released waters of non Ag containing control samples (TENT1_NoAg and TENT2_NoAg) in all the cases presented Ag concentration values below the limit of detection (0.2 ppb). Thus, for simplicity, they were not included in the chart.

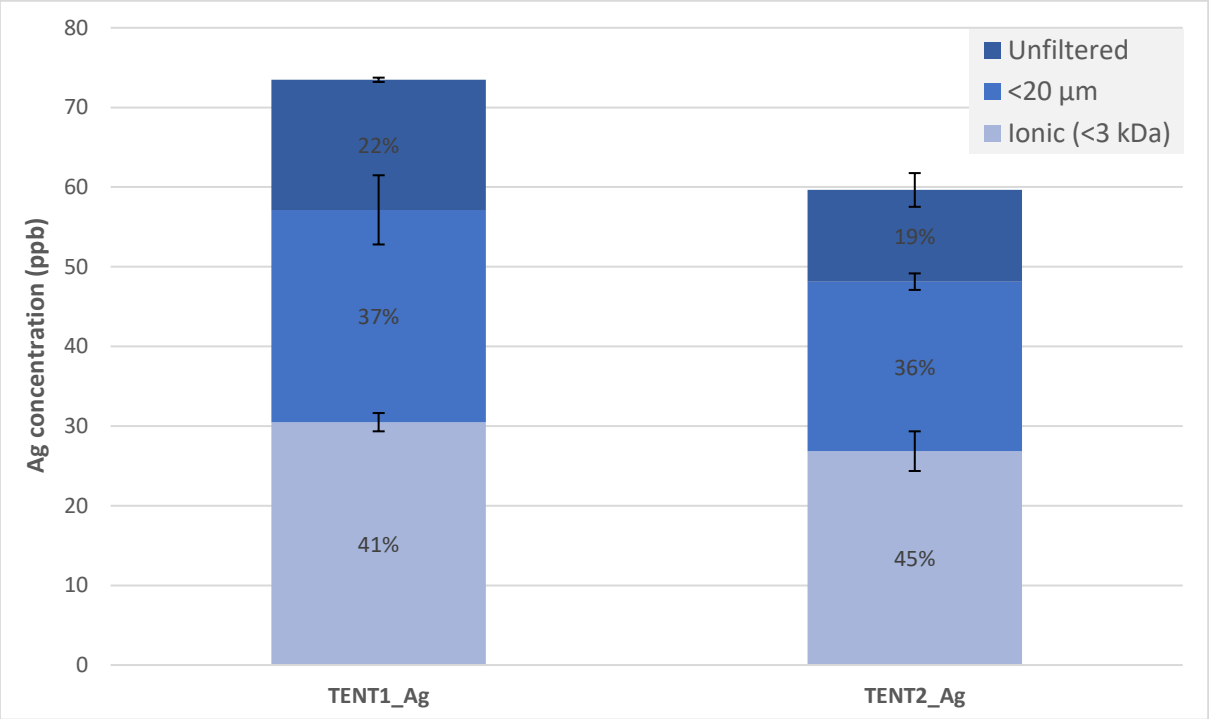

Figure 34 – Ag concentration in camping tents leaching waters.

For both samples (TENT1_Ag and TENT2_Ag) the results obtained were quite similar. Around 20% of the released silver was present in fragments bigger than 20µm, probably Ag that was embedded in released coating fragments or attached to released yarns bigger than 20 µm. 36% – 37% of the released silver was smaller than 20µm but it was not ionic (>3 kDa). In this category are included small coating fragments containing Ag, small cotton yarns with Ag attached and maybe freely released NPs, although no evidence for this was found in electron microscopy. The ionic content was higher than 40%, being the main Ag release form for the camping tents in the leaching study.

The total concentration of released Ag for both samples was relatively low, 73.5 ± 1.1 ppb for TENT1_Ag and 59.6 ± 2.5 ppb for TENT2_Ag. A fact that can seem surprising is that TENT1_Ag (which contains less silver) presents a higher Ag concentration than TENT2_Ag. However, it must be considered that for both samples the weight tested was the same. Thus, since TENT2_Ag density is higher, in order to have the same weight the volume tested was lower, so the coating area from where the release was coming from was smaller too. To delete the area factor release rates were normalized with the area and are presented in Table 7.

Table 7 – Camping tent case study release rates

SAMPLE	RELEASE RATE (Ag µg / textile m^2)
TENT1_Ag	183 ± 3

TENT2_Ag	161 ± 7

With the area correction, TENT1_Ag still presents a higher release. In any case, the release rate difference between both samples is very small suggesting that, as expected, their release behaviour is very similar. Indeed, since only the superficial layers of the coating containing the Ag-PEI NPs are being released, there should not be difference on the release rate per area.

Considering that the starting concentrations were 68.9 ± 0.2 ppm for TENT1_Ag and 111.9 ± 2.0 ppm for TENT2_Ag (Table 6) and knowing the total amount of Ag released, the released percentage can be determined. The values obtained are 1.07 ± 0.02% and 0.53 ± 0.02% released of total silver for TENT1_Ag and TENT2_Ag respectively. Since TENT1_Ag sample presents almost the same release than TENT2_Ag sample although it had almost the half of initial silver content, it makes sense that the total release percentage is the half than for TENT2_Ag.

Conclusion

Leaching experiments proved that silver is released from camping tents, although the amounts were relatively low. Electron microscopy helped in understanding the impact of the experimental conditions on the samples. This was so small that changes before and after the leaching experiment were not observed. As proved by the ICPMS analysis, the Ag amount (%) released was 1.07 ± 0.02% for TENT1_Ag and 0.53 ± 0.02% for TENT2_Ag. With such small releases, as expected, no significant changes in the coating surface were observed and no Ag NPs were detected. Moreover, 40% of the silver released was in ionic form, which decreased, even more, the chances of finding Ag NPs in leaching waters since dissolution of any released silver NPs could have occurred. In addition, the release of Ag embedded in the coating and/or attached to fibres is also a possibility, which would explain why 36% – 37% of the released silver was smaller than 20µm but it was not ionic, and that 20% of the released silver was present in fragments bigger than 20µm.

3.2.7. Conductive inks for printed circuits

Introduction

During production and manufacturing stages of conductive inks containing nano-Ag release is not expected, and during use, the circuits are generally protected by the hardware (external casing) to ensure their durability, which also limits the release. In addition, it is worth recalling that after the printing process the ink is submitted to a sintering process to fuse the silver nanoparticles together. Therefore, from that stage, NPs are not present, only bulk silver.

However, potential release could occur once the electronic devices are disposed in landfills, which could be in bulk, ionic or even nanoparticulate form. Given that electronic printing is one of the main applications of nano-Ag (Kuenen et al., 2020)(European Standards, 2003), its potential release needs to be assessed.

The nano-Ag conductive ink studied was provided by AMEPOX Enterprise Ltd., a Small-to-Medium Enterprise (SME) that synthesises conductive formulations. Although AMEPOX only synthesizes the ink they were able to provide printed circuits such as the ones shown in Figure 35, which were used to test the silver release.

Materials and methods

The ink printed in the circuits provided by AMEPOX is the Nano Ink JP, which contains 60 nm Ag particles. The substrate used was polyethylene terephthalate (PET), a material on which conductive inks are commonly printed. As stated in the introduction, after the printing process the nanoparticles are sintered. This is a process by which the individual nanoparticles fuse together removing nanoscale characteristics. However, it was decided to perform a leaching experiment simulating an end-of-life process in landfill to determine the release rate and form of Ag released from the printed circuit. The experiments were performed following the standardized protocol EN – 12457-4: Test for leaching of granular waste materials and sludges (European Standards, 2003), the same protocol as described in INOTEX's camping tents case study.

From the two circuits provided, the one on the right side (Figure 35) was selected because it presented a higher number of repeated patterns, which were used to perform experimental replicates. The circuit was cut through the red dashed lines shown in Figure 35, providing 5 pieces with the same structure. Three of them were used to perform the experiments and one of them was digested with an acid solution in an analytical microwave digestion system (MARS, CEM, 1600W) and later analysed by ICPMS (Agilent 7500, Agilent Technologies) to determine the initial Ag content. The piece left (the one from the top) was discarded because part of the printed pattern was a bit damaged. The printed area in each of the three replicates was the same. Weight differences were expected to be only due to differences in the amount of substrate present as a result of manually cutting the starting circuit into pieces.

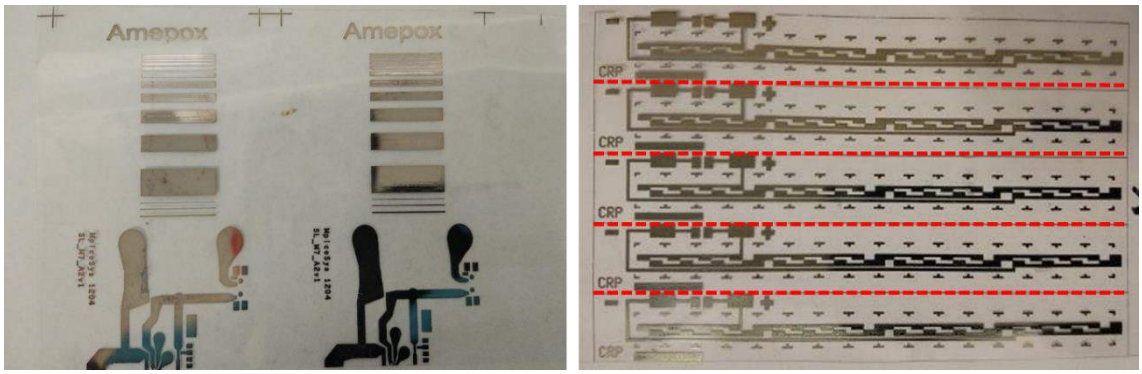

Figure 35 – Electric circuits printed with Ag Ink provided by AMEPOX.

The weight of the cut circuits was around 0.4 g each, as a consequence, in order to maintain the 10L/g ratio proposed by the standardized protocol, the leaching experiment was performed with 4 ml of water. Each of the cut pieces were cut in fragments smaller than 10 mm diameter (Figure 36A). Then, they were put into 15 ml falcon tubes where 4 ml of ultrapure water was added. Then, the samples were shaken with an end-over-end shaker (OVAN, NR50 E) at 10 ± 3 rpm for 24h at ambient temperature (25ºC). From each replicate 1 mL was directly collected for Ag determination through ICPMS; 1.5 ml were collected, diluted up to 15 ml (with 13.5 ml of ultrapure water) and filtered through a filter paper of approximately 20 µm pore size (Filter-Lab quantitative filter paper, ANOIA); from the filtered water 5 ml were digested and analyzed through ICPMS and the 10ml left were filtered through a Nylon 0.45µm syringe filter (Phenex). 5 ml were digested and analyzed through ICPMS and the rest (around 4ml) was centrifugated with 3kDa centricons (Amicon Ultra-4 Centrifugal Filter Units, Millipore). The filtrate from the centricons was analyzed through ICPMS to determine the ionic content.

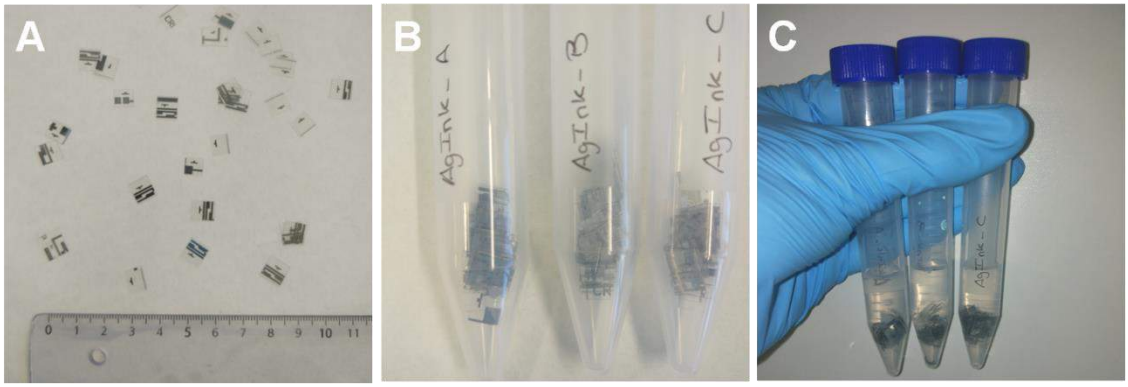

Figure 36 – Printed circuit: A) Cut in pieces; B) replicates inside the vial; C) replicates inside the vial with 4 ml of water.

Results

Leaching waters

Inductively Coupled Plasma Mass Spectrometry

From the ICPMS results of the Ag concentration total amount, the one collected directly from the vial (without passing through any filter) and the concentration of the digested circuit, the release rate was calculated. The Ag amount in each circuit was estimated in 2.05 Ag mg. In this case, since there was only one printed circuit to analyze, there were no replicates and thus no standard deviation. The measured Ag concentration in the leaching waters was 57.2 ± 11.9 ppm (Ag mg/leaching water L). Since all the experiments were conducted with 4ml of ultrapure water, the amount of Ag leached from the printed circuits is 0.229 ± 0.047 mg which gives a calculated release rate of Ag from the printed circuit due to leaching of **11.1 ± 2.3%.**

As is seen in Figure 37A, the release of the ink from the substrate occurs very fast, detached fragments of ink were already observed at the start of the experiment. After 24h, at the end of the experiment (Figure 37B) some Ag small fragments were also observed, but not as many or as big as in the beginning. In the 24h that the experiment lasts most of the Ag fragments released were partially dissolved reducing their size.

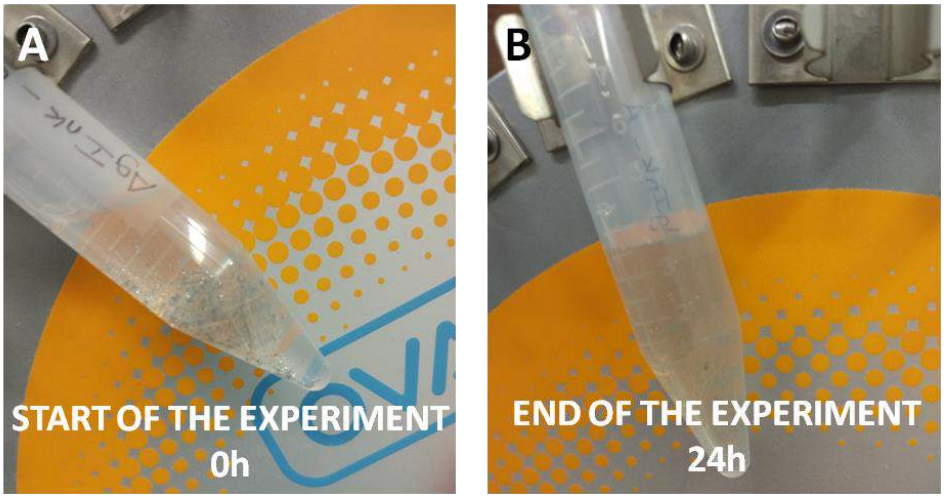

Figure 37 – Leaching waters at the start and at the end of the experiment.

From the ICPMS results from the leaching waters filtered through different pore sizes, a quantitative value of the amount of Ag in different range sizes was determined. The main result was that 81.1 ± 3.9% of the silver was bigger than 20µm. i.e. around 81% of silver was lost when the leaching waters were filtered with paper filter (pore size

Table 8 – AMEPOX ink release forms

RELEASE FORM
Ionic (Ag^+): 0.3 ± 0.1%
<0.45 µm: 6.4 ± 0.7%
<20 µm: 12.1 ± 3.0%
>20 µm: 81.1 ± 3.9%

~20µm), as can be seen in Figure 38. For the rest of the sized ranges the percentage is represented in Table 8.

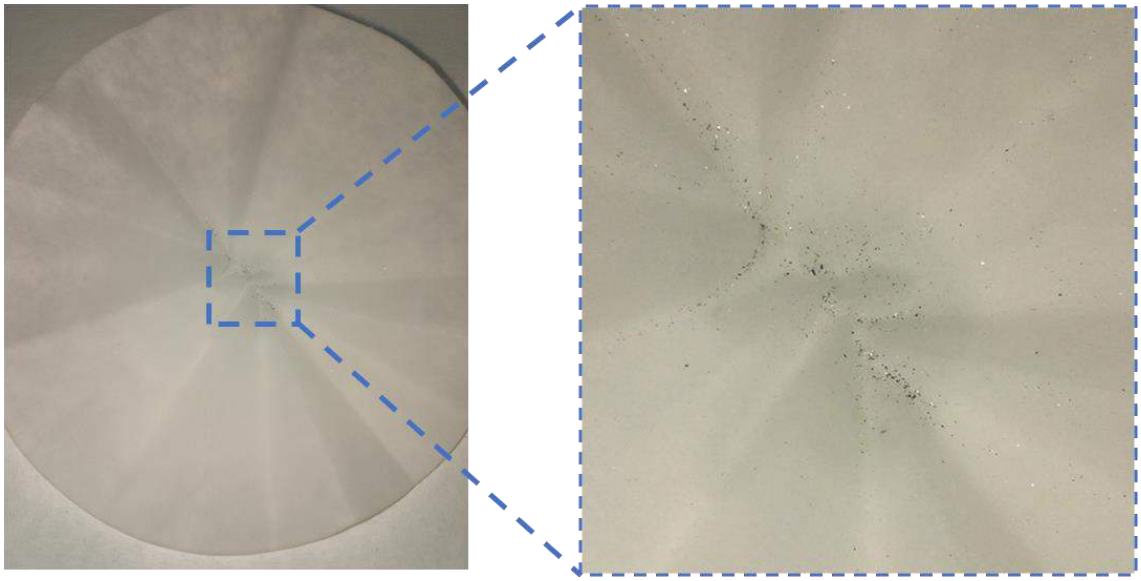

Figure 38 – Paper filter presenting Ag fragments after filtering the leaching waters in contact with the printed circuit.

Conclusion

The main outcome of these experiments is that most of Ag is released in fragments bigger than 20 µm. This is understandable since the ink is sintered for the nanoparticles to form a continuous film, necessary to improve the conductivity. When Ag is released due to leaching most of it remains as intact fragments. During the experiment, the size of some of the fragments can be reduced, but it still presents a large (>20µm) size. Indeed, in Figure 38, in the paper filter magnification it is clearly appreciated how a high amount of Ag was remaining in the filter during the filtration process.

Some of the Ag released could be in a nanometre size range or ionic form, but the amount would be very small. For example, the silver passing through 0.45 µm filter but not ionic, which corresponds to the 6.4% of the Ag released, from the total Ag in the circuit, the amount released would be 6.4% of the 11.1%, which is 0.7%.

Nanosafety research in Europe – Towards a focus on nano-enabled products

V. Pomar-Portillo,[a] B. Park,[b] A. Crossley,[a] and S. Vázquez-Campos[a]*

[a] *LEITAT Technological Center, C/de la Innovació 2, 08225 Terrassa (Barcelona), Spain*

[b] *GBP Consulting Ltd, Purton, Swindon SN5 4EJ, United Kingdom*

[c] *Department of Materials, Oxford University Begbroke Science Park, Begbroke Hill, Yarnton, Oxford OX5 1PF, United Kingdom*

*Corresponding author e-mail address: svazquez@leitat.org

Contribution to the peer-reviewed publication within the context of this thesis: In this paper substantial contributions to the conception of the work were provided and, as first author of the publication, the lead was taken in the acquisition, analysis, and interpretation of the data, as well as the writing of the manuscript.

The following manuscript is a version of record reproduced from NanoImpact 22 (2021) 100323 with permission from Elsevier.

The online version can be accessed from:

https://doi.org/10.1016/j.impact.2021.100323

NanoImpact 22 (2021) 100323

Contents lists available at ScienceDirect

NanoImpact

journal homepage: www.elsevier.com/locate/nanoimpact

Research Paper

Nanosafety research in Europe – Towards a focus on nano-enabled products

Vicenç Pomar-Portillo [a], Barry Park [b], Alison Crossley [c], Socorro Vázquez-Campos [a,*]

[a] LEITAT Technological Center, Carrer de la Innovació 2, 08225 Terrassa, Barcelona, Spain
[b] GBP Consulting Ltd, Purton, Swindon SN5 4EJ, United Kingdom
[c] Department of Materials, Oxford University Begbroke Science Park, Begbroke Hill, Yarnton, Oxford OX5 1PF, United Kingdom

ARTICLE INFO

Editor: Bernd Nowack

Keywords:
Nanosafety
Framework programmes
Nano-enabled products
Inventory
Market relevance

ABSTRACT

In the nanosafety projects funded by the European Commission a large amount of data has been generated on hazard and exposure for a variety of engineered nanomaterials (ENMs) and nano-enabled products (NEPs). However, not all the data generated has been published, nor has all the data been stored in an organised manner (e. g. database) which makes it very difficult for researchers, industry and other stakeholders to use it. This paper provides an inventory of NEPs studied in each of these projects, including relevant information on the NEPs, the life-cycle stages evaluated for each of them and an overview of the projects, which can be used for identifying areas in which there might be data gaps. The purpose of analyzing the nanosafety research done on NEPs was to provide an overview of the products studied compare to what can realistically be found in the market (i.e. the exposure relevant materials that workers, consumers and the environment may be exposed to). The analysis done in all the projects included in the inventory allowed the identification of the need to increase the number of studies with well-established commercialized NEPs, such as ENMs used in tyres or sunscreens. In addition, it was found that, in general, there was a correlation of the different ENMs studied with their respective production relevance (i.e. production volumes), except for silver, which was vastly over-represented, and on the other hand carbon black, which was under-represented. Addittionally, there is a need to improve accessibility to relevant and high quality data produced in all these projects to provide transparency and support to different stakeholder needs.

1. Introduction

Due to the ongoing recognition of nanotechnology as a key enabling technology and increasing introduction of nanotechnology-based products in the market (Allied Market Research, 2016; Future Markets Inc., 2016), the European Commission (EC) and the National Nanotechnology Initiative in the United States have funded many nanosafety research projects to identify and understand any potential risks that engineered nanomaterials (ENMs) may pose to humans and the environment. Nano-enabled products (NEPs) are defined in the ISO/TS 80004–1:2015 as those products exhibiting a specific function or performance only possible with nanotechnology; while nano-enhanced products are those improving or enhancing their function or performance by applying nanotechnology or by inclusion of nanosized materials (International Standards Organization, 2015). However, the projects generally do not discriminate between both terms. Therefore, in this paper, all references to products incorporating engineered nanomaterials will be referred to as nano-enabled products (NEPs).

The need for assessing the safety of nanotechnology-based products must be emphasized since ENMs now encompass an enormous array of sizes, shapes and chemical compositions. They are produced using a wide variety of manufacturing processes and are incorporated in a large number of matrices for many different applications (Giese et al., 2018). In addition, ENMs can be modified during the multiple activities that they might experience throughout their life cycle and, if they are released to the environment, further transformations may occur due to interactions with different substances and the biological media. As a result of all these possible transformations, which in some cases are not evident or easy to predict, a very wide diversity of materials may be generated inadvertently, with some of them potentially posing risks for humans and/or the environment (Schug et al., 2013). Therefore, the assessment of the potential human and environmental risks of nano-enabled products implies studies not only focused on pristine (as-synthesized) ENM, but also on the products during different life cycle stages (Mitrano et al., 2016).

In the last 20 years there have been many nanosafety studies, largely

* Corresponding author.
E-mail address: svazquez@leitat.org (S. Vázquez-Campos).

https://doi.org/10.1016/j.impact.2021.100323
Received 5 February 2021; Received in revised form 9 April 2021; Accepted 6 May 2021
Available online 15 May 2021

focussed on ENMs, independent of their potential applications. However, the context for such studies has been initiatives on both sides of the Atlantic with governments in Europe and in the US developing programmes that have driven the nano-based science and technology through these past 20 years. In the US, President Clinton unveiled the National Nanotechnology Initiative (NNI) in a major science policy address at Caltech on January 21, 2000. The initiative significantly increased investment with a view to strengthening scientific disciplines and creating critical interdisciplinary opportunities. The focus was on long-term fundamental nanoscience and engineering research and on a series of Grand Challenges representing significant technical and commercial breakthroughs (National Science and Technology Council, 2000). Around the same time in Europe, the European Commission noted in a document entitled *Towards a European Strategy for Nanotechnology* that it was essential that industry can bring nanotechnology based products and services to the market so as to generate wealth, employment and sustainable growth (European Commission, 2004a).

In 2004, the seminal report, Nanoscience and nanotechnologies: opportunities and uncertainties, from the Royal Society and the Royal Academy of Engineering in the UK talked about the need to balance the commercialisation of engineered nanomaterials with an understanding of any potential negative health and environmental impacts (The Royal Society and The Royal Academy of Engineering, 2004). The specific ENMs used in NEPs can determine the implications of their use and this requires access to commercial information that is not generally available. Some countries, principally in Europe, have started to realise the importance of reporting the production volumes and are working on establishing registration processes for nanomaterials (Pavlicek et al., 2020). France and Denmark were the first ones leading this initiative (Agence nationale de sécurité sanitaire (ANSES), 2020; Gottschalk et al., 2015) with Belgium (Innovationsgesellschaft GmbH, 2021) and Sweden (Swedish Chemicals Agency, 2021) following. Regulatory bodies like the European Chemical Agency (ECHA) together with the European Commission (EC) also started making important efforts in this direction. In December 2016 an agreement was signed to establish the European Union Observatory for Nanomaterials (EU-ON), which is intended to provide direct access to the most recent developments and scientific knowledge about nanomaterials and their potential impacts on human and environmental health (Bergeson and Hutton, 2016). The EC had concluded that the observatory was the best tool to increase transparency on nanomaterials on the EU market (European Chemicals Agency (ECHA), 2020).

Besides ENMs' production volumes, many attempts have also been made to identify commercialized NEPs and their associated ENMs. Different countries have approached this in different ways. The US Project on Emerging Nanotechnologies, launched in 2005 as a partnership between the Woodrow Wilson International Center for Scholars and the Pew Charitable Trusts, represented a major effort to provide such a source of information (Woodrow Wilson International Center for Scholars, 2020). It provided an inventory that collected NEPs examples through to 2010, but relied on submissions of such examples so could not be considered as comprehensive, but rather representative of what was available on the market in the late 2000s. Since the project was based in Washington DC and was US-centric, European based NEPs may have been missed. A revised version of the inventory was updated in 2013, when it contained 1814 products (Vance et al., 2015). At the moment of writing this document, after approximately 7 years, the inventory contains 1833 products (only 19 more), which means that, unfortunately, in recent years it has not been further updated/ maintained. Nowadays, different institutions are also trying to compile information on nano-enabled products in online databases categorizing the products by engineered nanomaterial, nano-enabled product application, or even by potential impact, i.e. environmental or human (DTU Environment, 2020; Nanotechnology Products Database, 2020, Nanowerk Catalog - Nanotechnology Materials and Equipment, 2020). However, the inventories provided by the online databases and market reports not only use different bases as sources of data (e.g. voluntary reporting, marketing claims, legally mandatory reporting), but also use different definitions of "nano" leading to many of the discrepancies and related confusion about which ENMs have been used in which NEPs and what testing has been conducted on each ENM or NEP.

The objective of this paper is therefore to provide an inventory of the nano-enabled products studied in the EC-funded nanosafety projects, including relevant information on the types of studies performed and ENMs studied. The information generated during nanosafety projects funded by the European Commission via their Sixth and Seventh Framework Programmes (FP6 and FP7 respectively) and Horizon 2020 (H2020) has been considered. Within the projects, a large amount of data has been generated on hazard and exposure for a variety of ENMs and NEPs. However, not all the data generated has been published, nor has all the data been stored in an organised manner (e. g. database) which makes it very difficult for researchers, industry and other stakeholders to conduct effective impact and risk assessments.

It should be noted that to the authors' knowledge, this paper presents the first comprehensive review of NEPs studied in nanosafety projects funded by the European Commission. Collating information on the type of data generated in all these projects on NEPs and ENMs provides an overview on how much could be achieved and offers an opportunity to identify where the gaps are with respect to the following key aims:

(i) commercialisation balance against risk,
(ii) transparency on use of NEPs/ENMs including production volumes and
(iii) clarity on the safe use and identified risks.

2. Methodology

2.1. Data collection

The inventory generation required collecting data from multiple sources. For the purpose of the study, the first step was identifying the nanosafety projects funded by the European Commission. The information was initially obtained through the NanoSafety Cluster (NSC) compendiums (Lynch, 2017; Lynch, 2016; Lynch, 2015; Lynch, 2014; Riediker, 2013), annual reports that documented the status of EC-funded projects on nanomaterial toxicity and exposure monitoring, integrated risk management, research infrastructure and coordination and support activities as well as regulatory-focussed research on nanosafety (EU NanoSafety Cluster, 2020). Projects belonging to the Sixth and Seventh Framework Programme (FP6 and FP7) and Horizon 2020 (H2020) covered from 2002 to 2006, from 2007 to 2013 and from 2014 to 2020, respectively. Projects starting in 2018 were the latest projects considered. Thus, projects initiated over a total time period of 16 years (from 2002 to 2018) were covered. Comparisons have been made of the scope and the focus of each of the Framework programmes and these are noted in the discussion section together with comments on the outcomes from the projects funded as part of the three framework programmes. It should also be noted that over this time period several EU Members States have also funded their own projects, but those initiatives are not considered in this analysis.

Since the last published compendium is from 2017, to account for more recent projects, the community research and development information service (CORDIS) from the EC website was consulted (European Commission, 2020). All the projects under the H2020-EU.2.1.2.2. programme (i.e. *Ensuring the safe and sustainable development and application of nanotechnologies*) and H2020-EU.2.1.2.4. programme (i.e. *Efficient and sustainable synthesis and manufacturing of nanomaterials, components and systems*) were considered. In addition, projects not mentioned in the compendiums nor in the two H2020 calls, but potentially containing studies on NEPs, were also examined after identification through personal communication with members of the NanoSafety Cluster or direct involvement of the authors in the projects. A complete list of the projects

considered under the different framework programmes is included in the Supporting Information (Table S1), indicating from which source (i.e. compendiums, CORDIS or *others*) the information from the different projects was extracted together with their main safety focus (i.e. exposure, hazard or *others*).

Once the nanosafety projects funded by the EC were identified, information available for each of them was evaluated to determine if nano-enabled products were studied and to discard those projects following a theoretical approach. Projects including experimental work with NEPs were further reviewed to extract all the information on: the ENMs incorporated, the NEP provider, and its commercialization state. In the evaluation of the experimental data generated in these projects, further information could be extracted: the life cycle stages considered (i.e. synthesis, manufacturing, use, recycling and end-of-life) and the type of assessments considered by the projects (i.e. environmental and/or human hazard and/or exposure assessment). Additionally, more general information about the projects was also included in the inventory: the elapsed time for each project and the funding provided.

This comprehensive evaluation was conducted based on the information on the projects available in the NSC compendiums, CORDIS, the projects' websites and if available, peer-reviewed literature (identified through CORDIS) containing data on the NEPs of interest. In the cases in which information was incomplete or unclear, the project coordinator and/or the specific partner in charge of the experiments with NEPs was contacted to complete and to verify the information. The authors' collaboration within the nanosafety cluster and contacts with other members facilitated the information exchange. Furthermore, the fact that the authors participated in and coordinated some of the projects included in the inventory facilitated the information collection. The persons contacted to provide and verify the information are mentioned in the Acknowledgements section together with an indication of the relevant projects for which they have or had responsibilties.

2.2. Data treatment

Once all the information about the selected projects was compiled in the inventory, some relevant conclusions could be extracted. Each NEP was allocated to one of the 9 product categories defined as: cement, coating, electronics, metal, paints, paper, polymeric composites, textiles and others. Paints, due to its high presence, was considered as a category by itself and not included within coatings. Under the category "*others*" have been included those product categories in which less than 5 NEPs were studied. It included categories such as lubricants, pesticides, sunscreens, membranes and food additives. A table indicating the category to which each nano-enabled product was assigned is included in the supporting information (Table S2).

In some cases, the specific purpose of the ENM incorporation into a product was known (e.g. antibacterial coating, photocatalytic paint), while for others, such information was not available. An analysis of the most common purposes was made and eight different categories were considered: antibacterial, antifouling, electrical, fire retardant, mechanical, optical, photocatalytic and others. In cases in which the purpose to incorporate the ENM into a product could cover double function (e.g. carbon nanotubes providing mechanical reinforcement and enhanced conductivity) both categories were considered. Under the category "*others*", have been included those purpose of incorporation categories that contained less than 4 NEPs. It included categories such as sun blockers or fuel and food additives. A table indicating the purpose category to which each nano-enabled product was assigned to is included in the supporting information (Table S3).

Special attention was paid to determine which ENMs were incorporated in each of the NEPs. The share of each ENM (i.e. in how many NEPs it was incorporated divided by the total amount of NEPs included in the inventory) was calculated. This information provides an indication of the types of ENMs studied in the projects funded by the European Commission, which can then be compared with the most commercialized products and determine if there is an alignment. Thirteen categories of ENMs were considered in the projects included in the inventory: aluminium oxide, carbon-based ENMs, cerium dioxide, copper-based ENMs, iron oxides, nanocellulose, nanoclays, others, quantum dots, silicon compounds, silver, titanium dioxide and zinc oxide. Under the category "*others*", ENMs that were incorporated in less than two NEPs, like zirconium dioxide (ZrO_2), gold (Au) or calcium carbonate ($CaCO_3$) were considered. Some ENMs were included in multiple categories (e.g. Al_2O_3-SiO_2 was included in aluminium oxide and silicon compounds categories.) In addition, for all the NEPs, information on the provider was reported. Further exploitation of the information included in the inventory allows potential tracking of specific properties of a material by checking the product (if it is a commercial product) or obtaining a contact point for further information needed. In some cases, one institution was the ENM provider while a second one was the provider of the final product.

Great efforts were devoted to determining the commercialization state of the different NEPs studied in all the projects selected. In some cases the ENMs incorporated were commercial but the NEP was not (it was exclusively made for the purpose of the project). In these cases, the product was considered as non-commercial. Even if the producers were providing similar commercialized NEP products (e.g. antifouling paints), if the specific product used for the studies in the project was not the one being commercialized, the NEP was rated as non-commercial. The life-cycle stage studied for each NEP was also indicated. The stages considered were synthesis (S), manufacturing (M), use (U), recycling (R) and end-of-life (EoL). Indications on the type of assessments (environmental and/or human hazard and/or exposure assessment) considered in the project were also reported in the inventory. For this last categorization, the project was considered as a whole, not each NEP individually. The purpose was to determine which was the main focus of the project on the NEP risk assessment (i.e. environmental or human risk assessment). Finally, the inventory also includes the total funding and the EC contribution received for each project evaluated.

3. Results

A total of 101 projects were reviewed. Many projects only studied pristine (as-synthesized) nanomaterials or surface modified versions of those, but were not incorporated into any product. Other projects were more theoretical, focusing for example on ontology or databases. This has resulted in a limited amount of projects which performed studies on NEP. From the 101 projects studied, 25 of them contained studies with NEPs and were included in the inventory (Table 1).

Having analysed each of the calls individually an increase of the number of nano-enabled products studied could be observed over the period reviewed. For FP7 and H2020, the ratio of projects studying NEP is the same, 26% in both cases, but for FP6, no projects on NEP were found – see Table 2.

3.1. Type of nano-enabled products studied

According to the information extracted from the data compiled, the most studied nano-enabled products in nanosafety projects funded by the European commission were polymeric nanocomposites. In most of the cases, the ENMs were incorporated to improve the mechanical properties, but incorporation for other functions like colouring (with pigments) or antibacterial activity (with Ag) was also identified. The second largest category was coatings, with photocatalytic and antibacterial properties being the main reasons for ENM incorporation into different products like ceramic tiles, wood or even asphalt. Paints was the third largest category and studies with different ENMs were reported (e.g. SiO_2, ZnO, TiO_2, pigments or Cu_2O). Applications ranged from indoor to outdoor paints and included antifouling paints for marine applications. The electronics category was represented by products such as conductive inks, displays and solar cells. Many of these products

Table 1
Inventory of NEP studied in nanosafety projects funded by the European Commission. Projects from FP7 and H2020 are shown in blue and red, respectively.

PROJECT	NANO-ENABLED PRODUCT	ENMs	PROVIDER	COMMERCIAL (Yes/No)	LC STAGE STUDIED					ASSESSMENT		TOTAL COST (€) EU CONTRIB. (€)
					S	M	U	R	EoL	E	H	
CALIBRATE (H2020) 2016.05.01 to 2019.10.31	**Paint**	Titanium Dioxide (TiO2)	Beck & Jørgensen	Yes		X	X		X	Yes	Yes	9.828.106 7.999.688
	Tiles coating	Silver (Ag)	Colorobbia, ISTEC CNR	No			X					
		TiO2	Colorobbia, ISTEC CNR	No			X					
		TiO2 + Silicon Dioxide (SiO2)	Colorobbia, ISTEC CNR	No			X					
CERASAFE (H2020) 2016.01.01 to 2018.12.31	**Ceramic coatings**	TiO2-Aluminium Oxide (Al2O3) blend	TMComas SLU	Yes		X				Yes	Yes	751.510 751.510
		Chromium (Cr)-Nickel (Ni) blend	Oerlikon, TMComas SLU	Yes		X						
		Tungsten Carbide (WC)–Cobalt (Co)–Cr–Ni blend	Oerlikon, TMComas SLU	Yes		X						
		WC–Chromium carbide (CrC)–Ni blend	Oerlikon, TMComas SLU	Yes		X						
FAST (H2020) 2015.12.01 to 2019 11.30	**Scaffolds from additive manufacturing**	Reduced graphene oxide (rGO)	Abalonyx	No	X					No	Yes	4.916.750 4.916.750
		Hydroxyapatite (HA)	Fluidinova	No		X						
		Hydrotalcite (HT)	Prolabin & Tefarms	No		X						
FUTURENANONEEDS (FP7) 2014.01.01 to 2017.12.31	**Thermoelectric materials**	SiO2 doped with Boron (B)	Institut für Energie und Umwelttechnik e.V (IUTA)	No	X	X				Yes	No	8.934.731 6.799.997
	Antimicrobial coatings	Ag	IUTA, Universidad de Santiago de Compostela (USC)	No	X	X						
		TiO2	IUTA, USC	No	X	X						
	Displays	QDs	Philipps Universität Marburg, USC	No	X	X						
	Motor oil	Molybdenum disulfide (MoS2), Fullerenes and graphene flakes	Institut Català de Nanotecnologia (ICN), French Alternative Energies and Atomic Energy Commission (CEA), IUTA	No	X	X						
	Lithium ion battery system	Silicon (Si) nanowires (NW)	NANOGAP, IUTA	No	X	X						
	Automotive heat recovery systems	Silicide nanocomposites (e.g. as MnSi and Mg2SiSn)	IUTA	No	X	X						
	Solar cells	Perovskites containing lead (Pb) and Zinc Oxide (ZnO)	École polytechnique fédérale de Lausanne (EPLF), USC	No	X	X						
GRACIOUS (H2020) 2018.01.01 to 2021.06.30	**Paint**	SiO2	Nouryon	Yes			X		X	Yes	No	7.180.119 6.999.369
		Cu-based pigments	BASF, Nouryon	Yes			X		X			
	Polymer	Cu-based pigments	BASF, LEITAT	No			X		X			
	Paper board	SiO2	Nouryon	No			X		X			
		Fe-based pigments	BASF, Nouryon	No			X		X			
	Commercial paper	SiO2	Nouryon	Yes			X		X			
GUIDENANO (FP7)	**Ceramic tiles with photocatalytic activity**	TiO2	Torrecid	Yes			X			Yes	No	11.143.364 8.150.000
		Al_2O_3-SiO_2	Torrecid	Yes			X					
	Food industry packaging and paper reinforcement	Nanocellulose	Innventia	Yes								
	Polymers Nanocomposites	TiO2 in PP matrix	Lati	Yes			X					
		Multi-Walled Carbon Nanotubes (MWCNT) in PP matrix	Lati	Yes			X					
		TiO2 in PA matrix	Lati	Yes			X					

2013.11.01 to 2017.04.30		MWCNT in PA matrix	Lati	Yes			X					
	Self-cleaning agent	TiO2 + Ag	Nser	Yes								
	Antifouling paints for marine activities	ZnO	Hempel	No			X					
	Textiles with antimicrobial properties	Silver Chloride (AgCl)	Inotex	No			X					
NANOFARM (H2020) 2016.03.01 to 2019.02.28	Nanopesticides	Copper Hydroxide $Cu(OH)_2$	Dupont (Kocide 3000)	Yes			X		X	Yes	No	968.394 968.394
NANOFASE (H2020) 2015.09.01 to 2019.08.31	Antifouling paints for marine activities	Copper (Cu^0)	Hempel	No			X			Yes	No	11.296.701 9.954.476
		Copper (I) Oxide (Cu2O)					X					
	Photocatalytic coating for roads	TiO2	FCCCO	No			X					
	Conductive ink	Ag	Amepox	Yes					X			
	Textiles with antimicrobial properties	Ag	Inotex	No			X					
	Textiles with photocatalytic activity	TiO2	Inotex	No			X					
	Additive for anaerobic digestors	Iron (II,III) Oxide (Fe3O4)	Applied Nanoparticles	Yes					X			
	Paint	TiO2	Beck & Jørgensen	Yes		X						
	Additive for soil and ground remediation	Nano-zero valent iron (Fe^0)	Nanoiron	Yes					X			
NANOFATE (FP7) 2010.04.01 to 2014.03.31	Fuel Additive	Cerium Dioxide (CeO2)	Energenics	Yes			X		X	Yes	No	3.251.135 2.497.100
	Sunscreen	ZnO	Microniser Pty Ltd	Yes			X		X			
	Conductive ink	Ag	Amepox	Yes			X		X			
	Antimicrobial textile	Ag	Nanotrade	Yes			X		X			
NANOGECO (FP7) 2015.01.01 to 2017.12.31	Paints	Carbon Black (CB)	Dothee SA	No			X			No	Yes	902.950 902.950
		TiO2	Dothee SA	No			X					
		ZnO	Wörwag	No			X					
NANOHOUSE (FP7) 2010.01.01 to 2013.06.30	Paints for indoor and outdoor applications	TiO2	Project Partners	No			X		X	Yes	No	3.143.207 2.400.100
		SiO2	Project Partners	No			X		X			
		Ag	Project Partners	No			X		X			
NANOMICEX (FP7) 2012.04.01 to 2015.03.31	Paints	Surface Modified ZnO (ZnO-BSA)	Plasmachem, Pinturas Montó SAU	No	X	X				Yes	Yes	4.800.478 3.535.290
		Al2O3	Plasmachem, Torrecid	No	X	X						
		Iron (III) Oxide (Fe2O3)	Tec-Star	No	X	X						
	Ceramic coating	TiO2 and ZnO water based mixtures	Plasmachem, Torrecid, Tec-Star	No	X	X						
		TiO2-ZnO dispersions	Plasmachem, Torrecid, Tec-Star	No	X	X						
	Ink	QDs coated with SiO2	Plasmachem, Ardeje	No	X	X						
		Ag	Plasmachem, Ardeje	No	X	X						
NANOPOLYTOX (FP7) 2010.05.01 to 2013.05.31	Plastic Industry, mainly outdoor applications: Polypropylene (PP), ethyl vinyl acetate (EVA), polyamide 6 (PA-6)	MWCNT	Lati, Glonatech	No			X	X		Yes	Yes	3.298.279 2.433.555
		ZnO	Lati, Urederra/Polyrise	No			X	X				
		TiO2	Lati, Urederra/Polyrise	No			X	X				
		SiO2	Lati, Urederra/Polyrise	No			X	X				
		Montmorillonite (MMT)	Lati, Laviosa	No			X	X				
		MMT (smaller size)	Lati, Laviosa	No			X	X				
NANOREG (FP7) 2013.03.01 to 2017.02.28	Concrete	TiO2	Confidential	No			X			Yes	Yes	49.586.318 10.000.000
	Electrodes for Lithium Ion Batteries	Lithium Iron Phosphate (LFP)	CEA pilot line	No		X		X	X			
		C-based ENMs with lithium nickel manganese cobalt oxide (NMC)	CEA pilot line	No		X						
	Photocatalytic Paints	TiO2	Allios	No			X					
	Preservative Wood Stain coating	Cerium Dioxide (CeO2)	Cerege	No			X					

NANOSAFEPACK (FP7) 2011.2.01 to 2014.11.30	**Polymeric matrices for the packaging sector: polypropylene (PP), polyethylene (PE), polyethylene terephthalate (PET), and poly-lactic acid (PLA)**	Layered Nanoclays	Tecni-Plasper, Tec-Star	No		X				Yes	Yes	2.240.594 1.626.339
		Ag	Tecni-Plasper, Tec-Star	No		X						
		SiO2	Tecni-Plasper, Tec-Star	No		X						
		ZnO	Tecni-Plasper, Tec-Star	No		X						
		Calcium carbonate (CaCO3)	Tecni-Plasper, Tec-Star	No		X						
NANOSOLUTIONS (FP7) 2013.04.01 to 2017.03.31	**Textiles with antimicrobial properties**	Ag	Polysistec	Yes			X			Yes	Yes	13.765.734 10.000.000
		TiO2	Polysistec	Yes			X					
		Copper oxide (CuO)	Polysistec	No			X					
	Engine oil	Nanodiamonds	PlasmaChem, Addo	Yes			X					
	Car arm-rest coating	MWCNT	Nanocyl	Yes			X					
	Ink	Cadmium Telluride (CdTe) QDs	PlasmaChem	No			X					
	Medical applications	Gold (Au)	Ubourdeaux	No			X					
NANOSUSTAIN (FP7) 2010.05.01 to 2013.05.31	**Paints**	TiO2	Nanoamor, Nabond	No	X	X	X	X	X	Yes	Yes	3.299.958 2.475.054
	Glazing products	ZnO	Nanogate	Yes	X	X	X	X	X			
	Plastics for structural or electrical/antistatic applications	Carbon nanotubes (CNT) epoxy resin	Nanocyl	Yes	X	X	X	X	X			
	Paper additive	Nanocellulose	UPM (The Biofore Company)	Yes	X	X	X	X	X			
NANOTUN3D (H2020) 2015.10.01 to 2019.09.30	**Materials for additive manufacturing**	Silicon Carbide (SiC) nanoparticles with TiO2/Fe2O3/Fe3O4 shell	Universitat Politecnica de Valencia (UPV), Laurentia Technologies SL	No	X					Yes	Yes	2.936.657 2.936.656
		Silicon Carbide (SiC) nanoparticles with TiO2 shell	ZOZ GmbH	No	X							
		Silicon Carbide (SiC) nanoparticles with TiO2 shell mixed with Ti-6Al-4V	ZOZ GmbH	No	X	X						
		Silicon Carbide (SiC) nanoparticles with TiO2 shell mixed with Ti-6Al-4V	TLS Technik GmbH & Co. Spezialpulver KG	No	X							
		Silicon Carbide (SiC) nanoparticles with TiO2 shell mixed with Ti-6Al-4V	Asociacion Centro Tecnologico CEIT-IK4	No	X							
		Silicon Carbide (SiC) nanoparticles with TiO2 shell mixed with Ti-6Al-4V	AIDIMME	No	X							
NEPHH (FP7) 2009.09.01 to 2012.08.31	**Plastic Industry, mainly for outdoor applications: Polypropylene (PP), polyurethane (PU), polyamide 6 (PA-6)**	SiO2	Degussa	No	X	X	X	X	X	Yes	Yes	3.096.159 2.428.496
		MMT	Laviosa	No	X	X	X	X	X			
		Glass Fibers (GF)	Taiwan Glass Ind. Corp.	No	X	X	X	X	X			
		Foam Glass Crystal Material (FGC)	Dennert Poraver GmbH	No	X	X	X	X	X			
OPTINANOPRO (H2020) 2015.10.01 to 2018.09.30	**Polymeric composite**	Nanoclay	MBN nanomaterialia s.p.a, HPX Polymers GmbH	No		X				Yes	Yes	6.920.685 5.516.910
		Nanotalc		No		X						
	Coating (electrospray)	SiO2	Bioinicia	No		X						
PLATFORM (H2020) 2015.02.01 to 2018.02.31	**Buckypaper**	CNT	Nanocyl	No		X				Yes	Yes	7.797.728 7.797.728
	Prepreg	CNT	Nanocyl	No		X						
	Non-woven veils	CNT	Nanocyl	No		X						
POROUS4APP (H2020) 2016.03.01 to 2020.02.29	**Support for energy storage, chemical catalysis and biomass conversion**	Nanoporous carbonaceous material (NCM)	Biorenewables Development Center	No	X	X				Yes	Yes	7,944,717 6.535.878
SANOWORK (FP7)	**Antibacterial nanosols**	Ag	Colorobbia	Yes		X				Yes	Yes	4.787.695
	Photocatalitic nanosols	TiO2	Colorobbia	Yes		X						
	Ceramics for improved flowability	Zirconium Dioxide (ZrO2)	GEA Niro	Yes	X							

2012.03.01 to 2015.02.28	**Nanofibers as photocatalytic components in Solar Cells**	Nanofibers (NF) containning TiO2	Elmarco/Bayer	Yes		X						3.409.185
	Nanofibers as membrane components for filter industry	Polyamide Nanofibers (NF)	Elmarco/Bayer	Yes	X	X						
	Plastic Industry	CNT	GLONATECH	No		X						
SCAFFOLD (FP7) 2012.05.01 to 2015.04.30	**Depollutant mortar**	TiO2	Acciona	Yes	X	X				No	Yes	3.710.015 2.537.000
	Self-cleaning mortar		Acciona	Yes	X	X						
	Self-compacting concrete	SiO2	Acciona	Yes	X	X						
	Bitominous Road Surface	Carbon Nanofibers/Nanoclay	Acciona	Yes		X						
	Fire retardant panels	Nanoclay	Acciona	Yes		X			X			
	Insulation panels	Cellulose nanofibers (NF)	Acciona	Yes		X						
SUN (FP7) 2013.10.01 to 2017.03.31	**Wear resistant metal coatings**	Tungsten Carbide-Cobalt (WC-Co)	MBN nanomaterialia s.p.a	Yes	X					Yes	Yes	13.585.305 10.249.962
	Antimicrobial wood impregnation	Basic Copper Carbonate (Cu2(OH)2CO3)	BASF	No		X	X		X			
	Antimicrobial wood coating	Copper Oxide (CuO)	Plasmachem, BASF	No	X		X		X			
	Lightweight conductive plastics	MWCNT	Nanocyl	Yes			X	X	X			
	Anti-fouling coatings	MWCNT	Nanocyl	No								
	Food additives	SiO2	Evonik (ENM), RIKILT(product)	No	X		X					
	Self-cleaning coatings for ceramic tiles	TiO2	Colorobbia	Yes	X	X	X		X			
	Coloured plastic composites	Iron Oxide (Fe2O3) inorganic pigment (Red 101)	BASF, PCMA	Yes	X		X		X			
		Organic pigment (Red 254)	BASF, PCMA	Yes	X	X	X	X	X			

contained silver or quantum dots (QDs), although ENMs like multi-walled carbon nanotubes (MWCNT) or perovskites based on lead (Pb) and zinc (Zn) were also studied. Numerous projects also studied nano-enabled textiles, many of them with Ag for antibacterial purposes or TiO_2 providing photocatalytic activity. Cement, metal and paper were also studied in different projects but less frequently than other products considered herein. The share of each type of NEP is represented in Fig. 1, for more details on the NEPs assigned to each category see Table S2.

3.2. Purpose of ENM incorporation

Mechanical properties improvement was identified as the main purpose of ENM incorporation. This was in line with polymeric nanocomposites being the main NEP studied. In addition, concrete or paper-based NEPs were also studied in the projects, where nanoclays and nanocellulose were incorporated to improve the mechanical performance. The second largest category was NEPs with photocatalytic activity, which is used on the one hand to provide self-cleaning properties and on the other hand to eliminate atmospheric harmful substances such as volatile organic compounds (VOCs) (Schneider et al., 2014). Most of the photocatalytic products contained TiO_2, although some ZnO-based NEPs were also reported. In antibacterial applications, the third largest category, ENMs were mainly applied as a coating component or impregnated on textiles. Ag was the main ENM in the studies for antibacterial applications, although NEPs incorporating copper-based compounds or cerium oxide (CeO_2) were also studied. For applications where the ENMs were incorporated for their electrical properties, different ENMs were used, for example silver, lithium iron phosphate (LFP) or MWCNTs among others. Polymeric nanocomposites and inks were some of the products in which those ENMs were incorporated to obtain specific electrical properties. NEPs in which the incorporation of ENMs was used to provide optical properties were mainly NEPs containing pigments and QDs. Studies for applications like fire retardancy and antifouling were less common. The share of each purpose of ENM incorporation category is represented in Fig. 2, for more details on the category in which each NEP was assigned see Table S3.

3.3. Engineered nanomaterials

Although there was a significant number of different engineered nanomaterials included in the nano-enabled products, three of them (TiO_2, carbon-based compounds and Silicon compounds) were incorporated in 68% of the total number of NEPs studied. The most studied nanomaterial was titanium dioxide (TiO_2), which in the context of the studies was mainly used in its anatase crystal form for its photocatalytic activity (Schneider et al., 2014). The second most studied ENMs were carbon-based materials. Different nanomaterials fell in this category, specifically different forms of carbon nanotubes, which are well known

for their electrical conductivity and for their ability to provide enhanced mechanical performance and these have been highly studied in European Projects. Nanodiamonds also were included in this category, based on their use as additives in lubricants. The third largest category was comprised of silicon compounds, mainly silicon dioxide (SiO_2) which can be incorporated in polymeric composites (Meer et al., 2016), concrete (Sanchez and Sobolev, 2010) or paper to improve mechanical performance. Silicides such as MnSi were also included in this category and these are used as thermoelectric materials. Silicon also fell into this category, and at the nanoscale can provide conductive properties.

With a smaller share, ENMs like Ag and ZnO were studied: In fourth place was silver (Ag), mainly used for its antibacterial properties (Marambio-Jones and Hoek, 2010) and also for its electrical conductive properties (in inks for example). Zinc oxide was used in many different products, for example as a component of solar cells (containing perovskites), as a component in paints (both construction and antifouling for marine applications) and in sunscreens, textiles or coatings. The share of each ENM is represented in Fig. 3, and for more details on the ENMs assigned to each category see Table S4.

3.4. Other results

Other results extracted from the information compiled in the inventory are summarized in Table 3. As shown in the table, only around one-third of the NEPs from all the studies in the different projects selected were commercial. The rest were specifically developed to be tested in the projects or were in a development stage. The implications of these results will be further discussed in the discussion section. The most studied life cycle stage was the product service life (i.e. use), with more than half of the NEPs studies considering it. Similarly, the manufacturing stage was also studied in almost half of the NEPs. Most of those studies were occupational measurements performed to cover the needs from industry concerning the potential health impact of ENMs on their workers. The least studied Life Cycle stage (LCS) was recycling and given that not all the products can be recycled, studying this particular stage was out of the scope of most of the projects. Synthesis and End-of-Life were each studied for around one-third of the NEPs included in the inventory.

Information on the type of assessment was project-specific, it was not compiled for each NEP individually. As shown in Table 3, around 85% of the projects included human assessment, 73% environmental assessment and 58% considered both. These data suggest that human risk assessment studies were slightly prioritized over environmental risk assessment studies. More than half of the projects considered in the inventory included both human and environmental assessments. Regarding the funding devoted to these projects, from the 25 projects listed in Table 2, the consortia have been in receipt of 127 M€ from the EC with total project funding of 190 M€.

4. Discussion

4.1. Main focus of nanosafety studies

4.1.1. Differences among EC calls

To fully understand the potential risks of nanotechnology, all the factors affecting the release and consequent exposure of ENMs and their hazard profile must be considered. Therefore, having a good understanding of the products in which the ENMs are incorporated and the processes to which they are submitted along the whole life cycle is essential. For this reason, the present study was focused on the inventory of studies on NEPs and not on pristine ENMs.

As observed in the results section, a significant number of projects from the framework Programmes H2020 and FP7 included studies with NEPs compared to the studies in projects from the sixth framework programme (FP6), where no studies with NEPs were identified (Table 1). In the FP6, the EC emphasized the need for increasing the understanding of the interaction of engineered nanoparticles with the environment and the living world. Accordingly, the funded projects had to address interdisciplinary toxicological and eco-toxicological research, i.e. exposure, including intake, uptake, time scale, dose-response monitoring, including cellular and molecular mechanisms, bio-persistence, biokinetics, etc. (European Commission, 2004b). Therefore, a lack of studies with NEPs could be justified since the focus was in understanding more fundamental aspects, which led to studies being focused on pristine ENMs, creating the basis for future studies with higher complexity (impact of NEP along their life cycle in humans and the environment).

In the objectives of the seventh framework programme, the EC stated that in nanosafety related research the emphasis was shifting from toxicology studies of individual nanomaterials towards more holistic safety assessments and management of overall risks (European Commission, 2010). In addition, the increase of NEPs placed in the market over the years (Allied Market Research, 2016; Future Markets Inc, 2016) may have fostered the acceptability of including them in the studies, which would explain the increase of projects considering NEPs. In the objectives for the Horizon 2020 programme, the EC indicated to support the safe development of nanotechnologies, risk management should become an integral part of the culture of the organisations involved in the supply chain, including regulatory support and risk governance, which should be achieved by fostering Safe-by-design strategies and grouping approaches (European Commission, 2019; European Commission, 2015). Therefore, many projects focused their efforts on compiling, analyzing and using the data generated in previous studies.

Although an increase of NEPs studies was observed along the different framework programmes, aligning with their general objectives, its consideration in only one-quarter of the projects seems insufficient. Therefore, the increase of their presence in future projects should be encouraged.

Table 2
Amount of European projects considered in the Nanosafety Cluster including nano-enabled products in their studies.

Project Call	Total number of projects	Projects with NEP	% of projects with NEP
FP6	6	0	0%
FP7	57	15	26%
H2020	38	10	26%
TOTAL	101	25	25%

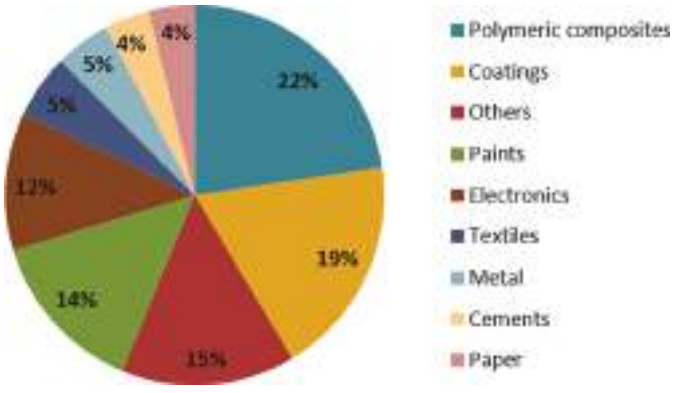

Fig. 1. Type of NEP studied in European Nanosafety projects.

4.1.2. Life cycle stages considered

When analyzing the Life Cycle Stages considered in the inventory projects, a greater tendency to perform studies on use phase and manufacturing stages was observed. A major focus on these two stages was expected, since for most of the products these were the stages where critical exposure scenarios (release of ENMs is more likely to occur) could be identified, e.g. manufacturing processes for ENMs incorporation in the matrix; service life processes-abrasion, ageing, washing. Thus, a major number of studies on these scenarios is justified. Nevertheless, around one-third of the NEPs based projects in the inventory also considered evaluation of risks during the synthesis and end-of-life stages. In those stages, although critical exposure scenarios were not initially identified in most of the cases included the inventory, for specific products and applications may represent higher concern. Thus, their consideration in multiple evaluations was considered as positive, being recycling the least studied stage. That fact can be justified since not all the products are intended to be recycled and their evaluation is not always needed. However, 13% of the NEPs studies evaluated risks during recycling processes. All in all, the efforts devoted to each of the LCS is directly linked to the identified critical exposure scenarios for each product-application.

At the life cycle stages considered in the projects of the inventory, slighly greater attention was devoted to human than to environmental exposure and hazard assessment. Additionally, 58% of the projects considered both assessments, which is a very encouraging statistic.

4.1.3. Balancing hazard and exposure assessment

In order to assess risks associated to ENMs, both exposure and hazard must be considered. The main safety focus of all the 101 projects in the inventory is indicated in Table S1. According to the information compiled from the table, 23% of the projects were considering other aspects apart from hazard or exposure (e.g ontology, stakeholders communication or analytical methods), 14% were mainly considering exposure, 31% hazard and 33% both hazard and exposure.

For regular chemicals, in Europe, REACH (Registration, Evaluation, Authorisation and Restriction of Chemicals) provides the possibility to waive the toxicity testing of a substance based on exposure scenarios (ES) developed in the exposure assessment, a concept termed 'Exposure-Based Waiving' (EBW) (Rowbotham and Gibson, 2011). However, REACH only allows EBW in a limited number of cases with constraints on tonnage levels, types of tests to be waived and the need for a thorough ES and exposure assessment throughout the life cycle of a chemical and for all human exposure routes and environmental pathways (European Chemicals Agency (ECHA), 2015). In US, EPA (United States Environmental Protection Agency) has also prioritzed exposure-based assessment, recognizing that regulators need reliable approaches to screen and prioritize chemicals based on their likelihood of exposure (Egeghy et al., 2011). A similar approach should be applied for ENMs. However, as extracted from table S1 and already highlighted in previous publications, in the last years a higher focus was on hazard than on exposure assessment (Ellenbecker and Tsai, 2015). Therefore, based on this information and as already pointed out by Maynard and Aitken in 2016, in future projects a higher emphasis should be given to exposure (Maynard and Aitken, 2016).

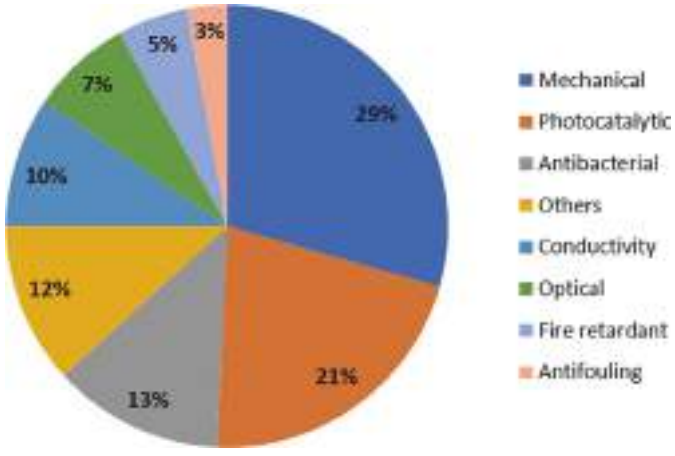

Fig. 2. Purpose of the ENMs incorporation in the products studied.

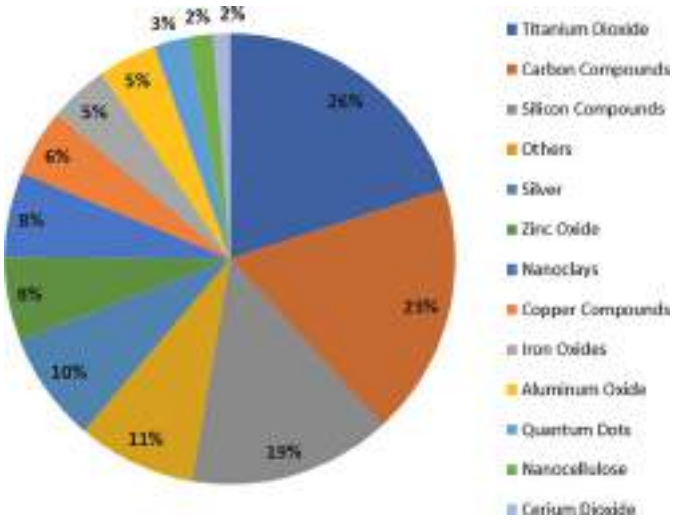

Fig. 3. Percentage of nano-enabled products that incorporated each ENM (since one nano-enabled product can contain more than one ENM, the total addition of values is higher than 100%).

4.2. Studies performed and real-world relevance

4.2.1. Correlation between most studied and most produced ENMs and NEPs

When the production volumes of the different ENMs are compared with the ENMs studied (Fig. 3), conclusions on the correlation of the studies performed and their industrial relevance can be extracted. In Table S5, the production volumes provided by different sources for several ENMs are included. Since estimations on production volumes for ENMs present high uncertainties on the exact volumes produced (Future

Table 3
Overview of the use of commercial and non-commercial NEP, the life cycle stages studied and the type of assessment (i.e. environmental and human) in the projects. The percentages can be calculated dividing by the quantity of NEP or projects by the total number of NEP (127) and the total number of projects (25). All the data has been extracted from the inventory.

	Commercialization state	
	Commercial	*Non-commercial*
Quantity of NEP	48	79
Percentage	38%	62%

	Life cycle stage studied				
	Synt.	*Manuf.*	*Use*	*Recyc.*	*E-o-L*
Quantity of NEP	42	60	65	17	34
Percentage	33%	47%	51%	13%	27%

	Type of assessment in the project		
	Human	*Environmental*	*Both*
Quantity of projects	22	19	15
Percentage	88%	76%	60%

Markets Inc, 2016; Janković and Plata, 2019; Sun et al., 2014), the authors acknowledge that the values dicsussed below are approximations. It should be emphasized that the aim of this paper is not to conduct research on production volumes, but given the large differences in the quoted values, they provide clear evidence for comparative purposes. The authors compiled production volumes from different sources, which can be of interest and they are reported in Table S5 to provide an overview of the commercially relevant ENMs for comparison with the results extracted from the inventory.

The most produced ENM in the world is estimated to be carbon black (CB), with European production of nearly 2 million tonnes per year (Mt) in 2018 (Grand View Research, 2020). Its high production is based on its use in rubber applications, especially manufacture of tyres, with approximately 70% of carbon black's production used for this application (Grand View Research, 2020). Although carbon black is by far the largest volume ENM in terms of commercial tonnage, only one project listed in Table 1 included carbon black-based NEP and it was in paints (Table S4). Coatings (including paints) are a common application for CB, with around 5 to 10% of carbon's black production used for this application (Grand View Research, 2020). It should be noted that CB in rubber for tyres (its main application) was not studied in nanosafety projects funded by the EC. However, Carbon black has been extensively studied, including toxicological studies and human risk assessment (Levy, 1995). Further research considering the whole nano-enabled product (i.e tyres) is still needed concerning emission factors, long-term monitoring, fate in surface waters and soils, (eco)toxicological impacts and degradation under realistic conditions (Baensch-Baltruschat et al., 2020).

The second most produced nanomaterial is estimated to be nano-SiO_2. Based on information from the French nano-registry (Agence nationale de sécurité sanitaire (ANSES), 2013), Wigger et al. identified that the entire production of silica is actually all nano-silica, which has an estimated production volume in Europe of 0.459 Mt. (Wigger et al., 2018). Its main application (with a share around 40%) is as a reinforcement additive in composites (including tyres) (Future Markets Inc, 2016; Wigger et al., 2018). 19% of the NEPs studied in the projects included in the inventory contained silicon-based materials (Fig. 3). From the materials included in this category, 46% belong to nano-SiO_2 (the other 54% were other types of Si compounds), which means that 8.7% of NEPs studied contained SiO_2 ENMs. Similarly to CB, any NEP incorporating nano-SiO_2 in tyres were not considered in any of the projects in the inventory. However, unlike CB, multiple studies with other NEPs incorporating nano-SiO_2 were performed. It was not surprising that the most studied NEPs were polymeric nano-SiO_2 composites considering the high number of potential applications for these materials. As reviewed in other publications, many polymeric nanocomposite studies focused on accelerated ageing and/or mechanical treatment (Koivisto et al., 2017). Polymeric nanocomposites have been highly studied in different projects because of their high industrial relevance, their multiple applications, the wide number of nanomaterials aiming at improving their performance (Dallas et al., 2011; El-Fattah et al., 2015; Lonkar et al., 2012; Ophir et al., 2010; Paul and Robeson, 2008; Sharma et al., 2010) and given that their composition facilitates monitoring of a high variety of ENMs.

Nano-TiO_2 is estimated to be the third most produced ENM (0.042 Mt), with nano-ZnO following (0.019 Mt) (Future Markets Inc, 2016). The applications of these ENMs were recently reviewed by Kuenen et al. after considering a comprehensive market report supplemented with nano-registration databases. For both ENMs, sunscreens were identified as their main application (with 57% and 64% of the ENMs used for this application being nano-TiO_2 and nano-ZnO, respectively) (Kuenen et al., 2020). It is interesting to note that although personal care products, especially sunscreens, are the main commercial application of the rutile form of nano-TiO_2 and of nano-ZnO and have been extensively commercialized for several decades, those NEPs were only studied in one of the reviewed projects (see NANOFATE in Table 1). This is in contrast to the many studies reported on the inclusion of anatase nano-TiO_2 (see Fig. 3), which was incorporated to exploit its photocatalytic characteristics. Therefore, although nano-TiO_2 and nano-ZnO were broadly studied in the projects, their main application was not represented as much as expected.

In contrast, in the case of nano-Ag, based on its production volume (240 Tonnes (Himly et al., 2020)), such a high number of studies (present in 10% of the NEPs, Fig. 3) may not be justified. Interestingly enough, when the NEPs databases are evaluated (Table S6) (DTU Environment, 2020; Nanotechnology Products Database, 2020; Woodrow Wilson International Center for Scholars, 2020), a high number of registered NEPs incorporating nano-Ag are identified (Hansen et al., 2020). Even more NEPs are registered than for other ENMs like nano-SiO_2, nano-ZnO or CB, which present production volumes up to 4 orders of magnitude higher. However, it should be emphasized that, since the NEPs databases do not include an estimation of the market relevance (i.e commercialized NEPs) for any of the listed items, a high number of registered NEPs is not necessarily correlated with a high presence in the market. For this reason, the approach followed with releases to the environment estimated through mass flow models using ENMs production volumes and corresponding product allocation of each ENM(Adam et al., 2021; Dumont et al., 2015). In any case, such a high number of registered NEPs containing nano-Ag in the databases provides evidence of the wide range of different products where it can be incorporated and the interest of some companies to develop such products. Overall, the ease to detect Ag, in comparison with Si or C, which are highly present in the environment and may lead to potential difficulty in differentiation from background elements, together with the wide range of NEPs that can be found (each of them presenting different release pathways), may have been the reason why despite the low commercial relevance of nano-Ag, it has been so broadly studied.

4.2.2. *Commercialization state of the NEPs studied*

As shown in Table 3, only about one-third of the NEPs studied were commercial. The other two-thirds were not in production, and thus, were subject to further modifications, or were specifically designed for the projects without any further intention of commercialization. Furthermore, some of the NEPs classified as commercial belonged to small and medium-sized enterprises (SMEs) including start-ups and universities' spin-offs with low turnovers. Although these NEPs were commercialized, they were not representing established products in the market and thus, not completely representative of the potential risks that NEPs may pose on humans or the environment. On the one hand, the studies with non-commercial (and low level to be commercialized) NEPs have been very useful for the nanosafety community. These case studies have provided the opportunity to gain knowledge on mechanisms of release, mechanisms of toxicity, optimizing and establishing experimental protocols for testing purposes (e.g. establishing experimental set-ups and interlaboratory comparisons). All these studies are extremely relevant contributing to the understanding of the mechanisms leading to potential risks of NEPs along their life cycle. However, on the other hand, there is a need to perform more studies on highly commercialized products to obtain a real picture of the potential effects caused by NEPs on human health and on the environment.

It should be highlighted that the projects are greatly influenced by the availability of industrial partners providing the NEPs, which can impose limitations in the selection of case studies. The requirements for industrial partners to be involved in Nanosafety projects may be demanding. Very often, the individual components (e.g. ENMs, matrix) of the materials constituting the NEP are required in sufficient quantities to enable testing across many different types of experiments, which can impose an additional constraint. In addition, it can be challenging to involve certain companies in the projects if there is not a relevant benefit for their participation. Nevertheless, with the increasing introduction of NEPs in the market (Allied Market Research, 2016; Future Markets Inc., 2016), the number of companies producing NEPs has increased, which

enhances the connection between industry and academia. Finally, since many of the mechanisms of release have already been studied in previous projects with well-known (produced within the project) materials, testing of highly commercialized NEPs, even from providers outside the project consortiums, should be encouraged to increase the real-world relevance of the studies performed.

4.3. Data accessibility

As mentioned in the methodology section, the data included in the inventory was compiled from the NanoSafety Cluster compendiums, CORDIS, the projects websites, peer-reviewed literature and personal communication. During the information collection process, a need for organizing and accessing data produced on NEPs was identified.

The project deliverables contain the information and all the data generated within the projects. Sometimes the data included are confidential, but even when deliverables were public, the accessibility to NEPs data was very limited. Especially for recent projects (i.e. H2020) some deliverables were found in CORDIS, but the number of deliverables available was quite limited. Other deliverables were obtained from the projects' websites, but many websites were closed shortly after the project ended, making all the information generated during the projects inaccessible which is at best unfortunate and at worst indefensible. As a consequence, the analysis on data generated on NEPs was extremely time demanding and most of the times the information had to be obtained by direct communication with the partners involved in the studies and from data accessible due to the authors' contribution in the projects. However, it is important that the information should also be accessible for people outside the consortia. Thus, a repository for the projects' outcomes (i.e. deliverables) would be extremely beneficial for the nanosafety community.

NanoSafety Cluster compendiums were a great source to extract a lot of information about the projects, but the last version published is from 2017. Therefore, accessibility to an extended abstract of project progress for future nanosafety projects may even be more limited. Other efforts for data compilation from nanosafety studies carried out in the different projects are being made by launching knowledge infrastructure projects to facilitate the storage and management of knowledge (data, methods, tools, models) in a common space. In the case of nanosafety the recent project, Nanocommons, provides the infrastructure needed by the nanosafety community to store and manage all the data generated in the different areas and makes this data publicly available and accessible to everyone (Himly et al., 2020). Similr efforts far data management were done in the project eNanoMapper by creating a modular and extensible infrastructure for data sharing, data analysis, and building computational toxicology models for ENMs (Jeliazkova et al., 2015), which continues growing the capacities to integrate data that can be used for different purposes. A common problem in all this efforts is the issue on how to manage the confidentiality on the data. During the inventory generation, some information could not be included due to its confidentiality or because the personal communication was not always effective. However, the maximum amount of information was compiled to provide an inventory as exhaustive as possible, without compromising the veracity and reliability of the data included.

5. Conclusions

To the authors' knowledge, this paper presents the first comprehensive review of NEPs studied in nanosafety projects funded by the European Commission. It therefore provides a picture of the recent priorities of both the EC in funding the projects and also the researchers in terms of their testing capabilities and their perception of the needs of the business community. Although in this work the authors have extracted highly relevant and useful conclusions for the nanosafety community, the inventory also provides a rich source of information from which readers with different data needs can extract their own conclusions.

The inventory of nano-enabled products thus provides an insight into the current status of nanosafety research in Europe and an overview to identify where the gaps are with respect to the following key aims:

(i) commercialisation balance against risk,
(ii) transparency on use of NEPs/ENMs including production volumes and
(iii) clarity on the safe use and identified risks.

In the first place, given the limited number of studies on NEPs, future projects should be focussed on commercialized products with specific attention paid to the ENMs that form part of these NEPs and that constitute the largest volumes produced and used in the EU and elsewhere.

In the second place, greater transparency of the commercialization of NEPs/ENMs would be beneficial to provide reinforcement of the view of their presence in the market leading to prioritization of the studies. To maximize the impact of the studies, the selection of materials (or NEPs) should consider aligning their position in the market, their application and the preidentified potential impacts in humans or the environment. NEPs registration may promote transparency on the wide range of applications of nanotechnology in society.

In the third place, the outcomes of the studies should provide indications on the safe use of the NEPs. As reflected in the inventory, multiple studies on NEPs have been performed providing knowledge on the mechanisms and behaviour of at least some ENMs. However, the outcomes of the proposed studies should be focussed on providing clear guidance specifying any associated risks of NEPs and their use and advising on how they should be safely manufactured, handled and disposed. For that purpose, exposure-based assessments should be prioritized. Thus, key factors such as intrinsic toxicity (hazard) and exposure can be considered alongside product performance and costs leading to a more balanced view on risk/benefit that can then be communicated to stakeholders including consumers of the products in question.

It should also be noted that in Europe, a major recent project, NanoReg2 focused on the challenge of coupling Safe by Design to the regulatory process, and sought to demonstrate and establish new principles and ideas based on data from industrial value chain implementation studies so that Safe by Design can become a fundamental pillar in the discovery, screening and commercialization of novel ENMs (Organization for Economic Co-operation and Development (OECD), 2020). Thus, regulation will potentially play an important role in reinforcing the need for safety to be considered as part of NEPs' commercialization i.e. through implementation of the safe-by-design concept in the industrial innovation process.

Declaration of Competing Interest

The authors declare that they have no known competing financial interests or personal relationships that could have appeared to influence the work reported in this paper.

Acknowledgements

This work was funded by the project "Nanomaterial Fate and Speciation in the Environment (NANOFASE)" from the European

Community's Horizon2020 Programme (H2020) under Grant Agreement number 646002. The authors acknowledge the following people for providing contributions for the data compiled in the inventory: Adam Laycock (NANOFARM), Alejandro Vilchez (GUIDENANO, NANOFASE, NANOSOLUTIONS), Apostolos Salmatonidis (CERASAFE), Armand Masion (NANOREG), Bernd Nowack (NANOHOUSE), Camila Delpivo (CALIBRATE, GRACIOUS, NANOREG), Celina Vaquero Morelejo (FAST, PLATFORM), Claus Svendsen (NANOFATE), Evelin Frijns (NANOTUN3D), Henk Goede (FUTURENANONEEDS), Jesús Lopez de Ipiña Peña (FAST), Julie Laloy (NANOGECO), Kenneth A. Dawson (FUTURENANONEEDS), Lorenzo Moroni (FAST), Mar Viana (CERASAFE), Nathan Bossa (GRACIOUS), Simon Clavaguera (NANOREG), Tardif François (NANOHOUSE), Víctor Puntes (FUTURENANONEEDS), William Peijnenburg (FUTURENANONEEDS).

Appendix A. Supplementary data

Supplementary data to this article can be found online at https://doi.org/10.1016/j.impact.2021.100323.

References

Adam, V., Wu, Q., Nowack, B., 2021. Integrated dynamic probabilistic material flow analysis of engineered materials in all European countries. NanoImpact 100312. https://doi.org/10.1016/j.impact.2021.100312.

Agence nationale de sécurité sanitaire (ANSES), 2013. Éléments Issus Des Déclarations Des Substances À L'État Nanoparticulaire. RAPPORT D'ETUDE.

Agence nationale de sécurité sanitaire (ANSES), 2020. Éléments Issus Des Déclarations Des Substances À L'État Nanoparticulaire - RAPPORT D'ETUDE 2019.

Allied Market Research, 2016. Europe nanomaterials market: trends, share, opportunities and forecasts 2014–2022. Allied Market Research.

Baensch-Baltruschat, B., Kocher, B., Stock, F., Reifferscheid, G., 2020. Tyre and road wear particles (TRWP) - a review of generation, properties, emissions, human health risk, ecotoxicity, and fate in the environment. Sci. Total Environ. https://doi.org/10.1016/j.scitotenv.2020.137823.

Bergeson, L.L., Hutton, C.N., 2016. ECHA Announces Signed Agreement for EU Observatory for Nanomaterials | Nano and Other Emerging Chemical Technologies Blog [WWW document]. URL. http://nanotech.lawbc.com/2016/12/echa-announces-signed-agreement-for-eu-observatory-for-nanomaterials/.

Dallas, P., Sharma, V.K., Zboril, R., 2011. Silver polymeric nanocomposites as advanced antimicrobial agents: classification, synthetic paths, applications, and perspectives. Adv. Colloid Interf. Sci. 166, 119–135. https://doi.org/10.1016/j.cis.2011.05.008.

DTU Environment, the D.E.C. and D.C.C, 2020. The Nanodatabase [WWW Document]. URL. http://nanodb.dk/ (accessed 1.11.21).

Dumont, E., Johnson, A.C., Keller, V.D.J., Williams, R.J., 2015. Nano silver and nano zinc-oxide in surface waters e exposure estimation for Europe at high spatial and temporal resolution. Environ. Pollut. 196, 341–349. https://doi.org/10.1016/j.envpol.2014.10.022.

Egeghy, P.P., Vallero, D.A., Cohen Hubal, E.A., 2011. Exposure-based prioritization of chemicals for risk assessment. Environ. Sci. Pol. 14, 950–964. https://doi.org/10.1016/j.envsci.2011.07.010.

El-Fattah, M.A., El Saeed, A.M., Dardir, M.M., El-Sockary, M.A., 2015. Studying the effect of organo-modified nanoclay loading on the thermal stability, flame retardant, anti-corrosive and mechanical properties of polyurethane nanocomposite for surface coating. Prog. Org. Coatings 89, 212–219. https://doi.org/10.1016/j.porgcoat.2015.09.010.

Ellenbecker, M.J., Tsai, C.S.-J., 2015. Exposure Assessment and Safety Considerations for Working with Engineered Nanoparticles. John Wiley & Sons, Inc, Hoboken, NJ. https://doi.org/10.1002/9781118998694.

EU NanoSafety Cluster, 2020. About the NanoSafety Cluster. WWW Document. URL. https://www.nanosafetycluster.eu/ (accessed 1.11.21).

European Chemicals Agency (ECHA), 2015. Guidance on Information Requirements and Chemical Safety Assessment, Chapter R.12: Use Description.

European Commission, 2004a. Towards a European Strategy for Nanotechnology.

European Commission, 2004b. THE SIXTH FRAMEWORK WORK PROGRAMME - Nanotechnology and Nanosciences, Knowledge-Based Multifunctional Materials, New Production Processes and Devices.

European Commission, 2010. The Seventh Framework Work Programme - Nanosciences, Nanotechnologies, Materials And New Production Technologies -NMP.

European Commission, 2015. HORIZON 2020 WORK PROGRAMME 2014–2015: Nanotechnologies, Advanced Materials, Biotechnology and Advanced Manufacturing and Processing.

European Commission, 2019. HORIZON 2020 WORK PROGRAMME 2018–2020: Nanotechnologies, Advanced Materials, Biotechnology and Advanced Manufacturing and Processing.

European Commission, 2020. CORDIS. WWW Document. URL. http://cordis.europa.eu/home_en.html (accessed 1.11.21).

Future Markets Inc, 2016. The Global Nanotechnology and Nanomaterials Market Opportunity Report.

Giese, B., Klaessig, F., Park, B., Kaegi, R., Steinfeldt, M., Wigger, H., Von Gleich, A., Gottschalk, F., 2018. Risks, release and concentrations of engineered nanomaterial in the Environment. Sci. Rep. 8 https://doi.org/10.1038/s41598-018-19275-4.

Gottschalk, F., Nowack, B., Lassen, C., Kjølholt, J., Christensen, F., 2015. Nanomaterials in the Danish Environment. The Danish Environmental Protection Agency.

Grand View Research, 2020. Carbon Black Market Report.

Hansen, S.F., Hansen, O.F.H., Nielsen, M.B., 2020. Advances and challenges towards consumerization of nanomaterials. Nat. Nanotechnol. 15, 964–965. https://doi.org/10.1038/s41565-020-00819-7.

Himly, M., Farcal, L., Papadiamantis, A., Duschl, A., Lynch, I., 2020. The NanoCommons e-Infrastructure – A Quick Guide to What and how of Nanoinformatics in Safety Assessment Suiting Basic to Expert Users in Academia, Industry, and Regulatory Agencies.

European Chemicals Agency (ECHA), 2020. European Union Observatory for Nanomaterials [WWW Document]. URL. https://euon.echa.europa.eu/ (accessed 1.11.21).

Innovationsgesellschaft GmbH, 2021. Belgium to Introduce Nano-Reporting [WWW Document]. URL. https://innovationsgesellschaft.ch/en/belgium-to-introduce-nano-reporting/.

International Standards Organization, 2015. ISO/TS 80004–1:2015 Nanotechnologies — Vocabulary — Part 1: Core terms.

Janković, N.Z., Plata, D.L., 2019. Engineered nanomaterials in the context of global element cycles. Environ. Sci. Nano 6, 2697–2711. https://doi.org/10.1039/c9en00322c.

Jeliazkova, N., Chomenidis, C., Doganis, P., Fadeel, B., Grafström, R., Hardy, B., Hastings, J., Hegi, M., Jeliazkov, V., Kochev, N., Kohonen, P., Munteanu, C.R., Sarimveis, H., Smeets, B., Sopasakis, P., Tsiliki, G., Vorgrimmler, D., Willighagen, E., 2015. The eNanoMapper database for nanomaterial safety information. Beilstein J. Nanotechnol. 6, 1609–1634. https://doi.org/10.3762/bjnano.6.165.

Koivisto, A.J., Jensen, A.C.Ø., Kling, K.I., Nørgaard, A., Brinch, A., Christensen, F., Jensen, K.A., 2017. Quantitative material releases from products and articles containing manufactured nanomaterials: towards a release library. NanoImpact 5, 119–132. https://doi.org/10.1016/j.impact.2017.02.001.

Kuenen, J., Pomar-Portillo, V., Vilchez, A., Visschedijk, A., Denier Van Der Gon, H., Vázquez-Campos, S., Nowack, B., Adam, V., 2020. Inventory of country-specific emissions of engineered nanomaterials throughout the life cycle. Environ. Sci. Nano 7, 3824–3839. https://doi.org/10.1039/d0en00422g.

Levy, L.S., 1995. Review: inhalation toxicology and human risk assessment of carbon black. Indoor Built Environ. https://doi.org/10.1177/1420326X9500400504.

Lonkar, S.P., Kushwaha, O.S., Leuteritz, A., Heinrich, G., Singh, R.P., Winey, K.I., Kappes, M., Hirsch, A., Heath, J.R., 2012. Self photostabilizing UV-durable MWCNT/polymer nanocomposites. RSC Adv. 2, 12255. https://doi.org/10.1039/c2ra21583g.

Lynch, I., 2014. Compendium of Projects in the European NanoSafety Cluster.

Lynch, I., 2015. Compendium of Projects in the European NanoSafety Cluster.

Lynch, I., 2016. Compendium of Projects in the European NanoSafety Cluster.

Lynch, I., 2017. Compendium of Projects in the European NanoSafety Cluster.

Marambio-Jones, C., Hoek, E.M.V., 2010. A review of the antibacterial effects of silver nanomaterials and potential implications for human health and the environment. J. Nanopart. Res. 12, 1531–1551. https://doi.org/10.1007/s11051-010-9900-y.

Maynard, A.D., Aitken, R.J., 2016. "Safe handling of nanotechnology" ten years on. Nat. Nanotechnol. 11, 998–1000. https://doi.org/10.1038/nnano.2016.270.

Meer, S., Kausar, A., Iqbal, T., 2016. Attributes of polymer and silica nanoparticle composites: a review. Polym. Plast. Technol. Eng. 55, 826–861. https://doi.org/10.1080/03602559.2015.1103267.

Mitrano, D.M., Limpiteeprakan, P., Babel, S., Nowack, B., Cheever, B., Frost, P.C., Xenopoulos, M.A., Hintelmann, H., Metcalfe, C.D., Thiel, S., 2016. Durability of nano-enhanced textiles through the life cycle: releases from landfilling after washing. Environ. Sci. Nano 3, 375–387. https://doi.org/10.1039/C6EN00023A.

Nanotechnology Products Database, 2020. WWW Document. http://product.statnano.com/ (accessed 1.11.21).

Nanowerk Catalog - Nanotechnology Materials and Equipment, 2020. WWW Document. URL. http://nanowerk.com/nanocatalog/ (accessed 1.11.21).

National Science and Technology Council, 2000. National Nanotechnology Initiative - the Initiative and its Implementation Plan.

Ophir, A., Dotan, A., Belinsky, I., Kenig, S., 2010. Barrier and mechanical properties of nanocomposites based on polymer blends and organoclays. J. Appl. Polym. Sci. 116, 72–83. https://doi.org/10.1002/app.31285.

Organisation for Economic Co-operation and Development (OECD), 2020. Moving Towards a Safe(r) Innovation Approach (SIA) for More Sustainable Nanomaterials and Nano-enabled Products.

Paul, D.R., Robeson, L.M., 2008. Polymer nanotechnology: nanocomposites. Polymer (Guildf). 49, 3187–3204. https://doi.org/10.1016/j.polymer.2008.04.017.

Pavlicek, A., Part, F., Rose, G., Praetorius, A., Miernicki, M., Gazsó, A., Huber-Humer, M., 2020. A European nano-registry as a reliable database for quantitative risk assessment of nanomaterials? A comparison of national approaches. NanoImpact 21, 100276. https://doi.org/10.1016/j.impact.2020.100276.

Riediker, M., 2013. Compendium of Projects in the European NanoSafety Cluster.

Rowbotham, A.L., Gibson, R.M., 2011. Exposure-driven risk assessment: applying exposure-based waiving of toxicity tests under REACH. Food Chem. Toxicol. https://doi.org/10.1016/j.fct.2011.03.050.

Sanchez, F., Sobolev, K., 2010. Nanotechnology in Concrete - A Review. https://doi.org/10.1016/j.conbuildmat.2010.03.014.

Schneider, J., Matsuoka, M., Takeuchi, M., Zhang, J., Horiuchi, Y., Anpo, M., Bahnemann, D.W., 2014. Understanding TiO2 Photocatalysis: mechanisms and materials. Chem. Rev. https://doi.org/10.1021/cr5001892.

Schug, T.T., Johnson, A.F., Balshaw, D.M., Garantziotis, S., Walker, N.J., Weis, C., Nadadur, S.S., Birnbaum, L.S., 2013. ONE Nano: NIEHS's strategic initiative on the health and safety effects of engineered nanomaterials. Environ. Health Perspect. 121, 410–414. https://doi.org/10.1289/ehp.1206091.

Sharma, A., Tripathi, B., Vijay, Y.K., 2010. Dramatic improvement in properties of magnetically aligned CNT/polymer nanocomposites. J. Memb. Sci. 361, 89–95. https://doi.org/10.1016/j.memsci.2010.06.005.

Sun, T.Y., Gottschalk, F., Hungerbühler, K., Nowack, B., 2014. Comprehensive probabilistic modelling of environmental emissions of engineered nanomaterials. Environ. Pollut. 185, 69–76. https://doi.org/10.1016/j.envpol.2013.10.004.

Swedish Chemicals Agency, 2021. Compulsory Declaration for Nanomaterial [WWW Document]. URL. https://www.kemi.se/en/products-register/products-obliged-to-be-reported/compulsory-declaration-for-nanomaterial.

The Royal Society & The Royal Academy of Engineering, 2004. Nanoscience and Nanotechnologies: Opportunities and Uncertainties.

Vance, M.E., Kuiken, T., Vejerano, E.P., McGinnis, S.P., Hochella, M.F., Rejeski, D., Hull, M.S., 2015. Nanotechnology in the real world: redeveloping the nanomaterial consumer products inventory. Beilstein J. Nanotechnol. 6, 1769–1780. https://doi.org/10.3762/bjnano.6.181.

Wigger, H., Wohlleben, W., Nowack, B., 2018. Redefining environmental nanomaterial flows: consequences of the regulatory nanomaterial definition on the results of environmental exposure models. Environ. Sci. Nano 5, 1372–1385. https://doi.org/10.1039/c8en00137e.

Woodrow Wilson International Center for Scholars, 2020. Project on Emerging Nanotechnologies [WWW Document]. URL. https://www.wilsoncenter.org/publication-series/project-emerging-nanotechnologies (accessed 1.11.21).

Nanosafety research in Europe – Towards a focus on nano-enabled products

Projects considered

Table S1: List of projects funded by the EC considered. The projects are sorted by call (i.e. FP6, FP7, H2020) and the resource by which they were identified is indicated. (i.e. compendiums, CORDIS or others). The main safety focus (i.e. Exposure [E], Hazard [H] or Others [O] was identified and also incorporated in the table. Projects included in the inventory are highlighted in green. The project's name contain a link to CORDIS from where more information on each of them can be consulted.

		PROJECT NAME	PROJECT TITLE	MAIN SAFETY FOCUS	COMPENDIUMS WHERE THEY ARE MENTIONED								CORDIS (2.1.X.X)		Others
					'10	'11	'12	'13	'14	'15	'16	'17	2.2	2.4	
1	FP6	CELLNANOTOX	Cellular Interaction and Toxicology with Engineered Nanoparticles	H	X										
2		DIPNA	Development of an Integrated Platform for Nanoparticle Analysis to verify their possible toxicity and the eco-toxicity	H	X										
3		NANOINTERACT	Development of a platform and toolkit for understanding interactions between nanoparticles and the living world	H	X										
4		NANOSAFE2	Safe production and use of nanomaterials	E, H		X									
5		NANOSH	Inflammatory and genotoxic effects of engineered nanomaterials	H	X										
6		NANOTRANSPORT	Behavior of Aerosols Released to Ambient Air from Nanoparticle Manufacturing – A pre-normative study	E	X										
7	FP7	ENANOMAPPER	A Database and Ontology Framework for Nanomaterials Design and Safety Assessment	O					X	X	X	X			
8		ENNSATOX	Engineered Nanoparticle Impact on Aquatic Environments: Structure, Activity and Toxicology	H	X	X	X	X							
9		ENPRA	Risk Assessment of EngineeredNanoParticles	E, H	X	X	X	X							
10		ENRHES	Engineered Nanoparticles: Review of Health and Environmental Safety	E, H											X
11		FIBRALSPEC	Fuctionalised Innovative Carbon Fibres Developed from Novel Precursors With Cost Efficiency and Tailored Properties	E						X		X			
12		FUTURENANONEEDS	Framework to respond to regulatory needs of future nanomaterials and markets	E, H					X	X	X	X			
13		GUIDENANO	Assessment and mitigation of nano-enabled product risks on human and environmental health: Development of new strategies and creation of a digital guidance tool for nanotech industries	E, H					X	X	X	X			
14		HINAMOX	Health Impact of Engineered Metal and Metal Oxide Nanoparticles: Response, Bioimaging and Distribution at Cellular and Body Level	H	X	X	X	X							
15		INLIVETOX	Intestinal, Liver and Endothelial Nanoparticle Toxicity - development and evaluation of a novel tool for high-throughput data generation	H	X	X	X								
16		INSTANT	Innovative Sensor for the fast Analysis of Nanoparticles in Selected Target Products	O			X	X	X						
17		ITS-NANO	Intelligent testing strategy for engineered nanomaterials	E, H			X	X							
18		LICARA	Life cycle approach and human risk impact assessment, product stewardship and stakeholder risk/benefit communication of nanomaterials	O				X							
19		MARINA	Managing Risks of Nanoparticles	E,H		X	X	X	X	X	X				
20		MEMBRANENANOPART	Modelling the mechanisms of nanoparticle-lipid interactions and nanoparticle effects on cell membrane structure and function	H				X	X	X					
21		MOD-ENP-TOX	"Modeling Assays Platform ""MAP"" for hazard ranking of engineered nanoparticles (ENPs)"	H						X					
22		MODERN	MODeling the EnviRonmental and human health effects of Nanomaterials	H				X							
23		MODNANOTOX	Modelling nanoparticle toxicity: principles, methods, novel approaches	H		X	X	X	X	X					

24		NANEX	Development of Exposure Scenarios for Manufactured Nanomaterials	E	X	X									
25		NANODEFINE	Development of an integrated approach based on validated and standardized methods to support the implementation of the EC recommendation for a definition of nanomaterial	O					X	X	X	X			
26		NANODETECTOR	Engineered Nanoparticle Impact on New methods for measuring, detection and identification of nanoparticles in products and/or in the environment	O			X	X	X	X					
27		NANODEVICE	Novel Concepts, Methods, andTechnologies for the Production ofPortable, Easy-to-Use Devices for theMeasurement and Analysis of Airborne Engineered Nanoparticles in Workplace Air	O	X	X	X	X							
28		NANOEIS	Nanotechnology Education for Industry and Society	O							X				
29		NANOFATE	Nanoparticle Fate Assessment and Toxicity in the Environment	E, H	X	X	X	X	X	X					
30		NANOGECO (SIINN)	Nanoparticle generation by atomization process in spray coating	E											X
31		NANOHETER (SIINN)	Fate of engineered nanoparticles in the water column under natural conditions. Role of the heteroaggregation with naturally occurring suspended matter.	E					X	X					
32		NANOHOUSE	Life Cycle of Nanoparticle-based Products used in House Coating	E, H	X	X	X	X							
33		NANOIMPACTNET	European Network on the Health andEnvironmental Impact of Nanomaterials	O	X	X	X				X				
34		NANOLYSE	NANOPARTICLES IN FOOD: Analytical methods for detection and characterisation	O		X	X	X							
35		NANOMICEX	Mitigation of risk and control of exposure in nanotechnology based inks and pigments	E, H			X	X	X	X					
36		NANOMILE	Engineered nanomaterial mechanisms of interactions with living systems and the environment	H				X	X	X	X	X			
37		NANOMMUNE	Comprehensive Assessment of Hazardous Effects of Engineered Nanomaterials on the Immune System	H	X	X	X								
38		NANOPLAST	A computational study of the interaction between nanoplastic and model biological membranes	H	X										
39		NANOPOLYTOX	Toxicological impact of nanomaterials derived from processing, weathering and recycling of polymer nanocomposites used in various industrial applications	E, H	X	X	X	X	X						
40		NANOPUZZLES	Modelling properties, interactions, toxicity and environmental behaviour of engineered nanoparticles	H				X	X	X					
41		NANOREG	A common European approach to the regulatory testing of nanomaterials	E, H					X	X	X	X			
42		NANORETOX	The Reactivity and Toxicity of Engineered Nanoparticles	H	X	X	X	X		X					
43		NANOSAFEPACK	Development of a best practices guide for the safe handling and use of nanoparticles in packaging industries	E, H			X	X		X					
44		NANOSOLUTIONS	Biological Foundation for the Safety Classification of Engineered Nanomaterials (ENM): Systems Biology Approaches to Understand Interactions of ENM with Living Organisms and the Environment	E, H					X	X	X	X			
45		NANOSTAIR	Establishing a process and a platform to support standardization for nanotechnologies implementing the STAIR approach	O				X	X						
46		NANOSUSTAIN	Development of sustainable solutions for nanotechnology-based products based on hazard characterization and LCA	E, H	X	X	X	X	X	X					
47		NANOTEST	Development of methodology for alternative testing strategies for the assessment of the toxicological profile of nanoparticles used in medical diagnostics	H							X				
48		NANOTOES	Training Of Experts in Safety	O							X				
49		NANOTOXCLASS (SIINN)	Establishing nanomaterial grouping / classification strategies according to toxicity and biological effects for supporting risk assessment	H							X	X			
50		NANOTRANSKINETICS	Modelling basis and kinetics of nanoparticle interaction with membranes, uptake into cells, and sub-cellular and inter-compartmental transport	H		X	X	X	X						

51		NANOVALID	Development of reference methods for hazard identification, risk assessment and LCA of engineered nanomaterials	E, H		X	X	X	X	X	X				
52		NANOXIMET (SIINN)	Oxidant generating capacity as a metric to allow grouping of nanomaterials and prediction of human health effects	H					X	X					
53		NEPHH	Nanomaterials-related environmental pollution and health hazards throughout their life-cycle	E, H	X	X	X								
54		NEURONANO	Understanding the origin of reactiveoxidative species and protein aggregation and mis-folding	H	X	X	X								
55		NHECD	Creation of a critical and commented database on the health, safety and environmental impact of nanoparticles	O		X	X								
56		OBSERVATORYNANO	European observatory for science-based and economic expert analysis of nanotechnologies, cognisant of barriers and risks, to engage with relevant stakeholders regarding benefits and opportunities	O	X										
57		PRENANOTOX	Predictive toxicology of engineered nanoparticles	H					X	X					
58		QUALITYNANO	A pan-European infrastructure for quality in nanomaterials safety testing	O		X	X	X	X	X					
59		SANOWORK	Safe Nano Worker Exposure Scenarios	E			X	X	X	X					
60		SCAFFOLD	Innovative strategies, methods and tools for occupational risks management of manufactured nanomaterials (MNMs) in the construction industry	E			X	X	X						
61		SIINN	Safe Implementation of Innovative Nanoscience and Nanotechnology	E, H		X	X	X	X	X		X			
62		SMARTNANO	Sensitive MeAsuRemenT, detection, and identification of engineered NANOparticles	O			X	X							
63		SUN	Sustainable Nanotechnologies	E, H					X	X	X	X			
64	H2020	ACENANO	Analytical and Characterisation Excellence in nanomaterial risk assessment: A tiered approach	O								X	X		
65		CALIBRATE	Performance testing, calibration and implementation of a next generation system-of-systems Risk Governance Framework for nanomaterials	E, H							X	X	X		
66		CERASAFE (SIIN)	Safe production and Use of Nanomaterials in the Ceramic Industry	E								X			
67		CO-PILOT	Flexible Pilot Scale Manufacturing of Cost-Effective Nanocomposites through Tailored Precision Nanoparticles in Dispersion	O										X	
68		DIMAP	Novel nanoparticle enhanced Digital Materials for 3D Printing and their application shown for the robotic and electronic industry	E									X		
69		EC4SAFENANO	European Centre for Risk Management and Safe Innovation in Nanomaterials & Nanotechnologies	O							X	X	X		
70		FAST	Functionally graded Additive Manufacturing scaffolds by hybrid manufacturing	E									X		
71		FOLSMART	Folate-Target Nanodevices To Activated Macrophages For Rheumatoid Arthritis	H									X		
72		GRACIOUS	Grouping, Read-Across, CharacterIsation and classificatiOn framework for regUlatory risk assessment of manufactured nanomaterials and Safer design of nano-enabled products	E, H									X		
73		GONANO	Governing Nanotechnologies through societal engagement	O											X
74		HISENTS	High level Integrated SEnsor for NanoToxicity Screening	H							X	X	X		
75		IZADI-NANO2INDUSTRY	Injection moulding, casting and coating PILOTS for the production of improved components with nano materials for automotive, construction and agricultural machinery	E, H									X	X	
76		LORCENIS	Long Lasting Reinforced Concrete for Energy Infrastructure under Severe Operating Conditions	E, H							X	X			
77		MODCOMP	Modified cost effective fibre based structures with improved multi-functionality andperformance	E, H								X			
78		MOZART	MesopOrous matrices for localiZed pH-triggered releAse of theRapeuTic ions and drugs	H									X		
79		NANOCOMMONS	The European Nanotechnology Community Informatics Platform: Bridging data and disciplinary gaps for industry and regulators (NanoCommons)	O											X

80		NANOFARM (SIINN)	Fate & Effects of Agriculturally Relevant Nanomaterials	E, H								X			
81		NANOFASE	Nanomaterial FAte and Speciation in the Environment	E, H						X	X	X	X		
82		NANOGENTOOLS	Developing and implementation of a new generation of nanosafety assessment tools	H							X	X			
83		NANOHYBRIDS	New generation of nanoporous organic and hybrid aerogels for industrial applications: from the lab to pilot scale production	E, H										X	
84		NANOINFORMATIX	Development and Implementation of a Sustainable Modelling Platform for NanoInformatics	E, H											X
85		NANOLEAP	Nanocomposite for building constructions and civil infraestructures: European network pilot production line to promote industrial application cases	E, H										X	
86		NANOREG II	Development and implementation of Grouping and Safe-by-Design approaches within regulatory frameworks	E, H						X	X	X	X		
87		NANOTUN3D	Development of the complete workflow for producing and using a novel nanomodified Ti-based alloy for additive manufacturing in special applications	E									X		
88		NECOMADA	Nano-Enabled Conducting Materials Accelerating Device Applicability	E, H								X			
89		NPSCOPE	A new integrated instrument for accurate and reproducible physicochemical characterisation of nanoparticles	O								X	X		
90		OPTINANOPRO	Processing and control of novel nanomaterials in packaging, automotive and solar panel processing lines	E									X	X	
91		PATROLS	Physiologically Anchored Tools for Realistic nanOmaterial hazard aSsessment	H									X		
92		PANDORA	Probing safety of nano-objects by defining immune responses of environmental organisms	H							X	X			
93		PEPTICAPS	Design of polyPEPTIdes diblock copolymers as emulsifiers to produce safe, controlled and reliable novel stimuli-responsive nanoCAPSules for skin care applications	H									X		
94		PLATFORM	Open access pilot plants for sustainable industrial scale nanocomposites manufacturing based on buckypapers, doped veils and prepregs	E										X	
95		POROUS4APP	Pilot plant production of controlled doped nanoporous carbonaceous materials for energy and catalysis applications	E										X	
96		PROCETS	PROtective composite Coatings via Electrodeposition and Thermal Spraying	O									X	X	
97		PRODIA	Production, control and Demonstration of structured hybrid nanoporous materials for Industrial adsorption Applications	E, H										X	
98		REFINE	Regulatory Science Framework for Nano(bio)material-based Medical Products and Devices	H									X		
99		SKHINCAP	SKin Healthcare by Innovative NanoCAPsuleS	E, H							X	X	X		
100		SMARTNANOTOX	Smart Tools for Gauging Nano Hazards	H							X	X	X		
101		PROSAFE	Promoting the Implementation of Safe by Design	O						X	X	X	X		

Products category

Table S2 – Overview of the product category where each of the NEPs were assigned.

PROJECT (Starting date) (Ending date)	NANO-ENABLED PRODUCT	ENMs	Products Category								
			Metal	Coatings	Textiles	Paints	Polymers	Electronics	Cements	Paper	Others
CALIBRATE (H2020) 2016.05.01 2019.10.31	Paint	Titanium Dioxide (TiO2)				1					
	Tiles coating	Silver (Ag)		1							
		TiO2		1							
		TiO2 + Silicon Dioxide (SiO2)		1							
CERASAFE (H2020) 2016.01.01 2018.12.31	Ceramic coatings	TiO2-Aluminum Oxide (Al2O3) blend		1							
		Chromium (Cr)-Nickel (Ni) blend		1							
		Tungsten Carbide (WC)–Cobalt (Co)–Cr–Ni blend		1							
		WC–Chromium carbide (CrC)–Ni blend		1							
FAST (H2020) 2015.12.01 2019 11.30	Scaffolds from additive manufacturing	Reduced graphene oxide (rGO)					1				
		Hydroxyapatite (HA)					1				
		Hydrotalcite					1				
FUTURENANONEEDS (FP7) 2014.01.01 2017.12.31	Thermoelectric materials	SiO2 doped with Boron (B)						1			
	Antimicrobial coatings	Ag		1							
		TiO2		1							
	Displays	QDs						1			
	Motor oil	Molybdenum disulfide (MoS2), Fullerenes and graphene flakes									1
	Lithium ion battery system	Silicon (Si) nanowires (NW)						1			
	Automotive heat recovery systems	Silicide nanocomposites (e.g. MnSi and Mg2SiSn)						1			
	Solar cells	Perovskites containing lead (Pb) and Zinc Oxide (ZnO)						1			
GRACIOUS (H2020) 2018.01.01 2021.06.30	Paint	SiO2				1					
		Cu-based pigments				1					
	Polymer	Cu-based pigments					1				
	Paper board	SiO2								1	
		Fe-based pigments								1	
	Commercial paper	SiO2								1	
GUIDENANO (FP7) 2013.11.01 2017.04.30	Ceramic tiles with photocatalytic activity	TiO2		1							
		Al_2O_3-SiO_2		1							
	Food industry packaging and paper reinforcement	Nanocellulose								1	
	Polymers Nanocomposites	TiO2 in PP matrix					1				
		Multi-Walled Carbon Nanotubes (MWCNT) in PP matrix					1				
		TiO2 in PA matrix					1				
		MWCNT in PA matrix					1				
	Self-cleaning agent	TiO2 + Ag		1							
	Antifouling paints for marine activities	ZnO				1					
	Textiles with antimicrobial properties	Silver Chloride (AgCl)			1						
NANOFARM (H2020) 2016.03.01 2019.02.28	Nanopesticides	Copper Hydroxide $Cu(OH)_2$									1
NANOFASE (H2020) 2015.09.01 2019.08.31	Antifouling paints for marine activities	Copper (Cu^0)				1					
		Copper (I) Oxide (Cu2O)				1					
	Photocatalytic coating for roads	TiO2		1							
	Conductive ink	Ag						1			
	Textiles with antimicrobial properties	Ag			1						

	Textiles with photocatalytic activity	TiO2			1						
	Additive for anaerobic digestors	Iron (II,III) Oxide (Fe3O4)									1
	Paint	TiO2				1					
	Additive for soil and ground remediation	Nano-zero valent iron (Fe^0)									1
NANOFATE (FP7) 2010.04.01 2014.03.31	**Fuel Additive**	Cerium Dioxide (CeO2)									1
	Sunscreen	ZnO									1
	Conductive ink	Ag						1			
	Antimicrobial textile	Ag			1						
NANOGECO (FP7) 2015.01.01 2017.12.31	**Paints**	Carbon Black (CB)				1					
		TiO2				1					
		ZnO				1					
NANOHOUSE (FP7) 2010.01.01 2013.06.30	**Paints for indoor and outdoor applications**	TiO2				1					
		SiO2				1					
		Ag				1					
NANOMICEX (FP7) 2012.04.01 2015.03.31	**Paints**	Surface Modified ZnO (ZnO-BSA)				1					
		Al2O3				1					
		Iron (III) Oxide (Fe2O3)				1					
	Ceramic coating	TiO2 and ZnO water based mixtures		1							
		TiO2-ZnO dispersions		1							
	Ink	QDs coated with SiO2						1			
		Ag						1			
NANOPOLYTOX (FP7) 2010.05.01 2013.05.31	**Plastic Industry, mainly outdoor applications: Polypropylene (PP), ethyl vinyl acetate (EVA), polyamide 6 (PA-6)**	MWCNT					1				
		ZnO					1				
		TiO2					1				
		SiO2					1				
		Montmorillonite (MMT)					1				
		MMT (smaller size)					1				
NANOREG (FP7) 2013.03.01 2017.02.28	**Concrete**	TiO2							1		
	Electrodes for Lithium Ion Batteries	Lithium Iron Phosphate (LFP)						1			
		C-based ENMs with lithium nickel manganese cobalt oxide (NMC)						1			
	Photocatalytic Paints	TiO2				1					
	Preservative Wood Stain coating	CeO2		1							
NANOSAFEPACK (FP7) 2011.12.01 2014.11.30	**Polymeric matrices for the packaging sector: polypropylene (PP), polyethylene (PE), polyethylene terephthalate (PET), and poly-lactic acid (PLA)**	Layered Nanoclays					1				
		Ag					1				
		SiO2					1				
		ZnO					1				
		Calcium carbonate (CaCO3)					1				
NANOSOLUTIONS (FP7) 2013.04.01 2017.03.31	**Textiles with antimicrobial properties**	Ag			1						
		TiO2			1						
		Copper oxide (CuO)			1						
	Engine oil	Nanodiamonds									1
	Car arm-rest coating	MWCNT		1							
	Ink	Cadmium Telluride (CdTe) QDs									1
	Medical applications	Gold (Au)									1
NANOSUSTAIN (FP7) 2010.05.01 2013.05.31	**Paints**	TiO2				1					
	Glazing products	ZnO		1							
	Plastics for structural or electrical/antistatic applications	Carbon nanotubes (CNT) epoxy resin					1				
	Paper additive	Nanocellulose								1	
NANOTUN3D (H2020) 2015.10.01 2019.09.30	**Materials for additive manufacturing**	Silicon Carbide (SiC) nanoparticles with TiO2/Fe2O3/Fe3O4 shell	1								
		SiC nanoparticles with TiO2 shell	1								
		SiC nanoparticles with TiO2 shell mixed with Ti-6Al-4V	1								
		SiC nanoparticles with TiO2 shell mixed with Ti-6Al-4V	1								
		SiC nanoparticles with TiO2 shell mixed with Ti-6Al-4V	1								
		SiC nanoparticles with TiO2 shell mixed with Ti-6Al-4V	1								
NEPHH (FP7)	**Plastic Industry, mainly for outdoor applications: Polypropylene (PP),**	SiO2					1				
		MMT					1				
		Glass Fibers (GF)					1				

2009.09.01 2012.08.31	**polyurethane (PU), polyamide 6 (PA-6)**	Foam Glass Crystal Material (FGC)					1				
OPTINANOPRO (H2020) 2015.10.01 2018.09.30	**Polymeric composite**	Nanoclay					1				
		Nanotalc					1				
	Coating (electrospray)	SiO2		1							
PLATFORM (H2020) 2015.02.01 2018.02.31	**Buckypaper**	CNT									1
	Prepreg	CNT									1
	Non-woven veils	CNT									1
POROUS4APP (H2020) 2016.03.01 2020.02.29	**Support for energy storage, chemical catalysis and biomass conversion**	Nanoporous carbonaceous material (NCM)						1			
SANOWORK (FP7) 2012.03.01 2015.02.28	**Antibacterial nanosols**	Ag									1
	Photocatalitic nanosols	TiO2									1
	Ceramics for improved flowability	Zirconium Dioxide (ZrO2)									1
	Nanofibers as photocatalytic components in Solar Cells	Nanofibers (NF) containning TiO2						1			
	Nanofibers as membrane components for filter industry	Polyamide NF									1
	Plastic Industry	CNT					1				
SCAFFOLD (FP7) 2012.05.01 2015.04.30	**Depollutant mortar**	TiO2							1		
	Self-cleaning mortar								1		
	Self-compacting concrete	SiO2							1		
	Bitominous Road surface	Carbon Nanofibers/Nanoclay							1		
	Fire retardant panels	Nanoclay									1
	Insulation panels	Cellulose NF									1
SUN (FP7) 2013.10.01 2017.03.31	**Wear resistant metal coatings**	WC-Co		1							
	Antimicrobial wood impregnation	Basic Copper Carbonate (Cu2(OH)2CO3)		1							
	Antimicrobial wood coating	CuO		1							
	Lightweight conductive plastics	MWCNT						1			
	Anti-fouling coatings	MWCNT		1							
	Food additives	SiO2									1
	Self-cleaning coatings for ceramic tiles	TiO2		1							
	Coloured plastic composites	Iron Oxide (Fe2O3) inorganic pigment (Red 101)					1				
		Organic pigment (Red 254)					1				
			6 5% Metal	24 19% Coatings	7 6% Textiles	18 14% Paints	29 23% Polymeric C.	14 11% Electronics	5 4% Cements	5 4% Paper	19 15% Others

Purpose of ENM incorporation

Table S3 – Overview of the purpose of ENM incorporation category where each of the NEPs were assigned.

PROJECT (Starting date) (Ending date)	NANO-ENABLED PRODUCT	ENMs	Purpose of incorporation								
			Antibacterial	Photocatalityc	Mechanical	Fire retardant	Antifouling	Electrical	Colouring	Others	Unknown
CALIBRATE (H2020) 2016.05.01 2019.10.31	Paint	Titanium Dioxide (TiO2)		1							
	Tiles coating	Silver (Ag)	1								
		TiO2		1							
		TiO2 + Silicon Dioxide (SiO2)		1							
CERASAFE (H2020) 2016.01.01 2018.12.31	Ceramic coatings	TiO2-Aluminum Oxide (Al2O3) blend									1
		Chromium (Cr)-Nickel (Ni) blend									1
		Tungsten Carbide (WC)–Cobalt (Co)–Cr–Ni blend									1
		WC–Chromium carbide (CrC)–Ni blend									1
FAST (H2020) 2015.12.01 2019 11.30	Scaffolds from additive manufacturing	Reduced graphene oxide (rGO)			1					1	
		Hydroxyapatite (HA)			1					1	
		Hydrotalcite (HT)			1					1	
FUTURENANONEEDS (FP7) 2014.01.01 2017.12.31	Thermoelectric materials	SiO2 doped with Boron (B)						1			
	Antimicrobial coatings	Ag	1								
		TiO2	1								
	Displays	QDs							1		
	Motor oil	Molybdenum disulfide (MoS2), Fullerenes and graphene flakes			1						
	Lithium ion battery system	Silicon (Si) nanowires (NW)						1			
	Automotive heat recovery systems	Silicide nanocomposites (e.g. MnSi and Mg2SiSn)						1			
	Solar cells	Perovskites containing lead (Pb) and Zinc Oxide (ZnO)						1			
GRACIOUS (H2020) 2018.01.01 2021.06.30	Paint	SiO2			1						
		Cu-based pigments							1		
	Polymer	Cu-based pigments							1		
	Paper board	SiO2			1						
		Fe-based pigments							1		
	Commercial paper	SiO2			1						
GUIDENANO (FP7) 2013.11.01 2017.04.30	Ceramic tiles with photocatalytic activity	TiO2		1							
		Al_2O_3-SiO_2		1							
	Food industry packaging and paper reinforcement	Nanocellulose			1						
	Polymers Nanocomposites	TiO2 in PP matrix		1							
		Multi-Walled Carbon Nanotubes (MWCNT) in PP matrix			1						
		TiO2 in PA matrix		1							
		MWCNT in PA matrix			1						
	Self-cleaning agent	TiO2 + Ag	1	1							
	Antifouling paints for marine activities	ZnO					1				
	Textiles with antimicrobial properties	Silver Chloride (AgCl)	1								
NANOFARM (H2020) 2016.03.01 2019.02.28	Nanopesticides	Copper Hydroxide $Cu(OH)_2$	1								
NANOFASE (H2020)	Antifouling paints for marine activities	Copper (Cu^0)					1				
		Copper (I) Oxide (Cu2O)					1				
	Photocatalytic coating for roads	TiO2		1							
	Conductive ink	Ag						1			

2015.09.01 2019.08.31	**Textiles with antimicrobial properties**	Ag	1								
	Textiles with photocatalytic activity	TiO2		1							
	Additive for anaerobic digestors	Iron (II,III) Oxide (Fe3O4)								1	
	Paint	TiO2		1							
	Additive for soil and ground remediation	Nano-zero valent iron (Fe^0)								1	
NANOFATE (FP7) 2010.04.01 2014.03.31	**Fuel Additive**	Cerium Dioxide (CeO2)								1	
	Sunscreen	ZnO								1	
	Conductive ink	Ag						1			
	Antimicrobial textile	Ag	1								
NANOGECO (FP7) 2015.01.01 2017.12.31	**Paints**	Carbon Black (CB)							1		
		TiO2		1							
		ZnO		1							
NANOHOUSE (FP7) 2010.01.01 2013.06.30	**Paints for indoor and outdoor applications**	TiO2		1							
		SiO2			1						
		Ag	1								
NANOMICEX (FP7) 2012.04.01 2015.03.31	**Paints**	Surface Modified ZnO (ZnO-BSA)		1							
		Al2O3									1
		Iron (III) Oxide (Fe2O3)							1		
	Ceramic coating	TiO2 and ZnO water based mixtures		1							
		TiO2-ZnO dispersions		1							
	Ink	QDs coated with SiO2							1		
		Ag						1			
NANOPOLYTOX (FP7) 2010.05.01 2013.05.31	**Plastic Industry, mainly outdoor applications: Polypropylene (PP), ethyl vinyl acetate (EVA), polyamide 6 (PA-6)**	MWCNT			1						
		ZnO		1							
		TiO2		1							
		SiO2			1						
		Montmorillonite (MMT)			1						
		MMT (smaller size)			1						
NANOREG (FP7) 2013.03.01 2017.02.28	**Concrete**	TiO2		1							
	Electrodes for Lithium Ion Batteries	Lithium Iron Phosphate (LFP)						1			
		C-based ENMs with lithium nickel manganese cobalt oxide (NMC)						1			
	Photocatalytic Paints	TiO2		1							
	Preservative Wood Stain coating	CeO2	1								
NANOSAFEPACK (FP7) 2011.12.01 2014.11.30	**Polymeric matrices for the packaging sector: polypropylene (PP), polyethylene (PE), polyethylene terephthalate (PET), and poly-lactic acid (PLA)**	Layered Nanoclays			1						
		Ag	1								
		SiO2			1						
		ZnO			1						
		Calcium carbonate (CaCO3)			1						
NANOSOLUTIONS (FP7) 2013.04.01 2017.03.31	**Textiles with antimicrobial properties**	Ag	1								
		TiO2	1								
		Copper oxide (CuO)	1								
	Engine oil	Nanodiamonds			1						
	Car arm-rest coating	MWCNT			1						
	Ink	Cadmium Telluride (CdTe) QDs							1		
	Medical applications	Gold (Au)								1	
NANOSUSTAIN (FP7) 2010.05.01 2013.05.31	**Paints**	TiO2		1							
	Glazing products	ZnO		1							
	Plastics for structural or electrical/antistatic applications	Carbon nanotubes (CNT) epoxy resin			1						
	Paper additive	Nanocellulose			1						
NANOTUN3D (H2020) 2015.10.01 2019.09.30	**Materials for additive manufacturing**	Silicon Carbide (SiC) nanoparticles with TiO2/Fe2O3/Fe3O4 shell			1						
		SiC nanoparticles with TiO2 shell			1						
		SiC nanoparticles with TiO2 shell mixed with Ti-6Al-4V			1						
		SiC nanoparticles with TiO2 shell mixed with Ti-6Al-4V			1						
		SiC nanoparticles with TiO2 shell mixed with Ti-6Al-4V			1						
		SiC nanoparticles with TiO2 shell mixed with Ti-6Al-4V			1						
NEPHH (FP7)		SiO2			1						

2009.09.01 2012.08.31	**Plastic Industry, mainly for outdoor applications: Polypropylene (PP), polyurethane (PU), polyamide 6 (PA-6)**	MMT				1					
		Glass Fibers (GF)				1					
		Foam Glass Crystal Material (FGC)				1					
OPTINANOPRO (H2020) 2015.10.01 2018.09.30	**Polymeric composite**	Nanoclay			1						
		Nanotalc			1						
	Coating (electrospray)	SiO2									1
PLATFORM (H2020) 2015.02.01 2018.02.31	**Buckypaper**	CNT			1	1		1		1	
	Prepreg	CNT			1	1		1		1	
	Non-woven veils	CNT			1	1		1		1	
POROUS4APP (H2020) 2016.03.01 2020.02.29	**Support for energy storage, chemical catalysis and biomass conversion**	Nanoporous carbonaceous material (NCM)								1	
SANOWORK (FP7) 2012.03.01 2015.02.28	**Antibacterial nanosols**	Ag	1								
	Photocatalitic nanosols	TiO2		1							
	Ceramics for improved flowability	Zirconium Dioxide (ZrO2)								1	
	Nanofibers as photocatalytic components in Solar Cells	Nanofibers (NF) containning TiO2		1							
	Nanofibers as membrane components for filter industry	Polyamide NF								1	
	Plastic Industry	CNT		1							
SCAFFOLD (FP7) 2012.05.01 2015.04.30	**Depollutant mortar**	TiO2		1							
	Self-cleaning mortar			1							
	Self-compacting concrete	SiO2			1						
	Bitominous Road surface	Carbon Nanofibers/Nanoclay			1						
	Fire retardant panels	Nanoclay				1					
	Insulation panels	Cellulose NF			1						
SUN (FP7) 2013.10.01 2017.03.31	**Wear resistant metal coatings**	WC-Co			1						
	Antimicrobial wood impregnation	Basic Copper Carbonate (Cu2(OH)2CO3)	1								
	Antimicrobial wood coating	CuO	1								
	Lightweight conductive plastics	MWCNT			1			1			
	Anti-fouling coatings	MWCNT					1				
	Food additives	SiO2								1	
	Self-cleaning coatings for ceramic tiles	TiO2		1							
	Coloured plastic composites	Iron Oxide (Fe2O3) inorganic pigment (Red 101)							1		
		Organic pigment (Red 254)							1		
			17 13% Antibacterial	29 21% Photocatalityc	40 30% Mechanical	7 5% Fire retardant	4 3% Antifouling	13 10% Electrical	10 7% Colouring	15 11% Others	6 Unknown

ENMs studied

Table S4 – Overview of the ENM category where each of the NEPs were assigned.

PROJECT (Starting date) (Ending date)	ENMs	ENM												
		Ag	Ti	C-based	Zn	Nanoclay	Nanocellulose	Cu	Si	Fe	Ce	Quantum Dots	Al	Others
CALIBRATE (H2020) 2016.05.01 2019.10.31	Titanium Dioxide (TiO2)		1											
	Silver (Ag)	1												
	TiO2		1											
	TiO2 + Silicon Dioxide (SiO2)		1						1					
CERASAFE (H2020) 2016.01.01 2018.12.31	TiO2-Aluminum Oxide (Al2O3) blend		1										1	
	Chromium (Cr)-Nickel (Ni) blend													1
	Tungsten Carbide (WC)–Cobalt (Co)–Cr–Ni blend			1										1
	WC–Chromium carbide (CrC)–Ni blend			1										1
FAST (H2020) 2015.12.01 2019 11.30	Reduced graphene oxide (rGO)			1										
	Hydroxyapatite (HA)					1								
	Hydrotalcite					1								
FUTURENANONEEDS (FP7) 2014.01.01 2017.12.31	SiO2 doped with Boron (B)								1					
	Ag	1												
	TiO2		1											
	QDs											1		
	Molybdenum disulfide (MoS2), Fullerenes and graphene flakes			1										1
	Silicon (Si) nanowires (NW)								1					
	Silicide nanocomposites (e.g. MnSi and Mg2SiSn)								1					
	Perovskites containing lead (Pb) and Zinc Oxide (ZnO)		1		1									1
GRACIOUS (H2020) 2018.01.01 2021.06.30	SiO2								1					
	Cu-based pigments							1						
	Cu-based pigments							1						
	SiO2								1					
	Fe-based pigments									1				
	SiO2								1					
GUIDENANO (FP7) 2013.11.01 2017.04.30	TiO2		1											
	Al_2O_3-SiO_2								1				1	
	Nanocellulose						1							
	TiO2 in PP matrix		1											
	Multi-Walled Carbon Nanotubes (MWCNT) in PP matrix			1										
	TiO2 in PA matrix		1											
	MWCNT in PA matrix			1										
	TiO2 + Ag	1	1											
	ZnO				1									
	Silver Chloride (AgCl)	1												
NANOFARM (H2020) 2016.03.01 2019.02.28	Copper Hydroxide $Cu(OH)_2$							1						
NANOFASE (H2020) 2015.09.01 2019.08.31	Copper (Cu^0)							1						
	Copper (I) Oxide (Cu2O)							1						
	TiO2		1											
	Ag	1												
	Ag	1												
	TiO2		1											
	Iron (II,III) Oxide (Fe3O4)									1				
	TiO2		1											

	Nano-zero valent iron (Fe^0)									1				
NANOFATE (FP7) 2010.04.01 2014.03.31	Cerium Dioxide (CeO2)										1			
	ZnO				1									
	Ag	1												
	Ag	1												
NANOGECO (FP7) 2015.01.01 2017.12.31	Carbon Black (CB)			1										
	TiO2		1											
	ZnO				1									
NANOHOUSE (FP7) 2010.01.01 2013.06.30	TiO2		1											
	SiO2								1					
	Ag	1												
NANOMICEX (FP7) 2012.04.01 2015.03.31	Surface Modified ZnO (ZnO-BSA)				1									
	Al2O3												1	
	Iron (III) Oxide (Fe2O3)									1				
	TiO2 and ZnO water based mixtures		1		1									
	TiO2-ZnO dispersions		1		1									
	QDs coated with SiO2								1			1		
	Ag	1												
NANOPOLYTOX (FP7) 2010.05.01 2013.05.31	MWCNT			1										
	ZnO				1									
	TiO2		1											
	SiO2								1					
	Montmorillonite (MMT)					1								
	MMT (smaller size)					1								
NANOREG (FP7) 2013.03.01 2017.02.28	TiO2		1											
	Lithium Iron Phosphate (LFP)									1				
	C-based ENMs with lithium nickel manganese cobalt oxide (NMC)			1										
	TiO2		1											
	CeO2										1			
NANOSAFEPACK (FP7) 2011.12.01 2014.11.30	Layered Nanoclays					1								
	Ag	1												
	SiO2								1					
	ZnO				1									
	Calcium carbonate (CaCO3)													1
NANOSOLUTIONS (FP7) 2013.04.01 2017.03.31	Ag	1												
	TiO2		1											
	Copper oxide (CuO)							1						
	Nanodiamonds			1										
	MWCNT			1										
	Cadmium Telluride (CdTe) QDs											1		
	Gold (Au)													1
NANOSUSTAIN (FP7) 2010.05.01 2013.05.31	TiO2		1											
	ZnO				1									
	Carbon nanotubes (CNT) epoxy resin			1										
	Nanocellulose						1							
NANOTUN3D (H2020) 2015.10.01 2019.09.30	Silicon Carbide (SiC) nanoparticles with TiO2/Fe2O3/Fe3O4 shell		1	1					1	1				
	SiC nanoparticles with TiO2 shell		1	1					1					
	SiC nanoparticles with TiO2 shell mixed with Ti-6Al-4V		1	1					1				1	1
	SiC nanoparticles with TiO2 shell mixed with Ti-6Al-4V		1	1					1				1	1
	SiC nanoparticles with TiO2 shell mixed with Ti-6Al-4V		1	1					1				1	1
	SiC nanoparticles with TiO2 shell mixed with Ti-6Al-4V		1	1					1				1	1
NEPHH (FP7) 2009.09.01 2012.08.31	SiO2								1					
	MMT					1								
	Glass Fibers (GF)								1					
	Foam Glass Crystal Material (FGC)								1					
OPTINANOPRO (H2020)	Nanoclay					1								
	Nanotalc					1								

2015.10.01 2018.09.30	SiO2								1					
PLATFORM (H2020) 2015.02.01 2018.02.31	CNT			1										
	CNT			1										
	CNT			1										
POROUS4APP (H2020) 2016.03.01 2020.02.29	Nanoporous carbonaceous material (NCM)			1										
SANOWORK (FP7) 2012.03.01 2015.02.28	Ag	1												
	TiO2		1											
	Zirconium Dioxide (ZrO2)													1
	Nanofibers (NF) containning TiO2		1	1										
	Polyamide NF			1										
	CNT			1										
SCAFFOLD (FP7) 2012.05.01 2015.04.30	TiO2		1											
			1											
	SiO2								1					
	Carbon Nanofibers/Nanoclay			1		1								
	Nanoclay					1								
	Cellulose NF						1							
SUN (FP7) 2013.10.01 2017.03.31	WC-Co			1										1
	Basic Copper Carbonate (Cu2(OH)2CO3)			1				1						
	CuO							1						
	MWCNT			1										
	MWCNT			1										
	SiO2								1					
	TiO2		1											
	Iron Oxide (Fe2O3) inorganic pigment (Red 101)									1				
	Organic pigment (Red 254)													1
		13 10% Ag	33 26% Ti	30 24% C-based	10 8% Zn	10 8% Nanoclay	3 2% Nanocellulose	8 6% Cu	24 19% Si	7 6% Fe	2 2% Ce	3 2% Quantum Dots	7 6% Al	14 11% Others

ENMs production volumes

In Table S5, the production volumes estimated for several ENMs from two market reports, two French repositories for nanomaterials (ANSES, French) reports and two documents from the European commission are included. For the R-Nano, apart from the more recent report (2020), the one from the year 2013 was included because only in the first year (2013) the actual tonnages were reported. In later years, only a range with a factor of 10 was provided. It should be highlighted that the different reports included in the table estimated the production volumes for different geographical areas (i.e. Global, European and France) and the years are not the same for all. Therefore, the values do not serve for direct comparison, but allow obtaining an estimation of the relative production volume of the ENMs among them.

It should be emphasized that the aim of the paper is not to perform a research on production volumes. The values shown in section 4.2.1 were only included to provide an overview of the most commercially relevant ENMs to be compared with the results extracted from the inventory. However, the authors compiled production volumes from different sources, which can be of interest for the readers and for this reason are included in Table S5.

Table S5 – Production volumes provided by different sources for several ENMs. The values in bold are the ones used in the paper. The value used for nano-SiO2 used in the report was obtained from Wigger et al., not from a report. The reference for each of the reports is included at the end of the section.

ENM	CB market report (Europe, 2018) [Mt]	Future market report (Europe, 2018) [kt]	French repository (France, 2013) [kt]	French repository (France, 2019) [kt]	2nd regulatory review on NMs (Global, 2012) [kt]	3rd regulatory review on NMs (Europe, 2015) [kt]
Carbon Black	**2**	/	275	>10	9600	1480
Nano-SiO2	/	93	155	>10	1500	22
Nano-TiO2	/	**42**	14	>10	10	92
Nano-ZnO	/	**19**	0.29	0.10 – 0.01	8	0.2
Nanoclays	/	**10**	/	/	/	/
Nano-Ag	/	**0.24**	/	0.00010 – 0.00001	0.02	0.1

Agence nationale de sécurité sanitaire (ANSES), 2020. Éléments Issus Des Déclarations Des Substances À L'État Nanoparticulaire - RAPPORT D'ETUDE 2019.

Agence nationale de sécurité sanitaire (ANSES), 2013. Éléments Issus Des Déclarations Des Substances À L'État Nanoparticulaire, RAPPORT d'étude.

European Commission, 2016. Support for 3rd regulatory review on nanomaterials - Environmental legislation.

European Commission, 2012. Commission Staff Working Paper - Types and uses of nanomaterials, indcluding safety aspects. Accompanying the Communication from the Commission to the European Parliament, the Council and the European Economic and Social Committee on the Second Regulatory.

Future Markets Inc., 2016. The Global Nanotechnology and Nanomaterials Market Opportunity Report.

Grand View Research, 2020. Carbon Black Market Report.

NEPs registered in databases

In Table S6 the number of NEPs registered in different databases for different ENMs are compiled. The values are not aimed to be compared among databases, since the amount of the total products registered differ.

Table S6 – Number of NEPs, incorporating specific ENMs, registered in different databases. N.R. states for non-registered. Last check on 30/03/2021. The reference for each database is included at the end of the section.

ENM	The Nanodatabase	STATnano	Project on Emerging Nanotechnologies
Carbon Black	18	N.R	N.R
Nano-SiO2	58	364	44
Nano-TiO2	145	379	93
Nano-ZnO	26	2	38
Nanoclays	N.R	222	7
Nano-Ag	543	981	443

DTU Environment, the D.E.C. and D.C.C., 2020. The Nanodatabase [WWW Document]. URL http://nanodb.dk/ (accessed 1.11.21).

Nanotechnology Products Database [WWW Document], 2020. URL http://product.statnano.com/ (accessed 1.11.21).

Woodrow Wilson International Center for Scholars, 2020. Project on Emerging Nanotechnologies [WWW Document]. URL https://www.wilsoncenter.org/publication-series/project-emerging-nanotechnologies (accessed 1.11.21).

4. DISCUSSION

This discussion aims to highlight the implications of the most relevant outcomes from the results, as well as to integrate the scientific results included in the different sections, with the aim to produce targeted and applied research in line with the objectives of this PhD thesis.

In the first section of the discussion, the main contributions from each of the three different perspectives from which the risks associated to ENM and nano-enabled products have been studied are highlighted. Its relevance, as well as its potential impact, are discussed. In the second section, taking advantage that the last section of the results (3.3 – Nanosafety research in Europe and prioritization of studies) provides indications on which materials research should be prioritized, the outputs generated in the thesis are compared with those recommendations. Finally, in the last section of the discussion, the focus of the thesis on environmental exposure is described, as well as how the outputs are also relevant for hazard and human exposure.

4.1. Contributions to understanding the risks associated to ENM and NEP

4.1.1. Material flow model contributions

Within the context of this thesis, three main contributions were provided to the MF model:

Firstly, the incorporation of ENM production allocation in European countries based on the identification of the main producers and the countries where their production facilities are located. This innovative approach allows providing more realistic estimates than previous studies, in which for example, Gross Domestic Product (GDP) was used. Furthermore, an added value of this approach is that it not only allows allocating the production to a specific country but also to specific geographical coordinates (i.e. the production facility location). Although the updated model only provides values for countries as a whole, this advantage could be fully exploited in future work. The geographical resolution obtained in the updated model was possible thanks to the contributions of one of the institutions involved in the publication, the Nederlandse Organisatie voor Toegepast Natuurwetenschappelijk Onderzoek (TNO; English: Netherlands Organisation for Applied Scientific Research), who has previously demonstrated the capacity to integrate geographical resolutions around 7x7 km^2 in other models, using an approach previously applied for air quality (Kuenen et al., 2014). In addition, future work is foreseen by applying this methodology to other ENM, not only the three (nano-TiO_2, nano-ZnO and nano-Ag) considered in the publication.

Secondly, the product (nano-enabled products) distributions were also updated based on a market report (Adam and Nowack, 2017) supplemented with nanoregistration databases (Bund für Umwelt und Naturschutz Deutschland (BUND), 2011; DTU Environment - Danish Ecological Council and Danish Consumer Council, 2021; "StatNano - Nanotechnology Products Database," 2021; Woodrow Wilson International Center for Scholars, 2021). Product distributions are critical to further determine the potential releases. For this reason, its refinement is very relevant for the models to be able to provide more realistic outputs (predictions of the concentrations of ENM that will end up in the different environmental compartments). The importance of this upgrade should be highlighted because when MF models are upgraded (and presented in new publications), while new efforts are focused on the specific upgrades (e.g. incorporation of release forms, refinement of release rates), it is common to use the product allocations established in previous publications. Therefore, the values refined in the context of this thesis will also feed future and more upgraded MF models (as later explained), which increases the significance of the refinements presented.

Thirdly, in agreement with the co-authors and with the recommendations from the consortium of the project under which this study was performed (NANOFASE), a new European production volume for nano-Ag was established. This new consideration resulted in a prediction of environmental releases of nano-Ag about one order of magnitude lower than previously assessed, providing more realistic insights on the environmental releases of silver.

In the peer-reviewed publication, more upgrades on the MF model were presented, but since the contributions were provided by the co-authors, they are not included in this thesis. For more information and discussions on the other refinements, the publication can be consulted.

All these upgrades were built on top of the code developed by Bernd Nowack's research group and their collaborators over the years, which is one of the most advanced and complete MF models for predicting environmental releases of ENM and are among the co-authors. From the time of publishing, new versions of the model with new refinements, like the one described in Adam et al. 2021, have been published (Adam et al., 2021). As indicated in the extract from Adam et al. 2021, included in Figure 39, the new upgrades are adding up to the work presented in this thesis. As indicated by the pink arrow and text, not only the allocation to countries during production and manufacturing were reused, but also the product allocations (i.e. product categories). As indicated in Figure 39, information from MF models published in 2016 (Sun et al., 2016) is still relevant and is being considered, which is an example of how the data generated

and refined within the context of this thesis can have an impact on future upgrades of MF models.

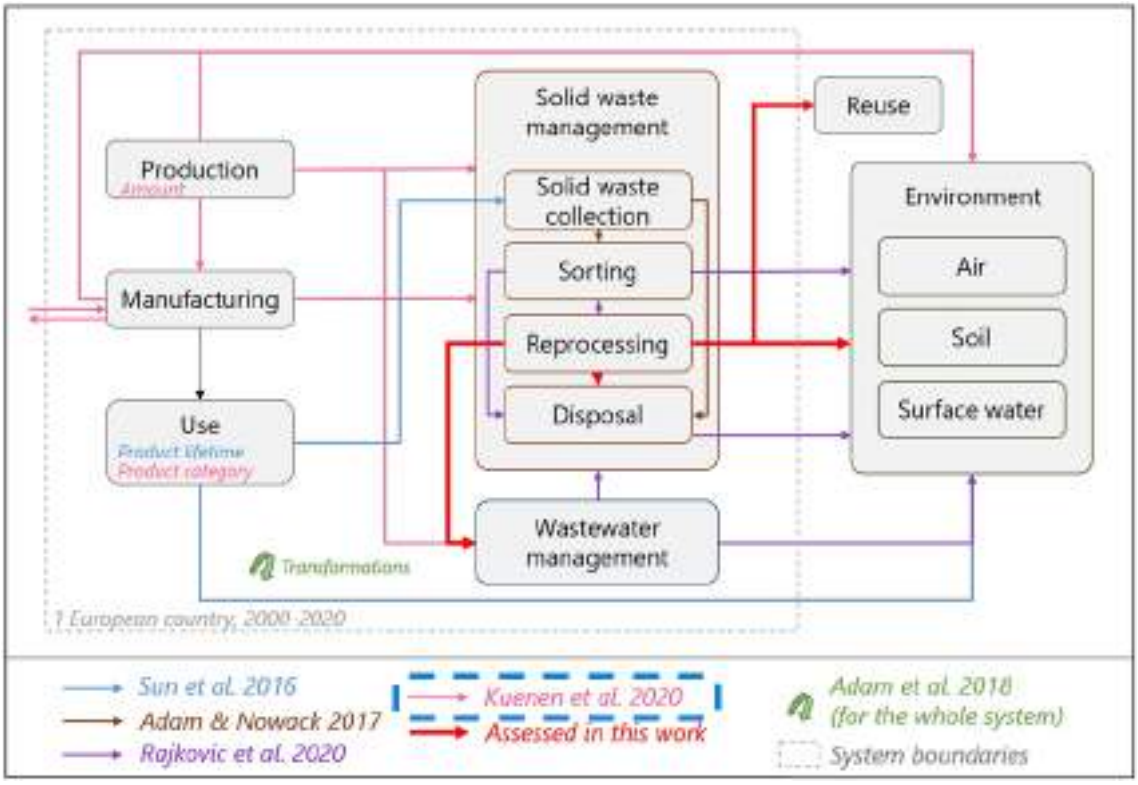

Figure 39 - Figure adapted from Adam et al. 2021 (Adam et al., 2021), representing the models in which the corresponding data were assessed by the colours of arrows and text. The model in the context of this thesis is represented in pink (Kuenen et al. 2020).

4.1.2. Release data generation from experimental simulations

An overview of the ENM, nano-enabled products and scenarios studied in this thesis, evaluating the critical scenarios to monitor potential ENM releases by experimental simulations is included in Figure 40. A total of seven different nano-enabled products were studied: asphalt coatings, camping tents, curtains, ink, polymeric nanocomposites, printed circuits and textiles. For each of the NEP, the most critical scenario was identified and evaluated accordingly, which resulted in five studies during the use phase stage and two during the end-of-life. In all the cases, the methodology was based on standardized protocols which were adapted to determine the release rates and release forms in each scenario.

Five different scenarios were experimentally evaluated in this thesis: leaching, printing, washing, weathering and a combination of weathering and abrasion. Exposure to humans was only evaluated during the printing experiments using ink containing PEG-CdTe QDs. For the rest of the scenarios, the evaluation was focused on assessing the potential environmental exposure of

the nano-enabled products under study. Therefore, the experimental work was mainly focused on assessing environmental exposure, although human exposure assessment was also considered.

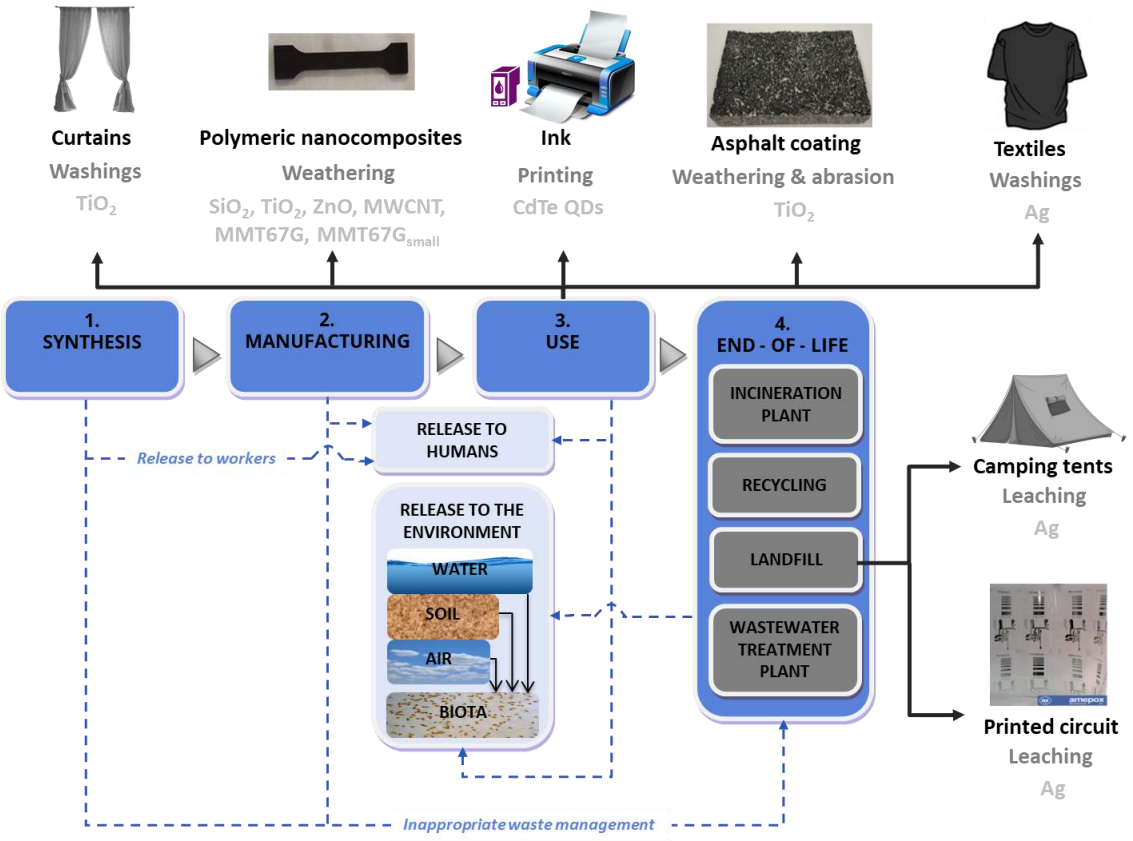

Figure 40 – Overview of the ENM, NEP and scenarios.

The main outcomes from the studies presented in this section of the thesis are release rates and release forms during the life cycle of different nano-enabled products, which then can be used to determine the potential risks (via realistic fate and exposure assessment determination) that ENM may pose to humans and the environment. The main uses of the data generated are described here below:

- ***Inputs for nano-specific modelling tools***: The values generated experimentally can be used to generate and refine the inputs for material flow models like the one developed in the first peer-reviewed publication included in this thesis. However, MF models are not the only modelling tools available to generate information for further predicting the potential risks of ENM. Multiple initiatives are focusing on the development of tools for ENM risk assessment and risk management during their whole life cycle, which require inputs from the experimental studies (Koivisto et al., 2017; Pietroiusti et al., 2018). Whereas the release rates values generated are needed to determine the exposure, the

release forms contribute to determining the hazard. Therefore, the data generated is needed to run those models and assessing the potential risks of ENM.

- ***Safe-by-design***: Release data provides to ENM producers and manufacturers information on the potential risk that specific NEP can present in further stages of the life cycle. This information provides insights to tackle safety issues that can then be addressed from the design phase, what is known as safe-by-design (SbD) (van de Poel and Robaey, 2017). The development of materials that are safe to humans and the environment from the early stages of the innovation process offers tremendous advantages (e.g. lower uncertainty of the risks, higher product value, increased stakeholder confidence, preparedness for future regulation, etc) (Sánchez Jiménez et al., 2020). In addition, release data from different nano-enabled products provide insights for the search for safer solutions and alternatives for those materials causing a problem of high release. Consequently, all the knowledge compiled on safety issues of ENM, including release data is currently being used to contribute to the development of new SbD approaches, becoming a central concern of several EU-funded nanosafety projects (Schwarz-Plaschg et al., 2017), highlighting the relevance of data generation.

- ***Release assessment methodology***: As previously stated, the protocols used in the experimental studies are based on standardized protocols adapted to monitor ENM releases. Since comprehensive methodologies for release determination are not available yet for many scenarios (Koivisto et al., 2017), release simulation studies offer the possibility to test different approaches and to disseminate the knowledge on specific adaptations to generate relevant data in a reliable and reproducible way. Knowledge of relevant characterisation techniques, as well as release sample preparation for its characterization are also significant outputs for the nanosafety field.

Release data is scarce and generally scattered among multiple publications and reports, which makes it difficult for its applicability for human and environmental exposure modelling to ENM and the associated risks (Koivisto et al., 2017). Thus, with the aim of facilitating the data usage, the most relevant outcomes from all the experimental results generated within the thesis have been compiled in Table 9. In the table, the NEP, the ENM incorporated and the scenarios studied are summarized, including the respective release rates (indicating when possible the time or process variable – e.g. in one year, in 10 washing), the release forms and the compartment

(human or environmental) where release is more likely to go. This data was also included in publically accessible databases to be used by the entire nanosafety community. Thus, following the FAIR (findability, accessibility, interoperability, and reusability) data policies implemented by the European Commission.

Table 9 – Summary table of experimental results generated within the thesis containing the release rates, release forms and compartments where release from the different case studies is more likely to go to. NEP: Nano-enabled product; ENM: Engineered nanomaterial; LCS: Life cycle stage.

NEP	ENM	LCS STUDIED	RELEASE RATE	RELEASE FORM	COMPARTMENT
Camping tents (1 coating)	Ag-PEI NPs	End of life (leaching)	183 ± 3 (Ag µg / textile m^2) 1.07 ± 0.02%	Ionic (Ag^+): 41 ± 0% <20 µm: 37 ± 6% >20 µm: 22 ± 2%	Soil
Camping tents (2 coatings)	Ag-PEI NPs	End of life (leaching)	161 ± 7 (Ag µg / textile m^2) 0.53 ± 0.02%	Ionic (Ag^+): 45 ± 4% <20 µm: 36 ± 2% >20 µm: 19 ± 4%	Soil
Curtains	TiO_2	Use (washing)	9 ± 2 % (in 10 washings)	TiO_2 Aggregate	WWTP
Antibacterial textile	Ag-PVP NPs	Use (washing)	70 ± 2 % (in 10 washings)	Ionic (Ag^+)	WWTP
Antibacterial textile	Ag-PVP NWs (~3 µm)	Use (washing)	59 ± 9 % (in 10 washings)	Ionic (Ag^+) and free NWs	WWTP
Antibacterial textile	Ag-PVP NWs (~30 µm)	Use (washing)	73 ± 2 % (in 10 washings)	Ionic (Ag^+) and free NWs	WWTP
Asphalt coating	TiO_2	Use (weathering	38% (the first year)	0.5 – 5 µm TiO_2 aggregates	WWTP or directly to

		and wheel abrasion)			rivers and soil
Printed circuit	Ag	End of life (leaching)	11.1 ± 2.3 %	Ionic (Ag^+): 0.3 ± 0.1% <0.45 µm: 6.4 ± 0.7% <20 µm: 12.1 ± 3.0% >20 µm: 81.1 ± 3.9%	Soil
Fluorescent ink	PEG-CdTe QDs	Use (printing)	453 (particles / cm^3) (in 10 min)	PEG-CdTe QDs aggregates in ink droplets	Humans
Polymeric nanocomposite	SiO_2	Use (weathering)	62 ± 9 (SiO_2 mg / polymer m^2) 0.0057 ± 0.0009% (the first year)	Embedded in polymer	WWTP or directly to rivers and soil
Polymeric Nanocomposite	TiO_2	Use (weathering)	47 ± 9 (TiO_2 mg / polymer m^2) 0.0043 ± 0.0008% (the first year)	Embedded in polymer	WWTP or directly to rivers and soil
Polymeric Nanocomposite	ZnO	Use (weathering)	474 ± 26 (ZnO mg / polymer m^2) 0.0429 ± 0.0023% (the first year)	Embedded in polymer and free aggregates	WWTP or directly to rivers and soil
Polymeric Nanocomposite	MWCNT	Use (weathering)	865 ± 75 (MWCNT mg / polymer m^2) 0.0765 ± 0.0065% (the first year)	Embedded in polymer and free MWCNT	WWTP or directly to rivers and soil

Polymeric Nanocomposite	Nanoclay (MMT67G)	Use (weathering)	71 ± 22 (67G mg / polymer m^2) 0.0067 ± 0.0021% (the first year)	Free nanoclays	WWTP or directly to rivers and soil
Polymeric Nanocomposite	Nanoclay (MMT67G_{small})	Use (weathering)	139 ± 35 (67G_{small} mg / polymer m^2) 0.0130 ± 0.0032% (the first year)	Free nanoclays	WWTP or directly to rivers and soil

4.1.3. Nanosafety research in Europe – Towards a focus on nano-enabled products

In the work presented in the fourth peer-reviewed publication, the data compiled can not be specifically used to perform any risk assessment. However, the outcomes can be used to increase the relevance of future studies and to evaluate the impact that data previously generated can have, as is described in the next section.

4.2. Materials prioritization in the studies

The information compiled in the fourth peer-reviewed publication regarding Nanosafety research in Europe presented the opportunity to analyze where most of the efforts were focused on the past, at the same time providing indications on where future research should aim and which are still the main gaps.

The fourth peer-reviewed publication is the last one published (available online 15 May 2021). Therefore, when it was written, the knowledge and information gathered during the previous years of the PhD could be used and described in the manuscript. Furthermore, since the aim was to provide an overview of Nanosafety research in Europe, it allowed to reflect on general aspects of nanosafety, and consequently, on most of the topics included in this thesis. For this reason, it is a useful paper to take as a basis for discussion on the information generated within the context of the whole PhD and its relevance for the nanosafety field.

As discussed in Pomar-Portillo et al. (fourth peer-reviewed publication) (Pomar-Portillo et al., 2021), studies should be prioritized on those materials with higher market relevance, which can

be identified by analyzing the ENM's production volumes and their main applications (summarized in Table 10).

Table 10 – Annual production volumes and main applications of most produced ENM and nano-silver in Europe. Data extracted from Pomar-Portillo et al. (Pomar-Portillo et al., 2021).

ENM	Annual production volume in Europe (Kilotonnes)	Main application
Carbon Black	2000	Tyres manufacture
SiO_2	459	Reinforcement additive (including tyres)
TiO_2	42	Sunscreens
ZnO	19	Sunscreens
Ag	0.240	Printed electronics

In the MF model presented in the first peer-reviewed publication, two of the four most relevant ENM were considered (nano-TiO_2 and nano-ZnO), reflecting the relevance of the analysis performed. In the case of nano-Ag (the third ENM considered in the MF model presented), although its market relevance is not high, it is among the most studied ENM, both in terms of release monitoring in different exposure scenarios along their life cycle and of material flow analysis, which allowed building the model on available information from previous studies. Furthermore, the main outputs of the work remain in the methodology developed, which can be applied to any ENM and even to other chemicals or substances.

Regarding the relevance of the experimental studies, as shown in Figure 40, a total of eight different ENM were studied in this thesis. When those ENM are compared with most produced ENM in Europe compiled in Table 10, all the ENM except Carbon Black are represented. Regarding its main applications, nano-SiO_2 was incorporated in a polymeric nanocomposite as a reinforcement additive. Thus, representing its main application. However, in the case of nano-TiO_2 and nano-ZnO, they were incorporated in polymeric nanocomposites (both nano-TiO_2 and nano-ZnO), curtains (only nano-TiO_2) and asphalt coating (only nano-TiO_2) due to its photocatalytic activity. Therefore, its main application (as sunscreen) was not considered. Nevertheless, it should be highlighted that release studies on commercial sunscreens containing nano-TiO_2 and nano-ZnO were performed within the research group (LEITAT – Materials Safety group) but not performed by the author of the thesis, for this reason they were not included in the results section. The studies were reported as part of an European Project deliverable

(together with some of the studies included in this thesis) (Pomar-Portillo, 2019) and are being refined for publication in a peer-reviewed journal.

Three of the seven NEP studied contained nano-Ag (textiles, camping tents and printed circuits). As argumented in Pomar-Portillo et al., such a high amount of studies may not be justified given the low production volumes of nano-Ag. However, since in the projects industrial partners were producing the NEP containing nano-Ag, it was a good opportunity to perform experiments with well-known materials since information as composition or production processes was available. At the same time, control materials (without ENM) could also be obtained, which were extremely important for the studies and are not generally available for commercial NEP. Furthermore, printed electronics, which is nano-Ag's main application was included, providing more relevance to the studies performed.

All in all, most of the ENM and NEP selected during the different experimental release studies included in the thesis were in line with the principle of focusing on those materials with higher market relevance. When those requirements were not accomplished (mainly in studies involving nano-Ag), the reasoning for performing such studies was justified.

4.3. Focus on environmental exposure

In order to characterise the risk of a specific substance both exposure and hazard need to be assessed, as described in the introduction (section 1.2.1 – Risk definition and assessment). In this thesis, the focus has been put on exposure, not on hazard, although some of the outcomes generated are useful for both. Furthermore, the emphasis was on exposure to the environment, more than to humans, although both have been considered.

The MF model provided insights on potential exposure to the environment. The outcomes from the model were ENM concentrations (tonnes/km^2) in different environmental compartments due to release. From these data, via realistic fate and exposure assessment, PEC could be derived, which combined with PNEC values generated from hazard studies, could be used to determine the potential risk that nano-TiO_2, -ZnO and -Ag releases could pose to the environment. In this case, only concentrations in the environment were reported. However, a similar approach could be applied to determine exposure to humans. Therefore, although the peer-reviewed publication does not provide exposure values to humans, part of the methodology developed and the values refined could be used for that purpose.

Regarding the release data generation from the experimental studies, as mentioned in section 4.2, from the 7 experimental studies, one of them was focused on humans (i.e. exposure to ink containing QDs during household printing), while for the other six, the compartment where release was expected to arrive was the environment. The main outputs from the experiments were release rates and release forms. Whereas release rates are used to determine the exposure, release forms provide relevant insights for both hazard and exposure. Regarding hazard, different release forms imply different physicochemical properties, which has a direct impact on the hazard that the substance may produce. In terms of exposure, the physicochemical properties dictate the behaviour of the substance in the compartments it goes through (e.g. air, water, soil) before reaching humans or the environment, which provides information on the potential exposure. For example, depending on the physicochemical properties, a substance will experience different sedimentation rates and heteroaggregation in natural waters, which will impact the potential transport of this substance and further exposure to specific organisms (Fang et al., 2017; Quik et al., 2014). For this reason, an exhaustive characterization of the released materials generated in the experiments is extremely beneficial to determine the risk.

The work presented in the last peer-reviewed publication (Nanosafety research in Europe - Towards a focus on nano-enabled products) does not specifically contribute to neither exposure nor hazard. It provides a general picture that can be beneficial for the whole nanosafety community (whether it is focused on hazard, exposure or other nanosafety-related topics).

5. CONCLUSIONS

As presented in the results section and further described in the discussion, multiple outcomes have been generated towards the achievement of the objective - "*to provide relevant information on engineered nanomaterials release from nano-enabled products in order to increase the knowledge on the potential risks that ENM may pose to humans and the environment*". Therefore, the objective is considered as achieved. The main conclusions that can be derived from this Thesis are described here below.

Material Flow models are a very useful tool for predicting the environmental concentrations of ENM since they have the capacity to consider the complexity and variations that ENM may experience along their life cycle (e.g. physicochemical transformations, incorporation in different products). The environmental concentrations predictions provided in the publication are useful and together with toxicity data can help to determine the risk that specific ENM can produce. However, the main outcomes of the work on the MF model remains on the Methodology developed, which can further be applied to other ENM or even other types of substances. Indeed, the refinements presented are already being used in upgraded versions of the MF model to determine environmental concentrations of different ENM.

Release experiments were performed with a high variety of nano-enabled products. An exhaustive characterisation was done in all the cases on both starting materials (ENM before being incorporated in the product), in the nano-enabled products before and after the respective experiments, and also on the released materials. The main outcomes were release rates and release forms, which were included in publically accessible databases to be used by the entire nanosafety community.

To the author's knowledge, the review of NEP studied in nanosafety projects funded by the European Commission presented within the context of this thesis, was the first comprehensive review made on this topic. Based on the data compiled, the current status of nanosafety research in Europe and an overview to identify where the gaps are with respect to the following key aims were provided: (i) commercialisation balance against risk, (ii) transparency on use of NEPs/ENMs including production volumes and (iii) clarity on the safe use and identified risks. In addition, the inventory also provided a rich source of information from which readers with different data needs can extract their own conclusions, providing relevant insights for the nanosafety community.

Although there are many uncertainties yet about the risks that ENMs may present, the nanosafety community is devoting many efforts to understanding its potential impacts. The purpose is to predict the potential risks before they occur, which have not been the case for many of the substances which are of concern nowadays (e.g. microplastics or pesticides). Nevertheless, it is important that a big focus on nanosafety studies does not lead to the general public to unjustified concern about ENM and NEP, but to foster its development by ensuring with a scientific basis that the advantages that it can provide are not in return of negative impacts to humans and the environment.

6. REFERENCES

Abbott, L.C., Maynard, A.D., 2010. Exposure Assessment Approaches for Engineered Nanomaterials. Risk Analysis 30, 1634–1644. https://doi.org/10.1111/J.1539-6924.2010.01446.X

Adam, V., Caballero-Guzman, A., Nowack, B., 2018. Considering the forms of released engineered nanomaterials in probabilistic material flow analysis. Environmental Pollution 243, 17–27. https://doi.org/10.1016/j.envpol.2018.07.108

Adam, V., Nowack, B., 2017. European country-specific probabilistic assessment of ENM flows towards landfilling, incineration and recycling, Environ. Sci.: Nano. https://doi.org/10.1039/C7EN00487G

Adam, V., Wu, Q., Nowack, B., 2021. Integrated dynamic probabilistic material flow analysis of engineered materials in all European countries. NanoImpact 100312. https://doi.org/10.1016/j.impact.2021.100312

Alenius, H., Norppa, H., Pylkkänen, L., Tuomi, T., Kasper, G., 2010. Risk assessment of engineered nanomaterials and nanotechnologies—A review. Toxicology 269, 92–104. https://doi.org/10.1016/J.TOX.2010.01.013

American Chemistry Council, 2021. Exposure | Terms and Definitions [WWW Document]. URL https://www.endocrinescience.org/glossary/exposure/ (accessed 9.7.21).

Bach, S., Schmidt, E., 2008. Determining the dustiness of powders--a comparison of three measuring devices. The Annals of occupational hygiene 52, 717–25. https://doi.org/10.1093/annhyg/men062

Baran, P., Quicker, P., 2017. Verbleib und Verhalten von Nanopartikeln bei der Abfallverbrennung. Österreichische Wasser- und Abfallwirtschaft 69, 51–65. https://doi.org/10.1007/s00506-016-0362-z

Besinis, A., de Peralta, T., Handy, R.D., 2014. The antibacterial effects of silver, titanium dioxide and silica dioxide nanoparticles compared to the dental disinfectant chlorhexidine on *Streptococcus mutans* using a suite of bioassays. Nanotoxicology 8, 1–16. https://doi.org/10.3109/17435390.2012.742935

Binnig, G., Rohrer, H., 1983. Scanning tunneling microscopy. Surface Science 126, 236–244. https://doi.org/10.1016/0039-6028(83)90716-1

Bornhöft, N.A., Sun, Y., Hilty, L.M., Nowack, B., 2016. A dynamic probabilistic material flow modeling method. Environmental Modelling and Software 76, 69–80. https://doi.org/10.1016/j.envsoft.2015.11.012

Bouillard, J.X., R'Mili, B., Moranviller, D., Vignes, A., le Bihan, O., Ustache, A., Bomfim, J.A.S., Frejafon, E., Fleury, D., 2013. Nanosafety by design: Risks from nanocomposite/nanowaste combustion. Journal of Nanoparticle Research 15. https://doi.org/10.1007/s11051-013-1519-3

Bund für Umwelt und Naturschutz Deutschland (BUND), 2011. Datenbank für Nano-Produkte [WWW Document]. URL http://archiv.bund.net/nc/themen_und_projekte/nanotechnologie/nanoproduktdatenbank/produktsuche/ (accessed 1.14.20).

Caballero-Guzman, A., Sun, T., Nowack, B., 2015. Flows of engineered nanomaterials through the recycling process in Switzerland. Waste Management 36, 33–43. https://doi.org/10.1016/j.wasman.2014.11.006

Dale, A.L., Casman, E.A., Lowry, G. v, Lead, J.R., Viparelli, E., Baalousha, M., 2015. Modeling Nanomaterial Environmental Fate in Aquatic Systems. Environ. Sci. Technol 25, 5. https://doi.org/10.1021/es505076w

Dallas, P., Sharma, V.K., Zboril, R., 2011. Silver polymeric nanocomposites as advanced antimicrobial agents: Classification, synthetic paths, applications, and perspectives. Advances in Colloid and Interface Science 166, 119–135. https://doi.org/10.1016/j.cis.2011.05.008

Ding, Y., Kuhlbusch, T.A.J., van Tongeren, M., Jiménez, A.S., Tuinman, I., Chen, R., Alvarez, I.L., Mikolajczyk, U., Nickel, C., Meyer, J., Kaminski, H., Wohlleben, W., Stahlmecke, B., Clavaguera, S., Riediker, M., 2017a. Airborne engineered nanomaterials in the workplace—a review of release and worker exposure during nanomaterial production and handling processes. Journal of Hazardous Materials 322, 17–28. https://doi.org/10.1016/j.jhazmat.2016.04.075

Ding, Y., Wohlleben, W., Boland, M., Vilsmeier, K., Riediker, M., 2017b. Nano-object Release During Machining of Polymer-Based Nanocomposites Depends on Process Factors and the Type of Nanofiller. Annals of Work Exposures and Health 61, 1132–1144. https://doi.org/10.1093/annweh/wxx081

Drexler, K.E., 1981. Molecular engineering: An approach to the development of general capabilities for molecular manipulation. Proceedings of the National Academy of Sciences 78, 5275–5278. https://doi.org/10.1073/pnas.78.9.5275

DTU Environment - Danish Ecological Council and Danish Consumer Council, 2021. The Nanodatabase [WWW Document]. URL http://nanodb.dk/ (accessed 1.11.21).

Dulger, M., Sakallioglu, T., Temizel, I., Demirel, B., Copty, N.K., Onay, T.T., Uyguner-Demirel, C.S., Karanfil, T., 2016. Leaching potential of nano-scale titanium dioxide in fresh municipal solid waste. Chemosphere 144, 1567–1572. https://doi.org/10.1016/j.chemosphere.2015.10.037

EcoMole, 2021. REACH Online - RISK CHARACTERISATION [WWW Document]. URL https://reachonline.eu/reach/en/annex-i-6.html?kw=exposure-scenario#anch--exposure-scenario (accessed 9.17.21).

European Chemicals Agency (ECHA), 2016. Guidance on information requirements and chemical safety assessment chapter R.16: Environmental exposure estimation. 3.0 ed. Helsinki, Finland.

European Commission, 2008. Directive 2008/98/EC of the European Parliament and of the Council of 19 November 2008 on Waste and Repealing Certain Directives.

European Commission, 2006. Regulation (EC) No 1907/2006 - Registration, Evaluation, Authorisation and Restriction of Chemicals (REACH).

European Commission, 2004. THE SIXTH FRAMEWORK WORK PROGRAMME - Nanotechnology and nanosciences, knowledge-based multifunctional materials, new production processes and devices.

European Environment Agency, 2018. Air quality in Europe — 2018 report.

European Standards, 2003. EN 12457-4: Characterisation of waste. Leaching. Compliance test for leaching of granular waste materials and sludges. Part 4: One stage batch test at a liquid to solid ratio of 10 l/kg for materials with particle size below 10mm.

Fang, J., Shijirbaatar, A., Lin, D. hui, Wang, D. jun, Shen, B., Sun, P. de, Zhou, Z. qing, 2017. Stability of co-existing ZnO and TiO2 nanomaterials in natural water: Aggregation and sedimentation mechanisms. Chemosphere 184, 1125–1133. https://doi.org/10.1016/J.CHEMOSPHERE.2017.06.097

Ferraris, S., Perero, S., Miola, M., Vernè, E., Rosiello, A., Ferrazzo, V., Valletta, G., Sanchez, J., Ohrlander, M., Tjörnhammar, S., Fokine, M., Laurell, F., Blomberg, E., Skoglund, S., Odnevall Wallinder, I., Ferraris, M., 2014. Chemical, mechanical and antibacterial properties of silver nanocluster/silica composite coated textiles for safety systems and aerospace applications. Applied Surface Science 317, 131–139. https://doi.org/10.1016/j.apsusc.2014.07.196

Fonseca, A.S., Viitanen, A.-K., Kanerva, T., Säämänen, A., Aguerre-Chariol, O., Fable, S., Dermigny, A., Karoski, N., Fraboulet, I., Koponen, I.K., Delpivo, C., Vilchez Villalba, A., Vázquez-Campos, S., Østerskov Jensen, A.C., Hjortkjær Nielsen, S., Sahlgren, N., Clausen, P.A., Xuan Nguyen Larsen, B., Kofoed-Sørensen, V., Alstrup Jensen, K., Koivisto, J., 2021. Occupational Exposure and Environmental Release: The Case Study of Pouring TiO2 and Filler Materials for Paint Production. International Journal of Environmental Research and Public Health . https://doi.org/10.3390/ijerph18020418

Giese, B., Klaessig, F., Park, B., Kaegi, R., Steinfeldt, M., Wigger, H., von Gleich, A., Gottschalk, F., 2018. Risks, Release and Concentrations of Engineered Nanomaterial in the Environment. Scientific Reports 8. https://doi.org/10.1038/s41598-018-19275-4

Golanski, L., Gaborieau, A., Guiot, A., Uzu, G., Chatenet, J., Tardif, F., 2011. Characterization of abrasion-induced nanoparticle release from paints into liquids and air. Journal of Physics: Conference Series 304, 012062. https://doi.org/10.1088/1742-6596/304/1/012062

Gottschalk, F., Lassen, C., Kjoelholt, J., Christensen, F., Nowack, B., 2015. Modeling Flows and Concentrations of Nine Engineered Nanomaterials in the Danish Environment. Int. J. Environ. Res. Public Health International Journal of Environmental Research and Public Health 12, 5581–5602. https://doi.org/10.3390/ijerph120505581

Gottschalk, F., Scholz, R.W., Nowack, B., 2010. Probabilistic material flow modeling for assessing the environmental exposure to compounds: Methodology and an application to engineered nano-TiO2 particles. Environmental Modelling & Software 25, 320–332. https://doi.org/10.1016/j.envsoft.2009.08.011

Gottschalk, F., Sonderer, T., Scholz, R.W., Nowack, B., 2009. Modeled Environmental Concentrations of Engineered Nanomaterials (TiO2, ZnO, Ag, CNT, Fullerenes) for Different Regions. Environmental Science & Technology 43, 9216–9222. https://doi.org/10.1021/es9015553

Hajipour, M.J., Fromm, K.M., Akbar Ashkarran, A., Jimenez de Aberasturi, D., Larramendi, I.R. de, Rojo, T., Serpooshan, V., Parak, W.J., Mahmoudi, M., 2012. Antibacterial properties of nanoparticles. Trends in Biotechnology 30, 499–511. https://doi.org/10.1016/j.tibtech.2012.06.004

Hamelmann, F., Schmidt, E., 2003. Methods of estimating the dustiness of industrial powders – A review. KONA Powder and Particle Journal. https://doi.org/10.14356/kona.2003006

Hochella, M.F., Mogk, D.W., Ranville, J., Allen, I.C., Luther, G.W., Marr, L.C., McGrail, B.P., Murayama, M., Qafoku, N.P., Rosso, K.M., Sahai, N., Schroeder, P.A., Vikesland, P., Westerhoff, P., Yang, Y., 2019. Natural,

incidental, and engineered nanomaterials and their impacts on the Earth system. Science. https://doi.org/10.1126/science.aau8299

Holder, A.L., Vejerano, E.P., Zhou, X., Marr, L.C., 2013. Nanomaterial disposal by incineration. Environ. Sci.: Processes Impacts 15, 1652–1664. https://doi.org/10.1039/C3EM00224A

International Standards Organization, 2019. ISO 21546:2019 Paints and varnishes -- Determination of the resistance to rubbing using a linear abrasion tester (crockmeter).

International Standards Organization, 2018. ISO 45001:2018 Occupational health and safety management systems — Requirements with guidance for use.

International Standards Organization, 2016. ISO 5470-1:2016 Rubber- or plastics-coated fabrics -- Determination of abrasion resistance -- Part 1: Taber abrader.

International Standards Organization, 2015. ISO/TS 80004-1:2015 Nanotechnologies — Vocabulary — Part 1: Core terms.

International Standards Organization, 2013. ISO 4892-2:2013 Plastics – Methods of exposure to laboratory light sources – Part 2: Xenon-arc lamps. International Standards Organization.

International Standards Organization, 2010. ISO 105-C06:2010 Textiles -- Tests for colour fastness -- Part C06: Colour fastness to domestic and commercial laundering.

International Standards Organization, 2007. EN 12697-22:2003 +A1:2007 Bituminous mixtures. Test methods for hot mix asphalt - Part 22: wheel tracking.

International Standards Organization, 2003. ISO 5470-2:2003 Rubber- or plastics-coated fabrics -- Determination of abrasion resistance -- Part 2: Martindale abrader.

International Union of Pure and Applied Chemistry (IUPAC), 2001. Hazard and Risk.

Kaegi, R., Englert, A., Gondikas, A., Sinnet, B., von der Kammer, F., Burkhardt, M., 2017. Release of TiO2 – (Nano) particles from construction and demolition landfills. NanoImpact 8, 73–79. https://doi.org/10.1016/j.impact.2017.07.004

Kaegi, R., Voegelin, A., Sinnet, B., Zuleeg, S., Hagendorfer, H., Burkhardt, M., Siegrist, H., 2011. Behavior of metallic silver nanoparticles in a pilot wastewater treatment plant. Environmental Science and Technology 45, 3902–3908. https://doi.org/10.1021/es1041892

Keller, A.A., McFerran, S., Lazareva, A., Suh, S., 2013. Global life cycle releases of engineered nanomaterials. Journal of Nanoparticle Research 15, 1692. https://doi.org/10.1007/s11051-013-1692-4

Kiser, M.A., Westerhoff, P., Benn, T., Wang, Y., Pérez-Rivera, J., Hristovski, K., 2009. Titanium nanomaterial removal and release from wastewater treatment plants. Environmental Science and Technology 43, 6757–6763. https://doi.org/10.1021/es901102n

Koivisto, A.J., Jensen, A.C.Ø., Kling, K.I., Nørgaard, A., Brinch, A., Christensen, F., Jensen, K.A., 2017. Quantitative material releases from products and articles containing manufactured nanomaterials: Towards a release library. NanoImpact 5, 119–132. https://doi.org/10.1016/j.impact.2017.02.001

Kuenen, J., Pomar-Portillo, V., Vilchez, A., Visschedijk, A., Denier Van Der Gon, H., Vázquez-Campos, S., Nowack, B., Adam, V., 2020. Inventory of country-specific emissions of engineered nanomaterials throughout the life cycle. Environmental Science: Nano 7, 3824–3839. https://doi.org/10.1039/d0en00422g

Kuenen, J.J.P., Visschedijk, A.J.H., Jozwicka, M., Denier Van Der Gon, H.A.C., 2014. TNO-MACC_II emission inventory; a multi-year (2003-2009) consistent high-resolution European emission inventory for air quality modelling. Atmos. Chem. Phys 14, 10963–10976. https://doi.org/10.5194/acp-14-10963-2014

Kuijpers, E., Pronk, A., Koivisto, A.J., Jensen, K.A., Vermeulen, R., Fransman, W., 2019. Relative Differences in Concentration Levels during Sawing and Drilling of Car Bumpers Containing MWCNT and Organic Pigment. Annals of Work Exposures and Health 63, 148–157. https://doi.org/10.1093/annweh/wxy101

Kvitek, L., Panacek, A., Prucek, R., Soukupova, J., Vanickova, M., Kolar, M., Zboril, R., 2011. Antibacterial activity and toxicity of silver – nanosilver versus ionic silver. Journal of Physics: Conference Series 304, 012029. https://doi.org/10.1088/1742-6596/304/1/012029

Lombi, E., Donner, E., Tavakkoli, E., Turney, T.W., Naidu, R., Miller, B.W., Scheckel, K.G., 2012. Fate of zinc oxide nanoparticles during anaerobic digestion of wastewater and post-treatment processing of sewage sludge. Environmental Science and Technology 46, 9089–9096. https://doi.org/10.1021/es301487s

Memon, H., Yasin, S., Ali Khoso, N., Hussain, M., 2015. Indoor Decontamination Textiles by Photocatalytic Oxidation: A Review. Journal of Nanotechnology 2015, 1–9. https://doi.org/10.1155/2015/104142

Mitrano, D.M., Limpiteeprakan, P., Babel, S., Nowack, B., Cheever, B., Frost, P.C., Xenopoulos, M.A., Hintelmann, H., Metcalfe, C.D., Thiel, S., 2016. Durability of nano-enhanced textiles through the life cycle: releases from landfilling after washing. Environ. Sci.: Nano 3, 375–387. https://doi.org/10.1039/C6EN00023A

Morimoto, Y., Kobayashi, N., Shinohara, N., Myojo, T., Tanaka, I., Nakanishi, J., 2010. Hazard Assessments of Manufactured Nanomaterials. Journal of Occupational Health 52, 325–334. https://doi.org/10.1539/JOH.R10003

Muñoz-García, J., Vázquez, L., Castro, M., Gago, R., Redondo-Cubero, A., Moreno-Barrado, A., Cuerno, R., 2014. Self-organized nanopatterning of silicon surfaces by ion beam sputtering. Materials Science and Engineering: R: Reports 86, 1–44. https://doi.org/10.1016/J.MSER.2014.09.001

Nored, A.W., Chalbot, M.-C.G., Kavouras, I.G., 2018. Characterization of paint dust aerosol generated from mechanical abrasion of TiO_2 -containing paints. Journal of Occupational and Environmental Hygiene 15, 629–640. https://doi.org/10.1080/15459624.2018.1484126

Norio, T., 1974. On the Basic Concept of “Nano-Technology,” in: Proceedings of the International Conference on Production Engineering (Ed.), . Proceedings of the International Conference on Production Engineering, Tokyo.

Oberdörster, G., Maynard, A., Donaldson, K., Castranova, V., Fitzpatrick, J., Ausman, K., Carter, J., Karn, B., Kreyling, W., Lai, D., Olin, S., Monteiro-Riviere, N., Warheit, D., Yang, H., 2005. Principles for characterizing the potential human health effects from exposure to nanomaterials: Elements of a screening strategy. Particle and Fibre Toxicology. https://doi.org/10.1186/1743-8977-2-8

OECD Glossary of Statistical Terms - Toxicity Definition [WWW Document], 2021. URL https://stats.oecd.org/glossary/detail.asp?ID=2734 (accessed 9.9.21).

Ogura, I., Kotake, M., Ata, S., 2019. Quantitative evaluation of carbon nanomaterial releases during electric heating wire cutting and sawing machine cutting of expanded polystyrene-based composites using thermal carbon analysis. Journal of Occupational and Environmental Hygiene 16, 165–178. https://doi.org/10.1080/15459624.2018.1540874

Oischinger, J., Meiller, M., Daschner, R., Hornung, A., Warnecke, R., 2019. Fate of nano titanium dioxide during combustion of engineered nanomaterial-containing waste in a municipal solid waste incineration plant. Waste Management & Research 37, 1033–1042. https://doi.org/10.1177/0734242X19862603

Organisation for Economic Co-operation and Development (OECD), 2008. Measuring material flows and resource productivity - The OECD Guide.

Oxford Advanced Learner's Dictionary, 2021a. Hazard - Definition [WWW Document]. URL https://www.oxfordlearnersdictionaries.com/definition/english/hazard_1?q=hazard (accessed 5.26.21).

Oxford Advanced Learner's Dictionary, 2021b. Exposure - Definition [WWW Document]. URL https://www.oxfordlearnersdictionaries.com/definition/english/exposure?q=exposure (accessed 5.27.21).

Part, F., Berge, N., Baran, P., Stringfellow, A., Sun, W., Bartelt-Hunt, S., Mitrano, D., Li, L., Hennebert, P., Quicker, P., Bolyard, S.C., Huber-Humer, M., 2018. A review of the fate of engineered nanomaterials in municipal solid waste streams. Waste Management. https://doi.org/10.1016/j.wasman.2018.02.012

Part, F., Zecha, G., Causon, T., Sinner, E.K., Huber-Humer, M., 2015. Current limitations and challenges in nanowaste detection, characterisation and monitoring. Waste Management 43, 407–420. https://doi.org/10.1016/j.wasman.2015.05.035

Pietroiusti, A., Stockmann-Juvala, H., Lucaroni, F., Savolainen, K., 2018. Nanomaterial exposure, toxicity, and impact on human health. Wiley Interdisciplinary Reviews: Nanomedicine and Nanobiotechnology. https://doi.org/10.1002/wnan.1513

Pomar-Portillo, V., 2019. NanoFASE report D4.2. - Identification and quantification of ENM releases from nano-enabled products - Release estimations during ENMs and nano-enabled products value chain.

Pomar-Portillo, V., Park, B., Crossley, A., Vázquez-Campos, S., 2021. Nanosafety research in Europe – Towards a focus on nano-enabled products. NanoImpact 22, 100323. https://doi.org/10.1016/j.impact.2021.100323

Quik, J.T.K., Velzeboer, I., Wouterse, M., Koelmans, A.A., van de Meent, D., 2014. Heteroaggregation and sedimentation rates for nanomaterials in natural waters. Water Research 48, 269–279. https://doi.org/10.1016/J.WATRES.2013.09.036

Rajkovic, S., Bornhöft, N.A., van der Weijden, R., Nowack, B., Adam, V., 2020. Dynamic probabilistic material flow analysis of engineered nanomaterials in European waste treatment systems. Waste Management 113, 118–131. https://doi.org/10.1016/j.wasman.2020.05.032

Salmatonidis, A., Viana, M., Biskos, G., Bezantakos, S., 2020. Particle size distributions and hygroscopic restructuring of ultrafine particles emitted during thermal spraying. Aerosol Science and Technology 54, 1359–1372. https://doi.org/10.1080/02786826.2020.1784837

Sánchez Jiménez, A., Puelles, R., Pérez-Fernández, M., Gómez-Fernández, P., Barruetabeña, L., Jacobsen, N.R., Suarez-Merino, B., Micheletti, C., Manier, N., Trouiller, B., Navas, J.M., Kalman, J., Salieri, B., Hischier, R., Handzhiyski, Y., Apostolova, M.D., Hadrup, N., Bouillard, J., Oudart, Y., Merino, C., Garcia, E., Liguori, B., Sabella, S., Rose, J., Masion, A., Galea, K.S., Kelly, S., Štěpánková, S., Mouneyrac, C., Barrick, A., Châtel, A., Dusinska, M., Rundén-Pran, E., Mariussen, E., Bressot, C., Aguerre-Chariol, O., Shandilya, N., Goede, H., Gomez-Cordon, J., Simar, S., Nesslany, F., Jensen, K.A., van Tongeren, M., Rodríguez Llopis, I., 2020. Safe(r) by design implementation in the nanotechnology industry. NanoImpact 20, 100267. https://doi.org/10.1016/j.impact.2020.100267

Schindelin, J., Arganda-Carreras, I., Frise, E., Kaynig, V., Longair, M., Pietzsch, T., Preibisch, S., Rueden, C., Saalfeld, S., Schmid, B., Tinevez, J.-Y., White, D.J., Hartenstein, V., Eliceiri, K., Tomancak, P., Cardona, A., 2012. Fiji: an open-source platform for biological-image analysis. Nature Methods 9, 676–682. https://doi.org/10.1038/nmeth.2019

Schneider, J., Matsuoka, M., Takeuchi, M., Zhang, J., Horiuchi, Y., Anpo, M., Bahnemann, D.W., 2014. Understanding TiO2 Photocatalysis: Mechanisms and Materials. Chemical Reviews. https://doi.org/10.1021/cr5001892

Schug, T.T., Johnson, A.F., Balshaw, D.M., Garantziotis, S., Walker, N.J., Weis, C., Nadadur, S.S., Birnbaum, L.S., 2013. ONE Nano: NIEHS's strategic initiative on the health and safety effects of engineered nanomaterials. Environmental health perspectives 121, 410–4. https://doi.org/10.1289/ehp.1206091

Schulte, P.A., Geraci, C.L., Murashov, V., Kuempel, E.D., Zumwalde, R.D., Castranova, V., Hoover, M.D., Hodson, L., Martinez, K.F., 2014. Occupational safety and health criteria for responsible development of nanotechnology. Journal of Nanoparticle Research 16, 2153. https://doi.org/10.1007/s11051-013-2153-9

Schwarz-Plaschg, C., Kallhoff, A., Eisenberger, I., 2017. Making Nanomaterials Safer by Design? NanoEthics 11, 277–281. https://doi.org/10.1007/s11569-017-0307-4

Scott, K., Pomar-Portillo, V., Vázquez-Campos, S., 2017. Nanomaterials in Textiles, in: Metrology and Standardization of Nanotechnology. Wiley-VCH Verlag GmbH & Co. KGaA, Weinheim, Germany, pp. 559–572. https://doi.org/10.1002/9783527800308.ch31

Shandilya, N., Kuijpers, E., Tuinman, I., Fransman, W., 2019. Powder Intrinsic Properties as Dustiness Predictor for an Efficient Exposure Assessment? Annals of Work Exposures and Health 63, 1029–1045. https://doi.org/10.1093/annweh/wxz065

Stark, W.J., Stoessel, P.R., Wohlleben, W., Hafner, A., 2015. Industrial applications of nanoparticles. Chemical Society Reviews 44, 5793–5805. https://doi.org/10.1039/c4cs00362d

Starost, K., Frijns, E., van Laer, J., Faisal, N., Egizabal, A., Elizextea, C., Blazquez, M., Nelissen, I., Njuguna, J., 2017. Assessment of nanoparticles release into the environment during drilling of carbon nanotubes/epoxy and carbon nanofibres/epoxy nanocomposites. Journal of Hazardous Materials 340, 57–66. https://doi.org/10.1016/j.jhazmat.2017.06.057

StatNano - Nanotechnology Products Database [WWW Document], 2021. URL http://product.statnano.com/ (accessed 1.11.21).

Sun, T.Y., Bornhöft, N.A., Hungerbühler, K., Nowack, B., 2016. Dynamic Probabilistic Modeling of Environmental Emissions of Engineered Nanomaterials. Environmental Science and Technology. https://doi.org/10.1021/acs.est.5b05828

Sun, T.Y., Gottschalk, F., Hungerbühler, K., Nowack, B., 2014. Comprehensive probabilistic modelling of environmental emissions of engineered nanomaterials. Environmental Pollution 185, 69–76. https://doi.org/10.1016/j.envpol.2013.10.004

Suzuki, S., Part, F., Matsufuji, Y., Huber-Humer, M., 2018. Modeling the fate and end-of-life phase of engineered nanomaterials in the Japanese construction sector. Waste Management 72, 389–398. https://doi.org/10.1016/j.wasman.2017.11.037

Syberg, K., Foss Hansen, S., 2016. Environmental risk assessment of chemicals and nanomaterials-The best foundation for regulatory decision-making? Science of the Total Environment 541, 784–794. https://doi.org/10.1016/j.scitotenv.2015.09.112

The Royal Society & The Royal Academy of Engineering, 2004. Nanoscience and nanotechnologies: opportunities and uncertainties.

United States Environmental Protection Agency (EPA), 1992. Test Method 1311: Toxicity characterization leaching procedure. Washington DC.

United States National Nanotechnology Initiative (NNI), 2021. What Is Nanotechnology? | National Nanotechnology Initiative [WWW Document]. URL https://www.nano.gov/nanotech-101/what/definition (accessed 5.25.21).

van de Poel, I., Robaey, Z., 2017. Safe-by-Design: from Safety to Responsibility. NanoEthics 11, 297–306. https://doi.org/10.1007/s11569-017-0301-x

Vejerano, E.P., Leon, E.C., Holder, A.L., Marr, L.C., 2014. Characterization of particle emissions and fate of nanomaterials during incineration. Environmental Science: Nano. https://doi.org/10.1039/c3en00080j

Walser, T., Limbach, L.K., Brogioli, R., Erismann, E., Flamigni, L., Hattendorf, B., Juchli, M., Krumeich, F., Ludwig, C., Prikopsky, K., Rossier, M., Saner, D., Sigg, A., Hellweg, S., Günther, D., Stark, W.J., 2012. Persistence of engineered nanoparticles in a municipal solid-waste incineration plant. Nature Nanotechnology 7, 520–524. https://doi.org/10.1038/nnano.2012.64

Wang, L., Hu, C., Shao, L., 2017. The antimicrobial activity of nanoparticles: present situation and prospects for the future. International journal of nanomedicine 12, 1227–1249. https://doi.org/10.2147/IJN.S121956

Wang, Y., Kalinina, A., Sun, T., Nowack, B., 2016. Probabilistic modeling of the flows and environmental risks of nano-silica 545–546, 67–76. https://doi.org/10.1016/j.scitotenv.2015.12.100

Woodrow Wilson International Center for Scholars, 2021. The project on emerging nanotechnologies - Consumer Products Inventory [WWW Document]. URL https://www.nanotechproject.org/cpi/ (accessed 1.14.20).

Ya, X., Jingcai, L., Lu, D., Yuqiang, L., Weishi, L., Changxing, N., Qifei, H., 2019. Buffering distance between hazardous waste landfill and water supply wells in a shallow aquifer. Journal of Cleaner Production 211, 1180–1189. https://doi.org/10.1016/j.jclepro.2018.11.161

Zielińska, A., Costa, B., Ferreira, M. v, Miguéis, D., S Louros, J.M., Durazzo, A., Lucarini, M., Eder, P., Chaud, M. v, Morsink, M., Willemen, N., Severino, P., Santini, A., Souto, E.B., 2020. Nanotoxicology and Nanosafety: Safety-by-Design and Testing at a Glance. Int. J. Environ. Res. Public Health 17, 4657. https://doi.org/10.3390/ijerph17134657

7. ANNEX: ABBREVIATIONS AND ACRONYMS

Abbreviations and Acronyms	Description
ALI	Air-liquid interface
ANOVA	Analysis of Variance
ANSES	Agence nationale de sécurité sanitaire
ATR	Attenuated total reflection
BET	Brunauer–Emmett–Teller
BSE	Backscattered electron
CB	Carbon black
CNT	Carbon nanotubes
CORDIS	Community research and development information service
CPS	Counts per second
DLS	Dynamic light scattering
DMF	N,N-dimethylformamide
DNEL	Derived No-Effect Level
DSC	Differential Scanning Calorimetry
EBW	Exposure Based Waiving
EC	European Commission
ECHA	European Chemical Agency
EDX	Energy dispersive X-ray analysis
ENM	Engineered nanomaterial
EoL	End-of-life
EPA	United States Environmental Protection Agency
ES	Exposure scenarios
EU	European Union
EU-ON	European Union Observatory for Nanomaterials
FAIR	Findability, accessibility, interoperability, and reusability
FE-SEM	Field emission scanning electron microscopy
FP	Framework Programmes
FT-IR	Fourier Transform Infrared Spectroscopy
GDP	Gross Domestic Product
HBM	Hot Bituminous Mix
HR-TEM	High resolution transmission electron microscopy
ICDD	International Centre for Diffraction Data
ICPMS	Inductively coupled plasma mass spectrometry
ICPOES	Inductively coupled plasma optical emission spectroscopy
ISO	International Standards Organization
IUPAC	International Union of Pure and Applied Chemistry
LC	Life-cycle
LCS	Life-cycle stage
LFP	Lithium iron phosphate
MF	Material Flow
MFA	Material Flow Analysis
MMT	Montmorillonites
MPPD	Multiple particle path dosimetry model
Mt	Million tonnes per year

MWCNT	Multi-walled carbon nanotubes
NC	Nanocomposite
NEP	Nano-enabled products
NF	Nanofiber
NIST	National Institute of Standards and Technology
NM	Nanomaterial
NMC	Nickel manganese cobalt oxide
NNI	National Nanotechnology Initiative
NP	Nanoparticle
NSC	NanoSafety Cluster
NW	Nanowire
OECD	The Organisation for Economic Co-operation and Development
OPS	Optical particle sizer
PA6	Polyamide 6
PEC	Predicted environmental concentration
PEG	Polyethylene glycol
PEI	Polyethylenimine
PES	Polyester
PET	Polyethylene terephthalate
PNC	Particle number concentration
PNEC	Predicted no-effect concentration
PPB	Parts per billion
PPM	Parts per million
PVP	Polyvinylpyrrolidone
QDs	Quantum dots
REACH	Registration, Evaluation, Authorisation and Restriction of Chemicals
ROS	Reactive oxygen species
RSD	Relative standard deviation
SbD	Safe-by-design
SE	Secondary electron
SEM	Scanning electron microscopy
SI	Supplementary information
SME	Small-to-Medium Enterprise
SMPS	Scanning Mobility Particle Sizer
STM	Scanning tunneling microscope
TDMA	Titanium Dioxide Manufacturers Association
TEM	Transmission Electron Microscopy
TGA	Thermogravimetric Analysis
TNO	Nederlandse Organisatie voor Toegepast Natuurwetenschappelijk Onderzoek (English: Netherlands Organisation for Applied Scientific Research)
UV	Ultraviolet
VOC	Volatile Organic Compounds
WWTP	Wastewater Treatment Plants
XRD	X-Ray Diffraction
ZOPA	Zinc Oxide Producers Association

8. ACKNOWLEDGEMENTS

Most of the work performed in the PhD Thesis was carried out in the framework of NANOFASE project (grant agreement 646002). I am extremely grateful to the whole NANOFASE consortium, with whom along the 4 years that the project lasted, allowed me to learn from them and supported me with the development of this thesis. I would specially like to thank to the partners involved in Work Package 4 with whom we shared tasks and maintained very interesting discussions. Furthermore, I would also like to acknowledge the other projects that provided funding for some of the studies presented: NANOPOLYTOX (grant agreement 247899), QUALITY NANO (grant agreement 262163), NANOSOLUTIONS (grant agreement 309329).

I am extremely grateful to my supervisor, Dr. Socorro Vázquez for her mentoring, not only through the Thesis, but in all research-related subjects to which she has provided guidance along the years that we have been working together. I also want to thank her for all the opportunities given and, among all, for generating a comfortable and friendly environment to work in. I also want to acknowledge Dr. Keana Scott for making my internship in the United States possible and guiding and helping me during all this period. I would also like to thank my tutor at the University of Barcelona (Faculty of Chemistry) Dr. Daniel Sainz Garcia for his kind support and advice every time I requested his assistance.

Kind acknowledgements to all the co-authors of the scientific papers included in this Thesis. My sincere gratitude to Prof. Dr. Barry Park from GBP and to Dr. Alison Crossley from Oxford University for sharing their vast expertise and their help and cooperation during the writing of the paper and execution of NANOFASE project. My honest thanks to Maria Blázquez from INKOA and to Jeroen Kuenen from TNO, for leading the peer-reviewed publication preparation of two of the papers included in this thesis. My warmest appreciations to Dr. Elisabeth Fernandez and David González from LEITAT, for always giving assistance and providing excellent research contributions to the work.

To my trustworthy co-workers, Dr. Nathan Bossa, Dr. Apostolos (Tolis) Salmatonidis and David Burrueco for all their help and support, specially for creating a wonderful working environment. My sincere appreciation to Dr. Alejandro Vilchez, Dr. Camilla Delpivo and Dr. Joan Cabellos for always having my back in the difficult moments and being a source of inspiration. I would also like to express my thanks to Dr. Bea Guerrero, Dr. Aleix Conesa and Clara Bagan for all the support provided with analytical services and their always excellent contribution to the results and discussions.

I owe gratitude to my parents for supporting my education throughout the years. Above all, I am entirely grateful to my family and friends, which I thank for everything.